First principles methods using CASTEP

Zeitschrift Fur Kristallographie - Crystalline Materials
220,
DOI: 10.1524/zkri.220.5.567.65075

Citation Report

#	Article	IF	Citations
1	Variational density-functional perturbation theory for dielectrics and lattice dynamics. Physical Review B, 2006, 73, .	1.1	735
2	Spectroscopic and Ab Initio Characterization of the [ReH9]2-Ion. Inorganic Chemistry, 2006, 45, 10951-10957.	1.9	25
3	Screened-exchange stress tensor in density functional theory. Physical Review B, 2006, 73, .	1.1	15
4	Density Functional Theory Based Ab Initio Molecular Dynamics Using the Car-Parrinello Approach. , 2006, , 223-285.		9
5	Implementation of linear-scaling plane wave density functional theory on parallel computers. Physica Status Solidi (B): Basic Research, 2006, 243, 973-988.	0.7	44
6	Lattice dynamical and dielectric properties of L-amino acids. Physical Review B, 2006, 74, .	1.1	24
7	When is H2O not water?. Journal of Chemical Physics, 2007, 127, 244503.	1.2	28
8	Achieving plane wave accuracy in linear-scaling density functional theory applied to periodic systems: A case study on crystalline silicon. Journal of Chemical Physics, 2007, 127, 164712.	1.2	46
9	Graphite intercalation compounds under pressure: A first-principles density functional theory study. Physical Review B, 2007, 75, .	1.1	35
10	A density functional study of the effect of hydrogen on the strength of an epitaxial Ag/ZnO interface. Journal of Applied Physics, 2007, 102, 103513.	1.1	12
11	Exchange-correlation holes in metal surfaces using nonlocal density-functional theory. Physical Review B, 2007, 76, .	1.1	5
12	Coupled Al/Si and O/N order/disorder in BaYb[Si4â€“xAlxOxN7â€“x]sialon: neutron powder diffraction and Monte Carlo simulations. Zeitschrift FÃ¼r Kristallographie, 2007, 222, .	1.1	11
13	Resolving Structures from Powders by NMR Crystallography Using Combined Proton Spin Diffusion and Plane Wave DFT Calculations. Journal of the American Chemical Society, 2007, 129, 8932-8933.	6.6	120
14	NMRcrystallography of oxybuprocaine hydrochloride, Modification IIÂ°. Physical Chemistry Chemical Physics, 2007, 9, 360-368.	1.3	102
15	Density functional theory study of flat and stepped NaCl(001). Physical Review B, 2007, 76, .	1.1	40
16	WO₃₋_x Nanorods Synthesized on a Thermal Hot Plate. Journal of Physical Chemistry C, 2007, 111, 17193-17199.	1.5	32
17	Carbon-13 Chemical Shift Tensors of Disaccharides:Â Measurement, Computation and Assignment. Journal of Physical Chemistry A, 2007, 111, 13126-13132.	1.1	44
18	Influence of the R-substituents on the properties of [Ni(R2pipdt)(dmit)] complexes and crystal structure where R = CH2C6H5. Dalton Transactions, 2007, , 5453.	1.6	19

#	Article	IF	Citations
19	Crystallinity and surface effects on Youngâ€™s modulus of CuO nanowires. Applied Physics Letters, 2007, 90, 163112.	1.5	92
20	Metallization of aluminum hydride at high pressures: A first-principles study. Physical Review B, 2007, 76, .	1.1	116
21	A first principles theory of nuclear magnetic resonance J-coupling in solid-state systems. Journal of Chemical Physics, 2007, 127, 204107.	1.2	76
22	Local Atomic Order and Infrared Spectra of Biogenic Calcite. Angewandte Chemie - International Edition, 2007, 46, 291-294.	7.2	76
24	Applications of Terahertz Spectroscopy in Biosystems. ChemPhysChem, 2007, 8, 2412-2431.	1.0	268
25	Chemical shift computations on a crystallographic basis: some reflections and comments. Magnetic Resonance in Chemistry, 2007, 45, S174-S186.	1.1	197
26	Ice formation on kaolinite: Lattice match or amphoterism?. Surface Science, 2007, 601, 5378-5381.	0.8	101
27	Precise ab-initio prediction of terahertz vibrational modes in crystalline systems. Chemical Physics Letters, 2007, 442, 275-280.	1.2	157
28	Experimental equilibrium crystal structures: Molecular dynamics as a probe for atomic probability density functions. Chemical Physics Letters, 2007, 448, 61-64.	1.2	15
29	Li and Na in diamond: A comparison of DFT models. Physica B: Condensed Matter, 2007, 401-402, 57-61.	1.3	8
30	Structure of phase III of solid hydrogen. Nature Physics, 2007, 3, 473-476.	6.5	593
31	High-pressure properties of diaspore, AlO(OH). Physics and Chemistry of Minerals, 2007, 34, 145-157.	0.3	45
32	A Theoretical Study of 51V Electric Field Gradient Tensors in Pyrovanadates and Metavanadates. Applied Magnetic Resonance, 2007, 32, 691-708.	0.6	12
33	A structure refinement strategy for NMR crystallography: An improved crystal structure of silica-ZSM-12 zeolite from 29Si chemical shift tensors. Journal of Magnetic Resonance, 2008, 194, 136-146.	1.2	66
34	Performance improvement of LiMn2O4 as cathode material for lithium ion battery with bismuth modification. Journal of Power Sources, 2008, 184, 408-413.	4.0	39
35	Study of high-pressure and high-temperature behaviors and Î±-to-Î² phase transition of forsterite by first-principles and quasi-harmonic Debye model. Computer Physics Communications, 2008, 179, 417-423.	3.0	14
36	Formation of impurity bands in iodine cation substitutionally doped TiO2 and its effects on photoresponse and photogenerated carriers. Physics Letters, Section A: General, Atomic and Solid State Physics, 2008, 372, 5901-5904.	0.9	8
37	How strong is the bond between water and salt?. Surface Science, 2008, 602, L135-L138.	0.8	21

#	Article	IF	Citations
38	First principles study of the adhesion asymmetry of a metal/oxide interface. Journal of Materials Science, 2008, 43, 3960-3968.	1.7	19
39	First principles study of three-component SrTiO3/BaTiO3/PbTiO3 ferroelectric superlattices. Journal of Materials Science, 2008, 43, 3750-3760.	1.7	22
40	Defect properties of albite. Physics and Chemistry of Minerals, 2008, 35, 129-135.	0.3	9
41	First atomistic studies of epitaxial growth of Na_{0.5}Bi_{0.5}TiO₃ on SrTiO₃. Physica Status Solidi (B): Basic Research, 2008, 245, 2649-2656.	0.7	6
42	Electronic properties of chemically modi.ed graphene ribbons. Physica Status Solidi (B): Basic Research, 2008, 245, 2068-2071.	0.7	22
43	Highâ€precision calculation of Hartreeâ€Fock energy of crystals. Journal of Computational Chemistry, 2008, 29, 2098-2106.	1.5	25
44	Reaction dynamics of H2 on Si. Ab initio supported model calculations. Progress in Surface Science, 2008, 83, 263-336.	3.8	36
45	Virtual crystal approximation study of nitridosilicates and oxonitridoaluminosilicates. Journal of Physics and Chemistry of Solids, 2008, 69, 1861-1868.	1.9	12
46	wannier90: A tool for obtaining maximally-localised Wannier functions. Computer Physics Communications, 2008, 178, 685-699.	3.0	2,947
47	13C CP MAS NMR and DFT study of vascular-selective drugs felodipine and amlodipine. Chemical Physics Letters, 2008, 463, 195-200.	1.2	13
48	Photocatalytic activities of AgSbO3 under visible light irradiation. Catalysis Today, 2008, 131, 197-202.	2.2	121
49	The vibrational spectrum of indole: An inelastic neutron scattering study. Chemical Physics, 2008, 345, 230-238.	0.9	16
50	Water on the hydroxylated (001) surface of kaolinite: From monomer adsorption to a flat 2D wetting layer. Surface Science, 2008, 602, 960-974.	0.8	155
51	Calculated loss function of C60: The effect of bond length. Ultramicroscopy, 2008, 108, 1476-1477.	0.8	0
52	The electronic structure and ferromagnetism of TM (TM=V, Cr, and Mn)-doped BN(5,5) nanotube: A first-principles study. Physica B: Condensed Matter, 2008, 403, 4213-4216.	1.3	26
53	Electronic Structures of Manganese-Doped Rutile TiO₂ from First Principles. Journal of Physical Chemistry C, 2008, 112, 18677-18685.	1.5	135
54	Reversible Structural Transition in MIL-53 with Large Temperature Hysteresis. Journal of the American Chemical Society, 2008, 130, 11813-11818.	6.6	402
55	Graphitic carbon nitride materials: variation of structure and morphology and their use as metal-free catalysts. Journal of Materials Chemistry, 2008, 18, 4893.	6.7	2,891

#	Article	IF	Citations
56	Modeling the interplay of inter- and intramolecular hydrogen bonding in conformational polymorphs. Journal of Chemical Physics, 2008, 128, 244708.	1.2	83
57	Computational prediction of organic crystal structures and polymorphism. International Reviews in Physical Chemistry, 2008, 27, 541-568.	0.9	103
58	Highly compressed ammonia forms an ionic crystal. Nature Materials, 2008, 7, 775-779.	13.3	166
60	Structure-Mechanical Property of Individual Cobalt Oxide Nanowires. Nano Letters, 2008, 8, 3226-3232.	4.5	57
61	Edge-functionalized and substitutionally doped graphene nanoribbons: Electronic and spin properties. Physical Review B, 2008, 77, .	1.1	503
62	First-principles calculations of boron-rich compounds of B13N2and B12C2X (X = Si, Ge). Journal of Physics Condensed Matter, 2008, 20, 505211.	0.7	9
63	Recent progress in linear-scaling density functional calculations with plane waves and pseudopotentials: the ONETEP code. Journal of Physics Condensed Matter, 2008, 20, 064209.	0.7	19
64	Density Functional Study of the ¹³C NMR Chemical Shifts in Single-Walled Carbon Nanotubes with Stoneâ^'Wales Defects. Journal of Physical Chemistry C, 2008, 112, 11744-11750.	1.5	56
65	Characterization of Layered Î³-Titanium Phosphate (C2H5NH3)[Ti(H1.5PO4)(PO4)]2Â·H2O Intercalate: A Combined NMR, Synchrotron XRD, and DFT Calculations Study. Chemistry of Materials, 2008, 20, 3944-3953.	3.2	27
66	Mechanism of linear and nonlinear optical effects of chalcopyrites LiGaX2 (X=S, Se, and Te) crystals. Journal of Applied Physics, 2008, 103, 083111.	1.1	60
67	Comparison of the Adsorption of Ni, Pd, and Pt on the (0001) Surface of Î±-Alumina. Journal of Physical Chemistry C, 2008, 112, 18948-18954.	1.5	32
68	Density-functional investigation of the rhombohedral to simple-cubic phase transition of arsenic. Physical Review B, 2008, 78, .	1.1	18
69	Hydrogen in<mml:math xmlns:mml="http://www.w3.org/1998/Math/MathML" display="inline"><mml:mi>Î±</mml:mi></mml:math>-iron: Stress and diffusion. Physical Review B, 2008, 78, .	1.1	67
70	Theory of core-hole effects in<mml:math xmlns:mml="http://www.w3.org/1998/Math/MathML" display="inline"><mml:mrow><mml:mn>1</mml:mn><mml:mi>s</mml:mi></mml:mrow></mml:math>core-level spectroscopy of the first-row elements. Physical Review B, 2008, 77, .	1.1	102
71	Strong physisorption site for H2 in K- and Li-doped porous carbons. Journal of Chemical Physics, 2008, 129, 224701.	1.2	23
72	NMR crystallography of p-tert-butylcalix[4]arene hostâ€"guest complexes using 1H complexation-induced chemical shifts. Physical Chemistry Chemical Physics, 2008, 10, 3857.	1.3	45
73	Structure and NMR assignment in calcined and as-synthesized forms of AlPO-14: a combined study by first-principles calculations and high-resolution 27Alâ€"31P MAS NMR correlation. Physical Chemistry Chemical Physics, 2008, 10, 5754.	1.3	95
74	Crystal Structures of Calcium IV and V under High Pressure. Physical Review Letters, 2008, 101, 095503.	2.9	47

#	Article	IF	Citations
75	Pressure effect on the structural and elastic properties of ternary compounds M₂AlC (M) Tj ETQq0 0 0 rgBT /Overlock 10 T	0.8	6
76	The influence of pressure on the structure and dynamics of hydrogen bonds in zoisite and clinozoisite. Physics and Chemistry of Minerals, 2008, 35, 25-35.	0.3	15
77	Theory: Periodic Electronic Structure Calculations. , 0, , 323-389.		1
78	Characterization of Polymorphs and Solvates of Terbutaline Sulfate. Crystal Growth and Design, 2008, 8, 80-90.	1.4	36
79	First-principles calculation of the effect of stress on the chemical activity of graphene. Applied Physics Letters, 2008, 93, .	1.5	50
80	Physical methods and techniques : NMR spectroscopy. Annual Reports on the Progress of Chemistry Section B, 2008, 104, 312.	0.8	2
81	Interatomic potentials for strontium titanate: An assessment of their transferability and comparison with density functional theory. Physical Review B, 2008, 78, .	1.1	70
82	A computational study of order-disorder phenomena in Mg2TiO4 spinel (qandilite). American Mineralogist, 2008, 93, 1363-1372.	0.9	16
83	Subsolidus phase relations in Ca2Mo2O8â€“NaEuMo2O8-powellite solid solution predicted from static lattice energy calculations and Monte Carlo simulations. Physical Chemistry Chemical Physics, 2008, 10, 3509.	1.3	19
84	Calcium-43 Chemical Shift Tensors as Probes of Calcium Binding Environments. Insight into the Structure of the Vaterite CaCO₃ Polymorph by ⁴³Ca Solid-State NMR Spectroscopy. Journal of the American Chemical Society, 2008, 130, 9282-9292.	6.6	92
85	NMR Crystallography of Zeolites: Refinement of an NMR-Solved Crystal Structure Using ab Initio Calculations of ²⁹Si Chemical Shift Tensors. Journal of the American Chemical Society, 2008, 130, 6306-6307.	6.6	96
86	Arsenate Incorporation in Gypsum Probed by Neutron, X-ray Scattering and Density Functional Theory Modeling. Journal of Physical Chemistry A, 2008, 112, 5159-5166.	1.1	47
87	Vibrational Spectra of Î±-Amino Acids in the Zwitterionic State in Aqueous Solution and the Solid State: DFT Calculations and the Influence of Hydrogen Bonding. Journal of Physical Chemistry A, 2008, 112, 10333-10347.	1.1	63
88	Hydrogen/silicon complexes in silicon from computational searches. Physical Review B, 2008, 78, .	1.1	46
89	Determining the Diameter of Functionalized Single-Walled Carbon Nanotubes with 13C NMR: A Theoretical Study. Journal of Physical Chemistry C, 2008, 112, 9267-9271.	1.5	30
90	The Phonon Spectrum of Phase-I Ammonia:â€‰ Reassignment of Lattice Mode Symmetries from Combined Molecular and Lattice Dynamics Calculations. Journal of Physical Chemistry A, 2008, 112, 1322-1329.	1.1	11
91	The Complex Excited-state Behavior of a Polyspirobifluorene Derivative: The Role of Spiroconjugation and Mixed Charge Transfer Character on Excited-state Stabilization and Radiative Lifetime. Journal of Physical Chemistry B, 2008, 112, 16300-16306.	1.2	33
92	Characterization of the High-Pressure Structural Transition and Thermodynamic Properties in Sodium Chloride: A Computational Investigation on the Basis of the Density Functional Theory. Journal of Physical Chemistry B, 2008, 112, 13898-13905.	1.2	9

#	Article	IF	Citations
93	Thermodynamics of oxygen defective MagnÃ©li phases in rutile: A first-principles study. Physical Review B, 2008, 77, .	1.1	92
94	Density Functional Theory Calculations of Hydrogen-Bond-Mediated NMR J Coupling in the Solid State. Journal of the American Chemical Society, 2008, 130, 12663-12670.	6.6	63
95	Structure and thermal fluctuation of one-dimensional AgO chains on Ag(110) surfaces studied with density functional theory and Monte Carlo simulations. Journal of Chemical Physics, 2008, 129, 154709.	1.2	4
96	Reaction of rhenium and carbon at high pressures and temperatures. Zeitschrift Fur Kristallographie - Crystalline Materials, 2008, 223, 492-501.	0.4	40
97	Applications and theoretical simulation of low-loss electron energy-loss spectra. Materials Science and Technology, 2008, 24, 651-659.	0.8	12
98	Defect structures in the silver halides. Physical Review B, 2008, 77, .	1.1	15
99	Mechanism of the linear electro-optic effect in potassium dihydrogen phosphate crystals. Journal of Applied Physics, 2008, 104, 073116.	1.1	7
100	Analysis of periodic SchrÃ¶dinger operators: Regularity and approximation of eigenfunctions. Journal of Mathematical Physics, 2008, 49, 083501.	0.5	12
101	Dielectric property analysis for the different charge defects in SiO<inf>2</inf> based on the first principles. , 2008, , .		1
102	Many-flavor electron gas approach to electron-hole drops. Physical Review B, 2008, 78, .	1.1	2
103	Diffusion Monte Carlo study of a valley-degenerate electron gas and application to quantum dots. Physical Review B, 2008, 78, .	1.1	0
104	Quantum Delocalization of Molecular Hydrogen in Alkali-Graphite Intercalates. Physical Review Letters, 2008, 101, 126101.	2.9	32
105	Defect-Induced Photoconductivity in Layered Manganese Oxides: A Density Functional Theory Study. Physical Review Letters, 2008, 100, 146601.	2.9	98
106	First principles investigation of polarisation at interfaces in multilayered strontium titanate. Journal of Physics: Conference Series, 2008, 94, 012005.	0.3	6
107	Chemically selective modification of spin polarization in ultrathin ferromagnetic films: Microscopic theory and macroscopic experiment. Physical Review B, 2009, 80, .	1.1	7
108	Structural, energetic, and electronic trends in low-dimensional late-transition-metal systems. Physical Review B, 2009, 79, .	1.1	31
109	Ultrafast electron and lattice dynamics at potassium-covered Cu(111) surfaces. Physical Review B, 2009, 80, .	1.1	14
110	Carbon nitride:Ab initioinvestigation of carbon-rich phases. Physical Review B, 2009, 80, .	1.1	48

#	Article	IF	Citations
111	Azobenzene at coinage metal surfaces: Role of dispersive van der Waals interactions. Physical Review B, 2009, 80, .	1.1	462
112	Evidence for hydrogen transport in deuterated<mml:math xmlns:mml="http://www.w3.org/1998/Math/MathML" display="inline"><mml:mrow><mml:msub><mml:mrow><mml:mtext>LiBH</mml:mtext></mml:mrow><mml:mn>4</mml:mn></mml:msub></mml:mrow></mml:math> low-temperature Raman-scattering measurements and first-principles calculations. Physical Review B, 2009, 80, .	1.1	87
113	Post-cotunnite phase ofTeO2obtained from first-principles density-functional theory methods with random-structure searching. Physical Review B, 2009, 80, .	1.1	10
114	Solid phases of phosphorus carbide: Anab initiostudy. Physical Review B, 2009, 79, .	1.1	37
115	First-principles study of native point defects in crystalline indium gallium zinc oxide. Journal of Applied Physics, 2009, 105, .	1.1	72
116	Tunability of the piezoelectric fields in strained III-V semiconductors. Applied Physics Letters, 2009, 95, 041912.	1.5	18
117	A study of the vibrational and thermoelectric properties of silicon type I and II clathrates. Journal of Applied Physics, 2009, 105, .	1.1	27
118	Atomic Positional Versus Electronic Order in Semiconducting ZnSe Nanoparticles. Physical Review Letters, 2009, 103, 136802.	2.9	59
119	Surface Stress of Stepped Chiral Metal Surfaces. Physical Review Letters, 2009, 102, 026102.	2.9	9
120	Core-level spectroscopy calculation and the plane wave pseudopotential method. Journal of Physics Condensed Matter, 2009, 21, 104203.	0.7	78
121	Ab initio modeling of layered materials with the CRYSTAL code: an overview. Zeitschrift FÃ¼r Kristallographie, 2009, 224, 241-250.	1.1	8
122	Isolation and aggregation of substituent Co in ZnO:Co diluted magnetic semiconductors. Journal of Physics Condensed Matter, 2009, 21, 175802.	0.7	14
123	First principles studies of an Si tip on an Si(100)2 Ã— 1 reconstructed surface. Journal of Physics Condensed Matter, 2009, 21, 185006.	0.7	3
124	Density functional theory, molecular dynamics, and differential scanning calorimetry study of the RbFâ€“CsF phase diagram. Journal of Chemical Physics, 2009, 130, 134716.	1.2	13
125	N codoping induced ferromagnetism in ZnO:Co (101Â¯) thin films. Journal of Applied Physics, 2009, 106, .	1.1	11
126	First-principles calculation of spectral features, chemical shift and absolute threshold of ELNES and XANES using a plane wave pseudopotential method. Journal of Physics Condensed Matter, 2009, 21, 104204.	0.7	88
127	Time and Frequency Resolved Hydrogen Dynamics in deuterated LiBH₄. Materials Research Society Symposia Proceedings, 2009, 1216, 1.	0.1	0
128	The Structure of (SCN)_x: A Study Using Molecular and Solidâ€State Density Functional Theory Calculations. Chemistry - A European Journal, 2009, 15, 2687-2692.	1.7	7

#	Article	IF	Citations
129	Natural Abundance ²⁵Mg Solidâ€State NMR of Mg Oxyanion Systems: A Combined Experimental and Computational Study. Chemistry - A European Journal, 2009, 15, 9785-9798.	1.7	53
130	Where does Hydrogen Adsorb on Ru Nanoparticles? A Powerful Joint ²H MASâ€NMR/DFT Approach. ChemPhysChem, 2009, 10, 2939-2942.	1.0	30
131	Vibrational spectroscopy of a compound with a CS₇ ring. Journal of Raman Spectroscopy, 2009, 40, 703-708.	1.2	3
132	Measurement of Î”1J(199Hg, 31P) in [HgPCy3(OAc)2]2 and relativistic ZORA DFT investigations of mercuryâ€“phosphorus coupling tensors. Solid State Nuclear Magnetic Resonance, 2009, 36, 182-191.	1.5	13
133	Pressure-induced structural transformations of the Zintl phase sodium silicide. Journal of Solid State Chemistry, 2009, 182, 2535-2542.	1.4	12
134	Structures at high pressure from random searching. Physica Status Solidi (B): Basic Research, 2009, 246, 536-540.	0.7	71
135	NMR shifts for polycyclic aromatic hydrocarbons from firstâ€principles. International Journal of Quantum Chemistry, 2009, 109, 3336-3342.	1.0	39
136	Orderâ€“disorder of oxygen anions and vacancies in solid solutions of La₂TiO₅ and La₄Ga₂O₉. Acta Crystallographica Section B: Structural Science, 2009, 65, 558-566.	1.8	6
137	Crystal structure and charge-transport properties of N-trimethyltriindole: Novel p-type organic semiconductor single crystals. Organic Electronics, 2009, 10, 643-652.	1.4	56
138	Boronâ€“hydrogen complexes in diamond: Energy levels and metastable states. Physica B: Condensed Matter, 2009, 404, 4525-4528.	1.3	1
139	Electronic structure of LiGaS2. Solid State Communications, 2009, 149, 572-575.	0.9	28
140	Structural, elastic and electronic properties of ACTi3 (A=Al, In and Tl) antiperovskite. Solid State Communications, 2009, 149, 919-922.	0.9	9
141	A first-principles study on the structural, elastic and electronic properties of AlCSc3 and AlNSc3. Solid State Communications, 2009, 149, 1840-1842.	0.9	8
142	Adsorbate influence on the coercive field of ultrathin Co/Cu{110}. Surface Science, 2009, 603, L45-L48.	0.8	7
143	Achieving sub-nanometre particle mapping with energy-filtered TEM. Ultramicroscopy, 2009, 109, 1217-1228.	0.8	57
144	A systematic approach to choosing parameters for modelling fine structure in electron energy-loss spectroscopy. Ultramicroscopy, 2009, 109, 1374-1388.	0.8	23
145	Photoluminescence of gold, copper and niobium as a function of temperature. Journal of Luminescence, 2009, 129, 1610-1614.	1.5	4
146	High-pressure behavior of the ternary bismuth oxides , and. Journal of Solid State Chemistry, 2009, 182, 767-777.	1.4	30

#	Article	IF	Citations
147	First-principles determination of the ground-state structure of Mg(BH4)2. Chemical Physics Letters, 2009, 480, 203-209.	1.2	38
148	Active anatase (001)-like surface of hydrothermally synthesized titania nanotubes. Chemical Physics Letters, 2009, 482, 134-138.	1.2	4
149	Influence of vibrational entropy on structural stability of Nbâ€“Si and Moâ€“Si systems at elevated temperatures. Acta Materialia, 2009, 57, 2657-2664.	3.8	57
150	First-principles study of the electronic and optical properties of ZnO nanowires. Chinese Physics B, 2009, 18, 2508-2513.	0.7	25
151	A Density Functional Study of the 13C NMR Chemical Shifts in Fluorinated Single-Walled Carbon Nanotubes. Journal of Physical Chemistry A, 2009, 113, 4117-4124.	1.1	28
152	Application of Solid-State ²⁰⁹Bi NMR to the Structural Characterization of Bismuth-Containing Materials. Journal of the American Chemical Society, 2009, 131, 8271-8279.	6.6	63
153	3DÂImaging of the Fermi Surface by Thermal Diffuse Scattering. Physical Review Letters, 2009, 103, 076403.	2.9	14
154	Structural Characterization of Interlayer Expanded Zeolite Prepared From Ferrierite Lamellar Precursor. Chemistry of Materials, 2009, 21, 2904-2911.	3.2	70
155	Ab initio calculations on the borate nonlinear optical crystal BaAlBO3F2. Journal of Applied Physics, 2009, 106, .	1.1	25
156	Synthesis, Characterization, and Photocatalytic Properties of ZrMo₂O₈. Journal of Physical Chemistry C, 2009, 113, 10661-10666.	1.5	23
157	²⁷Al NMR Chemical Shifts in Oxide Crystals: A First-Principles Study. Journal of Physical Chemistry C, 2009, 113, 3869-3873.	1.5	53
158	First Principles Studies of Fe-Containing Aluminosilicate and Aluminogermanate Nanotubes. Journal of Chemical Theory and Computation, 2009, 5, 3224-3231.	2.3	19
159	Combined 135/137Ba Solid-State NMR at an Ultrahigh Magnetic Field and Computational Study of Î²-Barium Borate. Journal of Physical Chemistry C, 2009, 113, 21196-21201.	1.5	25
160	Probing Heteronuclear ¹⁵Nâ€“¹⁷O and ¹³Câ€“¹⁷O Connectivities and Proximities by Solid-State NMR Spectroscopy. Journal of the American Chemical Society, 2009, 131, 1820-1834.	6.6	76
161	Platinum Group Metal Adsorption on Clean and Hydroxylated Corundum Surfaces. Journal of Physical Chemistry C, 2009, 113, 16747-16756.	1.5	25
162	ELASTIC AND ELECTRONIC PROPERTIES OFHf₂SnCANDHf₂SnN. International Journal of Modern Physics B, 2009, 23, 5155-5161.	1.0	2
163	Stabilizing a molecular switch at solid surfaces: A density functional theory study of azobenzene on Cu(111), Ag(111), and Au(111). Physical Review B, 2009, 80, .	1.1	48
164	Initial Structure Memory of Pressure-Induced Changes in the Phase-Change Memory Alloy<mml:math xmlns:mml="http://www.w3.org/1998/Math/MathML" display="inline"><mml:msub><mml:mi>Ge</mml:mi><mml:mn>2</mml:mn></mml:msub><mml:msub><mml:mi>Sb</mml:mi><mml:mi>Physical Review Letters, 2009, 103, 115502.	2.9	51

#	Article	IF	Citations
165	Corrosion of barium aluminosilicates by water-vapour: An investigation from first principles. Corrosion Science, 2009, 51, 2126-2129.	3.0	35
166	First-principles calculations of structural, electronic and elastic properties of Ca2MgSi2O7. Computational Materials Science, 2009, 47, 35-40.	1.4	5
167	Zinc surface complexes on birnessite: A density functional theory study. Geochimica Et Cosmochimica Acta, 2009, 73, 1273-1284.	1.6	63
168	On the role of Mn(IV) vacancies in the photoreductive dissolution of hexagonal birnessite. Geochimica Et Cosmochimica Acta, 2009, 73, 4142-4150.	1.6	87
169	Elastic properties of hydrous forsterites under high pressure: First-principle calculations. Physics of the Earth and Planetary Interiors, 2009, 176, 89-97.	0.7	24
170	A concerted rational crystallization/amorphization mechanism of Ge2Sb2Te5. Journal of Non-Crystalline Solids, 2009, 355, 2122-2126.	1.5	10
171	Reaction of titanium with carbon in a laser heated diamond anvil cell and reevaluation of a proposed pressure-induced structural phase transition of TiC. Journal of Alloys and Compounds, 2009, 478, 392-397.	2.8	32
172	Stability field of the high-(P, T) Re2C phase and properties of an analogous osmium carbide phase. Journal of Alloys and Compounds, 2009, 481, 577-581.	2.8	50
173	First-principles calculations of mechanical properties of TiC and TiN. Journal of Alloys and Compounds, 2009, 485, 542-547.	2.8	225
174	Density functional theory for transition metals and transition metal chemistry. Physical Chemistry Chemical Physics, 2009, 11, 10757.	1.3	1,431
175	Dense Low-Coordination Phases of Lithium. Physical Review Letters, 2009, 102, 146401.	2.9	103
177	A converse approach to the calculation of NMR shielding tensors. Journal of Chemical Physics, 2009, 131, 101101.	1.2	54
178	Predicting the Band Structure of Mixed Transition Metal Oxides: Theory and Experiment. Journal of Physical Chemistry C, 2009, 113, 2014-2021.	1.5	116
179	Calculation of NMR chemical shifts in organic solids: Accounting for motional effects. Journal of Chemical Physics, 2009, 130, 104701.	1.2	93
180	Red Shift in Manganese- and Iron-Doped TiO₂: A DFT+U Analysis. Journal of Physical Chemistry C, 2009, 113, 6800-6808.	1.5	154
181	Lattice dynamics of stishovite from powder inelastic Xâ€ray scattering. Geophysical Research Letters, 2009, 36, .	1.5	18
182	Density functional theory study of Fe(II) adsorption and oxidation on goethite surfaces. Physical Review B, 2009, 79, .	1.1	59
183	Structural, electronic and vibrational properties of tetragonal zirconia under pressure: a density functional theory study. Journal of Physics Condensed Matter, 2009, 21, 485404.	0.7	97

#	Article	IF	Citations
184	High-Pressure Phases of Nitrogen. Physical Review Letters, 2009, 102, 125702.	2.9	226
185	Stable phases of iron at terapascal pressures. Journal of Physics Condensed Matter, 2009, 21, 452205.	0.7	38
186	Intermolecular shielding contributions studied by modeling the C13 chemical-shift tensors of organic single crystals with plane waves. Journal of Chemical Physics, 2009, 131, 144503.	1.2	75
187	First principles determination of structural, electronic and lattice dynamical properties of a model dipeptide molecular crystal. Molecular Physics, 2009, 107, 2201-2212.	0.8	6
188	27Al NMR spectroscopy at multiple magnetic fields and ab initio quantum modeling for kaolinite. American Mineralogist, 2009, 94, 865-871.	0.9	18
189	First principles study ofÎ±-boron: can the B12cage host hetero-atoms?. Molecular Physics, 2009, 107, 1831-1842.	0.8	16
190	Chapter 5 Chlorine, Bromine, and Iodine Solid-State NMR Spectroscopy. Annual Reports on NMR Spectroscopy, 2009, 66, 195-326.	0.7	43
191	Hydrogen/nitrogen/oxygen defect complexes in silicon from computational searches. Physical Review B, 2009, 80, .	1.1	25
192	Optical properties of LiGaS₂: anab initiostudy and spectroscopic ellipsometry measurement. Journal of Physics Condensed Matter, 2009, 21, 455502.	0.7	18
193	Crystal Structure of Ammonia Monohydrate Phase II. Journal of the American Chemical Society, 2009, 131, 13508-13515.	6.6	59
194	A natural abundance³³S solid-state NMR study of layered transition metaldisulfides at ultrahigh magnetic field. Chemical Communications, 2009, , 186-188.	2.2	31
195	Vibrational Spectroscopy via Inelastic Neutron Scattering. , 2009, , 597-622.		5
196	Experimental and modelling techniques for assessing the adhesion of very thin coatings on glass. Journal Physics D: Applied Physics, 2009, 42, 214003.	1.3	22
197	Powder NMR crystallography of thymol. Physical Chemistry Chemical Physics, 2009, 11, 2610.	1.3	180
198	Growth of boehmite particles in the presence of xylitol: morphology oriented by the nest effect of hydrogen bonding. Physical Chemistry Chemical Physics, 2009, 11, 11310.	1.3	53
199	Characterizing Slight Structural Disorder in Solids by Combined Solid-State NMR and First Principles Calculations. Journal of Physical Chemistry A, 2009, 113, 902-911.	1.1	47
200	Static solid-state 14N NMR and computational studies of nitrogen EFG tensors in some crystalline amino acids. Physical Chemistry Chemical Physics, 2009, 11, 7069.	1.3	66
201	Supercell size scaling of density functional theory formation energies of charged defects. Physical Review B, 2009, 79, .	1.1	180

#	Article	IF	Citations
202	First-principles calculations of enhanced ferromagnetism in ZnO codoped with cobalt and nitrogen. Journal of Applied Physics, 2009, 105, 043906.	1.1	26
203	Vibrational Dynamics of LiBH₄ by Infrared Pumpâ˜Probe and 2D Spectroscopy. Journal of Physical Chemistry A, 2009, 113, 12838-12846.	1.1	33
204	A first principles study of the properties of Al:ZnO and its adhesion to Ag in an optical coating. Journal of Applied Physics, 2009, 106, .	1.1	14
205	Structure and stability of high pressure synthesized Mgâ€“TM hydrides (TM = Ti, Zr, Hf, V, Nb and Ta) as possible new hydrogen rich hydrides for hydrogen storage. Journal of Materials Chemistry, 2009, 19, 8150.	6.7	77
206	Nanoscale Phase Separation and Building Blocks of Ge₂Sb₂Te₅N and Ge₂Sb₂Te₅N₂ Thin Films. Chemistry of Materials, 2009, 21, 5244-5251.	3.2	39
207	High-resolution 17O double-rotation NMR characterization of ring and non-ring oxygen in vitreous B2O3. Physical Chemistry Chemical Physics, 2009, 11, 7061.	1.3	16
208	Study on conductivity property of quartz based on molecular simulation. , 2009, , .		0
209	Probing local structures of siliceous zeolite frameworks by solid-state NMR and first-principles calculations of 29Siâ€“Oâ€“29Si scalar couplings. Physical Chemistry Chemical Physics, 2009, 11, 1825.	1.3	76
210	Determining relative protonâ€“proton proximities from the build-up of two-dimensional correlation peaks in 1H double-quantum MAS NMR: insight from multi-spin density-matrix simulations. Physical Chemistry Chemical Physics, 2009, 11, 6941.	1.3	66
211	Mg-25 ultra-high field solid state NMR spectroscopy and first principles calculations of magnesium compounds. Physical Chemistry Chemical Physics, 2009, 11, 11487.	1.3	92
212	Two-Step Mechanism for Low-Temperature Oxidation of Vacancies in Graphene. Physical Review Letters, 2009, 102, 166104.	2.9	122
213	Application of multinuclear magnetic resonance and gauge-including projector-augmented-wave calculations to the study of solid group 13 chlorides. Physical Chemistry Chemical Physics, 2009, 11, 6987.	1.3	44
214	Crystallographic structure refinement with quadrupolar nuclei: a combined solid-state NMR and GIPAW DFT example using MgBr2. Physical Chemistry Chemical Physics, 2009, 11, 7120.	1.3	60
215	Structure and superconductivity of the intercalation compounds of TiNCl with pyridine and alkali metals as intercalants. Journal of Materials Chemistry, 2009, 19, 2573.	6.7	61
216	First-Principles calculations of structural, thermodynamic and electronic properties of intermetallic compounds in solder. , 2009, , .		2
217	Tin Oxide Nanoribbons with Vacancy Structures in Luminescence-Sensitive Oxygen Sensing. Nano Letters, 2009, 9, 1926-1931.	4.5	89
218	Boronâ€“hydrogen complexes in diamond and their vibrational properties. Diamond and Related Materials, 2009, 18, 835-838.	1.8	7
219	Pressure-Induced Metallization of a Single-Component Molecular Crystal. Journal of Physical Chemistry C, 2009, 113, 19310-19316.	1.5	11

#	Article	IF	Citations
220	Understanding the optical spectroscopy of amphiphilic molecular rectifiers: A density functional approach. Journal of Chemical Physics, 2010, 133, 244702.	1.2	1
221	Estimation of linear thermal expansion coefficient from cohesive energy obtained by ab-initio calculation of metals and ceramics. Journal of the Ceramic Society of Japan, 2010, 118, 241-245.	0.5	17
222	Atomistic model of diopside-K-jadeite (CaMgSi2O6-KAlSi2O6) solid solution. Petrology, 2010, 18, 447-459.	0.2	3
223	Piezoelastic properties of retgersite determined by ultrasonic measurements. European Physical Journal B, 2010, 73, 167-175.	0.6	15
224	Electronic and optical properties of aluminium-doped anatase and rutile<mml:math xmlns:mml="http://www.w3.org/1998/Math/MathML" display="inline"><mml:mrow><mml:msub><mml:mrow><mml:mtext>TiO</mml:mtext></mml:mrow><mml:mn>2</mml:mn></mml:msu initio</i>calculations. Physical Review B, 2010, 81, .	1.1	121
225	Stability and Decomposition of NaBH₄. Journal of Physical Chemistry C, 2010, 114, 7173-7177.	1.5	174
226	Powder Crystallography by Combined Crystal Structure Prediction and High-Resolution ¹H Solid-State NMR Spectroscopy. Journal of the American Chemical Society, 2010, 132, 2564-2566.	6.6	201
227	Can Na2[B12H12] be a decomposition product of NaBH4?. Physical Chemistry Chemical Physics, 2010, 12, 15093.	1.3	49
228	Very large scale wavefunction orthogonalization in Density Functional Theory electronic structure calculations. Computer Physics Communications, 2010, 181, 1057-1068.	3.0	13
229	Vibrational spectra and structures of urazole and 4-methylurazole: DFT calculations of the normal modes in aqueous solution and in the solid state, and the influence of hydrogen bonding. Chemical Physics, 2010, 373, 219-227.	0.9	7
230	New superconducting RbFe2As2: A first-principles investigation. Physica C: Superconductivity and Its Applications, 2010, 470, 202-205.	0.6	6
231	Density functional theory study of doping effects in monoclinic clinobisvanite BiVO4. Physics Letters, Section A: General, Atomic and Solid State Physics, 2010, 374, 4919-4927.	0.9	95
232	Changes in structure and proton conductivity at IIâ€“III phase transition of Rb3H(SO4)2. Solid State Ionics, 2010, 181, 567-571.	1.3	4
233	Solid-state NMR calculations for metal oxides and gallates: Shielding and quadrupolar parameters for perovskites and related phases. Journal of Magnetic Resonance, 2010, 204, 1-10.	1.2	44
234	KBiMS4 (M=Si, Ge): Synthesis, structure, and electronic structure. Journal of Solid State Chemistry, 2010, 183, 1640-1644.	1.4	25
235	Density Functional Study of Benzoquinone Sulfonate Adsorbed on a Pd(111) Electrode Surface. Electrocatalysis, 2010, 1, 159-162.	1.5	3
236	A first-principles study of the size-dependent electronic properties of SiC nanotubes. Science China: Physics, Mechanics and Astronomy, 2010, 53, 1333-1338.	2.0	4
237	Electronic structure and magnetism of Fe-doped SiC nanotubes. Science China: Physics, Mechanics and Astronomy, 2010, 53, 1582-1589.	2.0	23

#	Article	IF	Citations
238	Additive Occupancy in the Cu6Sn5-Based Intermetallic Compound Between Sn-3.5Ag Solder and Cu Studied Using a First-Principles Approach. Journal of Electronic Materials, 2010, 39, 426-432.	1.0	47
239	Thermoelectric Properties of Polycrystalline SrZn2Sb2 Prepared by Spark Plasma Sintering. Journal of Electronic Materials, 2010, 39, 1772-1776.	1.0	24
240	Elastic Moduli of (Ni,Cu)3Sn4 Ternary Alloys from First-Principles Calculations. Journal of Electronic Materials, 2010, 39, 2429-2434.	1.0	15
241	The effects of hydroxyl groups on Ca adsorption on rutile surfaces: a first-principles study. Journal of Materials Science: Materials in Medicine, 2010, 21, 1-10.	1.7	25
242	The ideal strength of transition metal diborides TMB2 (TM=Ti, Zr, Hf): Plastic anisotropy and the role of prismatic slip. Scripta Materialia, 2010, 62, 625-628.	2.6	62
243	First-principles comparative study of multiferroic compound PbVO3. Solid State Sciences, 2010, 12, 938-945.	1.5	21
244	X-ray photoelectron spectroscopic investigation on the elemental chemical shifts in multiferroic BiFeO3 and its valence band structure. Solid State Sciences, 2010, 12, 1803-1808.	1.5	39
245	In situ synchrotron X-ray diffraction study of the formation of TaB2 from the elements in a laser heated diamond anvil cell. Solid State Sciences, 2010, 12, 2059-2064.	1.5	15
246	Modulation of catalyst particle structure upon support hydroxylation: Ab initio insights into Pd13 and Pt13/Î³-Al2O3. Journal of Catalysis, 2010, 274, 99-110.	3.1	137
247	Calculation and Measurement of Terahertz Active Normal Modes in Crystalline PETN. ChemPhysChem, 2010, 11, 368-378.	1.0	30
248	Acidity of Amorphous Silicaâ€“Alumina: From Coordination Promotion of Lewis Sites to Proton Transfer. ChemPhysChem, 2010, 11, 105-108.	1.0	56
249	A ⁹³Nb Solidâ€State NMR and Density Functional Theory Study of Fourâ€and Sixâ€Coordinate Niobate Systems. Chemistry - A European Journal, 2010, 16, 3222-3239.	1.7	56
250	Probing the Electronic Effect of Carbon Nanotubes in Catalysis: NH₃ Synthesis with Ru Nanoparticles. Chemistry - A European Journal, 2010, 16, 5379-5384.	1.7	164
251	Dynamic Vapochromic Behaviors of Organic Crystals Based on the Openâ€“Close Motions of Sâ€Shaped Donorâ€“Acceptor Folding Units. Chemistry - A European Journal, 2010, 16, 4793-4802.	1.7	73
252	A computational investigation of J couplings involving 27Al, 17O, and 31P. Magnetic Resonance in Chemistry, 2010, 48, S69-S75.	1.1	7
253	New perspectives in the PAW/GIPAW approach: JP-O-Si coupling constants, antisymmetric parts of shift tensors and NQR predictions. Magnetic Resonance in Chemistry, 2010, 48, S86-S102.	1.1	42
254	Computation and NMR crystallography of terbutaline sulfate. Magnetic Resonance in Chemistry, 2010, 48, S103-S112.	1.1	76
255	Comparing quantum-chemical calculation methods for structural investigation of zeolite crystal structures by solid-state NMR spectroscopy. Magnetic Resonance in Chemistry, 2010, 48, S113-S121.	1.1	56

#	Article	IF	Citations
256	Contribution of first-principles calculations to multinuclear NMR analysis of borosilicate glasses. Magnetic Resonance in Chemistry, 2010, 48, S159-S170.	1.1	49
257	Lattice dynamics and elastic properties of Mg3As2 and Mg3Sb2 compounds from first-principles calculations. Physica B: Condensed Matter, 2010, 405, 4219-4225.	1.3	41
258	High pressure synthesis and properties of ternary titanium (III) fluorides in the system KFâ€“TiF3 containing regular pentagonal bipyramids [TiF7]. Journal of Solid State Chemistry, 2010, 183, 256-261.	1.4	4
259	Formation of scandium carbides and scandium oxycarbide from the elements at high-(P, T) conditions. Journal of Solid State Chemistry, 2010, 183, 975-983.	1.4	15
260	AlH3 between 65 and 110GPa: Implications of electronic band and phonon structures. Physica C: Superconductivity and Its Applications, 2010, 470, 403-406.	0.6	8
261	Elastic properties of mono- and poly-crystalline PbO-type FeSe1â^'xTex (x=0â€“1.0): A first-principles study. Physica C: Superconductivity and Its Applications, 2010, 470, 2072-2075.	0.6	28
262	Glassy ferromagnetism in Al-doped 4H-SiC: AlSiâ€“ complexes. Physics Letters, Section A: General, Atomic and Solid State Physics, 2010, 374, 3230-3233.	0.9	9
263	Testing the sensitivity limits of 33S NMR: An ultra-wideline study of elemental sulfur. Journal of Magnetic Resonance, 2010, 207, 345-347.	1.2	33
264	Elastic behavior of (MgxFe1â^'x)2SiO4 olivine at high pressure from first-principles simulations. Journal of Physics and Chemistry of Solids, 2010, 71, 1094-1097.	1.9	8
265	Counterintuitive charge distribution in Ba8Si6Sn â€“ A new tetralide Zintl phase containing -units. Inorganica Chimica Acta, 2010, 363, 4355-4360.	1.2	4
266	Electronic structures of silicon doped ZnO. Physica B: Condensed Matter, 2010, 405, 1980-1985.	1.3	25
267	Lattice dynamics of Î²-FeSi2 from first-principles calculations. Physica B: Condensed Matter, 2010, 405, 2200-2204.	1.3	18
268	Structural, electronic and optical properties of SrHfO3 (I4/mcm, Imma, Cmcm, P4/mbm and P4mm) phases. Physica B: Condensed Matter, 2010, 405, 3862-3868.	1.3	18
269	Optical properties of silicon doped ZnO. Physica B: Condensed Matter, 2010, 405, 4763-4767.	1.3	51
270	Theoretical ELNES using one-particle and multi-particle calculations. Micron, 2010, 41, 695-709.	1.1	79
271	Synergistic effect of different phase on the photocatalytic activity of visible light sensitive silver antimonates. Journal of Molecular Catalysis A, 2010, 320, 79-84.	4.8	21
272	Electron and vibrational spectroscopies using DFT, plane waves and pseudopotentials: CASTEP implementation. Computational and Theoretical Chemistry, 2010, 954, 22-35.	1.5	205
273	Structural, elastic, electronic and optical properties of the cubic perovskites (and Sn). Solid State Communications, 2010, 150, 350-355.	0.9	19

#	Article	IF	Citations
274	First-principles investigations of the band structure and optical properties of -boron. Solid State Communications, 2010, 150, 605-608.	0.9	21
275	Ab initio comparative study of the structural, elastic and electronic properties of antiperovskite cubic compounds. Solid State Communications, 2010, 150, 782-787.	0.9	10
276	Theoretical study on the electronic structures and optical properties of crystal with interstitial oxygen atom. Solid State Communications, 2010, 150, 897-900.	0.9	16
277	Theoretical investigations of the physical properties of tetragonal CaSiO3 perovskite. Solid State Communications, 2010, 150, 943-948.	0.9	21
278	The electronic and optical properties of mixed alloys. Solid State Communications, 2010, 150, 1413-1418.	0.9	19
279	Electronic structure and decomposition pathways of monoammoniate of lithium borohydride : A first-principles investigation. Solid State Communications, 2010, 150, 1552-1555.	0.9	2
280	Mechanism of the linear and nonlinear optical effects of and crystals. Solid State Communications, 2010, 150, 2318-2321.	0.9	12
281	Oxygen adatoms at SrTiO3(001): A density-functional theory study. Surface Science, 2010, 604, 372-376.	0.8	20
282	The structure and bonding of furan on Pd(111). Surface Science, 2010, 604, 920-925.	0.8	72
283	Ab initio study of water adsorption on TiO2-terminated (100) surface of SrTiO3 with and without Cr doping. Surface Science, 2010, 604, 1987-1995.	0.8	16
284	Analysis of computational EELS modelling results for MgO-based systems. Ultramicroscopy, 2010, 110, 1059-1069.	0.8	5
285	Mechanism of incorporation of zinc into hydroxyapatite. Acta Biomaterialia, 2010, 6, 2289-2293.	4.1	122
286	Element segregation on the surfaces of pure aluminum foils. Applied Surface Science, 2010, 256, 7300-7304.	3.1	22
287	The electronic transparency of a single CO molecule at contact. Chemical Physics Letters, 2010, 484, 237-241.	1.2	2
288	Distinguishing hydrogen bonding networks in Î±-d-galactose using NMR experiments and first principles calculations. Chemical Physics Letters, 2010, 498, 270-276.	1.2	33
289	Bulky spacer groups â€“ A valid strategy to control the coupling of functional molecules to surfaces?. Chemical Physics Letters, 2010, 499, 247-249.	1.2	24
290	Optical polarized properties of the F2 center in YAlO3 crystal. Journal of Electron Spectroscopy and Related Phenomena, 2010, 182, 47-50.	0.8	0
291	1-[2-(2,6-Diisopropylanilino)-1-naphthyl]isoquinoline. Acta Crystallographica Section C: Crystal Structure Communications, 2010, 66, o310-o312.	0.4	2

#	Article	IF	Citations
292	Persistence of the stereochemical activity of the Bi³⁺lone electron pair in Bi₂Ga₄O₉up to 50â€...GPa and crystal structure of the high-pressure phase. Acta Crystallographica Section B: Structural Science, 2010, 66, 323-337.	1.8	27
293	Structural polymorphism of pyrazinium hydrogen sulfate: extending chemistry of the pyrazinium salts with small anions. Acta Crystallographica Section B: Structural Science, 2010, 66, 451-457.	1.8	5
294	Synthesis, Crystal Structure and Lithium Motion of Li₈SeN₂ and Li₈TeN₂ÂÂ. Zeitschrift Fur Anorganische Und Allgemeine Chemie, 2010, 636, 936-946.	0.6	17
295	The Highâ€Pressure Phase of MgB₂C₂. Zeitschrift Fur Anorganische Und Allgemeine Chemie, 2010, 636, 2543-2549.	0.6	9
296	Stability and band gaps of InGaP, BGaP, and BInGaP alloys: Density-functional supercell calculations. Physica Status Solidi (B): Basic Research, 2010, 247, 59-66.	0.7	10
297	Ab initiocalculation of ELNES/XANES of BeO polymorphs. Physica Status Solidi (B): Basic Research, 2010, 247, 2190-2194.	0.7	9
298	The screenedâ€exchange approximation as alternative method for DFT calculations on graphene structures. Physica Status Solidi (B): Basic Research, 2010, 247, 2945-2948.	0.7	8
299	Chemical surface passivation of 3Câ€SiC nanocrystals: A firstâ€principle study. International Journal of Quantum Chemistry, 2010, 110, 2455-2461.	1.0	15
300	A genetic algorithm for predicting the structures of interfaces in multicomponent systems. Nature Materials, 2010, 9, 418-422.	13.3	152
301	Aluminium at terapascal pressures. Nature Materials, 2010, 9, 624-627.	13.3	202
302	Applications of the three-dimensional visualization system VESTA in mineralogical sciences. Ganseki Kobutsu Kagaku, 2010, 39, 136-145.	0.1	1
303	Crystal structure of antimony oxalate hydroxide, Sb(C2O4)OH. Powder Diffraction, 2010, 25, 19-24.	0.4	11
304	The role of vacancies in the pressure amorphisation phenomenon observed in Ge-Sb-Te phase change alloys. Materials Research Society Symposia Proceedings, 2010, 1251, 10.	0.1	0
305	An Efficient Cluster Expansion Method for Binary Solid Solutions: Application to the Halite-Silvite, NaCl-KCl, System. Reviews in Mineralogy and Geochemistry, 2010, 71, 413-436.	2.2	14
306	Temperature Dependence of Transistor Characteristics and Electronic Structure for Amorphous Inâ€“Gaâ€“Zn-Oxide Thin Film Transistor. Japanese Journal of Applied Physics, 2010, 49, 03CB04.	0.8	55
307	Methoxy Species on Cu(110): Understanding the Local Structure of a Key Catalytic Reaction Intermediate. Physical Review Letters, 2010, 105, 086101.	2.9	17
308	An ab initio study of the elastic behavior of single crystal group (IV) diborides at elevated temperatures. Applied Physics Letters, 2010, 97, .	1.5	9
309	Phase Stability and Electronic Structure of In-Free Photovoltaic Materials: Cu₂ZnSiSe₄, Cu₂ZnGeSe₄, and Cu₂ZnSnSe₄. Japanese Journal of Applied Physics, 2010, 49, 121203.	0.8	73

#	Article	IF	Citations
310	Vibrational properties ofRe3Nfrom experiment and theory. Physical Review B, 2010, 82, .	1.1	24
311	Asymmetric relief of surface stress induced by a chiral adsorbate: Alaninate adsorption on Cu(110). Physical Review B, 2010, 81, .	1.1	12
312	Photoemission core-level shifts reveal the thiolate-Au(111) interface. Physical Review B, 2010, 82, .	1.1	20
313	First-principles and experimental analysis of<mml:math xmlns:mml="http://www.w3.org/1998/Math/MathML" display="inline"><mml:mrow><mml:msup><mml:mi>f</mml:mi><mml:mi>n</mml:mi></mml:msup><mml:mtext>â^'</mml:mtext><mml:m spectra and multiplet energy levels of<mml:math xmlns:mml="http://www.w3.org/1998/Math/MathM. Physical Review B, 2010, 81, .	1.1	17
314	Eliminating ultraviolet optical absorption through Fe-impurity engineering:Ab initiostudy of the nonlinear optical crystalK2Al2B2O7. Physical Review B, 2010, 82, .	1.1	11
315	Density functional theory study of the relative stability of the iron disulfide polymorphs pyrite and marcasite. Physical Review B, 2010, 81, .	1.1	35
316	Structural assignments of NMR chemical shifts in<mml:math xmlns:mml="http://www.w3.org/1998/Math/MathML" display="inline"><mml:mrow><mml:msub><mml:mrow><mml:mtext>Ge</mml:mtext></mml:mrow><mml:mi>x</mml:mi></mml:msub> via first-principles calculations for<mml:math xmlns:mml="http://www.w3.org/1998/Math/MathML" display="inline"><mml:mrow><m. Physical Review B, 2010, 82, .	1.1	40
317	Design of three-dimensional solid-state boron oxide networks:Ab initiocalculations using density functional theory. Physical Review B, 2010, 82, .	1.1	13
318	Ab initioinvestigation of lithium on the diamond C(100) surface. Physical Review B, 2010, 82, .	1.1	49
319	An ab initio investigation of boron nanotube in ringlike cluster form. Applied Physics Letters, 2010, 96, 131901.	1.5	4
320	First-Principles Determination of the Ground-State Structure of<mml:math xmlns:mml="http://www.w3.org/1998/Math/MathML" display="inline"><mml:msub><mml:mi>LiBH</mml:mi><mml:mn>4</mml:mn></mml:msub></mml:math>. Physical Review Letters, 2010, 104, 215501.	2.9	45
321	Tunable electronic properties of Pt-doped zigzag graphene nanoribbons. , 2010, , .		0
322	Non-melting super-resolution near-field apertures in Sbâ€“Te alloys. Applied Physics Letters, 2010, 97, 161906.	1.5	33
323	Vibrational and thermal properties of small diameter silicon nanowires. Journal of Applied Physics, 2010, 108, .	1.1	14
324	Water adsorption and dissociation on<mml:math xmlns:mml="http://www.w3.org/1998/Math/MathML" display="inline"><mml:mrow><mml:msub><mml:mrow><mml:mtext>SrTiO</mml:mtext></mml:mrow><mml:mn>3</mml:mn></mml:msub></mml:mrow></mml:m A density functional theory study. Physical Review B, 2010, 81, .	3.1	67
325	Density functional theory screened-exchange approach for investigating electronical properties of graphene-related materials. Physical Review B, 2010, 82, .	1.1	22
326	Structure and Energetics of Azobenzene on Ag(111): Benchmarking Semiempirical Dispersion Correction Approaches. Physical Review Letters, 2010, 104, 036102.	2.9	222
327	First-principles method for impurities in quantum fluids: Positron in an electron gas. Physical Review B, 2010, 82, .	1.1	15

#	Article	IF	Citations
328	Influence of exchange correlation on the symmetry and properties of siderite according to density-functional theory. Physical Review B, 2010, 82, .	1.1	16
329	Trapping of electrons near chemisorbed hydrogen on graphene. Physical Review B, 2010, 81, .	1.1	18
330	Dynamics of quantum tunneling: Effects on the rate and transition path of OH on Cu(110). Physical Review B, 2010, 81, .	1.1	14
332	Electronic structure of oxide fuels from experiment and first principles calculations. Journal of Physics: Conference Series, 2010, 241, 012062.	0.3	5
333	Computational EELS modelling of magnesium oxide systems. Journal of Physics: Conference Series, 2010, 241, 012063.	0.3	0
334	ELECTRONIC, MECHANICAL AND OPTICAL PROPERTIES OFSi₃P₄ANDGe₃P₄: ANAB INITIOSTUDY. International Journal of Modern Physics B, 2010, 24, 5487-5494.	1.3	6
335	Dynamical effects in ab initio NMR calculations: Classical force fields fitted to quantum forces. Journal of Chemical Physics, 2010, 133, 084109.	1.2	39
336	A simple model for large-scale simulations of fcc metals with explicit treatment of electrons. Philosophical Magazine Letters, 2010, 90, 51-60.	0.5	3
337	Anab initiostudy of xenon retention in Î±-quartz. Journal of Physics Condensed Matter, 2010, 22, 025501.	0.7	19
338	Surface stress in d-band metal surfaces. Journal of Physics Condensed Matter, 2010, 22, 135007.	0.7	12
339	Calculation of anharmonic OH phonon dispersion curves for the Mg(OH)2 crystal. Journal of Chemical Physics, 2010, 133, 034120.	1.2	3
340	Linear-scaling density-functional simulations of charged point defects in Al2O3 using hierarchical sparse matrix algebra. Journal of Chemical Physics, 2010, 133, 114111.	1.2	38
341	Direct assessment of quantum nuclear effects on hydrogen bond strength by constrained-centroid ab initio path integral molecular dynamics. Journal of Chemical Physics, 2010, 133, 174306.	1.2	26
342	A first principles based polarizable O(N) interatomic force field for bulk silica. Journal of Chemical Physics, 2010, 133, 094102.	1.2	26
343	First-principles investigation of the relation between structural and NMR parameters in vitreous GeO2. Journal of Physics Condensed Matter, 2010, 22, 145501.	0.7	11
344	Electronic Structures and Optical Properties of Ga-Rich In_xGa_{1â^'x}N Nanotubes. Journal of Physical Chemistry C, 2010, 114, 21943-21947.	1.5	3
345	Hydrogen on graphene under stress: Molecular dissociation and gap opening. Physical Review B, 2010, 81, .	1.1	77
346	A study into the effect of subtle structural details and disorder on the terahertz spectrum of crystalline benzoic acid. Physical Chemistry Chemical Physics, 2010, 12, 5329.	1.3	78

#	Article	IF	Citations
347	Screened exchange density functional applied to solids. Physical Review B, 2010, 82, .	1.1	189
348	Solid-State ^{79/81}Br NMR and Gauge-Including Projector-Augmented Wave Study of Structure, Symmetry, and Hydration State in Alkaline Earth Metal Bromides. Journal of Physical Chemistry A, 2010, 114, 2102-2116.	1.1	43
349	Modelling nano-clusters and nucleation. Physical Chemistry Chemical Physics, 2010, 12, 786-811.	1.3	174
350	Quantum Nature of the Proton in Water-Hydroxyl Overlayers on Metal Surfaces. Physical Review Letters, 2010, 104, 066102.	2.9	101
351	Structure determination of adsorbed hydrogen on a real catalyst. Chemical Communications, 2010, 46, 2959.	2.2	22
352	Structural compression and vibrational properties of Bi₁₂SiO₂₀sillenite from experiment and theory. Journal of Physics Condensed Matter, 2010, 22, 505401.	0.7	33
353	Electron spin resonance parameters of bulk oxygen vacancy in semiconducting tin dioxide. Physical Review B, 2010, 81, .	1.1	21
354	Large-scale first principles and tight-binding density functional theory calculations on hydrogen-passivated silicon nanorods. Journal of Physics Condensed Matter, 2010, 22, 025303.	0.7	9
355	Structure and energetics of imogolite: a quantum mechanical ab initio study with B3LYP hybrid functional. Journal of Materials Chemistry, 2010, 20, 10417.	6.7	41
356	Surface properties and electronic structure of low-index stoichiometric anatase TiO₂surfaces. Journal of Physics Condensed Matter, 2010, 22, 175008.	0.7	54
357	BaM(BS₃)S (M = Sb, Bi): Two New Thioborate Compounds with One-Dimensional Polymeric Chain Structure. Inorganic Chemistry, 2010, 49, 6609-6615.	1.9	16
358	The structure and growth direction of rare earth silicide nanowires on Si(100). Applied Physics Letters, 2010, 96, 241903.	1.5	13
359	Far infrared spectra of solid state aliphatic amino acids in different protonation states. Journal of Chemical Physics, 2010, 132, 115105.	1.2	23
360	Time Averaging of NMR Chemical Shifts in the MLF Peptide in the Solid State. Journal of the American Chemical Society, 2010, 132, 5993-6000.	6.6	65
361	Role of Clay Minerals in Oil-Forming Reactions. Journal of Physical Chemistry A, 2010, 114, 3569-3575.	1.1	30
363	An investigation of the electronic properties of MgO doped with group III, IV, and V elements: trends with varying dopant atomic number. Journal of Physics Condensed Matter, 2010, 22, 046002.	0.7	24
364	Hypothetical low-energy chiral framework structure of group 14 elements. Physical Review B, 2010, 81, .	1.1	84
365	Electronic structure of a graphene/hexagonal-BN heterostructure grown on Ru(0001) by chemical vapor deposition and atomic layer deposition: extrinsically doped graphene. Journal of Physics Condensed Matter, 2010, 22, 302002.	0.7	50

#	Article	IF	Citations
366	Experimental and theoretical analysis of magnetic moment enhancement in oxygen-deficient EuO. Physical Review B, 2010, 81, .	1.1	38
367	Ab initiostudy of the formation of transparent carbon under pressure. Physical Review B, 2010, 82, .	1.1	119
368	Characterization of Hydrous Palladium Oxide: Implications for Low-Temperature Carbon Monoxide Oxidation. Journal of Physical Chemistry C, 2010, 114, 14164-14172.	1.5	34
369	Graphene nanoribbon band-gap expansion: Broken-bond-induced edge strain and quantum entrapment. Nanoscale, 2010, 2, 2160.	2.8	38
370	First-principles study of the paths of the decomposition reaction of LiBH₄. Molecular Physics, 2010, 108, 1263-1276.	0.8	17
371	Utilizing high performance computing for chemistry: parallel computational chemistry. Physical Chemistry Chemical Physics, 2010, 12, 6896.	1.3	84
372	Molecular self-organization: Predicting the pattern diversity and lowest energy state of competing ordering motifs. Physical Review B, 2010, 82, .	1.1	15
373	Elasticity of SrTiO₃ perovskite under high pressure in cubic, tetragonal and orthorhombic phases. Physica Scripta, 2010, 82, 025602.	1.2	37
374	Structural, Electronic, and Transport Properties of Gd/Eu Atomic Chains Encapsulated in Single-Walled Carbon Nanotubes. Journal of Physical Chemistry C, 2010, 114, 15347-15353.	1.5	19
375	Elastic Properties, Thermal Expansion, and Polymorphism of Acetylsalicylic Acid. Crystal Growth and Design, 2010, 10, 3132-3140.	1.4	47
376	Molecular Jigsaw: Pattern Diversity Encoded by Elementary Geometrical Features. Nano Letters, 2010, 10, 833-837.	4.5	15
377	DFT Calculations of Adsorption and Decomposition of N₂O on Rh(100). Journal of Physical Chemistry C, 2010, 114, 21444-21449.	1.5	21
378	Ca-VI: A high-pressure phase of calcium above 158 GPa. Physical Review B, 2010, 81, .	1.1	39
379	Ab Initio Elasticity of Poly(lactic acid) Crystals. Journal of Physical Chemistry B, 2010, 114, 3133-3139.	1.2	28
380	Proton transfer in adsorbed water dimers. Physical Chemistry Chemical Physics, 2010, 12, 3953.	1.3	28
381	Thermochemistry of Organic Reactions in Microporous Oxides by Atomistic Simulations: Benchmarking against Periodic B3LYP. Journal of Physical Chemistry A, 2010, 114, 7391-7397.	1.1	21
382	Chemistry-Controlled Structural Relaxation and Enhanced Redox Abilities in Vanadium-Doped Two-Dimensional Semiconductive TeMo5O16 Catalyst. Journal of Physical Chemistry C, 2010, 114, 13277-13286.	1.5	1
383	Photoelectrochemical Response of TlVO₄ and InVO₄:TlVO₄ Composite. Chemistry of Materials, 2010, 22, 2555-2562.	3.2	21

#	Article	IF	Citations
384	Interplay between Fast Diffusion and Molecular Interaction in the Formation of Self-Assembled Nanostructures of S-Cysteine on Au(111). Langmuir, 2010, 26, 4113-4118.	1.6	38
385	Alumina as a Simultaneous Support and Co Catalyst: Cationic Hafnium Complex Evidenced by Experimental and DFT Analyses. Journal of Physical Chemistry C, 2010, 114, 18516-18528.	1.5	23
386	Investigation of Mixed Conductor BaCo_{0.7}Fe_{0.3â^'x}Y_xO_{3â^'Î´} with High Oxygen Permeability. Journal of Physical Chemistry C, 2010, 114, 17975-17981.	1.5	65
387	Ultra-wideline 14N NMR spectroscopy as a probe of molecular dynamics. Chemical Communications, 2010, 46, 6774.	2.2	23
388	Phase Transition Analysis of 5-Aminotetrazole from Room Temperature to the Melting Point. Journal of Physical Chemistry B, 2010, 114, 12572-12576.	1.2	7
389	Predicting crystal structures ab initio: group 14 nitrides and phosphides. Physical Chemistry Chemical Physics, 2010, 12, 8620.	1.3	12
390	Molecular Dynamics Study of the Electrical Double Layer at Silver Chlorideâ^'Electrolyte Interfaces. Journal of Physical Chemistry C, 2010, 114, 8905-8916.	1.5	30
391	Diamond toÎ²-tin phase transition in Si within diffusion quantum Monte Carlo. Physical Review B, 2010, 82, .	1.1	30
392	Geometric, electronic and elastic properties of dental silver amalgam Î³-(Ag3Sn), Î³1-(Ag2Hg3), Î³2-(Sn8Hg) phases, comparison of experiment and theory. Intermetallics, 2010, 18, 756-760.	1.8	21
393	Thermodynamic assessment of Mo-Ni-Ti ternary system by coupling first-principle calculations with CALPHAD approach. Intermetallics, 2010, 18, 1713-1721.	1.8	35
394	In situ observation of the reaction of tantalum with nitrogen in a laser heated diamond anvil cell. Journal of Alloys and Compounds, 2010, 502, 5-12.	2.8	48
395	Charge disproportionation in AlV2O4: A first-principles study. Journal of Alloys and Compounds, 2010, 505, L23-L26.	2.8	8
396	First principles calculations of electronic and optical properties of Mo-doped rutile TiO2. Journal of Alloys and Compounds, 2010, 507, 33-37.	2.8	60
397	High-pressure behavior of otavite (CdCO3). Journal of Alloys and Compounds, 2010, 508, 251-257.	2.8	28
398	Mechanisms of nickel sorption by a bacteriogenic birnessite. Geochimica Et Cosmochimica Acta, 2010, 74, 3076-3089.	1.6	117
399	Surface complexation of Pb(II) by hexagonal birnessite nanoparticles. Geochimica Et Cosmochimica Acta, 2010, 74, 6731-6740.	1.6	73
400	Thermodynamic optimization of the Coâ€“Zr system. Calphad: Computer Coupling of Phase Diagrams and Thermochemistry, 2010, 34, 200-205.	0.7	27
401	First principles study of structural, elastic and electronic properties of ACY3 (A=Al, In and Tl). Computational Materials Science, 2010, 47, 973-976.	1.4	8

#	Article	IF	Citations
402	Electronic properties and pressure effect on the structural behaviour of M2AC (M=V, Nb and A=P, As). Computational Materials Science, 2010, 48, 174-178.	1.4	5
403	Ground state of spin chain system by Density Functional Theory. Computational Materials Science, 2010, 49, S348-S354.	1.4	2
404	Nuclear magnetic resonance in one-dimensional spin chains. Computational Materials Science, 2010, 49, S341-S347.	1.4	1
405	First principles study on electronic structures and properties of Sn-doped rutile TiO2. Computational Materials Science, 2010, 49, 430-434.	1.4	24
406	Structural identification, electronic and optical properties of ZnSnO3: First principle calculations. Computational Materials Science, 2010, 49, 552-555.	1.4	34
407	Crystal structure and elastic properties of ZrB compared with ZrB2: A first-principles study. Computational Materials Science, 2010, 49, 814-819.	1.4	79
408	(Ca,Sr)CO3 aqueousâ€“solid solution systems: From atomistic simulations to thermodynamic modelling. Physics and Chemistry of the Earth, 2010, 35, 217-232.	1.2	38
409	The Polar Phase of NaNbO₃: A Combined Study by Powder Diffraction, Solid-State NMR, and First-Principles Calculations. Journal of the American Chemical Society, 2010, 132, 8732-8746.	6.6	178
410	Solid-State ¹²⁷I NMR and GIPAW DFT Study of Metal Iodides and Their Hydrates: Structure, Symmetry, and Higher-Order Quadrupole-Induced Effects. Journal of Physical Chemistry A, 2010, 114, 10810-10823.	1.1	63
411	High-Resolution ¹⁹F MAS NMR Spectroscopy: Structural Disorder and Unusual J Couplings in a Fluorinated Hydroxy-Silicate. Journal of the American Chemical Society, 2010, 132, 15651-15660.	6.6	83
412	Evaluation of Linear Thermal Expansion Coefficients of Perovskite Oxides Using Ab-initio Molecular Dynamics with Small Cell Sizes for Materials Design. Japanese Journal of Applied Physics, 2010, 49, 045701.	0.8	11
413	Gaussian Approximation Potentials: The Accuracy of Quantum Mechanics, without the Electrons. Physical Review Letters, 2010, 104, 136403.	2.9	1,777
414	Hydroxyapatite as a key biomaterial: quantum-mechanical simulation of its surfaces in interaction with biomolecules. Physical Chemistry Chemical Physics, 2010, 12, 6309.	1.3	136
415	First principles nuclear magnetic resonance signatures of graphene oxide. Journal of Chemical Physics, 2010, 133, 034502.	1.2	51
416	The structure of schwertmannite, a nanocrystalline iron oxyhydroxysulfate. American Mineralogist, 2010, 95, 1312-1322.	0.9	96
417	Identification of Protonation State by XPS, Solid-State NMR, and DFT: Characterization of the Nature of a New Theophylline Complex by Experimental and Computational Methods. Journal of Physical Chemistry B, 2010, 114, 13961-13969.	1.2	72
418	Solid-State ^{47/49}Ti NMR of Titanocene Chlorides. Journal of Physical Chemistry Letters, 2010, 1, 2989-2998.	2.1	20
419	BaGa₄Se₇: A New Congruent-Melting IR Nonlinear Optical Material. Inorganic Chemistry, 2010, 49, 9212-9216.	1.9	339

#	Article	IF	Citations
420	Mechanical and electronic properties of B₁₂-based ternary crystals of orthorhombic phase. Journal of Physics Condensed Matter, 2010, 22, 315503.	0.7	51
421	Interaction of Ethanol and Water with the {101Ì…4} Surface of Calcite. Langmuir, 2010, 26, 14520-14529.	1.6	115
422	High Field 33S Solid State NMR and First-Principles Calculations in Potassium Sulfates. Journal of Physical Chemistry A, 2010, 114, 309-316.	1.1	28
423	Solid-State ¹³⁷Ba NMR Spectroscopy: An Experimental and Theoretical Investigation of ¹³⁷Ba Electric Field Gradient Tensors and Their Relation to Structure and Symmetry. Journal of Physical Chemistry B, 2010, 114, 6014-6022.	1.2	35
424	Ab initiomolecular dynamics simulation of hydrogen diffusion in<mml:math xmlns:mml="http://www.w3.org/1998/Math/MathML" display="inline"><mml:mi>Î±</mml:mi></mml:math>-iron. Physical Review B, 2010, 81, .	1.1	46
425	Calculation of NMR parameters in ionic solids by an improved self-consistent embedded cluster method. Physical Chemistry Chemical Physics, 2010, 12, 583-603.	1.3	52
426	Ordered Vacancy Network Induced by the Growth of Epitaxial Graphene on Pt(111). Physical Review Letters, 2010, 105, 216102.	2.9	70
427	Complete 1H resonance assignment of Î²-maltose from 1Hâ€“1H DQ-SQ CRAMPS and 1H (DQ-DUMBO)â€“13C SQ refocused INEPT 2D solid-state NMR spectra and first principles GIPAW calculations. Physical Chemistry Chemical Physics, 2010, 12, 6970.	1.3	83
428	Novel Rhenium Nitrides. Physical Review Letters, 2010, 105, 085504.	2.9	148
429	NMR Crystallography of Campho[2,3-c]pyrazole (Zâ€² = 6): Combining High-Resolution ¹H-¹³C Solid-State MAS NMR Spectroscopy and GIPAW Chemical-Shift Calculations. Journal of Physical Chemistry A, 2010, 114, 10435-10442.	1.1	127
430	First-principles density functional study of polarizationâ€“strain coupling in bismuth titanate. Journal of Physics Condensed Matter, 2010, 22, 385902.	0.7	8
431	Ferromagnetism in Carbon-Doped Zinc Oxide Systems. Journal of Physical Chemistry A, 2010, 114, 2689-2696.	1.1	52
432	Soft modes in strained and unstrained rutileTiO2. Physical Review B, 2010, 81, .	1.1	44
433	Inelastic neutron scattering of Na-zeolite A with in situ ammoniation: an examination of initial coordination. Physical Chemistry Chemical Physics, 2010, 12, 9661.	1.3	4
434	Databases of virtual inorganic crystal structures and their applications. Physical Chemistry Chemical Physics, 2010, 12, 8521.	1.3	6
435	Azobenzene versus 3,3â€²,5,5â€²-tetra-tert-butyl-azobenzene (TBA) at Au(111): characterizing the role of spacer groups. Physical Chemistry Chemical Physics, 2010, 12, 6404.	1.3	48
436	Exploring the limits of 73Ge solid-state NMR spectroscopy at ultrahigh magnetic field. Chemical Communications, 2010, 46, 2817.	2.2	19
437	The effect of pressure on the crystal structure of l-alanine. CrystEngComm, 2010, 12, 2573.	1.3	65

#	Article	IF	Citations
438	Calcium binding environments probed by 43Ca NMR spectroscopy. Dalton Transactions, 2010, 39, 8593.	1.6	56
439	Natural abundance high field 43Ca solid state NMR in cement science. Physical Chemistry Chemical Physics, 2010, 12, 6961.	1.3	29
440	Structures and Phase Transitions in (MoO₂)₂P₂O₇. Inorganic Chemistry, 2010, 49, 2290-2301.	1.9	27
441	Static equation of state of bcc iron. Physical Review B, 2010, 82, .	1.1	35
442	Characterization of thin silicon overlayers on rutile<mml:math xmlns:mml="http://www.w3.org/1998/Math/MathML" display="inline"><mml:mrow><mml:msub><mml:mrow><mml:mtext>TiO</mml:mtext></mml:mrow><mml:mn>2</mml:mn></mml:msu Physical Review B, 2010, 82, .	1.1	22
443	Effects of the reaction cavity on metastable optical excitation in ruthenium-sulfur dioxide complexes. Physical Review B, 2010, 82, .	1.1	41
444	Calculation of terahertz active normal modes in organic crystals. , 2010, , .		0
445	The structure of furan reaction products on Pd(111). Physical Chemistry Chemical Physics, 2011, 13, 7975.	1.3	10
446	Chemical bonding and properties of â€œlayeredâ€•quaternary antimonide oxide REOZnSb (RE = La, Ce, Pr,) Tj ETQq0 0 0 rgBT /Overlock	1.6	19
447	A multinuclear NMR and quantum chemical study of solid trimethylammonium chloride. Canadian Journal of Chemistry, 2011, 89, 1036-1046.	0.6	19
448	A combined experimental inelastic neutron scattering, Raman and ab initio lattice dynamics study of Î±-lithium amidoborane. Physical Chemistry Chemical Physics, 2011, 13, 12249.	1.3	11
449	Alanine at 13.6 GPa and its pressure-induced amorphisation at 15 GPa. CrystEngComm, 2011, 13, 5841.	1.3	48
450	Nonspectral Methods for Solving the SchrÃ¶dinger Equation for Electronic and Vibrational Problems. Journal of Physical Chemistry Letters, 2011, 2, 2193-2199.	2.1	11
451	Switching on the Electrocatalytic Ethene Epoxidation on Nanocrystalline RuO₂. Journal of the American Chemical Society, 2011, 133, 5882-5892.	6.6	55
452	Hydroxide oxidation and peroxide formation at embedded binuclear transition metal sites; TM = Cr, Mn, Fe, Co. Physical Chemistry Chemical Physics, 2011, 13, 15062.	1.3	26
453	Structure and energetics of low-index stoichiometric monoclinic clinobisvanite BiVO4 surfaces. RSC Advances, 2011, 1, 874.	1.7	58
454	Interplay between structure, stoichiometry and properties of technetium nitrides. Dalton Transactions, 2011, 40, 6738.	1.6	20
455	Weak Intermolecular Interactions in an Ionically Bound Molecular Adsorbate:Cyclopentadienyl/Cu(111). Physical Review Letters, 2011, 106, 186101.	2.9	20

#	Article	IF	Citations
456	First-Principle Study of Hydrogen Adsorption on Na-Coated Carbon Nanotubes. , 2011, , .		1
457	Probing the binding and spatial arrangement of molecular hydrogen in porous hosts via neutron Compton scattering. Faraday Discussions, 2011, 151, 171.	1.6	30
458	95Mo nuclear magnetic resonance parameters of molybdenum hexacarbonyl from density functional theory: appraisal of computational and geometrical parameters. Physical Chemistry Chemical Physics, 2011, 13, 19471.	1.3	12
459	Growth and interface phase stability of barium hexaferrite films on SiC(0001). Journal of Applied Physics, 2011, 109, 07E520.	1.1	9
460	Syntheses, crystal structures and characterizations of two new quaternary thioborates: PbMBS4 (M) Tj ETQq0 0 0 rgBT /Overlock 10 Tf 5	1.6	9
461	Measurement and calculation of 13C chemical shift tensors in Î±-glucose and Î±-glucose monohydrate. Canadian Journal of Chemistry, 2011, 89, 737-744.	0.6	11
462	Relativistic many-electron calculations of Cr3+â€ˆL2,3-edge x ray absorption near-edge structures for Cr3+:Î±-Al2O3 and Î±-Cr2O3 and magnetic circular dichroism of Cr3+L2,3-edge x ray absorption near-edge structures for Cr3+:Î±-Al2O3. Journal of Applied Physics, 2011, 110, .	1.1	13
463	Metastable De-excitation Spectroscopy and Density Functional Theory Study of the Selective Oxidation of Crotyl Alcohol over Pd(111). Journal of Physical Chemistry C, 2011, 115, 25290-25297.	1.5	11
464	The high-pressure structural transition in MnS: anab initiostudy. Molecular Physics, 2011, 109, 251-256.	0.8	6
465	Effect of lattice strain on hydrogen diffusion in Pd: A density functional theory study. Physical Review B, 2011, 84, .	1.1	35
466	Phonon, IR, and Raman Spectra, NMR Parameters, and Elastic Constant Calculations for AlH₃ Polymorphs. Journal of Physical Chemistry A, 2011, 115, 10708-10719.	1.1	20
467	Formate Ion: Structure and Spectroscopic Properties. Journal of Physical Chemistry A, 2011, 115, 70-75.	1.1	17
468	Structural Properties and Halogen Bonds of Cyanuric Chloride under High Pressure. Journal of Physical Chemistry B, 2011, 115, 4639-4644.	1.2	21
469	Complete Structural Characterization of Ni₃Si₂O₅(OH)₄ Nanotubes: Theoretical and Experimental Comparison. Journal of Physical Chemistry C, 2011, 115, 11442-11446.	1.5	35
470	Probing the atomic structure of amorphous Ta2O5 coatings. Applied Physics Letters, 2011, 98, .	1.5	50
471	Temperature Behavior of the AlH₃ Polymorph by in Situ Investigation Using High Resolution Raman Scattering. Journal of Physical Chemistry A, 2011, 115, 691-699.	1.1	7
472	Mode-Specific Chemisorption of CH₄ on Pt{110}-(1 Ã— 2) Explored by First-Principles Molecular Dynamics. Journal of Physical Chemistry C, 2011, 115, 21832-21842.	1.5	37
473	77Se Solid-State NMR of Inorganic and Organoselenium Systems: A Combined Experimental and Computational Study. Journal of Physical Chemistry C, 2011, 115, 10859-10872.	1.5	25

#	Article	IF	Citations
474	Syntheses, Crystal and Electronic Structures, and Characterizations of Quaternary Antiferromagnetic Sulfides: Ba₂MFeS₅(M = Sb, Bi). Inorganic Chemistry, 2011, 50, 2378-2384.	1.9	23
475	Novel approaches to multiscale modelling in materials science. International Materials Reviews, 2011, 56, 207-225.	9.4	107
476	Photocatalytic activity of Laâ€“N-codoped NaTaO₃ for H₂ evolution from water under visible-light irradiation. Journal Physics D: Applied Physics, 2011, 44, 165401.	1.3	23
477	Structure Resolution of Ba5Al3F19and Investigation of Fluorine Ion Dynamics by Synchrotron Powder Diffraction, Variable-Temperature Solid-State NMR, and Quantum Computations. Inorganic Chemistry, 2011, 50, 2644-2653.	1.9	35
478	Electronic Structure and Bonding of an Ionic Molecular Adsorbate: c-C5H5 on Cu{111}. Journal of Physical Chemistry C, 2011, 115, 16134-16141.	1.5	9
479	First-Principles Calculations on the LiMSO4F/MSO4F (M = Fe, Co, and Ni) Systems. Journal of Physical Chemistry C, 2011, 115, 7032-7037.	1.5	32
480	Thermal Transport in Suspended and Supported Few-Layer Graphene. Nano Letters, 2011, 11, 113-118.	4.5	246
481	Vibrational Properties of CaAlH₅ and Î±-AlH₃ with Different AlH₆ Networks Studied by Inelastic Neutron Scattering. Inorganic Chemistry, 2011, 50, 8007-8011.	1.9	7
482	Molecular Engineering Design to Resolve the Layering Habit and Polymorphism Problems in Deep UV NLO Crystals: New Structures in MMâ€²Be₂B₂O₆F (Mâ•Na, Mâ€²â•Ca; Mâ•K,	0.7	0
483	Magnetic Response of Single-Walled Carbon Nanotubes Induced by an External Magnetic Field. ACS Nano, 2011, 5, 537-545.	7.3	46
484	Band Structure and Optical Characteristics of TDA Crystals. Ferroelectrics, 2011, 417, 9-13.	0.3	0
485	Synthesis, Crystal Structure, and Thermal Properties of the First Mixed-Metal and Anion-Substituted Rare Earth Borohydride LiCe(BH₄)₃Cl. Journal of Physical Chemistry C, 2011, 115, 23591-23602.	1.5	50
486	Structural Composition of First-Neighbor Shells in GeSe₂ and GeSe₄ Glasses from a First-Principles Analysis of NMR Chemical Shifts. Journal of Physical Chemistry C, 2011, 115, 7755-7759.	1.5	36
487	A variable temperature solid-state nuclear magnetic resonance, electron paramagnetic resonance and Raman scattering study of molecular dynamics in ferroelectric fluorides. Journal of Physics Condensed Matter, 2011, 23, 315402.	0.7	4
489	Electronic structure, optical properties and lattice dynamics of MgSO3â‹…6H2O. Journal of Physics Condensed Matter, 2011, 23, 485401.	0.7	0
490	Magnetic ordering in tetragonal FeS: Evidence for strong itinerant spin fluctuations. Physical Review B, 2011, 83, .	1.1	57
491	System-size convergence of point defect properties: The case of the silicon vacancy. Physical Review B, 2011, 84, .	1.1	62
492	Phase Stability and Electronic Structure of In-Free Photovoltaic Materials Cu₂IISnSe₄ (II: Zn, Cd, Hg). Japanese Journal of Applied Physics, 2011, 50, 05FF01.	0.8	17

#	Article	IF	Citations
493	Twist-boat conformation in graphene oxides. Nanoscale, 2011, 3, 192-195.	2.8	37
494	BaAl4Se7: a new infrared nonlinear optical material with a large band gap. Dalton Transactions, 2011, 40, 3610.	1.6	51
495	Functionalized Graphene for High-Performance Two-Dimensional Spintronics Devices. ACS Nano, 2011, 5, 2601-2610.	7.3	116
497	Obtaining accurate chemical shifts for all magnetic nuclei (¹H, ¹³C,) Tj ETQq1 1 0.784314 rgBT /Overlock 10 solid-state NMR case study. Canadian Journal of Chemistry, 2011, 89, 1087-1094.	0.6	23
498	93Nb NMR and DFT investigation of the polymorphs of NaNbO3. Physical Chemistry Chemical Physics, 2011, 13, 7565.	1.3	50
499	Structure and Electronic and Transport Properties of Transition Metal Intercalated Graphene and Graphene-Hexagonal-Boron-Nitride Bilayer. Journal of Physical Chemistry C, 2011, 115, 25273-25280.	1.5	23
500	Limits to doping in oxides. Physical Review B, 2011, 83, .	1.1	248
501	Ab Initio Transition State Searching in Complex Systems: Fatty Acid Decarboxylation in Minerals.. Journal of Physical Chemistry A, 2011, 115, 2658-2667.	1.1	11
502	Multinuclear solid-state NMR of square-planar platinum complexesÂâ€" Cisplatin and related systems. Canadian Journal of Chemistry, 2011, 89, 919-937.	0.6	65
503	High-field multinuclear solid-state nuclear magnetic resonance (NMR) and first principle calculations in MgSO4 polymorphs. Canadian Journal of Chemistry, 2011, 89, 1076-1086.	0.6	11
504	Body-centered tetragonal B2N2: a novel sp3 bonding boron nitride polymorph. Physical Chemistry Chemical Physics, 2011, 13, 14565.	1.3	77
505	NMR parameters in alkali, alkaline earth and rare earth fluorides from first principle calculations. Physical Chemistry Chemical Physics, 2011, 13, 18539.	1.3	114
506	Thermal phase transformation of In2Se3 nanowires studied by in situ synchrotron radiation X-ray diffraction. Journal of Materials Chemistry, 2011, 21, 6944.	6.7	40
507	Theoretical Study of the Decomposition and Hydrogenation of H₂O₂ on Pd and Au@Pd Surfaces: Understanding toward High Selectivity of H₂O₂ Synthesis. Journal of Physical Chemistry C, 2011, 115, 7392-7398.	1.5	90
508	High temperature elastic properties of Mg-cordierite: experimental studies and atomistic simulations. Zeitschrift FÃ¼r Kristallographie, 2011, 226, 236-253.	1.1	11
509	Band Structures and Optical Properties of CBOB Crystal Material Based on First-Principles Study. Advanced Materials Research, 0, 216, 1-5.	0.3	0
510	High-Resolution Solid-State²H NMR Spectroscopy of Polymorphs of Glycine. Journal of Physical Chemistry A, 2011, 115, 12201-12211.	1.1	32
511	Ab initioenergetics of lanthanum substitution in ferroelectric bismuth titanate. Journal of Physics Condensed Matter, 2011, 23, 155902.	0.7	12

#	Article	IF	Citations
512	Atomistic Simulation of the Structural, Thermodynamic, and Elastic Properties of Li₂TiO₃. Journal of Physical Chemistry C, 2011, 115, 21874-21881.	1.5	37
513	Ab initiorandom structure searching. Journal of Physics Condensed Matter, 2011, 23, 053201.	0.7	832
514	Electronic structure and optical properties of monoclinic clinobisvanite BiVO4. Physical Chemistry Chemical Physics, 2011, 13, 4746.	1.3	327
515	Energetic stability, structural transition, and thermodynamic properties of ZnSnO3. Applied Physics Letters, 2011, 98, .	1.5	34
516	Identification and Quantification of Defects in the Cation Ordering in Mg/Al Layered Double Hydroxides. Chemistry of Materials, 2011, 23, 2821-2831.	3.2	114
517	Visible-light-driven photocatalysts: (La/Bi‰+â€‰N)-codoped NaNbO3 by first principles. Journal of Applied Physics, 2011, 109, 063103.	1.1	26
518	Bi₂(IO₄)(IO₃)₃: A New Potential Infrared Nonlinear Optical Material Containing [IO₄]^{3â€“} Anion. Inorganic Chemistry, 2011, 50, 12818-12822.	1.9	102
519	Syntheses and Characterization of New Mid-Infrared Transparency Compounds: Centric Ba₂BiGaS₅ and Acentric Ba₂BiInS₅. Inorganic Chemistry, 2011, 50, 5679-5686.	1.9	90
520	Cr in diamond: A first-principles study. Physical Review B, 2011, 84, .	1.1	12
521	Computational searches for iron carbide in the Earth's inner core. Physical Review B, 2011, 84, .	1.1	35
522	Ultra-high resolution 17O solid-state NMR spectroscopy of biomolecules: A comprehensive spectral analysis of monosodium L-glutamateÂ·monohydrate. Physical Chemistry Chemical Physics, 2011, 13, 12213.	1.3	30
523	Impact of stress on band-to-band tunneling current in SOI MOSFET based on first-principles calculation. , 2011, , .		0
524	Testing the limits of sensitivity in a solid-state structural investigation by combined X-ray powder diffraction, solid-state NMR, and molecular modelling. Physical Chemistry Chemical Physics, 2011, 13, 17978.	1.3	27
525	Characterization and Properties of Novel Gallium-Doped Calcium Phosphate Ceramics. Inorganic Chemistry, 2011, 50, 8252-8260.	1.9	60
526	Exploration of optical and electronic parameters of lithium thiogallate (LiGaS<inf>2</inf>). , 2011, , .		0
527	Combined Experimental and Computational Hydrostatic Compression Study of Crystalline Ammonium Perchlorate. Journal of Physical Chemistry C, 2011, 115, 18782-18788.	1.5	29
528	Calculating optical absorption spectra for large systems using linear-scaling density functional theory. Physical Review B, 2011, 84, .	1.1	52
529	Crystal structure of anhydrous 5-aminotetrazole and its high-pressure behavior. CrystEngComm, 2011, 13, 99-102.	1.3	21

#	Article	IF	Citations
530	Dynamically Stabilized Growth of Polar Oxides: The Case of MgO(111). Physical Review Letters, 2011, 107, 056101.	2.9	27
531	Anomalous Scaling in Heteroepitaxial Island Dynamics on Ag(100). Physical Review Letters, 2011, 107, 046101.	2.9	12
532	Crystal Structure Based Design of Signal Enhancement Schemes for Solid-State NMR of Insensitive Half-Integer Quadrupolar Nuclei. Journal of Physical Chemistry A, 2011, 115, 747-752.	1.1	23
533	Predicted Pressure-Induced<mml:math xmlns:mml="http://www.w3.org/1998/Math/MathML" display="inline"><mml:mi>s</mml:mi></mml:math>-Band Ferromagnetism in Alkali Metals. Physical Review Letters, 2011, 107, 087201.	2.9	59
534	The crystal structure of the first borohydride borate, Ca3(BD4)3(BO3). Journal of Materials Chemistry, 2011, 21, 7188.	6.7	25
535	Complete assignment of the vibrational modes of C60 by inelastic neutron scattering spectroscopy and periodic-DFT. Physical Chemistry Chemical Physics, 2011, 13, 7789.	1.3	32
536	Molecular Understanding of the Adhesive Force between a Metal Oxide Surface and an Epoxy Resin. Journal of Physical Chemistry C, 2011, 115, 11701-11708.	1.5	126
537	Strong Coupling of Cr and N in Crâ€“N-doped TiO2 and Its Effect on Photocatalytic Activity. Journal of Physical Chemistry C, 2011, 115, 17392-17399.	1.5	75
538	Estimating internuclear distances between half-integer quadrupolar nuclei by central-transition double-quantum sideband NMR spectroscopy. Canadian Journal of Chemistry, 2011, 89, 892-899.	0.6	18
539	Natural abundance solid-state 67Zn NMR characterization of microporous zinc phosphites and zinc phosphates at ultrahigh magnetic field. Physical Chemistry Chemical Physics, 2011, 13, 16606.	1.3	18
540	High-Yield Synthesis of Ultrathin and Uniform Bi₂WO₆ Square Nanoplates Benefitting from Photocatalytic Reduction of CO₂ into Renewable Hydrocarbon Fuel under Visible Light. ACS Applied Materials & Interfaces, 2011, 3, 3594-3601.	4.0	359
541	Second-order piezoelectricity in wurtzite III-N semiconductors. Physical Review B, 2011, 84, .	1.1	88
543	Correlation between hardness and elastic moduli of the covalent crystals. Computational Materials Science, 2011, 50, 2287-2290.	1.4	163
544	Properties of KNTN [100] surfaces: A first-principles study. Computational Materials Science, 2011, 50, 2354-2358.	1.4	1
545	Electronic and optical properties of ultrathin single walled boron nanotubes â€“ An ab initio study. Computational Materials Science, 2011, 50, 3038-3042.	1.4	18
546	Structural analysis of lanthanum-containing battery materials using ¹³⁹La solid-state NMR. Canadian Journal of Chemistry, 2011, 89, 1105-1117.	0.6	20
547	High-pressure crystal structure prediction of calcium borohydride using density functional theory. Physical Review B, 2011, 83, .	1.1	20
548	Photoelectrochemical Investigation and Electronic Structure of ap-Type CuNbO₃Photocathode. Journal of Physical Chemistry C, 2011, 115, 13534-13539.	1.5	82

#	Article	IF	Citations
549	Impurity Gas Analysis of the Decomposition of Complex Hydrides. Journal of Physical Chemistry C, 2011, 115, 17220-17226.	1.5	35
550	Structural Chemistry, Monoclinic-to-Orthorhombic Phase Transition, and CO₂ Adsorption Behavior of the Small Pore Scandium Terephthalate, Sc₂(O₂CC₆H₄CO₂)₃, and Its Nitro- And Amino-Functionalized Derivatives. Inorganic Chemistry, 2011, 50, 10844-10858.	1.9	75
551	Polymorph Prediction of Small Organic Molecules, Co-crystals and Salts. RSC Drug Discovery Series, 2011, , 44-88.	0.2	2
552	Accurate ionic forces and geometry optimization in linear-scaling density-functional theory with local orbitals. Physical Review B, 2011, 83, .	1.1	75
553	First principles investigation of the substitutional doping of Mn in Mg2Ni phase and the electronic structure of Mg3MnNi2 phase. Journal of Alloys and Compounds, 2011, 509, S328-S333.	2.8	22
554	Syntheses and characterization of two new selenides Ba5Al2Se8 and Ba5Ga2Se8. Journal of Alloys and Compounds, 2011, 509, 2981-2985.	2.8	25
555	Electronic structure and thermal properties of doped CaMnO3 systems. Journal of Alloys and Compounds, 2011, 509, 4171-4175.	2.8	44
556	First principles calculations on elasticity, electronic structure and bonding properties of antiperovskites ANTi3 (A=Al, In and Tl). Journal of Alloys and Compounds, 2011, 509, 4357-4362.	2.8	8
557	Hardness, isomer shifts and chemical bond properties of rare earth orthoferrites. Journal of Alloys and Compounds, 2011, 509, 6876-6879.	2.8	1
558	Half-metallic ferromagnetism in the half-Heusler compounds GeKCa and SnKCa from first-principles calculations. Journal of Alloys and Compounds, 2011, 509, 10172-10178.	2.8	67
559	Theoretical Revisit of the Direct Synthesis of H₂O₂ on Pd and Au@Pd Surfaces: A Comprehensive Mechanistic Study. Journal of Physical Chemistry C, 2011, 115, 25359-25367.	1.5	89
560	Interaction Tensors and Local Dynamics in Common Structural Motifs of Nitrogen: A Solid-State ¹⁴N NMR and DFT Study. Journal of the American Chemical Society, 2011, 133, 527-546.	6.6	77
561	Density functional theory study of influence of impurity on electronic properties and reactivity of pyrite. Transactions of Nonferrous Metals Society of China, 2011, 21, 1887-1895.	1.7	53
562	ZnAlF5Â·[TAZ]: an Al fluorinated MOF of MIL-53(Al) topology with cationic {Zn(1,2,4 triazole)}2+ linkers. Journal of Materials Chemistry, 2011, 21, 3949.	6.7	32
563	Computational Studies on the Crystal Structure, Thermodynamic Properties, Detonation Performance, and Pyrolysis Mechanism of 2,4,6,8-Tetranitro-1,3,5,7-tetraazacubane as a Novel High Energy Density Material. Journal of Physical Chemistry A, 2011, 115, 11788-11795.	1.1	63
564	First-principles generalized gradient approximation + U study of cubic CuAl2O4. Applied Physics Letters, 2011, 99, 091902.	1.5	14
565	First-principles study of indium-free photovoltaic compounds Ag<inf>2</inf>ZnSnSe<inf>4</inf> and Cu<inf>2</inf>ZnSnSe<inf>4</inf>. , 2011, , .		1
566	Computer simulation of Na-bearing majoritic garnet. Doklady Earth Sciences, 2011, 441, 1508-1511.	0.2	4

#	Article	IF	Citations
567	Influence of Doping Effect on Zinc Oxide by First-Principles Studies. Journal of Physical Chemistry C, 2011, 115, 7706-7716.	1.5	29
568	Quantum nature of the hydrogen bond. Proceedings of the National Academy of Sciences of the United States of America, 2011, 108, 6369-6373.	3.3	360
569	Insight into sodium silicate glass structural organization by multinuclear NMR combined with first-principles calculations. Geochimica Et Cosmochimica Acta, 2011, 75, 2453-2469.	1.6	120
570	A fast, stable method for density functional simulations of nanostructures. Journal of Physics: Conference Series, 2011, 286, 012034.	0.3	0
571	Molecular Theory of Adhesion of Metal/Epoxy Resin Interface. Kobunshi Ronbunshu, 2011, 68, 72-80.	0.2	14
572	DETERMINATION OF NONLOCAL CONSTITUTIVE EQUATIONS FROM PHONON DISPERSION RELATIONS. International Journal for Multiscale Computational Engineering, 2011, 9, 623-634.	0.8	24
573	Study on atomic and electronic structures of ceramic materials using spectroscopy, microscopy, and first principles calculation. Journal of the Ceramic Society of Japan, 2011, 119, 325-333.	0.5	7
574	Structural and Hydrogen Desorption Properties of Aluminum Hydride. Materials Transactions, 2011, 52, 598-601.	0.4	12
575	Distortion-triggered loss of long-range order in solids with bonding energy hierarchy. Nature Chemistry, 2011, 3, 311-316.	6.6	178
576	Pressure-induced phase transformation and magnetism transition in BaRuO3: A first-principles study. Solid State Sciences, 2011, 13, 350-355.	1.5	9
577	Growth and structure redetermination of a nonlinear BaAlBO3F2 crystal. Solid State Sciences, 2011, 13, 875-878.	1.5	57
578	First-principles study of the structural, electronic, and magnetic properties of InCCo3 and InNCo3. Solid State Communications, 2011, 151, 1916-1919.	0.9	7
579	Observation of â€œhiddenâ€•magnesium: First-principles calculations and 25Mg solid-state NMR of enstatite. Solid State Nuclear Magnetic Resonance, 2011, 40, 91-99.	1.5	25
580	NMR crystallography of 2-acylamino-6-[1H]-pyridones: Solid-state NMR, GIPAW computational, and single crystal X-ray diffraction studies. Journal of Molecular Structure, 2011, 1006, 678-683.	1.8	12
581	Elastic, electronic, and optical properties of hypothetical SnNNi3 and CuNNi3 in comparison with superconducting ZnNNi3. Physica B: Condensed Matter, 2011, 406, 4564-4568.	1.3	26
582	Half-metallic antiferromagnetism in the ordered Cr1â^'xCaxSb alloy from first-principles calculations. Physics Letters, Section A: General, Atomic and Solid State Physics, 2011, 375, 4053-4057.	0.9	1
583	Large shear strength enhancement of gamma-boron by normal compression. Journal of Superhard Materials, 2011, 33, 401-408.	0.5	10
584	Theoretical insights into the surface growth of rutile TiO2. Combustion and Flame, 2011, 158, 1868-1876.	2.8	22

#	Article	IF	Citations
585	Ab initio modeling of fused silica, crystal quartz, and water Raman spectra. Chemical Physics Letters, 2011, 512, 54-59.	1.2	33
586	14N magic angle spinning overtone NMR spectra. Chemical Physics Letters, 2011, 514, 168-173.	1.2	48
587	Hydrogen-doped cubic diamond and the crystal structure of n-diamond. Chemical Physics Letters, 2011, 516, 230-232.	1.2	12
588	Prediction of crystal structure, lattice dynamical, and mechanical properties of CaB2H2. International Journal of Hydrogen Energy, 2011, 36, 10149-10158.	3.8	16
589	Ab initio and thermodynamic investigation on the Caâ€“H system. International Journal of Hydrogen Energy, 2011, 36, 13632-13639.	3.8	8
590	Electronic, optical and lattice dynamic properties of the novel diamond-like semiconductors Li₂CdGeS₄and Li₂CdSnS₄. Journal of Physics Condensed Matter, 2011, 23, 225401.	0.7	23
591	Identifying Guanosine Self Assembly at Natural Isotopic Abundance by High-Resolution ¹H and ¹³C Solid-State NMR Spectroscopy. Journal of the American Chemical Society, 2011, 133, 19777-19795.	6.6	72
592	Ab initiostudy on band-gap narrowing in SrTiO<mml:math xmlns:mml="http://www.w3.org/1998/Math/MathML" display="inline"><mml:msub><mml:mrow /><mml:mn>3</mml:mn></mml:msub></mml:math>with Nb-C-Nb codoping. Physical Review B, 2011, 84, .	1.1	54
593	A DFT study on the interaction between europium, uranium and SWCNT. Open Physics, 2011, 9, .	0.8	1
594	First-principle calculations for electronic structure and bonding properties in layered Na2Ti3O7. Open Physics, 2011, 9, .	0.8	11
595	A solid-state ^{35/37}Cl NMR study of a chloride ion receptor and a GIPAW-DFT study of chlorine NMR interaction tensors in organic hydrochlorides. Canadian Journal of Chemistry, 2011, 89, 822-834.	0.6	28
596	Defects in Doped LaGaO₃ Anionic Conductors: Linking NMR Spectral Features, Local Environments, and Defect Thermodynamics. Journal of the American Chemical Society, 2011, 133, 17662-17672.	6.6	43
597	Electronic, elastic and optical properties on the Zn1â^'x Mg x Se mixed alloys. Journal of Materials Science, 2011, 46, 1007-1014.	1.7	22
598	Investigation of Trimetallic Ligand-Pillared Oxyfluorides: Ag2Cu(pzc)2MO x F6â^'x (MÂ=ÂMo, Nb, and W). Journal of Chemical Crystallography, 2011, 41, 1552-1559.	0.5	1
599	Calculation of infrared and Raman vibration modes of magnesite at high pressure by density-functional perturbation theory and comparison with experiments. Physics and Chemistry of Minerals, 2011, 38, 193-202.	0.3	6
600	Pressure dependence of the lattice dynamics of diaspore, Î±-AlO(OH), from Raman spectroscopy and density functional perturbation theory. Physics and Chemistry of Minerals, 2011, 38, 693-700.	0.3	15
601	Dicarboxylate assisted synthesis of the monoclinic heterometallic tetrathiocyanato bridged copper(II) and mercury(II) coordination polymer {Cu[Hg(SCN)4]} : Synthesis, structural, vibration, luminescence, EPR studies and DFT calculations. Journal of Solid State Chemistry, 2011, 184, 379-386.	1.4	8
602	Ab-initio crystal structure prediction. A case study: NaBH4. Journal of Solid State Chemistry, 2011, 184, 1622-1630.	1.4	21

#	Article	IF	Citations
603	Effects of rare-earth substitution on the stability and electronic structure of REZnOSb (RE=Laâ€“Nd,) Tj ETQq0 0 0 rgBT /Overlock 10 Tf	0.9	11
604	Lateral interaction and structures in Cl adlayers on the Ag(111) surface. Chemical Physics, 2011, 383, 35-40.	0.9	6
605	Density functional theory study of 3Râ€“ and 2Hâ€“CuAlO2 in tensile stress. Physics Letters, Section A: General, Atomic and Solid State Physics, 2011, 375, 1608-1611.	0.9	12
606	Multinuclear NMR study of silica fiberglass modified with zirconia. Solid State Nuclear Magnetic Resonance, 2011, 39, 47-57.	1.5	20
607	The electron structure and photocatalytic activity of Ti(IV) doped Bi2O3. Science China Chemistry, 2011, 54, 180-185.	4.2	32
608	First principle calculation of lithiation/delithiation voltage in Li-ion battery materials. Science Bulletin, 2011, 56, 3229.	1.7	20
609	Substitution effects on the hydrogen storage behavior of AB2 alloys by first principles. Frontiers of Physics, 2011, 6, 214-219.	2.4	7
610	Research on the Lattice Stability of Elemental Be, Mg, Ca, Sr, Ba and Ra by the Ultra-Soft Pseudo-Potential Method in First Principles. Journal of Phase Equilibria and Diffusion, 2011, 32, 428-434.	0.5	0
611	Synthesis, Crystal Structure and Chemical Bonding of the Zintl Phase Rb₇NaSi₈. Zeitschrift Fur Anorganische Und Allgemeine Chemie, 2011, 637, 1982-1991.	0.6	17
612	VESTAâ€...3for three-dimensional visualization of crystal, volumetric and morphology data. Journal of Applied Crystallography, 2011, 44, 1272-1276.	1.9	16,580
613	The effect of pressure on the crystal structure of bianthrone. Acta Crystallographica Section B: Structural Science, 2011, 67, 226-237.	1.8	12
614	Towards crystal structure prediction of complex organic compounds â€“ a report on the fifth blind test. Acta Crystallographica Section B: Structural Science, 2011, 67, 535-551.	1.8	358
615	Calculations for the linear and nonlinear optical coefficients of ZCTC crystals. Physica Status Solidi (B): Basic Research, 2011, 248, 1483-1489.	0.7	4
616	Structural and Electronic Properties of Fluorographene. Small, 2011, 7, 965-969.	5.2	194
617	Effects of Water Molecules on Photoluminescence from Hierarchical Peptide Nanotubes and Water Probing Capability. Small, 2011, 7, 2801-2807.	5.2	43
618	Terahertz spectroscopy and imaging â€“ Modern techniques and applications. Laser and Photonics Reviews, 2011, 5, 124-166.	4.4	1,525
619	A singleâ€crystal Raman and infrared study of the nonlinear optical crystal MBANP. Journal of Raman Spectroscopy, 2011, 42, 1174-1184.	1.2	12
620	A Versatile FrÃ©chetâ€Dendron Compound Unifies Hostâ€Guest and Templated Heterogeneous Selfâ€Assembly. Advanced Materials, 2011, 23, 2195-2198.	11.1	7

#	Article	IF	Citations
621	Tautomerism and the Protonation/Deprotonation of Isocytosine in Liquidâ€•and Solidâ€States Studied by NMR Spectroscopy and Theoretical Calculations. European Journal of Organic Chemistry, 2011, 2011, 1544-1551.	1.2	37
626	Semiempirical Rate Constants for Complex Chemical Kinetics: Firstâ€Principles Assessment and Rational Refinement. Angewandte Chemie - International Edition, 2011, 50, 1194-1197.	7.2	42
627	Oxygen Defects and Novel Transport Mechanisms in Apatite Ionic Conductors: Combined ¹⁷Oâ€...NMR and Modeling Studies. Angewandte Chemie - International Edition, 2011, 50, 9328-9333.	7.2	57
628	NaSr₃Be₃B₃O₉F₄: A Promising Deepâ€Ultraviolet Nonlinear Optical Material Resulting from the Cooperative Alignment of the [Be₃B₃O₁₂F]^{10â^'} Anionic Group. Angewandte Chemie - International Edition, 2011, 50, 9141-9144.	7.2	342
629	The Effect of High Pressure on MOFâ€5: Guestâ€Induced Modification of Pore Size and Content at High Pressure. Angewandte Chemie - International Edition, 2011, 50, 11138-11141.	7.2	128
630	Discriminative generation and hydrogen modulation of the Dirac-Fermi polarons at graphene edges and atomic vacancies. Carbon, 2011, 49, 3615-3621.	5.4	47
631	Light emission from several-atom Inâ€“N clusters in wurtzite Ga-rich InGaN alloys and InGaN/GaN strained quantum wells. Acta Materialia, 2011, 59, 2773-2782.	3.8	14
632	Understanding atomic structures of amorphous C-doped Ge2Sb2Te5 phase-change memory materials. Acta Materialia, 2011, 59, 4335-4342.	3.8	49
633	DFT study on surface properties and dissolution trends of Al(100) surfaces doped with Zn, Ga, In, Sn and Pb. Applied Surface Science, 2011, 257, 4004-4009.	3.1	28
634	Carbon-doped K4 nitrogen: A novel high energy density material. Chemical Physics Letters, 2011, 506, 175-178.	1.2	6
635	Magnetism induced by D3-symmetry tetra-vacancy defects in graphene. Chemical Physics Letters, 2011, 510, 246-251.	1.2	19
636	Effect of spin polarization on the optical properties of Co-doped TiO2 thin films. Physica B: Condensed Matter, 2011, 406, 1429-1435.	1.3	8
637	Influence of valence electron concentration on elastic, electronic and optical properties of the alkaline-earth tin oxides A3SnO (A=Ca, Sr and Ba): A comparative study with ASnO3 compounds. Physica B: Condensed Matter, 2011, 406, 2714-2722.	1.3	30
638	Magnetic state of the bulk, surface and nanoclusters of CaMnO3: A DFT study. Physica B: Condensed Matter, 2011, 406, 3613-3621.	1.3	15
639	Characterization of the Landau expansion equation for SrTiO3 under pressure. Physica B: Condensed Matter, 2011, 406, 3922-3925.	1.3	0
640	CO adsorption on oxygen-modified molybdenum surfaces. Journal of Physics and Chemistry of Solids, 2011, 72, 744-748.	1.9	1
641	On the identification of the oxygen vacancy in HfO2. Microelectronic Engineering, 2011, 88, 1464-1466.	1.1	23
642	Doping induced electronic structure and estimated thermoelectric properties of CaMnO3 system. Physica B: Condensed Matter, 2011, 406, 1258-1262.	1.3	27

#	Article	IF	Citations
643	Electronic structure and optical properties of substitutional and interstitial phosphor-doped ZnO. Physics Letters, Section A: General, Atomic and Solid State Physics, 2011, 375, 939-945.	0.9	22
644	Understanding the interaction of water with anatase TiO2 (101) surface from density functional theory calculations. Physics Letters, Section A: General, Atomic and Solid State Physics, 2011, 375, 2939-2945.	0.9	27
645	First-principles study of the structural, vibrational, phonon and thermodynamic properties of transition metal carbides TMC (, Zr and Hf). Solid State Communications, 2011, 151, 61-66.	0.9	36
646	Structural, elastic and electronic properties of transition metal carbides TMC (TM=Ti, Zr, Hf and Ta) from first-principles calculations. Solid State Communications, 2011, 151, 602-606.	0.9	92
647	Prediction of the phase transition from ferromagnetic perovskite to non-magnetic post-perovskite in SrRuO3 : A first-principles study. Solid State Communications, 2011, 151, 798-801.	0.9	5
648	Semi-ab initio interionic potential for gadolinia-doped ceria. Solid State Ionics, 2011, 187, 8-18.	1.3	29
649	The structure of methoxy species on Cu(110): A combined photoelectron diffraction and density functional theory determination. Surface Science, 2011, 605, 193-205.	0.8	13
650	First principles study of ZnO adsorption on stressed metal surfaces. Surface Science, 2011, 605, 450-455.	0.8	1
651	DFT study of carbon monoxide adsorption on Î±-Al2O3(0001). Surface Science, 2011, 605, 1694-1703.	0.8	28
652	Electronâ€“hole pairs during the adsorption dynamics of O₂on Pd(100): exciting or not?. New Journal of Physics, 2011, 13, 085010.	1.2	48
653	A high pressure Ca-VI phase between 158 and 180 GPa: stability, electronic structure and superconductivity. Journal of Physics Condensed Matter, 2011, 23, 105701.	0.7	6
654	Fluctuations of tensile strength and hardness of c-BC₂N crystals induced by difference in atomic configuration. Journal of Physics Condensed Matter, 2011, 23, 465401.	0.7	0
655	Energetics of hydrogen/lithium complexes in silicon analyzed using the Maxwell construction. Physical Review B, 2011, 84, .	1.1	21
656	Influences of twist boundaries on optical effects: Ab initio studies of the deep ultraviolet nonlinear optical crystal KBe₂BO₃F₂. Journal of Applied Physics, 2011, 109, 073721.	1.1	8
657	Mechanism for suppression of ferroelectricity in Cd1â^'xCaxTiO3. Physical Review B, 2011, 84, .	1.1	40
658	Optimization mechanism of CaSi₂O₂N₂â€‰:â€‰Eu²⁺phosphor by La³⁺ion doping. Journal Physics D: Applied Physics, 2011, 44, 355403.	1.3	19
659	Adsorption of polyaromatic heterocycles on pyrophyllite surface by means of different theoretical approaches. Environmental Chemistry, 2011, 8, 429.	0.7	18
660	Particle-hole symmetry breaking in the pseudogap state ofPb0.55Bi1.5Sr1.6La0.4CuO6+Î´: A quantum chemical perspective. Physical Review B, 2011, 83, .	1.1	5

#		IF	Citations
661	Electronic band structure of SrCu<mml:math xmlns:mml="http://www.w3.org/1998/Math/MathML" display="inline"><mml:msub><mml:mrow /><mml:mn>4</mml:mn></mml:msub></mml:math>As<mml:math xmlns:mml="http://www.w3.org/1998/Math/MathML" display="inline"><mml:msub><mml:mrow /><mml:mn>2</mml:mn></mml:msub></mml:math>and KCu<mml:math xmlns:mml="http://www.w3.org/1998/Math/MathML" display="inline"><mml:msub><mml:mrow /><mml:mml:	1.1	4
662	A multinuclear solid-state magnetic resonance and GIPAW DFT study of anhydrous calcium chloride and its hydrates. Canadian Journal of Chemistry, 2011, 89, 754-763.	0.6	20
663	Controlling the Bonding and Band Gaps of Solid Carbon Monoxide with Pressure. Physical Review Letters, 2011, 106, 145502.	2.9	60
664	Structural and Valence Changes of Europium Hydride Induced by Application of High-Pressure<mml:math xmlns:mml="http://www.w3.org/1998/Math/MathML" display="inline"><mml:msub><mml:mi mathvariant="normal">H</mml:mi><mml:mn>2</mml:mn></mml:msub></mml:math>. Physical Review Letters, 2011, 107, 025501.	2.9	34
665	Surface stress changes in the Ir(001)/H system: Density functional theory study. Physical Review B, 2011, 84, .	1.1	4
666	Face-Dependent Bond Lengths in Molecular Chemisorption: The Formate Species on Cu(111) and Cu(110). Physical Review Letters, 2011, 107, 046102.	2.9	25
667	Phase stability and the arsenic vacancy defect in In<mml:math xmlns:mml="http://www.w3.org/1998/Math/MathML" display="inline"><mml:msub><mml:mrow /><mml:mi>x</mml:mi></mml:msub></mml:math>Ga<mml:math xmlns:mml="http://www.w3.org/1998/Math/MathML" display="inline"><mml:msub><mml:mrow /><mml:mrow><mml:mn>1</mml:mn><mml:mo>â^’</mml:mo><mml:mi>x</mml:mi></mml:mrow></mml:msub></mml:math>As. Physical Review B, 2011, 84, .	1.1	26
668	Na-Au intermetallic compounds formed under high pressure at room temperature. Physical Review B, 2011, 84, .	1.1	7
669	Local atomic order of crystalline Ge<mml:math xmlns:mml="http://www.w3.org/1998/Math/MathML" display="inline"><mml:msub><mml:mrow /><mml:mn>8</mml:mn></mml:msub></mml:math>Sb<mml:math xmlns:mml="http://www.w3.org/1998/Math/MathML" display="inline"><mml:msub><mml:mrow /><mml:mn>2</mml:mn></mml:msub></mml:math>Te<mml:math xmlns:mml="http://www.w3.org/1998/Math/MathML" display="inline"><mml:msub><mml:mrow /><mml:mml:	1.1	18
670	Experimental evidence of librational vibrations determining the stability of calcium borohydride. Physical Review B, 2011, 83, .	1.1	24
671	A Principled Approach to Distributed Multiscale Computing, from Formalization to Execution. , 2011, , .		11
672	First-principles calculations of electronic, optical, and thermodynamic properties of SrSi2. Journal of Applied Physics, 2011, 109, .	1.1	20
673	Ab initiostudy of the cubic-to-hexagonal phase transition promoted by interstitial hydrogen in iron. Physical Review B, 2011, 84, .	1.1	15
674	Oxidation and reduction of Pd(100) and aerosol-deposited Pd nanoparticles. Physical Review B, 2011, 83, .	1.1	79
675	Theory and hierarchical calculations of the structure and energetics of [0001] tilt grain boundaries in graphene. Physical Review B, 2011, 84, .	1.1	84
676	Carbonate formation on<mml:math xmlns:mml="http://www.w3.org/1998/Math/MathML" display="inline"><mml:mrow><mml:mi>p</mml:mi><mml:mo>(</mml:mo><mml:mn>4</mml:mn><mml:mo>Ã—</mml:mo><mml:mml:mo><mml:mml:mn> Physical Review B, 2011, 84, .	1.1	20
677	Parallel Efficiency and Parametric Optimization in CASTEP. , 2011, , .		1
678	Ab initioelectronic and geometrical structures of tripotassium-intercalated phenanthrene. Physical Review B, 2011, 84, .	1.1	34

#	Article	IF	Citations
679	Crystal structure and electronic states of tripotassium picene. Physical Review B, 2011, 83, .	1.1	45
680	Dense close-packed phase of tin above 157 GPa observed experimentally via angle-dispersive x-ray diffraction. Physical Review B, 2011, 84, .	1.1	30
681	Adsorbate modification of the structural, electronic, and magnetic properties of ferromagnetic fcc{110}surfaces. Physical Review B, 2011, 83, .	1.1	7
682	Effect of carbon concentration on shear modulus of (W1/2Al1/2)CZ. Journal of Applied Physics, 2011, 109, 073519.	1.1	1
683	Ab Inito Study of Absorption Spectra in Ultra Small Diameter Single Walled Boron Nanotubes. Advanced Materials Research, 2011, 217-218, 16-20.	0.3	0
684	First-Principles Study of the Properties of Clean and Ni-Doped TiC/Fe Interfaces. Advanced Materials Research, 0, 415-417, 166-169.	0.3	1
685	Ab Initio Phonon Dispersion Curves Used to Check Experimentally Determined Elastic Constants of the MAX Phase Ti₃SiC₂. Advanced Materials Research, 2011, 275, 135-138.	0.3	1
686	Prediction of a Low-Dense BC ₂ N Phase. Chinese Physics Letters, 2011, 28, 057101.	1.3	5
687	A density functional study on dielectric properties of acrylic acid grafted polypropylene. Journal of Chemical Physics, 2011, 134, 134904.	1.2	7
688	Non-Dissociative Adsorption of Carbonaceous Gases on Ni Containing Group-13, 14, and 15 Elements. Journal of the Electrochemical Society, 2011, 158, C403.	1.3	2
689	Electrical Properties of Hydrous Forsterite Derived from First-Principles Calculations. Chinese Physics Letters, 2011, 28, 059101.	1.3	1
690	First-Principles Study of Fe-Doped ZnO Nanowires. Chinese Physics Letters, 2011, 28, 126102.	1.3	13
691	The pressureâ€“temperature phase diagram of MgH₂and isotopic substitution. Journal of Physics Condensed Matter, 2011, 23, 305403.	0.7	16
692	An Experimental and Theoretical Multi-Mbar Study of Ti-6Al-4V. Materials Research Society Symposia Proceedings, 2011, 1369, 1.	0.1	2
693	Synthesis of Binary Transition Metal Nitrides, Carbides and Borides from the Elements in the Laser-Heated Diamond Anvil Cell and Their Structure-Property Relations. Materials, 2011, 4, 1648-1692.	1.3	100
694	Crystal structure determination of the silver carboxylate dimer [Ag(O₂C₂₂H₄₃)]₂, silver behenate, using powder X-ray diffraction methods. Powder Diffraction, 2011, 26, 313-320.	0.4	23
695	Bandgap shift by quantum confinement effect in ã€˜100ã€‰ Si-nanowires derived from threshold-voltage shift of fabricated metal-oxide-semiconductor field effect transistors and theoretical calculations. Journal of Applied Physics, 2011, 109, 064312.	1.1	6
696	Structural transition, dielectric and bonding properties of BeCN 2. Chinese Physics B, 2011, 20, 016201.	0.7	15

#	Article	IF	Citations
697	Terahertz normal mode relaxation in pentaerythritol tetranitrate. Journal of Chemical Physics, 2011, 134, 014513.	1.2	18
698	Simulated pressure response of crystalline indole. Journal of Chemical Physics, 2011, 135, 164508.	1.2	15
699	Influence of deuteration on lithium acetate dihydrate studied by inelastic X-ray scattering, density functional theory, thermal expansion, elastic and thermodynamic measurements. Dalton Transactions, 2011, 40, 1737.	1.6	3
700	Assignment of the vibrational spectra of lithium hydroxide monohydrate, LiOHÂ·H2O. Journal of Chemical Physics, 2011, 134, 084503.	1.2	24
701	First Principles Investigations on the Supramolecular Structure of 1,5-Diaminotetrazole. Advanced Materials Research, 0, 554-556, 65-69.	0.3	0
702	High pressure ionic and molecular crystals of ammonia monohydrate within density functional theory. Journal of Chemical Physics, 2012, 137, 064506.	1.2	21
703	Temperature dependence in interatomic potentials and an improved potential for Ti. Journal of Physics: Conference Series, 2012, 402, 012001.	0.3	12
704	Strain dependence of internal displacement and effective charge in wurtzite III-N semiconductors. Journal of Physics: Conference Series, 2012, 367, 012006.	0.3	1
705	Investigation of the hydrogen bonding in ice Ih by first-principles density function methods. Journal of Chemical Physics, 2012, 137, 044504.	1.2	33
706	Structureâ€“property relations and thermodynamic properties of monoclinic petalite, LiAlSi₄O₁₀. Journal of Physics Condensed Matter, 2012, 24, 345402.	0.7	14
707	Experimental and theoretical study of electron-beam-induced spin-reorientation transition reversal in the CO/Co(1â€‰1â€‰0) system. Journal Physics D: Applied Physics, 2012, 45, 275003.	1.3	2
708	Linear-scaling density functional theory simulations of polar semiconductor nanorods. Journal of Physics: Conference Series, 2012, 367, 012002.	0.3	10
709	Crystal Structure of High-Pressure Phases V and VI of Potassium Dihydrogen Phosphate. Journal of the Physical Society of Japan, 2012, 81, 064706.	0.7	2
710	Electron microscopy of nuclear graphite: A modelling approach. Journal of Physics: Conference Series, 2012, 371, 012061.	0.3	2
711	Study on rare-earthâ€“doped type-I germanium clathrates. Journal of Applied Physics, 2012, 111, 07E305.	1.1	9
712	Phase transitions in KIO₃. Journal of Physics Condensed Matter, 2012, 24, 325401.	0.7	12
713	Adjustable nitrogen-vacancy induced magnetism in AlN. Applied Physics Letters, 2012, 100, .	1.5	35
714	Effect of iron on high pressure elasticity of hydrous wadsleyite and ringwoodite by first-principles simulation. High Pressure Research, 2012, 32, 385-395.	0.4	7

#	Article	IF	Citations
715	Study on Î±-Î² quartz phase transition and its effect on dielectric properties. Journal of Applied Physics, 2012, 111, .	1.1	9
716	Surface structure of GaP(110): Ion scattering and density functional theory study. Physical Review B, 2012, 85, .	1.1	4
717	Cubic MnSb: Epitaxial growth of a predicted room temperature half-metal. Physical Review B, 2012, 85, .	1.1	50
718	Effect of alloying element Al substitution on Ni-Mn-Sn shape memory alloy by first-principle calculations. Journal of Applied Physics, 2012, 112, .	1.1	17
719	Mechanism for reversed photoemission core-level shifts of oxidized Ag. Physical Review B, 2012, 85, .	1.1	34
720	Experimental and theoretical study of Ti-6Al-4V to 220 GPa. Physical Review B, 2012, 85, .	1.1	16
721	Influence of oxygen vacancy on the electronic structure of CaCu3Ti4O12 and its deep-level vacancy trap states by first-principle calculation. Journal of Applied Physics, 2012, 111, .	1.1	28
723	Optimized effective potential using the Hylleraas variational method. Physical Review B, 2012, 85, .	1.1	19
724	Density functional theory analysis of flexural modes, elastic constants, and corrugations in strained graphene. Physical Review B, 2012, 86, .	1.1	26
725	Bulk and surface half-metallicity: Metastable zinc-blende TiSb. Journal of Applied Physics, 2012, 112, .	1.1	23
726	Selective observation of local carrier dynamics at step bunches on vicinal TiO<mml:math xmlns:mml="http://www.w3.org/1998/Math/MathML" display="inline"><mml:msub><mml:mrow /><mml:mn>2</mml:mn></mml:msub></mml:math>(110) by time-resolved pump-probe second harmonic generation method. Physical Review B, 2012, 86, .	1.1	4
727	Fermi-level pinning can determine polarity in semiconductor nanorods. Physical Review B, 2012, 85, .	1.1	15
728	Ab initiostudies on the optical effects in the deep ultraviolet nonlinear optical crystals of the KBe₂BO₃F₂family. Journal of Physics Condensed Matter, 2012, 24, 335503.	0.7	40
729	First principle study of the electronic structure of hafnium-doped anatase TiO₂. Journal of Semiconductors, 2012, 33, 012002.	2.0	10
730	Multi-scale order in amorphous transparent oxide thin films. Journal of Applied Physics, 2012, 112, 054907.	1.1	10
731	Effect of Ca-Substitution on CdTiO3Studied by Raman Scattering and First Principles Calculations. Ferroelectrics, 2012, 426, 268-273.	0.3	7
732	The effect of MgO(111) interlayer on the interface phase stability and structure of BaFe12O19/SiC(0001). Journal of Applied Physics, 2012, 111, 07A515.	1.1	3
733	Electronic structure of polyethylene — Crystalline and amorphous phases of pure polyethylene and their interfaces. , 2012, , .		18

#	Article	IF	Citations
734	Ab Initio Molecular Dynamics Study of Plutonium (IV) Solvation. Materials Research Society Symposia Proceedings, 2012, 1475, 593.	0.1	0
735	Surface concentration dependent structures of iodine on Pd(110). Journal of Chemical Physics, 2012, 137, 204703.	1.2	9
736	OptaDOS - a new tool for EELS calculations. Journal of Physics: Conference Series, 2012, 371, 012062.	0.3	44
737	Superhard transition metal tetranitrides: XN₄(X = Re, Os, W). Journal of Materials Research, 2012, 27, 1705-1715.	1.2	20
738	The structure and magnetism of graphone. AIP Advances, 2012, 2, .	0.6	34
739	Anisotropic transport properties of zinc-blend ZnTe/CrTe heterogeneous junction nanodevices. Journal of Applied Physics, 2012, 112, .	1.1	3
740	Reduced density function analysis of titanium dioxide doped tantalum pentoxide. Journal of Physics: Conference Series, 2012, 371, 012058.	0.3	6
741	Ab-initio modelling, polarity and energetics of clean rutile surfaces in vacuum and comparison with water environment. Journal of Physics: Conference Series, 2012, 371, 012059.	0.3	4
742	Molecular Understanding of the Adhesive Force between a Metal Oxide Surface and an Epoxy Resin: Effects of Surface Water. Bulletin of the Chemical Society of Japan, 2012, 85, 672-678.	2.0	57
743	Reinterpretation of the monohydrate of clarithromycin from X-ray powder diffraction data as a trihydrate. Acta Crystallographica Section C: Crystal Structure Communications, 2012, 68, o369-o372.	0.4	3
744	A solid-state NMR investigation of the colossal expansion material, Ag3Co(CN)6. Canadian Journal of Chemistry, 2012, 90, 891-901.	0.6	4
745	New insights into the structure and chemistry of Titanâ€™s tholins via 13C and 15N solid state nuclear magnetic resonance spectroscopy. Icarus, 2012, 221, 844-853.	1.1	39
746	Mechanism of Morphology Transformation of Tetragonal Phase LaVO₄ Nanocrystals Controlled by Surface Chemistry: Experimental and Theoretical Insights. Crystal Growth and Design, 2012, 12, 5042-5050.	1.4	22
747	Hydrothermal growths, optical features and first-principles calculations of sillenite-type crystals comprising discrete MO4tetrahedra. CrystEngComm, 2012, 14, 1063-1068.	1.3	30
748	CuNb₃O₈: A p-Type Semiconducting Metal Oxide Photoelectrode. Journal of Physical Chemistry Letters, 2012, 3, 1577-1581.	2.1	114
749	Preparation and Photoelectrochemical Properties of p-type Cu₅Ta₁₁O₃₀ and Cu₃Ta₇O₁₉ Semiconducting Polycrystalline Films. Journal of Physical Chemistry C, 2012, 116, 10490-10497.	1.5	57
750	New Insights into the Molecular Structures, Compositions, and Cation Distributions in Synthetic and Natural Montmorillonite Clays. Chemistry of Materials, 2012, 24, 4376-4389.	3.2	79
751	Structure and decomposition of zinc borohydride ammonia adduct: towards a pure hydrogen release. Energy and Environmental Science, 2012, 5, 7590.	15.6	82

#	Article	IF	Citations
752	Effects of surface chemistry on the morphology transformation of ZnWO₄nanocrystals: investigated from experiment and theoretical calculations. CrystEngComm, 2012, 14, 920-928.	1.3	14
753	A novel aided-cation strategy to advance the dehydrogenation of calcium borohydride monoammoniate. Journal of Materials Chemistry, 2012, 22, 5312.	6.7	44
754	Van der Waals forces in the perfluorinated metalâ€“organic framework zinc 1,2-bis(4-pyridyl)ethane tetrafluoroterephthalate. Physical Chemistry Chemical Physics, 2012, 14, 7059.	1.3	20
755	Exotic Cubic Carbon Allotropes. Journal of Physical Chemistry C, 2012, 116, 24233-24238.	1.5	53
756	LiGaGe₂Se₆: A New IR Nonlinear Optical Material with Low Melting Point. Inorganic Chemistry, 2012, 51, 1035-1040.	1.9	103
757	Models for incomplete nucleophilic attack on a protonated carbonyl group and electron-deficient alkenes: salts and zwitterions from 1-dimethylamino-naphthalene-8-carbaldehyde. Organic and Biomolecular Chemistry, 2012, 10, 7763.	1.5	11
758	An effective structure prediction method for layered materials based on 2D particle swarm optimization algorithm. Journal of Chemical Physics, 2012, 137, 224108.	1.2	275
759	Extraordinarily Long-Ranged Structural Relaxation in Defective Achiral Carbon Nanotubes. Physical Review Letters, 2012, 109, 265502.	2.9	7
760	Structures and lattice energies of molecular crystals using density functional theory: Assessment of a local atomic potential approach. Chemical Physics Letters, 2012, 550, 94-98.	1.2	22
761	First-Principles Calculation of NMR Parameters Using the Gauge Including Projector Augmented Wave Method: A Chemistâ€™s Point of View. Chemical Reviews, 2012, 112, 5733-5779.	23.0	446
762	A New Mixed Halide, Cs₂HgI₂Cl₂: Molecular Engineering for a New Nonlinear Optical Material in the Infrared Region. Journal of the American Chemical Society, 2012, 134, 14818-14822.	6.6	130
763	Synthesis, Crystal Structure, and Properties of a New Lead Aluminum Fluoride Borate, Pb6AlB2O7F7. Zeitschrift Fur Anorganische Und Allgemeine Chemie, 2012, 638, n/a-n/a.	0.6	4
764	Many-body potential for nitrogen in Î±-iron. Philosophical Magazine Letters, 2012, 92, 656-667.	0.5	3
766	Bistability Loss as a Key Feature in Azobenzene (Nonâ€)Switching on Metal Surfaces. Angewandte Chemie - International Edition, 2012, 51, 12009-12011.	7.2	31
767	Effect of Platinum Incorporation on the Energetics and Oxygen Chemisorption Properties of the Ni(1â€‰1â€‰1) Surface. ChemCatChem, 2012, 4, 2005-2012.	1.8	4
768	Firstâ€Principles Calculations on Electronic Structures of N/Vâ€Doped and Nâ€Vâ€Dodoped Anatase TiO₂ (101) Surfaces. ChemPhysChem, 2012, 13, 3836-3847.	1.0	21
769	The Interaction of Noble Metal With La_{1â€“}_xSr_xMnO₃ (001) Surface and Catalytic Role for Oxygen Adsorption: A Density Functional Theory Study. Fuel Cells, 2012, 12, 1048-1055.	1.5	0
770	Isoglitter. Journal of Mathematical Chemistry, 2012, 50, 2281-2290.	0.7	3

#	Article	IF	Citations
771	Stable structures and electronic properties of 6-atom noble metal clusters using density functional theory. Journal of Nanoparticle Research, 2012, 14, 1.	0.8	8
772	Theoretic insights into the Ag doping in monolayer and bilayer ZnO armchair nanoribbons: edge effect and position-dependent properties. Journal of Nanoparticle Research, 2012, 14, 1.	0.8	5
773	First-principles molecular dynamics simulations to study the crystal-to-amorphous transition in the Mgâ€“Zn system. Intermetallics, 2012, 29, 75-79.	1.8	13
774	Systematic study of the elastic properties of Mn3AC antiperovskite with A=Zn, Al, Ga, In, Tl, Ge and Sn. Journal of Alloys and Compounds, 2012, 541, 75-78.	2.8	7
775	First-principles study of doping effect on the phase transition of zinc oxide with transition metal doped. Journal of Alloys and Compounds, 2012, 541, 250-255.	2.8	32
776	Formation of LiBH4 hydrate with dihydrogen bonding. Journal of Alloys and Compounds, 2012, 541, 111-114.	2.8	16
777	Mechanical stabilities of K4 carbon and K4-like NaC2. Journal of Physics and Chemistry of Solids, 2012, 73, 1264-1267.	1.9	3
778	Structure, growth and properties of a novel polar material, KSr4B3O9. Journal of Solid State Chemistry, 2012, 195, 73-78.	1.4	18
779	Thermoelectric and thermodynamic properties of half-Heulser alloy YPdSb from first principles calculations. Journal of Solid State Chemistry, 2012, 196, 511-517.	1.4	30
780	Energy band gap engineering in borate ultraviolet nonlinear optical crystals:ab initiostudies. Journal of Physics Condensed Matter, 2012, 24, 145503.	0.7	32
781	Importance of anisotropic Coulomb interactions and exchange to the band gap and antiferromagnetism of<mml:math xmlns:mml="http://www.w3.org/1998/Math/MathML" display="inline"><mml:mi>Î²</mml:mi></mml:math>-MnO<mml:math xmlns:mml="http://www.w3.org/1998/Math/MathML" display="inline"><mml:msub><mml:mrow /><mml:mn>2</mml:mn></mml:msub></mml:math>from DFT+<mml:math xmlns:mml="http://www.w3.org/1998/Math/MathML" display="inline"><mml:mi>U</mml:mi></mml:math>	1.1	72
782	The high-pressure electronic structure of the [Ni(ptdt)2] organic molecular conductor. Journal of Chemical Physics, 2012, 137, 024701.	1.2	1
785	Multinuclear Magnetic Resonance Crystallographic Structure Refinement and Cross-Validation Using Experimental and Computed Electric Field Gradients: Application to Na₂Al₂B₂O₇. Journal of Physical Chemistry C, 2012, 116, 19472-19482.	1.5	52
786	First-Principles Calculations on the Electronic Structure of ZnO Nanowires. Applied Mechanics and Materials, 2012, 198-199, 23-27.	0.2	0
787	Materials Properties of Ultra-Incompressible Re₂P. Chemistry of Materials, 2012, 24, 3240-3246.	3.2	15
788	First-principles studies of structural, mechanical, electronic, optical properties and pressure-induced phase transition of CuInO2 polymorph. Physica B: Condensed Matter, 2012, 407, 4665-4670.	1.3	6
789	Synthesis, crystal structure and properties of a new strontium cadmium diborate. Inorganica Chimica Acta, 2012, 392, 459-464.	1.2	3
790	First principles investigation of scandium-based borohydride NaSc(BH4)4. Journal of Alloys and Compounds, 2012, 536, S546-S549.	2.8	11

#	Article	IF	Citations
791	Phase stability, elastic, electronic, thermal and optical properties of Ti3Al1â˜xSixC2 (0â‰¤xâ‰¤1): First principle study. Physica B: Condensed Matter, 2012, 407, 4221-4228.	1.3	38
792	First principles study on mechanical properties of Mgâ€“MgCd interface micro-zone. Molecular Simulation, 2012, 38, 200-203.	0.9	1
793	A novel deep UV nonlinear optical crystal Ba3B6O11F2, with a new fundamental building block, B6O14 group. Journal of Materials Chemistry, 2012, 22, 9665.	6.7	177
794	Crystal and electronic structure, lattice dynamics and thermal properties of Ag(i)(SO3)R (R = F, CF3) Lewis acids in the solid state. Dalton Transactions, 2012, 41, 2034-2047.	1.6	28
795	A new noncentrosymmetric vanadoborate: synthesis, crystal structure and characterization of K2SrVB5O12. Dalton Transactions, 2012, 41, 9202.	1.6	16
796	Structure and hydrogenstorage properties of the first rare-earth metal borohydride ammoniate: Y(BH₄)₃Â·4NH₃. Journal of Materials Chemistry, 2012, 22, 1061-1068.	6.7	55
797	Mode-specificity and transition state-specific energy redistribution in the chemisorption of CH4 on Ni{100}. Physical Chemistry Chemical Physics, 2012, 14, 15879.	1.3	33
798	Ab initiopredictions of structural and elastic properties of struvite: contribution to urinary stone research. Computer Methods in Biomechanics and Biomedical Engineering, 2012, 15, 1329-1336.	0.9	10
799	Structure and electronic structure of S-doped graphitic C ₃ N ₄ investigated by density functional theory. Chinese Physics B, 2012, 21, 107101.	0.7	38
800	Experimental evidence for the structural models of Re<mml:math xmlns:mml="http://www.w3.org/1998/Math/MathML" display="inline"><mml:msub><mml:mrow /><mml:mn>2</mml:mn></mml:msub></mml:math>N and Re<mml:math xmlns:mml="http://www.w3.org/1998/Math/MathML" display="inline"><mml:msub><mml:mrow /><mml:mn>2</mml:mn></mml:msub></mml:math>C from micro-Raman spectroscopy. Physical Review B, 2012, 86, .	1.1	10
801	The hidden force opposing ice compression. Chemical Science, 2012, 3, 1455.	3.7	80
802	SMARTER crystallography of the fluorinated inorganicâ€“organic compound Zn3Al2F12Â·[HAmTAZ]6. Dalton Transactions, 2012, 41, 6232.	1.6	43
803	Lattice distortion and its role in the magnetic behavior of the Mn-doped ZnO system. New Journal of Physics, 2012, 14, 013033.	1.2	15
804	Unusual intermediate spin Fe3+ ion in antiferromagnetic Li3FeN2. Journal of Applied Physics, 2012, 111, 063704.	1.1	4
805	Rare earth induced formation of Î´-BiB3O6 at ambient pressure with strong second harmonic generation. Journal of Materials Chemistry, 2012, 22, 17934.	6.7	27
806	Atomic layer deposition of lithium nitride and carbonate using lithium silylamide. RSC Advances, 2012, 2, 6315.	1.7	42
807	NaGe₃P₃: a new ternary germanium phosphide featuring an unusual [Ge₃P₇] ring. Dalton Transactions, 2012, 41, 484-489.	1.6	19
808	A novel structural form of MIL-53 observed for the scandium analogue and its response to temperature variation and CO₂adsorption. Dalton Transactions, 2012, 41, 3937-3941.	1.6	95

#	Article	IF	Citations
809	Epitaxy of Prestrained Graphene on a Si-Terminated SiC(0001) Surface. Journal of Physical Chemistry C, 2012, 116, 13928-13934.	1.5	2
810	²⁵Mg Solid-State NMR of Magnesium Phosphates: High Magnetic Field Experiments and Density Functional Theory Calculations. Journal of Physical Chemistry C, 2012, 116, 19984-19995.	1.5	29
811	Chemical-State Analysis of Organic Semiconductors Using Soft X-ray Absorption Spectroscopy Combined with First-Principles Calculation. Journal of Physical Chemistry A, 2012, 116, 1527-1531.	1.1	5
812	First-Principles Study on Intrinsic Point Defects in Rhombohedral LaAlO$_{3}$ and Their Effects on Electrical Properties. Japanese Journal of Applied Physics, 2012, 51, 041103.	0.8	6
813	Periodic-DFT of a Disordered System: Mg₂(FeH₆)_{0.5}(CoH₅)_{0.5}. Journal of Physical Chemistry C, 2012, 116, 25206-25212.	1.5	3
814	Lattice Dynamics of Î²-V₂O₅: Raman Spectroscopic Insight into the Atomistic Structure of a High-Pressure Vanadium Pentoxide Polymorph. Inorganic Chemistry, 2012, 51, 3194-3201.	1.9	129
815	Variable-Temperature ¹⁷O NMR Studies Allow Quantitative Evaluation of Molecular Dynamics in Organic Solids. Journal of the American Chemical Society, 2012, 134, 14609-14617.	6.6	55
816	Pillared Covalent Organic Frameworks with Balanced Volumetric and Gravimetric Hydrogen Uptake. Journal of Physical Chemistry C, 2012, 116, 1479-1484.	1.5	19
817	Potential-Dependent Structural Memory Effects in Auâ€“Pd Nanoalloys. Journal of Physical Chemistry Letters, 2012, 3, 315-321.	2.1	39
818	Modification of the structural and electronic properties of graphene by the benzene molecule adsorption. Physica B: Condensed Matter, 2012, 407, 4557-4561.	1.3	21
819	Ab-initio study of active lone pair of Ge²⁺ cation in novel perovskite GeTiO<inf>3</inf> compound. , 2012, , .		0
820	A Theoretical Study of Water Adsorption and Decomposition on the Low-Index Stoichiometric Anatase TiO₂ Surfaces. Journal of Physical Chemistry C, 2012, 116, 7430-7441.	1.5	70
821	First-Principle Studies on the Pressure-Induced Structural Changes in Energetic Ionic Salt 3-Azido-1,2,4-triazolium Nitrate Crystal. Journal of Physical Chemistry C, 2012, 116, 16144-16153.	1.5	28
822	Cagelike Diamondoid Nitrogen at High Pressures. Physical Review Letters, 2012, 109, 175502.	2.9	176
823	NMR Crystallography Comparative Studies of Chiral (1R,2S,3R,5R)-3-Amino-6,6-dimethylbicyclo[3.1.1]heptan-2-ol and Its p-Toluenesulfonamide Derivative. Crystal Growth and Design, 2012, 12, 5956-5965.	1.4	4
824	High Pressure Synthesis and Superconductivity of the Ternary Compounds Mg(Mg1â€“xAlx)Si with the Anticotunnite Structure. Inorganic Chemistry, 2012, 51, 10300-10305.	1.9	16
825	Applications of NMR Crystallography to Problems in Biomineralization: Refinement of the Crystal Structure and ³¹P Solid-State NMR Spectral Assignment of Octacalcium Phosphate. Journal of the American Chemical Society, 2012, 134, 12508-12515.	6.6	80
826	A meta-GGA Made Free of the Order of Limits Anomaly. Journal of Chemical Theory and Computation, 2012, 8, 2078-2087.	2.3	49

#	Article	IF	Citations
827	Structural properties of PbVO₃perovskites under hydrostatic pressure conditions up to 10.6 GPa. Journal of Physics Condensed Matter, 2012, 24, 435403.	0.7	16
828	High-pressure ionic and molecular phases of ammonia within density functional theory. Physical Review B, 2012, 86, .	1.1	23
829	A Multinuclear Solid-State NMR Study of Templated and Calcined Chabazite-Type GaPO-34. Journal of Physical Chemistry C, 2012, 116, 15048-15057.	1.5	24
830	First-Principles Investigation of ThO₂. Advanced Materials Research, 2012, 535-537, 2531-2534.	0.3	1
831	Raman Spectra of Ammonia Borane: Low Frequency Lattice Modes. Journal of Physical Chemistry A, 2012, 116, 8827-8832.	1.1	12
832	Monomer Adsorption on Kaolinite: Modeling the Essential Ingredients. Journal of Physical Chemistry C, 2012, 116, 22365-22374.	1.5	33
833	Structural Investigation of Î±- and Î²-Sodium Hexafluoroarsenate, NaAsF6, by Variable Temperature X-ray Powder Diffraction and Multinuclear Solid-State NMR, and DFT Calculations. Journal of Physical Chemistry C, 2012, 116, 11682-11693.	1.5	20
834	Multinuclear Solid-State Nuclear Magnetic Resonance and Density Functional Theory Characterization of Interaction Tensors in Taurine. Journal of Physical Chemistry A, 2012, 116, 1008-1014.	1.1	35
835	First-Principle Study on High-Pressure Behavior of Crystalline Polyazido-1,3,5-triazine. Journal of Physical Chemistry C, 2012, 116, 6745-6753.	1.5	23
836	Deprotonated Glycine on Cu(111): Quantitative Structure Determination by Energy-Scanned Photoelectron Diffraction. Journal of Physical Chemistry C, 2012, 116, 9985-9995.	1.5	18
837	Ar adsorptions on Al (111) and Ir (111) surfaces: a first-principles study. Chinese Physics B, 2012, 21, 026802.	0.7	4
838	Bi<mml:math xmlns:mml="http://www.w3.org/1998/Math/MathML" display="inline"><mml:msub><mml:mrow /><mml:mn>2</mml:mn></mml:msub></mml:math>-based layered superconductor Bi<mml:math xmlns:mml="http://www.w3.org/1998/Math/MathML" display="inline"><mml:msub><mml:mrow /><mml:mn>4</mml:mn></mml:msub></mml:math>O<mml:math xmlns:mml="http://www.w3.org/1998/Math/MathML" display="inline"><mml:msub><mml:mrow	1.1	373
839	Combining Multinuclear High-Resolution Solid-State MAS NMR and Computational Methods for Resonance Assignment of Glutathione Tripeptide. Journal of Physical Chemistry A, 2012, 116, 6711-6719.	1.1	40
840	Insights into Changes in Voltage and Structure of Li₂FeSiO₄ Polymorphs for Lithium-Ion Batteries. Chemistry of Materials, 2012, 24, 2155-2161.	3.2	128
841	⁸⁷Sr Solid-State NMR as a Structurally Sensitive Tool for the Investigation of Materials: Antiosteoporotic Pharmaceuticals and Bioactive Glasses. Journal of the American Chemical Society, 2012, 134, 12611-12628.	6.6	68
842	The Importance of Attractive Three-Point Interaction in Enantioselective Surface Chemistry: Stereospecific Adsorption of Serine on the Intrinsically Chiral Cu{531} Surface. Journal of the American Chemical Society, 2012, 134, 9615-9621.	6.6	47
843	Influence of Crystal Structure of Bulk Phase on the Stability of Nanoscale Phases: Investigation on MgH₂ Derived Nanostructures. Journal of Physical Chemistry C, 2012, 116, 18965-18972.	1.5	30
844	Coverage-Dependent Structural Evolution in the Interaction of NO₂ with Au{111}. Journal of Physical Chemistry C, 2012, 116, 5637-5645.	1.5	5

#	Article	IF	Citations
845	The effect of pressure on the elastic properties and seismic anisotropy of diopside and jadeite from atomic scale simulation. Physics of the Earth and Planetary Interiors, 2012, 192-193, 81-89.	0.7	28
846	First-principles study on the structural, electronic and optical properties of BiOX (X=Cl, Br, I) crystals. Physica B: Condensed Matter, 2012, 407, 3364-3370.	1.3	167
847	Electronic and optical properties of pure and Mo doped anatase TiO2 using GGA and GGA+U calculations. Physica B: Condensed Matter, 2012, 407, 3610-3616.	1.3	38
848	Structure, elasticity, thermodynamics and high pressure behavior of ZnB4O7 and CdB4O7. Solid State Sciences, 2012, 14, 1080-1085.	1.5	12
849	Synthesis, crystal structure and characterization of a new compound, Li3NaBaB6O12. Solid State Sciences, 2012, 14, 1186-1190.	1.5	22
850	Synthesis, structure, physical properties, and electronic structure of KGaSe2. Solid State Sciences, 2012, 14, 1152-1156.	1.5	22
851	First principles study of the structural, elastic, electronic and optical properties of CaSrTt (Tt=Si, Ge,) Tj ETQq0 0 0 rgBT /Overlock 10 Tf 5	0.9	4
852	Crystal structures and band gap characters of h-BN polytypes predicted by the dispersion corrected DFT and GW method. Solid State Communications, 2012, 152, 1817-1820.	0.9	59
853	Surface composition of clean and oxidized Pd75Ag25(100) from photoelectron spectroscopy and density functional theory calculations. Surface Science, 2012, 606, 1777-1782.	0.8	34
854	Assignment of Metalâ€“Ligand Modes in Pt(II) Diimine Complexes Relevant to Solar Energy Conversion. Inorganic Chemistry, 2012, 51, 9748-9756.	1.9	10
855	Calculation of point defects in rutile TiO<mml:math xmlns:mml="http://www.w3.org/1998/Math/MathML" display="inline"><mml:msub><mml:mrow /><mml:mn>2</mml:mn></mml:msub></mml:math>by the screened-exchange hybrid functional. Physical Review B, 2012, 86, .	1.1	88
856	Density functional calculations of the enthalpies of formation of rare-earth orthophosphates. American Mineralogist, 2012, 97, 791-799.	0.9	47
857	Two-Dimensional Boron Monolayer Sheets. ACS Nano, 2012, 6, 7443-7453.	7.3	690
858	Hidden polymorphs drive vitrification in B2O3. Nature Materials, 2012, 11, 925-929.	13.3	60
859	Theoretical Insight into the Structural Stability of KZnB3O6Polymorphs with Different BOxPolyhedral Networks. Inorganic Chemistry, 2012, 51, 6762-6770.	1.9	11
860	Hydrogen adsorption on Naâ€“SWCNT systems. Journal of Materials Chemistry, 2012, 22, 22013.	6.7	8
861	Photoluminescence induced by twinning interface in CdS nanocrystals. Applied Physics Letters, 2012, 100, 171911.	1.5	12
862	Ammine bimetallic (Na, Zn) borohydride for advanced chemical hydrogen storage. Journal of Materials Chemistry, 2012, 22, 7300.	6.7	52

#	Article	IF	Citations
863	Computational Methods for the Assignment of Vibrational Modes in Crystalline Materials. Springer Series in Optical Sciences, 2012, , 151-190.	0.5	3
864	Electronic band structure and optical phonons of BaSnO3 and Ba0.97La0.03SnO3 single crystals: Theory and experiment. Journal of Applied Physics, 2012, 112, .	1.1	75
865	Ab-initio modeling of oxygen on the surface passivation of 3CSiC nanostructures. Applied Surface Science, 2012, 258, 8360-8365.	3.1	14
866	A Density Functional Theory study of the chemical surface modification of Î²-SiC nanopores. Materials Science and Engineering B: Solid-State Materials for Advanced Technology, 2012, 177, 1482-1486.	1.7	6
867	Band gap of C3N4 in the GW approximation. International Journal of Hydrogen Energy, 2012, 37, 11072-11080.	3.8	208
868	First-principles study of pressure-induced magnetic transition in siderite FeCO3. Journal of Alloys and Compounds, 2012, 510, L1-L4.	2.8	13
869	First principle calculations of the electronic and optical properties of pure and (Mo, N) co-doped anatase TiO2. Journal of Alloys and Compounds, 2012, 513, 539-545.	2.8	115
870	On the effect of thermal treatment and hydrogen vibrational dynamics in sodium alanates: An inelastic neutron scattering study. Journal of Alloys and Compounds, 2012, 523, 108-113.	2.8	8
871	A relationship to estimate the excess entropy of mixing: Application in silicate solid solutions and binary alloys. Journal of Alloys and Compounds, 2012, 527, 127-131.	2.8	25
872	Electronic structure and impurity states of S-doped cBN: A first-principle study. Journal of Alloys and Compounds, 2012, 531, 82-85.	2.8	15
873	Thermodynamical analysis of polytype stability during PVT growth of SiC using 2D nucleation theory. Journal of Crystal Growth, 2012, 352, 177-180.	0.7	19
874	Growth and characterisation of NiSb(0001)/GaAs(111)B epitaxial films. Journal of Crystal Growth, 2012, 357, 1-8.	0.7	13
875	Strategy for the optical property studies in ultraviolet nonlinear optical crystals from density functional theory. Computational Materials Science, 2012, 60, 99-104.	1.4	71
876	First-principles study of the Al(001)/Al3Ti(001) interfacial properties. Computational Materials Science, 2012, 62, 136-141.	1.4	30
877	Elastic, thermodynamic, electronic and optical properties of U2Ti. Computational Materials Science, 2012, 63, 256-260.	1.4	18
878	Bond-selective energy redistribution in the chemisorption of CH3D and CD3H on Pt{110}-(1Ã—2): A first-principles molecular dynamics study. Computational and Theoretical Chemistry, 2012, 990, 144-151.	1.1	20
879	Structural, elastic, electronic and magnetic properties of Mn3ZnC and Mn3GeC. Computational and Theoretical Chemistry, 2012, 991, 161-164.	1.1	10
880	On the ability of periodic dispersion-corrected DFT calculations to predict molecular crystal polymorphism in para-diiodobenzene. Chemical Physics Letters, 2012, 541, 12-15.	1.2	18

#	Article	IF	Citations
881	Pseudopotential errors in titanium. Computational Materials Science, 2012, 52, 2-6.	1.4	9
882	Lattice dynamics of PbTe polymorphs from first principles. Computational Materials Science, 2012, 56, 18-24.	1.4	10
883	Iron reduction in nontronite-type clay minerals: Modelling a complex system. Geochimica Et Cosmochimica Acta, 2012, 81, 13-27.	1.6	14
884	Lithium defects and diffusivity in forsterite. Geochimica Et Cosmochimica Acta, 2012, 91, 32-39.	1.6	8
885	Enhanced visible-light photocatalytic activity of g-C3N4â€“ZnWO4 by fabricating a heterojunction: investigation based on experimental and theoretical studies. Journal of Materials Chemistry, 2012, 22, 23428.	6.7	227
886	Complementing High-Throughput X-ray Powder Diffraction Data With Quantumâ€“Chemical Calculations: Application to Piroxicam Form III. Journal of Pharmaceutical Sciences, 2012, 101, 4214-4219.	1.6	30
887	NMR characterisation of structure in solvates and polymorphs of formoterol fumarate. Magnetic Resonance in Chemistry, 2012, 50, 680-690.	1.1	14
888	pâ€type conductivity of GeTe: The role of loneâ€pair electrons. Physica Status Solidi (B): Basic Research, 2012, 249, 1902-1906.	0.7	14
889	Superâ€atom properties of 13 atom clusters of group 13 elements. Physica Status Solidi (B): Basic Research, 2012, 249, 2179-2189.	0.7	7
890	The Silicides M₄Si₄ with M = Na, K, Rb, Cs, and Ba₂Si₄ â€“ NMR Spectroscopy and Quantum Mechanical Calculations. Zeitschrift Fur Anorganische Und Allgemeine Chemie, 2012, 638, 1437-1445.	0.6	26
891	Rare earth rhodium borides RRh3B (R = Y, Zr, and Nb): mechanical, thermal and optical properties. European Physical Journal B, 2012, 85, 1.	0.6	20
892	UKRmol: a low-energy electron- and positron-molecule scattering suite. European Physical Journal D, 2012, 66, 1.	0.6	169
893	Computational simulation of the effects of oxygen on the electronic states of hydrogenated 3C-porous SiC. Nanoscale Research Letters, 2012, 7, 471.	3.1	17
894	Low-loss EELS of 2D boron nitride. Journal of Physics: Conference Series, 2012, 371, 012060.	0.3	5
895	BaGa2MQ6 (M = Si, Ge; Q = S, Se): a new series of promising IR nonlinear optical materials. Dalton Transactions, 2012, 41, 5653.	1.6	174
896	Synthesis and Characterization of Sr₂Cu(W_{1â€“x}Mo_x)O₆: A Quasi-Two-Dimensional Magnetic System. Chemistry of Materials, 2012, 24, 2764-2774.	3.2	32
897	Weak Halogen Bonding in Solid Haloanilinium Halides Probed Directly via Chlorine-35, Bromine-81, and Iodine-127 NMR Spectroscopy. Crystal Growth and Design, 2012, 12, 1641-1653.	1.4	45
898	Prediction of structural, lattice dynamical, and mechanical properties of CaB2. RSC Advances, 2012, 2, 11687.	1.7	15

#	Article	IF	Citations
899	<scp><scp>Ti</scp></scp>₅<scp><scp>Al</scp></scp>₂<scp><scp>C</scp></scp>₃: A New Ternary Carbide Belonging to <scp>MAX</scp> Phases in the <scp><scp>Ti</scp></scp>â€“<scp><scp>Al</scp></scp>â€“<scp><scp>C</scp></scp> System. Journal of the American Ceramic Society, 2012, 95, 1508-1510.	1.9	29
900	Low temperature measurements by infrared spectroscopy in CoFe2O4 ceramic. Open Physics, 2012, 10, .	0.8	7
901	Oxygen Activation on Nanometer-Size Gold Nanoparticles. Journal of Physical Chemistry C, 2012, 116, 15992-16000.	1.5	39
902	Optical transitions due to native defects in nonlinear optical crystals LiGaS2. Journal of Applied Physics, 2012, 111, .	1.1	22
903	Optical isotropy in structurally anisotropic halide scintillators:Ab initiostudy. Physical Review B, 2012, 86, .	1.1	27
904	Quantum Monte Carlo investigations of adsorption energetics on graphene. Journal of Physics Condensed Matter, 2012, 24, 395002.	0.7	8
905	Superconductivity in LaTMBN and La3TM2B2N3 (TM = Transition Metal) Synthesized under High Pressure. Journal of the American Chemical Society, 2012, 134, 2516-2519.	6.6	14
906	HALF-METALLIC SILICENE AND GERMANENE NANORIBBONS: TOWARDS HIGH-PERFORMANCE SPINTRONICS DEVICE. Nano, 2012, 07, 1250037.	0.5	105
907	Hybrid functional calculations of the Al impurity in<mml:math xmlns:mml="http://www.w3.org/1998/Math/MathML" display="inline"><mml:mi>Î±</mml:mi></mml:math>quartz: Hole localization and electron paramagnetic resonance parameters. Physical Review B, 2012, 85, .	1.1	16
908	Synthesis and Structure Resolution of RbLaF4. Inorganic Chemistry, 2012, 51, 2272-2282.	1.9	32
909	Crystal structure of ammonia dihydrate II. Journal of Chemical Physics, 2012, 136, 174512.	1.2	17
910	Elastic stiffness coefficients of thenardite and their pressure and temperature dependence. Zeitschrift Fur Kristallographie - Crystalline Materials, 2012, 227, 503-513.	0.4	4
912	Metalâ€“organic frameworks for visible light absorption via anion substitution. Journal of Materials Chemistry, 2012, 22, 10144.	6.7	22
913	Sequential multiscale modelling of SiC/Al nanocomposites reinforced with WS<mml:math xmlns:mml="http://www.w3.org/1998/Math/MathML" display="inline"><mml:msub><mml:mrow /><mml:mn>2</mml:mn></mml:msub></mml:math>nanoparticles under static loading. Physical Review B, 2012, 86, .	1.1	6
914	First-principles study of O-BN: A sp3-bonding boron nitride allotrope. Journal of Applied Physics, 2012, 112, .	1.1	53
915	Mg2â^'xTixNi (xÂ=Â0, 0.5) alloys prepared by mechanical alloying for electrochemical hydrogen storage: Experiments and first-principles calculations. International Journal of Hydrogen Energy, 2012, 37, 14248-14256.	3.8	27
916	Reaction pathways derived from DFT for understanding catalytic decomposition of formic acid into hydrogen on noble metals. International Journal of Hydrogen Energy, 2012, 37, 15956-15965.	3.8	91
917	Thermodynamic study and re-assessment of the Ge-Ni system. Calphad: Computer Coupling of Phase Diagrams and Thermochemistry, 2012, 38, 23-34.	0.7	23

#	Article	IF	Citations
918	Structure and electronic properties of lead-free KTa1â^'xNbxO3: Accurate Wuâ€“Cohen and screened-exchange study. Computational Materials Science, 2012, 65, 100-103.	1.4	11
919	Structural and electronic properties of oxygen vacancy in lead-free KTa1â^'xNbxO3: Comparative first-principles calculations. Computational Materials Science, 2012, 65, 193-196.	1.4	3
920	Structural, elastic and thermodynamic properties of anti-ReO3 type Cu3N under pressure from first principles. Computational Materials Science, 2012, 65, 247-253.	1.4	13
921	MAX phases Nb2AC (A=S, Sn): An ab initio study. Computational Materials Science, 2012, 65, 365-371.	1.4	22
922	First-principles calculations of Zn substitutions in Cu6Sn5. Computational Materials Science, 2012, 65, 490-493.	1.4	17
923	2,4-Diazido-5-iodo-pyrimidine crystal under high pressure: A comparison of DFT and DFT-D studies. Computational and Theoretical Chemistry, 2012, 1000, 60-69.	1.1	10
924	Effects of the orientation of the 23Naâ€“29Si dipolar vector on the dipolar mediated heteronuclear solid state NMR correlation spectrum of crystalline sodium silicates. Solid State Nuclear Magnetic Resonance, 2012, 45-46, 1-10.	1.5	11
925	Superatom representation of high-TC superconductivity. Physica C: Superconductivity and Its Applications, 2012, 480, 137-143.	0.6	4
926	First-principles calculation of structure and mechanical property of IrY. Procedia Engineering, 2012, 31, 665-670.	1.2	0
927	Terahertz and mid-infrared spectroscopy of benzene-1,2-diol. Journal of Molecular Spectroscopy, 2012, 281, 13-17.	0.4	10
928	Athermal component of amorphisation in phase-change alloys and chalcogenide glasses. Journal of Non-Crystalline Solids, 2012, 358, 2398-2401.	1.5	7
929	Ab initio, crystal field and experimental spectroscopic studies of pure and Ni2+-doped KZnF3 crystals. Materials Chemistry and Physics, 2012, 136, 90-102.	2.0	21
930	Experimental and theoretical studies of second harmonic generation for Bi2O2[NO3(OH)]. Materials Research Bulletin, 2012, 47, 2573-2578.	2.7	39
931	First-principles study of Ge dangling bonds with different oxygen backbonds at Ge/GeO2 interface. Journal of Applied Physics, 2012, 111, .	1.1	13
932	Calculation of Infrared/Raman Spectra and Dielectric Properties of Various Crystalline Poly(lactic) Tj ETQq0 0 0 rgBT /Overlock 10 Tf 50 1 116, 1524-1535.	1.2	34
933	Syntheses, Structures, Physical Properties, and Electronic Structures of Ba₂MLnTe₅ (M = Ga and Ln = Sm, Gd, Dy, Er, Y; M = In and Ln = Ce, Nd, Sm, Gd, Dy,) Tj ETQq1 1 0.784314 rgB	1.1	38
934	Electrically tunable band gap in silicene. Physical Review B, 2012, 85, .	1.1	997
935	Theoretical Study of the Electronic Properties of Silicon Nanocrystals Partially Passivated with Cl and F. Journal of Physical Chemistry C, 2012, 116, 3988-3994.	1.5	29

#	Article	IF	Citations
936	Probing Cation and Vacancy Ordering in the Dry and Hydrated Yttrium-Substituted BaSnO₃ Perovskite by NMR Spectroscopy and First Principles Calculations: Implications for Proton Mobility. Journal of the American Chemical Society, 2012, 134, 14483-14498.	6.6	46
937	First-Principles Calculations of Potassium Amidoborane KNH₂BH₃: Structure and ³⁹K NMR Spectroscopy. Journal of Physical Chemistry C, 2012, 116, 20666-20672.	1.5	9
938	MgH₂ in Carbon Scaffolds: A Combined Experimental and Theoretical Investigation. Journal of Physical Chemistry C, 2012, 116, 21139-21147.	1.5	28
939	Probing intermolecular interactions and nitrogen protonation in pharmaceuticals by novel 15N-edited and 2D 14N-1H solid-state NMR. CrystEngComm, 2012, 14, 2654.	1.3	85
940	First principles study of two-dimensional early transition metal carbides. MRS Communications, 2012, 2, 133-137.	0.8	429
941	Recent Advances in Nuclear Shielding Calculations. Annual Reports on NMR Spectroscopy, 2012, 77, 1-80.	0.7	19
942	Non-adiabatic effects during the dissociative adsorption of O₂at Ag(111)? A first-principles divide and conquer study. New Journal of Physics, 2012, 14, 013050.	1.2	48
943	Temperature-Dependent Infrared Spectroscopy Studies of a Novel Antiferroelectric Liquid-Crystalline Thiobenzoate. Journal of Physical Chemistry B, 2012, 116, 11332-11343.	1.2	5
944	Repair and stabilization in confined nanoscale systems â€" inorganic nanowires within single-walled carbon nanotubes. Nano Research, 2012, 5, 833-844.	5.8	12
945	Complex Vibrational Analysis of an Antiferroelectric Liquid Crystal Based on Solid-State Oriented Quantum Chemical Calculations and Experimental Molecular Spectroscopy. Journal of Physical Chemistry A, 2012, 116, 7809-7821.	1.1	10
946	Solution and Solid-State Effects on NMR Chemical Shifts in Sesquiterpene Lactones: NMR, X-ray, and Theoretical Methods. Journal of Physical Chemistry A, 2012, 116, 680-688.	1.1	21
947	Comparative theoretical studies of high pressure effect on polymorph I of 2,2â€²,4,4â€²,6,6â€²-hexanitroazobenzene crystal. Structural Chemistry, 2012, 23, 1631-1642.	1.0	4
948	Interatomic potential to predict the favored and optimized compositions for ternary Cu-Zr-Hf metallic glasses. Journal of Applied Physics, 2012, 112, .	1.1	5
949	Polymorphism in co-crystals: a metastable form of the ionic co-crystal 2 HBzÂ·1 NaBz crystallised by flash evaporation. CrystEngComm, 2012, 14, 6744.	1.3	32
950	Thermodynamically Stable Phases of Carbon at Multiterapascal Pressures. Physical Review Letters, 2012, 108, 045704.	2.9	102
951	MOSFET performance and scalability enhancement by insertion of oxygen layers. , 2012, , .		12
952	Elucidation of the Al/Si Ordering in Gehlenite Ca₂Al₂SiO₇ by Combined ²⁹Si and ²⁷Al NMR Spectroscopy/Quantum Chemical Calculations. Chemistry of Materials, 2012, 24, 4068-4079.	3.2	95
953	Phase stability and superconductivity of strontium under pressure. Applied Physics Letters, 2012, 101, 052604.	1.5	6

#	Article	IF	Citations
954	Band gap engineering by functionalization of BN sheet. Physical Review B, 2012, 85, .	1.1	135
955	Zeolite Structure Direction by Simple Bis(methylimidazolium) Cations: The Effect of the Spacer Length on Structure Direction and of the Imidazolium Ring Orientation on the ¹⁹F NMR Resonances. Journal of the American Chemical Society, 2012, 134, 3845-3856.	6.6	39
956	Nucleation of Rh_n (n = 1â€“5) Clusters on Î³-Al₂O₃ Surfaces: A Density Functional Theory Study. Journal of Physical Chemistry C, 2012, 116, 10623-10631.	1.5	45
957	Persistence and Eventual Demise of Oxygen Molecules at Terapascal Pressures. Physical Review Letters, 2012, 108, 045503.	2.9	55
958	Theoretical aspects of indirect spin-spin couplings. Nuclear Magnetic Resonance, 2012, , 119-147.	0.1	2
959	First-principles investigation of ammonia borane for hydrogen storage. Physica Scripta, 2012, 86, 015606.	1.2	9
960	The electronic structure of RbTiOPO₄and the effects of the A-site cation substitution in KTiOPO₄-family crystals. Journal of Physics Condensed Matter, 2012, 24, 405503.	0.7	32
961	The interaction of iron pyrite with oxygen, nitrogen and nitrogen oxides: a first-principles study. Physical Chemistry Chemical Physics, 2012, 14, 3627.	1.3	27
962	Tetragonal Allotrope of Group 14 Elements. Journal of the American Chemical Society, 2012, 134, 12362-12365.	6.6	170
963	Effect of Indium Doping of Î³-Alumina on the Stabilization of PtSn Alloyed Clusters Prepared by Surface Organostannic Chemistry. Journal of Physical Chemistry C, 2012, 116, 10073-10083.	1.5	25
964	Tailoring microstructure and phase segregation for low friction carbon-based nanocomposite coatings. Journal of Materials Chemistry, 2012, 22, 15782.	6.7	53
965	Lithium Dihydroborate: First-Principles Structure Prediction of LiBH2. Inorganic Chemistry, 2012, 51, 9757-9765.	1.9	13
966	High-pressure studies on azido-tetrazole chainâ€“ring conversion in crystalline 2-azido-4,6-dichloro-1,3,5-triazine. Theoretical Chemistry Accounts, 2012, 131, 1.	0.5	2
967	The bonding in thiolate protected gold nanoparticles from Au4f photoemission core level shifts. Nanoscale, 2012, 4, 4178.	2.8	16
968	The Structure of Benzoquinone Chemisorbed on Pd(111): Simulation of EC-STM Images and HREELS Spectra by Density Functional Theory. Electrocatalysis, 2012, 3, 353-359.	1.5	4
969	Raman Scattering Study on the Phase Transition Dynamics of Ferroelectric Oxides. , 2012, , .		1
970	Where does tight binding go from here?. Physica Status Solidi (B): Basic Research, 2012, 249, 231-236.	0.7	8
971	Boehmite (Î³â€AlOOH) nanoparticles: Hydrothermal synthesis, characterization, pHâ€controlled morphologies, optical properties, and DFT calculations. Physica Status Solidi (B): Basic Research, 2012, 249, 1264-1270.	0.7	52

#	Article	IF	Citations
972	The Zintl Phases Eu3Mg5Si5and Eu3Mg5Ge5. Zeitschrift Fur Anorganische Und Allgemeine Chemie, 2012, 638, 1976-1985.	0.6	10
973	Pressureâ€dependent properties of a multifunctional material: Lithium platinum boride (LiPt₃B). Physica Status Solidi (B): Basic Research, 2012, 249, 1744-1755.	0.7	3
974	Phase transition between cubic and monoclinic polymorphs of the tetracyanoethylene crystal: the role of temperature and kinetics. CrystEngComm, 2012, 14, 4656.	1.3	21
975	Stability of hydrogenation states of graphene and conditions for hydrogen spillover. Physical Review B, 2012, 85, .	1.1	39
976	A Structural and Stability Evaluation of Au₁₂ from an Isolated Cluster to the Deposited Material. Journal of Physical Chemistry C, 2012, 116, 11507-11518.	1.5	28
977	Structure and Properties of Water on the Anatase TiO₂(101) Surface: From Single-Molecule Adsorption to Interface Formation. Journal of Physical Chemistry C, 2012, 116, 11054-11061.	1.5	64
978	Evolution of Structure and of Grafting Properties of Î³-Alumina with Pretreatment Temperature. Journal of Physical Chemistry C, 2012, 116, 834-843.	1.5	37
979	A high connectivity metalâ€“organic framework with exceptional hydrogen and methane uptake capacities. Chemical Science, 2012, 3, 3032.	3.7	75
980	Structure and Dynamics of the Functionalized MOF Type UiO-66(Zr): NMR and Dielectric Relaxation Spectroscopies Coupled with DFT Calculations. Chemistry of Materials, 2012, 24, 2168-2177.	3.2	200
981	Density functional theory study of highâ€pressure effect on crystalline 4,4â€²,6,6â€²â€tetra(azido)hydrazoâ€1,3,5â€triazine. Journal of Computational Chemistry, 2012, 33, 1820-1830.	1.5	10
982	Probing Intermolecular Hydrogen Bonding in Sibenadet Hydrochloride Polymorphs by High-Resolution 1H Double-Quantum Solid-State NMR Spectroscopy. Journal of Pharmaceutical Sciences, 2012, 101, 1821-1830.	1.6	20
983	Solidâ€state ¹¹B and ¹³C NMR, IR, and Xâ€ray crystallographic characterization of selected arylboronic acids and their catechol cyclic esters. Magnetic Resonance in Chemistry, 2012, 50, 388-401.	1.1	30
984	The Question of cis versus trans Configuration in Octahedral Metal Diketonates: An In-Depth Investigation on Diorganobis(4-acyl-5-pyrazolonato)tin(IV) Complexes. European Journal of Inorganic Chemistry, 2012, 2012, 1369-1379.	1.0	12
985	Structural and Electronic Properties of<mml:math xmlns:mml="http://www.w3.org/1998/Math/MathML" display="inline"><mml:mi>T</mml:mi></mml:math>Graphene: A Two-Dimensional Carbon Allotrope with Tetrarings. Physical Review Letters, 2012, 108, 225505.	2.9	377
986	CALYPSO: A method for crystal structure prediction. Computer Physics Communications, 2012, 183, 2063-2070.	3.0	2,085
987	New Twists on the Perovskite Theme: Crystal Structures of the Elusive Phases R and S of NaNbO₃. Inorganic Chemistry, 2012, 51, 6876-6889.	1.9	78
988	Relative strength of phase stabilizers in titanium alloys. Physical Review B, 2012, 85, .	1.1	29
989	New insights into the lattice dynamics ofÎ±-quartz. Zeitschrift FÃ¼r Kristallographie, 2012, 227, 84-91.	1.1	20

#	Article	IF	Citations
990	Solid-State ⁹¹Zr NMR Characterization of Layered and Three-Dimensional Framework Zirconium Phosphates. Journal of Physical Chemistry C, 2012, 116, 17070-17081.	1.5	20
991	Developing a second nearest-neighbor modified embedded atom method interatomic potential for lithium. Modelling and Simulation in Materials Science and Engineering, 2012, 20, 015014.	0.8	56
992	Li5Rb2B7O14: a new congruently melting compound with two kinds of Bâ€“O one-dimensional chains and short UV absorption edge. CrystEngComm, 2012, 14, 6720.	1.3	23
993	High-precision imaging of an encapsulated Lindqvist ion and correlation of its structure and symmetry with quantum chemical calculations. Nanoscale, 2012, 4, 1190.	2.8	11
997	Inorganic Doubleâ€Helix Structures of Unusually Simple Lithiumâ€“Phosphorus Species. Angewandte Chemie - International Edition, 2012, 51, 8330-8333.	7.2	60
998	Direct Detection of Discharge Products in Lithiumâ€“Oxygen Batteries by Solidâ€State NMR Spectroscopy. Angewandte Chemie - International Edition, 2012, 51, 8560-8563.	7.2	75
999	A New Ammine Dualâ€Cation (Li, Mg) Borohydride: Synthesis, Structure, and Dehydrogenation Enhancement. Chemistry - A European Journal, 2012, 18, 6825-6834.	1.7	62
1000	Piezochromism in Nickel Salicylaldoximato Complexes: Tuning Crystalâ€Field Splitting with High Pressure. Chemistry - A European Journal, 2012, 18, 7738-7748.	1.7	33
1001	Bandâ€Edge Electronic Structure of Î²â€In₂S₃: The Role of s or p Orbitals of Atoms at Different Lattice Positions. ChemPhysChem, 2012, 13, 1551-1556.	1.0	33
1002	The Influence of Defects on Moâ€Doped TiO₂ by Firstâ€Principles Studies. ChemPhysChem, 2012, 13, 1514-1521.	1.0	31
1003	Density functional theory study of phase IV of solid hydrogen. Physical Review B, 2012, 85, .	1.1	134
1004	Molecular Dynamics Simulation: From â€œAb Initioâ€•to â€œCoarse Grainedâ€•, 2012, , 195-238.		11
1005	Nature and Structure of Aluminum Surface Sites Grafted on Silica from a Combination of High-Field Aluminum-27 Solid-State NMR Spectroscopy and First-Principles Calculations. Journal of the American Chemical Society, 2012, 134, 6767-6775.	6.6	71
1006	Importance of non linear piezoelectric effect in Wurtzite III-N semiconductors. Optical and Quantum Electronics, 2012, 44, 195-203.	1.5	15
1007	Origin of significant visible-light absorption properties of Mn-doped TiO2 thin films. Acta Materialia, 2012, 60, 1974-1985.	3.8	56
1008	Molecular-level understanding of WGS and reverse WGS reactions on Rh through hierarchical multiscale approach. Chemical Engineering Science, 2012, 74, 296-299.	1.9	35
1009	Lattice contraction of cerium hydrides from first-principles LDAÂ+ÂU calculations. International Journal of Hydrogen Energy, 2012, 37, 5108-5113.	3.8	23
1010	Mapping application performance to HPC architecture. Computer Physics Communications, 2012, 183, 520-529.	3.0	6

#	Article	IF	Citations
1011	Introducing k-point parallelism into VASP. Computer Physics Communications, 2012, 183, 1696-1701.	3.0	33
1012	Terahertz absorption spectra of benzene-1,2-diol, benzene-1,3-diol and benzene-1,4-diol. Chemical Physics Letters, 2012, 525-526, 140-143.	1.2	27
1013	Benchmarks for the 13C NMR chemical shielding tensors in peptides in the solid state. Chemical Physics Letters, 2012, 527, 31-35.	1.2	15
1014	Boron nitride substrate-induced reversible hydrogen storage in bilayer solid matrix via interlayer spacing. International Journal of Hydrogen Energy, 2012, 37, 9677-9687.	3.8	13
1015	Calculating the diffusivity of Cu and Sn in Cu3Sn intermetallic by molecular dynamics simulations. Materials Letters, 2012, 73, 92-94.	1.3	48
1016	Effects of surface structure and Agâ€“Sb nanodots on electronic properties of PbTe (100) facets from first-principles calculations. Scripta Materialia, 2012, 67, 17-20.	2.6	2
1017	Molecular structure refinement by direct fitting of atomic coordinates to experimental ESR spectra. Journal of Magnetic Resonance, 2012, 216, 62-68.	1.2	4
1018	First-principles LDA+U calculations investigating the lattice contraction of face-centered cubic Pu hydrides. Journal of Nuclear Materials, 2012, 424, 183-189.	1.3	26
1019	A theoretical study for thorium monocarbide (ThC). Journal of Nuclear Materials, 2012, 429, 55-69.	1.3	23
1020	A second nearest-neighbor embedded atom method interatomic potential for Liâ€“Si alloys. Journal of Power Sources, 2012, 207, 150-159.	4.0	170
1021	Oxygen adsorption on the Ag/La1â^'xSrxMnO3(001) catalysts surfaces: A first-principles study. Journal of Power Sources, 2012, 209, 158-162.	4.0	15
1022	Synthesis, structure, and electronic structure of CsAgGa2Se4. Journal of Solid State Chemistry, 2012, 186, 54-57.	1.4	6
1023	Exploration on anion ordering, optical properties and electronic structure in K3WO3F3 elpasolite. Journal of Solid State Chemistry, 2012, 187, 159-164.	1.4	95
1024	Li2Sr4B12O23: A new alkali and alkaline-earth metal mixed borate with [B10O18]6â^' network and isolated [B2O5]4â^' unit. Journal of Solid State Chemistry, 2012, 190, 92-97.	1.4	21
1025	Phonon optical modes and electronic properties in diamond nanowires. Microelectronic Engineering, 2012, 90, 92-95.	1.1	10
1026	The near edge structure of cubic boron nitride. Micron, 2012, 43, 43-48.	1.1	19
1027	First principles pseudopotential calculation of electron energy loss near edge structures of lattice imperfections. Micron, 2012, 43, 37-42.	1.1	14
1028	Computation of magnetic shielding to simultaneously validate a crystal structure and assign a solid-state NMR spectrum. Journal of Molecular Structure, 2012, 1015, 192-201.	1.8	22

#	Article	IF	Citations
1029	Investigation on terahertz vibrational modes of crystalline benzoic acid. Optics Communications, 2012, 285, 1593-1598.	1.0	19
1030	Study of the surface segregation of carbon vacancies in. Solid State Communications, 2012, 152, 185-188.	0.9	9
1031	A solid-state NMR study of C70: A model molecule for amorphous carbons. Solid State Nuclear Magnetic Resonance, 2012, 42, 81-86.	1.5	12
1032	Thermal phase transformations in LaGaO3 and LaAlO3 perovskites: An experimental and computational solid-state NMR study. Solid State Nuclear Magnetic Resonance, 2012, 42, 87-97.	1.5	29
1033	ELNES for boron, carbon, and nitrogen K-edges with different chemical environments in layered materials studied by density functional theory. Ultramicroscopy, 2012, 112, 61-68.	0.8	15
1034	Under-coordinated atoms induced local strain, quantum trap depression and valence charge polarization at W stepped surfaces. Physica B: Condensed Matter, 2012, 407, 49-53.	1.3	5
1035	Structural, electronic and vibrational properties of InN under high pressure. Physica B: Condensed Matter, 2012, 407, 1008-1013.	1.3	19
1036	First-principles study of electronic and optical properties of N-doped SrHfO3. Physica B: Condensed Matter, 2012, 407, 2239-2242.	1.3	4
1037	Electronic structure, elastic and thermodynamic properties of Î±-phase Na3N under pressure from first principles. Physica B: Condensed Matter, 2012, 407, 2272-2277.	1.3	7
1038	Emission characteristics of SPAN-80 activated ZnS nanocolloids. Journal of Luminescence, 2012, 132, 2135-2142.	1.5	5
1039	Vibrational averaging of the chemical shift in crystalline Î±â€glycine. Journal of Computational Chemistry, 2012, 33, 1080-1089.	1.5	26
1040	Demonstration of Photoluminescence and Metalâ€Enhanced Fluorescence of Exfoliated MoS₂. ChemPhysChem, 2012, 13, 699-702.	1.0	28
1041	Milling-Induced Disorder of Pharmaceuticals: One-Phase or Two-Phase System?. Journal of Pharmaceutical Sciences, 2012, 101, 1475-1485.	1.6	22
1042	Detailed Reaction Paths for Zeolite Dealumination and Desilication From Density Functional Calculations. Angewandte Chemie - International Edition, 2012, 51, 652-655.	7.2	101
1043	First-Principles Investigations on Structural, Elastic, Electronic, and Optical Properties of Tetragonal HfSiO4. Brazilian Journal of Physics, 2012, 42, 20-27.	0.7	7
1044	Electronic and Lattice Vibrational Properties of Cubic SrHfO3 from First-Principles Calculations. Journal of Electronic Materials, 2012, 41, 535-539.	1.0	7
1045	New insights into oxidation properties and band structure of fluorescein dyes from ab initio calculations. Theoretical Chemistry Accounts, 2012, 131, 1.	0.5	92
1046	Structure of multilayer ZrO2/SrTiO3. Journal of Materials Science, 2012, 47, 1631-1640.	1.7	21

#	Article	IF	Citations
1047	The doping effect of N substituting for different atoms in orthorhombic SrHfO3. Journal of Materials Science, 2012, 47, 3046-3051.	1.7	1
1048	Role of cross section on the stability and electronic structure of Ag-doped ZnO nanowires. Journal of Nanoparticle Research, 2012, 14, 1.	0.8	6
1049	Transformation of the Î¸-phase in Mg-Li-Al alloys: a density functional theory study. Journal of Molecular Modeling, 2012, 18, 1123-1127.	0.8	10
1050	Solid-State ¹⁷O NMR of Pharmaceutical Compounds: Salicylic Acid and Aspirin. Journal of Physical Chemistry B, 2013, 117, 9643-9654.	1.2	56
1051	Absorbing a Little Water: The Structural, Thermodynamic, and Kinetic Relationship between Pyrogallol and Its Tetarto-Hydrate. Crystal Growth and Design, 2013, 13, 4071-4083.	1.4	39
1052	Effect of Ag doping concentration on the electronic and optical properties of anatase TiO2: a DFT-based theoretical study. Research on Chemical Intermediates, 2013, 39, 1633-1644.	1.3	20
1053	Density Functional Theory Models for Radiation Damage. Annual Review of Materials Research, 2013, 43, 35-61.	4.3	101
1054	Probing the Bonding in Nitrogen-Doped Graphene Using Electron Energy Loss Spectroscopy. ACS Nano, 2013, 7, 7145-7150.	7.3	69
1055	Electronic State of Oxidized Nanographene Edge with Atomically Sharp Zigzag Boundaries. ACS Nano, 2013, 7, 6868-6874.	7.3	24
1056	Formation of H₂O₂ on Au₂₀ and Au₁₉Pd Clusters: Understanding the Structure Effect on the Atomic Level. Journal of Physical Chemistry A, 2013, 117, 6817-6826.	1.1	48
1057	Design of Medium Band Gap Agâ€“Biâ€“Nbâ€“O and Agâ€“Biâ€“Taâ€“O Semiconductors for Driving Direct Water Splitting with Visible Light. Inorganic Chemistry, 2013, 52, 9192-9205.	1.9	9
1058	NMR crystallography of sodium diphosphates: combining dipolar, shielding, quadrupolar, diffraction, and computational information. CrystEngComm, 2013, 15, 8727.	1.3	24
1059	A molecular dynamics study of the effects of fast molecular motions on solid-state NMR parameters. CrystEngComm, 2013, 15, 8705.	1.3	77
1060	Influence of tungsten doping concentration on the electronic andÂoptical properties of anatase TiO2. Current Applied Physics, 2013, 13, 1376-1382.	1.1	22
1061	Orientation dependence of elastic constants and electronic properties of rhenium nitrides first-principle calculations. Journal of Materials Science, 2013, 48, 4284-4296.	1.7	6
1062	Synthesis, structure, optical property, and electronic structure of Ba7AgGa5Se15. Journal of Alloys and Compounds, 2013, 565, 115-119.	2.8	7
1063	Recent Advances in Solid-State NMR of Alkaline Earth Elements. Annual Reports on NMR Spectroscopy, 2013, , 129-240.	0.7	33
1064	Precision synthesis of colloidal inorganic nanocrystals using metal and metalloid amides. Nanoscale, 2013, 5, 8398.	2.8	42

#	Article	IF	Citations
1065	An ab initio study on the transition paths from graphite to diamond under pressure. Journal of Physics Condensed Matter, 2013, 25, 145402.	0.7	22
1066	Structural changes in zirconolite under Î±-decay. Journal of Physics Condensed Matter, 2013, 25, 055401.	0.7	4
1067	First-principles study on electronic structures and optical properties of the single-walled (n, 0) ZnO nanotubes. Science China: Physics, Mechanics and Astronomy, 2013, 56, 706-712.	2.0	4
1068	The first-principles study on the mechanical and electronic properties about rim phase and hard phase of Ti(C,N) based cermets. Computational Materials Science, 2013, 79, 417-423.	1.4	18
1069	Interpreting the Disordered Crystal Structure of Sodium Naproxen Tetrahydrate. Crystal Growth and Design, 2013, 13, 3665-3671.	1.4	11
1070	Dynamics of Ag⁺ Ions in RbAg₄I₅ Probed Indirectly via ⁸⁷Rb Solid-State NMR. Journal of Physical Chemistry C, 2013, 117, 9558-9565.	1.5	3
1071	Interfacial Properties of Bilayer and Trilayer Graphene on Metal Substrates. Scientific Reports, 2013, 3, 2081.	1.6	86
1072	First-principles calculations of elastic moduli of Tiâ€“Moâ€“Nb alloys using a cluster-plus-glue-atom model for stable solid solutions. Journal of Materials Science, 2013, 48, 3138-3146.	1.7	11
1073	Recent advances in computational predictions of NMR parameters for the structure elucidation of carbohydrates: methods and limitations. Chemical Society Reviews, 2013, 42, 8376.	18.7	113
1074	Multinuclear Solidâ€State Magnetic Resonance as a Sensitive Probe of Structural Changes upon the Occurrence of Halogen Bonding in Coâ€crystals. Chemistry - A European Journal, 2013, 19, 11949-11962.	1.7	41
1075	Understanding the role of vibrations, exact exchange, and many-body van der Waals interactions in the cohesive properties of molecular crystals. Journal of Chemical Physics, 2013, 139, 024705.	1.2	260
1076	A new strontium antimonateIII Sr5Sb22O38: Synthesis, crystal structure and characterizations. Journal of Solid State Chemistry, 2013, 203, 74-78.	1.4	6
1077	First-principles study on the doping effects of nitrogen on the electronic structure and optical properties of Cu₂O. RSC Advances, 2013, 3, 84-90.	1.7	35
1078	Suppression of thermal conductivity by rattling modes in thermoelectric sodium cobaltate. Nature Materials, 2013, 12, 1028-1032.	13.3	163
1079	Electronic properties of C-substituted boron nanotubes: a first principles study. European Physical Journal B, 2013, 86, 1.	0.6	1
1080	Molecular dynamics investigation of the disordered crystal structure of hexagonal LiBH4. Physical Chemistry Chemical Physics, 2013, 15, 8081.	1.3	18
1081	BaTiO3: Energy, geometrical and electronic structure, relationship between optical constant and density from first-principles calculations. Optical Materials, 2013, 35, 2629-2637.	1.7	69
1082	Ketoconazole Salt and Co-crystals with Enhanced Aqueous Solubility. Crystal Growth and Design, 2013, 13, 4295-4304.	1.4	78

#	Article	IF	Citations
1083	Anharmonic vibrational properties in periodic systems: energy, electron-phonon coupling, and stress. Physical Review B, 2013, 87, .	1.1	151
1085	Understanding the Structure and Electronic Properties of Molecular Crystals Under Pressure: Application of Dispersion Corrected DFT to Oligoacenes. Journal of Physical Chemistry A, 2013, 117, 8323-8331.	1.1	61
1087	An NMR crystallography DFT-D approach to analyse the role of intermolecular hydrogen bonding and Ï€â€“Ï€ interactions in driving cocrystallisation of indomethacin and nicotinamide. CrystEngComm, 2013, 15, 8797.	1.3	70
1088	Electronic properties of rutile TiO2 doped with 4d transition metals: First-principles study. Journal of Alloys and Compounds, 2013, 551, 118-124.	2.8	68
1089	Effects of pressure on PbWO4-III. Physics and Chemistry of Minerals, 2013, 40, 341-348.	0.3	2
1090	Lithium metasilicate and lithium disilicate nanomaterials: optical properties and density functional theory calculations. International Nano Letters, 2013, 3, 1.	2.3	12
1091	Excited-state potential-energy surfaces of metal-adsorbed organic molecules from linear expansion Î”-self-consistent field density-functional theory (Î”SCF-DFT). Journal of Chemical Physics, 2013, 139, 014708.	1.2	34
1092	A Study of Transitionâ€Metal Organometallic Complexes Combining ³⁵Cl Solidâ€State NMR Spectroscopy and ³⁵Clâ€…NQR Spectroscopy and Firstâ€Principles DFT Calculations. Chemistry - A European Journal, 2013, 19, 12396-12414.	1.7	34
1093	Nanostructured Inorganicâ€“Organic Hybrid Semiconductor Materials. , 2013, , 375-415.		2
1094	Lithium Insertion into Titanium Dioxide (Anatase): A Raman Study with ^{16/18}O and ^{6/7}Li Isotope Labeling. Chemistry of Materials, 2013, 25, 3710-3717.	3.2	17
1095	Optical properties of hexagonal boron nanotubes by first-principles calculations. Journal of Applied Physics, 2013, 114, 073514.	1.1	13
1096	Ab-initio study of anisotropic and chemical surface modifications of Î²-SiC nanowires. Journal of Molecular Modeling, 2013, 19, 2043-2048.	0.8	16
1097	Machine-learning approach for one- and two-body corrections to density functional theory: Applications to molecular and condensed water. Physical Review B, 2013, 88, .	1.1	177
1098	Anisotropic effects on the radial breathing mode of silicon nanowires: An ab initio study. Physica E: Low-Dimensional Systems and Nanostructures, 2013, 51, 10-14.	1.3	10
1099	The Electrical Conductivity of Strontium-Barium Niobate. Journal of Electronic Materials, 2013, 42, 1375-1376.	1.0	7
1100	Density functional theory study the effects of point defects in Î²-In2S3. Computational Materials Science, 2013, 73, 139-145.	1.4	14
1101	Synthesis, crystal structure and optical properties of a new beryllium borate, CsBe4(BO3)3. Solid State Sciences, 2013, 18, 105-109.	1.5	13
1102	Synthesis, structural and magnetic characterisation of the fluorinated compound 15R-BaFeO2F. Journal of Solid State Chemistry, 2013, 203, 218-226.	1.4	23

#	Article	IF	Citations
1103	Elastic anisotropy and phonon focusing in NiAl: Atomic study. Intermetallics, 2013, 42, 156-164.	1.8	7
1104	Exchange coupling and magnetic anisotropy at Fe/FePt interfaces. Physical Review B, 2013, 88, .	1.1	31
1105	InÂSituX-Ray Photoelectron Spectroscopy of Model Catalysts: At the Edge of the Gap. Physical Review Letters, 2013, 110, 117601.	2.9	107
1106	Lattice dynamics of Ti-based pnictide superconductors Ba1âˆ'xNaxTi2Sb2O. Physical Review B, 2013, 87, .	1.1	5
1107	Ultra soft pseudo potential investigation of fundamental physical properties of CaXO3 (X=Sn and Hf) distorted perovskites: A reference study to the perfect perovskites. Physica B: Condensed Matter, 2013, 429, 95-105.	1.3	32
1108	Solid-state DFT-assisted Raman study of titaniate nanostructures. Spectrochimica Acta - Part A: Molecular and Biomolecular Spectroscopy, 2013, 116, 646-650.	2.0	13
1109	A combined ultra-wideline solid-state NMR and DFT study of 137Ba electric field gradient tensors in barium compounds. Chemical Physics Letters, 2013, 565, 56-60.	1.2	14
1110	Syntheses, crystal structures, and optical properties of Pb6B3O10X (X=F, Cl, Br). Journal of Solid State Chemistry, 2013, 204, 64-69.	1.4	17
1111	First principles calculations of oxygen vacancy formation in barium-strontium-cobalt-ferrite. RSC Advances, 2013, 3, 12267.	1.7	33
1112	First-principles calculations on Hg-doped anatase TiO2 with and without O vacancy. Solid State Communications, 2013, 165, 15-18.	0.9	10
1113	14N overtone NMR spectra under magic angle spinning: Experiments and numerically exact simulations. Journal of Chemical Physics, 2013, 138, 064201.	1.2	47
1114	Unprecedented Electronâ€Poor Octahedral Ta₆ Clusters in a Solidâ€State Compound: Synthesis, Characterisations and Theoretical Investigations of Cs₂BaTa₆Br₁₅O₃. Chemistry - A European Journal, 2013, 19, 12711-12719.	1.7	14
1115	High thermoelectric performance of oxyselenides: intrinsically low thermal conductivity of Ca-doped BiCuSeO. NPG Asia Materials, 2013, 5, e47-e47.	3.8	349
1116	First principles investigation on the stability, magnetic and electronic properties of the fully and partially hydrogenated BN nanoribbons in different conformers. Journal of Materials Chemistry C, 2013, 1, 6890.	2.7	17
1117	Assignment of the vibrational spectrum of l-cysteine. Chemical Physics, 2013, 424, 75-79.	0.9	56
1118	Hydrogen Sensing with Ni-Doped TiO2 Nanotubes. Sensors, 2013, 13, 8393-8402.	2.1	54
1119	Linear and nonlinear optical properties of Na3La2(BO3)3 crystal. Optics and Laser Technology, 2013, 54, 407-412.	2.2	17
1120	Crystal Structure and Luminescent Properties of Eu3+-Doped A-La2Si2O7Tetragonal Phase Stabilized by Spray Pyrolysis Synthesis. Journal of Physical Chemistry C, 2013, 117, 20876-20886.	1.5	23

#	Article	IF	Citations
1121	Isolated catalyst sites on amorphous supports: A systematic algorithm for understanding heterogeneities in structure and reactivity. Journal of Chemical Physics, 2013, 138, 204105.	1.2	41
1122	Structural and vibrational stability of M and Z phases of silicon and germanium from first principles. Journal of Applied Physics, 2013, 113, .	1.1	14
1123	Optical properties of impact diamonds from the Popigai astrobleme. Diamond and Related Materials, 2013, 37, 8-16.	1.8	24
1124	Tunable Rashba Effect in Two-Dimensional LaOBiS₂ Films: Ultrathin Candidates for Spin Field Effect Transistors. Nano Letters, 2013, 13, 5264-5270.	4.5	100
1125	Structural assessment of anhydrous sulfates with high field 33S solid state NMR and first principles calculations. CrystEngComm, 2013, 15, 8808.	1.3	15
1126	Solid State Complex Chemistry: Formation, Structure, and Properties of Homoleptic Tetracyanamidogermanates RbRE[Ge(CN₂)₄] (RE = La, Pr, Nd, Gd). Inorganic Chemistry, 2013, 52, 12372-12382.	1.9	22
1127	Conductivity of boron-doped polycrystalline diamond films: influence of specific boron defects. European Physical Journal B, 2013, 86, 1.	0.6	55
1128	First-principles investigations of the physical properties of binary uranium silicide alloys. Journal of Nuclear Materials, 2013, 443, 195-199.	1.3	42
1129	Compressed carbon nanotubes: A family of new multifunctional carbon allotropes. Scientific Reports, 2013, 3, 1331.	1.6	80
1130	Variationally localized search direction method for constrained optimization of non-orthogonal, localized orbitals in electronic structure calculations. Journal of Chemical Physics, 2013, 139, 164110.	1.2	2
1131	Energy of Step Defects on the TiO₂ Rutile (110) Surface: An ab initio DFT Methodology. Journal of Physical Chemistry C, 2013, 117, 23766-23780.	1.5	13
1132	Ab initio crystal structure prediction by combining symmetry analysis representations and total energy calculations. An insight into the structure of Mg(BH₄)₂. Physical Chemistry Chemical Physics, 2013, 15, 1471-1480.	1.3	13
1133	Quantum Monte Carlo studies of 13-atom simple metallic clusters. Physical Review B, 2013, 88, .	1.1	19
1134	First-principles energetics of water clusters and ice: A many-body analysis. Journal of Chemical Physics, 2013, 139, 244504.	1.2	34
1135	Tailoring Two Polymorphs of LiFePO4 by Efficient Microwave-Assisted Synthesis: A Combined Experimental and Theoretical Study. Chemistry of Materials, 2013, 25, 3399-3407.	3.2	40
1136	Exploring the structureâ€“composition phase space of lithium borocarbide, LixBC for x â‰¤ 1. RSC Advances, 2013, 3, 10230.	1.7	4
1137	Non-linear piezoelectricity in wurtzite ZnO semiconductors. Nano Energy, 2013, 2, 1214-1217.	8.2	38
1138	Effect of alloying elements on <111> dislocation in NiAl: A first-principles study. Physica B: Condensed Matter, 2013, 417, 9-12.	1.3	10

#	Article	IF	Citations
1139	Modeling CO₂ Adsorption in Zeolites Using DFT-Derived Charges: Comparing System-Specific and Generic Models. Journal of Physical Chemistry C, 2013, 117, 24446-24454.	1.5	21
1140	A Spectroscopic and Diffractometric Study of Polymorphism in Ethyl 3-{3-[((2R)-3-{[2-(2,3-dihydro-1H-inden-2-yl)-1,1-dimethylethyl]amino}-2-hydroxypropyl)oxy]-4,5-difluorophenyl}propanoat Hydrochloride. Crystal Growth and Design, 2013, 13, 5353-5367.	1.4	4
1141	Effect of Ligand Coordination on the Structures and Visible-Light Photocatalytic Activity of Manganese Vanadate Hybrids. Crystal Growth and Design, 2013, 13, 5282-5288.	1.4	29
1142	Luminescence properties of Sm3+-doped TiO2 nanoparticles: Synthesis, characterization, and mechanism. Journal of Alloys and Compounds, 2013, 554, 12-20.	2.8	73
1143	Structural Characterization of Supported Rh^I(CO)₂/β^3-Al₂O₃Catalysts by Periodic DFT Calculations. Journal of Physical Chemistry C, 0, , 130911121850001.	1.5	5
1144	A nanoparticle Mg-doped Li4Ti5O12 for high rate lithium-ion batteries. Electrochimica Acta, 2013, 114, 198-204.	2.6	100
1145	De Novo Determination of the Crystal Structure of a Large Drug Molecule by Crystal Structure Prediction-Based Powder NMR Crystallography. Journal of the American Chemical Society, 2013, 135, 17501-17507.	6.6	173
1146	Oxygen K-edge electron energy loss spectra of hydrous and anhydrous compounds. Journal of Physics Condensed Matter, 2013, 25, 485401.	0.7	10
1147	Photoinduced features of energy bandgap in quaternary Cu₂CdGeS₄crystals. Journal of Physics Condensed Matter, 2013, 25, 505802.	0.7	17
1148	First-principles study of hydronitrogen compounds: Molecular crystalline NH4N3 and N2H5N3. Computational and Theoretical Chemistry, 2013, 1014, 37-42.	1.1	13
1149	Prospects for Fluoride Carbonate Nonlinear Optical Crystals in the UV and Deep-UV Regions. Journal of Physical Chemistry C, 2013, 117, 25684-25692.	1.5	92
1150	Bulk modulus for polar covalent crystals. Scientific Reports, 2013, 3, 3068.	1.6	35
1151	Hydrogen accommodation in Zr second phase particles: Implications for H pick-up and hydriding of Zircaloy-2 and Zircaloy-4. Corrosion Science, 2013, 69, 1-4.	3.0	43
1152	Ab initio study of dielectric function of C-substituted single walled boron nanotubes. European Physical Journal B, 2013, 86, 1.	0.6	1
1153	Dynamic Nuclear Polarization of17O: Direct Polarization. Journal of Physical Chemistry B, 2013, 117, 14894-14906.	1.2	62
1154	Combined Diffraction and Density Functional Theory Calculations of Halogen-Bonded Cocrystal Monolayers. Langmuir, 2013, 29, 14903-14911.	1.6	15
1155	High Energy Density Mixed Polymeric Phase from Carbon Monoxide and Nitrogen. Physical Review Letters, 2013, 111, 235501.	2.9	62
1156	Semiconducting ground-state of three polymorphs of Mg2NiH4 from first-principles calculations. International Journal of Hydrogen Energy, 2013, 38, 16471-16476.	3.8	8

#	Article	IF	Citations
1157	Behaviors and interactions of La atom with other foreign substitutional atoms (Al, Si, Ti, V, Cr, Mn,) Tj ETQq0 0 0 rgBT /Overlock 10 Tf 50 Science, 2013, 73, 120-127.	1.4	14
1158	Electronic structure of lanthanide oxide high K gate oxides. Microelectronic Engineering, 2013, 109, 72-74.	1.1	11
1159	Theoretical predictions of the two-dimensional solid-state NMR spectra: A case study of the 13Câ€“1H correlations in metergoline. Chemical Physics Letters, 2013, 586, 56-60.	1.2	18
1160	First-principles investigations on physical properties of NdN under high pressure. Journal of Physics and Chemistry of Solids, 2013, 74, 1504-1508.	1.9	5
1161	From 1D Chain to 3D Network: A New Family of Inorganicâ€“Organic Hybrid Semiconductors MO₃(L)_x (M = Mo, W; L = Organic Linker) Built on Perovskite-like Structure Modules. Journal of the American Chemical Society, 2013, 135, 17401-17407.	6.6	47
1162	Physical methods and techniques: NMR spectroscopy. Annual Reports on the Progress of Chemistry Section B, 2013, 109, 256.	0.8	5
1163	Mechanism for adsorption, dissociation and diffusion ofÂhydrogen in hydrogen permeation barrier of Î±-Al2O3: AÂdensity functional theory study. International Journal of Hydrogen Energy, 2013, 38, 1157-1165.	3.8	78
1164	Strong Intermolecular Ring Current Influence on ¹H Chemical Shifts in Two Crystalline Forms of Naproxen: a Combined Solid-State NMR and DFT Study. Journal of Physical Chemistry C, 2013, 117, 17731-17740.	1.5	35
1165	Broken Symmetry of an Adsorbed Molecular Switch Determined by Scanning Tunneling Spectroscopy. Angewandte Chemie - International Edition, 2013, 52, 11007-11010.	7.2	12
1166	Development of semi-ab initiointerionic potential for CaO and MgO. Molecular Simulation, 2013, 39, 956-967.	0.9	1
1167	13C chemical-shift anisotropy of alkyl-substituted aromatic carbon in anthracene derivatives. Solid State Nuclear Magnetic Resonance, 2013, 53, 1-12.	1.5	2
1168	Raman spectroscopic study of natural and synthetic brannerite. Journal of Nuclear Materials, 2013, 437, 149-153.	1.3	31
1169	Chemical Activity of Thin Oxide Layers: Strong Interactions with the Support Yield a New Thinâ€Film Phase of ZnO. Angewandte Chemie - International Edition, 2013, 52, 11925-11929.	7.2	158
1170	Simulations of nanocrystals under pressure: Combining electronic enthalpy and linear-scaling density-functional theory. Journal of Chemical Physics, 2013, 139, 084117.	1.2	7
1171	First-principles calculations of the electronic structure and defects of Al2O3. Journal of Applied Physics, 2013, 114, .	1.1	28
1172	Na₈Lu₂(CO₃)₆F₂ and Na₃Lu(CO₃)₂F₂: Rare Earth Fluoride Carbonates as Deep-UV Nonlinear Optical Materials. Chemistry of Materials, 2013, 25, 3147-3153.	3.2	123
1173	Ferromagnetism of V-doped ZnO nanowires. Chinese Physics B, 2013, 22, 027503.	0.7	4
1174	First-principles investigation on the electronic and magnetic properties of cubic Be0.75Mn0.25X (X=S,) Tj ETQq1 1 0.784314 rgBT /Ov	2.8	14

#	Article	IF	Citations
1175	Phonon and magnon Raman scattering in CuB<mml:math xmlns:mml="http://www.w3.org/1998/Math/MathML" display="inline"><mml:msub><mml:mrow /><mml:mn>2</mml:mn></mml:msub></mml:math>O<mml:math xmlns:mml="http://www.w3.org/1998/Math/MathML" display="inline"><mml:msub><mml:mrow /><mml:mn>4</mml:mn></mml:msub></mml:math>. Physical Review B, 2013, 88, .	1.1	10
1176	Electron-beam engineering of single-walled carbon nanotubes from bilayer graphene. Carbon, 2013, 65, 80-86.	5.4	26
1177	First principles selection and design of mid-IR nonlinear optical halide crystals. Journal of Materials Chemistry C, 2013, 1, 7363.	2.7	117
1178	High-pressure structural transformations of Sn up to 138 GPa: Angle-dispersive synchrotron x-ray diffraction study. Physical Review B, 2013, 88, .	1.1	54
1179	A variational method for density functional theory calculations on metallic systems with thousands of atoms. Journal of Chemical Physics, 2013, 139, 054107.	1.2	51
1180	A multinuclear solid state NMR, density functional theory and X-Ray diffraction study of hydrogen bonding in Group I hydrogen dibenzoates. CrystEngComm, 2013, 15, 8823.	1.3	24
1181	Study of the thermal processes in molecular crystals of peptides by means of NMR crystallography. CrystEngComm, 2013, 15, 8680.	1.3	14
1182	NMR crystallography driven structure determination: nanoporous materials. CrystEngComm, 2013, 15, 8613.	1.3	36
1183	Natural bond orbital analysis in the ONETEP code: Applications to large protein systems. Journal of Computational Chemistry, 2013, 34, 429-444.	1.5	27
1184	Noncentrosymmetric Cubic CsCdBO₃ with Bichromophore. European Journal of Inorganic Chemistry, 2013, 2013, 5528-5533.	1.0	22
1185	Adsorption of Sulfurâ€Containing Species on LaCrO₃ (001) Surface: A Firstâ€Principles Study. Fuel Cells, 2013, 13, 1040-1047.	1.5	3
1186	Intermolecular interactions, thermodynamic properties, crystal structure, and detonation performance of HMX/NTO cocrystal explosive. International Journal of Quantum Chemistry, 2013, 113, 1591-1599.	1.0	47
1187	Effective band gap reduction of titanium oxide semiconductors by codoping from first-principles calculations. International Journal of Quantum Chemistry, 2013, 113, 2546-2553.	1.0	14
1188	Experimental and theoretical studies of tetramethoxy-p-benzoquinone: infrared spectra, structural and lithium insertion properties. RSC Advances, 2013, 3, 19081.	1.7	21
1189	Structure and stress of Re(112Ì„1); chiral terraces at a racemic surface. Physical Chemistry Chemical Physics, 2013, 15, 20823.	1.3	2
1190	Triisobutylaluminum: bulkier and yet more reactive towards silica surfaces than triethyl or trimethylaluminum. Dalton Transactions, 2013, 42, 12681.	1.6	35
1191	Theoretical and experimental insights into applicability of solid-state 93Nb NMR in catalysis. Physical Chemistry Chemical Physics, 2013, 15, 5115.	1.3	48
1192	Computational studies on the adsorption of CO₂in the flexible perfluorinated metalâ€“organic framework zinc 1,2-bis(4-pyridyl)ethane tetrafluoroterephthalate. Physical Chemistry Chemical Physics, 2013, 15, 176-182.	1.3	11

#	Article	IF	Citations
1193	Syntheses, crystal and electronic structures, and characterizations of the mixed anions compounds Ba4In2Te2Q5 (Q = S, Se). CrystEngComm, 2013, 15, 4773.	1.3	5
1194	First principles study of Fe in diamond: A diamond-based half metallic dilute magnetic semiconductor. Journal of Applied Physics, 2013, 114, 223703.	1.1	6
1195	LaBeB3O7: a new phase-matchable nonlinear optical crystal exclusively containing the tetrahedral XO4 (X = B and Be) anionic groups. Journal of Materials Chemistry C, 2013, 1, 3616.	2.7	30
1196	Ab initio calculations of the optical absorption spectra of C60-conjugated polymer hybrids. Physical Chemistry Chemical Physics, 2013, 15, 13024.	1.3	17
1197	Pressure-Induced Local Lattice Distortions in Î±-Co[N(CN)₂]₂. Inorganic Chemistry, 2013, 52, 14148-14154.	1.9	8
1198	Identifying Hâ€“N proximities in solid-state NMR using 14N overtone irradiation under fast MAS. CrystEngComm, 2013, 15, 8657.	1.3	46
1199	Single-crystal adsorption calorimetry and density functional theory of CO chemisorption on fcc Co{110}. Physical Chemistry Chemical Physics, 2013, 15, 4059.	1.3	20
1200	Ensemble and ligand effects on the acetylene adsorption on ordered PdxAg1â^'x/Pd(100) surface alloys investigated by periodic DFT study. Physical Chemistry Chemical Physics, 2013, 15, 20345.	1.3	18
1201	CFA-1: the first chiral metalâ€“organic framework containing Kuratowski-type secondary building units. Dalton Transactions, 2013, 42, 10786.	1.6	55
1202	Adsorption structure determination of a large polyaromatic trithiolate on Cu(111): combination of LEED-I(V) and DFT-vdW. Physical Chemistry Chemical Physics, 2013, 15, 11054.	1.3	13
1203	First principle investigations of the physical properties of hydrogen-rich MgH₂. Physica Scripta, 2013, 88, 065704.	1.2	15
1204	First principles studies on the structural, elastic, electronic properties and heats of formation of Mgâ€“AE (AEÂ=ÂCa, Sr, Ba) intermetallics. Intermetallics, 2013, 32, 156-161.	1.8	16
1205	Structural stability, band structure and magnetic properties of ZnS and Zn0.75Cr0.25S under pressure. Journal of Alloys and Compounds, 2013, 549, 184-189.	2.8	13
1206	Validation of binuclear descriptor for mixed transition metal oxide supported electrocatalytic water oxidation. Catalysis Today, 2013, 202, 114-119.	2.2	32
1207	Structure of Li4B2O5: High-temperature monoclinic and low-temperature orthorhombic forms. Journal of Solid State Chemistry, 2013, 197, 466-470.	1.4	17
1208	Synthesis, crystal structures and optical properties of two congruent-melting isotypic diphosphates: LiM3P2O7 (M=Na, K). Journal of Solid State Chemistry, 2013, 197, 128-133.	1.4	55
1209	Raman and infrared spectra of brookite (TiO2): Experiment and theory. Vibrational Spectroscopy, 2013, 64, 148-152.	1.2	98
1210	Interactions of carbonâ€“nitrogen and carbonâ€“nitrogenâ€“vacancy in Î±-Fe from first-principles calculations. Computational Materials Science, 2013, 67, 222-228.	1.4	20

#	Article	IF	Citations
1211	Ab-initio calculation of C and CO adsorption on the Co (110) surface. Surface Science, 2013, 608, 282-291.	0.8	3
1212	NMR crystallography of Î±-poly(l-lactide). Physical Chemistry Chemical Physics, 2013, 15, 3137.	1.3	39
1213	Probing the Bonding and Electronic Structure of Single Atom Dopants in Graphene with Electron Energy Loss Spectroscopy. Nano Letters, 2013, 13, 4989-4995.	4.5	187
1214	Synthesis and Structure Determination of CaSi_{1/3}B_{2/3}O_{8/3}: A New Calcium Borosilicate. Inorganic Chemistry, 2013, 52, 4250-4258.	1.9	31
1215	Comparative studies on total energetics of nonequivalent hexagonal polytypes for group IV semiconductors and group III nitrides. Journal of Materials Research, 2013, 28, 7-16.	1.2	5
1216	Extraordinary Room-Temperature Photoluminescence in Triangular WS₂ Monolayers. Nano Letters, 2013, 13, 3447-3454.	4.5	1,375
1217	The first single-sized (â¼1 nm) and periodically ordered array of In2Te3semiconductor quantum dots self-assembled in solution. Journal of Materials Chemistry A, 2013, 1, 199-202.	5.2	21
1218	Pb2B5O9Cl: a chloride borate with second harmonic generation effect. Journal of Materials Science, 2013, 48, 2590-2596.	1.7	33
1219	Effect of chemical bond parmeters on hardness, isomer shift, and dielectric constant of rare earth ferroborates. Canadian Journal of Chemistry, 2013, 91, 177-180.	0.6	0
1220	Role of covalent hybridization in the martensitic structure and magnetic properties of shape-memory alloys: The case of Ni50Mn5+xGa35-xCu10. Applied Physics Letters, 2013, 102, .	1.5	20
1221	Four Polymorphs of Methyl Paraben: Structural Relationships and Relative Energy Differences. Crystal Growth and Design, 2013, 13, 1206-1217.	1.4	41
1222	M₂Cd₃B₁₆O₂₈ (M = Rb, Cs): Two Isostructural Alkali Cadmium Borates with a New Type of Borate Layer. European Journal of Inorganic Chemistry, 2013, 2013, 203-207.	1.0	28
1223	Ferroelectric behaviour in solid croconic acid using neutron scattering and first-principles density functional theory. Chemical Physics, 2013, 427, 95-100.	0.9	18
1224	Hydrogen solubility in zirconium intermetallic second phase particles. Journal of Nuclear Materials, 2013, 443, 502-506.	1.3	25
1225	First-principles calculations of zinc-blende GeC(001) surfaces. Computational Materials Science, 2013, 69, 121-127.	1.4	3
1226	Facile NOx interconversion over preoxidized Ag(111). Surface Science, 2013, 617, 167-174.	0.8	5
1227	Pb8M(BO3)6 (MÂ=ÂZn, Cd): Two new isostructural lead borates compounds with two-dimensional â^ž[Pb8B6O18]2â^' layer structure. Solid State Sciences, 2013, 15, 73-78.	1.5	10
1228	The comparison of approaches to the solid-state NMR-based structural refinement of vitamin B1 hydrochloride and of its monohydrate. Chemical Physics Letters, 2013, 555, 135-140.	1.2	20

#	Article	IF	Citations
1229	Metal cation-promoted hydrogen generation in activated aluminium borohydride ammoniates. Acta Materialia, 2013, 61, 4787-4796.	3.8	28
1230	Microscopic nature of mobile fluoride anions on sp2 carbon surfaces. Chemical Physics Letters, 2013, 570, 85-89.	1.2	4
1231	Theoretical study on the electronic and optical properties of B-doped zinc-blende GeC. Computational Materials Science, 2013, 71, 33-37.	1.4	5
1232	Inclusion behavior of Cs, Sr, and Ba impurities in LiCl crystal formed by layer-melt crystallization: Combined first-principles calculation and experimental study. Journal of Crystal Growth, 2013, 371, 84-89.	0.7	13
1233	Ab initio calculation of fundamental properties of CaxMg1â^'xA (A=Se and Te) alloys in the rock-salt structure. Physica E: Low-Dimensional Systems and Nanostructures, 2013, 49, 83-91.	1.3	1
1234	A new Sb-based polysulfide: Ba3Sb2S7 containing (S2)2â^' ligand. Journal of Molecular Structure, 2013, 1048, 482-486.	1.8	3
1235	Theoretical ELNES fingerprints of BC2N polytypes. Computational Materials Science, 2013, 68, 335-341.	1.4	1
1236	Ab-initio calculations of synergistic chromiumâ€“nitrogen codoping effects on the electronic and optical properties of anatase TiO2. Vacuum, 2013, 92, 32-38.	1.6	27
1237	Structures of cefradine dihydrate and cefaclor dihydrate from DFT-D calculations. Acta Crystallographica Section C: Crystal Structure Communications, 2013, 69, 1229-1233.	0.4	8
1238	Structure of NaYF₄ Upconverting Nanoparticles: A Multinuclear Solid-State NMR and DFT Computational Study. Journal of Physical Chemistry C, 2013, 117, 25733-25741.	1.5	32
1239	Self-Assembled Molecular Wires and Highly Ordered Monolayer: Thiazole on Ge(100). Journal of Physical Chemistry C, 2013, 117, 19115-19118.	1.5	2
1240	Monolayer MoS<mml:math xmlns:mml="http://www.w3.org/1998/Math/MathML" display="inline"><mml:msub><mml:mrow /><mml:mn>2</mml:mn></mml:msub></mml:math>: Trigonal warping, the<mml:math xmlns:mml="http://www.w3.org/1998/Math/MathML" display="inline"><mml:mi>Î“</mml:mi></mml:math>valley, and spin-orbit coupling effects. Physical Review B, 2013, 88, .	1.1	357
1241	Crystal structure, stability and spectroscopic properties of methane and CO2 hydrates. Journal of Molecular Graphics and Modelling, 2013, 44, 253-265.	1.3	44
1242	Boric acid flux synthesis, structure and magnetic property of MB12O14(OH)10 (M=Mn, Fe, Zn). Journal of Solid State Chemistry, 2013, 201, 29-34.	1.4	11
1243	Exploration of a new compound in the Mâ€“Bâ€“Oâ€“X (M: alkali metals; X: halogen) system: Preparation, crystal and electronic structures, and optical properties of Na3B6O10Br. Inorganica Chimica Acta, 2013, 406, 205-210.	1.2	16
1244	Insights into hydrogen generation from formic acid on PtRuBiOx in aqueous solution at room temperature. International Journal of Hydrogen Energy, 2013, 38, 8720-8731.	3.8	13
1245	Synthesis, crystal structure and optical properties of a new lithium dilead pentaborate, LiPb2B5O10. Journal of Molecular Structure, 2013, 1040, 180-183.	1.8	4
1246	The structure and desorption properties of the ammines of the group II halides. Chemical Physics, 2013, 427, 38-43.	0.9	19

#	Article	IF	Citations
1247	The effect of vanadium impurity on Nickel Î£5(012) grain boundary. Materials Science & Engineering A: Structural Materials: Properties, Microstructure and Processing, 2013, 577, 197-201.	2.6	44
1248	Solidâ€“aqueous equilibrium in the BaSO4â€“RaSO4â€“H2O system: First-principles calculations and a thermodynamic assessment. Geochimica Et Cosmochimica Acta, 2013, 122, 398-417.	1.6	48
1249	Synthesis, crystal structure, optical properties and theoretical calculations of a new potassium lead pentaborate, KPbB5O9. Journal of Molecular Structure, 2013, 1049, 473-478.	1.8	2
1250	First-principles calculations on elastic, electronic and optical properties for the alkaline platinum hydrides A2PtH6 (A=K, Rb and Cs). Materials Science in Semiconductor Processing, 2013, 16, 940-946.	1.9	5
1251	Ln3FeGaQ7: A new series of transition-metal rare-earth chalcogenides. Journal of Solid State Chemistry, 2013, 202, 269-275.	1.4	23
1252	Interaction of methanol with the flexible metal-organic framework MIL-53(Fe) observed by inelastic neutron scattering. Chemical Physics, 2013, 427, 30-37.	0.9	24
1253	Interfacial reaction between Snâ€“Agâ€“Cu solder and Coâ€“P films with various microstructures. Acta Materialia, 2013, 61, 4581-4590.	3.8	57
1254	Electronic and optical properties analysis on Bi/N-codoped anatase TiO2. Solid State Communications, 2013, 163, 7-10.	0.9	13
1255	In situ study of the formation of rhenium borides from the elements atÂhigh-(p, T) conditions: Extreme incompressibility of Re7B3 and formation of new phases. Solid State Sciences, 2013, 25, 85-92.	1.5	6
1256	Adhesion and fracture toughness at Î±-Ti(0001)/TiC(111): A first-principles investigation. Applied Surface Science, 2013, 286, 240-248.	3.1	59
1257	Sr3B6O11F2: a promising polar fluoroborate with short UV absorption edge and moderate second harmonic generation response. Scripta Materialia, 2013, 69, 449-452.	2.6	25
1258	Theoretical investigations on phase stability, elastic constants and electronic structures of D022- and L12-Al3Ti under high pressure. Journal of Alloys and Compounds, 2013, 556, 214-220.	2.8	48
1259	Correlations between the mechanical loss and atomic structure of amorphous TiO2-doped Ta2O5 coatings. Acta Materialia, 2013, 61, 1070-1077.	3.8	42
1260	NbF5 and TaF5: Assignment of 19F NMR resonances and chemical bond analysis from GIPAW calculations. Journal of Solid State Chemistry, 2013, 207, 208-217.	1.4	22
1261	Interactions of foreign interstitial and substitutional atoms in bcc iron from ab initio calculations. Physica B: Condensed Matter, 2013, 417, 57-69.	1.3	13
1262	The visible light absorption property of Cu-doped hydrogen titanate nanotube thin films: An experimental and theoretical study. Physica B: Condensed Matter, 2013, 429, 127-132.	1.3	8
1263	Extremely different structures and vibrational spectra of tetramethylpyrazine nitrate dihydrate in solid and solutions. Journal of Molecular Structure, 2013, 1037, 264-270.	1.8	6
1264	Electronic structure and optical properties of wurtzite-kesterite Cu2ZnSnS4. Physics Letters, Section A: General, Atomic and Solid State Physics, 2013, 377, 417-422.	0.9	31

#	Article	IF	Citations
1265	Structural Study of La_{1â€“x}Y_xScO₃, Combining Neutron Diffraction, Solid-State NMR, and First-Principles DFT Calculations. Journal of Physical Chemistry C, 2013, 117, 2252-2265.	1.5	39
1266	Effect of cation ordering on the electronic and lattice dynamic properties of Ag2CdGeS4 polytypes: First-principle calculation. Journal of Solid State Chemistry, 2013, 201, 48-55.	1.4	6
1267	K2FeGe3Se8: A New Antiferromagnetic Iron Selenide. Inorganic Chemistry, 2013, 52, 2022-2028.	1.9	24
1268	A theoretical study of the dielectric and magnetic responses of Fe-doped Î±-MnO2 based on quantum mechanical calculations. Journal of Materials Chemistry C, 2013, 1, 1990.	2.7	58
1269	Powder crystallography of pharmaceutical materials by combined crystal structure prediction and solid-state 1H NMR spectroscopy. Physical Chemistry Chemical Physics, 2013, 15, 8069.	1.3	155
1270	Structural, elastic, electronic and dynamical properties of Ba2MgWO6 double perovskite under pressure from first principles. European Physical Journal B, 2013, 86, 1.	0.6	19
1271	Seamless and Accurate Modeling of Organic Molecular Materials. Journal of Physical Chemistry Letters, 2013, 4, 1028-1033.	2.1	119
1272	Nitrogen passivation at GaAs:Al2O3 interfaces. Applied Physics Letters, 2013, 102, .	1.5	32
1273	First-principles calculations of electronic and optical properties of lead-free KTa1â^'xNbxO3 under high pressure. Computational Materials Science, 2013, 68, 1-4.	1.4	6
1274	Structural, Spectroscopic, and Electronic Properties of Cubic G0-Rb₂KTiOF₅ Oxyfluoride. Journal of Physical Chemistry C, 2013, 117, 7269-7278.	1.5	38
1275	Synthesis, Structure Characterization, and Optical Properties of the Aluminosilicate Li₂Na₃AlSi₂O₈. Zeitschrift Fur Anorganische Und Allgemeine Chemie, 2013, 639, 779-783.	0.6	6
1276	The stability of alloying additions in Zirconium. Journal of Nuclear Materials, 2013, 437, 122-129.	1.3	43
1277	Coverage- and Temperature-Controlled Isomerization of an Imine Derivative on Au(111). Journal of the American Chemical Society, 2013, 135, 4273-4281.	6.6	25
1278	First-Principles Study of Electronic, Elastic, and Lattice Vibrational Properties of Pbnm Orthorhombic SrHfO3. Journal of Electronic Materials, 2013, 42, 993-998.	1.0	5
1279	Synthesis and First Principles Investigation of HMX/NMP Cocrystal Explosive. Journal of Energetic Materials, 2013, 31, 261-272.	1.0	44
1280	Nature of the electronic band gap in lanthanide oxides. Physical Review B, 2013, 87, .	1.1	182
1281	Water Adsorption and Decomposition on N/V-Doped Anatase TiO₂ (101) Surfaces. Journal of Physical Chemistry C, 2013, 117, 6172-6184.	1.5	24
1282	Metastable Cu(I)-Niobate Semiconductor with a Low-Temperature, Nanoparticle-Mediated Synthesis. ACS Nano, 2013, 7, 1699-1708.	7.3	43

#	Article	IF	Citations
1283	Insights into Propranolol Adsorption on TiO₂: Spectroscopic and Molecular Modeling Study. Journal of Physical Chemistry C, 2013, 117, 5785-5791.	1.5	19
1284	Electrodynamic response and stability of molecular crystals. Physical Review B, 2013, 87, .	1.1	40
1285	{111}-specific twinning structures in nonstoichiometric ZrC_{0.6}with ordered carbon vacancies. Journal of Applied Crystallography, 2013, 46, 43-47.	1.9	15
1286	n-Diamond: Dynamical stability of proposed structures. Diamond and Related Materials, 2013, 34, 60-64.	1.8	12
1287	Probing Hydrogen Bonding in Cocrystals and Amorphous Dispersions Using ¹⁴Nâ€“¹H HMQC Solid-State NMR. Molecular Pharmaceutics, 2013, 10, 999-1007.	2.3	119
1288	Structure and thermodynamic studies of the LaMgNi4 compound and its hydrides by density functional theory. Intermetallics, 2013, 38, 30-35.	1.8	15
1289	Synthesis, Crystal Structure, and Solid-State NMR Investigations of Heteronuclear Zn/Co Coordination Networks â€" A Comparative Study. Inorganic Chemistry, 2013, 52, 4431-4442.	1.9	17
1290	Crystal Chemistry, Band Engineering, and Photocatalytic Activity of the LiNb₃O₈â€“CuNb₃O₈ Solid Solution. Inorganic Chemistry, 2013, 52, 4443-4450.	1.9	62
1291	Correlation between 13C chemical shifts and the halogen bonding environment in a series of solid para-diiodotetrafluorobenzene complexes. CrystEngComm, 2013, 15, 3168.	1.3	63
1292	Molecular Dynamics Simulation of the Solid-State Topochemical Polymerization of S₂N₂. Inorganic Chemistry, 2013, 52, 4648-4657.	1.9	19
1293	DFT+U investigation of the catalytic properties of ferruginous clay. American Mineralogist, 2013, 98, 132-140.	0.9	9
1294	Combined theoretical and experimental analysis of processes determining cathode performance in solid oxide fuel cells. Physical Chemistry Chemical Physics, 2013, 15, 5443.	1.3	240
1295	Atomistic structures and phase transition of In2Se3 nanowires studied by DFT calculations and synchrotron radiation X-ray diffraction. Solid State Communications, 2013, 162, 28-33.	0.9	4
1296	Accommodation of Lattice Mismatch in a Thiol Self-Assembled Monolayer. Journal of Physical Chemistry C, 2013, 117, 4647-4656.	1.5	6
1297	Raman spectroscopy and lattice dynamical calculations of Sc<mml:math xmlns:mml="http://www.w3.org/1998/Math/MathML" display="inline"><mml:msub><mml:mrow /><mml:mn>2</mml:mn></mml:msub></mml:math>O<mml:math xmlns:mml="http://www.w3.org/1998/Math/MathML" display="inline"><mml:msub><mml:mrow /><mml:mn>3</mml:mn></mml:msub></mml:math>single crystals. Physical Review B, 2013, 87, .	1.1	31
1298	ZnWO4/BiOI heterostructures with highly efficient visible light photocatalytic activity: the case of interface lattice and energy level match. Journal of Materials Chemistry A, 2013, 1, 3421.	5.2	153
1299	Complex Polymorphic System of Gallic Acidâ€"Five Monohydrates, Three Anhydrates, and over 20 Solvates. Crystal Growth and Design, 2013, 13, 19-23.	1.4	97
1300	Reply to â€œComment on â€˜Two-Dimensional Boron Monolayer Sheetsâ€™â€•. ACS Nano, 2013, 7, 880-881.	7.3	10

#	Article	IF	Citations
1301	A General Protocol for Determining the Structures of Molecularly Ordered but Noncrystalline Silicate Frameworks. Journal of the American Chemical Society, 2013, 135, 5641-5655.	6.6	70
1302	Electronic structure, optical properties and the mechanism of the B3â€“B8 phase transition of BeSe: insights from hybrid functionals, lattice dynamics andNPHmolecular dynamics. Journal of Physics Condensed Matter, 2013, 25, 125401.	0.7	18
1303	Ba₂Cd(B₃O₆)₂: A Congruentâ€Melting Compound with Isolated B₃O₆ Units. Zeitschrift Fur Anorganische Und Allgemeine Chemie, 2013, 639, 988-993.	0.6	4
1304	Quantum Influences in the Diffusive Motion of Pyrrole on Cu(111). Angewandte Chemie - International Edition, 2013, 52, 5085-5088.	7.2	16
1305	Adsorption of the OH Group on SnO₂(110) Oxygen Bridges: A Molecular Dynamics and Density Functional Theory Study. Journal of Physical Chemistry C, 2013, 117, 9962-9969.	1.5	45
1306	Na₁₁B₂₁O₃₆X₂ (X=Cl, Br): Halogen Sodium Borates with a New Grapheneâ€Like Borate Double Layer. Chemistry - A European Journal, 2013, 19, 7338-7341.	1.7	29
1307	Screened-exchange electronic structures and thermodynamic properties of the cubic perovskite BiAlO3. Physica B: Condensed Matter, 2013, 419, 32-36.	1.3	8
1308	Local instability of<mml:math xmlns:mml="http://www.w3.org/1998/Math/MathML" display="inline"><mml:mi>p</mml:mi></mml:math>-type bonding makes amorphous GeTe a lone-pair semiconductor. Physical Review B, 2013, 87, .	1.1	35
1309	Emergence of Crystal-like Atomic Dynamics in Glasses at the Nanometer Scale. Physical Review Letters, 2013, 110, 185503.	2.9	47
1310	Electronic structure and vibrational properties of KRbAl2B2O7. Materials Research Bulletin, 2013, 48, 929-934.	2.7	31
1311	Band structure and optical transitions in atomic layers of hexagonal gallium chalcogenides. Physical Review B, 2013, 87, .	1.1	181
1312	Decomposition and Terapascal Phases of Water Ice. Physical Review Letters, 2013, 110, 245701.	2.9	70
1313	Optical and energy-loss spectra of ZnS from ab initio molecular dynamics simulation: Temperature effect. Optik, 2013, 124, 5095-5098.	1.4	21
1314	Bandgaps in the deep ultraviolet borate crystals: Prediction and improvement. Applied Physics Letters, 2013, 102, 231904.	1.5	47
1315	A calculating proof on hydrogen bonding in ordinary ice by the first-principles density functional theory. RSC Advances, 2013, 3, 6646.	1.7	9
1316	First principle study on structural, elastic and electronic properties of cubic BiFeO3. Ceramics International, 2013, 39, S283-S286.	2.3	33
1317	Synthesis, structure, and optical properties of the quaternary diamond-like compounds I2â€“IIâ€“IVâ€“VI4 (I=Cu; II=Mg; IV=Si, Ge; VI=S, Se). Journal of Solid State Chemistry, 2013, 204, 251-256.	1.4	40
1318	Hg2Br3I: a new mixed halide nonlinear optical material in the infrared region. CrystEngComm, 2013, 15, 4196.	1.3	24

#	Article	IF	Citations
1319	Phonon probe of local strains in SnSxSe2â^'xmixed crystals. Physical Review B, 2013, 87, .	1.1	37
1320	Theoretical study of structural, elastic, electronic properties, and dispersion of optical functions of hexagonal ZnTiO₃. Physica Status Solidi (B): Basic Research, 2013, 250, 1810-1815.	0.7	14
1321	Nitrogen-rich transition metal nitrides. Coordination Chemistry Reviews, 2013, 257, 2063-2072.	9.5	114
1322	Mobile metal adatoms on single layer, bilayer, and trilayer graphene: Anab initioDFT study with van der Waals corrections correlated with electron microscopy data. Physical Review B, 2013, 87, .	1.1	84
1323	Leakage current in high dielectric oxides: Role of defect-induced energies. Journal of Applied Physics, 2013, 113, 184504.	1.1	10
1324	Computational modelling of inorganic solids. Annual Reports on the Progress of Chemistry Section A, 2013, 109, 421.	0.8	3
1325	Experimental visualization of the Biâ€"O covalency in ferroelectric bismuth ferrite (BiFeO3) by synchrotron X-ray powder diffraction analysis. Physical Chemistry Chemical Physics, 2013, 15, 6779.	1.3	49
1326	NMR crystallography methods to probe complex hydrogen bonding networks: application to structure elucidation of anhydrous quercetin. CrystEngComm, 2013, 15, 4131.	1.3	41
1327	Exploiting the Synergy of Powder X-ray Diffraction and Solid-State NMR Spectroscopy in Structure Determination of Organic Molecular Solids. Journal of Physical Chemistry C, 2013, 117, 12258-12265.	1.5	81
1328	Density functional theory study on the electronic and optical properties of three crystalline phases of BiVO4. Theoretical Chemistry Accounts, 2013, 132, 1.	0.5	51
1329	A Theoretical Study of Water Adsorption and Decomposition on Low-Index Spinel ZnGa2O4 Surfaces: Correlation between Surface Structure and Photocatalytic Properties. Langmuir, 2013, 29, 7025-7037.	1.6	22
1330	Experimental and DFT-D Studies of the Molecular Organic Energetic Material RDX. Journal of Physical Chemistry C, 2013, 117, 8062-8071.	1.5	56
1331	Structural investigation of Î±-LaZr2F11 by coupling X-ray powder diffraction, 19F solid state NMR and DFT calculations. Journal of Solid State Chemistry, 2013, 199, 326-333.	1.4	20
1332	K2Ta4O11 (â€œkalitantiteâ€): a wide band gap semiconductor synthesized in molybdate flux medium. CrystEngComm, 2013, 15, 5539.	1.3	5
1333	Toward Low Friction in High Vacuum for Hydrogenated Diamondlike Carbon by Tailoring Sliding Interface. ACS Applied Materials & Interfaces, 2013, 5, 5889-5893.	4.0	101
1334	Syntheses, Characterization, and Optical Properties of Ternary Baâ€"Snâ€"S System Compounds: Acentric Ba₇Sn₅S₁₅, Centric BaSn₂S₅, and Centric Ba₆Sn₇S₂₀. Inorganic Chemistry, 2013, 52, 273-279.	1.9	56
1335	Raman scattering study of Î±-MgH2 and Î³-MgH2. Solid State Communications, 2013, 154, 77-80.	0.9	13
1336	Multiscale Modeling of Barium Sulfate Formation from BaO. Industrial & Engineering Chemistry Research, 2013, 52, 9086-9098.	1.8	3

#	Article	IF	Citations
1337	Experimental and Theoretical Studies on the Linear and Nonlinear Optical Properties of Bi₂ZnOB₂O₆. Journal of Physical Chemistry C, 2013, 117, 14149-14157.	1.5	54
1338	The Structural, Electronic and Elastic Properties, and the Raman Spectra of Orthorhombic CaSnO ₃ through First Principles Calculations. Chinese Physics Letters, 2013, 30, 077101.	1.3	13
1339	¹⁷O Solid-State NMR as a Sensitive Probe of Hydrogen Bonding in Crystalline and Amorphous Solid Forms of Diflunisal. Molecular Pharmaceutics, 2013, 10, 3433-3446.	2.3	51
1340	Plasmon Absorption of Au-in-CoAl₂O₄ Linear Nanopeapod Chains. Journal of Physical Chemistry C, 2013, 117, 14142-14148.	1.5	20
1341	Influence of Interface Structure on the Properties of ZnO/Graphene Composites: A Theoretical Study by Density Functional Theory Calculations. Journal of Physical Chemistry C, 2013, 117, 10536-10544.	1.5	76
1342	Vacancymediated three-center four-electron bonds in GeTe-Sb<mml:math xmlns:mml="http://www.w3.org/1998/Math/MathML" display="inline"><mml:msub><mml:mrow /><mml:mn>2</mml:mn></mml:msub></mml:math>Te<mml:math xmlns:mml="http://www.w3.org/1998/Math/MathML" display="inline"><mml:msub><mml:mrow /><mml:mn>3</mml:mn></mml:msub></mml:math>phase-change memory alloys. Physical Review B, 2013, 87,.	1.1	76
1343	Spectral assignments and NMR parameterâ€“structure relationships in borates using high-resolution 11B NMR and density functional theory. Physical Chemistry Chemical Physics, 2013, 15, 8208.	1.3	20
1344	Accurate screened exchange band structures for the transition metal monoxides MnO, FeO, CoO and NiO. Journal of Physics Condensed Matter, 2013, 25, 165502.	0.7	66
1345	Simple and accurate determination of Xâ€“H distances under ultra-fast MAS NMR. Journal of Magnetic Resonance, 2013, 233, 56-63.	1.2	59
1346	Flux Growth of Single-Crystal Na₂Ta₄O₁₁ Particles and their Photocatalytic Hydrogen Production. Crystal Growth and Design, 2013, 13, 2322-2326.	1.4	41
1347	Dependence of the elastic properties of the early-transition-metal monoborides on their electronic structures: A density functional theory study. Physica B: Condensed Matter, 2013, 419, 105-111.	1.3	21
1348	Nuclear magnetic resonance predictions for graphenes: concentric finite models and extrapolation to large systems. Physical Chemistry Chemical Physics, 2013, 15, 4634.	1.3	26
1349	High photodegradation efficiency of Rhodamine B catalyzed by bismuth silicate nanoparticles. Catalysis Communications, 2013, 39, 65-69.	1.6	33
1350	Interatomic potential to predict favored composition for Hfâ€“Cuâ€“Ni metallic glasses formation. Journal of Alloys and Compounds, 2013, 552, 55-59.	2.8	6
1351	Hybrid QM/QM simulations of photochemical reactions in the molecular crystal N-salicylidene-2-chloroaniline. Physical Chemistry Chemical Physics, 2013, 15, 10803.	1.3	16
1352	Hybrid QM/QM Simulations of Excited-State Intramolecular Proton Transfer in the Molecular Crystal 7-(2-Pyridyl)-indole. Journal of Chemical Theory and Computation, 2013, 9, 1182-1192.	2.3	13
1353	Ultraâ€Flexible Boronâ€Oxygen 3D Solidâ€State Networks. Advanced Functional Materials, 2013, 23, 5887-5892.	7.8	7
1354	First-principles calculations of electronic and magnetic properties of carbon doped TiO2 clusters. Computational Materials Science, 2013, 68, 127-131.	1.4	6

#	Article	IF	Citations
1355	Electronic, elastic, acoustic and optical properties of cubic TiO2: A DFT approach. Physica B: Condensed Matter, 2013, 420, 74-80.	1.3	14
1356	Doping and compensation in Nb-doped anatase and rutile TiO2. Journal of Applied Physics, 2013, 113, .	1.1	67
1357	Microspheric Na₂Ti₃O₇consisting of tiny nanotubes: an anode material for sodium-ion batteries with ultrafast chargeâ€“discharge rates. Nanoscale, 2013, 5, 594-599.	2.8	167
1358	Synthesis, Crystal Structure, Magnetic Property, and Electronic Structure of Ba₂YbInSe₅. Zeitschrift Fur Anorganische Und Allgemeine Chemie, 2013, 639, 1021-1025.	0.6	5
1359	Effect of contact deformation on contact electrification: a first-principles calculation. Journal Physics D: Applied Physics, 2013, 46, 235304.	1.3	20
1360	Ca-VII: A Chain Ordered Host-Guest Structure of Calcium above 210ÂGPa. Physical Review Letters, 2013, 110, 235501.	2.9	38
1361	Lithiation of silicon via lithium Zintl-defect complexes from first principles. Physical Review B, 2013, 87, .	1.1	22
1362	Site-different structures from dilithium hexaboride (Li2b6) to dimagnesium hexaboride (Mg2B6) by first-principles. Journal of Alloys and Compounds, 2013, 569, 118-125.	2.8	3
1363	Newly synthesized nanolaminate Nb2GeC: Hardness, thermodynamic and optical properties by first-principles method. Computational Materials Science, 2013, 74, 119-123.	1.4	18
1364	Mechanical and optical properties of inverse-perovskites Sc3InX (X=B, C, N). Computational Materials Science, 2013, 73, 1-8.	1.4	13
1365	Electronic and lattice vibrational properties of cubic BaHfO3 from first principles calculations. Physics Letters, Section A: General, Atomic and Solid State Physics, 2013, 377, 927-931.	0.9	14
1366	Unravelling the interplay of crystal structure and electronic band structure of tantalum oxide (Ta₂O₅). Physical Chemistry Chemical Physics, 2013, 15, 1352-1357.	1.3	55
1367	A novel strategy for low-temperature synthesis of Ruddlesdenâ€“Popper type layered perovskite La3Mn2O7+Î´ for methane combustion. Journal of Materials Chemistry A, 2013, 1, 8411.	5.2	18
1368	Resolution of Organic Polymorphic Crystals by Raman Spectroscopy. Journal of Physical Chemistry B, 2013, 117, 7297-7307.	1.2	25
1369	Identifying the Azobenzene/Aniline Reaction Intermediate on TiO₂-(110): A DFT Study. Journal of Physical Chemistry C, 2013, 117, 12591-12599.	1.5	7
1370	Meso-scale modelling of shock wave propagation in a SiC/Al nanocomposite reinforced with WS2-inorganic fullerene nanoparticles. Composite Structures, 2013, 96, 601-605.	3.1	9
1371	Understanding the trends in transition metal sorption by vacancy sites in birnessite. Geochimica Et Cosmochimica Acta, 2013, 101, 222-232.	1.6	90
1372	CdB10O14(OH)4Â·H2O with an unprecedented decaborate fundamental building block. Materials Research Bulletin, 2013, 48, 270-276.	2.7	2

#	Article	IF	Citations
1373	An introduction to the calculation of valence EELS: Quantum mechanical methods for bulk solids. Micron, 2013, 44, 93-100.	1.1	22
1374	Theory studies on the linear and nonlinear optical properties of MnHg(SCN)4 crystal. Optics Communications, 2013, 286, 322-328.	1.0	3
1375	Valence band electronic structure characterization of the rutile TiO2 (110)-(1Ã—2) reconstructed surface. Surface Science, 2013, 608, 92-96.	0.8	19
1376	First-principles calculations of the structural and electronic properties of the cubic CaZrO3 (001) surfaces. Surface Science, 2013, 608, 146-153.	0.8	54
1377	Macroscopic scattering of cracks initiated at single impurity atoms. Nature Communications, 2013, 4, 2441.	5.8	42
1378	Theoretical Investigation of Ge(100) Nitridation by Nitric Oxide: Monomeric or Dimeric Dissociation?. Journal of Physical Chemistry C, 2013, 117, 17111-17118.	1.5	0
1379	MXene: A New Family of Promising Hydrogen Storage Medium. Journal of Physical Chemistry A, 2013, 117, 14253-14260.	1.1	389
1380	Structural Characterization of Magnesium-Based Compounds Mg₉Si₅ and Mg₄Si₃Al (Superconductor) Synthesized under High Pressure and High Temperature Conditions. Inorganic Chemistry, 2013, 52, 3953-3961.	1.9	18
1381	Pressure-induced effects on elastic and mechanical properties of TiC and TiN: A DFT study. Europhysics Letters, 2013, 101, 46002.	0.7	22
1382	BaClBF4: a new noncentrosymmetric pseudo-Aurivillius type material with transparency range from deep UV to middle IR and a high laser damage threshold. Journal of Materials Chemistry C, 2013, 1, 4740.	2.7	36
1383	Synthesis and Optical Properties of Ag(I), Pb(II), and Bi(III) Tantalate-Based Photocatalysts. ACS Catalysis, 2013, 3, 2943-2953.	5.5	45
1384	Two Novel Bi-Based Borate Photocatalysts: Crystal Structure, Electronic Structure, Photoelectrochemical Properties, and Photocatalytic Activity under Simulated Solar Light Irradiation. Journal of Physical Chemistry C, 2013, 117, 22986-22994.	1.5	334
1385	Effect of Molecular Size and Particle Shape on the Terahertz Absorption of a Homologous Series of Tetraalkylammonium Salts. Analytical Chemistry, 2013, 85, 7926-7934.	3.2	14
1386	First-principles calculations of electronic and magnetic properties of CeN: The LDA + U method. Chinese Physics B, 2013, 22, 107102.	0.7	4
1387	Role of Edge Oxygen Atoms on the Adhesive Interaction between Carbon Fiber and Epoxy Resin. Journal of Physical Chemistry C, 2013, 117, 24830-24835.	1.5	60
1388	Ring-Closing Reaction in Diarylethene Captured by Femtosecond Electron Crystallography. Journal of Physical Chemistry B, 2013, 117, 15894-15902.	1.2	79
1389	Electronic structure and optical properties of the nonlinear optical crystal Pb4O(BO3)2 by first-principles calculations. Journal of Solid State Chemistry, 2013, 198, 77-80.	1.4	9
1390	Anisotropic charge screening and supercell size convergence of defect formation energies. Physical Review B, 2013, 87, .	1.1	91

#	Article	IF	Citations
1391	Fluctuant magnetism in metal oxide nanocrystals capped with surfactants. Physical Review B, 2013, 88, .	1.1	10
1392	Selected-control hydrothermal growths of Î±- and Î²-PbO crystals and orientated pressure-induced phase transition. CrystEngComm, 2013, 15, 3513-3516.	1.3	18
1393	First-principles calculations of the structural, electronic, optical and elastic properties of the CuYS2 semiconductor. Journal of Physics Condensed Matter, 2013, 25, 345802.	0.7	18
1394	Water Oxidation on MnOx and IrOx: Why Similar Performance?. Journal of Physical Chemistry C, 2013, 117, 288-292.	1.5	38
1395	Jumping, Rotating, and Flapping: The Atomic-Scale Motion of Thiophene on Cu(111). Journal of Physical Chemistry Letters, 2013, 4, 1953-1958.	2.1	14
1396	Two novel nonlinear optical carbonates in the deep-ultraviolet region: KBeCO3F and RbAlCO3F2. Scientific Reports, 2013, 3, 1366.	1.6	79
1397	Sr₃BeB₆O₁₃: A New Borate in the SrO/BeO/B₂O₃ System with Novel Tri-Six-Membered Ring (BeB₆O₁₅)^{10â€“} Building Block. Inorganic Chemistry, 2013, 52, 6136-6141.	1.9	21
1398	Role of the Anchored Groups in the Bonding and Self-Organization of Macrocycles: Carboxylic versus Pyrrole Groups. Journal of Physical Chemistry C, 2013, 117, 7661-7668.	1.5	8
1399	Silver Exchange of Layered Metal Oxides and Their Photocatalytic Activities. ACS Catalysis, 2013, 3, 2547-2555.	5.5	46
1400	Lattice dynamics of coesite. Journal of Physics Condensed Matter, 2013, 25, 275401.	0.7	3
1401	Structural Characterization and Physical Properties of the New Transition Metal Oxyselenide La₂O₂ZnSe₂. Inorganic Chemistry, 2013, 52, 2078-2085.	1.9	24
1402	ELECTRONIC STRUCTURE AND LINEAR OPTICAL PROPERTIES OF MIXED ALKALI-METAL BOROPHOSPHATES (LiK2BP2O8, Li3K2BP4O14): A FIRST-PRINCIPLES STUDY. Functional Materials Letters, 2013, 06, 1350046.	0.7	0
1403	DFTâ€assisted interpretation of the Raman spectra of hydrogenâ€ordered ice XV. Journal of Raman Spectroscopy, 2013, 44, 290-298.	1.2	51
1404	Analysis of Phase Separation in High Performance PbTeâ€“PbS Thermoelectric Materials. Advanced Functional Materials, 2013, 23, 747-757.	7.8	52
1405	Room temperature single-crystal diffuse scattering andab initiolattice dynamics in CaTiSiO5. Journal of Physics Condensed Matter, 2013, 25, 315402.	0.7	8
1406	Hydrogen Bonding in the Organic Ferroelectric Croconic Acid: Insights from Experiment and First-Principles Modelling. Journal of the Physical Society of Japan, 2013, 82, SA001.	0.7	12
1407	Ab Initio Investigation of Nitride in Comparison with Carbide Phase of Superconducting InX (Xâ€‰=â€‰C, N). , 2013, 2013, 1-9.		14
1408	Cubic perovskite polymorph of strontium metasilicate at high pressures. American Mineralogist, 2013, 98, 2096-2104.	0.9	19

#	Article	IF	Citations
1409	Compression and structure of brucite to 31 GPa from synchrotron X-ray diffraction and infrared spectroscopy studies. American Mineralogist, 2013, 98, 33-40.	0.9	16
1410	First-Principles Calculations of Electronic and Structural Properties of LaN under High Pressure. Applied Mechanics and Materials, 0, 331, 563-566.	0.2	4
1411	A hybrid density functional view of native vacancies in gallium nitride. Journal of Physics Condensed Matter, 2013, 25, 405501.	0.7	22
1412	First-principles study of electronic properties of interfacial atoms in metal-metal contact electrification. Chinese Physics B, 2013, 22, 053403.	0.7	1
1413	First-principles study of Ar adsorptions on the (111) surfaces of Pd, Pt, Cu, and Rh. Chinese Physics B, 2013, 22, 066802.	0.7	3
1414	Classical and quantum ordering of protons in cold solid hydrogen under megabar pressures. Journal of Physics Condensed Matter, 2013, 25, 085402.	0.7	25
1415	Glass-Forming Region of Niâ€“Nbâ€“Ag System and the Corresponding Atomic Configuration Studied by Monte Carlo Simulation. Journal of the Physical Society of Japan, 2013, 82, 124603.	0.7	0
1416	Modelling the Elastic Constants of Cubic Zirconia Using Molecular Dynamics Simulations. Advanced Materials Research, 0, 845, 387-391.	0.3	4
1417	Exploring Pretreatmentâ€“Morphology Relationships: Abâ€…Initio Wulff Construction for RuO₂ Nanoparticles under Oxidising Conditions. ChemCatChem, 2013, 5, 3398-3403.	1.8	29
1418	A complementary experimental and computational study of loxapine succinate and its monohydrate. Acta Crystallographica Section C: Crystal Structure Communications, 2013, 69, 1273-1278.	0.4	5
1419	The interpretation of polycrystalline coherent inelastic neutron scattering from aluminium. Journal of Applied Crystallography, 2013, 46, 1755-1770.	1.9	3
1420	NaRb7(Si4-xGex)2- Soluble Zintl Phases Containing Heteroatomic Tetrahedral Â[Si4-xGex]4-Clusters. European Journal of Inorganic Chemistry, 2013, 2013, 5541-5546.	1.0	9
1421	QMX: A versatile environment for hybrid calculations applied to the grafting of Al₂Cl₃Me₃ on a silica surface. Journal of Computational Chemistry, 2013, 34, 1155-1163.	1.5	1
1422	The influence of neighboring vacancies and their charge state on the atomic migration of LaAlO3. Applied Physics Letters, 2013, 102, 211910.	1.5	6
1423	First-principles study of stability and properties on Î²-SiC/TiC(111) interface. Journal of Applied Physics, 2013, 114, .	1.1	31
1424	Structure, Stoichiometry, and Electrochemical Performance of Li₂CoTi₃O₈ as an Anode Material for Lithiumâ€ion Batteries. ChemPlusChem, 2013, 78, 1530-1535.	1.3	15
1425	Solid-State NMR Analysis of a Boron-Containing Pharmaceutical Hydrochloride Salt. Journal of Pharmaceutical Sciences, 2013, 102, 3705-3716.	1.6	31
1426	Ferromagnetism, adatom effect, and edge reconstruction induced by Klein boundary in graphene nanoribbons. Journal of Applied Physics, 2013, 113, 194302.	1.1	8

#	Article	IF	Citations
1427	Comment on â€œFirst-principles study of the influence of (110)-oriented strain on the ferroelectric properties of rutile TiO<mml:math xmlns:mml="http://www.w3.org/1998/Math/MathML" display="inline"><mml:msub><mml:mrow /><mml:mn>2</mml:mn></mml:msub></mml:math>â€• Physical Review B, 2013, 88, .	1.1	9
1428	Effect of C and H contamination on the MgO surface properties studied using the first-principles method. Journal of Information Display, 2013, 14, 97-102.	2.1	1
1429	Elastic and vibrational properties of group IV semiconductors in empirical potential modelling. Journal of Physics Condensed Matter, 2013, 25, 425801.	0.7	6
1430	Synthesis and Characterization of the First Tetracyanamidogallate. European Journal of Inorganic Chemistry, 2013, 2013, 6091-6096.	1.0	12
1431	Non-linear piezoelectricity in zinc blende GaAs and InAs semiconductors. Journal of Applied Physics, 2013, 114, 073515.	1.1	23
1432	The crystalline structure of the phenazine overlayer physisorbed on a graphite surface. Molecular Physics, 2013, 111, 3823-3830.	0.8	6
1433	Linking molecular level chemistry to macroscopic combustion behavior for nano-energetic materials with halogen containing oxides. Journal of Chemical Physics, 2013, 139, 074701.	1.2	19
1434	Molecular switches from benzene derivatives adsorbed on metal surfaces. Nature Communications, 2013, 4, 2569.	5.8	82
1435	First-principles study of structural phase transitions in CsSnI3. Journal of Applied Physics, 2013, 114, .	1.1	26
1436	Interfacial properties and electronic structure of Î²-SiC(111)/Î±-Ti(0001): A first principle study. Journal of Applied Physics, 2013, 113, .	1.1	28
1437	Measurements of THz absorption peaks in photo-degraded polyethylene and their assignment by quantum chemical calculations. , 2013, , .		2
1438	Quantification of finite-temperature effects on adsorption geometries of<mml:math xmlns:mml="http://www.w3.org/1998/Math/MathML" display="inline"><mml:mi>Ï€</mml:mi></mml:math>-conjugated molecules: Azobenzene/Ag(111). Physical Review B, 2013, 88, .	1.1	43
1439	STRUCTURAL, ELASTIC AND MECHANICAL PROPERTIES OFTMN(TM=Ti,V,Cr): A DFT STUDY. Modern Physics Letters B, 2013, 27, 1350158.	1.0	4
1440	BAND STRUCTURE, HARDNESS, THERMODYNAMIC AND OPTICAL PROPERTIES OF SUPERCONDUCTING Nb₂AsC, Nb₂InC AND Mo₂GaC. International Journal of Computational Materials Science and Engineering, 2013, 02, 1350007.	0.5	28
1441	Site occupation of doping La³⁺cations and phase transition in Na_{0.5}Bi_{0.5}TiO₃-BaTiO₃solid solution. Chinese Physics B, 2013, 22, 036401.	0.7	4
1442	Sulfur vacancies in monolayer MoS2 and its electrical contacts. Applied Physics Letters, 2013, 103, .	1.5	327
1443	Mechanical properties and electronic structures of VC, V₄C₃and V₈C₇from first principles. Physica Scripta, 2013, 88, 015301.	1.2	32
1444	Tensile properties of phase interfaces in Mgâ€”Li alloy: A first principles study. Chinese Physics B, 2013, 22, 126802.	0.7	4

#	Article	IF	Citations
1445	Ab initio studies of disorder in the full Heusler alloy Co2FexMn1â^'xSi. Journal of Applied Physics, 2013, 113, .	1.1	36
1446	A Bipodal Dicyano Anchor Unit for Singleâ€Molecule Spintronic Devices. ChemPhysChem, 2013, 14, 2470-2475.	1.0	7
1447	Identification of new pillared-layered carbon nitride materials at high pressure. Scientific Reports, 2013, 3, 2122.	1.6	15
1448	Understanding the influence of morphology on the terahertz spectra of a powdered ionic crystalline system. , 2013, , .		0
1449	A new cathode material for super-valent battery based on aluminium ion intercalation and deintercalation. Scientific Reports, 2013, 3, 3383.	1.6	286
1450	The transport properties of oxygen vacancy-related polaron-like bound state in HfOx. Scientific Reports, 2013, 3, 3246.	1.6	17
1451	Introduction to carbon-based nanostructures. , 0, , 1-10.		0
1452	Electronic properties of carbon-based nanostructures. , 0, , 11-90.		0
1455	Origin of the visible light absorption of Co²⁺ and <scp>NH</scp>₄⁺ coâ€doped hydrogen titanate nanotube thin films. Physica Status Solidi (B): Basic Research, 2013, 250, 1592-1598.	0.7	6
1457	Phase transition and elastic properties of beryllium sulfide semiconductor under high pressure. EPJ Applied Physics, 2013, 62, 20103.	0.3	4
1458	Computational Modeling of the Size Effects on the Optical Vibrational Modes of H-Terminated Ge Nanostructures. Molecules, 2013, 18, 4776-4785.	1.7	6
1459	An estimation of molecular dynamic behaviour in a liquid using core-loss spectroscopy. Scientific Reports, 2013, 3, 3503.	1.6	19
1460	Applications of Computational Chemistry to Designing Materials and Microstructure in Fuel Cell Technologies. Journal of Computer Chemistry Japan, 2013, 12, 1-7.	0.0	4
1461	Simulation of scanning tunneling microscope image of benzene chemisorbed on a Pd(111) electrode surface by density functional theory. Reports in Electrochemistry, 2013, , 1.	0.3	0
1462	Performance Analysis of Electronic Structure Codes on HPC Systems: A Case Study of SIESTA. PLoS ONE, 2014, 9, e95390.	1.1	13
1463	First-Principles Study of the Structural Stability and Electronic and Elastic Properties of Helium inÎ±-Zirconium. Advances in Condensed Matter Physics, 2014, 2014, 1-8.	0.4	15
1464	Optical Properties of Al- and Zr-Doped Rutile Single Crystals Grown by Tilting-Mirror-Type Floating Zone Method and Study of Structure-Property Relationships by First Principle Calculations. Chinese Journal of Inorganic Chemistry, 2014, 2014, 1-11.	0.2	2
1465	DFT Study of the Electronic Structure of Cubic-SiC Nanopores with a C-Terminated Surface. Journal of Nanomaterials, 2014, 2014, 1-7.	1.5	7

#	Article	IF	Citations
1466	Effect of Nitrogen Impurity on Electronic Properties of Boron Nanotubes. Advances in Condensed Matter Physics, 2014, 2014, 1-8.	0.4	0
1467	Interstellar ice analogs: band strengths of H₂O, CO₂, CH₃OH, and NH₃in the far-infrared region. Astronomy and Astrophysics, 2014, 565, A108.	2.1	25
1468	Density Functional Theory Study of Sulfur Poisoning on Nickel Anode in Solid Oxide Fuel Cells: Effects of Surface and Subsurface Sulfur Atoms. Journal of Chemical Engineering of Japan, 2014, 47, 793-800.	0.3	6
1469	Advanced study of hydrogen storage by substitutional doping of Mn and Ti in Mg2Ni phase. International Journal for Simulation and Multidisciplinary Design Optimization, 2014, 5, A24.	0.6	2
1470	B2 Atomic Disorder in Co2FeXMn1-XSi Heusler Alloys. Journal of the Magnetics Society of Japan, 2014, 38, 50-55.	0.5	7
1471	EELS from organic crystalline materials. Journal of Physics: Conference Series, 2014, 522, 012060.	0.3	5
1472	NMR Studies of Purines. Annual Reports on NMR Spectroscopy, 2014, 82, 59-113.	0.7	14
1473	FIRST-PRINCIPLES INVESTIGATION OF THE ELECTRONIC, ELASTIC AND THERMODYNAMIC PROPERTIES OF SUPERCONDUCTINGMgB₂. International Journal of Modern Physics B, 2014, 28, 1450057.	1.0	4
1474	Elastic and phonon instabilities in simple-cubic heavier alkali metals K, Rb and Cs under hydrostatic pressure studied using ab initio calculations. Modern Physics Letters B, 2014, 28, 1450158.	1.0	1
1475	Electronic structure, elastic and thermal properties of semiconductor GaX (X = N, P, As, Sb) with zinc blende from first-principles calculation. International Journal of Modern Physics B, 2014, 28, 1450183.	1.0	7
1476	²³Na magic-angle spinning and double-rotation NMR study of solid forms of sodium valproate. Canadian Journal of Chemistry, 2014, 92, 9-15.	0.6	13
1477	The electronic structures, Born effective charge tensors, and phonon properties of cubic, tetragonal, orthorhombic, and rhombohedral K_{0.5}Na_{0.5}NbO₃: A first-principles comparative study. Chinese Physics B, 2014, 23, 127102.	0.7	3
1478	Backâ€channelâ€etched thinâ€film transistor using câ€axisâ€aligned crystal Inâ€“Gaâ€“Zn oxide. Journal of the Society for Information Display, 2014, 22, 55-67.	0.8	51
1479	Pressure-Induced Enhancement of Superconductivity and Structural Transition in BiS₂-Layered LaO_{1â^'}_xF_xBiS₂. Journal of the Physical Society of Japan, 2014, 83, 063704.	0.7	111
1480	Correlations between atomic structure and giant magnetoresistance ratio in Co₂(Fe,Mn)Si spin valves. Journal Physics D: Applied Physics, 2014, 47, 322003.	1.3	7
1481	New observations on hydrogen bonding in ice by density functional theory simulations. Chinese Physics B, 2014, 23, 026103.	0.7	8
1482	Adsorptions and diffusions of carbon atoms on the surface and in the subsurface of Co (200): A first-principles density-functional study. Chinese Physics B, 2014, 23, 086802.	0.7	1
1483	Electronic structure and optical properties of Mg x Zn 1â^' x S bulk crystal using first-principles calculations. Chinese Physics B, 2014, 23, 107102.	0.7	3

#	Article	IF	Citations
1484	Automated effective band structures for defective and mismatched supercells. Journal of Physics Condensed Matter, 2014, 26, 485501.	0.7	6
1485	Diffuse scattering in Ih ice. Journal of Physics Condensed Matter, 2014, 26, 265401.	0.7	15
1486	Synthesis of TaC and Ta $$_2$$ 2 C from tantalum and graphite in the laser-heated diamond anvil cell. Science Bulletin, 2014, 59, 5283-5289.	1.7	2
1487	twins in the rolled Mgâ€“Znâ€“Ca alloy with high formability. Journal of Materials Research, 2014, 29, 3024-3031.	1.2	14
1488	Tritium Solubility in Li₂TiO₃ from First-Principles Simulations. Journal of Physical Chemistry C, 2014, 118, 29525-29532.	1.5	33
1489	Tuning the band gap and optical properties of Î³-Si3N4 with rare earth element Ce. RSC Advances, 2014, 4, 55452-55458.	1.7	5
1490	The investigation of dependences of mechanical and electronic properties of TiB₂on pressure using the first-principles method. Physica Scripta, 2014, 89, 115702.	1.2	16
1491	Zirconium metal-based MAX phases Zr₂AC (A =) Tj ETQq1 1 0.784314 rgBT /Overlock 10 Tf 5 International Journal of Modern Physics B, 2014, 28, 1550022.	1.0	41
1493	Structural, elastic, electronic and optical properties of various mineral phases of TiO₂from first-principles calculations. Physica Scripta, 2014, 89, 075703.	1.2	15
1494	Tunable luminescence of Bi³⁺-doped YP_xV_{1 â^' x}O₄(0 â‰¤ Tj ETQq1 1 0.784314 rg	0.7	36
1495	Phase transition trend of calcite on the molecular scale. Phase Transitions, 2014, 87, 1265-1270.	0.6	0
1496	The (√3X√3) R30° sulfur over layer on the iridium(111) surface: A DFT study. , 2014, , .		1
1497	Development of nonlinear optical materials promoted by density functional theory simulations. International Journal of Modern Physics B, 2014, 28, 1430018.	1.0	27
1498	First-principles Prediction for Mechanical and Optical Properties of Al ₃ BC ₃. Chinese Physics Letters, 2014, 31, 066201.	1.3	3
1499	Atomic study of fracture progress ofFe[110]/TMC[100] (TM=Ti,ZrandHf) semi-coherent interfaces. Modern Physics Letters B, 2014, 28, 1450192.	1.0	1
1500	Ab Initio Calculations of the Structural and Electronic Properties of Ca2La3Sb3O14Weberite at Ambient and Elevated Hydrostatic Pressure. ECS Journal of Solid State Science and Technology, 2014, 3, R1-R4.	0.9	5
1501	Temperature Dependence and Martensitic Transformation of Ti₅₀Pt₅₀ Shape Memory Alloys. Advanced Materials Research, 0, 1019, 379-384.	0.3	0
1502	Band gap expansion, shear inversion phase change behaviour and low-voltage induced crystal oscillation in low-dimensional tin selenide crystals. Dalton Transactions, 2014, 43, 7391-7399.	1.6	26

#	Article	IF	Citations
1503	Atomic Study of Semi-Coherent Interfacial Structure at Fe[110]/TMC[001] (TM=V, Nb and Ta) Interfaces. Advanced Materials Research, 2014, 1081, 232-236.	0.3	6
1504	Proton vibrations in 2,4,6-trimethylpyridinium pentachlorophenolate. Chemical Physics Letters, 2014, 608, 289-294.	1.2	0
1505	First-Principles Study of the Mechanical Properties of ScAl Microalloyed by 4d-Transition Metals. Advanced Materials Research, 0, 852, 198-202.	0.3	1
1506	Electronic Structures of S/C-Doped TiO₂Anatase (101) Surface: First-Principles Calculations. International Journal of Photoenergy, 2014, 2014, 1-7.	1.4	1
1507	Observation of high-spin mixed oxidation state of cobalt in ceramic Co3TeO6. Journal of Applied Physics, 2014, 116, .	1.1	21
1508	Does water dope carbon nanotubes?. Journal of Chemical Physics, 2014, 141, 164703.	1.2	14
1509	Study on Multiplet Energies of V²⁺, Cr³⁺, and Mn⁴⁺ in MgO Host Crystal Based on First-Principles Calculations with Consideration of Lattice Relaxation. Journal of the Physical Society of Japan, 2014, 83, 124707.	0.7	19
1510	Hydrogen-bond structure and anharmonicity in croconic acid. Physical Chemistry Chemical Physics, 2014, 16, 26234-26239.	1.3	13
1511	Citrate bridges between mineral platelets in bone. Proceedings of the National Academy of Sciences of the United States of America, 2014, 111, E1354-63.	3.3	234
1512	Validation of molecular crystal structures from powder diffraction data with dispersion-corrected density functional theory (DFT-D). Acta Crystallographica Section B: Structural Science, Crystal Engineering and Materials, 2014, 70, 1020-1032.	0.5	222
1513	Theory of vibrationally assisted tunneling for hydroxyl monomer flipping on Cu(110). Physical Review B, 2014, 90, .	1.1	4
1514	Structural and electronic properties of cubic boron nitride doped with zinc. Journal of Applied Physics, 2014, 116, .	1.1	14
1515	Ultra-high precision determination of site energy differences using a Bayesian method. Physical Review B, 2014, 89, .	1.1	10
1516	Density functional theory and evolution algorithm calculations of elastic properties of AlON. Journal of Applied Physics, 2014, 115, .	1.1	19
1517	Interlayer bonding in compounds with theThCr2Si2-type structure: Insight on the ferromagnetism ofSrCo2(Ge1â^'xPx)2from electronic structure calculations. Physical Review B, 2014, 90, .	1.1	8
1518	Direct imaging of monovacancy-hydrogen complexes in a single graphitic layer. Physical Review B, 2014, 89, .	1.1	44
1519	Martensitic transformation and phase stability of In-doped Ni-Mn-Sn shape memory alloys from first-principles calculations. Journal of Applied Physics, 2014, 115, 203703.	1.1	8
1520	Density functional investigation of intermolecular effects on 13C NMR chemical-shielding tensors modeled with molecular clusters. Journal of Chemical Physics, 2014, 141, 164121.	1.2	53

#	Article	IF	Citations
1521	First-principles investigation of the vacancy effect on the electronic properties in M2AlC(M = V and) Tj ETQq0 0 0 rgBT /Overlock 10 Tf 5	0.6	7
1522	Inelastic incoherent neutron scattering study of the molecular properties of pure hydrogen peroxide and its water mixtures of different concentration. Journal of Chemical Physics, 2014, 140, 164504.	1.2	15
1523	Theoretical study of molecular hydrogen and spiltover hydrogen storage on two-dimensional covalent-organic frameworks. Chinese Physics B, 2014, 23, 067303.	0.7	7
1524	Raman scattering from superhard rhenium diboride under high pressure. Applied Physics Letters, 2014, 104, .	1.5	4
1525	A comprehensive study on crystal structure, thermal behavior, and molecular dynamics of [Sr(DMSO)₄(NO₃)₂]. Journal of Coordination Chemistry, 2014, 67, 3135-3154.	0.8	5
1526	Thermodynamically stable lithium silicides and germanides from density functional theory calculations. Physical Review B, 2014, 90, .	1.1	71
1527	Unraveling Crystalline Structure of High-Pressure Phase of Silicon Carbonate. Physical Review X, 2014, 4, .	2.8	7
1528	Oxygen vacancy defects in Ta2O5 showing long-range atomic re-arrangements. Applied Physics Letters, 2014, 104, .	1.5	42
1529	Incisive Probing of Intermolecular Interactions in Molecular Crystals: Core Level Spectroscopy Combined with Density Functional Theory. Journal of Physical Chemistry B, 2014, 118, 12121-12129.	1.2	28
1530	Orbital resolution of molecules covalently attached to a clean semiconductor surface. Nature Communications, 2014, 5, 3721.	5.8	8
1531	Towards the mechanism of the accelerated corrosion of decorative nickelâ€“chromium coatings in the presence of metals and their salts. Materials and Corrosion - Werkstoffe Und Korrosion, 2014, 65, 959-967.	0.8	7
1532	Dissociative Chemisorption of<mml:math xmlns:mml="http://www.w3.org/1998/Math/MathML" display="inline"><mml:mrow><mml:msub><mml:mrow><mml:mi mathvariant="normal">O</mml:mi></mml:mrow><mml:mrow><mml:mn>2</mml:mn></mml:mrow></mml:msub></mml:mrow></mml Stress Corrosion Cracking in Silicon Crystals. Physical Review Letters, 2014, 112, 115501.	2.9	33
1533	Difference in the structures of alanine triâ€•and tetraâ€peptides with antiparallel Î²â€sheet assessed by Xâ€ray diffraction, solidâ€state NMR and chemical shift calculations by GIPAW. Biopolymers, 2014, 101, 13-20.	1.2	24
1534	Extracting semiconductor band gap zero-point corrections from experimental data. Physical Review B, 2014, 90, .	1.1	20
1535	Stabilizing reconstruction induced by O protrusions of the ZnO (0001) polar surface. RSC Advances, 2014, 4, 54249-54255.	1.7	2
1536	Pressure-induced ferroelastic phase transition in SnO2 from density functional theory. Journal of Chemical Physics, 2014, 140, 164706.	1.2	2
1537	Compression behavior of Sm2Ti2O7-pyrochlore up to 50ÂGPa: single-crystal X-ray diffraction and density functional theory calculations. Science Bulletin, 2014, 59, 5278-5282.	1.7	7
1538	Structural, mechanical, electronic and optical properties of layered ternary nitrides SrZrN 2 and SrHfN 2 : First-principles calculations. Computational Materials Science, 2014, 93, 249-254.	1.4	9

#	Article	IF	Citations
1539	Excitonic effects in oxyhalide scintillating host compounds. Journal of Applied Physics, 2014, 116, 133510.	1.1	7
1540	Investigating the significance of zero-point motion in small molecular clusters of sulphuric acid and water. Journal of Chemical Physics, 2014, 140, 024306.	1.2	2
1541	Framework flexibility and the negative thermal expansion mechanism of copper(I) oxide<mml:math xmlns:mml="http://www.w3.org/1998/Math/MathML"><mml:msub><mml:mi>Cu</mml:mi><mml:mn>2</mml:mn></mml:msub><mml:mathvariant="normal">O</mml:mi></mml:math>. Physical Review B, 2014, 89, .	1.1	34
1542	First-principles calculation on Î²-SiC(111)/Î±-WC(0001) interface. Journal of Applied Physics, 2014, 115, .	1.1	39
1543	Dispersion of the linear and nonlinear optical susceptibilities of the CuAl(S1â^'xSex)2 mixed chalcopyrite compounds. Journal of Applied Physics, 2014, 116, .	1.1	8
1544	Preparation, Structure, and Secondâ€order Nonlinear Optical Properties of a Borateâ€Carboxylic Acid Compound: NH₄B[<scp>dâ€</scp>(+)â€C₄H₄O₅]₂Â·H₂O. Zeitschrift Fur Anorganische Und Allgemeine Chemie, 2014, 640, 140-146.	0.6	3
1545	Accuracy and transferability of Gaussian approximation potential models for tungsten. Physical Review B, 2014, 90, .	1.1	219
1546	Predicting interface structures: From<mml:math xmlns:mml="http://www.w3.org/1998/Math/MathML"><mml:mi mathvariant="normal">SrTiO</mml:mi><mml:msub><mml:mrow /><mml:mn>3</mml:mn></mml:msub></mml:math>to graphene. Physical Review B, 2014, 90, .	1.1	52
1547	Phase stability limit of c-BN under hydrostatic and non-hydrostatic pressure conditions. Journal of Chemical Physics, 2014, 140, 164704.	1.2	9
1548	A new 12L-hexagonal perovskite Cs₄Mg₃CaF₁₂: structural transition derived from the partial substitution of Mg²⁺with Ca²⁺. RSC Advances, 2014, 4, 54194-54198.	1.7	8
1549	Structural, Electronic, and Optical Properties of Eu-Doped BiOX (X = F, Cl, Br, I): A DFT+U Study. Inorganic Chemistry, 2014, 53, 13001-13011.	1.9	117
1550	Slow and Very Fast MAS Solid State NMR Study of Biopolymers. Macromolecular Symposia, 2014, 339, 60-69.	0.4	2
1551	High-temperature Raman spectroscopy of microstructure around the growing Î²-BaB₂O₄crystal in the BaOâ€“B₂O₃â€“Na₂O system. Journal of Applied Crystallography, 2014, 47, 739-744.	1.9	4
1553	The Zintl Phase Cs₇NaSi₈ â€“ From NMR Signal Line Shape Analysis and Quantum Mechanical Calculations to Chemical Bonding. Zeitschrift Fur Anorganische Und Allgemeine Chemie, 2014, 640, 2169-2176.	0.6	8
1554	Local structure of CuxZn2â^'xTiO4 inverse spinel. Applied Physics Letters, 2014, 105, 071911.	1.5	8
1555	Ni-based nanoalloys: Towards thermally stable highly magnetic materials. Journal of Chemical Physics, 2014, 141, 214302.	1.2	7
1556	A Motif for Infinite Metal Atom Wires. Angewandte Chemie - International Edition, 2014, 53, 14087-14091.	7.2	25
1557	First Principles Calculations of the Relative Stability, Structure and Electronic Properties of Two Dimensional Metal Carbides and Nitrides. Key Engineering Materials, 0, 602-603, 527-531.	0.4	24

#	Article	IF	Citations
1558	Temperature effects in first-principles solid state calculations of the chemical shielding tensor made simple. Journal of Chemical Physics, 2014, 141, 134113.	1.2	28
1559	Properties of crystalline Inâ€“Gaâ€“Zn-oxide semiconductor and its transistor characteristics. Japanese Journal of Applied Physics, 2014, 53, 04ED18.	0.8	71
1560	Origin of structural and magnetic transitions in BaFe$_{2-x}$Ru_xAs₂materials. Superconductor Science and Technology, 2014, 27, 122003.	1.8	19
1561	Defect states of transition metal-doped MgO for secondary electron emission of plasma display panel. Journal of Information Display, 2014, 15, 157-161.	2.1	17
1562	Negative-U properties for substitutional Au in Si. Europhysics Letters, 2014, 105, 57006.	0.7	2
1563	A combined experimental-computational study on nitrogen doped Cu₂O as the wide-spectrum absorption material. Journal of Semiconductors, 2014, 35, 103001.	2.0	8
1564	First-Principles Studies on Electronic Structures of ZnO. Advanced Materials Research, 2014, 926-930, 444-447.	0.3	0
1565	Analysis of the electronic structures of 3d transition metals doped CuGaS₂based on DFT calculations. Journal of Semiconductors, 2014, 35, 013002.	2.0	9
1566	First principle calculations of hydrogen sulfide adsorption and dissociation on pure Pd (111) and Au (111), and alloy Pd/Au (111) and Au/Pd (111) surfaces. Journal of Theoretical and Computational Chemistry, 2014, 13, 1450065.	1.8	6
1567	Effect of Nitriding on the Hydrogen Diffusion Coefficient through AISI 4340. Journal of the Electrochemical Society, 2014, 161, C261-C267.	1.3	9
1568	Structural basis for the transformation pathways of the sodium naproxen anhydrateâ€“hydrate system. IUCrJ, 2014, 1, 328-337.	1.0	26
1569	Electrocatalysis - Basic Concepts, Theoretical Treatments in Electrocatalysis via DFT-Based Simulations. , 2014, , 397-402.		0
1570	Terahertz absorption spectra of oxidized polyethylene and their analysis by quantum chemical calculations. Japanese Journal of Applied Physics, 2014, 53, 092402.	0.8	35
1571	Effects of additive elements on structural and electronic properties of Sn-based intermetallics by first principles. Materials Research Express, 2014, 1, 025702.	0.8	10
1572	A theoretical study of the elastic and thermal properties of ScRu compound under pressure. Physica Scripta, 2014, 89, 065702.	1.2	23
1573	Collapse of CuO Double Chains and Suppression of Superconductivity in High-Pressure Phase of YBa₂Cu₄O₈. Journal of the Physical Society of Japan, 2014, 83, 093601.	0.7	10
1574	Comparison of intermolecular interactions in two phases of MeNSOF₂. Zeitschrift Fur Kristallographie - Crystalline Materials, 2014, 229, 649-660.	0.4	1
1575	Characterization and Physicochemical Evaluation of Molecular Complexes Formed Between Umifenovir and Dicarboxylic Acids. Latvian Journal of Chemistry, 2014, 52, 28-40.	0.1	2

#	Article	IF	Citations
1576	Distinguishing tautomerism in the crystal structure of (Z)-N-(5-ethyl-2,3-dihydro-1,3,4-thiadiazol-2-ylidene)-4-methylbenzenesulfonamide using DFT-D calculations and¹³C solid-state NMR. Acta Crystallographica Section C, Structural Chemistry, 2014, 70, 784-789.	0.2	17
1577	Study on Density Functional Theory of Zn_{1-x}Mg_xO Alloy. Applied Mechanics and Materials, 2014, 556-562, 177-180.	0.2	0
1578	INS, IR, RAMAN, 1H NMR and DFT investigations on dynamical properties of l-asparagine. Vibrational Spectroscopy, 2014, 72, 1-7.	1.2	13
1579	First-principles study of CO2 adsorption on KNTN (001) surfaces. Applied Surface Science, 2014, 308, 269-274.	3.1	10
1580	Characterization and first principle study of ball milled Tiâ€“Ni with Mg doping as hydrogen storage alloy. International Journal of Hydrogen Energy, 2014, 39, 9735-9743.	3.8	11
1581	Adsorption of water on the KNTN (001) surface: A density functional theory study. Applied Surface Science, 2014, 298, 102-108.	3.1	6
1582	An investigation on the crystal structures of Ti50Ni50â^'xCux shape memory alloys based on density functional theory calculations. Intermetallics, 2014, 53, 20-25.	1.8	29
1583	NMR parameters in column 13 metal fluoride compounds (AlF3, GaF3, InF3 and TlF) from first principle calculations. Solid State Nuclear Magnetic Resonance, 2014, 59-60, 1-7.	1.5	30
1584	The vibrational and configurational entropy of Î±-brass. Journal of Chemical Thermodynamics, 2014, 71, 126-132.	1.0	5
1585	Thermodynamic stability and electronic structure of Î·-Ni6Nb(Al,Ti) from first principles. Scripta Materialia, 2014, 77, 37-40.	2.6	19
1586	Relation between reactivity and electronic structure for Î±â€²L-, Î²- and Î³-dicalcium silicate: A first-principles study. Cement and Concrete Research, 2014, 57, 28-32.	4.6	59
1587	DFT studies on 7-nitrotetrazolo [1,5]furazano[4,5-b]pyridine 1-oxide: crystal structure, detonation properties, sensitivity and effect of hydrostatic compression. Structural Chemistry, 2014, 25, 239-249.	1.0	4
1588	First-Principles Study of Pressure-Induced Structural and Magnetic Phase Transitions of Binary Ferromagnets: MnSn and MnSb. Journal of Superconductivity and Novel Magnetism, 2014, 27, 1257-1264.	0.8	4
1589	Electronic and magnetic properties of double perovskite Dy2MnCoO6 by first-principles calculation. Journal of Applied Physics, 2014, 115, 17E106.	1.1	4
1590	Structural, mechanical and electronic properties of OsTM and TMOs2 (TM=Ti, Zr and Hf): First-principles calculations. Journal of Alloys and Compounds, 2014, 589, 278-282.	2.8	22
1591	Synthesis, Crystal Structure, and Characterization of a ÂCongruent Melting Compound Magnesium Strontium Diborate MgSrB2O5. Zeitschrift Fur Anorganische Und Allgemeine Chemie, 2014, 640, 1805-1809.	0.6	7
1592	Electronic and optical properties of SrTiO3 under pressure effect: Ab initio study. Solid State Communications, 2014, 189, 32-37.	0.9	14
1593	Density functional theory in the solid state. Philosophical Transactions Series A, Mathematical, Physical, and Engineering Sciences, 2014, 372, 20130270.	1.6	242

#	Article	IF	Citations
1594	Electron-Phonon Coupling and the Metallization of Solid Helium at Terapascal Pressures. Physical Review Letters, 2014, 112, 055504.	2.9	64
1595	The role of dipole moment in determining the nonlinear optical behavior of materials: ab initio studies on quaternary molybdenum tellurite crystals. Journal of Materials Chemistry C, 2014, 2, 530-537.	2.7	81
1596	Phase transition and elasticity of enstatite under pressure from experiments and first-principles studies. Physics of the Earth and Planetary Interiors, 2014, 228, 63-74.	0.7	23
1597	Electronic structures of Hg-doped anatase TiO2 with different O vacancy concentrations. Materials Science-Poland, 2014, 32, 93-97.	0.4	1
1598	First-principles study on transition metal-doped anatase TiO2. Nanoscale Research Letters, 2014, 9, 46.	3.1	177
1599	Quantum chemical calculations of pristine and modified crystalline cellulose surfaces: benchmarking interactions and adsorption of water and electrolyte. Cellulose, 2014, 21, 71-86.	2.4	9
1600	Pb3B6O11F2: the first non-centrosymmetric lead borate fluoride with a large second harmonic generation response. Journal of Materials Chemistry C, 2014, 2, 1704.	2.7	55
1601	First-principles studies of the structural, electronic, and optical properties of a novel thorium compound Rb2Th7Se15. Journal of Solid State Chemistry, 2014, 212, 37-41.	1.4	0
1602	A novel Bi-based phosphomolybdate photocatalyst K2Bi(PO4)(MoO4): Crystal structure, electronic structure and photocatalytic activity. Materials Research Bulletin, 2014, 51, 455-459.	2.7	20
1603	Site preference and alloying effect on elastic properties of ternary B2ÂRuAl-based alloys. Intermetallics, 2014, 51, 24-29.	1.8	21
1604	Analytical Transmission Electron Microscopy. Reviews in Mineralogy and Geochemistry, 2014, 78, 219-269.	2.2	17
1605	Synthesis, structure, and characterization of a new rubidium cadmium borate: RbCdB3O6. Journal of Alloys and Compounds, 2014, 588, 514-518.	2.8	8
1606	Chlorodiethylaluminum supported on silica: A dinuclear aluminum surface species with bridging Î¼2-Cl-ligand as a highly efficient co-catalyst for the Ni-catalyzed dimerization of ethene. Journal of Catalysis, 2014, 313, 46-54.	3.1	43
1607	Superconducting Double Perovskite Bismuth Oxide Prepared by a Lowâ€Temperature Hydrothermal Reaction. Angewandte Chemie - International Edition, 2014, 53, 3599-3603.	7.2	61
1608	On the Formation of Droperidol Solvates: Characterization of Structure and Properties. Crystal Growth and Design, 2014, 14, 2654-2664.	1.4	61
1609	Characterization of magnetic properties of<mml:math xmlns:mml="http://www.w3.org/1998/Math/MathML"><mml:msub><mml:mrow><mml:mi>Sr</mml:mi></mml:mrow><mml:mn>2</mml:mn> xmlns:mml="http://www.w3.org/1998/Math/MathML"><mml:msub><mml:mrow><mml:mi>CuWO</mml:mi></mml:mrow><mml:mn> xmlns:mml="http://www.w3.org/1998/Math/MathML"><mml:msub><mml:mrow><mml:mi>Sr</mml:mi></mml:mrow><mml:mn>2</mml:mn> xmlns:mml="http://www.w3.org/1998/Math/MathML"><mml:msub><mml:mrow><mml:mi>Ti</mml:mi></mml:mrow><mml:mn> Physical Review B, 2014, 89, .	1.1	35
1610	Ab initio studies of 1,3,5,7-tetranitro-1,3,5,7-tetrazocine/1,3-dimethyl-2-imidazolidinone cocrystal under high pressure using dispersion corrected density functional theory. Journal of Applied Physics, 2014, 115, .	1.1	24
1611	Specific features of the electronic structure of a novel ternary Tl3PbI5 optoelectronic material. Physical Chemistry Chemical Physics, 2014, 16, 12838.	1.3	21

#	Article	IF	Citations
1612	Density functional theory studies of electronic properties of PdAg/Pd surface alloys. Applied Surface Science, 2014, 288, 69-75.	3.1	12
1613	Calculation of metallic and insulating phases of V2O3 by hybrid density functionals. Journal of Chemical Physics, 2014, 140, 054702.	1.2	24
1614	TiO₂ Nanotube Arrays Modified with Crâ€Doped SrTiO₃ Nanocubes for Highly Efficient Hydrogen Evolution under Visible Light. Chemistry - A European Journal, 2014, 20, 2654-2662.	1.7	45
1615	{111} twinning structure and interfacial energy in nonstoichiometric TiCx with ordered carbon vacancies. Materials Characterization, 2014, 90, 94-98.	1.9	16
1616	Reactions of xenon with iron and nickel are predicted in the Earth's inner core. Nature Chemistry, 2014, 6, 644-648.	6.6	369
1617	Proton transfer and hydrogen bonding in the organic solid state: a combined XRD/XPS/ssNMR study of 17 organic acidâ€“base complexes. Physical Chemistry Chemical Physics, 2014, 16, 1150-1160.	1.3	153
1618	Solid-state NMR/NQR and first-principles study of two niobium halide cluster compounds. Solid State Nuclear Magnetic Resonance, 2014, 59-60, 20-30.	1.5	6
1619	Synthesis, structures, optical properties and electronic structures of two mixed metal borates MBaB5O9 (M=Na, K). Journal of Alloys and Compounds, 2014, 585, 602-607.	2.8	22
1620	Mapping functional groups on oxidised multi-walled carbon nanotubes at the nanometre scale. Chemical Communications, 2014, 50, 6744-6747.	2.2	12
1621	New Perovskite-Related Structure Family of Oxide-Ion Conducting Materials NdBaInO₄. Chemistry of Materials, 2014, 26, 2488-2491.	3.2	102
1622	First-principles studies on (001) surface electronic bonding and magnetic properties of ZnCMn3 and ZnNMn3 intermetallic antiperovskites type compounds. Journal of Alloys and Compounds, 2014, 586, 230-238.	2.8	2
1623	Theoretical Investigations of the Electronic, Elastic, Thermodynamics Properties and the Superconducting Transition Temperature of MNiBN (M = La, Ca). Journal of Superconductivity and Novel Magnetism, 2014, 27, 1671-1676.	0.8	2
1624	A DFT study on carbon monoxide adsorption onto hydroxylated Î±-Al₂O₃(0001) surfaces. Physical Chemistry Chemical Physics, 2014, 16, 14287-14297.	1.3	13
1625	Theoretical approach to the phonon modes and specific heat of germanium nanowires. Physica B: Condensed Matter, 2014, 453, 14-18.	1.3	2
1626	Reactivity of the calciteâ€“water-interface, from molecular scale processes to geochemical engineering. Applied Geochemistry, 2014, 45, 158-190.	1.4	90
1627	SHG Materials SnGa₄Q₇ (Q = S, Se) Appearing with Large Conversion Efficiencies, High Damage Thresholds, and Wide Transparencies in the Mid-Infrared Region. Chemistry of Materials, 2014, 26, 2743-2749.	3.2	118
1628	Dielectric response of pentagonal defects in multilayer graphene nano-cones. Nanoscale, 2014, 6, 1833-1839.	2.8	6
1629	A Nitrate Nonlinear Optical Crystal Pb₁₆(OH)₁₆(NO₃)₁₆ with a Large Second-Harmonic Generation Response. Inorganic Chemistry, 2014, 53, 3320-3325.	1.9	55

#	Article	IF	Citations
1630	Copper-Organic/Octamolybdates: Structures, Bandgap Sizes, and Photocatalytic Activities. Inorganic Chemistry, 2014, 53, 3464-3470.	1.9	35
1631	Cation-exchanged SAPO-34 for adsorption-based hydrocarbon separations: predictions from dispersion-corrected DFT calculations. Physical Chemistry Chemical Physics, 2014, 16, 21062-21072.	1.3	14
1632	Porous M^{II}/Pyrimidineâ€4,6â€Dicarboxylato Neutral Frameworks: Synthetic Influence on the Adsorption Capacity and Evaluation of CO₂â€Adsorbent Interactions. Chemistry - A European Journal, 2014, 20, 1554-1568.	1.7	22
1633	The optical properties of lead-free KTa1/2Nb1/2O3:M where M=Li, Na, H, Cu, Zn. Computational Materials Science, 2014, 83, 294-297.	1.4	5
1634	Theoretical study of the thermodynamic properties of cubic Zr3N4 and Hf3N4 under high pressures. Journal of Alloys and Compounds, 2014, 608, 90-94.	2.8	7
1635	Theoretical insight into the structural, elastic and electronic properties of N4H4 compounds. Computational Materials Science, 2014, 81, 582-586.	1.4	6
1636	Doping of ZnO nanowires using phosphorus diffusion from a spin-on doped glass source. Journal of Applied Physics, 2014, 115, 194302.	1.1	2
1637	Potential enhancement of superconductivity in MgB2 nanosheets: First-principles calculations. Chemical Physics Letters, 2014, 591, 185-188.	1.2	7
1638	First-principles study of the structural, elastic, and optical properties for Sr _{0.5} Ca _{0.5} TiO ₃. Chinese Physics B, 2014, 23, 026301.	0.7	5
1639	Infrared Spectroscopy of Ammonia on Iron: Thermal Stability and the Influence of Potassium. Journal of Physical Chemistry C, 2014, 118, 12184-12194.	1.5	9
1640	Contrasting Polymorphism of Related Small Molecule Drugs Correlated and Guided by the Computed Crystal Energy Landscape. Crystal Growth and Design, 2014, 14, 2056-2072.	1.4	72
1641	A first-principles study of As doping at a disordered Siâ€“SiO2interface. Journal of Physics Condensed Matter, 2014, 26, 055002.	0.7	3
1642	Joint experimental and computational 17O solid state NMR study of Brownmillerite Ba2In2O5. Physical Chemistry Chemical Physics, 2014, 16, 2597.	1.3	7
1643	Recent NMR developments applied to organicâ€“inorganic materials. Progress in Nuclear Magnetic Resonance Spectroscopy, 2014, 77, 1-48.	3.9	78
1644	Revised electronic structure, Raman and IR studies of AB2H2and ABCH (A = Sr, Ba; B = Al, Ga; C = Si, Ge) phases. RSC Advances, 2014, 4, 22-31.	1.7	2
1645	Band Gap Engineering and Layer-by-Layer Mapping of Selenium-Doped Molybdenum Disulfide. Nano Letters, 2014, 14, 442-449.	4.5	463
1646	Effect of trivalent dopants on local coordination and electronic structure in crystalline and amorphous ZnO. Thin Solid Films, 2014, 555, 117-121.	0.8	10
1647	Light Emission in Waterâ€Containing Cocrystals: the Influence of Water Molecules on the Fluorescence Properties of a Schiffâ€Base Molecule. Chemistry - an Asian Journal, 2014, 9, 223-228.	1.7	4

#	Article	IF	Citations
1648	An ab initio molecular dynamics study on the structural and electronic properties of AlB2, TiB2 and (Alx,Ti(1â^'x))B2 in Alâ€"Tiâ€"B master alloys. Journal of Alloys and Compounds, 2014, 585, 529-534.	2.8	13
1649	Origin of anisotropy of the near band gap absorption in Tl4HgBr6 single crystals. Journal of Materials Chemistry C, 2014, 2, 2779.	2.7	7
1650	First-principles investigation of half-metallic ferromagnetism of half-Heusler compounds XYZ. Journal of Magnetism and Magnetic Materials, 2014, 351, 92-97.	1.0	48
1651	Z-scan analysis and ab initio studies of Î²-BaTeMo2O9 single crystal. Solid State Sciences, 2014, 27, 30-35.	1.5	20
1652	Structural, elastic, electronic and optical properties of the newly synthesized monoclinic Zintl phase BaIn2P2. Solid State Sciences, 2014, 29, 12-23.	1.5	54
1653	The orbital minimization method for electronic structure calculations with finite-range atomic basis sets. Computer Physics Communications, 2014, 185, 873-883.	3.0	20
1654	Recent Advances in Solid-State 67Zn NMR Studies. Annual Reports on NMR Spectroscopy, 2014, 81, 1-46.	0.7	16
1655	Structure determination of the theophyllineâ€"nicotinamide cocrystal: a combined powder XRD, 1D solid-state NMR, and theoretical calculation study. CrystEngComm, 2014, 16, 3141-3147.	1.3	49
1656	Revealing lithiumâ€"silicide phase transformations in nano-structured silicon-based lithium ion batteries via in situ NMR spectroscopy. Nature Communications, 2014, 5, 3217.	5.8	332
1657	Strong band hybridization between silicene and Ag(111) substrate. Physica E: Low-Dimensional Systems and Nanostructures, 2014, 58, 38-42.	1.3	43
1658	Elastic and electronic properties of Pbca-BN: First-principles calculations. Computational Materials Science, 2014, 85, 80-87.	1.4	114
1659	Theoretical study of structural, elastic and thermodynamic properties of CZTX (X=S and Se) alloys. Journal of Alloys and Compounds, 2014, 589, 137-142.	2.8	19
1660	Hanoi Tower-like Multilayered Ultrathin Palladium Nanosheets. Nano Letters, 2014, 14, 7188-7194.	4.5	122
1661	Electronic structures of halogen-doped Cu ₂ O based on DFT calculations. Chinese Physics B, 2014, 23, 017401.	0.7	8
1662	Synthesis and photocatalytic properties of U<inf>3</inf>O<inf>8</inf>-type complex oxides Ag<inf>2</inf>M<inf>4</inf>O<inf>11</inf> (M = Nb, Ta). , 2014, , .		0
1663	Insight into the effects of surface oxidation and carbonization on the electronic properties of silicon quantum dots and silicon slabs: a density functional study. RSC Advances, 2014, 4, 60948-60952.	1.7	3
1664	Long- and Short-Range Constraints for the Structure Determination of Layered Silicates with Stacking Disorder. Chemistry of Materials, 2014, 26, 6994-7008.	3.2	24
1665	INS, DFT and temperature dependent IR investigations of dynamical properties of low temperature phase of choline chloride. Chemical Physics, 2014, 445, 31-37.	0.9	11

#	Article	IF	Citations
1666	Alloy Negative Electrodes for Li-Ion Batteries. Chemical Reviews, 2014, 114, 11444-11502.	23.0	1,675
1667	The Local Atomic Structures of Liquid CO at 3.6â€…GPa and Polymerized CO at 0 to 30â€…GPa from Highâ€Pressure Pair Distribution Function Analysis. Chemistry - A European Journal, 2014, 20, 11531-11539.	1.7	17
1668	Thermodynamics and density functional theory study of potassium dichromate interaction with galena. International Journal of Minerals, Metallurgy and Materials, 2014, 21, 947-954.	2.4	6
1669	Ferroelectric switching in epitaxial GeTe films. APL Materials, 2014, 2, .	2.2	67
1670	Quantum-size effect on the electronic and optical properties of hybrid TiO2/Au clusters. Journal of Chemical Physics, 2014, 141, 054301.	1.2	1
1671	Condensation of gold vapour on silicone oil â€“ effect of the liquid substrate. Philosophical Magazine, 2014, 94, 1967-1981.	0.7	3
1672	Communication: On the stability of ice 0, ice i, and Ih. Journal of Chemical Physics, 2014, 141, 161102.	1.2	25
1673	Relativistic nuclear magnetic resonance J-coupling with ultrasoft pseudopotentials and the zeroth-order regular approximation. Journal of Chemical Physics, 2014, 140, 234106.	1.2	35
1674	Interatomic potential to predict the glass-forming ability of Niâ€“Nbâ€“Mo ternary alloys. Journal of Materials Science, 2014, 49, 7263-7272.	1.7	4
1675	Fragment-Based Electronic Structure Approach for Computing Nuclear Magnetic Resonance Chemical Shifts in Molecular Crystals. Journal of Chemical Theory and Computation, 2014, 10, 4862-4872.	2.3	48
1676	First Principle Assisted Prediction of the Birefringence Values of Functional Inorganic Borate Materials. Journal of Physical Chemistry C, 2014, 118, 25651-25657.	1.5	67
1677	Tunable Cobalt Vacancies and Related Properties in LaCo_xAs₂. Chemistry of Materials, 2014, 26, 6221-6225.	3.2	15
1678	Assessing the performance of density functional theory in optimizing molecular crystal structure parameters. Acta Crystallographica Section B: Structural Science, Crystal Engineering and Materials, 2014, 70, 259-267.	0.5	28
1679	Electronic structure and magnetic properties of substitutional transition-metal atoms in GaN nanotubes. Chinese Physics B, 2014, 23, 017301.	0.7	14
1680	Raman Spectra of Monolayer, Few-Layer, and Bulk ReSe₂: An Anisotropic Layered Semiconductor. ACS Nano, 2014, 8, 11154-11164.	7.3	296
1681	The influence of hydrogen bonding on the nonlinear optical properties of a semiorganic material NH₄B[<scp>d</scp>-(+)-C₄H₄O₅]₂Â·H₂O: a theoretical perspective. Physical Chemistry Chemical Physics, 2014, 16, 20089.	1.6	17
1682	Câ€“H activation and metalation at electrode surfaces: 2,3-dimethyl-1,4-dihydroxybenzene on Pd(pc) and Pd(111) studied by TLE, HREELS and DFT. Dalton Transactions, 2014, 43, 14798-14805.	1.6	0
1683	First-principles investigations on the adsorption and diffusion of carbon atoms on the surface and in the subsurface of Co (111) related to the growth of graphene. RSC Advances, 2014, 4, 34237.	1.7	7

#	Article	IF	Citations
1684	O-vs. N-protonation of 1-dimethylaminonaphthalene-8-ketones: formation of aperiNâ€“C bond or a hydrogen bond to the pi-electron density of a carbonyl group. CrystEngComm, 2014, 16, 8363-8374.	1.3	15
1685	Calcium-43 chemical shift and electric field gradient tensor interplay: a sensitive probe of structure, polymorphism, and hydration. Physical Chemistry Chemical Physics, 2014, 16, 13340-13359.	1.3	22
1686	Choosing a proper exchangeâ€“correlation functional for the computational catalysis on surface. Physical Chemistry Chemical Physics, 2014, 16, 18563-18569.	1.3	21
1687	Spectroscopic study and electronic structure of prototypical iron porphyrins and their Î¼-oxo-dimer derivatives with different functional configurations. RSC Advances, 2014, 4, 46399-46406.	1.7	14
1688	Characterization and strong piezoelectric response of an organometallic nonlinear optical crystal: CdHg(SCN)₄(C₂H₆SO)₂. Journal of Materials Chemistry C, 2014, 2, 723-730.	2.7	10
1689	High-Pressure Phase Transition of Coffinite, USiO₄. Journal of Physical Chemistry C, 2014, 118, 25141-25149.	1.5	14
1690	Density Functional Theory Calculations of Pressure Effects on the Structure and Vibrations of 1,1-Diamino-2,2-dinitroethene (FOX-7). Journal of Physical Chemistry A, 2014, 118, 10002-10010.	1.1	35
1691	First-principles calculations of electronic, optical and elastic Properties of Y8CoIn3. , 2014, , .		0
1692	Supramolecular self-assembled network formation containing Nâ‹¯Br halogen bonds in physisorbed overlayers. Physical Chemistry Chemical Physics, 2014, 16, 19608-19617.	1.3	10
1693	Nitranilic acid hexahydrate, a novel benchmark system of the Zundel cation in an intrinsically asymmetric environment: spectroscopic features and hydrogen bond dynamics characterised by experimental and theoretical methods. Physical Chemistry Chemical Physics, 2014, 16, 998-1007.	1.3	14
1694	Structural skeleton of preferentially interpenetrated clusters and correlation with shear localization in Mgâ€“Cuâ€“Ni ternary metallic glasses. Physical Chemistry Chemical Physics, 2014, 16, 19590.	1.3	19
1695	Carbon coated face-centered cubic Ruâ€“C nanoalloys. Nanoscale, 2014, 6, 10370-10376.	2.8	17
1696	Direct evidence to support the restriction of intramolecular rotation hypothesis for the mechanism of aggregation-induced emission: temperature resolved terahertz spectra of tetraphenylethene. Materials Horizons, 2014, 1, 251-258.	6.4	117
1697	Probing halogen bonds with solid-state NMR spectroscopy: observation and interpretation of J(⁷⁷Se,³¹P) coupling in halogen-bonded Pî€Seâ‹¯I motifs. CrystEngComm, 2014, 16, 7285-7297.	1.3	43
1698	A semiconductive superhard FeB₄phase from first-principles calculations. Physical Chemistry Chemical Physics, 2014, 16, 22008-22013.	1.3	15
1699	Insight into insulator-to-metal transition of sulfur-doped silicon by DFT calculations. Physical Chemistry Chemical Physics, 2014, 16, 17499.	1.3	25
1700	First principles investigation of point defect-related properties in Ti₂AlN. RSC Advances, 2014, 4, 42014-42021.	1.7	17
1701	Structural transformation of confined iodine in the elliptical channels of AlPO4-11 crystals under high pressure. Physical Chemistry Chemical Physics, 2014, 16, 8301.	1.3	14

#	Article	IF	Citations
1702	Fe₄[Fe(CN)₆]₃: a cathode material for sodium-ion batteries. RSC Advances, 2014, 4, 42991-42995.	1.7	30
1703	Toward a Silverâ€“Alumina Model System for NO_x Reduction Catalysis. Journal of Physical Chemistry C, 2014, 118, 24556-24561.	1.5	3
1704	Study of CeO₂ and Its Native Defects by Density Functional Theory with Repulsive Potential. Journal of Physical Chemistry C, 2014, 118, 24248-24256.	1.5	86
1705	Effect by Doping and Surface Termination on c-BN Surface Reactivity: A Theoretical DFT Approach. Journal of Physical Chemistry C, 2014, 118, 10061-10075.	1.5	2
1706	Hydrogen Diffusion and Stabilization in Single-Crystal VO₂ Micro/Nanobeams by Direct Atomic Hydrogenation. Nano Letters, 2014, 14, 5445-5451.	4.5	65
1707	Spin-Orbit Coupling, Quantum Dots, and Qubits in Monolayer Transition Metal Dichalcogenides. Physical Review X, 2014, 4, .	2.8	222
1708	A Modular Approach for the Synthesis of Nanometer-Sized Polynitroxide Multi-Spin Systems. Journal of Organic Chemistry, 2014, 79, 8313-8323.	1.7	13
1709	Ca₃Be₆B₅O₁₆F: the first alkaline-earth beryllium borate with fluorine anions. Dalton Transactions, 2014, 43, 9998-10004.	1.6	10
1710	Y(IO₃)₃ as a Novel Photocatalyst: Synthesis, Characterization, and Highly Efficient Photocatalytic Activity. Inorganic Chemistry, 2014, 53, 8114-8119.	1.9	41
1711	Dissociation of High-Pressure Solid Molecular Hydrogen: A Quantum MonteÂCarlo and Anharmonic Vibrational Study. Physical Review Letters, 2014, 112, 165501.	2.9	102
1712	K₃MoPO₇: the first molybdenum phosphate with edge-sharing MoO₆octahedra and PO₄tetrahedra. RSC Advances, 2014, 4, 27122-27125.	1.7	8
1713	Central-transition double-quantum sideband NMR spectroscopy of half-integer quadrupolar nuclei: estimating internuclear distances and probing clusters within multi-spin networks. Physical Chemistry Chemical Physics, 2014, 16, 7037-7050.	1.3	14
1714	Dynamic nuclear polarisation enhanced14N overtone MAS NMR spectroscopy. Physical Chemistry Chemical Physics, 2014, 16, 12890-12899.	1.3	35
1715	Emergence of electric polarity in BiTeX (X = Br and I) monolayers and the giant Rashba spin splitting. Physical Chemistry Chemical Physics, 2014, 16, 17603.	1.3	73
1716	A combined⁷⁷Se NMR and molecular dynamics contribution to the structural understanding of the chalcogenide glasses. Physical Chemistry Chemical Physics, 2014, 16, 17975-17982.	1.3	19
1717	Interaction of hydrogen and carbon dioxide with sod-type zeolitic imidazolate frameworks: a periodic DFT-D study. CrystEngComm, 2014, 16, 1934.	1.3	44
1718	New Insights into the Short-Range Structures of Microporous Titanosilicates As Revealed by ^{47/49}Ti, ²³Na, ³⁹K, and ²⁹Si Solid-State NMR Spectroscopy. Journal of Physical Chemistry C, 2014, 118, 27353-27365.	1.5	25
1719	First-Principle Study of Atomic Structures of Fe/TMC (TM=Ti, Zr and Hf) Interface. Advanced Materials Research, 2014, 852, 193-197.	0.3	0

#	Article	IF	Citations
1720	High-Pressure Phase Transition of ZnO Nanorods Using Density Functional Theory. Integrated Ferroelectrics, 2014, 156, 122-128.	0.3	1
1721	Study of a magnetic-cooling material Gd(OH)CO₃. Journal of Materials Chemistry A, 2014, 2, 9851-9858.	5.2	173
1722	Electronic structure and optical properties of Siâ€“Oâ€“N compounds with different crystal structures. RSC Advances, 2014, 4, 36485-36493.	1.7	10
1723	Oxalyl dihydrazide polymorphism: a periodic dispersion-corrected DFT and MP2 investigation. CrystEngComm, 2014, 16, 102-109.	1.3	23
1724	Acoustic phonons and negative thermal expansion in MOF-5. Physical Chemistry Chemical Physics, 2014, 16, 21144-21152.	1.3	61
1725	Nasicon material NaZr₂(PO₄)₃: a novel storage material for sodium-ion batteries. Journal of Materials Chemistry A, 2014, 2, 1341-1345.	5.2	44
1726	Ba18F18In8S21 and Ba9F10In4S10: new kind of mixed anion compounds with the novel low-dimensional structure. CrystEngComm, 2014, 16, 2788.	1.3	8
1727	From semiconductors to semimetals: bismuth as a photocatalyst for NO oxidation in air. Journal of Materials Chemistry A, 2014, 2, 11065-11072.	5.2	88
1728	³⁵Cl solid-state NMR of HCl salts of active pharmaceutical ingredients: structural prediction, spectral fingerprinting and polymorph recognition. CrystEngComm, 2014, 16, 7334-7356.	1.3	51
1729	Ab initio investigations of dioctahedral interlayer-deficient mica: Modeling particles of illite found within gas shale. American Mineralogist, 2014, 99, 1962-1972.	0.9	5
1730	Electronic and optical properties of silicene nanomeshes. RSC Advances, 2014, 4, 37998-38003.	1.7	23
1731	A¹¹⁵In solid-state NMR study of low oxidation-state indium complexes. Chemical Science, 2014, 5, 982-995.	3.7	22
1732	On the fate of hydrogen during zirconium oxidation by water: effect of oxygen dissolution in Î±-Zr. RSC Advances, 2014, 4, 11050-11058.	1.7	12
1733	Dynamics of water molecules and sodium ions in solid hydrates of nucleotides. CrystEngComm, 2014, 16, 6756-6764.	1.3	12
1734	The roles of surface structure, oxygen defects, and hydration in the adsorption of CO₂on low-index ZnGa₂O₄surfaces: a first-principles investigation. Physical Chemistry Chemical Physics, 2014, 16, 7538-7547.	1.3	19
1735	Phase stability and elastic properties of (W0.5Al0.5)C phase with a novel NiAs-type structure. RSC Advances, 2014, 4, 42585-42590.	1.7	0
1736	Polycrystalline boron nitride constructed from hexagonal boron nitride. RSC Advances, 2014, 4, 38589-38593.	1.7	7
1737	On the infrared activation of the breathing mode of methane in ice. Physical Chemistry Chemical Physics, 2014, 16, 16694-16700.	1.3	11

#	Article	IF	Citations
1738	Bilayers of transition metal dichalcogenides: Different stackings and heterostructures. Journal of Materials Research, 2014, 29, 373-382.	1.2	40
1739	Elucidation of the reaction mechanism upon lithiation and delithiation of Cu_{0.5}TiOPO₄. Journal of Materials Chemistry A, 2014, 2, 12513-12518.	5.2	20
1740	Ba2B10O17: a new centrosymmetric alkaline-earth metal borate with a deep-UV cut-off edge. Dalton Transactions, 2014, 43, 8905-8910.	1.6	44
1741	Tunable ferromagnetic behavior in Cr doped ZnO nanorod arrays through defect engineering. Journal of Materials Chemistry C, 2014, 2, 2992-2997.	2.7	21
1742	Low energy structural dynamics and constrained libration of Li(NH₃)₄, the lowest melting point metal. Chemical Communications, 2014, 50, 10778-10781.	2.2	15
1743	Understanding compositionâ€“property relationships in Tiâ€“Crâ€“Vâ€“Mo alloys for optimisation of hydrogen storage in pressurised tanks. Physical Chemistry Chemical Physics, 2014, 16, 16563-16572.	1.3	8
1744	Creatine: Polymorphs Predicted and Found. Crystal Growth and Design, 2014, 14, 4895-4900.	1.4	33
1745	Manifestation of intrinsic defects in the band structures of quaternary chalcogenide Ag₂In₂SiSe₆and Ag₂In₂GeSe₆crystals. CrystEngComm, 2014, 16, 9534-9544.	1.3	10
1746	Unraveling the Polymorphism of [(p-cymene)Ru(ÎºN-INA)Cl₂] through Dispersion-Corrected DFT and NMR GIPAW Calculations. Inorganic Chemistry, 2014, 53, 7926-7935.	1.9	11
1747	Relative stability and phase transitions under pressure ofSrTiO₃:ab initioFP-LAPW within GGA-PBEsol+TB-mBJ calculations. International Journal of Modern Physics B, 2014, 28, 1450121.	1.0	3
1748	Pressureâ€induced sp ferromagnetism in electrideâ€like elemental potassium from firstâ€principles. Physica Status Solidi (B): Basic Research, 2014, 251, 527-532.	0.7	9
1749	Electronic and transport properties of LiCoO₂. Physical Chemistry Chemical Physics, 2014, 16, 23412-23420.	1.3	32
1750	Tungsten Carbide Supports for Single-Atom Platinum-Based Fuel-Cell Catalysts: First-Principles Study on the Metalâ€“Support Interactions and O₂ Dissociation on W_xC Low-Index Surfaces. Journal of Physical Chemistry C, 2014, 118, 13525-13538.	1.5	54
1751	The Stability, Electronic Structure, and Optical Property of TiO₂ Polymorphs. Journal of Physical Chemistry C, 2014, 118, 11385-11396.	1.5	223
1752	Effect of Interstitial Si on Different Boron Nitride Allotropes. Journal of Physical Chemistry C, 2014, 118, 20264-20274.	1.5	1
1753	Insights into Hydrate Formation and Stability of Morphinanes from a Combination of Experimental and Computational Approaches. Molecular Pharmaceutics, 2014, 11, 3145-3163.	2.3	38
1754	Investigating Relationships between the Crystal Structure and ³¹P Isotropic Chemical Shifts in Calcined Aluminophosphates. Journal of Physical Chemistry C, 2014, 118, 23285-23296.	1.5	23
1755	Spectroscopic Signatures for Interlayer Coupling in MoS₂â€“WSe₂ van der Waals Stacking. ACS Nano, 2014, 8, 9649-9656.	7.3	288

#	Article	IF	Citations
1756	High-Pressure-Induced Reversible Phase Transition in Sulfamide. Journal of Physical Chemistry C, 2014, 118, 18640-18645.	1.5	18
1757	New superconductor (Na 0.25 K 0.45) Ba 3 Bi 4 O 12 : A first-principles study. Physica C: Superconductivity and Its Applications, 2014, 506, 53-58.	0.6	22
1758	First-principles materials applications and design of nonlinear optical crystals. Journal Physics D: Applied Physics, 2014, 47, 253001.	1.3	201
1759	Effects of chalcogen substitution on electronic properties and chemical bondings of delafossite CuAlO₂. Physica Status Solidi (B): Basic Research, 2014, 251, 1630-1634.	0.7	11
1760	First-principles study of Cu-doping and oxygen vacancy effects on TiO2 for water splitting. Chemical Physics Letters, 2014, 612, 106-110.	1.2	31
1761	Superiority of DFT+U with non-linear core correction for open-shell binary rare-earth metal oxides: a case study of native point defects in cerium oxides. Philosophical Magazine, 2014, 94, 3052-3071.	0.7	24
1762	Synthesis of the Aluminophosphate ICP-1 by Self-Assembly of 1,3-Diphenylguanidine: Insights into Supramolecular Aggregation. Journal of Physical Chemistry C, 2014, 118, 4835-4845.	1.5	11
1763	Experimental and theoretical evidence for an ionic crystal of ammonia at high pressure. Physical Review B, 2014, 89, .	1.1	52
1764	Structure of Intermediate Phase II of LiNH₂ under High Pressure. Journal of Physical Chemistry B, 2014, 118, 9991-9996.	1.2	5
1765	Role of Ketoâ€“Enol Isomerization on Surface Chemistry and Hydrogenation of Acetone on Pt(111): A DFT study. Industrial & Engineering Chemistry Research, 2014, 53, 5451-5454.	1.8	17
1766	Self-Organized Overlayers Formed by Alanine on Cu{311} Surfaces. Journal of Physical Chemistry C, 2014, 118, 18589-18603.	1.5	14
1767	A promising new nonlinear optical crystal with high laser damage threshold for application in the IR region: synthesis, crystal structure and properties of noncentrosymmetric CsHgBr₃. Journal of Materials Chemistry C, 2014, 2, 6796-6801.	2.7	20
1768	Differential stress effect on the structural and elastic properties of forsterite by first-principles simulation. Physics of the Earth and Planetary Interiors, 2014, 233, 95-102.	0.7	5
1769	Raman Spectroscopy of Optical Transitions and Vibrational Energies of â¼1 nm HgTe Extreme Nanowires within Single Walled Carbon Nanotubes. ACS Nano, 2014, 8, 9044-9052.	7.3	33
1770	Comparative density functional theory study on the electronic and optical properties of BiMO4 (M =) Tj ETQq0 0 0 rgBT /Overlock 10 Tf	5.2	78
1771	Optical and magnetic properties of Ba₅(BO₃)₃F single crystals. Physical Chemistry Chemical Physics, 2014, 16, 24884-24891.	1.3	9
1772	Visibility of Al Surface Sites of Î³-Alumina: A Combined Computational and Experimental Point of View. Journal of Physical Chemistry C, 2014, 118, 15292-15299.	1.5	97
1773	Covalent-bonded graphyne polymers with high hardness. Journal of Superhard Materials, 2014, 36, 257-269.	0.5	13

#	Article	IF	Citations
1774	Theoretical Study of Pt Cocatalyst Loading on Anatase TiO₂(101) Surface: From Surface Doping to Interface Forming. Journal of Physical Chemistry C, 2014, 118, 24591-24602.	1.5	26
1775	Syntheses, structures, optical properties, and electronic structures of KBaMSe 3 (M = As, Sb). Journal of Alloys and Compounds, 2014, 617, 287-291.	2.8	19
1776	A₂BiI₅O₁₅(A = K⁺or Rb⁺): two new promising nonlinear optical materials containing [I₃O₉]^{3â^'}bridging anionic groups. Journal of Materials Chemistry C, 2014, 2, 4057-4062.	2.7	59
1777	Origin of Poor Cyclability in Li₂MnSiO₄ from First-Principles Calculations: Layer Exfoliation and Unstable Cycled Structure. Chemistry of Materials, 2014, 26, 3896-3899.	3.2	45
1778	Copper Deficiency in the p-Type Semiconductor Cu_{1â€“x}Nb₃O₈. Chemistry of Materials, 2014, 26, 2095-2104.	3.2	35
1779	Solid-State NMR Analysis of a Complex Crystalline Phase of Ronacaleret Hydrochloride. Journal of Physical Chemistry B, 2014, 118, 10266-10284.	1.2	29
1780	Stability of Pt near surface alloys under electrochemical conditions: a model study. Physical Chemistry Chemical Physics, 2014, 16, 16615-16622.	1.3	20
1781	Density functional theory calculations for the investigation of (Ag, N) codoping effect on the electronic and optical properties of anataseTiO₂. International Journal of Modern Physics B, 2014, 28, 1450112.	1.0	6
1782	Silicon Monoxide at 1 atm and Elevated Pressures: Crystalline or Amorphous?. Journal of the American Chemical Society, 2014, 136, 3410-3423.	6.6	26
1783	Effects of Quantum Nuclear Delocalisation on NMR Parameters from Path Integral Molecular Dynamics. Chemistry - A European Journal, 2014, 20, 2201-2207.	1.7	52
1784	Reinvestigation and Characterization of the Magnesium Borate Fluoride Mg₅(BO₃)F. Zeitschrift Fur Anorganische Und Allgemeine Chemie, 2014, 640, 2013-2018.	0.6	11
1785	Influence of Capping on the Atomistic Arrangement in Palladium Nanoparticles at Room Temperature. Journal of Physical Chemistry C, 2014, 118, 24641-24647.	1.5	20
1786	Novel three-dimensional boron nitride allotropes from compressed nanotube bundles. Journal of Materials Chemistry C, 2014, 2, 7022.	2.7	20
1787	Favored Composition Design and Atomic Structure Characterization for Ternary Alâ€“Cuâ€“Y Metallic Glasses via Proposed Interatomic Potential. Journal of Physical Chemistry B, 2014, 118, 4442-4449.	1.2	16
1788	Structural and optical properties of Î²-Si12â^'xCxN16 (x=0, 4, 6, 8, 12) crystals by first principles calculations. Physica E: Low-Dimensional Systems and Nanostructures, 2014, 64, 83-86.	1.3	2
1789	High-Pressure Structural Stability and Optical Properties of Scheelite-type ZrGeO4 and HfGeO4 X-ray Phosphor Hosts. Journal of Physical Chemistry C, 2014, 118, 4325-4333.	1.5	11
1790	Extreme deviations from stoichiometry in alumina nanopowders. Surface Science, 2014, 630, 182-186.	0.8	8
1791	Molecule VI: Sulfonimide or Sulfonamide?. Crystal Growth and Design, 2014, 14, 3704-3710.	1.4	16

#	Article	IF	Citations
1792	Effects of Structural Differences on the NMR Chemical Shifts in Isostructural Dipeptides. Journal of Physical Chemistry A, 2014, 118, 2618-2628.	1.1	2
1793	Fine Refinement of Solid-State Molecular Structures of Leu- and Met-Enkephalins by NMR Crystallography. Journal of Physical Chemistry B, 2014, 118, 3298-3309.	1.2	22
1795	First-principles investigation of elastic and thermodynamic properties of SiCN under pressure. Computational Materials Science, 2014, 95, 228-234.	1.4	5
1796	Theoretical two-atom thick semiconducting carbon sheet. Physical Chemistry Chemical Physics, 2014, 16, 18118-18123.	1.3	19
1797	The thermodynamics of hydride precipitation: The importance of entropy, enthalpy and disorder. Acta Materialia, 2014, 79, 351-362.	3.8	59
1798	Electronic and optical properties of Co-doped 3C-SiC from density functional calculations. Solid State Communications, 2014, 196, 28-31.	0.9	9
1799	The Role of Ti in Alanates and Borohydrides: Catalysis and Metathesis. Journal of Physical Chemistry C, 2014, 118, 77-84.	1.5	19
1800	Novel properties of Î³-Si3N4 with C, O and F dopants. Journal of Alloys and Compounds, 2014, 617, 518-524.	2.8	3
1801	Energy gap tuning and optical properties of Î³-Si3N4 doped with Fe, Co and Ni. Materials Science in Semiconductor Processing, 2014, 27, 474-481.	1.9	4
1802	Magnetism, band gap and stability of half-metallic property for the quaternary Heusler alloys CoFeTiZ (Z = Si, Ge, Sn). Journal of Alloys and Compounds, 2014, 616, 449-453.	2.8	76
1803	Synthesis, Crystal Structure, Magnetic and Electronic Properties of Bi2+xGaxPd4-3xO7+Î´ (x= 0.15, 0.30,) Tj ETQq0 0 0 rgBT /Overlock 1	1.2	0
1804	The interaction between cations and anionic groups inducing SHG enhancement in a series of apatite-like crystals: A first-principles study. Journal of Solid State Chemistry, 2014, 219, 138-142.	1.4	23
1805	Elastic properties and electronic structures of Y atom solid solute supercell Î³-Fe. Journal of Molecular Structure, 2014, 1076, 63-68.	1.8	6
1806	The effect of the stacking fault on the diffusion of chemisorbed hydrogen atoms inside few-layered graphene. RSC Advances, 2014, 4, 9223.	1.7	6
1807	Theoretical Approaches to Structure and Spectroscopy of Earth Materials. Reviews in Mineralogy and Geochemistry, 2014, 78, 691-743.	2.2	41
1808	Structural, elastic, and mechanical properties of germanium dioxide from first-principles calculations. Materials Science in Semiconductor Processing, 2014, 27, 765-776.	1.9	29
1809	Pressure-induced spin collapse of octahedrally coordinated<mml:math xmlns:mml="http://www.w3.org/1998/Math/MathML"><mml:msup><mml:mrow><mml:mi mathvariant="normal">Fe</mml:mi></mml:mrow><mml:mrow><mml:mn>3</mml:mn><mml:mo>+</mml:mo></mml:mrow></mml:msu	1.1	12
1810	xmlns:mml="http://www.w3.org/1998/Math/MathML"><mml:msub><mml:mrow><mml:mi mathvariant="normal">Ca</mml:mi></mml:mrow><mml:mn>3</mml:mn></mml:msub><mml:msub><mml:mrow><mml:mi mathvariant="normal">Fe</mml:mi></mml:mrow><mml:mn>2</mml:mn>. Physical Review B, 2014, 90, . Theoretical calculations on the adhesion, stability, electronic structure and bonding of SiC/W interface. Applied Surface Science, 2014, 314, 896-905.	3.1	25

#	Article	IF	Citations
1811	EELS modelling of graphitisation. Journal of Physics: Conference Series, 2014, 522, 012014.	0.3	1
1812	Electronic structure, optical properties, and lattice dynamics of orthorhombic<mml:math xmlns:mml="http://www.w3.org/1998/Math/MathML"><mml:mrow><mml:msub><mml:mi mathvariant="bold">Cu</mml:mi><mml:mn>2</mml:mn></mml:msub><mml:msub><mml:mi mathvariant="bold">CdGeS</mml:mi><mml:mn>4</mml:mn></mml:msub></mml:mrow></mml:math>and<mml:math xmlns:mml="http://www.w3.org/1998/Math/MathML"><mml:mrow><mml:msub><mml:mi mathvariant="bold">Cu</mml:mi><mml:mn>2</mml:mn></mml:msub><mml:msub><mml:mi mathvariant=	3.1	35
1813	Systematic Approach in Designing Rare-Earth-Free Hybrid Semiconductor Phosphors for General Lighting Applications. Journal of the American Chemical Society, 2014, 136, 14230-14236.	6.6	169
1814	First-principles high-pressure unreacted equation of state and heat of formation of crystal 2,6-diamino-3, 5-dinitropyrazine-1-oxide (LLM-105). Journal of Chemical Physics, 2014, 141, 064702.	1.2	36
1815	Spies Within Metal-Organic Frameworks: Investigating Metal Centers Using Solid-State NMR. Journal of Physical Chemistry C, 2014, 118, 23728-23744.	1.5	56
1816	Electronic and optical properties of anion-doped c-ZrO2 from first-principles calculations. Journal of Central South University, 2014, 21, 2584-2589.	1.2	8
1817	Structure and electronic properties of mixed (aâ€‰+â€‰c) dislocation cores in GaN. Journal of Applied Physics, 2014, 116, .	1.1	15
1818	Indirect doping effects from impurities inMoS2/h-BNheterostructures. Physical Review B, 2014, 90, .	1.1	39
1819	Synthesis of Crystalline Pyramidal Îµ-FeSi and Morphology- and Size-Dependent Ferromagnetism. Journal of Physical Chemistry C, 2014, 118, 2222-2228.	1.5	8
1820	Short-range structure of the brownmillerite-type oxide Ba₂In₂O₅and its hydrated proton-conducting form BaInO₃H. Journal of Materials Chemistry A, 2014, 2, 16915-16924.	5.2	37
1821	The electronic structure and photoluminescence properties of BiOCl:Eu 3+ from first-principles calculations. Journal of Luminescence, 2014, 156, 205-211.	1.5	26
1822	Noncentrosymmetric chalcohalide NaBa₄Ge₃S₁₀Cl with large band gap and IR NLO response. Journal of Materials Chemistry C, 2014, 2, 4590-4596.	2.7	96
1823	Polymorphism Arising from Differing Rates of Compression of Liquids. Crystal Growth and Design, 2014, 14, 3384-3391.	1.4	22
1824	L-glutamine: Dynamical properties investigation by means of INS, IR, RAMAN, 1H NMR and DFT techniques. Chemical Physics, 2014, 443, 17-25.	0.9	25
1825	An Investigation of Chlorine Ligands in Transition-Metal Complexes via ³⁵Cl Solid-State NMR and Density Functional Theory Calculations. Inorganic Chemistry, 2014, 53, 9581-9597.	1.9	28
1826	Structures and Physical Properties of Layered Oxyselenides Ba2MO2Ag2Se2(M = Co, Mn). Inorganic Chemistry, 2014, 53, 4154-4160.	1.9	21
1827	Experimental Characterization of the Hydride ¹H Shielding Tensors for HIrX₂(PR₃)₂ and HRhCl₂(PR₃)₂: Extremely Shielded Hydride Protons with Unusually Large Magnetic Shielding Anisotropies. Journal of Physical Chemistry A, 2014, 118, 1203-1212.	1.1	9
1828	Point defects and non-stoichiometry in thoria. Solid State Ionics, 2014, 267, 80-87.	1.3	39

#	Article	IF	Citations
1829	Study on spin polarization of non-magnetic atom in diluted magnetic semiconductor: The case of Al-doped 4Hâ€“SiC. Solid State Communications, 2014, 197, 44-48.	0.9	8
1830	Effect of Surface Termination on Diamond (100) Surface Electrochemistry. Journal of Physical Chemistry C, 2014, 118, 22995-23002.	1.5	28
1831	Beryllium-free Li4Sr(BO3)2 for deep-ultraviolet nonlinear optical applications. Nature Communications, 2014, 5, 4019.	5.8	384
1832	Na₄La₂(CO₃)₅ and CsNa₅Ca₅(CO₃)₈: Two New Carbonates as UV Nonlinear Optical Materials. Inorganic Chemistry, 2014, 53, 8098-8104.	1.9	58
1833	High-Coverage Oxygen-Induced Surface Structures on Ag(111). Journal of Physical Chemistry C, 2014, 118, 15324-15331.	1.5	46
1834	Molecular modeling studies of oleate adsorption on iron oxides. Applied Surface Science, 2014, 295, 115-122.	3.1	74
1835	Characterization of the Hydrides in Strykerâ€™s Reagent: [HCu{P(C₆H₅)₃}]₆. Inorganic Chemistry, 2014, 53, 2963-2967.	1.9	28
1836	Theoretical Study of the Energetic Stability and Geometry of Terminated and B-Doped Diamond (111) Surfaces. Journal of Physical Chemistry C, 2014, 118, 1944-1957.	1.5	50
1837	Half-metallic ferromagnetism in zinc-blende (CaX)1/(YX)1 (001)(Y=Al, Ga, and In; X=N, P, and As) superlattices: A first-principles study. Computational Materials Science, 2014, 84, 306-309.	1.4	6
1838	Specific features of band structure and optical anisotropy of Cu2CdGeSe4 quaternary compounds. Materials Chemistry and Physics, 2014, 147, 155-161.	2.0	21
1839	Mechanisms of charge transfer and redistribution in LaAlO3/SrTiO3 revealed by high-energy optical conductivity. Nature Communications, 2014, 5, 3663.	5.8	70
1840	Crystal growth and calculation of the electronic band structure and density of states of Li3Cs2B5O10. CrystEngComm, 2014, 16, 1978.	1.3	13
1841	First-principles calculations of water dissociation on the oxygen-deficient (010) surface of Fergusonite-type LaNbO4 crystal. International Journal of Hydrogen Energy, 2014, 39, 1457-1462.	3.8	1
1842	Insights from Arsenate Adsorption on Rutile (110): Grazing-Incidence X-ray Absorption Fine Structure Spectroscopy and DFT+U Study. Journal of Physical Chemistry A, 2014, 118, 4759-4765.	1.1	19
1843	AAg₂(Mâ€²_{1/3}M_{2/3})[VO₄]₂: Synthesis, Magnetic Properties, and Lattice Dynamics of Honeycomb-Type Lattices. Inorganic Chemistry, 2014, 53, 4994-5001.	1.9	14
1844	<scp>R</scp>aman scattering in orthorhombic Cu<scp>I</scp>n<scp>S</scp>₂ nanocrystals. Physica Status Solidi (A) Applications and Materials Science, 2014, 211, 195-199.	0.8	24
1845	Comparing electron-phonon coupling strength in diamond, silicon, and silicon carbide: First-principles study. Physical Review B, 2014, 89, .	1.1	77
1846	The Near Edge Structure of Hexagonal Boron Nitride. Microscopy and Microanalysis, 2014, 20, 1053-1059.	0.2	24

#	Article	IF	Citations
1847	Structure and stability of two polymorphs of creatine and its monohydrate. CrystEngComm, 2014, 16, 8197.	1.3	17
1848	Determination of the Crystal Structure of Hexaphenyldisilane from Powder Diffraction Data and Its Thermodynamic Properties. Crystal Growth and Design, 2014, 14, 2937-2944.	1.4	7
1849	CO Oxidation on Pd(100) Versus PdO(101)- $$(sqrt{5}imes sqrt{5})R27^{circ}$$ (5 Ã— 5) R 27 â˜ : First-Principles Kinetic Phase Diagrams and Bistability Conditions. Topics in Catalysis, 2014, 57, 159-170.	1.3	34
1850	Acoustic waves and phonon focus in Li crystal: the first principle study. European Physical Journal B, 2014, 87, 1.	0.6	3
1851	Direct Investigation of Halogen Bonds by Solid-State Multinuclear Magnetic Resonance Spectroscopy and Molecular Orbital Analysis. Journal of the American Chemical Society, 2014, 136, 6929-6942.	6.6	64
1852	Ferromagnetic spin-order in p-type N-doped SnO2 films prepared by thermal oxidation of SnNx. Journal of Magnetism and Magnetic Materials, 2014, 362, 14-19.	1.0	24
1853	Ab initio calculation of half-metallic ferromagnetism in zinc-blende (CaN)1/(AlN)x and (CaN)x/(AlN)1 (x=2, 3) (001) superlattices. Solid State Communications, 2014, 194, 43-47.	0.9	1
1854	Enhanced visible-light photocatalytic activity of g-C3N4/Zn2GeO4 heterojunctions with effective interfaces based on band match. Nanoscale, 2014, 6, 2649.	2.8	227
1855	Ab Initio Studies on the Structural and Electronic Properties of Bismuth Ferrite Based on Ferroelectric Hexagonal Phase and Paraelectric Orthorhombic Phase. Integrated Ferroelectrics, 2014, 155, 134-142.	0.3	13
1856	Theoretical prediction of the fundamental properties of ternary bismuth tellurohalides. Materials Science in Semiconductor Processing, 2014, 27, 605-610.	1.9	22
1857	A metallic carbon consisting of helical carbon triangle chains. Journal of Physics Condensed Matter, 2014, 26, 235402.	0.7	10
1858	Influences of Epitaxial Strain and Volume on BaTiO3: Ab Initio Total Energy Calculation. Integrated Ferroelectrics, 2014, 155, 91-99.	0.3	3
1859	Deep-Ultraviolet Transparent Phosphates RbBa₂(PO₃)₅ and Rb₂Ba₃(P₂O₇)₂ Show Nonlinear Optical Activity from Condensation of [PO₄]^{3â€“} Units. Journal of the American Chemical Society, 2014, 136, 8560-8563.	6.6	297
1860	Elastic, electronic and optical properties of baddeleyite TiO2 by first-principles. Materials Science in Semiconductor Processing, 2014, 27, 958-965.	1.9	3
1861	Atomic modeling to design favored compositions for the ternary Niâ€“Nbâ€“Zr metallic glass formation. Acta Materialia, 2014, 76, 482-492.	3.8	11
1862	Alloying-related trends in thermal properties of ternary TiN-based nitrides. International Journal of Modern Physics B, 2014, 28, 1450087.	1.0	3
1863	Ag₃Ga₃SiSe₈: a new infrared nonlinear optical material with a chalcopyrite structure. CrystEngComm, 2014, 16, 6836.	1.3	32
1864	Why the photocatalytic activity of Mo-doped BiVO4 is enhanced: a comprehensive density functional study. Physical Chemistry Chemical Physics, 2014, 16, 13465.	1.3	80

#	Article	IF	Citations
1865	The covariance of the differences between experimental and theoretical chemical shifts as an aid for assigning two-dimensional heteronuclear correlation solid-state NMR spectra. Chemical Physics Letters, 2014, 608, 334-339.	1.2	20
1866	Sodiumâ€“rare earth carbonates with shorite structure and large second harmonic generation response. CrystEngComm, 2014, 16, 4414.	1.3	41
1867	Role of Dispersion Interactions in the Polymorphism and Entropic Stabilization of the Aspirin Crystal. Physical Review Letters, 2014, 113, 055701.	2.9	156
1868	Exploration of new second-order nonlinear optical materials of the Csâ€“Hgâ€“Brâ€“I system. Dalton Transactions, 2014, 43, 8899-8904.	1.6	25
1869	New Assembly of Acetamidinium Nitrate Modulated by High Pressure. Journal of Physical Chemistry C, 2014, 118, 23443-23450.	1.5	10
1870	pâ€“(p,Ï€*) interaction mechanism revealing and accordingly designed new member in deep-ultraviolet NLO borates Li_nM_{nâ¯1}B_{2nâ¯1}O_{4nâ¯2}(M = Cs/Rb, n = 3, 4,)	2.7	61
1871	The Effect of the Ratio of [M/(B+P)] on the Configuration of Anionic Groups: Synthesis of the Borateâ€“Phosphate LiPb₄(BO₃)(PO₄)₂. European Journal of Inorganic Chemistry, 2014, 2014, 3467-3473.	1.0	13
1872	Ab initio investigations of dioctahedral interlayer-deficient mica: modelling 1 M polymorphs of illite found within gas shale. European Journal of Mineralogy, 2014, 26, 127-144.	0.4	17
1873	Pressure-Induced Diversity of Ï€-Stacking Motifs and Amorphous Polymerization in Pyrrole. Journal of Physical Chemistry C, 2014, 118, 12420-12427.	1.5	13
1874	Effect of Terminating Species on the Initial Growth of BN on Diamond Substrates. Journal of Physical Chemistry C, 2014, 118, 3490-3503.	1.5	4
1875	Experimental and Solid-State Computational Study of Structural and Dynamic Properties in the Equilibrium Form of Temazepam. Journal of Physical Chemistry B, 2014, 118, 6670-6679.	1.2	5
1876	A Fundamental Understanding of Catechol and Water Adsorption on a Hydrophilic Silica Surface: Exploring the Underwater Adhesion Mechanism of Mussels on an Atomic Scale. Langmuir, 2014, 30, 6906-6914.	1.6	89
1877	Linear and Nonlinear Optical Properties of K₃B₆O₁₀Br Single Crystal: Experiment and Calculation. Journal of Physical Chemistry C, 2014, 118, 11849-11856.	1.5	73
1878	Investigation of Acrylic Acid at High Pressure Using Neutron Diffraction. Journal of Physical Chemistry B, 2014, 118, 4044-4051.	1.2	14
1879	Electronic and vibrational properties of defective transition metal dichalcogenide Haeckelites: new 2D semi-metallic systems. 2D Materials, 2014, 1, 011003.	2.0	35
1880	First-principle study of adhesion, wetting and bonding on Al/Al3V(001) interface. Surface Science, 2014, 624, 1-7.	0.8	19
1881	Superhard and high-strength yne-diamond semimetals. Diamond and Related Materials, 2014, 46, 15-20.	1.8	18
1882	First-principle calculations of the elastic properties of semiconductors. Computational Materials Science, 2014, 87, 227-231.	1.4	20

#	Article	IF	Citations
1883	Syntheses, structures and characterizations of Rb3Na(MO4)2 (MÂ=ÂMo, W) crystals. Solid State Sciences, 2014, 33, 32-37.	1.5	13
1884	Layered B-site cation ordering: A key factor in ferrimagnetism of Y2MnCrO6. Journal of Alloys and Compounds, 2014, 601, 14-18.	2.8	17
1885	Terahertz spectral investigation of anhydrous and monohydrated glucose using terahertz spectroscopy and solid-state theory. Journal of Molecular Spectroscopy, 2014, 296, 9-13.	0.4	38
1886	Atomistic mechanism of Î±â€“Î² phase transition in vanadium pentoxide. Journal of Physics and Chemistry of Solids, 2014, 75, 115-122.	1.9	23
1887	Mechanisms for adsorption, dissociation and diffusion of hydrogen in hydrogen permeation barrier of Î±-Al2O3: The role of crystal orientation. International Journal of Hydrogen Energy, 2014, 39, 610-619.	3.8	40
1888	Can binary sp half-metallic ferromagnets maintain half-metallicity when they form superlattices? A first-principles approach. Physics Letters, Section A: General, Atomic and Solid State Physics, 2014, 378, 1208-1212.	0.9	9
1889	Theoretical insights into structuralâ€“electronic relationships and relative stability of the Cu-, Al- and O-terminated CuAlO2(0001) surfaces. Vacuum, 2014, 107, 90-98.	1.6	13
1890	Alloys based on Crâ€“Cr2Ta containing Si. Intermetallics, 2014, 48, 62-70.	1.8	19
1891	First-principles study of Al/A13Ti heterogeneous nucleation interface. Applied Surface Science, 2014, 307, 593-600.	3.1	74
1892	Phase changes in lithium amideâ€“borohydride complexes under high pressure. Solid State Ionics, 2014, 262, 490-494.	1.3	1
1893	A thermodynamic adsorption/entrapment model for selenium(IV) coprecipitation with calcite. Geochimica Et Cosmochimica Acta, 2014, 134, 16-38.	1.6	46
1894	Electronic structure, magnetism and phase stability of isostructural Ga2MnCoâ€“Ga2MnV Heusler alloys from first principles. Computational Materials Science, 2014, 89, 130-136.	1.4	15
1895	Structural and electrochemical properties of aluminium doped LiMn2O4 cathode materials for Li battery: Experimental and ab initio calculations. Sustainable Energy Technologies and Assessments, 2014, 5, 44-49.	1.7	38
1896	Density-functional theory study of the pressure-induced phase transition in hydronitrogen compound N4H4. Physics Letters, Section A: General, Atomic and Solid State Physics, 2014, 378, 1333-1335.	0.9	6
1897	Co-adsorption of water and glycine on Cu{110}. Physical Chemistry Chemical Physics, 2014, 16, 6101.	1.3	19
1898	In Situ Self-Assembled FeWO₄/Graphene Mesoporous Composites for Li-Ion and Na-Ion Batteries. Chemistry of Materials, 2014, 26, 3721-3730.	3.2	52
1899	Phosphorene Nanoribbons, Phosphorus Nanotubes, and van der Waals Multilayers. Journal of Physical Chemistry C, 2014, 118, 14051-14059.	1.5	544
1900	Single Water Molecule Adsorption and Decomposition on the Low-Index Stoichiometric Rutile TiO₂ Surfaces. Journal of Physical Chemistry C, 2014, 118, 4287-4295.	1.5	23

#	Article	IF	Citations
1901	In Situ Diffraction Study of Catalytic Hydrogenation of VO₂: Stable Phases and Origins of Metallicity. Journal of the American Chemical Society, 2014, 136, 8100-8109.	6.6	67
1902	Design and Syntheses of Electron-Transfer Photochromic Metalâ€“Organic Complexes Using Nonphotochromic Ligands: A Model Compound and the Roles of Its Ligands. Inorganic Chemistry, 2014, 53, 847-851.	1.9	84
1903	Crystal plane-dependent gas-sensing properties of zinc oxide nanostructures: experimental and theoretical studies. Physical Chemistry Chemical Physics, 2014, 16, 11471-11480.	1.3	168
1904	Optical phonons in the wurtzstanniteCu2ZnGeS4semiconductor: Polarized Raman spectroscopy and first-principle calculations. Physical Review B, 2014, 89, .	1.1	24
1905	Electrons and phonons in single layers of hexagonal indium chalcogenides fromab initiocalculations. Physical Review B, 2014, 89, .	1.1	281
1906	Two-dimensional Sc2C: A reversible and high-capacity hydrogen storage material predicted by first-principles calculations. International Journal of Hydrogen Energy, 2014, 39, 10606-10612.	3.8	163
1907	Theoretical prediction of the fundamental properties for the ternary MgYZn and Mg0.9YZn1.06 alloys. Computational Materials Science, 2014, 91, 315-319.	1.4	17
1908	First-principle calculations on the structural and electronic properties of hard C11N4. Physica B: Condensed Matter, 2014, 449, 90-94.	1.3	5
1909	First Principles LDA+U Calculations for ZnO Materials. Integrated Ferroelectrics, 2014, 155, 15-22.	0.3	71
1910	Comparison and Rationalization of Droperidol Isostructural Solvate Stability: An Experimental and Computational Study. Crystal Growth and Design, 2014, 14, 3639-3648.	1.4	24
1911	Ba₈Sn₄S₁₅: A Strong Second Harmonic Generation Sulfide with Zero-Dimensional Crystal Structure. Chemistry of Materials, 2014, 26, 1093-1099.	3.2	92
1912	Optical properties and electronic band structure of BiMg2PO6, BiMg2VO6, BiMg2VO6:Pr3+ and BiMg2VO6:Eu3+. Optical Materials, 2014, 36, 1724-1729.	1.7	56
1913	Prediction study on mechanical and thermodynamic properties of orthorhombic Mg2SiO4 under high temperature. Physica B: Condensed Matter, 2014, 449, 95-103.	1.3	2
1914	Three new chalcohalides, Ba4Ge2PbS8Br2, Ba4Ge2PbSe8Br2 and Ba4Ge2SnS8Br2: Syntheses, crystal structures, band gaps, and electronic structures. Journal of Alloys and Compounds, 2014, 611, 422-426.	2.8	3
1915	Feasibility of arsenic and antimony NMR spectroscopy in solids: An investigation of some group 15 compounds. Solid State Nuclear Magnetic Resonance, 2014, 61-62, 54-61.	1.5	25
1916	First-principles calculations of the dielectric and vibrational properties of ferroelectric and paraelectric BaAl2O4. Physics Letters, Section A: General, Atomic and Solid State Physics, 2014, 378, 1867-1870.	0.9	15
1917	Study of the effect of doped impurities on polytype stability during PVT growth of SiC using 2D nucleation theory. Journal of Crystal Growth, 2014, 385, 95-99.	0.7	23
1918	The theoretical study on electronic structure and electromagnetic properties ofÎ±-MnO2based on crystal defects. EPJ Applied Physics, 2014, 68, 30901.	0.3	3

#	Article	IF	Citations
1920	Defect formation energetics at the grain boundary in CuInSe₂ using first-principles calculations. Journal of the Ceramic Society of Japan, 2014, 122, 469-472.	0.5	7
1921	Pressureâ€Induced Intersite Bïf¿M (M=Ru,â€…Ir) Valence Transitions in Hexagonal Perovskites. Angewandte Chemie - International Edition, 2014, 53, 3414-3417.	7.2	14
1922	Modelling of amorphous poly-CO structure with N and He. Journal of Physics: Conference Series, 2014, 500, 022006.	0.3	2
1923	A Combined Metalâ€“Halide/Metal Flux Synthetic Route towards Typeâ€I Clathrates: Crystal Structures and Thermoelectric Properties of A₈Al₈Si₃₈ (A=K, Rb, and Cs). Chemistry - A European Journal, 2014, 20, 15077-15088.	1.7	26
1924	Analysis of energy gap opening in graphene oxide. Journal of Physics: Conference Series, 2014, 526, 012003.	0.3	13
1926	Mechanical and chemical effects of solute elements on generalized stacking fault energy of Mg. Journal of Materials Research, 2014, 29, 2576-2586.	1.2	13
1927	Crystal Structure and Desolvation Behaviour of the Tadalafil Monosolvates with Acetone and Methyl Ethyl Ketone. Journal of Pharmaceutical Sciences, 2015, 104, 3782-3788.	1.6	7
1928	The thermal stability and microwave electromagnetic properties of Mn4N. Applied Physics A: Materials Science and Processing, 2015, 120, 1075-1081.	1.1	12
1929	Copper accumulation in the sequestrum of medication-related osteonecrosis of the jaw. Bone Reports, 2015, 3, 40-47.	0.2	6
1930	¹¹B Solid-State NMR Interaction Tensors of Linear Two-Coordinate Boron: The Dimesitylborinium Cation. Inorganic Chemistry, 2015, 54, 11889-11896.	1.9	14
1931	Dopant effects on high temperature mechanical properties of zirconium carbide ceramics. Advances in Applied Ceramics, 2015, 114, 338-343.	0.6	13
1932	Crystal structures of eight mono-methyl alkanes (C₂₆â€“C₃₂)viasingle-crystal and powder diffraction and DFT-D optimization. IUCrJ, 2015, 2, 490-497.	1.0	13
1933	Elucidating the high-k insulator Î±-Al2O3 direct/indirect energy band gap type through density functional theory computations. Chemical Physics Letters, 2015, 637, 172-176.	1.2	40
1934	First-principles study of multiferroic material PbVO3 under uniaxial pressure. European Physical Journal B, 2015, 88, 1.	0.6	5
1935	The effect of atomic environment on Bâ€“O bonding state based on the ab initio calculations. Materials Research Innovations, 2015, 19, S283-S286.	1.0	0
1936	Tailored Nearâ€Infrared Photoemission in Fluoride Perovskites through Activator Aggregation and Superâ€Exchange between Divalent Manganese Ions. Advanced Science, 2015, 2, 1500089.	5.6	86
1937	Assignment of the Internal Vibrational Modes of C₇₀ by Inelastic Neutron Scattering Spectroscopy and Periodicâ€DFT. ChemistryOpen, 2015, 4, 620-625.	0.9	10
1939	Structure Prediction at High Pressures. , 2015, , 105-130.		1

#	Article	IF	Citations
1941	Two-dimensional Cs-vacancy superstructure in iron-based superconductor<mml:math xmlns:mml="http://www.w3.org/1998/Math/MathML"><mml:mrow><mml:msub><mml:mi>Cs</mml:mi><mml:mrow><mml:mn>0.8</mml:mn></m Physical Review B, 2015, 91, .	1.1	10
1942	Splitting of monolayer out-of-plane<mml:math xmlns:mml="http://www.w3.org/1998/Math/MathML"><mml:msubsup><mml:mi>A</mml:mi><mml:mrow><mml:mn>1</mml:mn></m mode in few-layer<mml:math xmlns:mml="http://www.w3.org/1998/Math/MathML"><mml:msub><mml:mi>WS</mml:mi><mml:mn>2</mml:mn></mml:msub></m Physical Review B, 2015, 91, .	1.1	78
1943	Ferroelectric soft mode of polarZnTiO3investigated by Raman spectroscopy at high pressure. Physical Review B, 2015, 91, .	1.1	15
1944	Two-dimensional inversion-asymmetric topological insulators in functionalized III-Bi bilayers. Physical Review B, 2015, 91, .	1.1	60
1945	Pressure-induced spin collapse of octahedrally coordinated<mml:math xmlns:mml="http://www.w3.org/1998/Math/MathML"><mml:msup><mml:mrow><mml:mi>Mn</mml:mi></mml:mrow><mml:mrow><m the tetragonal hydrogarnet henritermierite<mml:math xmlns:mml="http://www.w3.org/1998/Math/MathML"><mml:mrow><mml:msub><mml:mi>Ca</mml:mi><mml:mn>3</mml:mn></mml:m Physical Review B, 2015, 92, .	1.1	8
1946	Quantum spin Hall effect and topological phase transition in two-dimensional square transition-metal dichalcogenides. Physical Review B, 2015, 92, .	1.1	117
1947	Optical properties, lattice dynamics, and structural phase transition in hexagonal<mml:math xmlns:mml="http://www.w3.org/1998/Math/MathML"><mml:mrow><mml:mn>2</mml:mn><mml:mi>H</mml:mi><mml:mo>â^’</mml:m mathvariant="normal">O</mml:mi><mml:mn>3</mml:mn></mml:msub></mml:mrow></mml:math>single crystals. Physical Review B, 2015, 92, .	1.1	12
1948	Lattice dynamics and electron-phonon coupling calculations using nondiagonal supercells. Physical Review B, 2015, 92, .	1.1	99
1949	Steps or Terraces? Dynamics of Aromatic Hydrocarbons Adsorbed at Vicinal Metal Surfaces. Physical Review Letters, 2015, 115, 086101.	2.9	19
1950	Quantum MonteÂCarlo Calculation of the Binding Energy of Bilayer Graphene. Physical Review Letters, 2015, 115, 115501.	2.9	166
1951	Anharmonic Nuclear Motion and the Relative Stability of Hexagonal and Cubic ice. Physical Review X, 2015, 5, .	2.8	35
1952	First-principles structure determination of interface materials: The<mml:math xmlns:mml="http://www.w3.org/1998/Math/MathML"><mml:mrow><mml:msub><mml:mtext>Ni</mml:mtext><mml:mi>x</mml:mi> Physical Review B, 2015, 92, .	1.1	12
1953	Giant electron-phonon interactions in molecular crystals and the importance of nonquadratic coupling. Physical Review B, 2015, 92, .	1.1	42
1954	Defect-induced magnetism in SiC: Interplay between ferromagnetism and paramagnetism. Physical Review B, 2015, 92, .	1.1	31
1955	Electronic Friction-Based Vibrational Lifetimes of Molecular Adsorbates: Beyond the Independent-Atom Approximation. Physical Review Letters, 2015, 115, 046102.	2.9	65
1956	Low Speed Crack Propagation via Kink Formation and Advance on the Silicon (110) Cleavage Plane. Physical Review Letters, 2015, 115, 135501.	2.9	25
1957	Atomistic Design of Favored Compositions for Synthesizing the Al-Ni-Y Metallic Glasses. Scientific Reports, 2015, 5, 16218.	1.6	6
1958	Investigating crystalline-polarity-dependent electronic structures of GaN by hard x-ray photoemission and ab-initio calculations. Applied Physics Letters, 2015, 107, .	1.5	17

#	Article	IF	Citations
1959	Structure sensitivity in oxide catalysis: First-principles kinetic Monte Carlo simulations for CO oxidation at RuO2(111). Journal of Chemical Physics, 2015, 143, 204702.	1.2	9
1960	Ab initiostudy of anisotropic mechanical properties of LiCoO2 during lithium intercalation and deintercalation process. Journal of Applied Physics, 2015, 118, .	1.1	56
1961	Stable Gold Carbide Nanostructures. Materials Transactions, 2015, 56, 1383-1386.	0.4	2
1962	Fingerprints of energy dissipation for exothermic surface chemical reactions: O2 on Pd(100). Journal of Chemical Physics, 2015, 143, 034705.	1.2	19
1963	Understanding Phase-Change Memory Alloys from a Chemical Perspective. Scientific Reports, 2015, 5, 13698.	1.6	47
1964	Vibrational renormalisation of the electronic band gap in hexagonal and cubic ice. Journal of Chemical Physics, 2015, 143, 244708.	1.2	18
1965	Novel silicon allotropes: Stability, mechanical, and electronic properties. Journal of Applied Physics, 2015, 118, .	1.1	44
1966	The effect of atomic structure on interface spin-polarization of half-metallic spin valves: Co2MnSi/Ag epitaxial interfaces. Applied Physics Letters, 2015, 107, .	1.5	13
1967	Structure and spectroscopy of CuH preparedviaborohydride reduction. Acta Crystallographica Section B: Structural Science, Crystal Engineering and Materials, 2015, 71, 608-612.	0.5	11
1968	Ab-initio calculation study on the formation mechanism of boron-oxygen complexes in c-Si. AIP Advances, 2015, 5, .	0.6	6
1969	Effect of the tetrahedral groups on the optical properties of LaBRO5 (Râ€‰=â€‰Si and Ge): A first-principles study. Journal of Applied Physics, 2015, 118, .	1.1	9
1970	Fragment-based 13C nuclear magnetic resonance chemical shift predictions in molecular crystals: An alternative to planewave methods. Journal of Chemical Physics, 2015, 143, 102809.	1.2	65
1971	Solid-State 87Sr NMR Spectroscopy at Natural Abundance and High Magnetic Field Strength. Journal of Physical Chemistry A, 2015, 119, 11847-11861.	1.1	13
1972	Band Gap Characters and Ferromagnetic/Antiferromagnetic Coupling in Group-IV Monolayers Tuned by Chemical Species and Hydrogen Adsorption Configurations. Nanoscale Research Letters, 2015, 10, 1040.	3.1	46
1973	A theoretical and experimental study of the NMR spectra of 4,5,6,7-tetrafluorobenzazoles with special stress on PCM calculations of chemical shifts. Magnetic Resonance in Chemistry, 2015, 53, 353-362.	1.1	18
1974	Synthesis and Crystal Structures of the Calcium Silicon Phosphides Ca₂Si₂P₄, Ca₃Si₈P₁₄ and Ca₃Si₂P₄. Zeitschrift Fur Anorganische Und Allgemeine Chemie, 2015, 641, 1545-1549.	0.6	21
1976	Energy Migration Upconversion in Manganese(II)â€Doped Nanoparticles. Angewandte Chemie - International Edition, 2015, 54, 13312-13317.	7.2	64
1977	On the Thermal Stability and Structures of Layered Double Hydroxides Mg_{1â€“x}Al_x(OH)₂(NO₃)_xÂ·nH₂O (0.18â€‰â‰€â€‰xâ€‰â‰€â€‰0.38). European Journal of Inorganic Chemistry, 2015, 2015, 1775-1788.	2.4	109

#	Article	IF	Citations
1978	Ba₂B₆O₁₁, a Member of the BaOâ€B₂O₃ Family, Featuring a Layer Framework. European Journal of Inorganic Chemistry, 2015, 2015, 3328-3335.	1.0	16
1980	Monitoring and Understanding the Paraelectricâ€“Ferroelectric Phase Transition in the Metalâ€“Organic Framework [NH₄][M(HCOO)₃] by Solidâ€State NMR Spectroscopy. Chemistry - A European Journal, 2015, 21, 14348-14361.	1.7	36
1981	Nature of electrical resistivity and structural stability in N-doped GeTe models for reliable phase-change materials. Physica Status Solidi (B): Basic Research, 2015, 252, 431-441.	0.7	11
1982	A framework for machineâ€learningâ€augmented multiscale atomistic simulations on parallel supercomputers. International Journal of Quantum Chemistry, 2015, 115, 1129-1139.	1.0	31
1983	Crystal and Electronic Structure of Y₅Al₃C₄. Zeitschrift Fur Anorganische Und Allgemeine Chemie, 2015, 641, 1521-1526.	0.6	2
1984	YAlC: A Bonding Chameleon with Heteropolyacetylene Features. Angewandte Chemie - International Edition, 2015, 54, 9606-9609.	7.2	2
1985	Advances in the study of the deformation mechanism of stishovite. Physica Status Solidi (B): Basic Research, 2015, 252, 1486-1491.	0.7	13
1986	Supramolecular Frameworks Built up from Redâ€PhosphorÂescent transâ€Re₆ Cluster Building Blocks: One Pot Synthesis, Crystal Structures, and DFT Investigations. Zeitschrift Fur Anorganische Und Allgemeine Chemie, 2015, 641, 1156-1163.	0.6	21
1987	Crystallization Behavior of Amorphous Si₂BC₃N Ceramic Monolith Subjected to High Pressure. Journal of the American Ceramic Society, 2015, 98, 3788-3796.	1.9	16
1990	Nanostructured Ni₂P as a Robust Catalyst for the Hydrolytic Dehydrogenation of Ammoniaâ€“Borane. Angewandte Chemie - International Edition, 2015, 54, 15725-15729.	7.2	204
1991	First-principles simulation of Raman spectra and structural properties of quartz up to 5 GPa. Chinese Physics B, 2015, 24, 127401.	0.7	5
1992	Going clean: structure and dynamics of peptides in the gas phase and paths to solvation. Journal of Physics Condensed Matter, 2015, 27, 493002.	0.7	29
1993	Synthesis, Crystal Structure, and Properties of the Sodium Molybdate Fluoride Na₃MoO₄F. Zeitschrift Fur Anorganische Und Allgemeine Chemie, 2015, 641, 922-926.	0.6	4
1994	Ba₂In₂Q₅ (Q = S, Se): Synthesis, Crystal Structures, Electronic Structures, and Optical Properties. Zeitschrift Fur Anorganische Und Allgemeine Chemie, 2015, 641, 1329-1333.	0.6	8
1995	The Double Molybdate Rb₂Ba(MoO₄)₂: Synthesis, Crystal Structure, Optical, Thermal, Vibrational Properties, and Electronic Structure. Zeitschrift Fur Anorganische Und Allgemeine Chemie, 2015, 641, 2321-2325.	0.6	14
1997	Effect of Cu Content on Atomic Positions of Ti50Ni50â€™xCux Shape Memory Alloys Based on Density Functional Theory Calculations. Metals, 2015, 5, 2222-2235.	1.0	6
1998	Existence of the Î²-tin structure in Sr: First evidence from computational approach. AIP Advances, 2015, 5, .	0.6	10
1999	A Tale of Two Entangled Instabilitiesâ€”The Dual Role of Î´-O in HgBa2Can-1CunO2(n+1)+Î´. Entropy, 2015, 17, 6765-6782.	1.1	4

#	Article	IF	Citations
2000	Effects of nitrogen-related defects on visible light photocatalytic response in N+implanted TiO2: A first-principles study. Journal of Applied Physics, 2015, 118, 115702.	1.1	7
2001	Magnetic and Mechanical Properties of Deformed Iron Nitride<mml:math xmlns:mml="http://www.w3.org/1998/Math/MathML" id="M1"><mml:mrow><mml:msup><mml:mrow><mml:mi>Î³</mml:mi></mml:mrow><mml:mrow><mml:mi>â€²</mml:mi></mml:mrow></mml:msup></mml:mr Journal of Applied Mathematics, 2015, 2015, 1-9.	0.4	4
2002	First-principles Study of Hydrogen-induced Embrittlement in Fe Grain Boundary with Cr Segregation. ISIJ International, 2015, 55, 1131-1134.	0.6	15
2003	Interatomic Potential for xNa₂O-(1â^'x)SiO₂ Glasses. Journal of Computer Chemistry Japan, 2015, 14, 63-66.	0.0	3
2004	Confinement of massless Dirac fermions in the graphene matrix induced by the B/N heteroatoms. Physical Chemistry Chemical Physics, 2015, 17, 5586-5593.	1.3	4
2005	An outstanding second-harmonic generation material BiB₂O₄F: exploiting the electron-withdrawing ability of fluorine. Inorganic Chemistry Frontiers, 2015, 2, 170-176.	3.0	82
2006	Investigation of In-doped BaFeO_{3â^'Î´}perovskite-type oxygen permeable membranes. Journal of Materials Chemistry A, 2015, 3, 6202-6214.	5.2	68
2007	Synthesis, characterization and theoretical studies of nonlinear optical crystal Sr₂B₅O₉(OH)Â·H₂O. Physical Chemistry Chemical Physics, 2015, 17, 10489-10496.	1.3	26
2008	Synthesis and characterization of a new mid-infrared transparent compound: acentric Ba₅In₄Te₄S₇. Dalton Transactions, 2015, 44, 7673-7678.	1.6	14
2009	Pb6Ba2(BO3)5X (X = Cl, Br): new borate halides with strong predicted optical anisotropies derived from Pb2+and (BO3)3â^'. Dalton Transactions, 2015, 44, 7041-7047.	1.6	22
2010	The effect of the aliphatic carboxylate linkers on the electronic structures, chemical bonding and optical properties of the uranium-based metalâ€"organic frameworks. RSC Advances, 2015, 5, 26735-26748.	1.7	9
2011	K5Mo4O14F: A Novel Fluorinated Polyoxomolybdate and Its Structural Stability. Inorganic Chemistry, 2015, 54, 6066-6068.	1.9	7
2012	Further Search for Hydroxyl Nests in Acid Dealuminated Zeolite Y. Journal of Physical Chemistry C, 2015, 119, 8619-8625.	1.5	17
2013	Ab initio models for polycrystalline diamond constructed from cold-compressed disordered graphite. Materials Research Express, 2015, 2, 045601.	0.8	1
2014	Discovery of New Metastable Polymorphs in a Family of Urea Co-Crystals by Solid-State Mechanochemistry. Crystal Growth and Design, 2015, 15, 2901-2907.	1.4	34
2015	Experimental (X-ray, ¹³C CP/MAS NMR, IR, RS, INS, THz) and Solid-State DFT Study on (1:1) Co-Crystal of Bromanilic Acid and 2,6-Dimethylpyrazine. Journal of Physical Chemistry B, 2015, 119, 6852-6872.	1.2	18
2016	Structure of Pigment Yellow 181 dimethylsulfoxideN-methyl-2-pyrrolidone (1:1:1) solvate from XRPD + DFT-D. Acta Crystallographica Section B: Structural Science, Crystal Engineering and Materials, 2015, 71, 89-94.	0.5	6
2017	Complex physical properties of EuMgSi â€" a complementary study by neutron powder diffraction and¹⁵¹Eu MÃ¶ssbauer spectroscopy. Journal of Materials Chemistry C, 2015, 3, 7203-7215.	2.7	10

#	Article	IF	Citations
2018	Chalcogen vacancies in monolayer transition metal dichalcogenides and Fermi level pinning at contacts. Applied Physics Letters, 2015, 106, .	1.5	151
2019	Low-temperature physical properties and electronic structures of Ni ₃ Sb, Ni ₅ Sb ₂ , NiSb ₂ , and NiSb. Chinese Physics B, 2015, 24, 067201.	0.7	7
2020	Carrier-transport-path-induced switching parameter fluctuation in oxide-based resistive switching memory. Materials Research Express, 2015, 2, 046304.	0.8	10
2021	X-ray and NMR Crystallography Studies of Novel Theophylline Cocrystals Prepared by Liquid Assisted Grinding. Crystal Growth and Design, 2015, 15, 3674-3683.	1.4	57
2022	Pressure-induced semiconductor-to-metal transition in Mg ₂ Sn with the modified Becke-Johnson potential. Europhysics Letters, 2015, 109, 57002.	0.7	10
2023	A DFT-D study of the interaction of methane, carbon monoxide, and nitrogen with cation-exchanged SAPO-34. Zeitschrift Fur Kristallographie - Crystalline Materials, 2015, 230, 311-323.	0.4	2
2024	Synthesis, Crystal and Electronic Structure, and Optical Property of the Quaternary Selenide: La₃Sb_{0.33}SiSe₇. Zeitschrift Fur Anorganische Und Allgemeine Chemie, 2015, 641, 917-921.	0.6	5
2025	How focussing on hydrogen bonding interactions in amino acids can miss the bigger picture: a high-pressure neutron powder diffraction study of Îµ-glycine. CrystEngComm, 2015, 17, 5315-5328.	1.3	35
2026	Atomistic modeling to optimize composition and characterize structure of Niâ€“Zrâ€“Mo metallic glasses. Physical Chemistry Chemical Physics, 2015, 17, 13355-13365.	1.3	19
2027	A solid-state¹⁷O NMR study of platinum-carboxylate complexes: carboplatin and oxaliplatin. Canadian Journal of Chemistry, 2015, 93, 945-953.	0.6	19
2028	The effect of temperature and pressure on the crystal structure of piperidine. Chemistry Central Journal, 2015, 9, 18.	2.6	17
2029	High-Pressure Stability of Energetic Crystal of Dihydroxylammonium 5,5â€²-Bistetrazole-1,1â€²-diolate: Raman Spectroscopy and DFT Calculations. Journal of Physical Chemistry B, 2015, 119, 6836-6847.	1.2	51
2030	High thermoelectric and mechanical performance in highly dense Cu_{2â^'x}S bulks prepared by a melt-solidification technique. Journal of Materials Chemistry A, 2015, 3, 9432-9437.	5.2	176
2031	First-principle study of the electronic structures and optical properties of six typical hexaferrites. Computational Materials Science, 2015, 105, 27-31.	1.4	7
2032	Energetic stability, atomic and electronic structures of extended Î³-graphyne: A density functional study. Journal of Molecular Modeling, 2015, 21, 154.	0.8	7
2033	Introducing new half-integer quadrupolar nuclei for solid state NMR of inclusion compounds. Canadian Journal of Chemistry, 2015, 93, 1014-1024.	0.6	1
2034	Towards fully compensated ferrimagnetic spin gapless semiconductors for spintronic applications. Europhysics Letters, 2015, 111, 37009.	0.7	31
2035	First-principles Investigation on Diffusion Mechanism of Zinc in n-GaSb. Energy Procedia, 2015, 75, 2175-2180.	1.8	0

#	Article	IF	Citations
2036	Structural, elastic, and electronic properties of recently discovered ternary silicide superconductor Li₂IrSi₃: Anab-initiostudy. Chinese Physics B, 2015, 24, 117401.	0.7	33
2037	Self-interaction corrected LDA + U investigations of BiFeO₃properties: plane-wave pseudopotential method. Materials Research Express, 2015, 2, 116101.	0.8	30
2038	On the relaxation dynamics in active pharmaceutical ingredients: solid-state 1H NMR, quasi-elastic neutron scattering and periodic DFT study of acebutolol hydrochloride. RSC Advances, 2015, 5, 57502-57514.	1.7	4
2039	Vibrational Spectroscopy and Phonon-Related Properties of the <scp>l</scp>-Aspartic Acid Anhydrous Monoclinic Crystal. Journal of Physical Chemistry A, 2015, 119, 11791-11803.	1.1	22
2040	3D Behavior of Schottky Barriers of 2D Transition-Metal Dichalcogenides. ACS Applied Materials & Interfaces, 2015, 7, 25709-25715.	4.0	134
2041	On the Nb-Ge Binary System. Metallurgical and Materials Transactions A: Physical Metallurgy and Materials Science, 2015, 46, 5526-5536.	1.1	15
2042	Assessing distortion of the AF 6 â^' (A=As, Sb) octahedra in solid hexafluorometallates(V) via NMR spectroscopy. Canadian Journal of Chemistry, 2015, 93, 938-944.	0.6	8
2043	First-Principles Study on Ligand Binding and Positional Disorder in Pentlandite. Journal of Physical Chemistry C, 2015, 119, 25457-25468.	1.5	13
2044	Structural refinement of the RT LaOF phases by coupling powder X-Ray diffraction,¹⁹F and¹³⁹La solid state NMR and DFT calculations of the NMR parameters. Dalton Transactions, 2015, 44, 20675-20684.	1.6	21
2045	First-principles study on the electronic structure and optical properties of Mn-doped NaNbO3. , 2015, , .		0
2046	Exploring the low-friction mechanism of CN x films in inert atmospheres by first-principles calculations. Applied Surface Science, 2015, 356, 1082-1085.	3.1	8
2047	Crystal structures and properties of nitrogen oxides under high pressure. RSC Advances, 2015, 5, 103373-103379.	1.7	3
2048	Structural and electronic properties of Î£7 grain boundaries in Î±-Al2O3. Acta Materialia, 2015, 99, 16-28.	3.8	24
2049	In-between Bragg reflections: thermal diffuse scattering and vibrational spectroscopy with x-rays. Journal Physics D: Applied Physics, 2015, 48, 504003.	1.3	16
2050	Predicted Formation of H₃⁺ in Solid Halogen Polyhydrides at High Pressures. Journal of Physical Chemistry A, 2015, 119, 11059-11065.	1.1	19
2051	Mechanochemical Production of Halogen-Bonded Solids Featuring Pâ•ÖÂ·Â·Â·Iâ€“C Motifs and Characterization via X-ray Diffraction, Solid-State Multinuclear Magnetic Resonance, and Density Functional Theory. Journal of Physical Chemistry C, 2015, 119, 27104-27117.	1.5	45
2052	Computational searches for iron oxides at high pressures. Journal of Physics Condensed Matter, 2015, 27, 455501.	0.7	44
2053	Interfacial properties of<mml:math xmlns:mml="http://www.w3.org/1998/Math/MathML" altimg="si1.gif" overflow="scroll"><mml:mi>Î±</mml:mi><mml:mo stretchy="false">/</mml:mo><mml:mi>Î²</mml:mi></mml:math>-Bi 2 O 3 homo-junction from first-principles calculations. Physics Letters, Section A: General, Atomic and Solid State Physics, 2015, 379, 2766-2771.	0.9	30

#	Article	IF	Citations
2054	Current limitations of molecular dynamic simulations as probes of thermo-physical behavior of silicate melts. American Mineralogist, 2015, 100, 1866-1882.	0.9	14
2055	Interplay of Noncovalent Interactions in Ribbon-like Guanosine Self-Assembly: An NMR Crystallography Study. Crystal Growth and Design, 2015, 15, 5945-5954.	1.4	40
2056	QMC and phonon study of super-hard cubic boron carbon nitride. Materials Research Express, 2015, 2, 105902.	0.8	5
2057	A theoretical and experimental study of the crystal structure of H₂V₃O₈. RSC Advances, 2015, 5, 106543-106550.	1.7	17
2058	Electron behavior in hydrogen atom under electric fields. , 2015, , .		1
2059	Methylene Blue Adsorption on the Basal Surfaces of Kaolinite: Structure and Thermodynamics from Quantum and Classical Molecular Simulation. Clays and Clay Minerals, 2015, 63, 185-198.	0.6	45
2060	Characterization of M-O bonds in Y₂Ti₂O₇and Y₂TiO₅with EELS. Physica Status Solidi (B): Basic Research, 2015, 252, 206-211.	0.7	5
2061	Ab initio investigation of the intermetallics in the Nbâ€“Sn binary system. Acta Materialia, 2015, 86, 23-33.	3.8	39
2062	Phonon and electronic properties of Ti 2 SiC from first-principles calculations. Solid State Communications, 2015, 204, 37-40.	0.9	18
2063	Theoretical investigations on the elastic wave propagation and phonon focusing in AlLi crystal. Materials Chemistry and Physics, 2015, 152, 34-40.	2.0	2
2064	Modeling hydrogen storage in boron-substituted graphene decorated with potassium metal atoms. International Journal of Energy Research, 2015, 39, 524-528.	2.2	21
2065	Thermally accessible triplet state of Ï€-nucleophiles does exist. Evidence from first principles study of ethylene interaction with copper species. RSC Advances, 2015, 5, 11558-11569.	1.7	19
2066	Correlation between electronic properties and reactivity toward oxygen of tetrahedral goldâ€“silver clusters. Computational and Theoretical Chemistry, 2015, 1055, 61-67.	1.1	14
2067	Evidence of â€œnew hot spotsâ€•from determining the nonlinear optical behavior of materials: mechanistic studies of the vanadium borate crystal, Na₃VO₂B₆O₁₁. Physical Chemistry Chemical Physics, 2015, 17, 5338-5344.	1.3	15
2068	Anab initiostudy of the structural, elastic, electronic and optical properties of the newly synthesized nitridoaluminate LiCaAlN₂. Philosophical Magazine, 2015, 95, 41-63.	0.7	4
2069	Syntheses, structures, and optical properties of Ba₄Ga₄SnSe₁₂and Ba₆Ga₂SnSe₁₁. Dalton Transactions, 2015, 44, 2259-2266.	1.6	18
2070	The elastic, electronic and thermodynamic properties of PdTe under high pressure from first-principles calculations. Physica C: Superconductivity and Its Applications, 2015, 509, 34-41.	0.6	13
2071	First-principles and Monte Carlo studies on the magnetic stability of half-metallic zinc-blende CaC and similar compounds. Journal of Magnetism and Magnetic Materials, 2015, 378, 469-477.	1.0	13

#	Article	IF	Citations
2072	Structure and bonding nature of [PbCl]+ adsorption on the kaolinite(0 0 1) surface in aqueous system. Applied Surface Science, 2015, 330, 411-417.	3.1	7
2073	Room-temperature ferromagnetism with high magnetic moment in Cu-doped AlN single crystal whiskers. Chinese Physics B, 2015, 24, 027503.	0.7	3
2074	Phase transitions and mechanical stability of TiO2 polymorphs under high pressure. Journal of Alloys and Compounds, 2015, 631, 192-201.	2.8	70
2075	Study of the reaction products of SF6 and C in the laser heated diamond anvil cell by pair distribution function analysis and micro-Raman spectroscopy. Journal of Solid State Chemistry, 2015, 225, 141-148.	1.4	4
2076	Tailored Synthesis of a Nonlinear Optical Phosphate with a Short Absorption Edge. Angewandte Chemie - International Edition, 2015, 54, 4217-4221.	7.2	205
2077	On the possibility of p-type doping of SnO2 with Mg: A first-principles study. Computational Materials Science, 2015, 101, 62-65.	1.4	14
2078	Synthesis of nanocrystalline molybdenum carbide materials and their characterization. Catalysis Today, 2015, 250, 123-133.	2.2	50
2079	Correlation-induced metal-insulator transitions in d0 magnetic superlattices based on alkaline-earth monoxides: Insights from ab initio calculations. Journal of Magnetism and Magnetic Materials, 2015, 384, 33-39.	1.0	8
2080	Origin of electronic properties of PbGa2Se4 crystal: Experimental and theoretical investigations. Journal of Alloys and Compounds, 2015, 633, 415-423.	2.8	15
2081	PbGa₂MSe₆ (M = Si, Ge): Two Exceptional Infrared Nonlinear Optical Crystals. Chemistry of Materials, 2015, 27, 914-922.	3.2	110
2082	Structures and charge transport properties of â€œselenosulflowerâ€•and its selenium analogue â€œselfloweâ€• computer-aided design of high-performance ambipolar organic semiconductors. Journal of Materials Chemistry C, 2015, 3, 3472-3481.	2.7	25
2083	Polymorphism of Resorcinol Explored by Complementary Vibrational Spectroscopy (FT-RS, THz-TDS,) Tj ETQq1 1 0.784314 rgBT /Over 2015, 119, 1681-1695.	1.2	35
2084	Direct Validation of the Single Step Classical to Quantum Free Energy Perturbation. Journal of Physical Chemistry B, 2015, 119, 1017-1025.	1.2	45
2085	How the Surface Structure Determines the Properties of CuH. Inorganic Chemistry, 2015, 54, 2213-2220.	1.9	27
2086	Piezoelectric field enhancement in IIIâ€“V coreâ€“shell nanowires. Nano Energy, 2015, 14, 382-391.	8.2	46
2087	The Effects of Te^{2â¯} and I^{â¯} Substitutions on the Electronic Structures, Thermoelectric Performance, and Hardness in Meltâ€Quenched Highly Dense Cu_{2â€x}Se. Advanced Electronic Materials, 2015, 1, 1400015.	2.6	51
2088	Lithiation Behavior of High Capacity SiCO Anode Material for Lithium-ion Battery: A First Principle Study. Electrochimica Acta, 2015, 156, 115-120.	2.6	11
2089	Vibrational and electronic peculiarities of NiTiO₃nanostructures inferred from first principle calculations. RSC Advances, 2015, 5, 17396-17404.	1.7	37

#	Article	IF	Citations
2090	Robust Two-Dimensional Topological Insulators in Methyl-Functionalized Bismuth, Antimony, and Lead Bilayer Films. Nano Letters, 2015, 15, 1083-1089.	4.5	166
2091	First principle calculations of nitric oxide on metallic Pt (111) and Pt (100), and bimetallic Au/Pt (111) and Au/Pt (100) surfaces. Applied Surface Science, 2015, 328, 591-595.	3.1	9
2092	Study on electronic structures and mechanical properties of new predicted orthorhombic Mg2SiO4 under high pressure. Journal of Alloys and Compounds, 2015, 630, 11-22.	2.8	4
2093	The structural and magnetic properties of Fe2â^'xNiGa1+x Heusler alloys. Physica B: Condensed Matter, 2015, 462, 93-96.	1.3	6
2094	Fermiology of 122 family of Fe-based superconductors: An ab initio study. Physics Letters, Section A: General, Atomic and Solid State Physics, 2015, 379, 843-847.	0.9	16
2095	Are the amide bonds in N-acyl imidazoles twisted? A combined solid-state 17O NMR, crystallographic, and computational study. Canadian Journal of Chemistry, 2015, 93, 451-458.	0.6	10
2096	Computational Identification and Experimental Realization of Lithium Vacancy Introduction into the Olivine LiMgPO₄. Chemistry of Materials, 2015, 27, 2074-2091.	3.2	33
2097	Structural Stability, Electronic Structure and Mechanical Properties of Liâ€“Nâ€“H System. Acta Metallurgica Sinica (English Letters), 2015, 28, 550-558.	1.5	2
2098	BaMn₉[VO₄]₆(OH)₂: A Unique Canted Antiferromagnet with a Chiral â€œPaddle-Wheelâ€•Structural Feature. Inorganic Chemistry, 2015, 54, 898-904.	1.9	14
2099	Structural Analysis of Some High-Pressure Stable and Metastable Phases in Lithium Borohydride LiBH₄. Journal of Physical Chemistry C, 2015, 119, 3911-3917.	1.5	8
2100	Epitaxial Retrieval of a Disappearing Polymorph. Crystal Growth and Design, 2015, 15, 115-123.	1.4	10
2101	Light Metals on Oxygen-Terminated Diamond (100): Structure and Electronic Properties. Chemistry of Materials, 2015, 27, 1306-1315.	3.2	26
2102	A Theoretical Study of the Effect of Dopants on Diamond (100) Surface Stabilization for Different Termination Scenarios. Journal of Physical Chemistry C, 2015, 119, 2545-2556.	1.5	10
2103	Effects of different concentration S-doping on the structural stability and electronic structures of delafossite CuAlO2. Computational Materials Science, 2015, 101, 152-155.	1.4	14
2104	Polyaniline-Decorated {001} Facets of Bi₂O₂CO₃ Nanosheets: In Situ Oxygen Vacancy Formation and Enhanced Visible Light Photocatalytic Activity. ACS Applied Materials & Interfaces, 2015, 7, 730-737.	4.0	205
2105	Ab initio study on the mechanical and electronic properties of the Ti1-xNbxN alloys. European Physical Journal B, 2015, 88, 1.	0.6	7
2106	Simulated pressure-induced blue-shift of phase-matching region and nonlinear optical mechanism for K3B6O10X (Xâ€‰=â€‰Cl, Br). Applied Physics Letters, 2015, 106, .	1.5	121
2107	A Review of 91Zr Solid-State Nuclear Magnetic Resonance Spectroscopy. Annual Reports on NMR Spectroscopy, 2015, 84, 233-289.	0.7	12

#	Article	IF	Citations
2108	Novel superconducting skutterudite-type phosphorus nitride at high pressure from first-principles calculations. Scientific Reports, 2014, 4, 5889.	1.6	29
2109	A novel method of identifying the carrier transport path in metal oxide resistive random access memory. Journal Physics D: Applied Physics, 2015, 48, 065101.	1.3	25
2110	High-Pressure Experimental and DFT-D Structural Studies of the Energetic Material FOX-7. Journal of Physical Chemistry C, 2015, 119, 2322-2334.	1.5	69
2111	<scp>L</scp>â€Lysine: Exploiting Powder Xâ€ray Diffraction to Complete the Set of Crystal Structures of the 20 Directly Encoded Proteinogenic Amino Acids. Angewandte Chemie - International Edition, 2015, 54, 3973-3977.	7.2	55
2112	Radiolytic hydrogen generation from aluminum oxyhydroxide solids: theory and experiment. Journal of Radioanalytical and Nuclear Chemistry, 2015, 303, 81-86.	0.7	27
2113	New insights into the nitroaromatics-detection mechanism of the luminescent metalâ€“organic framework sensor. Dalton Transactions, 2015, 44, 2897-2906.	1.6	50
2114	First-principles calculation of the band structure, electronic states, and optical properties of Cr-doped ZnS double-wall nanotubes. Computational Materials Science, 2015, 101, 1-7.	1.4	18
2115	Hydrostatic pressure effects on the electronic, optical, and photocatalytic properties of ribbon-like Bi2S3: A DFT study. Superlattices and Microstructures, 2015, 81, 49-63.	1.4	32
2116	Magnetostructural relationship in the tetrahedral spin-chain oxideCsCoO2. Physical Review B, 2015, 91, .	1.1	2
2117	First-principles investigation of the elastic and thermodynamic properties of ReC2 (Re = Ho, Nd, Pr). Modern Physics Letters B, 2015, 29, 1450256.	1.0	2
2118	Beryllium-Free Rb₃Al₃B₃O₁₀F with Reinforced Interlayer Bonding as a Deep-Ultraviolet Nonlinear Optical Crystal. Journal of the American Chemical Society, 2015, 137, 2207-2210.	6.6	237
2119	Role of Oxygen Vacancy on the Photoluminescence of BaMgSiO₄:Eu Phosphors: Experimental and Theoretical Analysis. Inorganic Chemistry, 2015, 54, 1556-1562.	1.9	83
2120	High-pressure phases of SF6 up to 32GPa from X-ray diffraction and Raman spectroscopy. Journal of Physics and Chemistry of Solids, 2015, 80, 11-21.	1.9	4
2121	Origin of photocatalytic activity of nitrogen-doped germanium dioxide under visible light from first principles. Materials Science in Semiconductor Processing, 2015, 31, 517-524.	1.9	8
2122	Assessing the Viability of Extended Nonmetal Atom Chains in M_nF_{4n+2} (M=S and Se). Angewandte Chemie - International Edition, 2015, 54, 1476-1480.	7.2	15
2123	Effect of configuration and biaxial strain to electronic structure of half-fluorinated graphene. Surface Science, 2015, 635, 78-84.	0.8	13
2124	First-principles study of electronic structure of CuSbS2 and CuSbSe2 photovoltaic semiconductors. Thin Solid Films, 2015, 582, 401-407.	0.8	44
2125	Theoretical investigation of the electronic structure, optical, elastic, hardness and thermodynamics properties of jadeite. Materials Science in Semiconductor Processing, 2015, 31, 509-516.	1.9	14

#	Article	IF	Citations
2126	Elastic and electronic properties of Imm2- and I<mml:math xmlns:mml="http://www.w3.org/1998/Math/MathML" altimg="si1.gif" overflow="scroll"><mml:mrow><mml:mover accent="true"><mml:mrow><mml:mn>4</mml:mn></mml:mrow><mml:mrow><mml:mo>Â¯</mml:mo></mml:mrow></mml:mover></m Computational Materials Science, 2015, 97, 6-13.	1.4	25
2127	Three Alkali Metal Lead Orthophosphates â€“ Syntheses, Crystal Structures and Properties of APbPO₄ (A = K, Rb, Cs). European Journal of Inorganic Chemistry, 2015, 2015, 1490-1495.	1.0	17
2128	Solid state forms of 4-aminoquinaldine â€“ from void structures with and without solvent inclusion to close packing. CrystEngComm, 2015, 17, 2504-2516.	1.3	18
2129	Thermodynamic mixing properties of the UO2â€“HfO2 solid solution: Density functional theory and Monte Carlo simulations. Journal of Nuclear Materials, 2015, 458, 296-303.	1.3	3
2130	DFT study of structural, elastic properties and thermodynamic parameters of Bi2S3 under hydrostatic pressures. Computational Materials Science, 2015, 101, 301-312.	1.4	28
2131	Electronic structures and mechanical properties of Al(111)/ZrB₂(0001) heterojunctions from first-principles calculation. Molecular Physics, 2015, 113, 1794-1801.	0.8	21
2132	Comparative theoretical study of formic acid decomposition on PtAg(111) and Pt(111) surfaces. RSC Advances, 2015, 5, 21170-21177.	1.7	19
2133	Manipulating the orientation of an organic adsorbate on silicon: a NEXAFS study of acetophenone on Si(0â€‰0â€‰1). Journal of Physics Condensed Matter, 2015, 27, 054002.	0.7	10
2134	Exploring atomic defects in molybdenum disulphide monolayers. Nature Communications, 2015, 6, 6293.	5.8	1,124
2135	First-principles investigation of the electronic, mechanical, and thermodynamic properties of europium carbide. Canadian Journal of Physics, 2015, 93, 409-412.	0.4	16
2136	Ultrahardness: Measurement and Enhancement. Journal of Physical Chemistry C, 2015, 119, 5633-5638.	1.5	37
2137	Adsorption of Pb(II) on the kaolinite(001) surface in aqueous system: A DFT approach. Applied Surface Science, 2015, 339, 28-35.	3.1	47
2138	Molecular Dynamics with On-the-Fly Machine Learning of Quantum-Mechanical Forces. Physical Review Letters, 2015, 114, 096405.	2.9	470
2139	Strain tunable electronic and magnetic properties of pristine and semihydrogenated hexagonal boron phosphide. Applied Physics Letters, 2015, 106, .	1.5	35
2140	Bi₂Te(IO₃)O₅Cl: a novel polar iodate oxychloride exhibiting a second-order nonlinear optical response. Dalton Transactions, 2015, 44, 2469-2475.	1.6	28
2141	Terahertz Time-Domain and Low-Frequency Raman Spectroscopy of Organic Materials. Applied Spectroscopy, 2015, 69, 1-25.	1.2	153
2142	Crystallization and disorder of the polytypic Î±₁and Î±₂polymorphs of piroxicam. CrystEngComm, 2015, 17, 5266-5272.	1.3	23
2143	Concomitant conformational dimorphism in 1,2-bis(9-anthryl)acetylene. CrystEngComm, 2015, 17, 4877-4882.	1.3	10

#	Article	IF	Citations
2144	Chemical Descriptors of Yttria-Stabilized Zirconia at Low Defect Concentration: An ab Initio Study. Journal of Physical Chemistry A, 2015, 119, 6412-6420.	1.1	16
2145	Comparison of oxygen vacancy defects in crystalline and amorphous Ta2O5. Microelectronic Engineering, 2015, 147, 254-259.	1.1	25
2146	Prediction of 10-fold coordinated TiO ₂ and SiO ₂ structures at multimegabar pressures. Proceedings of the National Academy of Sciences of the United States of America, 2015, 112, 6898-6901.	3.3	54
2147	Graphene growth on Pt(111) and Au(111) using a MBE carbon solid-source. Diamond and Related Materials, 2015, 57, 58-62.	1.8	27
2148	Calculation of TiO₂ Surface and Subsurface Oxygen Vacancy by the Screened Exchange Functional. Journal of Physical Chemistry C, 2015, 119, 18160-18166.	1.5	136
2149	Structural and mechanic properties of RFeO3 with R = Y, Eu and La perovskites: a first-principles calculation. European Physical Journal D, 2015, 69, 1.	0.6	10
2150	Transition metal incorporation into mackinawite (tetragonal FeS). American Mineralogist, 2015, 100, 1509-1517.	0.9	26
2151	Probing the sorption reactivity of the edge surfaces in birnessite nanoparticles using nickel(II). Geochimica Et Cosmochimica Acta, 2015, 164, 191-204.	1.6	75
2152	Electronic band structure and optical properties of ferroelectric TGS, TGSe and TGFB crystals. Materials Chemistry and Physics, 2015, 162, 787-793.	2.0	4
2153	Thermal expansion of mullite-type Bi2Al4O9: A study by X-ray diffraction, vibrational spectroscopy and density functional theory. Journal of Solid State Chemistry, 2015, 229, 87-96.	1.4	29
2154	K₃LaTe₂O₉: a new alkali-rare earth tellurate with face-sharing TeO₆ octahedra. Dalton Transactions, 2015, 44, 15576-15582.	1.6	10
2155	Electronic transport calculations in the onetep code: Implementation and applications. Computer Physics Communications, 2015, 193, 78-88.	3.0	10
2156	NaIn3S5, a new compound from the CaSâ€“In2S3/NaBr system. Journal of Alloys and Compounds, 2015, 624, 279-283.	2.8	10
2157	Channel length dependence of field-effect mobility ofc-axis-aligned crystalline Inâ€“Gaâ€“Znâ€“O field-effect transistors. Japanese Journal of Applied Physics, 2015, 54, 041103.	0.8	13
2158	DFT study of the effects of interstitial impurities on the resistance of Cr-doped Î³-Fe(111) surface dissolution corrosion. Journal of Molecular Modeling, 2015, 21, 206.	0.8	6
2159	Two New Crystals in LimCsnBm+nO2(m+n)(m+n= 5, 7;m>n) Series: Noncentrosymmetric Li5Cs2B7O14and Centrosymmetric Li4CsB5O10. Inorganic Chemistry, 2015, 54, 7381-7387.	1.9	17
2160	Electronic structure, optical and dielectric properties of BaTiO₃/CaTiO₃/SrTiO₃ ferroelectric superlattices from first-principles calculations. Journal of Materials Chemistry C, 2015, 3, 8625-8633.	2.7	96
2161	Effects of alloying on oxidation and dissolution corrosion of the surface of Î³-Fe(111): a DFT study. Journal of Molecular Modeling, 2015, 21, 181.	0.8	17

#	Article	IF	Citations
2162	Study of the growth kinetics of biomimetically grown hydroxyapatite coatings in large gradient magnetic fields. Applied Surface Science, 2015, 351, 594-599.	3.1	2
2163	Spinâ€“Spin Coupling between Quadrupolar Nuclei in Solids: ¹¹Bâ€“⁷⁵As Spin Pairs in Lewis Acidâ€“Base Adducts. Journal of Physical Chemistry A, 2015, 119, 6949-6960.	1.1	6
2164	Solid-State 17O NMR of Oxygenâ€“Nitrogen Singly Bonded Compounds: Hydroxylammonium Chloride and Sodium Trioxodinitrate (Angeliâ€™s Salt). Journal of Physical Chemistry A, 2015, 119, 8133-8138.	1.1	13
2165	Spontaneous Local Symmetry Breaking: A Conformational Study of Glycine on Cu{311}. Journal of Physical Chemistry C, 2015, 119, 13041-13049.	1.5	12
2166	High-Field17O MAS NMR Reveals1J(17O-127I) with its Sign and the NMR Crystallography of the Scheelite Structures for NaIO4and KIO4. Journal of Physical Chemistry C, 2015, , 150612155518000.	1.5	9
2167	A furosemideâ€“isonicotinamide cocrystal: an investigation of properties and extensive structural disorder. CrystEngComm, 2015, 17, 6707-6715.	1.3	38
2168	An unusual density evolution between SrCdB2O5 polymorphs. Dalton Transactions, 2015, 44, 15823-15828.	1.6	5
2169	A trimetallic Vâ€“Coâ€“Fe oxide nanoparticle as an efficient and stable electrocatalyst for oxygen evolution reaction. Journal of Materials Chemistry A, 2015, 3, 17763-17770.	5.2	121
2170	Photocatalytic activity of ZnO/GaP_{1â^'x}N_xfor water splitting. Journal of Materials Chemistry A, 2015, 3, 18083-18089.	5.2	14
2171	C2/m-carbon: structural, mechanical, and electronic properties. Journal of Materials Science, 2015, 50, 7104-7114.	1.7	44
2172	Systematic Optimization of a Force Field for Classical Simulations of TiO₂â€“Water Interfaces. Journal of Physical Chemistry C, 2015, 119, 18110-18125.	1.5	53
2173	Pressure-Induced Amorphization and Recrystallization of SnI₂. Journal of Physical Chemistry C, 2015, 119, 19312-19317.	1.5	5
2174	Theoretical study on the structures and optical absorption of Si₁₇₂nanoclusters. Nanoscale, 2015, 7, 14444-14451.	2.8	15
2175	Novel optical properties of Î³-Si3N4 with B dopant. Materials Chemistry and Physics, 2015, 161, 170-174.	2.0	1
2176	Structural, elastic, electronic and optical properties of KAl Q 2 (Q Â=ÂSe, Te): A DFT study. Solid State Sciences, 2015, 48, 72-81.	1.5	24
2177	Two-Dimensional Ordering of Ionic Liquids Confined by Layered Silicate Plates via Molecular Dynamics Simulation. Journal of Physical Chemistry C, 2015, 119, 19244-19252.	1.5	27
2178	Are the Crystal Structures of Enantiopure and Racemic Mandelic Acids Determined by Kinetics or Thermodynamics?. Journal of the American Chemical Society, 2015, 137, 11095-11104.	6.6	57
2179	Magnetic and Electronic Properties of Selected Rare-Earth Chromium Germanides Compounds. Acta Physica Polonica A, 2015, 127, 385-387.	0.2	2

#	Article	IF	Citations
2180	Modification mechanism of praseodymium doping for the photocatalytic performance of TiO₂: a combined experimental and theoretical study. Physical Chemistry Chemical Physics, 2015, 17, 19087-19095.	1.3	15
2181	Structural stability and fission product behaviour in U3Si. Journal of Nuclear Materials, 2015, 466, 739-744.	1.3	22
2182	Flexible band gap tuning of hexagonal boron nitride sheets interconnected by acetylenic bonds. Physical Chemistry Chemical Physics, 2015, 17, 20376-20381.	1.3	11
2183	The new dimension of silver. Physical Chemistry Chemical Physics, 2015, 17, 19695-19699.	1.3	52
2184	Backbone NxH compounds at high pressures. Journal of Chemical Physics, 2015, 142, 214308.	1.2	38
2185	An Investigation of Structural and Electronic Properties of Novel Cathode Material Li₂MnP₂O₇ and its Delithiated Li_{2-x}MnP₂O₇ (x=1,2): A First Principle Study. Advanced Materials Research, 2015, 1107, 485-490.	0.3	0
2186	CO adsorption complexes in zeolites: How does the inclusion of dispersion interactions affect predictions made from DFT calculations? The case of Na-CHA. Theoretical Chemistry Accounts, 2015, 134, 1.	0.5	17
2187	An NMR crystallography study of the hemihydrate of 2â€², 3â€²-O-isopropylidineguanosine. Solid State Nuclear Magnetic Resonance, 2015, 65, 41-48.	1.5	48
2188	Pb₂Ba₃(BO₃)₃Cl: A Material with Large SHG Enhancement Activated by Pb-Chelated BO₃ Groups. Journal of the American Chemical Society, 2015, 137, 9417-9422.	6.6	255
2189	Synthesis and thermoelectric properties of half-Heusler alloy YNiBi. Journal of Applied Physics, 2015, 117, .	1.1	35
2190	Navigating the Waters of Unconventional Crystalline Hydrates. Molecular Pharmaceutics, 2015, 12, 3069-3088.	2.3	62
2191	Structural investigations in BaFe_{2â€…â^'â€…x}Ru_xAs₂as a function of Ru and temperature. Acta Crystallographica Section B: Structural Science, Crystal Engineering and Materials, 2015, 71, 61-67.	0.5	15
2192	First Principles Study on Structural and Electronic Properties of LiFeSO₄F Cathode Material for Lithium Ion Batteries. Advanced Materials Research, 0, 1107, 508-513.	0.3	3
2193	Sn2SiS4, synthesis, structure, optical and electronic properties. Optical Materials, 2015, 47, 379-385.	1.7	14
2194	A new phase from compression of carbon nanotubes with anisotropic Dirac fermions. Scientific Reports, 2015, 5, 10713.	1.6	23
2195	Effect of salt on the H-bond symmetrization in ice. Proceedings of the National Academy of Sciences of the United States of America, 2015, 112, 8216-8220.	3.3	58
2196	First-Principles Study of Electronic and Elastic Properties of Hexagonal Layered Crystal MoS₂ Under Pressure. Zeitschrift Fur Naturforschung - Section A Journal of Physical Sciences, 2015, 70, 529-537.	0.7	13
2197	Insight into the Segregation Phenomenon in Metal-Cation-Doped Aluminum Sol during the Drying Process with NO3â€“ as Counterions. Journal of Physical Chemistry C, 2015, 119, 13915-13921.	1.5	4

#	Article	IF	Citations
2198	Thermodynamic predicting and atomistic modeling the favored compositions for Mgâ€“Niâ€“Y metallic glasses. RSC Advances, 2015, 5, 60220-60229.	1.7	3
2199	Appraisal of the realistic accuracy of molecular dynamics of high-pressure hydrogen. Cogent Physics, 2015, 2, 1049477.	0.7	11
2200	Theoretical study of core-loss electron energy-loss spectroscopy at graphene nanoribbon edges. Journal of Physics Condensed Matter, 2015, 27, 305301.	0.7	5
2201	Electronic structure, magnetic and optical properties of the Ba7(BO3)4â˜F2+3 crystal. Journal of Solid State Chemistry, 2015, 229, 358-365.	1.4	7
2202	Lattice dynamics ofÎ±-cristobalite and the Boson peak in silica glass. Journal of Physics Condensed Matter, 2015, 27, 305401.	0.7	18
2203	Effect of oxygen and nitrogen functionalization on the physical and electronic structure of graphene. Nano Research, 2015, 8, 2620-2635.	5.8	47
2204	The synthesis and gas sensitivity of the Î²-Ti3O5 powder: Experimental and DFT study. Journal of Alloys and Compounds, 2015, 649, 939-948.	2.8	19
2205	Contribution of lone-pairs to birefringence affected by the Pb(<scp>ii</scp>) coordination environment: a DFT investigation. Physical Chemistry Chemical Physics, 2015, 17, 21968-21973.	1.3	55
2206	First principle calculations of elastic and thermodynamic properties of Ir3Nb and Ir3V with L12 structure under high pressure. Intermetallics, 2015, 66, 103-110.	1.8	11
2207	Manganeseâ€“Vanadate Hybrids: Impact of Organic Ligands on Their Structures, Thermal Stabilities, Optical Properties, and Photocatalytic Activities. Inorganic Chemistry, 2015, 54, 7388-7401.	1.9	16
2208	Performance of Frozen Density Embedding for Modeling Hole Transfer Reactions. Journal of Physical Chemistry B, 2015, 119, 7541-7557.	1.2	46
2209	Relationships among the structural topology, bond strength, and mechanical properties of single-walled aluminosilicate nanotubes. Nanoscale, 2015, 7, 16222-16229.	2.8	15
2210	Three dimensional graphdiyne polymers with tunable band gaps. Carbon, 2015, 91, 518-526.	5.4	35
2211	Elevated Curie temperature and half-metallicity in the ferromagnetic semiconductorLaxEu1â˜xO. Physical Review B, 2015, 92, .	1.1	5
2212	Identification of electrochemical reaction products in lithiumâ€“oxygen cells with ⁷Li nutation spectroscopy. Canadian Journal of Chemistry, 2015, 93, 976-982.	0.6	3
2213	Structural, elastic, electronic and optical properties of the quaternary nitridogallate LiCaGaN2: First-principles study. Materials Science in Semiconductor Processing, 2015, 40, 64-76.	1.9	19
2214	Methanol formation by catalytic hydrogenation of CO₂on a nitrogen doped zinc oxide surface: an evaluative study on the mechanistic pathway by density functional theory. RSC Advances, 2015, 5, 60524-60533.	1.7	7
2215	Role ofd-dandp-dhybridization in CoTi-based magnetic semiconductors with 21 and 26 valence electrons. Journal Physics D: Applied Physics, 2015, 48, 325001.	1.3	23

#	Article	IF	Citations
2216	Low-energy tetrahedral polymorphs of carbon, silicon, and germanium. Physical Review B, 2015, 91, .	1.1	90
2217	Optical properties of Î± -, Î² -, Î³ -, and 6,6,12-graphyne structures: First-principle calculations. Physica E: Low-Dimensional Systems and Nanostructures, 2015, 74, 438-442.	1.3	51
2218	Structural, Mechanical, and Electronic Properties of Monoclinic N2H5N3 Under Pressure. Brazilian Journal of Physics, 2015, 45, 399-403.	0.7	3
2219	Ab initio investigation of the Nbâ€“Al system. Computational Materials Science, 2015, 107, 116-121.	1.4	33
2220	Polar Polymorphism: Î±-, Î²-, and Î³-Pb₂Ba₄Zn₄B₁₄O₃₁â€“Synthesis, Characterization, and Nonlinear Optical Properties. Chemistry of Materials, 2015, 27, 4779-4788.	3.2	75
2221	Post-anti-van't Hoff-Le Bel motif in atomically thin germaniumâ€“copper alloy film. Physical Chemistry Chemical Physics, 2015, 17, 17545-17551.	1.3	81
2222	Reactive simulation of the chemistry behind the condensed-phase ignition of RDX from hot spots. Physical Chemistry Chemical Physics, 2015, 17, 18790-18801.	1.3	28
2223	First-Principles Electronic Transport. Springer Theses, 2015, , 63-86.	0.0	0
2224	Thiolate-Bonded Self-Assembled Monolayers on Ni(111): Bonding Strength, Structure, and Stability. Journal of Physical Chemistry C, 2015, 119, 15455-15468.	1.5	21
2225	Experimental evidence of new tetragonal polymorphs of silicon formed through ultrafast laser-induced confined microexplosion. Nature Communications, 2015, 6, 7555.	5.8	122
2226	First-principles calculations of Mg₂X (X = Si, Ge, Sn) semiconductors with the calcium fluorite structure. Journal of Semiconductors, 2015, 36, 053002.	2.0	5
2227	Lattice Vibrations and Spectroscopy of Mantle Phases. , 2015, , 203-231.		3
2228	Cocrystal or Salt: Solid State-Controlled Iodine Shift in Crystalline Halogen-Bonded Systems. Crystal Growth and Design, 2015, 15, 3464-3473.	1.4	76
2229	Reexamination of formic acid decomposition on the Pt(111) surface both in the absence and in the presence of water, from periodic DFT calculations. Catalysis Science and Technology, 2015, 5, 3322-3332.	2.1	13
2230	Ba₇(BO₃)₃GeO₄X (XÂ= Cl, Br): borogermanate halides with rigid GeO₄tetrahedra and flexible XBa₆octahedra. RSC Advances, 2015, 5, 53448-53454.	1.7	11
2231	Unusual Intermolecular â€œThrough-Spaceâ€•J Couplings in Pâ€“Se Heterocycles. Journal of the American Chemical Society, 2015, 137, 6172-6175.	6.6	24
2232	Characterization of the Dynamics in the Protonic Conductor CsH₂PO₄ by ¹⁷O Solid-State NMR Spectroscopy and First-Principles Calculations: Correlating Phosphate and Protonic Motion. Journal of the American Chemical Society, 2015, 137, 3867-3876.	6.6	53
2233	Synthesis and Characterization of Mid-Infrared Transparency Compounds: Acentric BaHgS2and Centric Ba8Hg4S5Se7. Inorganic Chemistry, 2015, 54, 2772-2779.	1.9	47

#	Article	IF	Citations
2234	PbGa₄S₇: a wide-gap nonlinear optical material. Journal of Materials Chemistry C, 2015, 3, 3060-3067.	2.7	80
2235	Synthesis, Crystal Structure and Properties of the Strontium Vanadate Fluoride Sr₅(VO₄)₃F. Zeitschrift Fur Anorganische Und Allgemeine Chemie, 2015, 641, 1211-1215.	0.6	11
2236	Zero Thermal Expansion in ZrMgMo₃O₁₂: NMR Crystallography Reveals Origins of Thermoelastic Properties. Chemistry of Materials, 2015, 27, 2633-2646.	3.2	90
2237	SnGa₂GeS₆: synthesis, structure, linear and nonlinear optical properties. Dalton Transactions, 2015, 44, 7404-7410.	1.6	40
2239	Electronic structure and optical properties of B/P-doped amorphous Si calculated by first-principles. Journal of Alloys and Compounds, 2015, 638, 59-66.	2.8	5
2240	AlN-GeO2 based gate stack for improved reliability of Ge MOSFETs. Microelectronic Engineering, 2015, 147, 168-170.	1.1	6
2241	Materials discovery via CALYPSO methodology. Journal of Physics Condensed Matter, 2015, 27, 203203.	0.7	93
2242	Hydrothermal synthesis of a new Bi-based (Ba0.82K0.18)(Bi0.53Pb0.47)O3 superconductor. Journal of Alloys and Compounds, 2015, 634, 208-214.	2.8	38
2243	Mapping Out Chemically Similar, Crystallographically Nonequivalent Hydrogen Sites in Metalâ€“Organic Frameworks by ¹H Solid-State NMR Spectroscopy. Chemistry of Materials, 2015, 27, 3306-3316.	3.2	46
2244	Modelling proton tunnelling in the adenineâ€“thymine base pair. Physical Chemistry Chemical Physics, 2015, 17, 13034-13044.	1.3	54
2245	Extraordinary diffusion in Co/Cu grain boundaries. Scripta Materialia, 2015, 101, 52-55.	2.6	0
2246	Homogeneous shear-driven reversible Î±-to-Î±â€³ phase transformation and superelasticity of titanium investigated by molecular dynamics simulations. Acta Materialia, 2015, 93, 105-113.	3.8	9
2247	Density functional study of Î±-graphyne derivatives: Energetic stability, atomic and electronic structure. Physica E: Low-Dimensional Systems and Nanostructures, 2015, 70, 190-197.	1.3	13
2248	Structural, elastic, electronic and optical properties of new layered semiconductor BaGa2P2. Optical Materials, 2015, 46, 122-130.	1.7	8
2249	Mechanical properties and electronic structures of the Hfâ€“Si system: First-principles calculations. Solid State Communications, 2015, 205, 39-45.	0.9	14
2250	Acid-base dissociation mechanisms and energetics at the silicaâ€“water interface: An activationless process. Journal of Colloid and Interface Science, 2015, 451, 231-244.	5.0	96
2251	Phase transitions, band structures, elastic and lattice dynamic properties of CdSnV2 (V=P, As, Sb) under pressure from first principles. Materials Science in Semiconductor Processing, 2015, 35, 149-161.	1.9	8
2252	Optimized molecular reconstruction procedure combining hybrid reverse Monte Carlo and molecular dynamics. Journal of Chemical Physics, 2015, 142, 114112.	1.2	24

#	Article	IF	Citations
2253	Effect of the cation size on the framework structures of magnesium tungstate, A₄Mg(WO₄)₃(A = Na, K), R₂Mg₂(WO₄)₃(R = Rb, Cs). Dalton Transactions, 2015, 44, 5810-5817.	1.6	23
2254	The lone-pairs enhanced birefringence and SHG response: A DFT investigation on M2B5O9Cl (M=Sr, Ba,) Tj ETQq1 1 0.784314 rgBT /O	0.9	36
2255	A new zinc(II) coordination compound of meta-aminobenzoate and 4,4â€²-bipyridine with broad-band photoluminescence emission. Inorganica Chimica Acta, 2015, 432, 46-49.	1.2	5
2256	Anomalous chemical shifts in X-ray photoelectron spectra of sulfur-containing compounds of silver (I) and (II). Journal of Electron Spectroscopy and Related Phenomena, 2015, 202, 38-45.	0.8	15
2257	High-Pressure Hydrogen Sulfide from First Principles: A Strongly Anharmonic Phonon-Mediated Superconductor. Physical Review Letters, 2015, 114, 157004.	2.9	377
2258	First-principles investigation of the lattice vibrations in the alkali feldspar solid solution. Physics and Chemistry of Minerals, 2015, 42, 243-249.	0.3	9
2259	Carbon p Electron Ferromagnetism in Silicon Carbide. Scientific Reports, 2015, 5, 8999.	1.6	38
2260	Calcium peroxide from ambient to high pressures. Physical Chemistry Chemical Physics, 2015, 17, 6889-6895.	1.3	28
2261	Tailored upconversion emission of Eu3+ in Sr2Ca(W,Mo)O6:Yb3+,Eu3+ by a laser via an electronic polarization mechanism. Journal of Materials Chemistry C, 2015, 3, 4997-5003.	2.7	12
2262	Oneâ€Step Selfâ€Assembly Fabrication of High Quality Ni_xMg_{1â€x}O Bowlâ€Shaped Array Film and Its Enhanced Photocurrent by Mg,²⁺ Doping. Advanced Functional Materials, 2015, 25, 3256-3263.	7.8	13
2263	Three-dimensional sp²-hybridized carbons consisting of orthogonal nanoribbons of graphene and net C. Physical Chemistry Chemical Physics, 2015, 17, 13028-13033.	1.3	22
2264	Simulation study of negative thermal expansion in yttrium tungstate Y₂W₃O₁₂. Journal of Physics Condensed Matter, 2015, 27, 185401.	0.7	14
2265	Template effect in TiN/AlN multilayered coatings from first principles. Ceramics International, 2015, 41, 10095-10101.	2.3	21
2266	Computationally Assisted (Solid-State Density Functional Theory) Structural (X-ray) and Vibrational Spectroscopy (FT-IR, FT-RS, TDs-THz) Characterization of the Cardiovascular Drug Lacidipine. Crystal Growth and Design, 2015, 15, 2817-2830.	1.4	21
2267	Growth, structure, and optical properties of a self-activated crystal: Na2Nd2O(BO3)2. Optical Materials, 2015, 46, 461-466.	1.7	7
2268	Biaxial crystal Î±-BaTeMo_2O_9: theory study of large birefringence and wide-band polarized prisms design. Optics Express, 2015, 23, 3851.	1.7	26
2269	Accommodation of tin in tetragonal ZrO2. Journal of Applied Physics, 2015, 117, .	1.1	36
2270	Advances in theory and their application within the field of zeolite chemistry. Chemical Society Reviews, 2015, 44, 7044-7111.	18.7	405

#	Article	IF	Citations
2271	Ba2GeS4and Mg2SnS4: synthesis, structures, optical properties and electronic structures. RSC Advances, 2015, 5, 33646-33652.	1.7	31
2272	Joint Experimental and Computational ¹⁷O and ¹H Solid State NMR Study of Ba₂In₂O₄(OH)₂ Structure and Dynamics. Chemistry of Materials, 2015, 27, 3861-3873.	3.2	27
2273	Predicting crystal structures and physical properties of novel superhard p-BN under pressure via first-principles investigation. Journal of Alloys and Compounds, 2015, 644, 638-644.	2.8	65
2274	k Â· p theory for two-dimensional transition metal dichalcogenide semiconductors. 2D Materials, 2015, 2, 022001.	2.0	676
2275	Correlated electron pseudopotentials for 3d-transition metals. Journal of Chemical Physics, 2015, 142, 064110.	1.2	32
2276	Synthesis, characterisation and properties of rare earth oxyselenides A4O4Se3(A = Eu, Gd, Tb, Dy, Ho,) Tj ETQq1 1 0.784314 rgBT /Ov	1.6	8
2277	Piezochromic luminescence behaviors of two new benzothiazoleâ€“enamido boron difluoride complexes: intra- and inter-molecular effects induced by hydrostatic compression. Chemical Communications, 2015, 51, 7497-7500.	2.2	105
2278	Relationship between structure and cleavage behavior in the nonlinear optical crystal MnTeMoO 6. Journal of Crystal Growth, 2015, 419, 25-30.	0.7	10
2279	CO oxidation catalysed by Pd-based bimetallic nanoalloys. Physical Chemistry Chemical Physics, 2015, 17, 28010-28021.	1.3	25
2280	Metallic Icosahedron Phase of Sodium at Terapascal Pressures. Physical Review Letters, 2015, 114, 125501.	2.9	75
2281	Theoretical investigation of lead vapor adsorption on kaolinite surfaces with DFT calculations. Journal of Hazardous Materials, 2015, 295, 43-54.	6.5	85
2283	Expanding the structural landscape of niclosamide: a highZâ€² polymorph, two new solvates and monohydrate H_A. Acta Crystallographica Section C, Structural Chemistry, 2015, 71, 394-401.	0.2	7
2284	Enhanced Visible-Light Photocatalytic Activity of BiOI/BiOCl Heterojunctions: Key Role of Crystal Facet Combination. ACS Catalysis, 2015, 5, 3540-3551.	5.5	307
2285	Conformational Stability and Thermal Pathways of Relaxation in Triclosan (Antibacterial/Excipient/Contaminant) in Solid-State: Combined Spectroscopic (¹H NMR) and Computational (Periodic DFT) Study. Journal of Physical Chemistry A, 2015, 119, 4864-4874.	1.1	21
2286	Synthesis of cyclotriphosphazene-containing polymeric nanotubes and their use as metal-free photocatalysts for methylene blue degradation. Applied Surface Science, 2015, 347, 541-547.	3.1	23
2287	Structural Characterization and Rationalization of Formation, Stability, and Transformations of Benperidol Solvates. Crystal Growth and Design, 2015, 15, 2337-2351.	1.4	38
2288	The electronic structure and luminescence properties of Ce3+ doped Sr10[(PO4)5.5(BO4)0.5]BO2 under UV/VUV and X-ray excitation. Optical Materials, 2015, 45, 13-21.	1.7	1
2289	Atomic-scale friction modulated by potential corrugation in multi-layered graphene materials. Journal of Applied Physics, 2015, 117, .	1.1	10

#	Article	IF	Citations
2290	Cs₆RE₂(PO₄)₄(RE = Y and Gd): two new members of the alkali rare-earth double phosphates. New Journal of Chemistry, 2015, 39, 4328-4333.	1.4	19
2291	Pb₇O(OH)₃(CO₃)₃(BO₃): First Mixed Borate and Carbonate Nonlinear Optical Material Exhibiting Large Second-Harmonic Generation Response. Inorganic Chemistry, 2015, 54, 4138-4142.	1.9	69
2292	Superhard-driven search of the covalent network in the B₃NO system. RSC Advances, 2015, 5, 35882-35887.	1.7	18
2293	Segregation of alloying elements to intrinsic and extrinsic stacking faults in Î³â€²-Ni3Al via first principles calculations. Scripta Materialia, 2015, 102, 87-90.	2.6	39
2294	Anatase TiO₂nanocubes for fast and durable sodium ion battery anodes. Journal of Materials Chemistry A, 2015, 3, 8800-8807.	5.2	163
2295	A metallic superhard boron carbide: first-principles calculations. Physical Chemistry Chemical Physics, 2015, 17, 9748-9751.	1.3	14
2296	Theoretical study of BTF/TNA cocrystal: Effects of hydrostatic pressure and temperature. Defence Technology, 2015, 11, 132-139.	2.1	15
2297	Structural Study of Mg-Based Metalâ€“Organic Frameworks by X-ray Diffraction, 1H, 13C, and 25Mg Solid-State NMR Spectroscopy, and First-Principles Calculations. Journal of Physical Chemistry C, 2015, 119, 7831-7841.	1.5	20
2298	N,F-monodoping and N/F-codoping effects on the electronic structures and optical performances of Zn2GeO4. Physical Chemistry Chemical Physics, 2015, 17, 5613-5623.	1.3	10
2299	Comparative investigations of the crystal structure and photoluminescence property of eulytite-type Ba₃Eu(PO₄)₃and Sr₃Eu(PO₄)₃. Dalton Transactions, 2015, 44, 7679-7686.	1.6	161
2300	Superstructure of a Substituted Zeolitic Imidazolate Metalâ€“Organic Framework Determined by Combining Proton Solidâ€state NMR Spectroscopy and DFT Calculations. Angewandte Chemie - International Edition, 2015, 54, 5971-5976.	7.2	38
2301	Origin of Dirac Cones in SiC Silagraphene: A Combined Density Functional and Tight-Binding Study. Journal of Physical Chemistry Letters, 2015, 6, 1333-1339.	2.1	41
2302	Syntheses, structures, and characterizations of a new second-order nonlinear optical material: Pb2(SeO3)(NO3)2. Journal of Alloys and Compounds, 2015, 640, 39-44.	2.8	29
2303	Na3B4O7X (X = Cl, Br): two new borate halides with a 1D Na-X (X = Cl, Br) chain formed by the face-sharing XNa6octahedra. RSC Advances, 2015, 5, 12416-12422.	1.7	10
2304	Half-metallic fully compensated ferrimagnetism in C1 b -type half Heusler compounds Mn 2 Si 1â^'x Ge x. Journal of Magnetism and Magnetic Materials, 2015, 387, 67-71.	1.0	25
2305	Understanding the run-in tribological behavior of amorphous carbon films against Al₂O₃balls under high vacuum. RSC Advances, 2015, 5, 32690-32697.	1.7	6
2306	The Raman spectrum of the Î³â€²-V₂O₅polymorph: a combined experimental and DFT study. Journal of Raman Spectroscopy, 2015, 46, 406-412.	1.2	57
2307	The physical properties of Li-doped g-C3N4 monolayer sheet investigated by the first-principles. Materials Research Bulletin, 2015, 66, 156-162.	2.7	72

#	Article	IF	Citations
2308	First-Principles Study on Electronic and Optical Properties of Kesterite and Stannite Cu₂ZnSnS₄ Photovoltaic Absorbers. Materials Science Forum, 2015, 815, 80-88.	0.3	7
2309	Synthesis and crystal structure of a novel layered barium antimonate Ba2Sb7O13(OH) with mixed-valence antimony. Solid State Sciences, 2015, 44, 27-31.	1.5	3
2310	Photoluminescence Tuning and Water Detection of Yttrium Diazinedicarboxylate Materials through Lanthanide Doping. European Journal of Inorganic Chemistry, 2015, 2015, 2650-2663.	1.0	12
2311	DFT study on microstructures and electronic structures of Pt mono-/bi-doped anatase TiO₂(101) surface. RSC Advances, 2015, 5, 17984-17992.	1.7	7
2312	A first-principles study of the vibrational properties of crystalline tetracene under pressure. Journal of Physics Condensed Matter, 2015, 27, 375402.	0.7	13
2313	Assignment of terahertz vibrational modes of L-glutamine using density functional theory within generalized-gradient approximation. Chinese Physics B, 2015, 24, 073301.	0.7	4
2314	Electronic, optical and photocatalytic properties of three-layer perovskite Dionâ€“Jacobson phase CsBa₂M₃O₁₀(M = Ta, Nb): a DFT study. RSC Advances, 2015, 5, 88725-88735.	1.7	15
2315	Tl4CdI6 â€“ Wide band gap semiconductor: First principles modelling of the structural, electronic, optical and elastic properties. Materials Chemistry and Physics, 2015, 163, 562-568.	2.0	8
2316	Probing the Charge Storage Mechanism of a Pseudocapacitive MnO₂ Electrode Using in Operando Raman Spectroscopy. Chemistry of Materials, 2015, 27, 6608-6619.	3.2	212
2317	Mercury Interaction with the Fine Fraction of Coal-Combustion Fly Ash in a Simulated Coal Power Plant Flue Gas Stream. Energy & Fuels, 2015, 29, 6025-6038.	2.5	37
2318	Enhanced Photocatalytic Activity of Ultrathin Ba₅Nb₄O₁₅ Two-Dimensional Nanosheets. ACS Applied Materials & Interfaces, 2015, 7, 21860-21867.	4.0	56
2319	Structural study by solid-state⁷¹Ga NMR of thin film transistor precursors. Dalton Transactions, 2015, 44, 17652-17659.	1.6	7
2320	Pressure-induced phase transition in hydrogen-bonded molecular crystal acetamide: combined Raman scattering and X-ray diffraction study. RSC Advances, 2015, 5, 84703-84710.	1.7	13
2321	Grafting trimethylaluminum and its halogen derivatives on silica: general trends for²⁷Al SS-NMR response from first principles calculations. Physical Chemistry Chemical Physics, 2015, 17, 26937-26945.	1.3	10
2322	Clathrate directed assembly of tetrapyridyl-tetraphenylethylene metalâ€“organic frameworks. RSC Advances, 2015, 5, 84134-84141.	1.7	20
2323	Measuring absolute spin polarization in dissolution-DNP by Spin PolarimetrY Magnetic Resonance (SPY-MR). Journal of Magnetic Resonance, 2015, 260, 127-135.	1.2	18
2324	Analysis of electronic structure and optical properties of N-doped SiO2 based on DFT calculations. Modern Physics Letters B, 2015, 29, 1550100.	1.0	3
2325	First-principles calculation of Mg/MgO interfacial free energies. Journal of Alloys and Compounds, 2015, 650, 228-238.	2.8	26

#	Article	IF	Citations
2326	Effects of inorganic acids and divalent hydrated metal cations (Mg2+, Ca2+, Co2+, Ni2+) on Î³-AlOOH solâ€“gel process. Physical Chemistry Chemical Physics, 2015, 17, 27391-27398.	1.3	1
2327	Pressure-induced reversible phase transition in thiourea dioxide crystal. Journal of Chemical Physics, 2015, 142, 244701.	1.2	11
2328	Understanding the Solid-State Phase Transitions of <scp>dl</scp>-Norleucine: An in Situ DSC, Microscopy, and Solid-State NMR Study. Crystal Growth and Design, 2015, 15, 5157-5167.	1.4	38
2329	Metal Thiophosphates with Good Mid-infrared Nonlinear Optical Performances: A First-Principles Prediction and Analysis. Journal of the American Chemical Society, 2015, 137, 13049-13059.	6.6	345
2330	Synthesis, structures, and properties of two magnesium silicate fluorides Mg₅(SiO₄)₂F₂and Mg₃SiO₄F₂. New Journal of Chemistry, 2015, 39, 8866-8873.	1.4	11
2331	Radial deformation of single-walled carbon nanotubes on quartz substrates and the resultant anomalous diameter-dependent reaction selectivity. Nano Research, 2015, 8, 3054-3065.	5.8	6
2332	The improvement of hole transport property and optical band gap forÂamorphous Cu2O films. Journal of Alloys and Compounds, 2015, 647, 585-589.	2.8	26
2333	First-Principles Design of a Deep-Ultraviolet Nonlinear-Optical Crystal from KBe₂BO₃F₂ to NH₄Be₂BO₃F₂. Inorganic Chemistry, 2015, 54, 10533-10535.	1.9	85
2334	Impact of Te on the structure and⁷⁷Se NMR spectra of Se-rich Geâ€“Teâ€“Se glasses: a combined experimental and computational investigation. Physical Chemistry Chemical Physics, 2015, 17, 29020-29026.	1.3	10
2335	Electronic, optical and thermal properties of TiCr2 and TiMn2 by ab initio simulations. International Journal of Modern Physics B, 2015, 29, 1550223.	1.0	5
2336	Computation assisted design of favored composition for ternary Mgâ€“Cuâ€“Y metallic glass formation. Physical Chemistry Chemical Physics, 2015, 17, 14879-14889.	1.3	3
2337	Aluminum environments in synthetic Ca-Tschermak clinopyroxene (CaAlAlSiO6) from Rietveld refinement,27Al NMR, and first-principles calculations. American Mineralogist, 2015, 100, 2219-2230.	0.9	12
2338	p-N,Nâ€²-tetraacetylodiaminodurene. The structure and vibrational spectra. Chemical Physics, 2015, 459, 148-154.	0.9	3
2339	Critical Analysis of Cluster Models and Exchange-Correlation Functionals for Calculating Magnetic Shielding in Molecular Solids. Journal of Chemical Theory and Computation, 2015, 11, 5229-5241.	2.3	60
2340	Polymorphs of Theophylline Characterized by DNP Enhanced Solid-State NMR. Molecular Pharmaceutics, 2015, 12, 4146-4153.	2.3	77
2341	Evaluation of the Stability of Trimethyl Phosphate as a Liâ€“O2 Battery Electrolyte via Multinuclear Solid-State NMR. Journal of Physical Chemistry C, 2015, 119, 26840-26848.	1.5	11
2342	Far infrared spectra of solid state l-serine, l-threonine, l-cysteine, and l-methionine in different protonation states. Spectrochimica Acta - Part A: Molecular and Biomolecular Spectroscopy, 2015, 150, 301-307.	2.0	22
2343	Enhancement of the thermoelectric properties of MnSb₂Se₄through Cu resonant doping. RSC Advances, 2015, 5, 99065-99073.	1.7	11

#	Article	IF	Citations
2344	A DFT study of Pt layer deposition on catalyst supports of titanium oxide, nitride and carbide. Journal of Materials Chemistry A, 2015, 3, 24504-24511.	5.2	14
2345	Electronic Structure and Optical Properties of BiOI Ultrathin Films for Photocatalytic Water Splitting. Inorganic Chemistry, 2015, 54, 10732-10737.	1.9	61
2346	Analysis of local molecular motions of aromatic sidechains in proteins by 2D and 3D fast MAS NMR spectroscopy and quantum mechanical calculations. Physical Chemistry Chemical Physics, 2015, 17, 28789-28801.	1.3	19
2347	An investigation of new infrared nonlinear optical material: BaCdSnSe₄, and three new related centrosymmetric compounds: Ba₂SnSe₄, Mg₂GeSe₄, and Ba₂Ge₂S₆. Dalton Transactions, 2015, 44, 19856-19864.	1.6	67
2348	First-principles investigation of possible martensitic transformation and magnetic properties of Heusler-type Pt2-xMn1+xIn alloys. Functional Materials Letters, 2015, 08, 1550064.	0.7	3
2349	Carbyne with finite length: The one-dimensional sp carbon. Science Advances, 2015, 1, e1500857.	4.7	131
2350	Electronic and magnetic properties of second main-group and second sub-group metals substitution for Al in delafossite CuAlO2. Chemical Physics Letters, 2015, 633, 181-185.	1.2	5
2351	High temperature CO₂sensing properties and mechanism of nanocrystalline LaCrO₃with rhombohedral structure: experiments and ab initio calculations. RSC Advances, 2015, 5, 54710-54716.	1.7	19
2352	A study on K2SbF2Cl3 as a new mid-IR nonlinear optical material: new synthesis and excellent properties. Journal of Materials Chemistry C, 2015, 3, 9588-9593.	2.7	41
2353	Stabilization of Pt monolayer catalysts under harsh conditions of fuel cells. Journal of Chemical Physics, 2015, 142, 194710.	1.2	11
2354	Structures and stability of calcium and magnesium carbonates at mantle pressures. Physical Review B, 2015, 91, .	1.1	70
2355	First-Principles Evaluation of the Alkali and/or Alkaline Earth Beryllium Borates in Deep Ultraviolet Nonlinear Optical Applications. ACS Photonics, 2015, 2, 1183-1191.	3.2	117
2356	Ten new predicted covalent organic frameworks with strong optical response in the visible and near infrared. Journal of Chemical Physics, 2015, 142, 244706.	1.2	11
2357	Self-assembled two-dimensional nanoporous molecular arrays and photoinduced polymerization of 4-bromo-4â€²-hydroxybiphenyl on Ag(111). Journal of Chemical Physics, 2015, 142, 101902.	1.2	21
2358	Mechanisms of Enhanced Electrocatalytic Activity for Oxygen Reduction Reaction on High-Index Platinum n(111)â€“(111) Surfaces. Journal of Physical Chemistry Letters, 2015, 6, 3346-3351.	2.1	36
2359	Effects of N on Electronic and Mechanical Properties of H-Type SiC. Chinese Physics Letters, 2015, 32, 087103.	1.3	1
2360	Effect of Mg doping on the structural and electrochemical performance of LiNi0.6Co0.2Mn0.2O2 cathode materials. Electrochimica Acta, 2015, 182, 795-802.	2.6	149
2361	Variable gradient refractive index engineering: design, growth and electro-deflective application of KTa_{1â^'x}Nb_xO₃. Journal of Materials Chemistry C, 2015, 3, 10968-10973.	2.7	30

#	Article	IF	Citations
2362	Atomic Disorders Induced by Silver and Magnesium Ion Migrations Favor High Thermoelectric Performance in Î±â€MgAgSbâ€Based Materials. Advanced Functional Materials, 2015, 25, 6478-6488.	7.8	70
2363	Delicate Distinction between OH Groups on Proton-Exchanged H-Chabazite and H-SAPO-34 Molecular Sieves. Journal of Physical Chemistry C, 2015, 119, 24046-24055.	1.5	21
2364	The first principle study: Electronic and optical properties in Bi2Se3. Computational Condensed Matter, 2015, 4, 59-63.	0.9	37
2365	Structural and electrochemical properties of Mg-doped nickel based cathode materials LiNi_{0.6}Co_{0.2}Mn_{0.2â^'x}Mg_xO₂for lithium ion batteries. RSC Advances, 2015, 5, 88773-88779.	1.7	47
2366	Electronic and optical properties of Er-doped Y₂O₂S phosphors. Journal of Materials Chemistry C, 2015, 3, 11486-11496.	2.7	23
2367	Reactivity Studies of Alkoxy-Substituted [2.2]Paracyclophane-1,9-dienes and Specific Coordination of the Monomer Repeating Unit during ROMP. Macromolecules, 2015, 48, 7435-7445.	2.2	27
2368	Theoretical model of the interaction of glycine with hydrogenated amorphous carbon (HAC). Physical Chemistry Chemical Physics, 2015, 17, 28966-28976.	1.3	6
2369	Combined theoretical and time-resolved photoluminescence investigations of [Mo₆Brⁱ₈Br^a₆]^{2â^'}metal cluster units: evidence of dual emission. Physical Chemistry Chemical Physics, 2015, 17, 28574-28585.	1.3	62
2370	Synthesis, characterization and modelling of zinc and silicate co-substituted hydroxyapatite. Journal of the Royal Society Interface, 2015, 12, 20150190.	1.5	41
2371	First-principles study on the structural, electronic and magnetic properties of the Ti2VZ (ZÂ=ÂSi, Ge, Sn) full-Heusler compounds. Materials Chemistry and Physics, 2015, 164, 177-182.	2.0	21
2372	Component-controllable synthesis of Co(S Se1â^')2 nanowires supported by carbon fiber paper as high-performance electrode for hydrogen evolution reaction. Nano Energy, 2015, 18, 1-11.	8.2	130
2373	Mechanical and electronic properties of Ca1â^'Mg O alloys. Materials Science in Semiconductor Processing, 2015, 40, 676-684.	1.9	18
2374	Solution-combustion synthesized aluminium-doped spinel (LiAl x Mn2â^'x O4) as a high-performance lithium-ion battery cathode material. Applied Physics A: Materials Science and Processing, 2015, 121, 51-57.	1.1	16
2375	Pressure-Induced Phase Transformation, Reversible Amorphization, and Anomalous Visible Light Response in Organolead Bromide Perovskite. Journal of the American Chemical Society, 2015, 137, 11144-11149.	6.6	303
2376	Local environments of boron heteroatoms in non-crystalline layered borosilicates. Physical Chemistry Chemical Physics, 2015, 17, 21664-21682.	1.3	11
2377	Enhanced photocatalytic H₂-evolution by immobilizing CdS nanocrystals on ultrathin Co_{0.85}Se/RGOâ€"PEI nanosheets. Journal of Materials Chemistry A, 2015, 3, 18711-18717.	5.2	51
2378	Isoxazolone-based single crystals with large second harmonic generation effect. CrystEngComm, 2015, 17, 7316-7322.	1.3	18
2379	Phonon anomalies predict superconducting T_cfor AlB₂-type structures. Physical Chemistry Chemical Physics, 2015, 17, 25090-25099.	1.3	28

#	Article	IF	Citations
2380	Ultra-wideline¹⁴N solid-state NMR as a method for differentiating polymorphs: glycine as a case study. CrystEngComm, 2015, 17, 5225-5236.	1.3	33
2381	First-principles study on the band structure, magnetic and elastic properties of half-metallic Cr2MnAl. Modern Physics Letters B, 2015, 29, 1550139.	1.0	14
2382	Uranyl Carboxyphosphonates Derived from Hydrothermal in Situ Ligand Reaction: Syntheses, Structures, and Computational Investigations. Inorganic Chemistry, 2015, 54, 8617-8624.	1.9	24
2383	Shell Model force field for Lead Zirconate Titanate Pb(Zr_{1â€“x}Ti_x)O₃. Journal of Physical Chemistry C, 2015, 119, 17784-17789.	1.5	20
2384	Atomic Description of the Interface between Silica and Alumina in Aluminosilicates through Dynamic Nuclear Polarization Surface-Enhanced NMR Spectroscopy and First-Principles Calculations. Journal of the American Chemical Society, 2015, 137, 10710-10719.	6.6	129
2385	Quantum Monte Carlo study of the phase diagram of solid molecular hydrogen at extreme pressures. Nature Communications, 2015, 6, 7794.	5.8	84
2386	Many-body dispersion effects in the binding of adsorbates on metal surfaces. Journal of Chemical Physics, 2015, 143, 102808.	1.2	69
2387	Structural, Elastic, and Electronic Properties of a New Phase of Carbon. Communications in Theoretical Physics, 2015, 64, 237-243.	1.1	17
2388	Electronic, optical, and mechanical properties of Cu₂ZnSnS₄with four crystal structures. Journal of Semiconductors, 2015, 36, 083004.	2.0	15
2389	Theoretical perspective of the lone pair activity influence on band gap and SHG response of lead borates. RSC Advances, 2015, 5, 79882-79887.	1.7	22
2390	Solid-state^{185/187}Re NMR and GIPAW DFT study of perrhenates and Re₂(CO)₁₀: chemical shift anisotropy, NMR crystallography, and a metalâ€“metal bond. Physical Chemistry Chemical Physics, 2015, 17, 10118-10134.	1.3	18
2391	BaGa₂SnSe₆: a new phase-matchable IR nonlinear optical material with strong second harmonic generation response. Journal of Materials Chemistry C, 2015, 3, 10998-11004.	2.7	54
2392	Theoretical study of surface dependence of NH₃adsorption and decomposition on spinel-type MgAl₂O₄. RSC Advances, 2015, 5, 77973-77985.	1.7	4
2393	First-principles study on alkali-metal effect of Li, Na, and K in CuInSe₂and CuGaSe₂. Japanese Journal of Applied Physics, 2015, 54, 08KC20.	0.8	38
2394	Synthesis and optical properties of the first lead borate bromide with isolated BO₃groups: Pb₂Ba₃(BO₃)₃Br. Dalton Transactions, 2015, 44, 16818-16823.	1.6	25
2395	Theoretical Investigation of the Newly Noncentrosymmetric Superconductor SrAuSi3 via First Principles. Journal of Superconductivity and Novel Magnetism, 2015, 28, 3235-3241.	0.8	8
2396	Supramolecular pairing among heteroaromatic compounds and the cationic surfactant C12TAC. Fuel, 2015, 149, 174-183.	3.4	8
2397	Target-Induced Nanocatalyst Deactivation Facilitated by Core@Shell Nanostructures for Signal-Amplified Headspace-Colorimetric Assay of Dissolved Hydrogen Sulfide. Analytical Chemistry, 2015, 87, 10153-10160.	3.2	93

#	Article	IF	Citations
2398	Water adsorption in SAPO-34: elucidating the role of local heterogeneities and defects using dispersion-corrected DFT calculations. Physical Chemistry Chemical Physics, 2015, 17, 25260-25271.	1.3	30
2399	Effect of cation substitution on structural transition: synthesis, characterization and theoretical studies of NaCa₄B₃O₉, NaCaBO₃, NaSrBO₃and Li₄CaB₂O₆. Physical Chemistry Chemical Physics, 2015, 17, 26359-26368.	1.3	16
2400	Glitter in a 2D monolayer. Physical Chemistry Chemical Physics, 2015, 17, 26036-26042.	1.3	68
2401	Revealing unusual chemical bonding in planar hyper-coordinate Ni₂Ge and quasi-planar Ni₂Si two-dimensional crystals. Physical Chemistry Chemical Physics, 2015, 17, 26043-26048.	1.3	95
2402	Theoretical and experimental studies on wide-band-gap p-type conductive BaCuSeF and related compounds. Japanese Journal of Applied Physics, 2015, 54, 08KC07.	0.8	10
2403	Thermodynamic description of the AgClâ€“CoCl2â€“InCl3â€“KCl system. Materials Chemistry and Physics, 2015, 163, 73-87.	2.0	14
2404	Simulating spin dynamics in organic solids under heteronuclear decoupling. Solid State Nuclear Magnetic Resonance, 2015, 70, 28-37.	1.5	5
2405	Native Point Defects in CaS: Focus on Intrinsic Defects and Rare Earth Ion Dopant Levels for Up-converted Persistent Luminescence. Inorganic Chemistry, 2015, 54, 11423-11440.	1.9	47
2406	The mechanism for the nonlinear optical properties in La₉Na₃B₈O₂₇, La₂Na₃B₃O₉and La₂CaB₁₀O₁₉:ab initiostudies. Journal of Physics Condensed Matter, 2015, 27, 485501.	0.7	7
2407	Structural and electronic properties of Cu-doped Zn5(OH)6(CO3)2 from first principles. Journal of Materials Science, 2015, 50, 6794-6807.	1.7	7
2408	Coverage-driven dissociation of azobenzene on Cu(111): a route towards defined surface functionalization. Chemical Communications, 2015, 51, 15324-15327.	2.2	13
2409	Bi₂O₂(OH)(NO₃) as a desirable [Bi₂O₂]²⁺layered photocatalyst: strong intrinsic polarity, rational band structure and {001} active facets co-beneficial for robust photooxidation capability. Journal of Materials Chemistry A, 2015, 3, 24547-24556.	5.2	352
2410	A Novel Approach to Identify the Carrier Transport Path and Its Correlation to the Current Variation in RRAM. , 2015, , .		0
2411	Electrically Tunable van der Waals Interaction in Grapheneâ€“Molecule Complex. Nano Letters, 2015, 15, 8176-8180.	4.5	53
2412	BaBi(SeO₃)₂Cl: a new polar material showing high second-harmonic generation efficiency enhanced by constructive alignment of chloride ions. Journal of Materials Chemistry C, 2015, 3, 12290-12296.	2.7	32
2413	Surface Charge Transfer Doping of Monolayer Phosphorene via Molecular Adsorption. Journal of Physical Chemistry Letters, 2015, 6, 4701-4710.	2.1	63
2414	Roles of Cu concentration in the photocatalytic activities of Cu-doped TiO 2 from GGA+ U calculations. Solid State Communications, 2015, 204, 23-27.	0.9	21
2415	Anomalous elastic properties in stishovite. RSC Advances, 2015, 5, 8974-8980.	1.7	15

#	Article	IF	Citations
2416	Synthesis, Crystal Structure, and Optical Properties of a New Sodiumâ€Cadmium Carbonate Na₄Cd₃(CO₃)₄(OH)₂. Zeitschrift Fur Anorganische Und Allgemeine Chemie, 2015, 641, 460-463.	0.6	3
2417	Platinumâ€“carbide interactions: coreâ€“shells for catalytic use. Physical Chemistry Chemical Physics, 2015, 17, 4250-4258.	1.3	23
2418	The atomistic mechanism of hcp-to-bcc martensitic transformation in the Tiâ€“Nb system revealed by molecular dynamics simulations. Physical Chemistry Chemical Physics, 2015, 17, 4184-4192.	1.3	8
2419	Supramolecular binding and separation of hydrocarbons within a functionalized porous metalâ€“organic framework. Nature Chemistry, 2015, 7, 121-129.	6.6	530
2420	New in situ solid-state NMR techniques for probing the evolution of crystallization processes: pre-nucleation, nucleation and growth. Faraday Discussions, 2015, 179, 115-140.	1.6	29
2421	Anomalous second-harmonic generation response in SrBPO₅and BaBPO₅. Journal of Materials Chemistry C, 2015, 3, 1557-1566.	2.7	34
2422	Synthesis, crystal growth, and second-order nonlinear optical properties of new configurationally locked polyene derivatives. CrystEngComm, 2015, 17, 1050-1055.	1.3	19
2423	A simulated annealing approach for solving zeolite crystal structures from two-dimensional NMR correlation spectra. Solid State Nuclear Magnetic Resonance, 2015, 65, 89-98.	1.5	13
2424	Structural and luminescence studies of the new nitridomagnesoaluminate CaMg₂AlN₃. Dalton Transactions, 2015, 44, 2819-2826.	1.6	10
2425	Theoretical investigation of the electronic structure, optical, elastic and thermodynamics properties of a newly binary boron nitride (T-B3N3). Physica B: Condensed Matter, 2015, 459, 134-139.	1.3	17
2426	First-principles calculations of phonon and thermodynamic properties of OsSi2. Materials Science in Semiconductor Processing, 2015, 31, 251-255.	1.9	2
2427	Revealing the interactions between pentagonâ€“octagonâ€“pentagon defect graphene and organic donor/acceptor molecules: a theoretical study. Physical Chemistry Chemical Physics, 2015, 17, 4919-4925.	1.3	22
2428	First-principles study on the ferrimagnetic half-metallic Mn2FeAs alloy. Journal of Solid State Chemistry, 2015, 225, 8-12.	1.4	21
2429	Roles of hydrogen bonds and Ï€â€“Ï€ stacking in the optical detection of nitro-explosives with a luminescent metalâ€“organic framework as the sensor. RSC Advances, 2015, 5, 3045-3053.	1.7	62
2430	First principles studies of the structural, electronic and optical properties of LiInSe2 and LiInTe2 chalcopyrite crystals. Solid State Communications, 2015, 203, 69-74.	0.9	25
2431	Strain-induced quantum spin Hall effect in methyl-substituted germanane GeCH3. Scientific Reports, 2014, 4, 7297.	1.6	68
2432	Diamond-based electrodes for organic photovoltaic devices. Solar Energy Materials and Solar Cells, 2015, 134, 73-79.	3.0	15
2433	Na₃Ba₂(B₃O₆)₂F: Next Generation of Deep-Ultraviolet Birefringent Materials. Crystal Growth and Design, 2015, 15, 523-529.	1.4	159

#	Article	IF	Citations
2434	Two-dimensional electron gas in the KNbO3:Y ultrathin film. Journal of Materials Science, 2015, 50, 74-78.	1.7	2
2435	Hydrogen-bond relaxation dynamics: Resolving mysteries of water ice. Coordination Chemistry Reviews, 2015, 285, 109-165.	9.5	136
2436	On the solid-state NMR spectra of naproxen. Chemical Physics Letters, 2015, 619, 230-235.	1.2	15
2437	Acid-functionalized UiO-66(Zr) MOFs and their evolution after intra-framework cross-linking: structural features and sorption properties. Journal of Materials Chemistry A, 2015, 3, 3294-3309.	5.2	174
2438	DFT and experimental studies of oxygen adsorption on galena surface bearing Ag, Mn, Bi and Cu impurities. Minerals Engineering, 2015, 71, 170-179.	1.8	17
2439	Theoretical characterization of quaternary iridium based hydrides NaAeIrH6 (AeÂ=ÂCa, Ba and Sr). Materials Chemistry and Physics, 2015, 149-150, 87-93.	2.0	2
2440	Phase stability, magnetism, elastic properties and hardness of binary iron nitrides from first principles. Journal of Alloys and Compounds, 2015, 625, 224-230.	2.8	39
2441	First-principles investigation of the elastic, Vickers hardness and thermodynamic properties of Alâ€“Cu intermetallic compounds. Superlattices and Microstructures, 2015, 79, 156-165.	1.4	70
2442	Atomic approach to the optimized compositions of Niâ€“Nbâ€“Ti glassy alloys with large glass-forming ability. RSC Advances, 2015, 5, 3054-3062.	1.7	12
2443	First-principle investigation of Kâ€“N dual-acceptor codoping for p-ZnO. Materials Science in Semiconductor Processing, 2015, 29, 245-249.	1.9	15
2444	New First Order Raman-active Modes in Few Layered Transition Metal Dichalcogenides. Scientific Reports, 2014, 4, 4215.	1.6	367
2445	Mechanistic aspects in the direct synthesis of hydrogen peroxide on PdAu catalyst from first principles. Catalysis Today, 2015, 248, 142-148.	2.2	35
2446	Synthesis of NiGa2O4Octahedron Nanocrystal with Exposed {111} Facets and Enhanced Efficiency of Photocatalytic Water Splitting. ChemPlusChem, 2015, 80, 223-230.	1.3	18
2447	Reversible Hydrophobic to Hydrophilic Transition in Graphene via Water Splitting Induced by UV Irradiation. Scientific Reports, 2014, 4, 6450.	1.6	105
2448	Low temperature phase transition and crystal structure of CsMgPO4. Journal of Solid State Chemistry, 2015, 221, 224-229.	1.4	10
2449	Mechanical, electronic, optical, thermodynamic properties and superconductivity of ScGa. Physica B: Condensed Matter, 2015, 457, 320-325.	1.3	24
2450	Allâ€Metallic Vertical Transistors Based on Stacked Dirac Materials. Advanced Functional Materials, 2015, 25, 68-77.	7.8	59
2451	Enhanced visible light photocatalytic activity of Cu₂O via cationicâ€“anionic passivated codoping. Physical Chemistry Chemical Physics, 2015, 17, 630-637.	1.3	42

#	Article	IF	Citations
2452	Synthesis, structures, optical properties and electronic structures of PbGa2Q4 (Q=S, Se) crystals. Journal of Molecular Structure, 2015, 1082, 174-179.	1.8	11
2453	Electronic structure of Î²-RbSm(MoO₄)₂and chemical bonding in molybdates. Dalton Transactions, 2015, 44, 1805-1815.	1.6	85
2454	First-principles Studies on Electronic and Magnetic Properties of I A â€“III A and I A â€“IV A Compounds with Zinc-Blende and Wurtzite Structures. Journal of Superconductivity and Novel Magnetism, 2015, 28, 1535-1541.	0.8	4
2455	First-principles calculation of W/WC interface: Atomic structure, stability and electronic properties. Applied Surface Science, 2015, 324, 205-211.	3.1	39
2456	Structures and optical properties of two phases of SrMgF₄. Physical Chemistry Chemical Physics, 2015, 17, 500-508.	1.3	9
2457	Prediction of molecular crystal structures by a crystallographic QM/MM model with full space-group symmetry. Acta Crystallographica Section A: Foundations and Advances, 2015, 71, 26-35.	0.0	8
2458	Synthesis, X-ray crystal structure, optical properties and DFT studies of a new 2D layered iodide bridged Pb(II) coordination polymer with 2,3-bis(2-pyridyl)pyrazine. Journal of Solid State Chemistry, 2015, 221, 433-440.	1.4	8
2459	First-principle investigation of electronic structure, magnetism and phase stability of Heusler-type Pt2â€²Mn1+Ga alloys. Journal of Magnetism and Magnetic Materials, 2015, 377, 40-43.	1.0	13
2460	Crystal Structure of the ZrO Phase at Zirconium/Zirconium Oxide Interfaces. Advanced Engineering Materials, 2015, 17, 211-215.	1.6	66
2461	DFT calculations study of structural, electronic, and optical properties of Cu2ZnSn(S1â€²Se)4 alloys. Journal of Alloys and Compounds, 2015, 618, 248-253.	2.8	11
2462	First-principles investigation on Cu/ZnO catalyst precursor: Energetic, structural and electronic properties of Zn-doped Cu2(OH)2CO3. Computational Materials Science, 2015, 96, 1-9.	1.4	15
2463	Thermodynamic reassessment of Nb-Ni-Ti system with orderâ€“disorder model. Journal of Alloys and Compounds, 2015, 619, 733-747.	2.8	25
2464	First-principles study of spin transition and seismic properties of ferric iron-bearing post-perovskite with oxygen vacancy. Physics and Chemistry of Minerals, 2015, 42, 163-169.	0.3	0
2465	Phase boundaries and molar volumes of high-temperature and high-pressure phase V of LiBH4. Journal of Physics and Chemistry of Solids, 2015, 76, 40-44.	1.9	5
2466	Growth mechanisms for spherical mixed hydroxide agglomerates prepared by co-precipitation method: A case of Ni1/3Co1/3Mn1/3(OH)2. Journal of Alloys and Compounds, 2015, 619, 846-853.	2.8	68
2467	Characterization of the physicochemical properties of novel SnS2 with cubic structure and diamond-like Sn sublattice. Acta Materialia, 2015, 82, 212-223.	3.8	20
2468	Enhancing the visible-light absorption of TiO2 with the use of key N, Co, and Na dopant concentrations. Solar Energy Materials and Solar Cells, 2015, 132, 94-100.	3.0	14
2469	Theoretical investigation on the interaction of subnano platinum clusters with graphene using DFT methods. Computational Materials Science, 2015, 96, 268-276.	1.4	21

#	Article	IF	Citations
2470	Solid-state NMR and computational investigation of solvent molecule arrangement and dynamics in isostructural solvates of droperidol. Solid State Nuclear Magnetic Resonance, 2015, 65, 12-20.	1.5	21
2471	Ab Initio Study of Binary and Ternary Nb3(X,Y) A15ÂIntermetallic Phases (X,YÂ=ÂAl, Ge, Si, Sn). Metallurgical and Materials Transactions A: Physical Metallurgy and Materials Science, 2015, 46, 566-576.	1.1	29
2472	Electronic Structures of Cu/S Co-doped/Anatase TiO 2 by First-principles. Revista Materia, 2016, 21, 599-605.	0.1	3
2473	Effects of Content of Network-Modifying Ion and Network Structure of Sodium Silicate Glasses by Molecular Dynamics Simulation. Journal of Computer Chemistry Japan, 2016, 14, 181-183.	0.0	0
2474	A New Phase of GaN. Journal of Chemistry, 2016, 2016, 1-9.	0.9	10
2475	Theoretical and Experimental Studies on the Crystal Structure, Electronic Structure and Optical Properties of SmTaO4. Materials, 2016, 9, 55.	1.3	20
2476	Photodesorption of NO from Au(100) using 3D surface-velocity map imaging. Journal of Chemical Physics, 2016, 145, 184201.	1.2	9
2477	Properties of the Free-Standing Two-Dimensional Copper Monolayer. Journal of Nanomaterials, 2016, 2016, 1-6.	1.5	13
2478	Multiscale, Multiphysics Computational Chemistry Methods Based on Artificial Intelligence Integrated Ultra-Accelerated Quantum Molecular Dynamics for the Application to Automotive Emission Control. SAE International Journal of Engines, 0, 9, 2434-2441.	0.4	2
2480	Electronic Structure and Optical Properties of BiOI as a Photocatalyst Driven by Visible Light. Catalysts, 2016, 6, 133.	1.6	28
2481	Computational Study of Quasi-2D Liquid State in Free Standing Platinum, Silver, Gold, and Copper Monolayers. Condensed Matter, 2016, 1, 1.	0.8	21
2482	Si96: A New Silicon Allotrope with Interesting Physical Properties. Materials, 2016, 9, 284.	1.3	26
2483	The Mechanical and Electronic Properties of Carbon-Rich Silicon Carbide. Materials, 2016, 9, 333.	1.3	19
2484	Two Novel C3N4 Phases: Structural, Mechanical and Electronic Properties. Materials, 2016, 9, 427.	1.3	34
2485	A Reinvestigation of a Superhard Tetragonal sp3 Carbon Allotrope. Materials, 2016, 9, 484.	1.3	18
2486	Crystal Structures and Mechanical Properties of Ca2C at High Pressure. Materials, 2016, 9, 570.	1.3	15
2487	Edge Structure of Montmorillonite from Atomistic Simulations. Minerals (Basel, Switzerland), 2016, 6, 25.	0.8	28
2488	Properties of the Sodium Naproxen-Lactose-Tetrahydrate Co-Crystal upon Processing and Storage. Molecules, 2016, 21, 509.	1.7	13

#	Article	IF	Citations
2489	Particulate Matter Formation Dynamics as Investigated by Ultra-Accelerated Quantum Chemical Molecular Dynamics Coupled with Canonical Monte Carlo Method. , 0, , .		0
2490	First Principles Investigation of Electronic Property and High Pressure Phase Stability of SmN. Chinese Journal of Chemical Physics, 2016, 29, 219-222.	0.6	1
2491	Instability and Spontaneous Reconstruction of Few-Monolayer Thick GaN Graphitic Structures. Nano Letters, 2016, 16, 4849-4856.	4.5	51
2492	Correlation and ordering of defects in the formation of conducting nanofilaments. Journal Physics D: Applied Physics, 2016, 49, 125303.	1.3	3
2493	Formation and Local Structure Analysis of Highâ€Valence Chromium Ion in Dicalcium Silicate. Journal of the American Ceramic Society, 2016, 99, 3151-3158.	1.9	6
2494	Structure Elucidation of an Yttrium Diethyldithiocarbamato-Phenanthroline Complex by X-ray Crystallography, Solid-State NMR, and ab-initio Quantum Chemical Calculations. European Journal of Inorganic Chemistry, 2016, 2016, 3278-3291.	1.0	7
2495	Simulations and measurements in scanning electron microscopes at low electron energy. Scanning, 2016, 38, 802-818.	0.7	12
2496	Microphase separation upon crystallization of small amphiphilic molecules: â€˜lowâ€™ temperature form II of sodium benzoate (E 211). CrystEngComm, 2016, 18, 5811-5817.	1.3	3
2497	Nuclear Magnetic Resonance of Metal-Organic Frameworks (MOFs). , 2016, , 607-628.		1
2498	Nuclear magnetic resonance study of sulfate reorientations in LiNaSO₄. Journal of Physics Condensed Matter, 2016, 28, 176003.	0.7	2
2499	The observation of oxygenâ€"oxygen interactions in ice. New Journal of Physics, 2016, 18, 023052.	1.2	21
2500	Predicting the electronic and optical properties of IB metals doped monoclinic BiVO₄: First principle calculations. International Journal of Quantum Chemistry, 2016, 116, 388-395.	1.0	12
2501	Recent advances in solidâ€state NMR computational spectroscopy: The case of aluminoâ€silicate glasses. International Journal of Quantum Chemistry, 2016, 116, 1520-1531.	1.0	23
2502	Donorâ€unsupported Phosphanylmethanides Li[CH₂PR₂] (R =) Tj ETQq1 1 0.784314 rgBT /O DFTâ€Ð Calculations. Zeitschrift Fur Anorganische Und Allgemeine Chemie, 2016, 642, 282-287.	0.6	7
2503	Modern solid state NMR techniques and concepts in structural studies of synthetic polymers. Polymers for Advanced Technologies, 2016, 27, 1143-1155.	1.6	10
2504	Modeling Ti/Ge Distribution in LiTi2â€"xGex(PO4)3 NASICON Series by 31P MAS NMR and First-Principles DFT Calculations. Journal of the American Chemical Society, 2016, 138, 9479-9486.	6.6	19
2505	Computational and experimental study of reversible hydration/dehydration processes in molecular crystals of natural products â€" a case of catechin. CrystEngComm, 2016, 18, 5267-5277.	1.3	15
2506	An overview of first-principles calculations of NMR parameters for paramagnetic materials. Materials Science and Technology, 2016, 32, 181-194.	0.8	5

#	Article	IF	Citations
2507	Design and Syntheses of Three Novel Carbonate Halides: Cs₃Pb₂(CO₃)₃I, KBa₂(CO₃)₂F, and RbBa₂(CO₃)₂F. Chemistry - A European Journal, 2016, 22, 2944-2954.	1.7	22
2508	PDielec: The calculation of infrared and terahertz absorption for powdered crystals. Journal of Computational Chemistry, 2016, 37, 1491-1504.	1.5	31
2510	Does the Dirac cone of germanene exist on metal substrates?. Physical Chemistry Chemical Physics, 2016, 18, 19451-19456.	1.3	39
2511	Electro-optical properties of the perfect reflector material: Poly(3-thiophene boronic acid) semiconducting polymer. Polymer Engineering and Science, 2016, 56, 707-714.	1.5	2
2512	Crystal structure and vibrational properties of Cu₂ZnSiSe₄quaternary semiconductor. Physica Status Solidi (B): Basic Research, 2016, 253, 1808-1815.	0.7	22
2513	Surface atomic relaxation and magnetism on hydrogen-adsorbed Fe(110) surfaces from first principles. Applied Surface Science, 2016, 387, 385-392.	3.1	9
2514	Synergistic Inhibition of Oxide Formation in Oxidation Catalysis: A First-Principles Kinetic Monte Carlo Study of NO + CO Oxidation at Pd(100). ACS Catalysis, 2016, 6, 5191-5197.	5.5	17
2515	Dendriteâ€Free Lithium Deposition Induced by Uniformly Distributed Lithium Ions for Efficient Lithium Metal Batteries. Advanced Materials, 2016, 28, 2888-2895.	11.1	877
2516	Crystallographic and Dynamic Aspects of Solidâ€State NMR Calibration Compounds: Towards ab Initio NMR Crystallography. ChemPhysChem, 2016, 17, 2496-2502.	1.0	12
2517	Analysis of the bondâ€valence method for calculating 29 Si and 31 P magnetic shielding in covalent network solids. Journal of Computational Chemistry, 2016, 37, 1704-1710.	1.5	14
2518	Rationalization of the Color Properties of Fluorescein in the Solid State: A Combined Computational and Experimental Study. Chemistry - A European Journal, 2016, 22, 10065-10073.	1.7	24
2519	4f fine-structure levels as the dominant error in the electronic structures of binary lanthanide oxides. Journal of Computational Chemistry, 2016, 37, 825-835.	1.5	49
2520	A theoretical and experimental NMR study of BODIPY 493/503: difluoro{2â€[1â€(3,5â€dimethylâ€2Hâ€pyrrolâ€2â€ylideneâ€N)ethyl]â€3,5â€dimethylâ€1Hâ€pyrrolatoâ€N Magnetic Resonance in Chemistry, 2016, 54, 684-688.	1.1	8
2521	Anab initiocharacterization of the electronic structure of LaCoxFe1-xO3forxâ€‰â‰â€‰0.5. Physica Status Solidi (B): Basic Research, 2016, 253, 1673-1687.	0.7	0
2522	Optical properties of quaternary kesterite-type Cu₂Zn(Sn_{1â^'x}Ge_x)S₄crystalline alloys: Raman scattering, photoluminescence and first-principle calculations. RSC Advances, 2016, 6, 67756-67763.	1.7	25
2523	Bandgap narrowing in the layered oxysulfide semiconductor Ba₃Fe₂O₅Cu₂S₂: Role of FeO₂layer. Chinese Physics B, 2016, 25, 026101.	0.7	5
2524	First-principles study of electronic and optical properties of Sr₂ZnN₂ under pressure. Modern Physics Letters B, 2016, 30, 1650139.	1.0	0
2525	Band gap and conductivity evaluation of carbon nanotube with hematite for green ammonia synthesis. AIP Conference Proceedings, 2016, , .	0.3	0

#	Article	IF	Citations
2526	Visible-Light-Responsive Chalcogenide Photocatalyst Ba₂ZnSe₃: Crystal and Electronic Structure, Thermal, Optical, and Photocatalytic Activity. Inorganic Chemistry, 2016, 55, 12783-12790.	1.9	40
2527	Structural and electronic structures of alkaline-earth transition metal oxynitride perovskites. Journal of the Ceramic Society of Japan, 2016, 124, 1056-1062.	0.5	3
2528	On the existence of the optimal order for wavefunction extrapolation in Born-Oppenheimer molecular dynamics. Journal of Chemical Physics, 2016, 144, 244103.	1.2	12
2529	O (N log N) scaling method to evaluate the ionâ€“electron potential of crystalline solids. Journal of Chemical Physics, 2016, 145, 184110.	1.2	7
2530	Intra- and inter-atomic optical transitions of Fe, Co, and Ni ferrocyanides studied using first-principles many-electron calculations. Journal of Applied Physics, 2016, 119, .	1.1	12
2531	Quasielastic neutron scattering measurements and ab initio MD-simulations on single ion motions in molten NaF. Journal of Chemical Physics, 2016, 144, 014503.	1.2	11
2532	Novel high-pressure phases of AlP from first principles. Journal of Applied Physics, 2016, 119, .	1.1	11
2533	The mechanism of the area negative thermal expansion in KBe2BO3F2 family crystals: A first-principles study. Journal of Applied Physics, 2016, 119, .	1.1	4
2534	Isotope tracer investigation and ab-initio simulation of anisotropic hydrogen transport and possible multi-hydrogen centers in tin dioxide. Journal of Applied Physics, 2016, 119, 225704.	1.1	4
2535	Effect of pressure on crystal structure and charge transport properties of 2,6-diphenylanthracene. Journal of Materials Research, 2016, 31, 3731-3744.	1.2	4
2536	Perspective: Role of structure prediction in materials discovery and design. APL Materials, 2016, 4, 053210.	2.2	114
2537	Electronic structure of O-doped SiGe calculated by DFT + U method. Chinese Physics B, 2016, 25, 127101.	0.7	2
2538	First-Principles Study of Electronic Structure of Type I Hybrid Carbonâ€“Silicon Clathrates. Journal of Electronic Materials, 2016, 45, 4246-4255.	1.0	4
2539	Realisation of magnetically and atomically abrupt half-metal/semiconductor interface: Co2FeSi0.5Al0.5/Ge(111). Scientific Reports, 2016, 6, 37282.	1.6	18
2540	Ab-initio simulations of higher Miller index Si:SiO2 interfaces for fin field effect transistor and nanowire transistors. Journal of Applied Physics, 2016, 119, .	1.1	6
2541	Band structure, Fermi surface, elastic, thermodynamic, and optical properties of AlZr₃, AlCu₃, and AlCu₂Zr: First-principles study. Chinese Physics B, 2016, 25, 083101.	0.7	11
2542	Communication: Towards catalytic nitric oxide reduction via oligomerization on boron doped graphene. Journal of Chemical Physics, 2016, 144, 151102.	1.2	10
2543	Crystallographic and optical properties and band structures of CuInSe₂, CuIn₃Se₅, and CuIn₅Se₈ phases in Cu-poor Cu₂Seâ€“In₂Se₃ pseudo-binary system. Japanese Journal of Applied Physics, 2016, 55, 04ES15.	0.8	59

#	Article	IF	Citations
2544	The screening effects of the screened exchange hybrid functional in surface systems: A case study on the CO/Pt(111) problem. AIP Advances, 2016, 6, 065309.	0.6	2
2545	Superhardsp2â€“sp3hybrid carbon allotropes with tunable electronic properties. AIP Advances, 2016, 6, 055020.	0.6	20
2546	Influence of the goethite (Î±-FeOOH) surface on the stability of distorted PuO₂ and PuO_{2â€“x} phases. Radiochimica Acta, 2016, 104, 821-841.	0.5	3
2547	Topotactic Transformation of Metalâ€“Organic Frameworks to Graphene-Encapsulated Transition-Metal Nitrides as Efficient Fenton-like Catalysts. ACS Nano, 2016, 10, 11532-11540.	7.3	253
2548	Insight into the mechanical, thermodynamics and superconductor properties of NbRuB via first-principles calculation. Scientific Reports, 2016, 6, 19055.	1.6	20
2549	Reversible switching between pressure-induced amorphization and thermal-driven recrystallization in VO2(B) nanosheets. Nature Communications, 2016, 7, 12214.	5.8	47
2550	Interfacial charge rearrangement and intermolecular interactions: Density-functional theory study of free-base porphine adsorbed on Ag(111) and Cu(111). Journal of Chemical Physics, 2016, 144, 024701.	1.2	23
2551	Bifunctional Ag/C₃N_{4.5}composite nanobelts for photocatalysis and antibacterium. Nanotechnology, 2016, 27, 395603.	1.3	16
2552	Band engineering in transition metal dichalcogenides: Stacked versus lateral heterostructures. Applied Physics Letters, 2016, 108, .	1.5	151
2553	Structural, anisotropic and thermodynamic properties of Imm2-BCN. Journal Wuhan University of Technology, Materials Science Edition, 2016, 31, 1272-1279.	0.4	1
2554	A universal preconditioner for simulating condensed phase materials. Journal of Chemical Physics, 2016, 144, 164109.	1.2	46
2555	Electronic structure and phase stability of low-temperature Ba(Fe1-xNix)2As2 superconductor. AIP Conference Proceedings, 2016, , .	0.3	1
2556	First-principles calculation of the elastic dipole tensor of a point defect: Application to hydrogen inÎ±-zirconium. Physical Review B, 2016, 94, .	1.1	24
2557	OPTICAL CONSTANTS AND BAND STRENGTHS OF CH₄:C₂H₆ ICES IN THE NEAR- AND MID-INFRARED. Astrophysical Journal, 2016, 825, 156.	1.6	15
2558	Enhanced ionic conductivity with Li7O2Br3 phase in Li3OBr anti-perovskite solid electrolyte. Applied Physics Letters, 2016, 109, .	1.5	48
2559	Structural, elastic and thermodynamic properties of A15-type compounds V₃X (X = Ir, Pt) Tj ETQq1 1 0.784314 rgBT /Ov	1.0	6
2560	Equiatomic quaternary Heusler alloys: A material perspective for spintronic applications. Applied Physics Reviews, 2016, 3, 031101.	5.5	242
2561	Folding of xylan onto cellulose fibrils in plant cell walls revealed by solid-state NMR. Nature Communications, 2016, 7, 13902.	5.8	287

#	Article	IF	Citations
2562	Pressure-induced structural transformation of CaC2. Journal of Chemical Physics, 2016, 144, 194506.	1.2	5
2563	AZn₂BO₃X₂(A = K, Rb, NH₄; X = Cl, Br): New Members of KBBF Family Exhibiting Large SHG Response and the Enhancement of Layer Interaction by Modified Structures. Chemistry of Materials, 2016, 28, 9122-9131.	3.2	134
2564	Raman fingerprint for semi-metal WTe2 evolving from bulk to monolayer. Scientific Reports, 2016, 6, 19624.	1.6	106
2565	Crystal-to-crystal photo-reversible polymerization mechanism of bis-thymine derivative. RSC Advances, 2016, 6, 107317-107322.	1.7	5
2566	The presence of CH3NH2 neutral species in organometal halide perovskite films. Applied Physics Letters, 2016, 108, .	1.5	50
2567	Hubbard U calculations on optical properties of 3d transition metal oxide TiO2. Results in Physics, 2016, 6, 891-896.	2.0	65
2568	The role of chemical structure on the magnetic and electronic properties of Co2FeAl0.5Si0.5/Si(111) interface. Applied Physics Letters, 2016, 108, .	1.5	15
2569	The antiphase boundary in half-metallic Heusler alloy Co2Fe(Al,Si): atomic structure, spin polarization reversal, and domain wall effects. Applied Physics Letters, 2016, 109, .	1.5	9
2570	Elastic anisotropy and electronic properties of Si3N4 under pressures. AIP Advances, 2016, 6, .	0.6	11
2571	Experimental and density functional study of Mn doped Bi2Te3 topological insulator. APL Materials, 2016, 4, .	2.2	14
2572	Mechanical characterization of nanoporous Au modified with self-assembled monolayers. Applied Physics Letters, 2016, 109, 261905.	1.5	5
2573	Coexistence of multiple metastable polytypes in rhombohedral bismuth. Scientific Reports, 2016, 6, 20337.	1.6	16
2575	Lattice dynamics and elasticity of SrCO₃. Journal of Applied Crystallography, 2016, 49, 1982-1990.	1.9	21
2576	Effect of metal oxide additions to quality on Ge/GeO2 interfaces. Journal of Applied Physics, 2016, 120, .	1.1	2
2577	Anomalous transition of major charge carriers from holes to electrons observed in single-crystal films of tungsten. Physical Review B, 2016, 94, .	1.1	3
2578	HRTEM low dose: the unfold of the morphed graphene, from amorphous carbon to morphed graphenes. Advanced Structural and Chemical Imaging, 2016, 2, 10.	4.0	33
2579	Robust high pressure stability and negative thermal expansion in sodium-rich antiperovskites Na3OBr and Na4OI2. Journal of Applied Physics, 2016, 119, .	1.1	13
2580	A Density Functional Theory Study of Codoping Characteristics of Sulfur with Alkaline Earth in Delafossite CuAlO 2. Communications in Theoretical Physics, 2016, 65, 527-530.	1.1	5

#	Article	IF	Citations
2581	Mirrored continuum and molecular scale simulations of the ignition of high-pressure phases of RDX. Journal of Chemical Physics, 2016, 144, 184111.	1.2	23
2582	Simulation of electron energy loss spectra of nanomaterials with linear-scaling density functional theory. Journal of Physics Condensed Matter, 2016, 28, 195202.	0.7	13
2583	Chemical trends of Schottky barrier behavior on monolayer hexagonal B, Al, and Ga nitrides. Journal of Applied Physics, 2016, 120, .	1.1	13
2584	Controlling the half-metallicity of Heusler/Si(1â€‰1â€‰1) interfaces by a monolayer of Siâ€“Coâ€“Si. Journal of Physics Condensed Matter, 2016, 28, 395003.	0.7	3
2585	Vibrational effects on surface energies and band gaps in hexagonal and cubic ice. Journal of Chemical Physics, 2016, 145, 044703.	1.2	7
2586	DFT study of gases adsorption on sharp tip nano-catalysts surface for green fertilizer synthesis. AIP Conference Proceedings, 2016, , .	0.3	1
2587	The normal modes of lattice vibrations of ice XI. Scientific Reports, 2016, 6, 29273.	1.6	22
2588	Controlled Exfoliation of MoS₂ Crystals into Trilayer Nanosheets. Journal of the American Chemical Society, 2016, 138, 5143-5149.	6.6	207
2589	Raman light scattering, infrared absorption and neutron scattering studies of the phase transition and reorientational dynamics of H2O ligands and ClO4â†™ anions in [Ca(H2O)4](ClO4)2. Vibrational Spectroscopy, 2016, 83, 26-35.	1.2	4
2590	The adsorbed state of a thiol on palladium nanoparticles. Physical Chemistry Chemical Physics, 2016, 18, 17265-17271.	1.3	6
2591	Chiral phosphorus nanotubes: structure, bonding, and electronic properties. Physical Chemistry Chemical Physics, 2016, 18, 12414-12418.	1.3	17
2592	Universal synthesis method for mixed phase TiO₂(B)/anatase TiO₂thin films on substrates via a modified low pressure chemical vapour deposition (LPCVD) route. Journal of Materials Chemistry A, 2016, 4, 5685-5699.	5.2	39
2593	Molecular structure of diethylaminoalane in the solid state: an X-ray powder diffraction, DFT calculation and Raman spectroscopy study. Acta Crystallographica Section B: Structural Science, Crystal Engineering and Materials, 2016, 72, 232-240.	0.5	6
2594	Modeling the effects of Si-X (XÂ=ÂF, Cl) bonds on the chemical and electronic properties of Si-surface terminated porous 3C-SiC. Theoretical Chemistry Accounts, 2016, 135, 1.	0.5	8
2595	Ab Initio Study of Phosphorus Anodes for Lithium- and Sodium-Ion Batteries. Chemistry of Materials, 2016, 28, 2011-2021.	3.2	182
2596	Monolayer MXenes: promising half-metals and spin gapless semiconductors. Nanoscale, 2016, 8, 8986-8994.	2.8	380
2597	Synthesis, crystal structure and optical properties of a new nocentrosymmetric borate: Ba7(BO3)3F5. Materials Research Bulletin, 2016, 81, 114-118.	2.7	3
2598	Elastic and electronic properties of M585 carbon under pressure. Chinese Journal of Physics, 2016, 54, 398-407.	2.0	2

#	Article	IF	Citations
2599	Structural, electronic and mechanical properties of (NbxTi1â^'x)2SC and (NbxZr1â^'x)2SC (0â©½xâ©½1) from first-principles investigations. Computational and Theoretical Chemistry, 2016, 1090, 58-66.	1.1	10
2600	On the predictions of the 11B solid state NMR parameters. Chemical Physics Letters, 2016, 655-656, 66-70.	1.2	12
2601	Transition metal coordination complexes of chrysazin. CrystEngComm, 2016, 18, 5121-5129.	1.3	7
2602	Structural stability, band structure and optical properties of different BiVO4 phases under pressure. Journal of Materials Science, 2016, 51, 6662-6673.	1.7	15
2603	Two-dimensional GeS with tunable electronic properties via external electric field and strain. Nanotechnology, 2016, 27, 274001.	1.3	85
2604	Luminescent, optical and electronic properties of La 3 Ta 0.5 Ga 5.5 O 14 single crystals grown in different atmospheres. Journal of Luminescence, 2016, 177, 152-159.	1.5	10
2605	Two novel Bi-based oxychloride photocatalysts: Synthesis, optical property and visible-light-responsive photocatalytic activity. Materials Science in Semiconductor Processing, 2016, 41, 317-322.	1.9	16
2606	Cs3W3PO13: A Tungsten Phosphate with One-Dimensional Zigzag Tunnels Exhibiting Strongly Anisotropic Thermal Expansion. Inorganic Chemistry, 2016, 55, 5113-5115.	1.9	2
2607	Surface-Induced Phase of Tyrian Purple (6,6â€²-Dibromoindigo): Thin Film Formation and Stability. Crystal Growth and Design, 2016, 16, 3647-3655.	1.4	15
2608	Switching of an Azobenzene-Tripod Molecule on Ag(111). Journal of Physical Chemistry Letters, 2016, 7, 2080-2084.	2.1	31
2609	Na₂ZnGe₂S₆: A New Infrared Nonlinear Optical Material with Good Balance between Large Second-Harmonic Generation Response and High Laser Damage Threshold. Journal of the American Chemical Society, 2016, 138, 7422-7428.	6.6	259
2610	Doped penta-graphene and hydrogenation of its related structures: a structural and electronic DFT-D study. Physical Chemistry Chemical Physics, 2016, 18, 15505-15509.	1.3	37
2611	Role of Tricoordinate Al Sites in CH₃ReO₃/Al₂O₃ Olefin Metathesis Catalysts. Journal of the American Chemical Society, 2016, 138, 6774-6785.	6.6	42
2612	Isomorphous template induced crystallisation: a robust method for the targeted crystallisation of computationally predicted metastable polymorphs. Chemical Communications, 2016, 52, 7384-7386.	2.2	57
2613	Graphene, Graphene Oxide and Silicon Irradiation by Cluster Ions of Argon and Highly Charged Ions. MRS Advances, 2016, 1, 1417-1422.	0.5	1
2614	Electronic structure and optical properties of CsI, CsI(Ag), and CsI(Tl). Journal of the Korean Physical Society, 2016, 68, 1069-1074.	0.3	14
2615	Nuclear Quantum Effects in Water and Aqueous Systems: Experiment, Theory, and Current Challenges. Chemical Reviews, 2016, 116, 7529-7550.	23.0	439
2616	Novel high-pressure phases of AlN: A first-principles study. Computational Materials Science, 2016, 117, 496-501.	1.4	29

#	Article	IF	Citations
2617	Complex doping chemistry owing to Mn incorporation in nanocrystalline anatase TiO₂powders. Physical Chemistry Chemical Physics, 2016, 18, 2818-2829.	1.3	19
2618	Metastabiles SalpetersÃuretrihydrat in Eiswolken. Angewandte Chemie, 2016, 128, 3334-3338.	1.6	0
2619	Transition from Diffusionâ€Controlled Intercalation into Extrinsically Pseudocapacitive Charge Storage of MoS₂ by Nanoscale Heterostructuring. Advanced Energy Materials, 2016, 6, 1501115.	10.2	185
2620	Structural, elastic and thermodynamic properties of tetragonal and orthorhombic polymorphs of Sr₂GeN₂: an ab initio investigation. High Pressure Research, 2016, 36, 198-219.	0.4	15
2621	Comparison of HfCl4, HfI4, TEMA-Hf, and TDMA-Hf as precursors in early growing stages of HfO2 films deposited by ALD: A DFT study. Chemical Physics, 2016, 472, 81-88.	0.9	13
2622	Electronic and Mechanical Properties of Tetragonal Nb2Al Under High Pressure: First-Principles Calculations. Brazilian Journal of Physics, 2016, 46, 213-219.	0.7	6
2623	Na₂Hg₃M₂S₈ (M = Si, Ge, and Sn): New Infrared Nonlinear Optical Materials with Strong Second Harmonic Generation Effects and High Laser-Damage Thresholds. Chemistry of Materials, 2016, 28, 2795-2801.	3.2	156
2624	Influence of main-group element on half-metallic properties in half-Heusler compound. Modern Physics Letters B, 2016, 30, 1650206.	1.0	3
2625	Structural and morphological studies of meso-ethylcarbazole F-BODIPY thin films. Monatshefte FÃ¼r Chemie, 2016, 147, 1915-1923.	0.9	5
2626	Cyanoacetohydrazide under Pressure: Chemical Changes in a Hydrogen-Bonded Material. Journal of Physical Chemistry A, 2016, 120, 2712-2719.	1.1	2
2627	Structural, elastic, electronic and optical properties of Cu3MTe4 (M = Nb, Ta) sulvanites â€" An abÂinitio study. International Journal of Modern Physics B, 2016, 30, 1650089.	1.0	18
2628	Density functional theory calculations, growth, structure, and optical properties of birefringent LiNaV₂O₆. Journal of Materials Research, 2016, 31, 488-494.	1.2	6
2629	Computational study of the structure, UV-vis absorption spectra and conductivity of biphenylene-based polymers and their boron nitride analogues. RSC Advances, 2016, 6, 49505-49516.	1.7	24
2630	Thermodynamics of mixing in an isostructural solid solution: Simulation methodologies and application to the rutile-cassiterite system. American Mineralogist, 2016, 101, 1197-1206.	0.9	8
2631	Strong compensation hinders the p-type doping of ZnO: a glance over surface defect levels. Solid State Communications, 2016, 237-238, 34-37.	0.9	22
2632	Effect of the [Ba2BO3F]âˆž Layer on the Band Gap: Synthesis, Characterization, and Theoretical Studies of BaZn2B2O6Â·nBa2BO3F (n = 0, 1, 2). Inorganic Chemistry, 2016, 55, 4806-4812.	1.9	21
2633	Interesting pressure dependence of power factor in BiTeI. Journal Physics D: Applied Physics, 2016, 49, 215107.	1.3	16
2634	First-Principles Investigations of the Structure, Electronic, and Optical Properties of Mullite-Type Orthorhombic Bi₂M₄O₉ (M = Al³⁺, Ga³⁺). Inorganic Chemistry, 2016, 55, 4824-4835.	1.9	23

#	Article	IF	Citations
2635	Counting vacancies and nitrogen-vacancy centers in detonation nanodiamond. Nanoscale, 2016, 8, 10548-10552.	2.8	33
2636	Narrow Red Emission Band Fluoride Phosphor KNaSiF₆:Mn⁴⁺ for Warm White Light-Emitting Diodes. ACS Applied Materials & Interfaces, 2016, 8, 11194-11203.	4.0	228
2637	Unraveling energy conversion modeling in the intrinsic persistent upconverted luminescence of solids: a study of native point defects in antiferromagnetic Er₂O₃. Physical Chemistry Chemical Physics, 2016, 18, 13564-13582.	1.3	29
2638	Electronic structures and magnetism for carbon doped CdSe: Modified Beckeâ€“Johnson density functional calculations. Journal of Magnetism and Magnetic Materials, 2016, 414, 10-13.	1.0	2
2639	Combining solid-state NMR spectroscopy with first-principles calculations â€“ a guide to NMR crystallography. Chemical Communications, 2016, 52, 7186-7204.	2.2	202
2640	Effects of alloying on the behavior of B and S at Î£5 (2 1 0) grain boundary in Î³-Fe. Computational Materials Science, 2016, 115, 170-176.	1.4	24
2641	Role of Sn impurity on electronic topological transitions in 122 Fe-based superconductors. Journal of Alloys and Compounds, 2016, 677, 245-251.	2.8	7
2642	Hierarchical active factors to band gap and nonlinear optical response in Ag-containing quaternary-chalcogenide compounds. Journal of Solid State Chemistry, 2016, 239, 30-35.	1.4	8
2643	First-principles study on the structural, elastic and electronic properties of Ti2SiN under high pressure. Solid State Communications, 2016, 237-238, 24-27.	0.9	12
2644	Single-Layered Hittorfâ€™s Phosphorus: A Wide-Bandgap High Mobility 2D Material. Nano Letters, 2016, 16, 2975-2980.	4.5	219
2645	Manipulation of birefringence via substitution of Sr²⁺by Pb²⁺based on the structure model of LiSr_{1â^'x}Pb_xBO₃(0 â‰¤ x â‰¤ 0.5). New Journal of Chemistry, 2016, 40, 6120-6126.	1.4	5
2646	Electronic structure and optical properties of Î±-RDX crystal under pressure from first-principles calculations. Molecular Physics, 2016, 114, 1931-1938.	0.8	2
2647	Optical vibrational modes of Ge nanowires: A computational approach. Microelectronic Engineering, 2016, 159, 215-220.	1.1	7
2648	Point defect interactions in iron lattice: a first-principles study. RSC Advances, 2016, 6, 45250-45258.	1.7	21
2649	First principles insights into improved catalytic performance of BaTiO3- graphene nanocomposites in conjugation with experimental investigations. Materials Science in Semiconductor Processing, 2016, 51, 33-41.	1.9	17
2650	³⁵Cl Solid-State NMR and Computational Study of Chlorine Halogen Bond Donors in Single-Component Crystalline Chloronitriles. Journal of Physical Chemistry C, 2016, 120, 11121-11130.	1.5	44
2651	Two-Dimensional Phosphorus Porous Polymorphs with Tunable Band Gaps. Journal of the American Chemical Society, 2016, 138, 7091-7098.	6.6	119
2652	Research on new rare-earth half-metallic ferromagnets X0.75Eu0.25O (X=Ca, Sr and Ba) based on the first-principles calculations. Solid State Communications, 2016, 242, 11-15.	0.9	10

#	Article	IF	Citations
2653	First principles investigation of helium physisorption on an Î±-Al₂O₃(0001) surface. Physical Chemistry Chemical Physics, 2016, 18, 15711-15718.	1.3	8
2654	Computational and Experimental Characterization of Five Crystal Forms of Thymine: Packing Polymorphism, Polytypism/Disorder, and Stoichiometric 0.8-Hydrate. Crystal Growth and Design, 2016, 16, 3480-3496.	1.4	34
2655	Aluminum Borohydride Complex with Ethylenediamine: Crystal Structure and Dehydrogenation Mechanism Studies. Journal of Physical Chemistry C, 2016, 120, 10192-10198.	1.5	9
2656	Flat-Band Potentials of Molecularly Thin Metal Oxide Nanosheets. ACS Applied Materials & Interfaces, 2016, 8, 11539-11547.	4.0	92
2657	Furosemide's one little hydrogen atom: NMR crystallography structure verification of powdered molecular organics. Chemical Communications, 2016, 52, 6685-6688.	2.2	49
2658	â€œXA6â€•octahedra influencing the arrangement of anionic groups and optical properties in inverse-perovskite [B6O10]XA3(X = Cl, Br; A = alkali metal). Physical Chemistry Chemical Physics, 2016, 18, 15394-15398.	1.3	16
2659	Wavelength-dependent optical transition mechanisms for light-harvesting of perovskite MAPbI3 solar cells using first-principles calculations. Journal of Materials Chemistry C, 2016, 4, 5248-5254.	2.7	11
2660	Electronic and optical properties of Mnâ€“S co-doped anatase TiO₂ from first-principles calculations. Materials Science-Poland, 2016, 34, 38-44.	0.4	4
2661	The microstructure of scale formed by oxynitriding of Ti and exhibiting significant apatite-forming ability. Journal of Materials Research, 2016, 31, 1004-1011.	1.2	7
2662	Influences of S, Se, Te and Po substitutions on structural, electronic and optical properties of hexagonal CuAlO₂using GGA and B3LYP functionals. Physical Chemistry Chemical Physics, 2016, 18, 14317-14322.	1.3	14
2663	First-Principles Study of Lattice Dynamics, Structural Phase Transition, and Thermodynamic Properties of Barium Titanate. Zeitschrift Fur Naturforschung - Section A Journal of Physical Sciences, 2016, 71, 759-768.	0.7	13
2664	Mononuclear, tetranuclear and polymeric cadmium(II) complexes with the 3,6-bis(2-pyridyl)-1,2,4,5-tetrazine ligand: Synthesis, crystal structure, spectroscopic and DFT studies. Polyhedron, 2016, 119, 160-174.	1.0	17
2665	Mechanical and electronic properties of Câ€“Si alloys in the P222 1 structure. Chinese Journal of Physics, 2016, 54, 700-710.	2.0	8
2666	First-principles study of the structural, elastic, mechanical, electronic, and optical properties of cubic Mg2TiO4. Moscow University Physics Bulletin (English Translation of Vestnik Moskovskogo) Tj ETQq1 1 0.784314 rgBT /Overlock	0.3	
2667	An Overview of Powder X-ray Diffraction and Its Relevance to Pharmaceutical Crystal Structures. Advances in Delivery Science and Technology, 2016, , 293-314.	0.4	2
2668	Structural Investigation of Zn(II) Insertion in Bayerite, an Aluminum Hydroxide. Inorganic Chemistry, 2016, 55, 9306-9315.	1.9	22
2669	AMgPO₄Â·6H₂O (A = Rb, Cs): strong SHG responses originated from orderly PO₄groups. Journal of Materials Chemistry C, 2016, 4, 9219-9226.	2.7	44
2670	Photoemission simulation for photocathode design: theory and application to copper and silver surfaces. Computational Materials Science, 2016, 122, 331-340.	1.4	19

#	Article	IF	Citations
2671	Si₁₀: A sp³ Silicon Allotrope with Spirally Connected Si₅ Tetrahedrons. Chemistry of Materials, 2016, 28, 6441-6445.	3.2	16
2672	Pressure-Induced Phase Transition of Hydrogen Storage Material Hydrazine Bisborane: Evolution of Dihydrogen Bonds. Journal of Physical Chemistry C, 2016, 120, 21293-21298.	1.5	8
2673	Growth, Properties, and Theoretical Analysis of KBa₂(PO₃)₅ Single Crystal. Crystal Growth and Design, 2016, 16, 5588-5592.	1.4	43
2674	Interfacial properties of staneneâ€“metal contacts. 2D Materials, 2016, 3, 035020.	2.0	26
2675	The structural, elastic, electronic and optical properties of MgCu under pressure: A first-principles study. International Journal of Modern Physics B, 2016, 30, 1650199.	1.0	73
2676	A Computational and Experimental Study on the Binding of Dithio Ligands to Sperrylite, Pentlandite, and Platinum. Journal of Physical Chemistry C, 2016, 120, 22476-22488.	1.5	16
2677	Using crystal structure prediction to rationalize the hydration propensities of substituted adamantane hydrochloride salts. Acta Crystallographica Section B: Structural Science, Crystal Engineering and Materials, 2016, 72, 551-561.	0.5	15
2678	The electronic and structural properties in Ca 2 TiMnO 6 double perovskite: The first principle study. Computational Condensed Matter, 2016, 9, 35-39.	0.9	9
2679	Prediction of indirect to direct band gap transition under tensile biaxial strain in type-I guest-free silicon clathrate Si46: A first-principles approach. Superlattices and Microstructures, 2016, 100, 296-305.	1.4	4
2680	Ammonia and iron cointercalated iron sulfide (NH₃)Fe_{0.25}Fe₂S₂: hydrothermal synthesis, crystal structure, weak ferromagnetism and crossover from a negative to positive magnetoresistance. RSC Advances, 2016, 6, 81886-81893.	1.7	11
2681	Why Do Hydrates (Solvates) Form in Small Neutral Organic Molecules? Exploring the Crystal Form Landscapes of the Alkaloids Brucine and Strychnine. Crystal Growth and Design, 2016, 16, 6405-6418.	1.4	32
2682	Highly active Ta₂O₅microcubic single crystals: facet energy calculation, facile fabrication and enhanced photocatalytic activity of hydrogen production. Journal of Materials Chemistry A, 2016, 4, 16562-16568.	5.2	16
2683	On the Crystal Structural Control of Sputtered TiO2 Thin Films. Nanoscale Research Letters, 2016, 11, 324.	3.1	30
2684	La₃Li₃W₂O₁₂: Ionic Diffusion in a Perovskite with Lithium on both A- and B-Sites. Chemistry of Materials, 2016, 28, 7833-7851.	3.2	27
2685	Phase Composition and Disorder in La₂(Sn,Ti)₂O₇ Ceramics: New Insights from NMR Crystallography. Journal of Physical Chemistry C, 2016, 120, 20288-20296.	1.5	15
2686	Electronic excitation-induced semiconductor-to-metal transition in monolayer<mml:math xmlns:mml="http://www.w3.org/1998/Math/MathML"><mml:msub><mml:mi>MoTe</mml:mi><mml:mn>2</mml:mn></mml:msub><m Physical Review B, 2016, 94, .	1.1	48
2687	Rb2SeOCl4Â·H2O: a polar material among the alkali metal selenite halides with a strong SHG response. Dalton Transactions, 2016, 45, 17723-17728.	1.6	15
2688	Evolutionary design of interfacial phase change van der Waals heterostructures. Nanoscale, 2016, 8, 18212-18220.	2.8	28

#	Article	IF	Citations
2689	Enhanced NMR Discrimination of Pharmaceutically Relevant Molecular Crystal Forms through Fragment-Based Ab Initio Chemical Shift Predictions. Crystal Growth and Design, 2016, 16, 6479-6493.	1.4	34
2690	Raman and IR Spectra of Ice Ih and Ice XI with an Assessment of DFT Methods. Journal of Physical Chemistry B, 2016, 120, 11043-11051.	1.2	18
2691	Hexagonal structure of phase III of solid hydrogen. Physical Review B, 2016, 94, .	1.1	44
2692	Three-Dimensional Non-Centrosymmetric Ba(II)/Li(I)â€“Imidazolecarboxylate Coordination Polymers: Second Harmonic Generation and Blue Fluorescence. Crystal Growth and Design, 2016, 16, 6654-6662.	1.4	11
2693	Effects of differential stress on the structure and Raman spectra of calcite from first-principles calculations. American Mineralogist, 2016, 101, 1892-1897.	0.9	7
2695	Firstâ€principles prediction of mechanical and bonding characteristics of new T₂ superconductor Ta₅GeB₂. Physica Status Solidi (B): Basic Research, 2016, 253, 2020-2026.	0.7	61
2696	Density functional theory study on Hg removal mechanisms of Cu-impregnated activated carbon prepared by simplified method. Korean Journal of Chemical Engineering, 2016, 33, 2869-2877.	1.2	4
2697	Experimental and First-Principles NMR Analysis of Pt(II) Complexes With O,Oâ€²-Dialkyldithiophosphate Ligands. Journal of Physical Chemistry A, 2016, 120, 8326-8338.	1.1	8
2698	LiSr_{2â€“x}Eu_xGe₃: Light on the Europium Site Preferences. Journal of Physical Chemistry C, 2016, 120, 23121-23128.	1.5	2
2699	Hybridization of inorganic CoB noncrystal with graphene and its Kubas-enhanced hydrogen adsorption at room temperature. RSC Advances, 2016, 6, 93238-93244.	1.7	7
2700	Superhard Semiconducting Phase of Osmium Tetraboride Stabilizing at 11 GPa. Journal of Physical Chemistry C, 2016, 120, 23165-23171.	1.5	14
2701	Testing the limits of NMR crystallography: the case of caffeineâ€“citric acid hydrate. CrystEngComm, 2016, 18, 6700-6707.	1.3	25
2702	K5Ba10(BO3)8F: A New Potassium Barium Borate Fluoride with a Perovskite-Like Structure. Journal of Physical Chemistry C, 2016, 120, 18763-18770.	1.5	38
2703	Eu³⁺-Doped Wide Band Gap Zn₂SnO₄ Semiconductor Nanoparticles: Structure and Luminescence. Journal of Physical Chemistry C, 2016, 120, 18887-18894.	1.5	43
2704	Explanation of Surface-Enhanced Raman Scattering Intensities of p-Aminobenzenethiol by Density Functional Computations. Journal of Physical Chemistry C, 2016, 120, 18275-18280.	1.5	13
2705	Applications of large-scale density functional theory in biology. Journal of Physics Condensed Matter, 2016, 28, 393001.	0.7	105
2706	Fundamental View of Electronic Structures of Î²-NaYF₄, Î²-NaGdF₄, and Î²-NaLuF₄. Journal of Physical Chemistry C, 2016, 120, 18858-18870.	1.5	42
2707	Role of the metal cation types around VO4 groups on the nonlinear optical behavior of materials: experimental and theoretical analysis. Dalton Transactions, 2016, 45, 14394-14402.	1.6	16

#	Article	IF	Citations
2708	Electronic properties of red and black phosphorous and their potential application as photocatalysts. RSC Advances, 2016, 6, 80872-80884.	1.7	33
2710	Role of the electronic structure in the morphotropic phase boundary of TbxDy1â^'xCo2 studied by first-principle calculation. Journal of Alloys and Compounds, 2016, 689, 1083-1087.	2.8	6
2711	DFT Based Theoretical Study about the Contributions of Fluorine to Nonlinear Optical Properties in Borate Fluoride Crystals. Crystal Growth and Design, 2016, 16, 5067-5073.	1.4	20
2712	K3B3O4(OH)4Â·2H2O: A UV Nonlinear Optical Crystal with Isolated [B3O4(OH)4]3â€“ Anion Groups. Inorganic Chemistry, 2016, 55, 8744-8749.	1.9	20
2713	A structurally flexible triazolate-based metalâ€“organic framework featuring coordinatively unsaturated copper(<scp>i</scp>) sites. Dalton Transactions, 2016, 45, 13853-13862.	1.6	26
2714	Alkali and Alkaline earth metal doped aluminum tetraborides containing intrinsic planar boron sheet: XAlB4 (X= Li, Mg, Ca, and Na). Computational Materials Science, 2016, 124, 130-141.	1.4	5
2715	A Multi-Technique Experimental and Computational Approach To Study the Dehydration Processes in the Crystals of Endomorphin Opioid Peptide Derivative. Crystal Growth and Design, 2016, 16, 5312-5322.	1.4	7
2716	Design Strategies in Hydrothermal Polymerization of Polyimides. Macromolecular Chemistry and Physics, 2016, 217, 485-500.	1.1	25
2717	Bottom-up Approach Design, Band Structure, and Lithium Storage Properties of Atomically Thin Î³-FeOOH Nanosheets. ACS Applied Materials & Interfaces, 2016, 8, 21334-21342.	4.0	49
2718	Crystal Structure Determination of Dimenhydrinate after More than 60 Years: Solving Saltâ€“Cocrystal Ambiguity via Solid-State Characterizations and Solubility Study. Crystal Growth and Design, 2016, 16, 5223-5229.	1.4	33
2719	Tunable Ambipolar Polarization-Sensitive Photodetectors Based on High-Anisotropy ReSe₂ Nanosheets. ACS Nano, 2016, 10, 8067-8077.	7.3	276
2720	Calculating EELS. , 2016, , 405-423.		1
2721	Influence of L2 1 B Disorder on the Spin-Gapless Semiconductor Character in Quaternary Heusler Alloys CoFeMnSi and CoFeVSi. Journal of Superconductivity and Novel Magnetism, 2016, 29, 3181-3186.	0.8	10
2722	A promising two-dimensional channel material: monolayer antimonide phosphorus. Science China Materials, 2016, 59, 648-656.	3.5	28
2723	Energy harvesting and conversion mechanisms for intrinsic upconverted mechano-persistent luminescence in CaZnOS. Physical Chemistry Chemical Physics, 2016, 18, 25946-25974.	1.3	46
2724	Fe/W Coâ€Đoped BiVO₄ Photoanodes with a Metalâ€“Organic Framework Cocatalyst for Improved Photoelectrochemical Stability and Activity. ChemSusChem, 2016, 9, 2824-2831.	3.6	81
2725	Structureâ€“Spectra Correlations in Anilate Complexes with Picolines. Crystal Growth and Design, 2016, 16, 6069-6083.	1.4	3
2726	Structure determination of Ba5AlF13 by coupling electron, synchrotron and neutron powder diffraction, solid-state NMR and ab initio calculations. Dalton Transactions, 2016, 45, 15565-15574.	1.6	12

#	Article	IF	Citations
2727	Electronic Structures of Germanene on MoS₂: Effect of Substrate and Molecular Adsorption. Journal of Physical Chemistry C, 2016, 120, 21691-21698.	1.5	40
2728	Hydrogen release reactions of Al-based complex hydrides enhanced by vibrational dynamics and valences of metal cations. Chemical Communications, 2016, 52, 11807-11810.	2.2	10
2729	High-Pressure-Induced Planarity of the Molecular Arrangement in Maleic Anhydride. Journal of Physical Chemistry C, 2016, 120, 18503-18509.	1.5	4
2730	Jastrow correlation factor for periodic systems. Physical Review B, 2016, 94, .	1.1	6
2731	Multinuclear NMR as a tool for studying local order and dynamics in CH₃NH₃PbX₃ (X = Cl, Br, I) hybrid perovskites. Physical Chemistry Chemical Physics, 2016, 18, 27133-27142.	1.3	78
2732	Theoretical exploration of novel catalyst support materials for fuel cell applications. Journal of Materials Chemistry A, 2016, 4, 15181-15188.	5.2	11
2733	Self-Supported Cedarlike Semimetallic Cu₃P Nanoarrays as a 3D High-Performance Janus Electrode for Both Oxygen and Hydrogen Evolution under Basic Conditions. ACS Applied Materials & Interfaces, 2016, 8, 23037-23048.	4.0	170
2734	First-principles study of martensitic transformation and magnetic properties of carbon doped Niâ€“Mnâ€“Sn Heusler alloys. Physics Letters, Section A: General, Atomic and Solid State Physics, 2016, 380, 3414-3420.	0.9	19
2735	First-principles prediction of a new planar hydrocarbon material: half-hydrogenated 14,14,14-graphyne. Physical Chemistry Chemical Physics, 2016, 18, 23954-23960.	1.3	11
2736	Pressure effect on the structural, electronic, and elastic properties and Debye temperature of Rh3Nb: first-principles calculations. RSC Advances, 2016, 6, 78028-78035.	1.7	6
2737	Selective Adsorption of Sulfur Dioxide in a Robust Metalâ€“Organic Framework Material. Advanced Materials, 2016, 28, 8705-8711.	11.1	214
2738	Crystal Growth, Structure, and Optical Properties of LiGaGe₂Se₆. Inorganic Chemistry, 2016, 55, 8672-8680.	1.9	37
2739	Structure and stability of pyrophyllite edge surfaces: Effect of temperature and water chemical potential. Geochimica Et Cosmochimica Acta, 2016, 190, 100-114.	1.6	32
2740	Effects of biaxial strains on the structural, electronic, elastic and lattice vibrational properties in t -BC 2 N and z -BC 2 N. Journal of Alloys and Compounds, 2016, 686, 914-922.	2.8	11
2741	Effects of Dopant Addition on Lattice and Luminescence Intensity Parameters of Eu(III)-Doped Lanthanum Orthovanadate. Journal of Physical Chemistry C, 2016, 120, 28497-28508.	1.5	50
2742	Approach using the electrical structure and optical properties of aluminium-doped zinc oxide for solar cells. RSC Advances, 2016, 6, 110943-110950.	1.7	11
2743	Room temperature detection of individual molecular physisorption using suspended bilayer graphene. Science Advances, 2016, 2, e1501518.	4.7	127
2744	Synthesis, X-ray powder diffraction and DFTÂcalculations of vasorelaxant active 3-(arylmethylidene)pyrrolidine-2,5-diones. RSC Advances, 2016, 6, 112950-112959.	1.7	9

#	Article	IF	Citations
2745	Epoxy-Carbonyl Conformation of Graphene Oxides. Journal of Physical Chemistry C, 2016, 120, 22739-22743.	1.5	19
2746	Carbon nitride frameworks and dense crystalline polymorphs. Physical Review B, 2016, 94, .	1.1	51
2747	Interplay of Pt and Crystal Facets of TiO₂: CO Oxidation Activity and Operando XAS/DRIFTS Studies. ACS Catalysis, 2016, 6, 7799-7809.	5.5	107
2748	Stability and migration of transmutation atoms (H/He) in Ti₃AlC₂: first principles calculations. RSC Advances, 2016, 6, 59875-59881.	1.7	13
2749	Deep-Ultraviolet Transparent Cs₂LiPO₄ Exhibits an Unprecedented Second Harmonic Generation. Chemistry of Materials, 2016, 28, 7110-7116.	3.2	130
2750	¹⁴N Solidâ€State NMR Spectroscopy of Amino Acids. ChemPhysChem, 2016, 17, 4011-4027.	1.0	20
2751	Copper(II) adsorption on the kaolinite(001) surface: Insights from first-principles calculations and molecular dynamics simulations. Applied Surface Science, 2016, 389, 316-323.	3.1	44
2752	A set of manganese ion activated fluoride phosphors (A₂BF₆:Mn⁴⁺, A = K, Na, B = Si, Ge, Ti): synthesis below 0 Â°C and efficient room-temperature photoluminescence. Journal of Materials Chemistry C, 2016, 4, 9561-9568.	2.7	75
2753	A simple melting-diffusing-reacting strategy to fabricate S/NiS₂â€“C for lithiumâ€“sulfur batteries. Nanoscale, 2016, 8, 17616-17622.	2.8	100
2754	Periodic vs. molecular cluster approaches to resolving glass structure and properties: Anorthite a case study. Journal of Non-Crystalline Solids, 2016, 451, 138-145.	1.5	20
2755	The solid state structures of the high and low temperature phases of dimethylcadmium. Chemical Communications, 2016, 52, 10144-10146.	2.2	7
2757	Synthesis and Characterization of Nanostructured Magnesium Oxide: Insight from Solid-State Density Functional Theory Calculations. Journal of Inorganic and Organometallic Polymers and Materials, 2016, 26, 1413-1420.	1.9	21
2758	Enclathration of CHF 3 and C 2 F 6 molecules in gas hydrates for potential application in fluorinated gas (F-gas) separation. Chemical Engineering Journal, 2016, 306, 298-305.	6.6	24
2759	On the molecular dynamics in long-acting calcium channel blocker lacidipine: solid-state NMR, neutron scattering and periodic DFT study. RSC Advances, 2016, 6, 66617-66629.	1.7	3
2760	Dynamical and elastic properties of MgSiO₃ perovskite (bridgmanite). Geophysical Research Letters, 2016, 43, 2568-2575.	1.5	15
2762	Investigating Unusual Homonuclear Intermolecular â€œThrough-Spaceâ€• Couplings in Organochalcogen Systems. Inorganic Chemistry, 2016, 55, 10881-10887.	1.9	15
2763	The outlook for platonic and cubic gauche nitrogens. Computational Materials Science, 2016, 123, 31-39.	1.4	5
2764	SnS₂- Compared to SnO₂-Stabilized S/C Composites toward High-Performance Lithium Sulfur Batteries. ACS Applied Materials & Interfaces, 2016, 8, 19550-19557.	4.0	102

#	Article	IF	Citations
2765	Electronic structure, first and second order physical properties of MPS4: a theoretical study. Materials Science-Poland, 2016, 34, 275-285.	0.4	3
2766	Structural, Elastic, and Electronic Properties of Newly Discovered Li2PtSi3 Superconductor: Effect of Transition Metals. Journal of Superconductivity and Novel Magnetism, 2016, 29, 2503-2508.	0.8	23
2767	Benchmark fragment-based¹H,¹³C,¹⁵N and¹⁷O chemical shift predictions in molecular crystals. Physical Chemistry Chemical Physics, 2016, 18, 21686-21709.	1.3	94
2768	Vibrational averages along thermal lines. Physical Review B, 2016, 93, .	1.1	48
2769	Dissociation products and structures of solid<mml:math xmlns:mml="http://www.w3.org/1998/Math/MathML"><mml:msub><mml:mi mathvariant="normal">H</mml:mi><mml:mn>2</mml:mn></mml:msub><mml:mi mathvariant="normal">S</mml:mi></mml:math>at strong compression. Physical Review B, 2016, 93, .	1.1	119
2770	Tucker-tensor algorithm for large-scale Kohn-Sham density functional theory calculations. Physical Review B, 2016, 93, .	1.1	7
2771	Supercell convergence of charge-transfer energies in pentacene molecular crystals from constrained DFT. Physical Review B, 2016, 93, .	1.1	18
2772	Property trends in simple metals: An empirical potential approach. Physical Review B, 2016, 93, .	1.1	37
2773	Interplay between nanometer-scale strain variations and externally applied strain in graphene. Physical Review B, 2016, 93, .	1.1	8
2774	Semiconductor-topological insulator transition of two-dimensional SbAs induced by biaxial tensile strain. Physical Review B, 2016, 93, .	1.1	118
2775	Spin Manipulation by Creation of Single-Molecule Radical Cations. Physical Review Letters, 2016, 116, 027201.	2.9	53
2776	Thermal and Electronic Fluctuations of Flexible Adsorbed Molecules: Azobenzene on Ag(111). Physical Review Letters, 2016, 116, 146101.	2.9	26
2777	Soft phonon modes in rutile<mml:math xmlns:mml="http://www.w3.org/1998/Math/MathML"><mml:msub><mml:mi>TiO</mml:mi><mml:mn>2</mml:mn></mml:msub></mml Physical Review B, 2016, 93, .	1.1	56
2778	DNA-stabilized Agâ€“Au bimetallic clusters: the effects of alloying and embedding on optical properties. Physical Chemistry Chemical Physics, 2016, 18, 22311-22322.	1.3	5
2779	Phase transition and equation of state of paratellurite (TeO₂) under high pressure. Materials Research Express, 2016, 3, 076206.	0.8	6
2780	Copper Selenidophosphates Cu4P2Se6, Cu4P3Se4, Cu4P4Se3, and CuP2Se, Featuring Zero-, One-, and Two-Dimensional Anions. Inorganic Chemistry, 2016, 55, 8031-8040.	1.9	4
2781	Impact of surface arrangement and composition on ethylene adsorption over Pdâ€“Ag surface alloys: a computational study. RSC Advances, 2016, 6, 70932-70942.	1.7	4
2782	First principles calculation of the stacking fault in (111) low-temperature metastable alumina. Journal of Structural Chemistry, 2016, 57, 294-300.	0.3	3

#	Article	IF	Citations
2783	Interface Engineering for Atomic Layer Deposited Alumina Gate Dielectric on SiGe Substrates. ACS Applied Materials & Interfaces, 2016, 8, 19110-19118.	4.0	34
2784	Observation of Binding and Rotation of Methane and Hydrogen within a Functional Metalâ€“Organic Framework. Journal of the American Chemical Society, 2016, 138, 9119-9127.	6.6	54
2785	A New Deep-Ultraviolet Transparent Orthophosphate LiCs₂PO₄ with Large Second Harmonic Generation Response. Journal of the American Chemical Society, 2016, 138, 9101-9104.	6.6	307
2786	The role of citric acid and ascorbic acid in morphology control of palladium nanocrystals: A molecular dynamics and density functional theory study. Chemical Physics Letters, 2016, 659, 159-163.	1.2	6
2787	Nonmagnetic 2 p -block elements (B, C, N, and O)-doped AgCl for potential halide spintronic applications: A first-principles perspective. Physics Letters, Section A: General, Atomic and Solid State Physics, 2016, 380, 2968-2973.	0.9	5
2788	Enhanced electrochemical reduction of CO₂to CO on Ag electrocatalysts with increased unoccupied density of states. Journal of Materials Chemistry A, 2016, 4, 12616-12623.	5.2	74
2789	High Energetic Polymeric Nitrogen Stabilized in the Confinement of Boron Nitride Nanotube at Ambient Conditions. Journal of Physical Chemistry C, 2016, 120, 16412-16417.	1.5	21
2791	Physical properties of the recently discovered Zr2(Al1â^'x Bi x)C MAX phases. Journal of Materials Science: Materials in Electronics, 2016, 27, 11925-11933.	1.1	71
2792	DFT Calculations with van der Waals Interactions of Hydrated Calcium Carbonate Crystals CaCO₃Â·(H₂O, 6H₂O): Structural, Electronic, Optical, and Vibrational Properties. Journal of Physical Chemistry A, 2016, 120, 5752-5765.	1.1	31
2793	High-pressure polymorphism of<mml:math xmlns:mml="http://www.w3.org/1998/Math/MathML"><mml:mrow><mml:mi>Pb</mml:mi><mml:msub><mml:mi mathvariant="normal">F</mml:mi><mml:mn>2</mml:mn></mml:msub></mml:mrow></mml:math>to 75 GPa. Physical Review B, 2016, 94, .	1.1	9
2794	The application of inelastic neutron scattering to investigate the interaction of methyl propanoate with silica. Physical Chemistry Chemical Physics, 2016, 18, 17210-17216.	1.3	6
2795	A copper-based sorbent with oxygen-vacancy defects from mechanochemical reduction for carbon disulfide absorption. Journal of Materials Chemistry A, 2016, 4, 17207-17214.	5.2	18
2796	Thermal expansion modeling of framework-type Na[AsW 2 O 9] and K[AsW 2 O 9]. Materials Research Bulletin, 2016, 84, 273-282.	2.7	11
2797	Edge preference and band gap characters of MoS2 and WS2 nanoribbons. Surface Science, 2016, 653, 107-112.	0.8	51
2798	Solving the Hydrogen and Lithium Substructure of Poly(triazine imide)/LiCl Using NMR Crystallography. Chemistry - A European Journal, 2016, 22, 16878-16890.	1.7	54
2799	Zintl Phases K_{4â€“x}Na_xSi₄ (1 â‰ x â‰ 2.2) and K₇NaSi₈: Synthesis, Crystal Structures, and Solidâ€State NMR Spectroscopic Investigations. European Journal of Inorganic Chemistry, 2016, 2016, 4674-4682.	1.0	8
2800	KPb₂(PO₃)₅: a novel nonlinear optical lead polyphosphate with a short deep-UV cutoff edge. Journal of Materials Chemistry C, 2016, 4, 10630-10637.	2.7	88
2801	Lu₂CaMg₂(Si_{1â^'x}Ge_x)₃O₁₂:Ce³⁺solid-solution phosphors: bandgap engineering for blue-light activated afterglow applicable to AC-LED. Journal of Materials Chemistry C, 2016, 4, 10329-10338.	2.7	92

#	Article	IF	Citations
2802	The plane-wave DFT investigations into the structure and the 11B solid-state NMR parameters of lithium fluorooxoborates. Chemical Physics Letters, 2016, 666, 22-27.	1.2	4
2803	Synthesis, Structure, and Local Molecular Dynamics for Crystalline Rotors Based on Hecogenin/Botogenin Steroidal Frameworks. Crystal Growth and Design, 2016, 16, 5698-5709.	1.4	12
2804	High-Pressure Structural Response of an Insensitive Energetic Crystal: 1,1-Diamino-2,2-dinitroethene (FOX-7). Journal of Physical Chemistry C, 2016, 120, 27600-27607.	1.5	22
2805	Synthesis of sodium polyhydrides at high pressures. Nature Communications, 2016, 7, 12267.	5.8	79
2806	Syntheses and structures of two [Au(I)PPh₃]-complexes with 2-aceneoxazolethiolates as ligands. Zeitschrift Fur Kristallographie - Crystalline Materials, 2016, 231, 709-714.	0.4	1
2807	Proton Probability Distribution in the OÂ·Â·Â·HÂ·Â·Â·O Low-Barrier Hydrogen Bond: A Combined Solid-State NMR and Quantum Chemical Computational Study of Dibenzoylmethane and Curcumin. Journal of Physical Chemistry B, 2016, 120, 11692-11704.	1.2	41
2808	Chemical engineering of mixed halide hexaborates as nonlinear optical materials. RSC Advances, 2016, 6, 107810-107815.	1.7	5
2809	Design of graphene-like gallium nitride and WS2/WSe2 nanocomposites for photocatalyst applications. Science China Materials, 2016, 59, 1027-1036.	3.5	65
2810	Mass Transport in Surface Diffusion of van der Waals Bonded Systems: Boosted by Rotations?. Journal of Physical Chemistry Letters, 2016, 7, 4819-4824.	2.1	14
2811	Pb₂Bi₂GaB₃O₁₁, a new congruent-melting galloborate containing two types of asymmetric cations with a moderate birefringence. Dalton Transactions, 2016, 45, 18977-18983.	1.6	2
2812	Dramatically Enhanced Visible Light Response of Monolayer ZrS2 via Non-covalent Modification by Double-Ring Tubular B20 Cluster. Nanoscale Research Letters, 2016, 11, 495.	3.1	25
2813	Structures of Nanoalloy Clusters Au_nAl_n (n = 1â€“10) and the Growth Patterns to the Bulk Phase. Journal of Physical Chemistry C, 2016, 120, 25588-25595.	1.5	9
2814	Optical Activity and Optical Anisotropy in Photomechanical Crystals of Chiral Salicylidenephenylethylamines. Journal of the American Chemical Society, 2016, 138, 15066-15077.	6.6	48
2815	Effect of crystal packing on the excitonic properties of rubrene polymorphs. CrystEngComm, 2016, 18, 7353-7362.	1.3	57
2816	Large-scale room-temperature synthesis and optical properties of perovskite-related Cs₄PbBr₆fluorophores. Journal of Materials Chemistry C, 2016, 4, 10646-10653.	2.7	183
2817	Predicting the Crystal Structure of Decitabine by Powder NMR Crystallography: Influence of Long-Range Molecular Packing Symmetry on NMR Parameters. Crystal Growth and Design, 2016, 16, 7102-7111.	1.4	23
2818	Irradiation Specified Conformational Change in a Small Organic Compound and Its Effect on Electrical Properties. Journal of Physical Chemistry C, 2016, 120, 25557-25563.	1.5	20
2819	Energy Dissipation during Diffusion at Metal Surfaces: Disentangling the Role of Phonons versus Electron-Hole Pairs. Physical Review Letters, 2016, 117, 196001.	2.9	29

#	Article	IF	Citations
2820	High near infrared absorption of hyperâ€doped silicon induced by coâ€doping of sulfur and nitrogen. Physica Status Solidi (A) Applications and Materials Science, 2016, 213, 2855-2860.	0.8	3
2821	Fast Magic-Angle Spinning Three-Dimensional NMR Experiment for Simultaneously Probing Hâ€"H and Nâ€"H Proximities in Solids. Analytical Chemistry, 2016, 88, 11412-11419.	3.2	38
2822	Experimental and First-Principles Investigations of Lattice Strain Effect on Electronic and Optical Properties of Biotemplated BiFeO₃ Nanoparticles. Journal of Physical Chemistry C, 2016, 120, 26012-26020.	1.5	16
2823	Diverse ruthenium nitrides stabilized under pressure: a theoretical prediction. Scientific Reports, 2016, 6, 33506.	1.6	23
2824	Magnetic moment collapse induced axial alternative compressibility of Cr2TiAlC2 at 420â€‰GPa from first principle. Scientific Reports, 2016, 6, 34092.	1.6	11
2825	Theoretical and experimental determination of the crystal structures of cesiumâ€“molybdenum chloride. Japanese Journal of Applied Physics, 2016, 55, 075502.	0.8	12
2827	Benchmarking DFT-GGA calculations for the structure optimisation of neutral-framework zeotypes. Theoretical Chemistry Accounts, 2016, 135, 1.	0.5	38
2828	Investigation of a solid oxide fuel cells catalyst LaSrNiO4: Electronic structure, surface segregation, and oxygen adsorption. International Journal of Hydrogen Energy, 2016, 41, 21497-21502.	3.8	5
2829	First-principles calculations of lattice dynamics and thermal properties of polar solids. Npj Computational Materials, 2016, 2, .	3.5	119
2830	Robustly photogenerating H2 in water using FeP/CdS catalyst under solar irradiation. Scientific Reports, 2016, 6, 19846.	1.6	94
2831	Structural, Electronic and Optical Properties of BiOX1â^'xYx (X, Yâ€‰=â€‰F, Cl, Br and I) Solid Solutions from DFT Calculations. Scientific Reports, 2016, 6, 31449.	1.6	28
2832	Nonlinear optical response mechanism of noncentrosymmetric lead borate Pb₆[B₄O₇(OH)₂]₃with three crystallographically independent [B₄O₇(OH)₂]^{4â^'}chains. RSC Advances, 2016, 6, 100849-100856.	1.7	6
2833	Influence of Ti and La Additions on the Formation of Intermetallic Compounds in the Al-Zn-Si Bath. Metallurgical and Materials Transactions A: Physical Metallurgy and Materials Science, 2016, 47, 6542-6554.	1.1	11
2834	New ordered MAX phase Mo₂TiAlC₂: Elastic and electronic properties from first-principles. Chinese Physics B, 2016, 25, 107103.	0.7	36
2835	Tuning near-gap electronic structure, interface charge transfer and visible light response of hybrid doped graphene and Ag3PO4 composite: Dopant effects. Scientific Reports, 2016, 6, 22267.	1.6	24
2836	Columnar shifts as symmetry-breaking degrees of freedom in molecular perovskites. Physical Chemistry Chemical Physics, 2016, 18, 31881-31894.	1.3	52
2837	Nanocluster-Assembled Materials. Series in Materials Science and Engineering, 2016, , 113-148.	0.1	3
2838	Structure, Vibrational Spectra and ¹¹B-NMR Chemical Shift of Na₈[AlSiO₄]₆(B(OH)₄)₂: Comparison of Theory and Experiment. Journal of Physical Chemistry A, 2016, 120, 7503-7509.	1.1	2

#	Article	IF	Citations
2839	Predicting Global Minimum in Complex Beryllium Borate System for Deep-ultraviolet Functional Optical Applications. Scientific Reports, 2016, 6, 34839.	1.6	24
2840	Strong Nonlinear-Optical Response in the Pyrophosphate CsLiCdP₂O₇ with a Short Cutoff Edge. Inorganic Chemistry, 2016, 55, 11626-11629.	1.9	55
2841	Low-Temperature Synthesis of Bismuth Chalcohalides: Candidate Photovoltaic Materialswith Easily, Continuously Controllable Band gap. Scientific Reports, 2016, 6, 32664.	1.6	49
2842	High-pressure phase of<mml:math xmlns:mml="http://www.w3.org/1998/Math/MathML"><mml:msub><mml:mi>LaPO</mml:mi><mml:mn>4</mml:mn></mml:msub></ by x-ray diffraction and second harmonic generation. Physical Review B, 2016, 94, .	1.1	21
2843	Trail-Needs pseudopotentials in quantum Monte Carlo calculations with plane-wave/blip basis sets. Physical Review B, 2016, 94, .	1.1	20
2844	Unexpected Cation Dynamics in the Low-Temperature Phase of Methylammonium Lead Iodide: The Need for Improved Models. Journal of Physical Chemistry Letters, 2016, 7, 4701-4709.	2.1	53
2845	Surface Charge Transfer Doping via Transition Metal Oxides for Efficient p-Type Doping of IIâ€“VI Nanostructures. ACS Nano, 2016, 10, 10283-10293.	7.3	31
2846	An unforeseen polymorph of coronene by the application of magnetic fields during crystal growth. Nature Communications, 2016, 7, 11555.	5.8	68
2847	Strain-engineered diffusive atomic switching in two-dimensional crystals. Nature Communications, 2016, 7, 11983.	5.8	85
2848	Chemically driven negative linear compressibility in sodium amidoborane, Na(NH2BH3). Scientific Reports, 2016, 6, 28745.	1.6	13
2850	Interdependence of spin structure, anion height and electronic structure of BaFe2As2. AIP Conference Proceedings, 2016, , .	0.3	1
2851	An effective and efficient approach to p-type AlN by Be2:O codoping from first-principles calculations. Modern Physics Letters B, 2016, 30, 1650257.	1.0	0
2852	Optical properties and lattice dynamics of CuZnGeSe quaternary semiconductor: A densityâ€functional study. Physica Status Solidi (B): Basic Research, 2016, 253, 323-328.	0.7	17
2853	Total pressureâ€controlled PVT SiC growth for polytype stability during using 2D nucleation theory. Crystal Research and Technology, 2016, 51, 344-348.	0.6	1
2854	Vibrational and reorientational dynamics, crystal structure and solidâ€“solid phase transition studies in [Ca(H₂O)₆]Cl₂ supported by theoretical (DFT) calculations. Journal of Raman Spectroscopy, 2016, 47, 591-601.	1.2	9
2855	Nature of Hydrogen Bonds and SÂ·Â·Â·S Interactions in the <scp>l</scp>-Cystine Crystal. Journal of Physical Chemistry A, 2016, 120, 4223-4230.	1.1	13
2856	High Pressure Behavior of Hydrogen Storage Material Guanidinium Borohydride. Journal of Physical Chemistry C, 2016, 120, 13414-13420.	1.5	8
2857	Mechanical alloying-spark plasma sintering synthesis and thermoelectric properties of n-type NiSe2+x semiconductors: analysis of intrinsic defects and phase structures. Journal of Materials Science: Materials in Electronics, 2016, 27, 8363-8369.	1.1	4

#	Article	IF	Citations
2858	Solâ€“gel synthesis, crystal structure, and characterization of Y x Bi2+x Cd4â^'3x O7 (0.05Ââ‰ÂxÂâ‰Â0.35) nano-oxides. Journal of Sol-Gel Science and Technology, 2016, 79, 596-605.	1.1	0
2859	Effect of Boron Doping on the CVD Growth Rate of Diamond. Journal of Physical Chemistry C, 2016, 120, 10658-10666.	1.5	19
2860	Adsorption structures and energetics of molecules on metal surfaces: Bridging experiment and theory. Progress in Surface Science, 2016, 91, 72-100.	3.8	121
2861	Spectroscopic Raman characterization of rutherfordine: a combined DFT and experimental study. Physical Chemistry Chemical Physics, 2016, 18, 16575-16584.	1.3	43
2862	A Deep-Ultraviolet Nonlinear Optical Crystal: Strontium Beryllium Borate Fluoride with Planar Be(O/F)₃ Groups. Chemistry of Materials, 2016, 28, 4563-4571.	3.2	47
2863	Hunting for hydrogen: random structure searching and prediction of NMR parameters of hydrous wadsleyite. Physical Chemistry Chemical Physics, 2016, 18, 10173-10181.	1.3	19
2864	DFT simulations of⁷Li solid state NMR spectral parameters and Li⁺ion migration barriers in Li₂ZrO₃. RSC Advances, 2016, 6, 41015-41024.	1.7	5
2865	Mechanical Anisotropy of the Energetic Crystal of 1,1-Diamino-2,2-dinitroethylene (FOX-7): A Study by Nanoindentation Experiments and Density Functional Theory Calculations. Journal of Physical Chemistry C, 2016, 120, 13434-13442.	1.5	18
2866	A DFT study of pressure-induced phase transitions, structural and electronic properties of Cu₂ZnSnS₄. Modern Physics Letters B, 2016, 30, 1650176.	1.0	4
2867	First-principles calculations of crystal and electronic structures and thermodynamic stabilities of Laâ€“Niâ€“H, Laâ€“Niâ€“Alâ€“H and Laâ€“Niâ€“Alâ€“Mnâ€“H hydrogen storage compounds. International Journal of Hydrogen Energy, 2016, 41, 12194-12204.	3.6	7
2868	Experimental and theoretical studies on the linear and nonlinear optical properties of lead phosphate crystals LiPbPO₄. Physical Chemistry Chemical Physics, 2016, 18, 19123-19129.	1.3	61
2869	First-Principles Calculations of the Mechanical and Elastic Properties of 2H_c- and 2H_a-WS₂/CrS₂ Under Pressure. Zeitschrift Fur Naturforschung - Section A Journal of Physical Sciences, 2016, 71, 517-524.	0.7	2
2870	Drugâ€“Drug Multicomponent Crystals as an Effective Technique to Overcome Weaknesses in Parent Drugs. Crystal Growth and Design, 2016, 16, 3577-3581.	1.4	52
2871	First principles studies on structural, elastic and electronic properties of new Ti Mo Nb Zr alloys for biomedical applications. Materials and Design, 2016, 108, 60-67.	3.3	42
2872	Structural, electronic, optical and elastic properties of the complex K₂PtCl₆-structure hydridesARuH₆(A= Mg, Ca, Sr and) Tj ETQq0 0 0 rgBT /Overlock	0.7	17
2873	High-field solid-state 35Cl NMR in selenium(IV) and tellurium(IV) hexachlorides. Journal of Structural Chemistry, 2016, 57, 308-318.	0.3	4
2874	Research on electronic structure and optical properties of Ga0.75Al0.25N with vacancy defects. Optik, 2016, 127, 8662-8669.	1.4	1
2875	Unusual Changes in Electronic Band-Edge Energies of the Nanostructured Transparent n-Type Semiconductor Zr-Doped Anatase TiO₂ (Ti_{1â€“x}Zr_xO₂; x < 0.3). Inorganic Chemistry, 2016, 55, 6574-6585.	1.9	14

#	Article	IF	Citations
2876	Be₂BO₃F: A Phase of Beryllium Fluoride Borate Derived from KBe₂BO₃F₂ with Short UV Absorption Edge. Inorganic Chemistry, 2016, 55, 6586-6591.	1.9	36
2877	How does the B,F-monodoping and B/F-codoping affect the photocatalytic water-splitting performance of g-C₃N₄?. Physical Chemistry Chemical Physics, 2016, 18, 19217-19226.	1.3	99
2878	Extra-Broad Band Orange-Emitting Ce³⁺-Doped Y₃Si₅N₉O Phosphor for Solid-State Lighting: Electronic, Crystal Structures and Luminescence Properties. Chemistry of Materials, 2016, 28, 4829-4839.	3.2	105
2879	Preparation, structure and properties of Na₂Mn₃(SO₄)₄: a new potential candidate with high voltage for Na-ion batteries. Journal of Materials Chemistry A, 2016, 4, 11870-11877.	5.2	24
2880	Effective masses, electronic and optical properties of (111)-layered B-site deficient hexagonal perovskite Ba5M4O15 (M = Ta, Nb): a DFT study using HSE06. RSC Advances, 2016, 6, 61150-61161.	1.7	7
2881	Quasiparticle and excitonic gaps of one-dimensional carbon chains. Physical Chemistry Chemical Physics, 2016, 18, 14810-14821.	1.3	31
2882	Synthesis and stability of xenon oxides Xe2O5 and Xe3O2 under pressure. Nature Chemistry, 2016, 8, 784-790.	6.6	89
2883	On the predictability of supramolecular interactions in molecular cocrystals â€“ the view from the bench. CrystEngComm, 2016, 18, 5434-5439.	1.3	47
2884	Interaction of water with (silico)aluminophosphate zeotypes: a comparative investigation using dispersion-corrected DFT. Physical Chemistry Chemical Physics, 2016, 18, 15738-15750.	1.3	29
2885	Electronic and magnetic properties of a new diluted magnetic semiconductor Li(Zn,TM)As (TM:V, Cr,) Tj ETQq1 1 0.784314 rgBT /Ove	1.2	2
2886	Nematicity, magnetic fluctuation and ferro-spin-orbital ordering in BaFe2As2 family. Journal of Alloys and Compounds, 2016, 675, 416-422.	2.8	7
2887	Study of Hypochlorite Reduction Related to the Sodium Chlorate Process. Electrocatalysis, 2016, 7, 326-335.	1.5	23
2888	Possible socket-plug standard connection for functionalized graphene â€“ Validation by DFT. Carbon, 2016, 104, 40-46.	5.4	6
2889	First-principles study of monolayer MoS2 with deficient and excessive Mo and S (n= â^'3 â†' 3) clusters on 5 Ã— 5 supercells. Computational Materials Science, 2016, 121, 124-130.	1.4	11
2890	Sodium Ion Transport Mechanisms in Antiperovskite Electrolytes Na₃OBr and Na₄OI₂: An in Situ Neutron Diffraction Study. Inorganic Chemistry, 2016, 55, 5993-5998.	1.9	68
2891	Strong influence of off-site symmetry positions of hydrogen atoms in ScH3 hcp phases. Solid State Communications, 2016, 225, 48-55.	0.9	3
2892	Density functional theory calculations of the nitrogen-rich energetic compound 3,4-diamino-1,2,4-triazolium 1-aminotetrazol-5-oneate. Computational Materials Science, 2016, 121, 225-231.	1.4	1
2893	Structure of ZnCl₂ Melt. Part I: Raman Spectroscopy Analysis Driven by Ab Initio Methods. Journal of Physical Chemistry B, 2016, 120, 4174-4181.	1.2	20

#	Article	IF	Citations
2894	Adding a new dimension to the chemistry of phosphorus and arsenic. Physical Chemistry Chemical Physics, 2016, 18, 17586-17591.	1.3	39
2895	Two-dimensional BX (X = P, As, Sb) semiconductors with mobilities approaching graphene. Nanoscale, 2016, 8, 13407-13413.	2.8	122
2896	Novel cobalt-free BaFe_{1â^'x}Gd_xO_{3â^'Î´} perovskite membranes for oxygen separation. Journal of Materials Chemistry A, 2016, 4, 10454-10466.	5.2	72
2897	Insight into Hydrogen Bonding of Uranyl Hydroxide Layers and Capsules by Use of ¹H Magic-Angle Spinning NMR Spectroscopy. Journal of Physical Chemistry C, 2016, 120, 10675-10685.	1.5	20
2898	Hierarchized band gap and enhanced optical responses of trivalent rare-earth metal nitrates due to (dâ€“p)Ï€ conjugation interactions. Journal of Materials Chemistry C, 2016, 4, 6295-6301.	2.7	16
2899	Systematic Theoretical Study of Ethylene Adsorption on Î´-MoC(001), TiC(001), and ZrC(001) Surfaces. Journal of Physical Chemistry C, 2016, 120, 13531-13540.	1.5	19
2900	Resolving the structure of TiBe₁₂. Acta Crystallographica Section B: Structural Science, Crystal Engineering and Materials, 2016, 72, 277-280.	0.5	11
2901	First-principles and molecular dynamics studies on structural, electronic, and magnetic characteristics of (CaC)1/(SiC)1and (KC)1/(SiC)1in wurtzite structure. Physica Status Solidi (B): Basic Research, 2016, 253, 1734-1742.	0.7	2
2902	Defect Physics of BiOI as High Efficient Photocatalyst Driven by Visible Light. Journal of the American Ceramic Society, 2016, 99, 3015-3024.	1.9	17
2903	A periodic DFT study of adsorption of water on sodium-montmorillonite (001) basal and (010) edge surface. Applied Surface Science, 2016, 387, 308-316.	3.1	94
2904	Reexamination of CO formation during formic acid decomposition on the Pt(1 1 1) surface in the gas phase. Chemical Physics Letters, 2016, 658, 207-209.	1.2	3
2905	High Pressure Structural Investigation of Benzoic Acid: Raman Spectroscopy and X-ray Diffraction. Journal of Physical Chemistry C, 2016, 120, 14758-14766.	1.5	60
2906	³⁵Cl solid-state NMR spectroscopy of HCl pharmaceuticals and their polymorphs in bulk and dosage forms. CrystEngComm, 2016, 18, 6213-6232.	1.3	43
2907	The bifurcation point of the oxygen reduction reaction on Auâ€“Pd nanoalloys. Faraday Discussions, 2016, 188, 257-278.	1.6	26
2908	The stability of B₆ octahedron in BaB₆ under high pressure. RSC Advances, 2016, 6, 18077-18081.	1.7	12
2909	Optical phonons in the kesterite Cu₂ZnGeS₄semiconductor: polarized Raman spectroscopy and first-principle calculations. RSC Advances, 2016, 6, 13278-13285.	1.7	35
2910	A new family of sp 3 -hybridized carbon phases. Chinese Physics B, 2016, 25, 016103.	0.7	8
2911	Ab initio path-integral molecular dynamics and the quantum nature of hydrogen bonds. Chinese Physics B, 2016, 25, 013104.	0.7	3

#	Article	IF	Citations
2912	The influence of alloying elements on the corrosion of Zr alloys. Corrosion Science, 2016, 105, 36-43.	3.0	40
2913	Structural, anisotropic and electronic properties of C96 under pressure. European Physical Journal B, 2016, 89, 1.	0.6	6
2914	Characterising the role of water in sildenafil citrate by NMR crystallography. CrystEngComm, 2016, 18, 1054-1063.	1.3	25
2915	Oxygen-17 NMR spectroscopy of water molecules in solid hydrates. Canadian Journal of Chemistry, 2016, 94, 189-197.	0.6	21
2916	Gate-opening effect in ZIF-8: the first experimental proof using inelastic neutron scattering. Chemical Communications, 2016, 52, 3639-3642.	2.2	106
2917	Tuning the electronic and optical properties of phosphorene by transition-metal and nonmetallic atom co-doping. RSC Advances, 2016, 6, 10919-10929.	1.7	53
2918	The first principle study of electronic and optical properties in rhombohedral BiAlO₃. Modern Physics Letters B, 2016, 30, 1650006.	1.0	8
2919	Fermi resonance in the phonon spectra of quaternary chalcogenides of the type Cu₂ZnGeS₄. Journal of Physics Condensed Matter, 2016, 28, 065401.	0.7	27
2920	Probing the thermal stability and the decomposition mechanism of a magnesiumâ€“fullerene polymer via X-ray Raman spectroscopy, X-ray diffraction and molecular dynamics simulations. Physical Chemistry Chemical Physics, 2016, 18, 5366-5371.	1.3	7
2921	Inter- versus Intramolecular Structural Manipulation of a Dichromium(II) Pacman Complex through Pressure Variation. Inorganic Chemistry, 2016, 55, 214-220.	1.9	6
2922	High pressure behaviour and elastic properties of a dense inorganicâ€“organic framework. Dalton Transactions, 2016, 45, 4303-4308.	1.6	26
2923	INS, DFT and temperature dependent IR studies on dynamical properties of acetylcholine chloride. Vibrational Spectroscopy, 2016, 82, 37-43.	1.2	10
2924	Role of Amineâ€“Cavity Interactions in Determining the Structure and Mechanical Properties of the Ferroelectric Hybrid Perovskite [NH₃NH₂]Zn(HCOO)₃. Chemistry of Materials, 2016, 28, 312-317.	3.2	55
2925	Structural variety beyond appearance: high-pressure phases of CrB4 in comparison with FeB4. Physical Chemistry Chemical Physics, 2016, 18, 2361-2368.	1.3	16
2926	Syntheses, crystal structures and physical properties of three new chalcogenides: NaGaGe₃Se₈, K₃Ga₃Ge₇S₂₀, and K₃Ga₃Ge₇Se₂₀. Dalton Transactions, 2016, 45, 532-538.	1.6	13
2927	Packing Interactions and Physicochemical Properties of Novel Multicomponent Crystal Forms of the Anti-Inflammatory Azelaic Acid Studied by X-ray and Solid-State NMR. Crystal Growth and Design, 2016, 16, 154-166.	1.4	30
2928	How TiO₂facets determine arsenic adsorption and photooxidation: spectroscopic and DFT studies. Catalysis Science and Technology, 2016, 6, 2419-2426.	2.1	36
2929	First-principles study of defect formation in the photovoltaic semiconductor Cu2SnS3for comparison with Cu2ZnSnS4and CuInSe2. Japanese Journal of Applied Physics, 2016, 55, 04ES08.	0.8	9

#	Article	IF	Citations
2930	Oxidation behaviour of lattice oxygen in Li-rich manganese-based layered oxide studied by hard X-ray photoelectron spectroscopy. Journal of Materials Chemistry A, 2016, 4, 5909-5916.	5.2	48
2931	Stabilization of 3d Transition Metal Hydrido Complexes in SrH₂Mg₂[Co(I)H₅], BaH₂Mg₅[Co(â"I)H₄]₂, and RbH₂Mg₅[Co(â"I)H₄ Ni(0)H₄] via Easily Polarizable Hydride Ligands. Inorganic Chemistry, 2016, 55, 3576-3582.	1.9	4
2932	Monoclinic C2/m-20 carbon: a novel superhard sp³carbon allotrope. RSC Advances, 2016, 6, 32740-32745.	1.7	29
2933	Reproducibility in density functional theory calculations of solids. Science, 2016, 351, aad3000.	6.0	1,113
2934	Two novel silicon phases with direct band gaps. Physical Chemistry Chemical Physics, 2016, 18, 12905-12913.	1.3	50
2935	Mixed Valence Tin Oxides as Novel van der Waals Materials: Theoretical Predictions and Potential Applications. Advanced Energy Materials, 2016, 6, 1501190.	10.2	79
2936	Electronic structures of efficient M BiO ₃ (M = Li, Na, K, Ag) photocatalyst. Chinese Physics B, 2016, 25, 037102.	0.7	15
2937	Metastable Nitric Acid Trihydrate in Ice Clouds. Angewandte Chemie - International Edition, 2016, 55, 3276-3280.	7.2	12
2938	Molecular Engineering as an Approach To Design a New Beryllium-Free Fluoride Carbonate as a Deep-Ultraviolet Nonlinear Optical Material. Chemistry of Materials, 2016, 28, 2301-2307.	3.2	85
2939	Midinfrared Nonlinear Optical Thiophosphates from LiZnPS₄ to AgZnPS₄: A Combined Experimental and Theoretical Study. Inorganic Chemistry, 2016, 55, 3724-3726.	1.9	78
2940	The interaction of reactants, intermediates and products with Cu ions in Cu-SSZ-13 NH₃SCR catalysts: an energetic and ab initio X-ray absorption modeling study. Catalysis Science and Technology, 2016, 6, 5812-5829.	2.1	23
2941	First-principles calculation of the effects of Li-doping on the structure and piezoelectricity of (K_{0.5}Na_{0.5})NbO₃lead-free ceramics. Physical Chemistry Chemical Physics, 2016, 18, 7702-7706.	1.3	20
2942	NaBa₄(GaB₄O₉)₂X₃ (X = Cl, Br) with NLO-Active GaO₄ Tetrahedral Unit: Experimental and ab Initio Studies. Journal of Physical Chemistry C, 2016, 120, 6190-6197.	1.5	22
2943	Optoelectronic properties of atomically thin ReSSe with weak interlayer coupling. Nanoscale, 2016, 8, 5826-5834.	2.8	32
2944	Investigation on the effect of Na doping on structure and Li-ion kinetics of layered LiNi0.6Co0.2Mn0.2O2 cathode material. Electrochimica Acta, 2016, 192, 120-126.	2.6	132
2945	Pressure effects on hydrogen atoms near the metal plane in the HCP phase of rare-earth metal trihydrides. Solid State Communications, 2016, 231-232, 48-52.	0.9	1
2946	Layered Perovskite Oxychloride Bi₄NbO₈Cl: A Stable Visible Light Responsive Photocatalyst for Water Splitting. Journal of the American Chemical Society, 2016, 138, 2082-2085.	6.6	364
2947	RbIO₃ and RbIO₂F₂: Two Promising Nonlinear Optical Materials in Mid-IR Region and Influence of Partially Replacing Oxygen with Fluorine for Improving Laser Damage Threshold. Chemistry of Materials, 2016, 28, 1413-1418.	3.2	107

#	Article	IF	Citations
2948	Liquidâ€“Liquid Phase Transition in Nanoconfined Silicon Carbide. Journal of the American Chemical Society, 2016, 138, 2815-2822.	6.6	29
2949	Active performance of tetrahedral groups to SHG response: theoretical interpretations of Ge/Si-containing borate crystals. Physical Chemistry Chemical Physics, 2016, 18, 6077-6084.	1.3	3
2950	Temperature Dependence of NMR Parameters Calculated from Path Integral Molecular Dynamics Simulations. Journal of Chemical Theory and Computation, 2016, 12, 968-973.	2.3	54
2951	Molecular docking sites designed for the generation of highly crystalline covalent organic frameworks. Nature Chemistry, 2016, 8, 310-316.	6.6	436
2952	Electronic and optical properties of new synthesized TTF-based azine derivatives â€“ Experimental and theoretical study. Optical Materials, 2016, 56, 27-35.	1.7	2
2953	A classical reactive potential for molecular clusters of sulphuric acid and water. Molecular Physics, 2016, 114, 172-185.	0.8	8
2954	Why Do Chemically Similar Pharmaceutical Molecules Crystallize in Different Structures: A Case of Droperidol and Benperidol. Crystal Growth and Design, 2016, 16, 1643-1653.	1.4	17
2955	Structural, elastic and thermodynamic properties of the tetragonal structure of germanium carbonitride. Journal of Physics and Chemistry of Solids, 2016, 91, 106-113.	1.9	12
2956	Flux Crystal Growth and the Electronic Structure of BaFe₁₂O₁₉ Hexaferrite. Journal of Physical Chemistry C, 2016, 120, 5114-5123.	1.5	96
2957	Muon-spin relaxation study of the double perovskite insulators Sr₂BOsO₆(Bâ€‰â€‰=â€‰â€‰Fe, Y, In). Journal of Physics Condensed Matter, 2016, 28, 076001.	2.2	9
2958	Structure-forming units of amino acid maleates. Case study of<scp>L</scp>-valinium hydrogen maleate. Acta Crystallographica Section B: Structural Science, Crystal Engineering and Materials, 2016, 72, 160-163.	0.5	14
2959	The comparative theoretical study of the LaBO3 (001) (BÂ=ÂMn, Fe, Co, and Ni) surface properties and oxygen adsorption mechanisms. Ionics, 2016, 22, 1153-1158.	1.2	6
2960	Benchmark Theoretical and Experimental Study on ¹⁵N NMR Shifts of Oxidatively Damaged Guanine. Journal of Physical Chemistry B, 2016, 120, 915-925.	1.2	10
2961	Combining the Advantages of Powder X-ray Diffraction and NMR Crystallography in Structure Determination of the Pharmaceutical Material Cimetidine Hydrochloride. Crystal Growth and Design, 2016, 16, 1798-1804.	1.4	55
2962	Nanostructured Co_xNi_{1â^'x}bimetallic alloys for high efficient and ultrafast adsorption: experiments and first-principles calculations. RSC Advances, 2016, 6, 9209-9220.	1.7	12
2963	Designing a Beryllium-Free Deep-Ultraviolet Nonlinear Optical Material without a Structural Instability Problem. Journal of the American Chemical Society, 2016, 138, 2961-2964.	6.6	220
2964	Thermodynamic description of the AgClâ€“CoCl2â€“InCl3â€“NaCl system. Journal of Alloys and Compounds, 2016, 663, 885-898.	2.8	11
2965	Mechanical and Electronic Properties of P4₂/mnm Silicon Carbides. Zeitschrift Fur Naturforschung - Section A Journal of Physical Sciences, 2016, 71, 387-396.	0.7	14

#	Article	IF	Citations
2966	Ca2O3Fe2.6S2: an antiferromagnetic Mott insulator at proximity to bad metal. Journal of Physics Condensed Matter, 2016, 28, 145701.	0.7	6
2967	First principle calculation of physical properties of barium based chalcogenides BaM 4 S 7 (M = Ga, Al); a DFT, DFT-D and hybrid functional HSE06 study. Optical Materials, 2016, 54, 269-275.	1.7	19
2968	Morphed graphene nanostructures: Experimental evidence for existence. Carbon, 2016, 102, 288-296.	5.4	37
2969	Unusual electronic and mechanical properties of sodium chlorides at high pressures. Physics Letters, Section A: General, Atomic and Solid State Physics, 2016, 380, 1556-1561.	0.9	2
2970	New Dionâ€“Jacobson Phase Three-Layer Perovskite CsBa₂Ta₃O₁₀ and Its Conversion to Nitrided Ba₂Ta₃O₁₀ Nanosheets via a Nitridationâ€“Protonationâ€“Intercalationâ€“Exfoliation Route for Water Splitting. Crystal Growth and Design, 2016, 16, 2302-2308.	1.4	47
2971	Syntheses, Structures, and Nonlinear Optical Properties of Two Sulfides Na₂In₂MS₆ (M = Si, Ge). Inorganic Chemistry, 2016, 55, 1480-1485.	1.9	50
2972	New ternary nanolaminated carbide Mo2Ga2C: A first-principles comparison with the MAX phase counterpart Mo2GaC. Computational Materials Science, 2016, 117, 422-427.	1.4	74
2973	Crystal structure of disordered nanocrystalline Î±^{II}-quinacridone determined by electron diffraction. CrystEngComm, 2016, 18, 529-535.	1.3	28
2974	From benzodithiophene to diethoxy-benzodithiophene covalent organic frameworks â€“ structural investigations. CrystEngComm, 2016, 18, 4295-4302.	1.3	27
2975	Characterisation of the surface of freshly prepared precious metal catalysts. Physical Chemistry Chemical Physics, 2016, 18, 17196-17201.	1.3	7
2976	Spectroscopic Investigation of Plasma-Fluorinated Monolayer Graphene and Application for Gas Sensing. ACS Applied Materials & Interfaces, 2016, 8, 8652-8661.	4.0	77
2977	Some new members of MAX family including light-elements: Nanolayered Hf2XY (X= Al, Si, P and Y=B, C,) Tj ETQq1 1 0.784314 rgBT /	1.5	23
2978	Insights into the behaviour of biomolecules on the early Earth: The concentration of aspartate by layered double hydroxide minerals. Geochimica Et Cosmochimica Acta, 2016, 176, 239-258.	1.6	18
2979	Reaction mechanism studies towards effective fabrication of lithium-rich anti-perovskites Li3OX (X=) Tj ETQq1 1 0.784314 rgBT /Over	1.3	89
2980	Influence of doping on chain-like TiO2 clusters: A DFT study. Current Applied Physics, 2016, 16, 197-206.	1.1	7
2981	Prediction of novel phase of silicon and Siâ€“Ge alloys. Journal of Solid State Chemistry, 2016, 233, 471-483.	1.4	37
2982	Li₃AlSiO₅: the first aluminosilicate as a potential deep-ultraviolet nonlinear optical crystal with the quaternary diamond-like structure. Physical Chemistry Chemical Physics, 2016, 18, 4362-4369.	1.3	40
2983	Theoretical investigation on the interfacial properties of carbon deposited on Î²-SiC(111) substrate. Diamond and Related Materials, 2016, 62, 22-29.	1.8	2

#	Article	IF	Citations
2984	Sodium modified molybdenum sulfide via molten salt electrolysis as an anode material for high performance sodium-ion batteries. Physical Chemistry Chemical Physics, 2016, 18, 3204-3213.	1.3	49
2985	Three-dimensional controlled growth of monodisperse sub-50â€‰nm heterogeneous nanocrystals. Nature Communications, 2016, 7, 10254.	5.8	267
2986	13C Chemical Shift in Natural Gas Hydrates from First-Principles Solid-State NMR Calculations. Journal of Physical Chemistry C, 2016, 120, 1130-1136.	1.5	6
2987	Density-functional theory study of high hydrogen content complex hydrides Mg(BH 4) 2 at low temperature. Renewable Energy, 2016, 90, 114-119.	4.3	16
2988	Structural Properties, Orderâ€“Disorder Phenomena, and Phase Stability of Orotic Acid Crystal Forms. Molecular Pharmaceutics, 2016, 13, 1012-1029.	2.3	31
2989	The bandgap distribution investigated across the strain-induced bending ZnO nanowire. Modern Physics Letters B, 2016, 30, 1650048.	1.0	4
2990	Three new phosphates with isolated P₂O₇units: noncentrosymmetric Cs₂Ba₃(P₂O₇)₂and centrosymmetric Cs₂BaP₂O₇and LiCsBaP₂O₇. Dalton Transactions, 2016, 45, 3936-3942.	1.6	62
2991	Hydrothermal Synthesis, Crystal Structure, and Superconductivity of a Double-Perovskite Bi Oxide. Chemistry of Materials, 2016, 28, 459-465.	3.2	54
2992	Engel-Vosko GGA Approach Within DFT Investigations of the Optoelectronic Structure of the Metal Chalcogenide Semiconductor CsAgGa2Se4. Journal of Electronic Materials, 2016, 45, 746-754.	1.0	4
2993	Density functional theory study of nitrogen-induced magnetism in rutile TiO 2. Materials Science in Semiconductor Processing, 2016, 41, 257-260.	1.9	2
2994	Characterization of Two Distinct Amorphous Forms of Valsartan by Solid-State NMR. Molecular Pharmaceutics, 2016, 13, 211-222.	2.3	30
2995	Theoretical investigation of cadmium vapor adsorption on kaolinite surfaces with DFT calculations. Fuel, 2016, 166, 333-339.	3.4	44
2996	Two New Series of Coordination Polymers and Evaluation of Their Properties by Density Functional Theory. Crystal Growth and Design, 2016, 16, 339-346.	1.4	6
2997	Bandgap engineering of the Lu Y1â^'PO4 mixed crystals. Journal of Luminescence, 2016, 171, 33-39.	1.5	21
2998	Inhomogeneous depletion of oxygen ions in metal oxide nanoparticles. Surface Science, 2016, 644, 141-147.	0.8	5
2999	Does p-type ohmic contact exist in WSe₂â€“metal interfaces?. Nanoscale, 2016, 8, 1179-1191.	2.8	166
3000	Investigation of an Amide-Pseudo Amide Hydrogen Bonding Motif within a Series of Theophylline:Amide Cocrystals. Crystal Growth and Design, 2016, 16, 51-58.	1.4	30
3001	Effects of Growth Temperature on Crystal Morphology and Size Uniformity in KTa1â€“xNbxO3 and K1â€“yNayNbO3 Single Crystals. Crystal Growth and Design, 2016, 16, 325-330.	1.4	24

#	Article	IF	Citations
3002	Self-assembly of mesoporous ZnCo₂O₄nanomaterials: density functional theory calculation and flexible all-solid-state energy storage. Journal of Materials Chemistry A, 2016, 4, 568-577.	5.2	73
3003	Theoretical study on temperature effect of electronic structure and spin state in LaCoO3 by using density functional theory. Solid State Ionics, 2016, 285, 195-201.	1.3	12
3004	Ca2SnS4: Crystal structure, optical property, and electronic structure. Journal of Crystal Growth, 2016, 434, 67-71.	0.7	2
3005	Structure and properties of Al-MIL-53-ADP, a breathing MOF based on the aliphatic linker molecule adipic acid. Dalton Transactions, 2016, 45, 4179-4186.	1.6	54
3006	Enhanced visible-light-driven photocatalytic activity in yellow and black orthorhombic NaTaO 3 nanocubes by surface modification and simultaneous N/Ta 4+ co-doping. Journal of Colloid and Interface Science, 2016, 461, 185-194.	5.0	18
3007	Synthesis, crystal structures, magnetic properties, and lattice dynamics of Ba2XCu(OH)[V2O7] with X=Cl, Br. Journal of Solid State Chemistry, 2016, 236, 69-77.	1.4	8
3008	Electronic band structure and related properties of Rb 2 ZnCl 4 crystals at different hydrostatic pressures. Computational Materials Science, 2016, 111, 257-262.	1.4	2
3009	4-Aminoquinaldine monohydrate polymorphism: prediction and impurity aided discovery of a difficult to access stable form. CrystEngComm, 2016, 18, 4053-4067.	1.3	39
3010	First-principles investigation of mechanical, thermodynamic and electronic properties of FeSn 5 and CoSn 5 phases. Computational Materials Science, 2016, 111, 175-180.	1.4	11
3011	A First-Principles Theoretical Study on the Thermoelectric Properties of the Compound Cu5AlSn2S8. Journal of Electronic Materials, 2016, 45, 1453-1458.	1.0	6
3012	DFT-based evaluation of porous metal formates for the storage and separation of small molecules. Microporous and Mesoporous Materials, 2016, 219, 249-257.	2.2	11
3013	Fast Relaxation of Photo-Excited Carriers in 2-D Transition Metal Dichalcogenides. IEEE Journal of Selected Topics in Quantum Electronics, 2017, 23, 168-172.	1.9	30
3014	Numerical simulation and a parametric study of inorganic nanowire solar cells. International Journal of Numerical Modelling: Electronic Networks, Devices and Fields, 2017, 30, e2176.	1.2	3
3015	Lead-free pseudo-three-dimensional organicâ€“inorganic iodobismuthates for photovoltaic applications. Sustainable Energy and Fuels, 2017, 1, 308-316.	2.5	90
3016	High Color Rendering Index of Rb₂GeF₆:Mn⁴⁺ for Light-Emitting Diodes. Chemistry of Materials, 2017, 29, 935-939.	3.2	172
3017	Insights into the composition exploration of novel hydrogen storage alloys: evaluation of the Mgâ€“Niâ€“Ndâ€“H phase diagram. Journal of Materials Chemistry A, 2017, 5, 3848-3864.	5.2	62
3018	Linear-scaling density functional simulations of the effect of crystallographic structure on the electronic and optical properties of fullerene solvates. Physical Chemistry Chemical Physics, 2017, 19, 5617-5628.	1.3	13
3019	Implanted muon spin spectroscopy on 2-O-adamantane: a model system that mimics the liquid$longrightarrow $ glasslike transitions. Journal of Physics Condensed Matter, 2017, 29, 085405.	0.7	6

#	Article	IF	Citations
3020	Fluoroethylene Carbonate Additives to Render Uniform Li Deposits in Lithium Metal Batteries. Advanced Functional Materials, 2017, 27, 1605989.	7.8	1,189
3021	The first quaternary diamond-like semiconductor with 10-membered LiS₄rings exhibiting excellent nonlinear optical performances. Chemical Communications, 2017, 53, 3010-3013.	2.2	96
3022	Ionicity and birefringence of Î±-LiNH₄SO₄crystals: ab initio DFT study, X-ray spectroscopy measurements. RSC Advances, 2017, 7, 6889-6901.	1.7	20
3023	Towards multifunctional coating in the boron-doped graphene/copper system. Carbon, 2017, 115, 375-379.	5.4	1
3024	Theoretical investigations on phase stability, elastic constants and electronic structures of Ga3Zr polymorphs under high pressure. Journal of Alloys and Compounds, 2017, 696, 1010-1018.	2.8	3
3025	Chemical beam epitaxy of GaAs 1-x N x using MMHy and DMHy precursors, modeled by ab initio study of GaAs(100) surfaces stability over As 2 , H 2 and N 2. Journal of Crystal Growth, 2017, 468, 557-561.	0.7	0
3026	Electronic structures and half-metallicity of carbon doped bulk and surface CdS: The modified Becke-Johnson potential calculation. Solid State Communications, 2017, 250, 108-111.	0.9	0
3027	Enhanced efficiency of solid-state NMR investigations of energy materials using an external automatic tuning/matching (eATM) robot. Journal of Magnetic Resonance, 2017, 275, 127-136.	1.2	41
3028	Internal dynamics in helical molecules studied by X-ray diffraction, NMR spectroscopy and DFT calculations. Physical Chemistry Chemical Physics, 2017, 19, 2900-2907.	1.3	33
3029	Structural evolution of (Ti0.5V0.5)+1GeC (n= 1â€“4) under pressure from first principles. Computational Materials Science, 2017, 127, 251-260.	1.4	18
3030	A Multinuclear NMR Study of Six Forms of AlPO-34: Structure and Motional Broadening. Journal of Physical Chemistry C, 2017, 121, 1781-1793.	1.5	25
3031	First-principles study of the Al(001)-Al3Nb(001) interfacial properties. Surface Science, 2017, 657, 104-110.	0.8	22
3032	Investigations on Magnetic Properties of Cr-Doped LiZnAs by First-Principle Calculations. Journal of Superconductivity and Novel Magnetism, 2017, 30, 1545-1549.	0.8	3
3033	First-Principles Studies on d 0 Magnetism in Zinc-Blende IV-IV Compounds-Based Short-Period Heterostructures (SiC)1/(KC)1, (GeC)1/(KC)1, (SiC)1/(CaC)1, and (GeC)1/(CaC)1. Journal of Superconductivity and Novel Magnetism, 2017, 30, 1619-1628.	0.8	0
3034	Superpolyhedron-Built Second Harmonic Generation Materials Exhibit Large Mid-Infrared Conversion Efficiencies and High Laser-Induced Damage Thresholds. Chemistry of Materials, 2017, 29, 1796-1804.	3.2	84
3035	Erbium ion implantation into diamond â€“ measurement and modelling of the crystal structure. Physical Chemistry Chemical Physics, 2017, 19, 6233-6245.	1.3	18
3036	Synthesis of Hf8O7, a new binary hafnium oxide, at high pressures and high temperatures. High Pressure Research, 2017, 37, 147-158.	0.4	3
3037	Equilibrium Fractionation of Non-traditional Isotopes: a Molecular Modeling Perspective. Reviews in Mineralogy and Geochemistry, 2017, 82, 27-63.	2.2	71

#	Article	IF	Citations
3038	Phonon dispersion anomalies and superconductivity in metal substituted MgB2. Computational Materials Science, 2017, 130, 191-203.	1.4	19
3039	Enhancing optical anisotropy of crystals by optimizing bonding electron distribution in anionic groups. Chemical Communications, 2017, 53, 2818-2821.	2.2	155
3040	Molecular Dynamics Simulation: From â€œAb Initioâ€• to â€œCoarse Grainedâ€• , 2017, , 337-396.		2
3041	An alkaline tin(II) halide compound Na 3 Sn 2 F 6 Cl: Synthesis, structure, and characterization. Journal of Solid State Chemistry, 2017, 248, 104-108.	1.4	7
3042	Super high-energy density single-bonded trigonal nitrogen allotropeâ€”a chemical twin of the cubic gauche form of nitrogen. Physical Chemistry Chemical Physics, 2017, 19, 6698-6706.	1.3	32
3043	Effects of oxygen vacancies on the structural and optical properties of Î²-Ga2O3. Scientific Reports, 2017, 7, 40160.	1.6	215
3044	The initial stages of melting of graphene between 4000 K and 6000 K. Physical Chemistry Chemical Physics, 2017, 19, 3756-3762.	1.3	72
3045	Band calculation of lonsdaleite Ge. Journal Physics D: Applied Physics, 2017, 50, 015107.	1.3	8
3046	Tuning the near-gap electronic structure of Cu2O by anionâ€“cation co-doping for enhanced solar energy conversion. Modern Physics Letters B, 2017, 31, 1650429.	1.0	4
3047	First-principle studies on the Liâ€“Te system. Materials Research Express, 2017, 4, 015701.	0.8	0
3048	Orbital driven impurity spin effect on the magnetic order of quasi-3D cupric oxide. Journal of Physics Condensed Matter, 2017, 29, 155802.	0.7	3
3049	Theoretical investigation on the balance between large band gap and strong SHG response in BMO₄(M = P and As) crystals. RSC Advances, 2017, 7, 2804-2809.	1.7	17
3050	Influence of high-temperature AlN intermediate layer on the optical properties of MOCVD grown AlGaN films. Materials Research Express, 2017, 4, 025903.	0.8	1
3051	Improvement of thermoelectric properties and their correlations with electron effective mass in Cu1.98SxSe1â^'x. Scientific Reports, 2017, 7, 40436.	1.6	31
3052	Silver(<scp>i</scp>) coordination polymers with 3,3â€²,5,5â€²-tetrasubstituted 4,4â€²-bipyridine ligands: towards new porous chiral materials. RSC Advances, 2017, 7, 7358-7367.	1.7	13
3053	Vibrational spectroscopy of orthorhombic Cu 2 ZnSiS 4 single crystal: Low-temperature polarized Raman scattering and first principle calculations. Vibrational Spectroscopy, 2017, 89, 81-84.	1.2	5
3054	A new cerium iodate infrared nonlinear optical material with a large second-harmonic generation response. Journal of Materials Chemistry C, 2017, 5, 2130-2134.	2.7	20
3055	Na₂CdGe₂Q₆(Q = S, Se): two metal-mixed chalcogenides with phase-matching abilities and large second-harmonic generation responses. Dalton Transactions, 2017, 46, 2778-2784.	1.6	69

#	Article	IF	Citations
3056	Effect of Ag and Pd promotion on CH₄selectivity in Fe(100) Fischerâ€“TrÃ¶psch catalysis. Physical Chemistry Chemical Physics, 2017, 19, 5495-5503.	1.3	4
3057	High mechanical strength in Zn₄B₆O₁₃with an unique sodalite-cage structure. RSC Advances, 2017, 7, 2038-2043.	1.7	7
3058	Solidâ€State ¹⁷Oâ€…NMR Reveals Hydrogenâ€Bonding Energetics: Not All Lowâ€Barrier Hydrogen Bonds Are Strong. Angewandte Chemie - International Edition, 2017, 56, 6166-6170.	7.2	33
3059	Structure and Characterization of a Zero-Dimensional Alkali Tin Dihalides Compound Cs₃Sn₃F₂Cl₇ with the [Sn₂F₂Cl₄]^{2â€“} Clusters. Inorganic Chemistry, 2017, 56, 3081-3086.	1.9	9
3060	Simulation calculations of efficiencies and silicon consumption for CH3NH3PbI3â^'xâ^'y Br x Cl y /crystalline silicon tandem solar cells. Journal Physics D: Applied Physics, 2017, 50, 155102.	1.3	3
3061	Structure and physicochemical characterization of a naproxenâ€“picolinamide cocrystal. Acta Crystallographica Section C, Structural Chemistry, 2017, 73, 168-175.	0.2	28
3062	Calculations of solidâ€state ⁴³Ca NMR parameters: A comparison of periodic and cluster approaches and an evaluation of DFT functionals. Journal of Computational Chemistry, 2017, 38, 949-956.	1.5	19
3063	Hydrothermal Synthesis, Structure, and Superconductivity of Simple Cubic Perovskite (Ba_{0.62}K_{0.38})(Bi_{0.92}Mg_{0.08})O₃ with T_c â^¼ 30 K. Inorganic Chemistry, 2017, 56, 3174-3181.	1.9	26
3064	First-Principles Calculations for the Energetics of the Hydration Reaction of Acceptor-Doped BaZrO₃. Chemistry of Materials, 2017, 29, 1518-1526.	3.2	60
3065	Controlling Surface Termination and Facet Orientation in Cu₂O Nanoparticles for High Photocatalytic Activity: A Combined Experimental and Density Functional Theory Study. ACS Applied Materials & Interfaces, 2017, 9, 8100-8106.	4.0	99
3066	Sb Doping of Metallic CuCr₂S₄ as a Route to Highly Improved Thermoelectric Properties. Chemistry of Materials, 2017, 29, 2988-2996.	3.2	68
3067	Zero Thermal Expansion and Semiconducting Properties in PbTiO₃â€“Bi(Co,) Tj ETQq1 1 0.784314 rgBT /Overlock 10 Tf 50	1.9	13
3068	Simulations and spectra of water in CO matrices. Physical Chemistry Chemical Physics, 2017, 19, 7280-7287.	1.3	1
3069	Extracting Crystal Chemistry from Amorphous Carbon Structures. ChemPhysChem, 2017, 18, 873-877.	1.0	80
3070	Solidâ€State 17 Oâ€…NMR Reveals Hydrogenâ€Bonding Energetics: Not All Lowâ€Barrier Hydrogen Bonds Are Strong. Angewandte Chemie, 2017, 129, 6262-6266.	1.6	9
3071	Thermodynamic and Mechanical Properties of the Rutherfordine Mineral Based on Density Functional Theory. Journal of Physical Chemistry C, 2017, 121, 5994-6001.	1.5	41
3072	Experimental and first-principles studies of high-pressure effects on the structural, electronic, and optical properties of semiconductors and lanthanide doped solids. Japanese Journal of Applied Physics, 2017, 56, 05FA02.	0.8	7
3073	First-principles study lone-pair effects of Sb (III)-S chromophore influence on SHG response in quaternary potassium containing silver antimony sulfides. Journal of Solid State Chemistry, 2017, 249, 215-220.	1.4	10

#	Article	IF	Citations
3074	ACaBO₃(A = Cs, Rb): two new cubic borates with isolated BO₃groups. Dalton Transactions, 2017, 46, 4968-4974.	1.6	19
3075	Stacking faults and the -surface on first-order pyramidal planes in -titanium. Philosophical Magazine, 2017, 97, 1129-1143.	0.7	21
3076	Physical mechanism of resistance switching in the co-doped RRAM. Journal of Semiconductors, 2017, 38, 014008.	2.0	2
3077	First-principles investigation of the equation of state and elastic properties of perovskite-type SrW(O,N)3 under hydrostatic pressures up to 139 GPa. European Physical Journal B, 2017, 90, 1.	0.6	1
3078	Energy conversion modeling of the intrinsic persistent luminescence of solids via energy transfer paths between transition levels. Physical Chemistry Chemical Physics, 2017, 19, 9457-9469.	1.3	8
3079	Structure and ionic diffusivity in an yttria-stabilised zirconia/strontium titanate multilayer. Acta Materialia, 2017, 129, 388-397.	3.8	2
3080	Origin of asymmetric broadening of Raman peak profiles in Si nanocrystals. Scientific Reports, 2017, 7, 43602.	1.6	35
3081	Atomic scale structure of amorphous aluminum oxyhydroxide, oxide and oxycarbide films probed by very high field²⁷Al nuclear magnetic resonance. Physical Chemistry Chemical Physics, 2017, 19, 8101-8110.	1.3	23
3082	Yttrium passivation of defects in GeO2 and GeO2/Ge interfaces. Applied Physics Letters, 2017, 110, .	1.5	12
3083	Elucidation of the helical spin structure of FeAs. Physical Review B, 2017, 95, .	1.1	10
3084	Fluorooxoborates: Berylliumâ€Free Deepâ€Ultraviolet Nonlinear Optical Materials without Layered Growth. Angewandte Chemie - International Edition, 2017, 56, 3916-3919.	7.2	674
3085	Detection of N-Te bonds in the as-deposited amorphous nitrogen-doped GeTe-based phase change alloys using N K-edge XANES spectroscopy and their impact on crystallization. Journal of Alloys and Compounds, 2017, 704, 254-259.	2.8	5
3086	Structural Evolution and Atom Clustering in Î²-SiAlON: Î²-Si_{6â€“z}Al_zO_zN_{8â€“z}. Inorganic Chemistry, 2017, 56, 2153-2158.	1.9	24
3087	Ab initio study of the mechanical and electronic properties of scheelite-type XWO₄(X = Ca, Sr, Ba) compounds. International Journal of Modern Physics B, 2017, 31, 1750086.	1.0	22
3088	Unravelling exceptional acetylene and carbon dioxide adsorption within a tetra-amide functionalized metal-organic framework. Nature Communications, 2017, 8, 14085.	5.8	193
3089	¹³C and¹⁹F solid-state NMR and X-ray crystallographic study of halogen-bonded frameworks featuring nitrogen-containing heterocycles. Acta Crystallographica Section C, Structural Chemistry, 2017, 73, 157-167.	0.2	34
3090	Investigation on the contact between graphdiyne and Cu (111) surface. Carbon, 2017, 117, 246-251.	5.4	26
3091	Machine learning based interatomic potential for amorphous carbon. Physical Review B, 2017, 95, .	1.1	431

#	Article	IF	Citations
3092	Thermodynamic, elastic, elastic anisotropy and minimum thermal conductivity of Î²-GaN under high temperature. Chinese Journal of Physics, 2017, 55, 400-411.	2.0	13
3093	Full Elasticity Tensor from Thermal Diffuse Scattering. Physical Review Letters, 2017, 118, 035502.	2.9	16
3094	Confirmation of the Structural Phase Transitions in XeF₂ under High Pressure. Journal of Physical Chemistry C, 2017, 121, 6264-6271.	1.5	17
3095	A new family of multifunctional silicon clathrates: Optoelectronic and thermoelectric applications. Journal of Applied Physics, 2017, 121, .	1.1	12
3096	Investigation of YIGâ€™s Active Site Using Density Functional Theory. Materials Science Forum, 0, 888, 76-80.	0.3	0
3097	Fluorooxoborates: Berylliumâ€Free Deepâ€Ultraviolet Nonlinear Optical Materials without Layered Growth. Angewandte Chemie, 2017, 129, 3974-3977.	1.6	94
3098	Structural Polymorphism in â€œKesteriteâ€•Cu₂ZnSnS₄: Raman Spectroscopy and First-Principles Calculations Analysis. Inorganic Chemistry, 2017, 56, 3467-3474.	1.9	84
3099	Adjusting the band structure and defects of ZnO quantum dots via tin doping. RSC Advances, 2017, 7, 11345-11354.	1.7	35
3100	First-principles prediction of magnetic salts: Case study of NaCl bulk and (0 0 1) surface doped with light non-metallic 2 p -block elements. Computational Materials Science, 2017, 132, 10-18.	1.4	2
3101	Theoretical study the electronic, elastic properties and thermodynamics properties of ternary phosphide SrPt 6 P 2. Journal of Physics and Chemistry of Solids, 2017, 106, 10-15.	1.9	2
3102	Improving methane gas sensing properties of multi-walled carbon nanotubes by vanadium oxide filling. Sensors and Actuators B: Chemical, 2017, 247, 11-18.	4.0	49
3103	Thermodynamic calculations and dynamics simulation on thermal-decomposition reaction of MoS 2 and Mo 2 S 3 under vacuum. Vacuum, 2017, 139, 143-152.	1.6	18
3104	Identifying Atomic Scale Structure in Undoped/Doped Semicrystalline P3HT Using Inelastic Neutron Scattering. Macromolecules, 2017, 50, 2424-2435.	2.2	52
3105	Structural inheritance and difference between Ti₂AlC, Ti₃AlC₂ÂandÂTi₅Al₂C₃ under pressure from first principles. Modern Physics Letters B, 2017, 31, 1750016.	1.0	10
3106	Pressureâ€Induced Photoluminescence Adjustment and Lattice Disorder in Monolayer WSe₂. ChemNanoMat, 2017, 3, 238-244.	1.5	9
3107	Tunable thermal expansion in framework materials through redox intercalation. Nature Communications, 2017, 8, 14441.	5.8	95
3108	Optimized multi-step NMR-crystallography approach for structural characterization of a stable quercetin solvate. Journal of Pharmaceutical and Biomedical Analysis, 2017, 138, 22-28.	1.4	14
3109	Single-crystal elasticity of SrCO₃ by Brillouin spectroscopy. High Pressure Research, 2017, 37, 181-192.	0.4	15

#	Article	IF	Citations
3110	Structural, electronic and optical properties of Bi₂O₃ polymorphs by first-principles calculations for photocatalytic water splitting. Materials Research Express, 2017, 4, 034002.	0.8	17
3111	Understanding the interfacial properties of graphene-based materials/BiOI heterostructures by DFT calculations. Applied Surface Science, 2017, 406, 8-20.	3.1	23
3112	Thermodynamic assessment of the Na-O and Na-U-O systems: Margin to the safe operation of SFRs. Journal of Chemical Thermodynamics, 2017, 114, 93-115.	1.0	11
3113	A terahertz study of taurine: Dispersion correction and mode couplings. Journal of Chemical Physics, 2017, 146, 124119.	1.2	12
3114	First-principles multiscale modelling of charged adsorbates on doped graphene. 2D Materials, 2017, 4, 025070.	2.0	11
3115	First-principles study of defect formation in the photovoltaic semiconductors Cu₂GeS₃and Cu₂ZnGeS₄for comparison with Cu₂SnS₃, Cu₂ZnSnS₄, and CuInSe₂. Japanese Journal of Applied Physics, 2017, 56, 04CS08.	0.8	14
3116	Pressure-Stabilized Cubic Perovskite Oxyhydride BaScO₂H. Inorganic Chemistry, 2017, 56, 4840-4845.	1.9	36
3117	Preparation-Dependent Composition and O/F Ordering in NbO₂F and TaO₂F. Inorganic Chemistry, 2017, 56, 5219-5232.	1.9	17
3118	Single-crystal X-ray diffraction and NMR crystallography of a 1:1 cocrystal of dithianon and pyrimethanil. Acta Crystallographica Section C, Structural Chemistry, 2017, 73, 149-156.	0.2	22
3119	BaAu₂S₂: A Au-Based Intrinsic Photocatalyst for High-Performance Visible-Light Photocatalysis. Inorganic Chemistry, 2017, 56, 5173-5181.	1.9	16
3120	Experimental and ab initio studies of two UV nonlinear optical materials. RSC Advances, 2017, 7, 20259-20265.	1.7	10
3121	Syntheses, crystal structures and characterization of three alkaline metal borates. CrystEngComm, 2017, 19, 2561-2569.	1.3	5
3122	First-Principles Assisted Prediction of the Nonlinear Optical Behavior of Mg₃B₇O₁₃Cl Crystal. Journal of the Physical Society of Japan, 2017, 86, 044401.	0.7	4
3123	Raman and DRIFT spectra, vibrational assignments and quantum mechanical calculations of centrosymmetric meso -2,3-Dimercaptosuccinic acid. Spectrochimica Acta - Part A: Molecular and Biomolecular Spectroscopy, 2017, 183, 275-283.	2.0	7
3124	Series of ZnSn(OH)₆ Polyhedra: Enhanced CO₂ Dissociation Activation and Crystal Facet-Based Homojunction Boosting Solar Fuel Synthesis. Inorganic Chemistry, 2017, 56, 5704-5709.	1.9	27
3125	High-pressure hydrogen sulfide by diffusion quantum Monte Carlo. Journal of Chemical Physics, 2017, 146, 084503.	1.2	14
3126	Prediction of novel ultra-incompressibility compounds TM2B (TM=Mo, W, Re and Os) by first-principles calculations. Philosophical Magazine, 2017, 97, 1729-1739.	0.7	3
3127	Fluorine Etching in Porous Silicon: An Ab-Initio Molecular Dynamics Study. ECS Journal of Solid State Science and Technology, 2017, 6, P172-P177.	0.9	2

#	Article	IF	Citations
3128	A Modular Implementation for the Simulation of 1D and 2D Solid-State NMR Spectra of Quadrupolar Nuclei in the Virtual Multifrequency Spectrometerâ€“Draw Graphical Interface. Journal of Chemical Theory and Computation, 2017, 13, 2215-2229.	2.3	18
3130	Semi-empirical refinements of crystal structures using 17O quadrupolar-coupling tensors. Journal of Chemical Physics, 2017, 146, 064201.	1.2	26
3131	Design of electric field controlled molecular gates mounted on metalâ€“organic frameworks. Journal of Materials Chemistry A, 2017, 5, 8690-8696.	5.2	51
3132	Effects of oxygen vacancy on the mechanical, electronic and optical properties of monoclinic BiVO4. Journal of Materials Science, 2017, 52, 8546-8555.	1.7	32
3133	SeO 2 adsorption on CaO surface: DFT study on the adsorption of a single SeO 2 molecule. Applied Surface Science, 2017, 413, 366-371.	3.1	45
3134	Mechanistic insights into complete hydrogenation of 1,3-butadiene over Pt/SiO₂: effect of Pt dispersion and kinetic analysis. Catalysis Science and Technology, 2017, 7, 2717-2728.	2.1	20
3135	Terahertz spectroscopy and solid-state density functional theory calculations of structural isomers: Nicotinic acid, isonicotinic acid and 2-picolinic acid. Modern Physics Letters B, 2017, 31, 1750149.	1.0	12
3136	Crystal structure and mechanical properties of a new ternary phase in Mg-Zn-Y alloy solidified under high pressure. Journal of Alloys and Compounds, 2017, 717, 214-218.	2.8	19
3137	A first-principles high-pressure study of Hf 2 PX (X=B, C, N). Solid State Communications, 2017, 259, 45-49.	0.9	0
3138	Lattice and Valence Electronic Structures of Crystalline Octahedral Molybdenum Halide Clusters-Based Compounds, Cs₂[Mo₆X₁₄] (X = Cl, Br, I), Studied by Density Functional Theory Calculations. Inorganic Chemistry, 2017, 56, 6234-6243.	1.9	16
3139	One-step fabrication of CdS:Moâ€“CdMoO4coreâ€“shell nanoribbons for nonvolatile memory devices with high resistance switching. Journal of Materials Chemistry C, 2017, 5, 6156-6162.	2.7	8
3140	Structures and Mechanical Properties of CH₄, SO₂, and H₂S Hydrates from Density Function Theory Calculations. Chemistry Letters, 2017, 46, 1141-1144.	0.7	12
3141	Engineering the Lattice Site Occupancy of Apatite-Structure Phosphors for Effective Broad-Band Emission through Cation Pairing. Inorganic Chemistry, 2017, 56, 5696-5703.	1.9	16
3142	Mechanism of CO₂ Reforming of CH₄ on a Pt₄/ZrO₂(101) Surface: A Density Functional Theory Study. Journal of Physical Chemistry B, 2017, 121, 5238-5246.	1.2	9
3143	Accurate structures and energetics of neutral-framework zeotypes from dispersion-corrected DFT calculations. Journal of Chemical Physics, 2017, 146, 174111.	1.2	30
3144	Raman studies in tetragonal structure PbTeO 3. Solid State Communications, 2017, 260, 1-5.	0.9	0
3145	Exploring Systematic Discrepancies in DFT Calculations of Chlorine Nuclear Quadrupole Couplings. Journal of Physical Chemistry A, 2017, 121, 4103-4113.	1.1	19
3146	DFT design of polyguanidine â€“ a unique two-dimensional material with high-energy density. Molecular Physics, 2017, 115, 2423-2430.	0.8	7

#	Article	IF	Citations
3147	In Situ Phaseâ€Induced Spatial Charge Separation in Coreâ€“Shell Oxynitride Nanocube Heterojunctions Realizing Robust Solar Water Splitting. Advanced Energy Materials, 2017, 7, 1700171.	10.2	39
3148	The effect of ions on the magnetic moment of vacancy for ion-implanted 4H-SiC. Journal of Applied Physics, 2017, 121, .	1.1	5
3149	Engineering Pt/Pd Interfacial Electronic Structures for Highly Efficient Hydrogen Evolution and Alcohol Oxidation. ACS Applied Materials & Interfaces, 2017, 9, 18008-18014.	4.0	111
3150	A Nitrogen Doping Method for CoS₂ Electrocatalysts with Enhanced Water Oxidation Performance. ACS Catalysis, 2017, 7, 4214-4220.	5.5	181
3151	Experimental investigation and DFT calculation of different amine/ammonium salts adsorption on kaolinite. Applied Surface Science, 2017, 419, 241-251.	3.1	54
3152	SeO 2 adsorption on CaO surface: DFT and experimental study on the adsorption of multiple SeO 2 molecules. Applied Surface Science, 2017, 420, 465-471.	3.1	44
3153	New hexagonal boron nitride polytypes with triple-layer periodicity. Journal of Applied Physics, 2017, 121, .	1.1	13
3154	Study of NaFâ€“AlF₃ Melts by Coupling Molecular Dynamics, Density Functional Theory, and NMR Measurements. Journal of Physical Chemistry C, 2017, 121, 10289-10297.	1.5	29
3155	Insulating characteristics of zinc niobium borate glassâ€ceramics. Journal of the American Ceramic Society, 2017, 100, 4066-4080.	1.9	22
3156	Clathrate Structure Determination by Combining Crystal Structure Prediction with Computational and Experimental ¹²⁹Xe NMR Spectroscopy. Chemistry - A European Journal, 2017, 23, 5258-5269.	1.7	18
3157	Investigating Sodium Storage Mechanisms in Tin Anodes: A Combined Pair Distribution Function Analysis, Density Functional Theory, and Solid-State NMR Approach. Journal of the American Chemical Society, 2017, 139, 7273-7286.	6.6	121
3158	Carbon dioxide binary crystals via the thermal decomposition of RDX at high pressure. Chemical Science, 2017, 8, 4872-4878.	3.7	6
3159	Single-Atom Scale Structural Selectivity in Te Nanowires Encapsulated Inside Ultranarrow, Single-Walled Carbon Nanotubes. ACS Nano, 2017, 11, 6178-6185.	7.3	69
3160	Tolterodine Tartrate. Profiles of Drug Substances, Excipients and Related Methodology, 2017, 42, 339-403.	3.5	3
3161	First-principles calculations of electronic and optical properties of aluminum-doped Î²-Ga2O3 with intrinsic defects. Results in Physics, 2017, 7, 1582-1589.	2.0	76
3162	DFT-Based Comparative Study about the Influence of Fluorine and Hydroxyl Anions on Opto-Electric Properties of Borate Crystals: Choice for Better Anion. Inorganic Chemistry, 2017, 56, 5636-5645.	1.9	9
3163	LiMCO3 (M = K, Rb, Cs): a series of mixed alkali carbonates with large birefringence. Dalton Transactions, 2017, 46, 6894-6899.	1.6	7
3164	Five low energy phosphorene allotropes constructed through gene segments recombination. Scientific Reports, 2017, 7, 46431.	1.6	31

#	Article	IF	Citations
3165	The effect of Nb on the corrosion and hydrogen pick-up of Zr alloys. Acta Materialia, 2017, 132, 425-431.	3.8	40
3166	First-principle study of graphyne-like BN sheet: Electronic structure and optical properties. Computational Materials Science, 2017, 136, 12-19.	1.4	44
3167	The application of tailor-made force fields and molecular dynamics for NMR crystallography: a case study of free base cocaine. IUCrJ, 2017, 4, 175-184.	1.0	10
3168	Cooperation of Three Chromophores Generates the Waterâ€Resistant Nitrate Nonlinear Optical Material Bi₃TeO₆OH(NO₃)₂. Angewandte Chemie - International Edition, 2017, 56, 540-544.	7.2	91
3169	The effect of saturation magnetization of nanocatalyst and oscillating magnetic field for green urea synthesis. Physica B: Condensed Matter, 2017, 507, 95-106.	1.3	12
3170	Cooperation of Three Chromophores Generates the Waterâ€Resistant Nitrate Nonlinear Optical Material Bi₃TeO₆OH(NO₃)₂. Angewandte Chemie, 2017, 129, 555-559.	1.6	12
3171	LiRb2LaB2O6: a new rare-earth borate with a MOF-5-like topological structure and a short UV cut-off edge. Dalton Transactions, 2017, 46, 193-199.	1.6	10
3172	Ba_{n+2}Zn_n(BO₃)_n(B₂O₅)F_n(n) Tj ETQq1 1 0 Inorganic Chemistry Frontiers, 2017, 4, 281-288.	3.0	29
3173	LiRb₂PO₄: a new deep-ultraviolet nonlinear optical phosphate with a large SHG response. Journal of Materials Chemistry C, 2017, 5, 269-274.	2.7	84
3174	Structure and infrared spectra of hydrocarbon interstellar dust analogs. Physical Chemistry Chemical Physics, 2017, 19, 1352-1360.	1.3	16
3175	Elastic and thermodynamic properties of new (Zr3âˆ'Ti)AlC2 MAX-phase solid solutions. Computational Materials Science, 2017, 137, 318-326.	1.4	119
3176	Nitrogen-Doped Graphene on Transition Metal Substrates as Efficient Bifunctional Catalysts for Oxygen Reduction and Oxygen Evolution Reactions. ACS Applied Materials & Interfaces, 2017, 9, 22578-22587.	4.0	128
3177	Theoretical evaluation on selective adsorption characteristics of alkali metal-based sorbents for gaseous oxidized mercury. Chemosphere, 2017, 184, 711-719.	4.2	38
3178	Does Zâ€² equal 1 or 2? Enhanced powder NMR crystallography verification of a disordered room temperature crystal structure of a p38 inhibitor for chronic obstructive pulmonary disease. Physical Chemistry Chemical Physics, 2017, 19, 16650-16661.	1.3	25
3179	Works of separation for (0 0 0 1)ZnO	(1 1 1)ZrO 2 interfaces: A first-principle study. Computational Materials Science, 2017, 136, 157-162.	1.4	11
3180	An ab initio study of the adsorption of Eu3+, Pu3+, Am3+, and Cm3+ hydroxide complexes on hematite (001) surface: Role of magnetism on adsorption. Surface Science, 2017, 664, 120-128.	0.8	10
3181	Experimental and Computational Hydrate Screening: Cytosine, 5-Flucytosine, and Their Solid Solution. Crystal Growth and Design, 2017, 17, 4347-4364.	1.4	21
3182	First-principles calculation of lithium insertion into homogeneous a-SiC2/5O6/5as high performance anode. RSC Advances, 2017, 7, 30559-30563.	1.7	0

#	Article	IF	Citations
3183	Vacuum referred binding energy scheme for rare earth ions in RE 2 BaZnO 5 [REÂ=ÂY, Gd, La]. Optical Materials, 2017, 70, 57-62.	1.7	8
3184	Insights into Antimony Adsorption on {001} TiO₂: XAFS and DFT Study. Environmental Science & Technology, 2017, 51, 6335-6341.	4.6	118
3185	Experimental and Theoretical Evaluation of the Stability of True MOF Polymorphs Explains Their Mechanochemical Interconversions. Journal of the American Chemical Society, 2017, 139, 7952-7957.	6.6	93
3186	Tuning magnetic properties in quasi-two-dimensional ferromagnetic Fe_{3â^'y}Ge_{1â^'x}As_xTe₂ (0â€‰â€‰â©½â€‰â€‰xâ€‰â€‰â©½â€‰â€‰1) Research Express, 2017, 4, 036103.		
3187	Na2ZnSn2S6: A mixed-metal thiostannate with large second-harmonic generation response activated by penta-tetrahedral [ZnSn4S14]10â^' clusters. Science China Technological Sciences, 2017, 60, 1465-1472.	2.0	9
3188	Improvements of thermoelectric properties for p-type Cu_{1.8}S bulk materials via optimizing the mechanical alloying process. Inorganic Chemistry Frontiers, 2017, 4, 1192-1199.	3.0	26
3189	The intriguing electronic and optical properties modulation in blue phosphorene/g-III-nitrides heterostructures. , 2017, , .		0
3190	Describing the anisotropic 133Cs solid state NMR interactions in cesium chromate. Chemical Physics Letters, 2017, 684, 8-13.	1.2	4
3191	Distinct effects of Al3+ doping on the structure and properties of hexagonal turbostratic birnessite: A comparison with Fe3+ doping. Geochimica Et Cosmochimica Acta, 2017, 208, 268-284.	1.6	26
3192	Structural, mechanical and vibrational study of uranyl silicate mineral soddyite by DFT calculations. Journal of Solid State Chemistry, 2017, 253, 249-257.	1.4	39
3193	An NMR Crystallographic Investigation of the Relationships between the Crystal Structure and ²⁹Si Isotropic Chemical Shift in Silica Zeolites. Journal of Physical Chemistry C, 2017, 121, 15198-15210.	1.5	28
3194	Atomistic dynamics of sulfur-deficient high-symmetry grain boundaries in molybdenum disulfide. Nanoscale, 2017, 9, 10312-10320.	2.8	18
3195	Theoretical prediction of new Câ€“Si alloys in ${oldsymbol{C}}2/{oldsymbol{m}}$-20 structure. Chinese Physics B, 2017, 26, 046101.	0.7	9
3196	Measuring and Modeling Highly Accurate 15 N Chemical Shift Tensors in a Peptide.. ChemPhysChem, 2017, 18, 2225-2232.	1.0	16
3197	Relationship between electronic properties of Fe3O4 substituted by Ca and Ba and their reactivity in chemical looping process: A first-principles study. Applied Energy, 2017, 202, 550-557.	5.1	34
3198	First-principles study of the structure, electronic, magnetic and elastic properties of half-Heusler compounds LiXGe (XÂ=ÂCa, Sr and Ba). Intermetallics, 2017, 89, 65-73.	1.8	44
3199	Molecular Construction Using (C₃N₃O₃)^{3â€“} Anions: Analysis and Prospect for Inorganic Metal Cyanurates Nonlinear Optical Materials. Crystal Growth and Design, 2017, 17, 4015-4020.	1.4	114
3200	Density Functional Theory Study of the Thermodynamic and Raman Vibrational Properties of Î³-UO₃ Polymorph. Journal of Physical Chemistry C, 2017, 121, 14507-14516.	1.5	43

#	Article	IF	Citations
3201	BaCu2MIVQ4(MIV= Si, Ge, and Sn; Q = S, Se): synthesis, crystal structures, optical performances and theoretical calculations. RSC Advances, 2017, 7, 29378-29385.	1.7	48
3202	Phase diagram of waterâ€“methane by first-principles thermodynamics: discovery of MH-IV and MH-V hydrates. Physical Chemistry Chemical Physics, 2017, 19, 15996-16002.	1.3	12
3203	Refractive index and extinction coefficient of NH₂CHâ€‰â€‰=â€‰â€‰NH₂PbI₃ perovskite photovoltaic material. Journal of Physics Condensed Matter, 2017, 29, 245702.	0.7	27
3204	Monolayer Bismuthene-Metal Contacts: A Theoretical Study. ACS Applied Materials & Interfaces, 2017, 9, 23128-23140.	4.0	73
3205	Electronic and Morphological Dual Modulation of Cobalt Carbonate Hydroxides by Mn Doping toward Highly Efficient and Stable Bifunctional Electrocatalysts for Overall Water Splitting. Journal of the American Chemical Society, 2017, 139, 8320-8328.	6.6	745
3206	Growth, Properties, and Theoretical Analysis of M2LiVO4 (Mâ€‰=â€‰Rb, Cs) Crystals: Two Potential Mid-Infrared Nonlinear Optical Materials. Scientific Reports, 2017, 7, 1901.	1.6	25
3207	Room-temperature methane gas sensing properties based on in situ reduced graphene oxide incorporated with tin dioxide. Journal of Materials Chemistry A, 2017, 5, 11131-11142.	5.2	40
3208	First-principle simulations of electronic structure in semicrystalline polyethylene. Journal of Chemical Physics, 2017, 146, 204901.	1.2	43
3209	Terahertz investigations on photoisomerisable compounds. Molecular Physics, 2017, 115, 2486-2494.	0.8	2
3210	Crystal structure of radium sulfate: An X-ray powder diffraction and density functional theory study. Journal of Solid State Chemistry, 2017, 253, 15-20.	1.4	18
3211	Structural and electronic properties of low-index surfaces of NbAl3 intermetallic with first-principles calculations. Applied Surface Science, 2017, 419, 811-816.	3.1	29
3212	A computational study of monolayer hexagonal WTe₂ to metal interfaces. Physica Status Solidi (B): Basic Research, 2017, 254, 1600837.	0.7	17
3213	Prediction of a new transition metal oxide MgRhO3 with SrTiO3-type structure: Stability, structure and physical characteristics. Chinese Journal of Physics, 2017, 55, 1489-1494.	2.0	18
3214	Electronic and optical properties of strained graphene and other strained 2D materials: a review. Reports on Progress in Physics, 2017, 80, 096501.	8.1	383
3215	Shape and energy consistent pseudopotentials for correlated electron systems. Journal of Chemical Physics, 2017, 146, 204107.	1.2	38
3216	Adsorption of heavy metals on a complex Al-Si-O bearing mineral system: Insights from theory and experiments. Separation and Purification Technology, 2017, 186, 28-38.	3.9	27
3217	Synthesis and Pharmacological Evaluation of a Novel Series of Cyclopentenone Derivatives. Journal of Chemical Research, 2017, 41, 50-56.	0.6	1
3218	Mechanical and thermodynamic properties of AlX (X = N, P, As) compounds. International Journal of Modern Physics B, 2017, 31, 1750167.	1.0	14

#	Article	IF	Citations
3219	Broadband Cooling Spectra of Hot Electrons and Holes in PbSe Quantum Dots. ACS Nano, 2017, 11, 6286-6294.	7.3	34
3220	Study of Structural, Electronic and Optical Properties of Lanthanum Doped Perovskite PZT Using Density Functional Theory. Applied Mechanics and Materials, 2017, 864, 127-132.	0.2	4
3221	Design and Synthesis of a Series of Novel Mixed Borate and Carbonate Halides. Chemistry - A European Journal, 2017, 23, 10451-10459.	1.7	14
3222	Computational study of structural, optoelectronic and nonlinear optical properties of dynamic solid-state chalcone derivatives. Journal of Molecular Graphics and Modelling, 2017, 75, 355-364.	1.3	16
3223	Carbon nitrides: synthesis and characterization of a new class of functional materials. Physical Chemistry Chemical Physics, 2017, 19, 15613-15638.	1.3	339
3224	Adsorption of atmospheric gases on cementite 010 surfaces. Journal of Chemical Physics, 2017, 146, 204703.	1.2	6
3225	Observation of deflagration wave in energetic materials using reactive molecular dynamics. Combustion and Flame, 2017, 184, 20-29.	2.8	18
3226	Prediction and experimental validation of solid solutions and isopolymorphs of cytosine/5-flucytosine. CrystEngComm, 2017, 19, 3566-3572.	1.3	12
3227	Structure Prediction of Liâ€“Sn and Liâ€“Sb Intermetallics for Lithium-Ion Batteries Anodes. Chemistry of Materials, 2017, 29, 5787-5795.	3.2	37
3228	Superhard sp2-sp3 hybridized BC2N: A 3D crystal with 1D and 2D alternate metallicity. Journal of Applied Physics, 2017, 121, .	1.1	13
3229	Structural, elastic, electronic and optical properties of the novel quaternary diamond-like semiconductors Cu2MgSiS4 and Cu2MgGeS4. Solid State Sciences, 2017, 70, 21-35.	1.5	24
3230	Li₆Zn₃(BO₃)₄: a new zincoborate featuring vertex-, edge- and face-sharing LiO₄tetrahedra and exhibiting reversible phase transitions. Inorganic Chemistry Frontiers, 2017, 4, 1100-1107.	3.0	17
3231	Phonon dispersion models for MgB 2 with application of pressure. Physica C: Superconductivity and Its Applications, 2017, 536, 11-17.	0.6	13
3232	Nonradiative Step Facets in Semiconductor Nanowires. Nano Letters, 2017, 17, 2454-2459.	4.5	17
3233	Effective calcium doping at the B-site of BaFeO_{3â^'Î´} perovskite: towards low-cost and high-performance oxygen permeation membranes. Journal of Materials Chemistry A, 2017, 5, 7999-8009.	5.2	53
3234	High Mobility 2D Palladium Diselenide Fieldâ€Effect Transistors with Tunable Ambipolar Characteristics. Advanced Materials, 2017, 29, 1602969.	11.1	251
3235	Triazolyl, Imidazolyl, and Carboxylic Acid Moieties in the Design of Molybdenum Trioxide Hybrids: Photophysical and Catalytic Behavior. Inorganic Chemistry, 2017, 56, 4380-4394.	1.9	20
3236	Molecular and Vibrational Dynamics in the Cholesterol-Lowering Agent Lovastatin: Solid-State NMR, Inelastic Neutron Scattering, and Periodic DFT Study. Journal of Physical Chemistry B, 2017, 121, 2776-2787.	1.2	15

#	Article	IF	Citations
3237	Insight into the hydrogen evolution reaction of nickel dichalcogenide nanosheets: activities related to non-metal ligands. Nanoscale, 2017, 9, 5538-5544.	2.8	97
3238	Interface formation energy, bonding, energy band alignment in Î±-NaYF 4 related core shell models: For future multi-layer core shell luminescence materials. Journal of Rare Earths, 2017, 35, 315-334.	2.5	7
3239	Stoner factors of doped 122 Fe-based superconductors: First principles results. Computational Materials Science, 2017, 132, 46-54.	1.4	2
3240	Synthesis, structure and electronic calculation of alkali metals borate Li 2 Na[B 5 O 8 (OH) 2]. Inorganic Chemistry Communication, 2017, 79, 104-108.	1.8	2
3241	Ab initio study of N-doped Î²-Ga 2 O 3 with intrinsic defects: the structural, electronic and optical properties. Journal of Alloys and Compounds, 2017, 712, 379-385.	2.8	88
3242	Influences of different surfaces on anisotropic impact sensitivity of hexahydro-1,3,5-trinitro-1,3,5-triazine. Vacuum, 2017, 139, 117-121.	1.6	4
3243	Structural, electronic and optical properties of brookite phase titanium dioxide. Materials Research Express, 2017, 4, 044003.	0.8	9
3244	Structural, elastic and thermodynamic properties of iron carbide Fe 7 C 3 phases: An ab initio study. Chinese Journal of Physics, 2017, 55, 977-988.	2.0	4
3245	Structure comparison and optical properties of Na₇Mg_{4.5}(P₂O₇)₄: a sodium magnesium phosphate with isolated P₂O₇units. New Journal of Chemistry, 2017, 41, 3399-3404.	1.4	17
3246	The atomic simulation environmentâ€"a Python library for working with atoms. Journal of Physics Condensed Matter, 2017, 29, 273002.	0.7	1,933
3247	Activation mechanism of ammonium ions on sulfidation of malachite (â€“201) surface by DFT study. Applied Surface Science, 2017, 410, 126-133.	3.1	50
3248	Band structure, electronic and optical features of Tl4SnX3 (XÂ=ÂS, Te) ternary compounds for optoelectronic applications. Journal of Alloys and Compounds, 2017, 710, 600-607.	2.8	21
3249	Practical principles of density functional theory for catalytic reaction simulations on metal surfaces â€“ from theory to applications. Molecular Simulation, 2017, 43, 861-885.	0.9	22
3250	Synthesis and Mechanical Character of Hexagonal Phase Î´â€²WN. Inorganic Chemistry, 2017, 56, 3970-3975.	1.9	25
3251	Structural insights into the polymorphism of bismuth(III) di-n-butyldithiocarbamate by X-ray diffraction, solid-state (13C/15N) CP-MAS NMR and DFT calculations. Polyhedron, 2017, 129, 123-132.	1.0	11
3252	Local Structure Evolution and Modes of Charge Storage in Secondary Liâ€"FeS₂ Cells. Chemistry of Materials, 2017, 29, 3070-3082.	3.2	42
3253	Metalâ€"Organic Nanosheets Formed via Defect-Mediated Transformation of a Hafnium Metalâ€"Organic Framework. Journal of the American Chemical Society, 2017, 139, 5397-5404.	6.6	224
3254	More accurate depiction of adsorption energy on transition metals using work function as one additional descriptor. Physical Chemistry Chemical Physics, 2017, 19, 12628-12632.	1.3	44

#	Article	IF	Citations
3255	Single isomerization selectivity of glucose in methanol over Sn-BEC zeolite of homogenous Sn distribution. Microporous and Mesoporous Materials, 2017, 247, 158-165.	2.2	28
3256	Adsorption of Zn(II) on the kaolinite(001) surfaces in aqueous environment: A combined DFT and molecular dynamics study. Applied Surface Science, 2017, 414, 405-412.	3.1	36
3257	Incipient FeO(1 1 1) monolayer formation during O-adsorption on Fe(1 1 0) surface. Computational Materials Science, 2017, 134, 109-115.	1.4	6
3258	Synthesis and Characterization of the High-Pressure Nickel Borate Î³-NiB₄O₇. Inorganic Chemistry, 2017, 56, 4217-4228.	1.9	22
3259	Physical properties of ternary silicide superconductors Li₂XSi₃ (X = Rh, Os): An ab initio study. International Journal of Modern Physics B, 2017, 31, 1750135.	1.0	5
3260	Temperature Dependence in the Terahertz Spectrum of Nicotinamide: Anharmonicity and Hydrogen-Bonded Network. Journal of Physical Chemistry A, 2017, 121, 2558-2564.	1.1	23
3261	Identification of single-site gold catalysis in acetylene hydrochlorination. Science, 2017, 355, 1399-1403.	6.0	380
3262	Efficiency evaluation on Cs x [NH 2 CH = NH 2] 1âˆ’ x Pb(I 1âˆ’ y Br y) 3 /crystalline silicon tandem solar cells. Solar Energy, 2017, 147, 432-438.	2.9	7
3263	Li₃VO₄: A Promising Mid-Infrared Nonlinear Optical Material with Large Laser Damage Threshold. Crystal Growth and Design, 2017, 17, 2792-2800.	1.4	33
3264	Understanding the Role of Molecular Diffusion and Catalytic Selectivity in Liquid-Phase Beckmann Rearrangement. ACS Catalysis, 2017, 7, 2926-2934.	5.5	30
3265	DFT study on the interfacial properties of vertical and in-plane BiOI/BiOIO₃hetero-structures. Physical Chemistry Chemical Physics, 2017, 19, 9900-9911.	1.3	17
3266	One-step synthesis, electronic structure, and photocatalytic activity of earth-abundant visible-light-driven FeAl₂O₄. Physical Chemistry Chemical Physics, 2017, 19, 9392-9401.	1.3	22
3267	Dirac's dream: Understanding metal sorption by geomedia using density functional theory. Chemical Geology, 2017, 464, 4-13.	1.4	16
3268	Determination of Crystal Structure of Graphitic Carbon Nitride: Ab Initio Evolutionary Search and Experimental Validation. Chemistry of Materials, 2017, 29, 2694-2707.	3.2	83
3269	A3Sr2P7O21 (A = Rb, Cs): Two Polyphosphates Based on Different Types of Pâ€“O Chains and Ring Structures. Inorganic Chemistry, 2017, 56, 3939-3945.	1.9	33
3270	High-Pressure Structural Response of an Insensitive Energetic Crystal: Dihydroxylammonium 5,5â€²-Bistetrazole-1,1â€²-diolate (TKX-50). Journal of Physical Chemistry C, 2017, 121, 5761-5767.	1.5	28
3271	Crystallographic, optical, and electronic properties of (Cu,Li)InS2 system. Thin Solid Films, 2017, 633, 172-178.	0.8	7
3272	Investigation of the post-annealing electromagnetic response of Cuâ€“Co oxide coatings via optical measurement and computational modelling. RSC Advances, 2017, 7, 16826-16835.	1.7	27

#	Article	IF	Citations
3273	Facile preparation of Prussian blue analogue Co₃[Co(CN)₆]₂with fine-tuning color transition temperature as thermochromic material. CrystEngComm, 2017, 19, 2057-2064.	1.3	32
3274	Determination of a complex crystal structure in the absence of single crystals: analysis of powder X-ray diffraction data, guided by solid-state NMR and periodic DFT calculations, reveals a new 2â€²-deoxyguanosine structural motif. Chemical Science, 2017, 8, 3971-3979.	3.7	62
3275	Mid-Infrared Nonlinear Optical Materials Based on Metal Chalcogenides: Structureâ€“Property Relationship. Crystal Growth and Design, 2017, 17, 2254-2289.	1.4	266
3276	NMR shieldings from density functional perturbation theory: GIPAW versus all-electron calculations. Journal of Chemical Physics, 2017, 146, 064115.	1.2	15
3277	Two-dimensional honeycomb (A7) and zigzag sheet (ZS) type nitrogen monolayers. A first principles study of structural, electronic, spectral, and mechanical properties. Computational Materials Science, 2017, 133, 122-129.	1.4	27
3278	Chiral penta-graphene nanotubes: Structure, bonding and electronic properties. Computational and Theoretical Chemistry, 2017, 1108, 70-75.	1.1	21
3279	Models of Aged Magnesiumâ€“Silicateâ€“Hydrate Cements Based on the Lizardite and Talc Crystals: A Periodic DFT-GIPAW Investigation. Journal of Physical Chemistry C, 2017, 121, 7319-7330.	1.5	21
3280	Nuclear dynamics and phase polymorphism in solid formic acid. Physical Chemistry Chemical Physics, 2017, 19, 9064-9074.	1.3	33
3281	Efficient noble metal nanocatalysts supported on HfC(001) for O2 dissociation. AIP Advances, 2017, 7, .	0.6	6
3282	Investigations of the magnetic, mechanical and thermodynamic properties of cubic phase LaMO₃ (M=Ti~Fe). Philosophical Magazine Letters, 2017, 97, 169-179.	0.5	11
3283	First-principles study of the dynamic Jahn-Teller distortion of the neutral vacancy in diamond. Physical Review B, 2017, 95, .	1.1	23
3284	Enhancement of the Thermoelectric Properties of FeGa3-type Structures with Group 6 Transition Metals: A Computational Exploration. Inorganic Chemistry, 2017, 56, 4229-4237.	1.9	9
3285	New pressure-induced polymorphic transitions of anhydrous magnesium sulfate. Dalton Transactions, 2017, 46, 5058-5068.	1.6	23
3286	LiSr₃Be₃B₃O₉F₄: a new ultraviolet nonlinear optical crystal for fourth-harmonic generation of Nd:YAG lasers. New Journal of Chemistry, 2017, 41, 4269-4272.	1.4	18
3287	Green urea synthesis catalyzed by hematite nanowires in magnetic field. Journal of Magnetism and Magnetic Materials, 2017, 428, 469-480.	1.0	18
3288	Piezochromism and hydrochromism through electron transfer: new stories for viologen materials. Chemical Science, 2017, 8, 2758-2768.	3.7	174
3289	Theoretical Evaluation of Terahertz Sources Generated From SnGa₄Q₇ (Q=S,) Tj ETQq0 0 0 rgBT /Overlock 10	1.0	6
3290	Shape-Controlled TiO₂ Nanocrystals for Na-Ion Battery Electrodes: The Role of Different Exposed Crystal Facets on the Electrochemical Properties. Nano Letters, 2017, 17, 992-1000.	4.5	162

#	Article	IF	Citations
3291	Unusual physical behaviour and polymorphic phase transitions in crystalline bicyclic anhydrides. CrystEngComm, 2017, 19, 276-284.	1.3	2
3292	Lattice dynamics and Mg/Ti order in orthorhombic pseudobrookite-type MgTi2 O5. Journal of Alloys and Compounds, 2017, 699, 16-24.	2.8	12
3293	Crystal and electronic structures of substituted halide perovskites based on density functional calculation and molecular dynamics. Chemical Physics, 2017, 485-486, 22-28.	0.9	12
3294	A new potential for methylammonium lead iodide. Physical Chemistry Chemical Physics, 2017, 19, 2313-2321.	1.3	24
3295	In-situhigh temperature Raman spectroscopic study on the structural evolution of Na₂W₂O₇from the crystalline to molten states. Journal of Raman Spectroscopy, 2017, 48, 298-304.	1.2	23
3296	Enhancement of Ferromagnetism in Nonmagnetic Metal Oxide Nanoparticles by Facet Engineering. Small, 2017, 13, 1602951.	5.2	12
3297	â€œEnergy Relay Centerâ€•for doped mechanoluminescence materials: a case study on Cu-doped and Mn-doped CaZnOS. Physical Chemistry Chemical Physics, 2017, 19, 1190-1208.	1.3	35
3298	Crystal chemical characterization of mullite-type aluminum borate compounds. Journal of Solid State Chemistry, 2017, 247, 173-187.	1.4	16
3299	Engineering stepped edge surface structures of MoS₂sheet stacks to accelerate the hydrogen evolution reaction. Energy and Environmental Science, 2017, 10, 593-603.	15.6	284
3300	Structural Modulation of Nitrate Group with Cations to Affect SHG Responses in RE(OH)₂NO₃ (RE = La, Y, and Gd): New Polar Materials with Large NLO Effect after Adjusting pH Values of Reaction Systems. Chemistry of Materials, 2017, 29, 896-903.	3.2	107
3301	AlN/BP Heterostructure Photocatalyst for Water Splitting. IEEE Electron Device Letters, 2017, 38, 145-148.	2.2	68
3302	2D-Layered Lithium Carboxylate Based on Biphenyl Core as Negative Electrode for Organic Lithium-Ion Batteries. Chemistry of Materials, 2017, 29, 546-554.	3.2	41
3303	Why does F-doping enhance the photocatalytic water-splitting performance of mBiVO₄? â€“ a density functional theory study. New Journal of Chemistry, 2017, 41, 1094-1102.	1.4	12
3304	Nano-sized graphene flakes: insights from experimental synthesis and first principles calculations. Physical Chemistry Chemical Physics, 2017, 19, 6338-6344.	1.3	9
3305	Metastable phases, phase transformation and properties of AlAs based on first-principle study. Computational Materials Science, 2017, 128, 337-342.	1.4	20
3306	A local Fock-exchange potential in Kohnâ€“Sham equations. Journal of Physics Condensed Matter, 2017, 29, 04LT01.	0.7	12
3307	(Oxo)(Fluoro)â€“Aluminates in KFâ€“Al₂O₃ System: Thermal Stability and Structural Correlation. Inorganic Chemistry, 2017, 56, 13349-13359.	1.9	11
3308	Towards lead-free perovskite photovoltaics and optoelectronics by ab-initio simulations. Scientific Reports, 2017, 7, 14025.	1.6	310

#	Article	IF	Citations
3309	Observing different modes of mobility in lithium titanate spinel by nuclear magnetic resonance. RSC Advances, 2017, 7, 25276-25284.	1.7	17
3310	Exceptional ring topology makes diamond allotropes as light-weight superhard materials. Diamond and Related Materials, 2017, 80, 140-146.	1.8	0
3311	Is C₃N₄ Chemically Stable toward Reactive Oxygen Species in Sunlight-Driven Water Treatment?. Environmental Science & Technology, 2017, 51, 13380-13387.	4.6	119
3312	Spectroscopy and DFT studies of uranyl carbonate, rutherfordine, UO2CO3: a model for uranium transport, carbon dioxide sequestration, and seawater species. Journal Physics D: Applied Physics, 2017, 50, 505501.	1.3	7
3314	Pressure-induced improvement in symmetry and change in electronic properties of SnSe. Journal of Molecular Modeling, 2017, 23, 319.	0.8	7
3315	Location and orientation of lone pairs in apatite-type materials: a computational study. Dalton Transactions, 2017, 46, 15996-15999.	1.6	6
3316	Role of Exact Exchange and Relativistic Approximations in Calculating ¹⁹F Magnetic Shielding in Solids Using a Cluster Ansatz. Journal of Chemical Theory and Computation, 2017, 13, 4741-4752.	2.3	20
3317	Synthesis, Structure, and Properties of Nonlinear Optical Crystal Na₂SiF₆. Zeitschrift Fur Anorganische Und Allgemeine Chemie, 2017, 643, 1739-1743.	0.6	10
3318	Solid solution and densification behavior of zirconium oxycarbide (ZrCxOy) ceramics via doping ZrO2 and Zr in ZrC. Journal of Alloys and Compounds, 2017, 729, 492-497.	2.8	15
3319	Charge transport, interfacial interactions and synergistic mechanisms in BiNbO₄/MWO₄ (M = Zn and Cd) heterostructures for hydrogen production: insights from a DFT+U study. Physical Chemistry Chemical Physics, 2017, 19, 28401-28413.	1.3	19
3320	Hydrostatic pressure effects on the structural, elastic and thermodynamic properties of the complex transition metal hydrides A₂OsH₆ (Aâ€‰=â€‰Mg, Ca, Sr and Ba). High Pressure Research, 2017, 37, 558-578.	0.4	13
3321	Synthesis of unexpected novel bis-coumarin derivatives via three component reactions of 4-hydroxycoumarin, aldehydes and cyclic secondary amines. Conformation in the solid state and pharmacological evaluation. Zeitschrift Fur Naturforschung - Section B Journal of Chemical Sciences, 2017, 72, 705-716.	0.3	11
3322	New Group 13 MIL-53 Derivates based on 2,5-Thiophenedicarboxylic Acid. Zeitschrift Fur Anorganische Und Allgemeine Chemie, 2017, 643, 1600-1608.	0.6	44
3323	First-principles investigation of H₂S adsorption and dissociation on titanium carbide surfaces. Physical Chemistry Chemical Physics, 2017, 19, 27116-27122.	1.3	8
3324	Structural convergence properties of amorphous InGaZnO4 from simulated liquid-quench methods. Dalton Transactions, 2017, 46, 15311-15316.	1.6	2
3325	Solvent-mediated purification of hexa-molybdenum cluster halide, Cs₂[Mo₆Cl₁₄] for enhanced optical properties. CrystEngComm, 2017, 19, 6028-6038.	1.3	8
3326	In Situ Ligand Modification Strategy for the Construction of One-, Two-, and Three-Dimensional Heterometallic Iodides. Inorganic Chemistry, 2017, 56, 13785-13793.	1.9	29
3327	Preferential S/Se occupation in an anisotropic ReS_{2(1â^'x)}Se_{2x}monolayer alloy. Nanoscale, 2017, 9, 18275-18280.	2.8	10

#	Article	IF	Citations
3328	Electronic correlation effects and orbital density wave in the layered compound <mml:math xmlns:mml="http://www.w3.org/1998/Math/MathML"><mml:mrow><mml:mn>1</mml:mn><mml:mi>T</mml:mi><mml:msub><mml:mt Physical Review B, 2017, 96, .	1.1	32
3329	Understanding the role of water in 1,10-phenanthroline monohydrate. CrystEngComm, 2017, 19, 6133-6145.	1.3	8
3330	Calculation of the electronic structure and exchange interaction in the InSb and GaAs semiconductors codoped with Mn and Ni. Inorganic Materials, 2017, 53, 1131-1135.	0.2	8
3331	Structure Evolution and Spin-Glass Transition of Layered Compounds ALiFeSe₂ (A = Na, K,) Tj ETQq1 1 0.784314 rgBT /O	1.9	14
3332	Three Mixed-Alkaline Borates: Na₂M₂B₂₀O₃₂ (M = Rb,) Tj ETQq0 0 0 rgBT /Overloc Li₄Cs₄B₄₀O₆₄ with Fundamental Building Block B₄₀O₇₇. Inorganic Chemistry, 2017, 56, 13456-13463.	1.9	29
3333	Enantioselective Recognition of Ammonium Carbamates in a Chiral Metalâ€“Organic Framework. Journal of the American Chemical Society, 2017, 139, 16000-16012.	6.6	82
3334	A superhard sp3 microporous carbon with direct bandgap. Chemical Physics Letters, 2017, 689, 68-73.	1.2	39
3335	A three-dimensional lead borate with a fluorite net constructed from different cluster building units. Inorganic Chemistry Communication, 2017, 86, 108-111.	1.8	5
3336	Influence of point defects on the near edge structure of hexagonal boron nitride. Physical Review B, 2017, 96, .	1.1	59
3337	Revealing phase relations between Fe2B7 and FeB4 and hypothetical Fe2B7-type Ru2B7 and Os2B7: first-principles calculations. RSC Advances, 2017, 7, 44860-44866.	1.7	2
3338	Electronic structure and photoluminescence property of a novel white emission phosphor Na 3 MgZr(PO 4) 3 :Dy 3+ for warm white light emitting diodes. Chinese Physics B, 2017, 26, 097801.	0.7	4
3339	Two KBBF-Type Beryllium Borates MBe₂B₂O₆ (M = Sr, Ba) with a Three-Dimensional (Be₂B₂O₆)_{âˆž} Network. Inorganic Chemistry, 2017, 56, 12090-12093.	1.9	8
3340	New Compressed Chalcopyrite-like Li₂BaM^{IV}Q₄ (M^{IV} =) Tj ETQq0 0 0 rgBT /Overloc Society, 2017, 139, 14885-14888.	6.6	201
3341	The Mechanism of In and Ge Occurrence in Sphalerite Crystal and the Influence on Properties: A DFT (Density Function Theory) Simulation. Solid State Phenomena, 2017, 262, 303-306.	0.3	0
3342	DFT study of anisotropy effects on the electronic properties of diamond nanowires with nitrogen-vacancy center. Journal of Molecular Modeling, 2017, 23, 292.	0.8	1
3343	Zerovalent Selenium Adsorption Mechanisms on CaO Surface: DFT Calculation and Experimental Study. Journal of Physical Chemistry A, 2017, 121, 7385-7392.	1.1	15
3344	ScMO(BO₃) (M = Ca and Cd): new Sc-based oxyborates featuring interesting edge-sharing sandwich-like chains and UV cut-off edges. Dalton Transactions, 2017, 46, 14839-14846.	1.6	13
3345	Enhancing the resolution of¹H and¹³C solid-state NMR spectra by reduction of anisotropic bulk magnetic susceptibility broadening. Physical Chemistry Chemical Physics, 2017, 19, 28153-28162.	1.3	29

#	Article	IF	Citations
3346	Disorder-order phase transition at high pressure in ammonium fluoride. Physical Review B, 2017, 96, .	1.1	7
3347	Two isomeric solid carbon nitrides with 1â€‰:â€‰1 stoichiometry which exhibit strong mechanical anisotropy. New Journal of Chemistry, 2017, 41, 13140-13148.	1.4	8
3348	First principles study of the structural, elastic, electronic, optical and thermodynamic properties of SrRh 2 laves phase intermetallic compound. Computational Condensed Matter, 2017, 13, 65-71.	0.9	16
3349	Confinement of Iodine Molecules into Triple-Helical Chains within Robust Metalâ€“Organic Frameworks. Journal of the American Chemical Society, 2017, 139, 16289-16296.	6.6	199
3350	<mml:math xmlns:mml="http://www.w3.org/1998/Math/MathML"><mml:mrow><mml:msub><mml:mi mathvariant="normal">C</mml:mi><mml:mn>3</mml:mn></mml:msub><mml:msub><mml:mi mathvariant="normal">H</mml:mi><mml:mn>2</mml:mn></mml:msub></mml:mrow></mml:math> : A wide-band-gap semiconductor with strong optical absorption. Physical Review B, 2017, 96, .	1.1	8
3351	Stability, elastic anisotropy, and electronic properties of Ca ₂ C ₃. Chinese Physics B, 2017, 26, 066201.	0.7	3
3352	Adsorption and dissociation of O₂on MoO₂(1Ì„11) surfaces: a DFT study. Physical Chemistry Chemical Physics, 2017, 19, 29244-29254.	1.3	7
3353	Unexpected Crystallization Patterns of Zinc Boron Imidazolate Framework ZBIFâ€1: NMR Crystallography of Integrated Metalâ€“Organic Frameworks. ChemPhysChem, 2017, 18, 3576-3582.	1.0	6
3354	LiGaGe₂S₆: A Chalcogenide with Good Infrared Nonlinear Optical Performance and Low Melting Point. Inorganic Chemistry, 2017, 56, 13267-13273.	1.9	51
3355	The origin of uniaxial negative thermal expansion in layered perovskites. Npj Computational Materials, 2017, 3, .	3.5	38
3356	Bipolar charge transfer induced by water: experimental and first-principles studies. Physical Chemistry Chemical Physics, 2017, 19, 29418-29423.	1.3	40
3357	Co-based alloys design based on first-principles calculations: Influence of transition metal and rare-earth alloying element on stacking fault energy. AIP Conference Proceedings, 2017, , .	0.3	4
3358	Investigation of energy band alignments and interfacial properties of rutile NMO₂/TiO₂ (NM = Ru, Rh, Os, and Ir) by first-principles calculations. Physical Chemistry Chemical Physics, 2017, 19, 29583-29593.	1.3	7
3359	The phase stability of terephthalic acid under high pressure. Chemical Physics Letters, 2017, 689, 56-61.	1.2	10
3360	DFT Investigation of Structural, Electronic, Elastic and Optical Properties of SrMO₄(M=Mo and W). Communications in Theoretical Physics, 2017, 68, 536.	1.1	8
3361	Structural Evolution in BaSn₂F₅X (X = Cl, Br, I): A Family of Alkaline Earth Metal Tin Mixed Halides. Inorganic Chemistry, 2017, 56, 13593-13599.	1.9	11
3362	Robust theoretical modelling of core ionisation edges for quantitative electron energy loss spectroscopy of B- and N-doped graphene. Journal of Physics Condensed Matter, 2017, 29, 225303.	0.7	8
3363	The GGA+U method studied the effects of Cu doping on the formation energy, electronic and optical properties of V-doped ZnO. Optical and Quantum Electronics, 2017, 49, 1.	1.5	3

#	Article	IF	Citations
3364	Acetylene and Ethylene Adsorption on a Î²-Mo₂C(100) Surface: A Periodic DFT Study on the Role of C- and Mo-Terminations for Bonding and Hydrogenation Reactions. Journal of Physical Chemistry C, 2017, 121, 19786-19795.	1.5	22
3365	Pressure-Induced Emission Enhancement of Carbazole: The Restriction of Intramolecular Vibration. Journal of Physical Chemistry Letters, 2017, 8, 4191-4196.	2.1	95
3366	Nature of the metallization transition in solid hydrogen. Physical Review B, 2017, 95, .	1.1	34
3367	Phase transition of tetragonal copper sulfide <mml:math xmlns:mml="http://www.w3.org/1998/Math/MathML"><mml:mrow><mml:msub><mml:mi>Cu</mml:mi><mml:mn>2</mml:mn></mml mathvariant="normal">S</mml:mi></mml:mrow></mml:math> at low temperatures. Physical Review B, 2017, 96, .	1.1	15
3368	Influence of Intramolecular Charge Transfer and Nuclear Quantum Effects on Intramolecular Hydrogen Bonds in Azopyrimidines. Journal of Organic Chemistry, 2017, 82, 10350-10359.	1.7	15
3370	Increase in Solubility of Poorly-Ionizable Pharmaceuticals by Salt Formation: A Case of Agomelatine Sulfonates. Crystal Growth and Design, 2017, 17, 5283-5294.	1.4	13
3371	Ammonia Synthesis on Wool-Like Au, Pt, Pd, Ag, or Cu Electrode Catalysts in Nonthermal Atmospheric-Pressure Plasma of N₂ and H₂. ACS Catalysis, 2017, 7, 6924-6929.	5.5	157
3372	Theoretical investigations on the phase transition of pure and Li-doped AlH₃. RSC Advances, 2017, 7, 42024-42029.	1.7	3
3373	Physical Properties of C-Si Alloys inC2/mStructure. Communications in Theoretical Physics, 2017, 68, 259.	1.1	16
3374	Hg-Based Infrared Nonlinear Optical Material KHg₄Ga₅Se₁₂ Exhibits Good Phase-Matchability and Exceptional Second Harmonic Generation Response. Chemistry of Materials, 2017, 29, 7993-8002.	3.2	85
3375	Experimental and ab initio studies of Cd₅(BO₃)₃Cl: the first cadmium borate chlorine NLO material with isolated BO₃groups. Dalton Transactions, 2017, 46, 15228-15234.	1.6	18
3376	Theoretical prediction of the mechanical properties of zeolitic imidazolate frameworks (ZIFs). RSC Advances, 2017, 7, 41499-41503.	1.7	18
3377	Exchange constants in molecule-based magnets derived from density functional methods. Physical Review B, 2017, 96, .	1.1	8
3378	Understanding the Solid Solutionâ€“Aqueous Solution Equilibria in the KClÂ+ÂRbClÂ+ÂH2O System from Experiments,ÂAtomistic Simulation and Thermodynamic Modeling. Journal of Solution Chemistry, 2017, 46, 1871-1902.	0.6	15
3379	The critical role of Si doping in enhancing the stability of M6C carbides. Journal of Alloys and Compounds, 2017, 728, 917-926.	2.8	38
3380	Molecular Level Understanding of the Reversible Phase Transformation between Forms III and II of Dapsone. Crystal Growth and Design, 2017, 17, 5054-5060.	1.4	19
3381	Quantum chemical calculations of thermodynamic and mechanical properties of the intermetallic phases in copperâ€“scandium alloy. Journal of Theoretical and Computational Chemistry, 2017, 16, 1750056.	1.8	4
3383	Syntheses, structures and properties of metal phosphates Pb2Mg(PO4)2, Pb4Zn8(PO4)8and Î±-BaZn2(PO4)2. Dalton Transactions, 2017, 46, 16034-16040.	1.6	4

#	Article	IF	Citations
3384	Theoretical investigations of Li+ and Co3+ positions for layered LiCoO2 Lithium ion battery cathode material using first principle method. AIP Conference Proceedings, 2017, , .	0.3	5
3385	Picoscale materials engineering. Nature Reviews Materials, 2017, 2, .	23.3	42
3386	A series of pentanary inorganic supramolecular sulfides (A₃X)[MB₁₂(MS₄)₃] (A = K, Cs; X = Cl, Br, I; M = Ga, In,) Tj ETQq0 0 0 rgBT /Overlo	2.0	8
3387	Second-order nonlinear optical switching with a record-high contrast for a photochromic and thermochromic bistable crystal. Chemical Science, 2017, 8, 7751-7757.	3.7	104
3388	Interaction of curcumin in a drug delivery system including a composite with poly(lactic-co-glycolic) Tj ETQq0 0 0 rgBT /Overlock 10 Tf 5 Materials Chemistry B, 2017, 5, 8070-8082.	2.9	45
3389	Enhanced photoelectric performance of (2Al, S) co-doped rutile SnO₂. RSC Advances, 2017, 7, 42940-42945.	1.7	11
3390	The development of a promising photosensitive Schottky barrier diode using a novel Cd(<scp>ii</scp>) based coordination polymer. Dalton Transactions, 2017, 46, 13531-13543.	1.6	49
3391	Atomic-scale friction behavior of layered graphene and graphene-like BN materials modulated by interaction potential. AIP Advances, 2017, 7, .	0.6	3
3392	Unraveling Complexity in the Solid Form Screening of a Pharmaceutical Salt: Why so Many Forms? Why so Few?. Crystal Growth and Design, 2017, 17, 5349-5365.	1.4	33
3393	Na₆Si₃S₈O: the first example of a sulfide silicate exhibiting unusual tri-polymerized [Si₃S₈O]^{6â^'}units without Sâ€“O bonds. Dalton Transactions, 2017, 46, 13356-13359.	1.6	6
3394	Understanding the breathing phenomena in nano-ZIF-7 upon gas adsorption. Journal of Materials Chemistry A, 2017, 5, 20938-20946.	5.2	50
3395	Structural, mechanical, electronic and thermal properties of the newly predicted NB2 from ab initio calculations. Chinese Journal of Physics, 2017, 55, 2540-2547.	2.0	5
3396	Luminescent, optical and electronic properties of Na2Mo2O7 single crystals. Journal of Luminescence, 2017, 192, 1264-1272.	1.5	23
3397	Preferential synthesis of (6,4) single-walled carbon nanotubes by controlling oxidation degree of Co catalyst. Scientific Reports, 2017, 7, 11149.	1.6	16
3398	CO₂ Dynamics in Pure and Mixed-Metal MOFs with Open Metal Sites. Journal of Physical Chemistry C, 2017, 121, 25778-25787.	1.5	59
3399	Structure of Carbon-Coated C12A7 Electride via Solid-State NMR and DFT Calculations. Journal of Physical Chemistry C, 2017, 121, 22268-22273.	1.5	9
3400	A new phase-matchable nonlinear optical silicate: Rb₂ZnSi₃O₈. Journal of Materials Chemistry C, 2017, 5, 11025-11029.	2.7	21
3401	Unexpected stable stoichiometries and superconductivity of potassium-rich sulfides. RSC Advances, 2017, 7, 44884-44889.	1.7	5

#	Article	IF	Citations
3402	Mechanical Anisotropic and Electronic Properties ofAmm2-carbon under Pressure[*]. Communications in Theoretical Physics, 2017, 68, 395.	1.1	8
3403	Tuning the electronic structure in stanene/graphene bilayers using strain and gas adsorption. Physical Chemistry Chemical Physics, 2017, 19, 25574-25581.	1.3	12
3404	Gauge-including projector augmented-wave NMR chemical shift calculations with DFT+ <mml:math xmlns:mml="http://www.w3.org/1998/Math/MathML"><mml:mi>U</mml:mi></mml:math>. Physical Review B, 2017, 96, .	1.1	7
3405	First principle and tight-binding study of strained SnC. Journal of Physics and Chemistry of Solids, 2017, 111, 458-463.	1.9	23
3406	High pressure elasticity of FeCO 3 -MgCO 3 carbonates. Physics of the Earth and Planetary Interiors, 2017, 271, 57-63.	0.7	22
3407	Violations of LÃ¶wenstein's rule in zeolites. Chemical Science, 2017, 8, 7483-7491.	3.7	84
3408	Toward Bi³⁺ Red Luminescence with No Visible Reabsorption through Manageable Energy Interaction and Crystal Defect Modulation in Single Bi³⁺-Doped ZnWO₄ Crystal. Chemistry of Materials, 2017, 29, 8412-8424.	3.2	148
3409	Vibrational spectra and physico-chemical properties of astrophysical analogs. Physical Chemistry Chemical Physics, 2017, 19, 26582-26588.	1.3	4
3410	Two-dimensional semiconducting gold. Physical Review B, 2017, 95, .	1.1	10
3411	Na2(H2en)[B5O8(OH)]2[B3O4(OH)]2and Na3(HCOO)[B5O8(OH)]: Two Borates Co-Templated by Inorganic Cations and Organic Compounds. European Journal of Inorganic Chemistry, 2017, 2017, 4061-4067.	1.0	14
3412	A New KBBF-Family Nonlinear Optical Material with Strong Interlayer Bonding. Crystal Growth and Design, 2017, 17, 4422-4427.	1.4	42
3413	Mechanical and Electronic Properties of Carbon Nitride Methanediide under High Pressure. Journal of Physical Chemistry C, 2017, 121, 16959-16963.	1.5	1
3414	Solvent Effect Inside the Nanocage of Zeolite Catalysts: A Combined Solid-State NMR Approach and Multiscale Simulation. Journal of Physical Chemistry C, 2017, 121, 16921-16931.	1.5	8
3415	A Cd(<scp>ii</scp>)-based MOF as a photosensitive Schottky diode: experimental and theoretical studies. Dalton Transactions, 2017, 46, 11239-11249.	1.6	66
3416	Electrons on the surface of 2D materials: from layered electrides to 2D electrenes. Journal of Materials Chemistry C, 2017, 5, 11196-11213.	2.7	45
3417	Interpretation of x-ray absorption spectroscopy in the presence of surface hybridization. Journal of Chemical Physics, 2017, 146, 214701.	1.2	31
3418	Germanium oxidation occurs by diffusion of oxygen network interstitials. Applied Physics Letters, 2017, 110, 222902.	1.5	9
3419	Rhodiumâ€onâ€Palladium Nanocatalysts for Selective Methanation of Carbon Dioxide. ChemNanoMat, 2017, 3, 639-645.	1.5	12

#	Article	IF	Citations
3420	Lowâ€Temperature Direct Catalytic Hydrothermal Conversion of Biomass Cellulose to Light Hydrocarbons over Pt/Zeolite Catalysts. ChemistrySelect, 2017, 2, 6201-6205.	0.7	8
3421	Fabrication and anisotropic electronic property for oriented Li1+â^'Nb1â^'â^'3Ti+4O3 solid solution by slip casting in a high magnetic field. Advanced Powder Technology, 2017, 28, 2373-2379.	2.0	6
3422	Single-component small-molecule white light organic phosphors. Chemical Communications, 2017, 53, 9269-9272.	2.2	55
3423	Toward a reverse hierarchy of halogen bonding between bromine and iodine. Faraday Discussions, 2017, 203, 389-406.	1.6	35
3424	Explorations of new UV nonlinear optical materials in the Na₂CO₃â€"CaCO₃system. Journal of Materials Chemistry C, 2017, 5, 8758-8764.	2.7	25
3425	Stabilizing Cesium Lead Halide Perovskite Lattice through Mn(II) Substitution for Air-Stable Light-Emitting Diodes. Journal of the American Chemical Society, 2017, 139, 11443-11450.	6.6	705
3426	Infrared Peak Splitting from Phonon Localization in Solid Hydrogen. Physical Review Letters, 2017, 118, 145701.	2.9	14
3427	Liquid Exfoliation Few-Layer SnSe Nanosheets with Tunable Band Gap. Journal of Physical Chemistry C, 2017, 121, 17530-17537.	1.5	75
3428	In situ stable crack growth at the micron scale. Nature Communications, 2017, 8, 108.	5.8	51
3429	The activity of lone pair contributing to SHG response in bismuth borates: a combination investigation from experiment and DFT calculation. Physical Chemistry Chemical Physics, 2017, 19, 25270-25276.	1.3	20
3430	Self-interaction free local exchange potentials applied to metallic systems. Journal of Physics Condensed Matter, 2017, 29, 374002.	0.7	4
3431	Pyrrolyl-silicon compounds with different alkyl spacer lengths: Synthesis, electrochemical behavior and binding properties. Synthetic Metals, 2017, 231, 127-136.	2.1	9
3432	Impact sensitivity of crystalline phenyl diazonium salts: A first-principles study of solid-state properties determining the phenomenon. International Journal of Quantum Chemistry, 2017, 117, e25430.	1.0	19
3433	Mechanical, Electronic, and Optical Properties of Î²-B₆O: First-Principles Calculations. Zeitschrift Fur Naturforschung - Section A Journal of Physical Sciences, 2017, 72, 805-810.	0.7	3
3434	Electric field-induced phase transitions and composition-driven nanodomains in rhombohedral-tetragonal potassium-sodium niobate-based ceramics. Acta Materialia, 2017, 140, 79-86.	3.8	36
3435	Faradaic processes beyond Nernst's law: density functional theory assisted modelling of partial electron delocalisation and pseudocapacitance in graphene oxides. Chemical Communications, 2017, 53, 10414-10417.	2.2	26
3436	Computational assignments of lattice vibrations of ice Ic. RSC Advances, 2017, 7, 36801-36806.	1.7	21
3437	Electro-optical properties, decomposition pathways and the hydrostatic pressure-dependent behaviours of a double-cation hydrogen storage material of $$hbox {Al}_{3}hbox {Li}_{4}(hbox) Tj ETQq1 1 0.784314 rgBT /Overloc	3.4	

#	Article	IF	Citations
3438	Rheniumâ€Loaded TiO₂: A Highly Versatile and Chemoselective Catalyst for the Hydrogenation of Carboxylic Acid Derivatives and the Nâ€Methylation of Amines Using H₂ and CO₂. Chemistry - A European Journal, 2017, 23, 14848-14859.	1.7	76
3439	A new polymorph of ciprofloxacin saccharinate: Structural characterization and pharmaceutical profile. Journal of Pharmaceutical and Biomedical Analysis, 2017, 146, 7-14.	1.4	12
3440	First hafnium-based MAX phase in the 312 family, Hf3AlC2: A first-principles study. Journal of Alloys and Compounds, 2017, 727, 616-626.	2.8	95
3441	Computing analysis of lattice vibrations of ice VIII. RSC Advances, 2017, 7, 31789-31794.	1.7	10
3442	High pressure effect on structural, electronic and elastic properties of topological half-Heusler LaPdBi compound. Materials Research Express, 2017, 4, 086511.	0.8	3
3443	Tuning the Electronic and Optical Properties of Monolayers As, Sb, and Bi via Surface Charge Transfer Doping. Journal of Physical Chemistry C, 2017, 121, 19530-19537.	1.5	35
3444	Vibrational spectra of buta-1,3-diene iron tricarbonyl: comparison to surface species. Journal of Lithic Studies, 2017, 3, 119-127.	0.1	2
3445	Ab-initio study of C15-type Laves phase superconductor LaRu2. Cogent Physics, 2017, 4, 1360461.	0.7	2
3446	Computational evaluation of aluminophosphate zeotypes for CO₂/N₂separation. Physical Chemistry Chemical Physics, 2017, 19, 22801-22812.	1.3	13
3447	Increased thermal stability of activated N2 adsorbed on K-promoted Ni{110}. Physical Chemistry Chemical Physics, 2017, 19, 21848-21855.	1.3	3
3448	Elastic properties of CaCO₃high pressure phases from first principles. Chinese Physics B, 2017, 26, 089101.	0.7	15
3449	Avalanche atomic switching in strain engineered Sb₂Te₃â€“GeTe interfacial phase-change memory cells. Nano Futures, 2017, 1, 025003.	1.0	37
3450	Phase transition sequences in tetramethylammonium tetrachlorometallates by X-ray diffraction and spectroscopic measurements. Acta Crystallographica Section B: Structural Science, Crystal Engineering and Materials, 2017, 73, 844-855.	0.5	8
3451	Computational study of dye adsorption onto Brookite TiO2surfaces for the applications in dye sensitized solar cells. Journal of Physics: Conference Series, 2017, 905, 012034.	0.3	2
3452	Predicting Raman Spectra of Condensed Polymer Phases from MD Simulations. Macromolecules, 2017, 50, 9773-9787.	2.2	2
3453	Hydrogen and the Light-Induced Bias Instability Mechanism in Amorphous Oxide Semiconductors. Scientific Reports, 2017, 7, 16858.	1.6	19
3454	A first-principles study of gas molecule adsorption on borophene. AIP Advances, 2017, 7, .	0.6	59
3455	Machine learning unifies the modeling of materials and molecules. Science Advances, 2017, 3, e1701816.	4.7	488

#	Article	IF	Citations
3456	Ab initio model for GaAs_{1â^'}_xN_xchemical beam epitaxy using GaAs(100) surface stability over As₂, H₂, and N₂. Japanese Journal of Applied Physics, 2017, 56, 060306.	0.8	1
3457	Superhard and superconducting B6C. Materials Today Physics, 2017, 3, 76-84.	2.9	13
3458	Effects of Extraframework Species on the Structure-Based Prediction of ³¹P Isotropic Chemical Shifts of Aluminophosphates. Journal of Physical Chemistry C, 2017, 121, 28065-28076.	1.5	12
3459	A Phosphosilicate Compound, NaCa₃PSiO₈: Structure Solution and Luminescence Properties. Inorganic Chemistry, 2017, 56, 15130-15137.	1.9	6
3460	Structural phase transitions of Ga(Mn)N under high pressure. Journal of Physics: Conference Series, 2017, 901, 012030.	0.3	1
3461	Valence Band Engineering of Layered Bismuth Oxyhalides toward Stable Visible-Light Water Splitting: Madelung Site Potential Analysis. Journal of the American Chemical Society, 2017, 139, 18725-18731.	6.6	144
3462	Design and Synthesis of Heteroleptic Iridium(III) Phosphors for Efficient Organic Light-Emitting Devices. Inorganic Chemistry, 2017, 56, 15304-15313.	1.9	20
3463	Changing the gap type of solid state boric acid by heating: a dispersion-corrected density functional study of Iâ±-, Iâ²-, and Iâ³-metaboric acid polymorphs. New Journal of Chemistry, 2017, 41, 15533-15544.	1.4	4
3464	Control of zeolite framework flexibility and pore topology for separation of ethane and ethylene. Science, 2017, 358, 1068-1071.	6.0	304
3465	Unravelling the energy transfer of Er³⁺-self-sensitized upconversion in Er³⁺â€“Yb³⁺â€“Er³⁺clustered core@shell nanoparticles. Nanoscale, 2017, 9, 18490-18497.	2.8	10
3466	Prediction of optically-active transitions in type-VIII guest-free silicon clathrate Si46: A comparative study of its physical properties with type-I counterpart through first-principles. Journal of Applied Physics, 2017, 122, .	1.1	7
3467	Insights into the increased degradation rate of CH₃NH₃PbI₃ solar cells in combined water and O₂ environments. Journal of Materials Chemistry A, 2017, 5, 25469-25475.	5.2	52
3468	Dirac cones in two-dimensional borane. Physical Review B, 2017, 96, .	1.1	17
3469	Robust Hydrogenation of Nitrile and Nitro Groups to Primary Amines Using Ni₂P as a Catalyst and Ammonia Borane under Ambient Conditions. Asian Journal of Organic Chemistry, 2017, 6, 1589-1593.	1.3	22
3470	Chemical Sensitivity of Valence-to-Core X-ray Emission Spectroscopy Due to the Ligand and the Oxidation State: A Computational Study on Cu-SSZ-13 with Multiple H₂O and NH₃ Adsorption. Journal of Physical Chemistry C, 2017, 121, 25759-25767.	1.5	12
3471	Structure and electronic states of a graphene double vacancy with an embedded Si dopant. Journal of Chemical Physics, 2017, 147, 194702.	1.2	9
3472	Structural and Mechanical Properties of TiN-TiC-TiO System: First Principle Study. Communications in Theoretical Physics, 2017, 68, 678.	1.1	6
3473	Open-boundary reflection of quantum well states at Pb(111). Physical Review B, 2017, 96, .	1.1	6

#	Article	IF	Citations
3474	Electronic structural properties of BiOF crystal and its oxygen vacancy from first-principles calculations. Russian Journal of Physical Chemistry A, 2017, 91, 2425-2430.	0.1	3
3475	Titanium-Based Hydrides as Heterogeneous Catalysts for Ammonia Synthesis. Journal of the American Chemical Society, 2017, 139, 18240-18246.	6.6	189
3476	Mechanism of enhancement of ferroelectricity of croconic acid with temperature. Physical Chemistry Chemical Physics, 2017, 19, 32216-32225.	1.3	7
3477	Direct response of the spin-density wave transition and superconductivity to anion height in SrFe2As2. Physical Review B, 2017, 96, .	1.1	2
3478	Applications of Solid-State 43 Ca Nuclear Magnetic Resonance: Superconductors, Glasses, Biomaterials, and NMR Crystallography. Annual Reports on NMR Spectroscopy, 2017, 92, 227-363.	0.7	7
3479	Electronic structure and optical properties of CsI under high pressure: a first-principles study. RSC Advances, 2017, 7, 52449-52455.	1.7	11
3480	Superhard B₂CO phases derived from carbon allotropes. RSC Advances, 2017, 7, 52192-52199.	1.7	12
3481	Stacking Characteristics of Close Packed Materials. Physical Review Letters, 2017, 119, 205701.	2.9	18
3482	In Situ Spectroscopic and Computational Studies on a MnO₂â€“CuO Catalyst for Use in Volatile Organic Compound Decomposition. ACS Omega, 2017, 2, 7424-7432.	1.6	6
3483	Raman and inelastic neutron scattering spectra of (NH4)2SO3, an intermediate for solar hydrogen production. International Journal of Hydrogen Energy, 2017, 42, 30216-30222.	3.8	1
3484	Reaction pathway for partial hydrogenation of 1,3-butadiene over Pt/SiO₂. Catalysis Science and Technology, 2017, 7, 5932-5943.	2.1	16
3485	Nonadiabatic Vibrational Damping of Molecular Adsorbates: Insights into Electronic Friction and the Role of Electronic Coherence. Physical Review Letters, 2017, 119, 176808.	2.9	18
3486	Difference of rate performance between discharge and charge reactions for bismuth fluoride electrode in lithium-ion battery. Journal of Electroanalytical Chemistry, 2017, 806, 82-87.	1.9	22
3487	Coordination Polymerization of Metal Azides and Powerful Nitrogen-Rich Ligand toward Primary Explosives with Excellent Energetic Performances. Chemistry of Materials, 2017, 29, 9725-9733.	3.2	92
3488	Ultrahigh-Field 25Mg NMR and DFT Study of Magnesium Borate Minerals. ACS Earth and Space Chemistry, 2017, 1, 299-309.	1.2	11
3489	Assessment on the structural, elastic and electronic properties of Nb3Ir and Nb3Pt: A first-principles study. AIP Advances, 2017, 7, 065012.	0.6	8
3490	The role of high oxygen vacancy concentration on modification of surface properties and H2S adsorption on the rutile TiO2 (110). Applied Surface Science, 2017, 422, 990-996.	3.1	23
3491	A two-dimensional van der Waals CdS/germanene heterojunction with promising electronic and optoelectronic properties: DFT + NEGF investigations. Physical Chemistry Chemical Physics, 2017, 19, 18330-18337.	1.3	26

#	Article	IF	Citations
3492	Spin-gapless and half-metallic ferromagnetism in potassium and calcium Î´-doped GaN digital magnetic heterostructures for possible spintronic applications: insights from first principles. Applied Physics A: Materials Science and Processing, 2017, 123, 1.	1.1	4
3493	Effects of Transition Metal (TM = V, Cr, Mn, Fe, Co, and Ni) Elements on Magnetic Mechanism of LiZnP with Decoupled Charge and Spin Doping. Journal of Superconductivity and Novel Magnetism, 2017, 30, 2823-2828.	0.8	4
3494	Semimetallic Two-Dimensional TiB₁₂: Improved Stability and Electronic Properties Tunable by Biaxial Strain. Chemistry of Materials, 2017, 29, 5922-5930.	3.2	41
3495	Scalable Mesoporous Platinum Diselenide Nanosheet Synthesis in Water. ACS Omega, 2017, 2, 3325-3332.	1.6	32
3496	Charge transfer doping of graphene without degrading carrier mobility. Journal of Applied Physics, 2017, 121, .	1.1	10
3497	Crystal structures and electronic properties of solid fluorine under high pressure. Chinese Physics B, 2017, 26, 076103.	0.7	21
3498	Adsorption properties of NO molecules on the hexagonal LaCoO₃(0 0 1) surface: a density functional theory study. RSC Advances, 2017, 7, 34714-34721.	1.7	4
3499	Ground state structure of high-energy-density polymeric carbon monoxide. Physical Review B, 2017, 95, .	1.1	22
3500	Thermal conductivities in NaSnAs, NaSnP, and<mml:math xmlns:mml="http://www.w3.org/1998/Math/MathML"><mml:mrow><mml:mi>NaS</mml:mi><mml:msub><mml:mi mathvariant="normal">n</mml:mi><mml:mn>2</mml:mn></mml:msub><mml:mi mathvariant="normal">A</mml:mi><mml:msub><mml:mi mathvariant="normal">s</mml:mi><mml:mn>2</mml:mn></mml:msub></mml:mrow></mml:math>: Effect of double lone-pair electrons. Physical Review B, 2017, 95, .	1.1	29
3501	Pharmaceutical aspects of salt and cocrystal forms of APIs and characterization challenges. Advanced Drug Delivery Reviews, 2017, 117, 86-110.	6.6	218
3502	Contribution to the study of structural and elastic properties of wÃ¼stite under pressure up to 140ÂGPa by pseudopotential calculations. Phase Transitions, 2017, , 1-12.	0.6	0
3503	Local structure of the crystalline and amorphous states of<mml:math xmlns:mml="http://www.w3.org/1998/Math/MathML"><mml:mrow><mml:msub><mml:mi>Ga</mml:mi><mml:mn>2</mml:mn></mml:msub></mml:mrow></mml:math> alloy without resonant bonding: A combined x-ray absorption andab initiostudy. Physical Review B, 2017, 95, .	1.1	14
3504	Pressure Effects on Structure and Optical Properties in Cesium Lead Bromide Perovskite Nanocrystals. Journal of the American Chemical Society, 2017, 139, 10087-10094.	6.6	214
3505	Modeling of amorphous SiCxO6/5 by classical molecular dynamics and first principles calculations. Scientific Reports, 2017, 7, 42705.	1.6	7
3506	Density functional theory study of a new Bi-based (K1.00)(Ba1.00)3(Bi0.89Na0.11)4O12 double perovskite superconductor. Computational Materials Science, 2017, 138, 160-165.	1.4	45
3507	â€œEnergy Selection Channelsâ€•for High-Performance Electrolyte: Anion-Frenkel Defect Pair as Dominant Source for O Ion Conductions in Pyrochlore-type Lanthanide Hafnium Oxides SOFC. Inorganic Chemistry, 2017, 56, 7975-7984.	1.9	25
3508	The Role of Auxiliary Alkali Metal Ions on Scheelite Structure Double Molybdate and Tungstate Phosphors. Inorganic Chemistry, 2017, 56, 8078-8086.	1.9	16
3509	Hidden Oceans? Unraveling the Structure of Hydrous Defects in the Earthâ€™s Deep Interior. Journal of the American Chemical Society, 2017, 139, 10499-10505.	6.6	23

#	Article	IF	Citations
3510	Theoretical study of PbZrTiO3and PbSnZrTiO3using a total-energy planewave-pseudopotential method. Materials Research Express, 2017, 4, 074001.	0.8	3
3511	Manipulating the Bulk Band Structure of Artificially Constructed van der Waals Chalcogenide Heterostructures. ACS Applied Materials & Interfaces, 2017, 9, 23918-23925.	4.0	17
3512	The Plot Thickens: Gelation by Phenylalanine in Water and Dimethyl Sulfoxide. Crystal Growth and Design, 2017, 17, 4100-4109.	1.4	22
3513	Understanding the Unusual Response to High Pressure in KBe2BO3F2. Scientific Reports, 2017, 7, 4027.	1.6	2
3514	Influence of transition metal doping on the electronic and optical properties of ReS₂and ReSe₂monolayers. Physical Chemistry Chemical Physics, 2017, 19, 19050-19057.	1.3	46
3515	Mirrored continuum and molecular scale simulations of the ignition of gamma phase RDX. AIP Conference Proceedings, 2017, , .	0.3	1
3516	Influences of pressure on methyl group, elasticity, sound velocity and sensitivity of solid nitromethane. European Physical Journal B, 2017, 90, 1.	0.6	14
3517	Reducing Pb concentration in Î±-CsPbI3 based perovskite solar cell materials via alkaline-earth metal doping: A DFT computational study. Ceramics International, 2017, 43, 13101-13112.	2.3	28
3518	Elastic, electronic and optical properties of anatase TiO2 under pressure: A DFT approach. Chinese Journal of Physics, 2017, 55, 1252-1263.	2.0	15
3519	Structural, elastic, and vibrational properties of phase H: A first-principles simulation. Chinese Physics B, 2017, 26, 067401.	0.7	5
3520	High-pressure phases of group-II difluorides: Polymorphism and superionicity. Physical Review B, 2017, 95, .	1.1	25
3521	Quantum Monte Carlo study of the energetics of the rutile, anatase, brookite, and columbite<mml:math xmlns:mml="http://www.w3.org/1998/Math/MathML"><mml:msub><mml:mi>TiO</mml:mi><mml:mn>2</mml:mn></mml:msub></m Physical Review B, 2017, 95, .	1.1	43
3522	A first principles investigation of electron transfer between Fe(II) and U(VI) on insulating Al- vs. semiconducting Fe-oxide surfaces via the proximity effect. Geochimica Et Cosmochimica Acta, 2017, 197, 305-322.	1.6	19
3523	Identification of the catalytically active component of Cuâ€“Zrâ€“O catalyst for the hydrogenation of levulinic acid to Î³-valerolactone. Green Chemistry, 2017, 19, 225-236.	4.6	68
3524	A combined NMR crystallographic and PXRD investigation of the structure-directing role of water molecules in orotic acid and its lithium and magnesium salts. CrystEngComm, 2017, 19, 224-236.	1.3	6
3525	Growth, structure, optical and thermal properties of three new organicâ€“inorganic hybrid crystals: (C2H7N4S)3BiCl6Â·H2O, (C2H7N4S)2BiBr5, and (C2H5N4S)2BiI5. Polyhedron, 2017, 127, 478-488.	1.0	13
3526	Fabrication of thin TEM sample of ionic liquid for high-resolution ELNES measurements. Ultramicroscopy, 2017, 178, 81-87.	0.8	19
3527	Surface charge transfer doping induced inversion layer for high-performance graphene/silicon heterojunction solar cells. Journal of Materials Chemistry A, 2017, 5, 285-291.	5.2	52

#	Article	IF	Citations
3528	Surface Hydroxyl OH Defects of Î·-Al₂O₃ and Ï‡-Al₂O₃ by Solid State NMR, XRD, and DFT Calculations. Zeitschrift Fur Physikalische Chemie, 2017, 231, 809-825.	1.4	13
3529	A comparative study of NbAl3 and Nb3Al intermetallic compounds under pressure. Computational Materials Science, 2017, 126, 280-286.	1.4	18
3530	The distribution analysis on the proton siting and the acid strength of the zeolite ferrierite: A computational study. Microporous and Mesoporous Materials, 2017, 239, 354-362.	2.2	11
3531	Pressure induced structural and optical properties of cubic phase SnSe: An investigation for the infrared/mid-infrared optoelectronic devices. Journal of Alloys and Compounds, 2017, 695, 194-201.	2.8	45
3532	Emulating Natural Product Conformation by Cooperative, Nonâ€Covalent Fluorine Interactions. Chemistry - A European Journal, 2017, 23, 6142-6149.	1.7	32
3533	Computational evaluation of sub-nanometer cluster activity of singly exposed copper atom with various coordinative environment in catalytic CO2 transformation. Applied Surface Science, 2017, 396, 444-454.	3.1	4
3534	Superhard orthorhombic phase of B 2 CO compound. Diamond and Related Materials, 2017, 73, 87-92.	1.8	18
3535	Synthetic mimetics of the endogenous gastrointestinal nanomineral: Silent constructs that trap macromolecules for intracellular delivery. Nanomedicine: Nanotechnology, Biology, and Medicine, 2017, 13, 619-630.	1.7	17
3536	A DFT-D Study on Structural, Electronic, Thermodynamic, and Mechanical Properties of HMX/MPNO Cocrystal under High Pressure. Journal of Energetic Materials, 2017, 35, 157-171.	1.0	10
3537	Structural, electronic and magnetic properties of CoFeTiGa1â^'Sb compounds. Journal of Magnetism and Magnetic Materials, 2017, 422, 32-36.	1.0	5
3538	WB2: not a superhard material for strong polarization character of interlayer Wâ€“B bonding. Physical Chemistry Chemical Physics, 2017, 19, 8919-8924.	1.3	28
3539	Experimental and DFT investigation of (Cr,Ti)₃AlC₂ MAX phases stability. Materials Research Letters, 2017, 5, 144-157.	4.1	27
3540	The adsorption and dissociation of water molecule on goethite (010) surface: A DFT approach. Applied Surface Science, 2017, 392, 760-767.	3.1	30
3541	Assignment of the vibrational spectra of the parent polysilsesquioxane (POSS): Octahydridosilasequioxane, H 8 Si 8 O 12. Spectrochimica Acta - Part A: Molecular and Biomolecular Spectroscopy, 2017, 171, 222-228.	2.0	0
3542	A new non-centrosymmetry compound: Synthesis, crystal structure and electronic structure study of hydrated sodium borate Na2[BO2(OH)]Â·H2O. Journal of Molecular Structure, 2017, 1127, 252-256.	1.8	4
3543	Analysis and prediction of mid-IR nonlinear optical metal sulfides with diamond-like structures. Coordination Chemistry Reviews, 2017, 333, 57-70.	9.5	278
3544	Optical properties of epitaxial Na0.5Bi0.5TiO3 lead-free piezoelectric thin films: Ellipsometric and theoretical studies. Applied Surface Science, 2017, 421, 367-372.	3.1	10
3545	Theoretical Aspects of Infrared and Raman Spectroscopies. Developments in Clay Science, 2017, 8, 6-33.	0.3	1

#	Article	IF	Citations
3546	Mechanical, elastic, anisotropy, and electronic properties of monoclinic phase of m -Si _x Ge _{3â^' x} N ₄. Chinese Physics B, 2017, 26, 126105.	0.7	3
3547	Potentiality of Density-Functional Theory in Analyzing the Devices Containing Graphene-Crystalline Solid Interfaces: A Review. IEEE Transactions on Electron Devices, 2017, 64, 4738-4745.	1.6	8
3549	Crystallographic and optical properties and band diagrams of CuGaS₂and CuGa₅S₈phases in Cu-poor Cu₂Sâ€“Ga₂S₃pseudo-binary system. Japanese Journal of Applied Physics, 2017, 56, 04CS12.	0.8	15
3550	Revealing Local Dynamics of the Protonic Conductor CsH(PO₃H) by Solid-State NMR Spectroscopy and First-Principles Calculations. Journal of Physical Chemistry C, 2017, 121, 27830-27838.	1.5	6
3551	Visualising crystal packing interactions in solid-state NMR: Concepts and applications. Journal of Chemical Physics, 2017, 147, 144203.	1.2	19
3552	Implications of X-ray thermal diffuse scattering in integrated Bragg intensities of silicon and cubic boron nitride. Journal of Applied Crystallography, 2017, 50, 1791-1799.	1.9	6
3553	Face Dependence of Schottky Barriers Heights of Silicides and Germanides on Si and Ge. Scientific Reports, 2017, 7, 16669.	1.6	14
3554	Simulation of crystal and electronic structures of octahedral molybdenum cluster complex compound Cs₂[Mo₆Cl₁₄] using various DFT functionals. Journal of the Ceramic Society of Japan, 2017, 125, 753-759.	0.5	5
3555	First-principles study on electronic and optical characteristics of zinc vanadate photocatalyst. , 2017, , .		0
3556	Enhanced Framework Rigidity of a Zeolitic Metal-Azolate via Ligand Substitution. Crystals, 2017, 7, 99.	1.0	11
3557	Deformation Modes and Anisotropy of Anti-Perovskite Ti3AN (A = Al, In and Tl) from First-Principle Calculations. Materials, 2017, 10, 362.	1.3	9
3558	A Novel Silicon Allotrope in the Monoclinic Phase. Materials, 2017, 10, 441.	1.3	14
3559	Theoretical Investigations of Si-Ge Alloys in P42/ncm Phase: First-Principles Calculations. Materials, 2017, 10, 599.	1.3	14
3560	Mechanical, Anisotropic, and Electronic Properties of XN (X = C, Si, Ge): Theoretical Investigations. Materials, 2017, 10, 912.	1.3	3
3561	New Half-Metallic Materials: FeRuCrP and FeRhCrP Quaternary Heusler Compounds. Materials, 2017, 10, 1367.	1.3	17
3562	Li-Decorated Î²12-Borophene as Potential Candidates for Hydrogen Storage: A First-Principle Study. Materials, 2017, 10, 1399.	1.3	21
3563	Two B-C-O Compounds: Structural, Mechanical Anisotropy and Electronic Properties under Pressure. Materials, 2017, 10, 1413.	1.3	23
3564	First-Principles Investigation of Structural, Electronic and Elastic Properties of HfX (X = Os, Ir and Pt) Compounds. Metals, 2017, 7, 317.	1.0	11

#	Article	IF	Citations
3565	Na-Montmorillonite Edge Structure and Surface Complexes: An Atomistic Perspective. Minerals (Basel,) Tj ETQq0 0 0 rgBT /Overlock 10 T	0.8	17
3566	Hydrogen Atomic Positions of Oâ€“HÂ·Â·Â·O Hydrogen Bonds in Solution and in the Solid State: The Synergy of Quantum Chemical Calculations with 1H-NMR Chemical Shifts and X-ray Diffraction Methods. Molecules, 2017, 22, 415.	1.7	51
3567	New Insights into Solid Form Stability and Hydrate Formation: o-Phenanthroline HCl and Neocuproine HCl. Molecules, 2017, 22, 2238.	1.7	8
3568	Pnma-BN: Another Boron Nitride Polymorph with Interesting Physical Properties. Nanomaterials, 2017, 7, 3.	1.9	41
3569	Corrosion Study of Mild Steel in Aqueous Sulfuric Acid Solution Using 4-Methyl-4H-1,2,4-Triazole-3-Thiol and 2-Mercaptonicotinic Acidâ€”An Experimental and Theoretical Study. Frontiers in Chemistry, 2017, 5, 61.	1.8	61
3570	Theoretical Prediction of Electronic Structures and Phonon Dispersion of Ce2XN2 (X = S, Se, and Te) Ternary. Computation, 2017, 5, 29.	1.0	2
3571	Enhanced Manifold of States Achieved in Heterostructures of Iron Selenide and Boron-Doped Graphene. Condensed Matter, 2017, 2, 34.	0.8	2
3572	Interior Melting of the C3B16 and C2B14â¯ Clusters Between 1000 K and 2000 K. Condensed Matter, 2017, 2, 35.	0.8	1
3573	Synthesis, Crystal Structure and Nonlinear Optical Property of RbHgI3. Crystals, 2017, 7, 148.	1.0	10
3574	A Multiscale Simulation Method and Its Application to Determine the Mechanical Behavior of Heterogeneous Geomaterials. Advances in Materials Science and Engineering, 2017, 2017, 1-12.	1.0	2
3575	First-Principles Study of Properties of Alpha Uranium Crystal and Seven Alpha Uranium Surfaces. Journal of Chemistry, 2017, 2017, 1-7.	0.9	6
3576	The Effect of Impurities in Nickel Grain Boundary: Density Functional Theory Study. , 2017, , .		1
3577	Local structure and stacking disorder of chloro(phthalocyaninato)aluminium. Acta Crystallographica Section B: Structural Science, Crystal Engineering and Materials, 2017, 73, 744-755.	0.5	3
3578	On the stacking disorder of DL-norleucine. Acta Crystallographica Section B: Structural Science, Crystal Engineering and Materials, 2017, 73, 1075-1084.	0.5	6
3579	Compare investigation of lithiation, sodiation, and magnesiation ion adsorptions and diffusions on monolayer MoS<inf>2</inf> for energy storages using first-principles. , 2017, , .		0
3580	Clustering and spin interactions in Fe-doped diamond. Journal of Physics: Conference Series, 2017, 905, 012033.	0.3	3
3581	Structure and Optical Properties of K0.67Rb1.33Al2B2O7 Crystal. Crystals, 2017, 7, 104.	1.0	3
3582	Atomic Quantum Dynamics in Materials Research. Experimental Methods in the Physical Sciences, 2017, , 403-457.	0.1	27

#	Article	IF	Citations
3584	New tetrahedral polymorphs of the group-14 elements. Journal of Physics: Conference Series, 2017, 950, 042010.	0.3	0
3586	The Mechanism of Skutterudite Acid Leaching: A DFT Study of H⁺ Effect on CoO (010) Surface. Solid State Phenomena, 0, 262, 408-412.	0.3	1
3587	Supported Ga-oxide Catalyst for Dehydrogenation of Ethane. Journal of the Japan Petroleum Institute, 2017, 60, 203-210.	0.4	9
3588	Structure, thermal expansion and incompressibility of MgSO₄Â·9H₂O, its relationship to meridianiite (MgSO₄Â·11H₂O) and possible natural occurrences. Acta Crystallographica Section B: Structural Science, Crystal Engineering and Materials, 2017, 73, 47-64.	0.5	19
3589	Two-site jumps in dimethyl sulfone studied by one- and two-dimensional 17O NMR spectroscopy. Journal of Magnetic Resonance, 2018, 288, 84-94.	1.2	16
3590	Influence of Relativistic Effects on the Contact Formation of Transition Metals. Physical Review Letters, 2018, 120, 076802.	2.9	15
3591	A first-principles prediction on the â€œhealing effectâ€•of graphene preventing carrier trapping near the surface of metal halide perovskites. Chemical Science, 2018, 9, 3341-3353.	3.7	19
3592	The electronic and optical properties of a narrow-band red-emitting nanophosphor K₂NaGaF₆:Mn⁴⁺for warm white light-emitting diodes. Journal of Materials Chemistry C, 2018, 6, 3016-3025.	2.7	78
3593	Enhanced magnetoelectric effect in M-type hexaferrites by Co substitution into trigonal bi-pyramidal sites. Applied Physics Letters, 2018, 112, 082401.	1.5	20
3594	Effect of Element Substitution on Structural Transformation and Optical Performances in I₂BaM^{IV}Q₄ (I = Li, Na, Cu, and Ag; M^{IV} =) Tj ETQq1 1 0.784314 rgBT	2.1	46
3595	Mechanochemical Synthesis of Methylammonium Lead Mixedâ€“Halide Perovskites: Unraveling the Solid-Solution Behavior Using Solid-State NMR. Chemistry of Materials, 2018, 30, 2309-2321.	3.2	85
3596	Electrical Conductivity of Copper Hexamers Tuned by their Ground-State Valences. Inorganic Chemistry, 2018, 57, 3443-3450.	1.9	10
3597	Inspecting the Structure and Formation of Molecular Sieve SAPO-34 via ¹⁷O Solid-State NMR Spectroscopy. Journal of Physical Chemistry C, 2018, 122, 7260-7277.	1.5	8
3598	Elastic and thermodynamic properties of zirconium- and hafnium-doped $$hbox {Rh}_{3}hbox {V}$$ Rh 3 V intermetallic compounds: potential aerospace material. Bulletin of Materials Science, 2018, 41, 1.	0.8	10
3599	Pushing Nonlinear Optical Oxides into the Mid-Infrared Spectral Region Beyond 10 Î¼m: Design, Synthesis, and Characterization of La₃SnGa₅O₁₄. Journal of the American Chemical Society, 2018, 140, 4684-4690.	6.6	117
3600	First-principles momentum distributions and vibrationally corrected permittivities of hexagonal and cubic ice. Physical Review B, 2018, 97, .	1.1	3
3601	P21/c-C2/c phase transition and mixing properties of the (Li,Na)FeGe2O6 solid solution: A calorimetric and thermodynamic study. Journal of Chemical Thermodynamics, 2018, 120, 123-140.	1.0	6
3602	K 3 B 6 O 9 F 3 : A New Fluorooxoborate with Four Different Anionic Units. Chemistry - A European Journal, 2018, 24, 4497-4502.	1.7	38

#	Article	IF	Citations
3603	Temperature dependent optical properties of red emitting Na₃GaF₆:Mn⁴⁺as a color converter for warm white LEDs. Zeitschrift Fur Kristallographie - Crystalline Materials, 2018, 233, 489-499.	0.4	6
3604	Thermodynamic Properties of Uranyl-Containing Materials Based on Density Functional Theory. Journal of Physical Chemistry C, 2018, 122, 5254-5267.	1.5	32
3605	A beryllium-free deep-UV nonlinear optical material CsNaMgP₂O₇with honeycomb-like topological layers. Journal of Materials Chemistry C, 2018, 6, 3910-3916.	2.7	48
3606	Experimental and Theoretical Investigation of Structures, Stoichiometric Diversity, and Bench Stability of Cocrystals with a Volatile Halogen Bond Donor. Crystal Growth and Design, 2018, 18, 2387-2396.	1.4	19
3607	Studying the properties of a predicted tetragonal silicon by first principles. Materials Research Express, 2018, 5, 035910.	0.8	1
3608	Novel 2D Layered Molybdenum Ditelluride Encapsulated in Fewâ€Łayer Graphene as Highâ€Performance Anode for Lithiumâ€Ion Batteries. Small, 2018, 14, e1703680.	5.2	52
3609	Dissociation reaction of the 1/3$$ leftlangle {ar{1}101} ightangle $$ edge dislocation in Î±-Al2O3. Journal of Materials Science, 2018, 53, 8049-8058.	1.7	4
3610	Water Confined in Nanocapillaries: Two-Dimensional Bilayer Squarelike Ice and Associated Solidâ€“Liquidâ€“Solid Transition. Journal of Physical Chemistry C, 2018, 122, 6704-6712.	1.5	27
3611	Elucidating an Amorphous Form Stabilization Mechanism for Tenapanor Hydrochloride: Crystal Structure Analysis Using X-ray Diffraction, NMR Crystallography, and Molecular Modeling. Molecular Pharmaceutics, 2018, 15, 1476-1487.	2.3	32
3612	Computational evaluation of metal pentazolate frameworks: inorganic analogues of azolate metalâ€“organic frameworks. Chemical Science, 2018, 9, 3367-3375.	3.7	39
3613	Atomistic Insight into the Correlation among Oxygen Vacancies, Protonic Defects, and the Acceptor Dopants in Sc-Doped BaZrO₃ Using First-Principles Calculations. Journal of Physical Chemistry C, 2018, 122, 6501-6507.	1.5	24
3614	Large-scale controlled synthesis of porous two-dimensional nanosheets for the hydrogen evolution reaction through a chemical pathway. Nanoscale, 2018, 10, 6168-6176.	2.8	23
3615	Magnetic and electronic properties of single-walled Mo₂C nanotube: a first-principles study. Journal of Physics Condensed Matter, 2018, 30, 155305.	0.7	6
3616	Structural complexity and wide application of two-dimensional S/O type antimonene. Applied Surface Science, 2018, 441, 77-84.	3.1	34
3617	Superficial-defect engineered nickel/iron oxide nanocrystals enable high-efficient flexible fiber battery. Energy Storage Materials, 2018, 13, 160-167.	9.5	48
3618	Thermodynamic investigation of phase equilibria in Alâ€“Siâ€“V system. Journal of Materials Science and Technology, 2018, 34, 1592-1601.	5.6	7
3619	Optically active derivatives of terephthalic acid: four crystal structures from two powder patterns. Acta Crystallographica Section C, Structural Chemistry, 2018, 74, 248-255.	0.2	7
3620	Beryllium-Free Nonlinear Optical Crystals A₃Ba₃Li₂Ga₄B₆O₂₀F (A = K) Tj ETQq1 1 0.784314 rgBT Strong Covalent Connection between the _{âˆž}²[Li₂Ga₄B₆O₂₀F]^{9â€“} Double Layers. Inorganic Chemistry, 2018, 57, 5669-5676.	1.9	23

#	Article	IF	Citations
3621	Design of Boron Doped C2N-C3N Coplanar Conjugated Heterostructure for Efficient HER Electrocatalysis. Scientific Reports, 2018, 8, 5661.	1.6	21
3622	Study of the structural, vibrational and thermodynamic properties of natroxalate mineral using density functional theory. Journal of Solid State Chemistry, 2018, 263, 131-140.	1.4	23
3623	Computational prediction of muon stopping sites using ab initio random structure searching (AIRSS). Journal of Chemical Physics, 2018, 148, 134114.	1.2	16
3624	Effect of thermal history on highâ€valence chromium ion dissolution in merwinite (3CaOÂ·MgOÂ·2SiO₂). Journal of the American Ceramic Society, 2018, 101, 2653-2665.	1.9	4
3625	Density Functional Theory Modeling of Solid-State Nuclear Magnetic Resonances for Polycyclic Aromatic Hydrocarbons. Journal of Physical Chemistry C, 2018, 122, 11008-11014.	1.5	0
3626	Stability and Pressure Dependent Properties of Ternary Lithium Borides of Gold and Silver. Physica Status Solidi (B): Basic Research, 2018, 255, 1700666.	0.7	0
3627	First-principles calculation of the optoelectronic properties of doped methylammonium lead halide perovskites: A DFT-based study. Computational Materials Science, 2018, 150, 439-447.	1.4	16
3628	AbINS: The modern software for INS interpretation. Physica B: Condensed Matter, 2018, 551, 443-448.	1.3	51
3629	A first-principles study of hydrogen storage capacity based on Liâ€“Na-decorated silicene. Physical Chemistry Chemical Physics, 2018, 20, 13903-13908.	1.3	19
3630	Spatially resolved proton momentum distributions in KDP from first-principles. Journal of Chemical Physics, 2018, 148, 144708.	1.2	3
3631	Magnesium doped Gallium Phosphonates Ga_{1â€“x}Mg_x[H_{3+x}(O₃PCH₂)₃N] (x = 0, 0.20) and the Influence on Proton Conductivity. Zeitschrift Fur Anorganische Und Allgemeine Chemie, 2018, 644, 86-91.	0.6	4
3632	A cation size effect on the framework structures in ABi₂SeO₃F₅ (A = K and Rb): first examples of alkali metal bismuth selenite fluorides. Dalton Transactions, 2018, 47, 6598-6604.	1.6	12
3633	Direct transition of a HfGeTe₄ ternary transition-metal chalcogenide monolayer with a zigzag van der Waals gap. APL Materials, 2018, 6, 046104.	2.2	17
3634	Pressure-induced changes of the structure and properties of monoclinic Î± -chalcocite Cu2S. Physical Review B, 2018, 97, .	1.1	9
3635	A new disodium hafnium borate Na2Hf(BO3)2: synthesis, crystal structure, DFT calculations and luminescent properties. Zeitschrift Fur Kristallographie - Crystalline Materials, 2018, 233, 753-760.	0.4	1
3636	ZnV2O4: A potential anode material for sodium-ion batteries. Journal of the Taiwan Institute of Chemical Engineers, 2018, 88, 161-168.	2.7	25
3637	Stabilization Mechanism of the Tetragonal Structure in a Hydrothermally Synthesized BaTiO₃ Nanocrystal. Inorganic Chemistry, 2018, 57, 5413-5419.	1.9	28
3638	CaB₅O₇F₃: A Beryllium-Free Alkaline-Earth Fluorooxoborate Exhibiting Excellent Nonlinear Optical Performances. Inorganic Chemistry, 2018, 57, 4820-4823.	1.9	136

#	Article	IF	Citations
3639	Ba₂ZnSc(BO₃)₃and Ba₄Zn₅Sc₂(BO₃)₈: first examples of borates in the Znâ€“Scâ€“Bâ€“O system featuring special structure configurations. Inorganic Chemistry Frontiers, 2018, 5, 1787-1794.	3.0	12
3640	How the H-Bond Layout Determines Mechanical Properties of Crystalline Amino Acid Hydrogen Maleates. Crystal Growth and Design, 2018, 18, 3366-3375.	1.4	19
3641	Chemical Bonding and Transport Properties in Clathrates-I with Cuâ€“Znâ€“P Frameworks. Chemistry of Materials, 2018, 30, 3419-3428.	3.2	21
3642	Surface Instability of Sn-Based Hybrid Perovskite Thin Film, CH₃NH₃SnI₃: The Origin of Its Material Instability. Journal of Physical Chemistry Letters, 2018, 9, 2293-2297.	2.1	45
3643	Local Environment Sensitivity of the Cu K-Edge XANES Features in Cu-SSZ-13: Analysis from First-Principles. Journal of Physical Chemistry Letters, 2018, 9, 3035-3042.	2.1	34
3644	Synthesis, crystal structure and optical properties of a new fluorocarbonate with an interesting sandwich-like structure. Dalton Transactions, 2018, 47, 6464-6469.	1.6	4
3645	Effect of strain on the intrinsic stacking fault energy of fcc Co: a first-principles study. Journal of Materials Science, 2018, 53, 10217-10230.	1.7	9
3646	Density Functional Theory Calculations of the Quantum Capacitance of Graphene Oxide as a Supercapacitor Electrode. ChemPhysChem, 2018, 19, 1579-1583.	1.0	50
3647	Quantum mechanical tunneling in the automerization of cyclobutadiene. Journal of Chemical Physics, 2018, 148, 104109.	1.2	5
3648	Structural Stability, Electronic, and Optical Properties of BiVO₄ With Oxygen Vacancy Under Pressure. Physica Status Solidi (B): Basic Research, 2018, 255, 1700653.	0.7	8
3649	Study of structural, elastic, electronic, mechanical, optical and thermodynamic properties of NdPb 3 intermetallic compound: DFT based calculations. Computational Condensed Matter, 2018, 15, 42-47.	0.9	24
3650	Implications of bond disorder in a S=1 kagome lattice. Scientific Reports, 2018, 8, 4745.	1.6	5
3651	Quantum diffusion of H/D on Ni(111)â€"A partially adiabatic centroid MD study. Journal of Chemical Physics, 2018, 148, 102339.	1.2	4
3652	Observation of direct evolution from antiferromagnetism to superconductivity in Cu1â^'xLixFeAs () Tj ETQq1 1 0.784314 rgBT /Overlo	1.1	3
3653	Raman scattering and phase transitions in <scp>(NH₄)₃TiF₇</scp>. Journal of Raman Spectroscopy, 2018, 49, 1230-1235.	1.2	3
3654	Structural prediction of host-guest structure in lithium at high pressure. Scientific Reports, 2018, 8, 5278.	1.6	21
3655	Gaussian approximation potential modeling of lithium intercalation in carbon nanostructures. Journal of Chemical Physics, 2018, 148, 241714.	1.2	71
3656	First-principles investigations on structural, elastic and mechanical properties of BNxAs1â^'x ternary alloys. International Journal of Modern Physics B, 2018, 32, 1850152.	1.0	1

#	Article	IF	Citations
3657	Low-energy 3D sp²carbons with versatile properties beyond graphite and graphene. Dalton Transactions, 2018, 47, 6233-6239.	1.6	7
3658	Quantum Confinement and Surface Effects on the Itinerant Ferromagnetism in Ni and Niâ€“Fe Nanowire Arrays: An Ab Initio Study. Physica Status Solidi (B): Basic Research, 2018, 255, 1700618.	0.7	3
3659	Na₆Zn₃MIII2Q₉ (M^{III} = Ga, In; Q = S, Se): four new supertetrahedron-layered chalcogenides with unprecedented vertex-sharing T₃-clusters and desirable photoluminescence performances. Inorganic Chemistry Frontiers, 2018, 5, 1415-1422.	3.0	26
3660	First-principles calculations of crystal structure, electronic structure and optical properties of Ba2RETaO6 (REâ€‰=â€‰Y, La, Pr, Sm, Gd). Journal of Materials Science, 2018, 53, 9401-9410.	1.7	10
3661	Improving Confidence in Crystal Structure Solutions Using NMR Crystallography: The Case of Î²-Piroxicam. Crystal Growth and Design, 2018, 18, 3339-3351.	1.4	34
3662	Excitation and characterization of image potential state electrons on quasi-free-standing graphene. Physical Review B, 2018, 97, .	1.1	7
3663	Data-Driven Learning of Total and Local Energies in Elemental Boron. Physical Review Letters, 2018, 120, 156001.	2.9	150
3664	A Multifaceted Study of Methane Adsorption in Metalâ€“Organic Frameworks by Using Three Complementary Techniques. Chemistry - A European Journal, 2018, 24, 7866-7881.	1.7	29
3665	Pressure-Tailored Band Gap Engineering and Structure Evolution of Cubic Cesium Lead Iodide Perovskite Nanocrystals. Journal of Physical Chemistry C, 2018, 122, 9332-9338.	1.5	67
3667	Data-driven learning and prediction of inorganic crystal structures. Faraday Discussions, 2018, 211, 45-59.	1.6	66
3668	Strong coupling superconductivity in a quasiperiodic host-guest structure. Science Advances, 2018, 4, eaao4793.	4.7	24
3669	Molecular Dynamics Study of Hydrophilic Sphalerite (110) Surface as Modified by Normal and Branched Butylthiols. Langmuir, 2018, 34, 3363-3373.	1.6	16
3670	The High-Pressure Superconducting Phase of Arsenic. Scientific Reports, 2018, 8, 3026.	1.6	16
3671	Pb₂BO₃Br: a novel nonlinear optical lead borate bromine with a KBBF-type structure exhibiting strong nonlinear optical response. Inorganic Chemistry Frontiers, 2018, 5, 916-921.	3.0	90
3672	¹⁷O solid-state NMR spectroscopy of A₂B₂O₇oxides: quantitative isotopic enrichment and spectral acquisition?. RSC Advances, 2018, 8, 7089-7101.	1.7	13
3673	Stochastic sampling of quadrature grids for the evaluation of vibrational expectation values. Physical Review B, 2018, 97, .	1.1	1
3674	DL_MG: A Parallel Multigrid Poisson and Poissonâ€“Boltzmann Solver for Electronic Structure Calculations in Vacuum and Solution. Journal of Chemical Theory and Computation, 2018, 14, 1412-1432.	2.3	31
3675	First-principles calculations of lattice dynamics and thermodynamic properties for Yb14MnSb11. Journal of Applied Physics, 2018, 123, .	1.1	10

#	Article	IF	Citations
3676	Ab initio Eliashberg Theory: Making Genuine Predictions of Superconducting Features. Journal of the Physical Society of Japan, 2018, 87, 041012.	0.7	72
3677	Structure and electronic properties of deformed single-walled carbon nanotubes: quantum calculations. Structural Chemistry, 2018, 29, 39-47.	1.0	2
3678	Diffusion mechanism in the sodium-ion battery material sodium cobaltate. Scientific Reports, 2018, 8, 3210.	1.6	31
3679	Structural, electronic, and mechanical properties of cubic TiO₂: A first-principles study. Chinese Physics B, 2018, 27, 017102.	0.7	11
3680	GaAs monolayer: Excellent SHG responses and semi metallic to metallic transition modulated by vacancy effect. Applied Surface Science, 2018, 441, 401-407.	3.1	11
3681	Experimental and Theoretical Insights into the Structure of Tellurium Chloride Glasses. Inorganic Chemistry, 2018, 57, 2517-2528.	1.9	4
3682	Three alkaline-rare earth cations carbonates with large birefringence in the deep UV range. Journal of Alloys and Compounds, 2018, 742, 587-593.	2.8	11
3683	Recently synthesized (Zr1-xTix)2AlC (0â€¯â‰¤â€¯xâ€¯â‰¤â€¯1) solid solutions: Theoretical study of the effects of M mixing on physical properties. Journal of Alloys and Compounds, 2018, 743, 146-154.	2.8	69
3684	Solid state NMR and XPS of ternary fluorido-zirconates of various coordination modes. Journal of Fluorine Chemistry, 2018, 208, 24-35.	0.9	24
3685	Experimental and computational investigations of LaNi 5-x Al x (xâ€¯=â€¯0, 0.25, 0.5, 0.75 and 1.0) tritium-storage alloys. Journal of Materials Science and Technology, 2018, 34, 1699-1712.	5.6	22
3686	Facile and Efficient Decontamination of Thorium from Rare Earths Based on Selective Selenite Crystallization. Inorganic Chemistry, 2018, 57, 1880-1887.	1.9	32
3687	Theoretical Evaluation on Terahertz Source Generators from Ternary Metal Chalcogenides of PbM₆Te₁₀ (M = Ga, In). Journal of Physical Chemistry C, 2018, 122, 4557-4564.	1.5	21
3688	Structural, vibrational, and electrical properties of <mml:math xmlns:mml="http://www.w3.org/1998/Math/MathML"><mml:mrow><mml:mn>1</mml:mn><mml:mi>T</mml:mi><mml:mtext>â^'</mml:mtext><mml:msub><mml:mi mathvariant="normal">e</mml:mi><mml:mn>2</mml:mn></mml:msub></mml:mrow></mml:math> under hydrostatic pressure: Experiments and theory. Physical Review B, 2018, 97, .	1.1	63
3689	Does the choice of the crystal structure influence the results of the periodic DFT calculations? A case of glycine alpha polymorph GIPAW NMR parameters computations. Journal of Computational Chemistry, 2018, 39, 853-861.	1.5	14
3690	Different copper species as active sites for NH3-SCR reaction over Cu-SAPO-34 catalyst and reaction pathways: A periodic DFT study. Microporous and Mesoporous Materials, 2018, 266, 223-231.	2.2	35
3691	Surface sensitization mechanism on negative electron affinity p-GaN nanowires. Superlattices and Microstructures, 2018, 115, 140-153.	1.4	11
3692	Synthesis, crystal structure and characterizations of a new diphosphate Rb2CaP2O7. Journal of Alloys and Compounds, 2018, 744, 370-374.	2.8	13
3693	Strain effects on the modulation of band gap and optical properties of direct band gap silicon. Materials Research Bulletin, 2018, 102, 1-7.	2.7	3

#	Article	IF	Citations
3694	LiNa₄B₁₅O₂₅: Featuring Unprecedented B₁₅O₃₀ Fundamental Building Block and Deep-UV Cutoff Edge. Inorganic Chemistry, 2018, 57, 2876-2882.	1.9	16
3695	Theoretical aspects in structural distortion and the electronic properties of lithium peroxide under high pressure. Physical Chemistry Chemical Physics, 2018, 20, 9488-9497.	1.3	4
3696	Design and synthesis of a nonlinear optical material BaAl₄S₇with a wide band gap inspired from SrB₄O₇. Journal of Materials Chemistry C, 2018, 6, 2684-2689.	2.7	51
3697	Characterization of Pharmaceutical Cocrystals and Salts by Dynamic Nuclear Polarization-Enhanced Solid-State NMR Spectroscopy. Crystal Growth and Design, 2018, 18, 2588-2601.	1.4	54
3698	Seâ€“C Cleavage of Hexane Selenol at Steps on Au(111). Langmuir, 2018, 34, 2630-2636.	1.6	2
3699	Structural, electronic, vibration and elastic properties of the layered AgInP₂S₆semiconducting crystal â€“ DFT approach. RSC Advances, 2018, 8, 6965-6977.	1.7	20
3700	Proton distribution in Sc-doped BaZrO₃: a solid state NMR and first principle calculations analysis. Physical Chemistry Chemical Physics, 2018, 20, 4317-4328.	1.3	21
3701	ZnO Functionalization: Metalâ€“Dithiol Superstructures on ZnO(0001) by Self-Assembly. Journal of Physical Chemistry C, 2018, 122, 2880-2889.	1.5	10
3702	LiCs₂La(BO₃)₂ and Li₃K₉La₃(BO₃)₇: new mixed alkali metal lanthanum borates with three-dimensional open frameworks and short cut-off edges. Dalton Transactions, 2018, 47, 3512-3520.	1.6	6
3703	Melilite-Type Oxide SrGdGa₃O₇: Bulk Crystal Growth and Theoretical Studies upon Both Chemical Bonding Theory of Single Crystal Growth and DFT Methods. Crystal Growth and Design, 2018, 18, 1598-1604.	1.4	9
3704	Completely flat 2D Zn3O2 monolayer with triangle and pentangle coordinated networks. Journal of Physics Condensed Matter, 2018, 30, 095301.	0.7	1
3705	First-principles Study of Mechanical and Electronic Properties of Co-Sn Intermetallics for Lithium Ion Battery Anode. Chemical Research in Chinese Universities, 2018, 34, 235-240.	1.3	14
3706	Effects of Biaxial Strains and High Pressure on the Structural, Electronic, and Vibrational Properties of DCâ€HgM₂Te₄ (Mâ€‰=â€‰Al, In). Physica Status Solidi (B): Basic Research, 2018, 255, 1700574.	1.5	3
3707	Different Atomic Terminations Affect the Photocatalytic Nitrogen Fixation of Bismuth Oxybromide: A First Principles Study. Chemistry - an Asian Journal, 2018, 13, 799-808.	1.7	21
3708	A Joint Strategy To Evaluate the Microscopic Origin of the Second-Harmonic-Generation Response in Nonpolar ABCO₃F Compounds. Inorganic Chemistry, 2018, 57, 1251-1258.	1.9	29
3709	Functional Materials Design via Structural Regulation Originated from Ions Introduction: A Study Case in Cesium Iodate System. Chemistry of Materials, 2018, 30, 1136-1145.	3.2	72
3710	Non-Centrosymmetric RbNaMgP₂O₇ with Unprecedented Thermo-Induced Enhancement of Second Harmonic Generation. Journal of the American Chemical Society, 2018, 140, 1592-1595.	6.6	200
3711	Exfoliation of Layered Na-Ion Anode Material Na₂Ti₃O₇ for Enhanced Capacity and Cyclability. Chemistry of Materials, 2018, 30, 1505-1516.	3.2	63

#	Article	IF	Citations
3712	Unique Zigzag-Shaped Buckling Zn₂C Monolayer with Strain-Tunable Band Gap and Negative Poisson Ratio. Inorganic Chemistry, 2018, 57, 1958-1963.	1.9	22
3713	In Situ Salt Formation during Melt Extrusion for Improved Chemical Stability and Dissolution Performance of a Meloxicamâ€“Copovidone Amorphous Solid Dispersion. Molecular Pharmaceutics, 2018, 15, 1226-1237.	2.3	20
3714	Room temperature solid state dual-ion batteries based on gel electrolytes. Journal of Materials Chemistry A, 2018, 6, 4313-4323.	5.2	40
3715	Band edge states, intrinsic defects, and dopants in monolayer HfS2 and SnS2. Applied Physics Letters, 2018, 112, .	1.5	22
3716	A new soluble and bioactive polymorph of praziquantel. European Journal of Pharmaceutics and Biopharmaceutics, 2018, 127, 19-28.	2.0	45
3717	Visible-Light-Responsive SillÃ©n-Structured Mixed-Cationic CdBiO₂Br Nanosheets: Layer Structure Design Promoting Charge Separation and Oxygen Activation Reactions. Journal of Physical Chemistry C, 2018, 122, 2661-2672.	1.5	60
3718	Rotator side chains trigger cooperative transition for shape and function memory effect in organic semiconductors. Nature Communications, 2018, 9, 278.	5.8	90
3719	Structural, elastic, electronic, optical and thermoelectric properties of the Zintl-phase Ae₃AlAs₃ (Ae = Sr, Ba). Philosophical Magazine, 2018, 98, 1217-1240.	0.7	17
3720	First-principles study of defect formation in a photovoltaic semiconductor Cu₂ZnGeSe₄. Japanese Journal of Applied Physics, 2018, 57, 02CE06.	0.8	5
3721	Combined Approach for the Structural Characterization of Alkali Fluoroscandates: Solid-State NMR, Powder X-ray Diffraction, and Density Functional Theory Calculations. Inorganic Chemistry, 2018, 57, 1184-1195.	1.9	14
3722	Tailored fabrication of a prospective acoustoâ€“optic crystal TiTe₃O₈endowed with high performance. Journal of Materials Chemistry C, 2018, 6, 2443-2451.	2.7	18
3723	Formation of<mml:math xmlns:mml="http://www.w3.org/1998/Math/MathML"><mml:msub><mml:mi mathvariant="normal">H</mml:mi><mml:mn>2</mml:mn></mml:msub></mml:math>-rich iodine-hydrogen compounds at high pressure. Physical Review B, 2018, 97, .	1.1	15
3724	Gas Adsorption and Urea Formation Using Magnetically Induced Environment. Green Energy and Technology, 2018, , 23-60.	0.4	0
3725	Engineering an N-doped TiO₂@N-doped C butterfly-like nanostructure with long-lived photo-generated carriers for efficient photocatalytic selective amine oxidation. Journal of Materials Chemistry A, 2018, 6, 2091-2099.	5.2	67
3726	Theoretical and experimental studies of Ba₂SmTaO₆on crystal structure, electronic structure and optical properties. Journal of Materials Chemistry C, 2018, 6, 1806-1814.	2.7	10
3727	C2x: A tool for visualisation and input preparation for Castep and other electronic structure codes. Computer Physics Communications, 2018, 225, 174-179.	3.0	45
3728	Manifestations of structural phase transition in ab initio molecular dynamics of (C3N2H5)2SbF5 crystal. Materials Chemistry and Physics, 2018, 205, 452-461.	2.0	1
3729	Theoretical investigation of the structural, elastic, electronic and optical properties of the ternary indium sulfide layered structures A InS 2 (A Â= K, Rb and Cs). Solid State Sciences, 2018, 76, 74-84.	1.5	12

#	Article	IF	Citations
3730	The sorption and diffusion of 133Ba in crushed and intact granitic rocks from the Olkiluoto and Grimsel in-situ test sites. Applied Geochemistry, 2018, 89, 138-149.	1.4	14
3731	Evidence of Intermediate Hydrogen States in the Formation of a Complex Hydride. Inorganic Chemistry, 2018, 57, 867-872.	1.9	11
3732	Synthesis of STW zeolites using imidazolium-based dications of varying length. Journal of Materials Chemistry A, 2018, 6, 1485-1495.	5.2	24
3733	Research on inhibitors and hindered groups in ultra-deep hydrodesulfurization based on density functional theory. Catalysis Today, 2018, 314, 170-178.	2.2	14
3734	Substituting Copper with Silver in the BiMOCh Layered Compounds (M = Cu or Ag; Ch = S, Se, or Te): Crystal, Electronic Structure, and Optoelectronic Properties. Chemistry of Materials, 2018, 30, 549-558.	3.2	31
3735	Pressure-dependent mechanical and thermodynamic properties of newly discovered cubic Na 2 He. Chinese Journal of Physics, 2018, 56, 231-237.	2.0	16
3736	Effects of Ti, Si, Mg and Cu additions on interfacial properties and electronic structure of Al(111)/4H-SiC(0001) interface: A first-principles study. Applied Surface Science, 2018, 437, 103-109.	3.1	62
3737	Magnetism and Optical Property of Mn-Doped Monolayer CrSi2 by First-Principle Study. Journal of Superconductivity and Novel Magnetism, 2018, 31, 2759-2765.	0.8	5
3738	Atomically Thin Mesoporous In₂O_{3â€“}_x/In₂S₃ Lateral Heterostructures Enabling Robust Broadbandâ€Light Photoâ€Electrochemical Water Splitting. Advanced Energy Materials, 2018, 8, 1701114.	10.2	106
3739	Thermodynamics and vibrational study of hydrogenated carbon nanotubes: A DFT study. Physica B: Condensed Matter, 2018, 530, 307-311.	1.3	7
3740	Quantifying Macroscopic Friction of Diamond-like Carbon Films by Microscopic Adsorption and Removal of Water Molecules. Langmuir, 2018, 34, 58-65.	1.6	20
3741	Theoretical Investigation of the Mechanical and Thermodynamic Properties of the Layered Yttrium Diborocarbides. Journal of Superconductivity and Novel Magnetism, 2018, 31, 2373-2379.	0.8	1
3742	First-principles investigation on the structures, energies, electronic and defective properties of Ti 2 AlN surfaces. Applied Surface Science, 2018, 433, 1056-1066.	3.1	25
3743	Charge Order and Negative Thermal Expansion in V₂OPO₄. Journal of the American Chemical Society, 2018, 140, 636-641.	6.6	45
3744	First-principle analysis of the structural, mechanical, optical and electronic properties of wollastonite monoclinic polymorph. Computational Condensed Matter, 2018, 14, 20-26.	0.9	38
3745	Kinetics of Molecular Diffusion and Self-Assembly: Glycine on Cu{110}. Journal of Physical Chemistry C, 2018, 122, 782-797.	1.5	4
3746	Investigations on magnetic properties of Cr-doped LiZnP by first principle calculations. Journal of Alloys and Compounds, 2018, 735, 355-358.	2.8	6
3747	Vibrational Properties of Bulk Boric Acid2Aand3TPolymorphs and Their Two-Dimensional Layers: Measurements and Density Functional Theory Calculations. Journal of Physical Chemistry A, 2018, 122, 1312-1325.	1.1	10

#	Article	IF	Citations
3748	Biosynthesis of palladium nanoparticles usingShewanella loihicaPV-4 for excellent catalytic reduction of chromium(<scp>vi</scp>). Environmental Science: Nano, 2018, 5, 730-739.	2.2	64
3749	Recent Advances in Solid-State Nuclear Magnetic Resonance Spectroscopy. Annual Review of Analytical Chemistry, 2018, 11, 485-508.	2.8	45
3750	How Vertical Compression Triggers Lateral Interlayer Slide for Metallic Molybdenum Disulfide?. Tribology Letters, 2018, 66, 1.	1.2	13
3751	Investigation of iron adsorption on composite transition metal carbides in steel by first-principles calculation. Journal of Physics and Chemistry of Solids, 2018, 116, 30-36.	1.9	11
3752	Oxyhalides: prospecting ore for optical functional materials with large laser damage thresholds. Journal of Materials Chemistry C, 2018, 6, 2435-2442.	2.7	56
3753	Hierarchical Nâ€Rich Carbon Sponge with Excellent Cycling Performance for Lithiumâ€Sulfur Battery at High Rates. Chemistry - A European Journal, 2018, 24, 5860-5867.	1.7	20
3754	Influence of Na and Nb co-substitution on electrochemical performance of ternary cathode materials for Li-ion batteries. New Journal of Chemistry, 2018, 42, 3444-3451.	1.4	23
3755	Electronic Band Structure Engineering and Enhanced Thermoelectric Transport Properties in Pb-Doped BiCuOS Oxysulfide. Chemistry of Materials, 2018, 30, 1085-1094.	3.2	18
3756	Study on the Electrochemical Oxidation Desulfurization Behavior of Model Diesel on Anodic Alumina Oxide and Ceria Nanotubes. Energy & Fuels, 2018, 32, 2612-2621.	2.5	16
3757	Biomimetic organization of a ruthenium-doped collagen-based carbon scaffold for hydrogen evolution. Journal of Materials Chemistry A, 2018, 6, 2311-2317.	5.2	36
3758	First-principles atomistic Wulff constructions for an equilibrium rutile TiO2 shape modeling. Applied Surface Science, 2018, 436, 989-994.	3.1	43
3759	Exploration for the stabilities of CHN 7 and CN 7 â^' : A theoretical study on the formation and dissociation mechanisms. Chemical Physics, 2018, 502, 27-32.	0.9	6
3760	The second-harmonic generation intensification derived from localization conjugated Ï€-orbitals in O₂^{2â^'}. Chemical Communications, 2018, 54, 1445-1448.	2.2	33
3761	The improvement of photocatalytic activity of monolayer g-C3N4via surface charge transfer doping. RSC Advances, 2018, 8, 1899-1904.	1.7	19
3762	Polarized Raman, <scp>FTIR,</scp> and <scp>DFT</scp> study of <scp>Na₂Ti₃O₇</scp> microcrystals. Journal of Raman Spectroscopy, 2018, 49, 538-548.	1.2	54
3763	PbGa₂GeS₆: An Infrared Nonlinear Optical Material Synthesized by an Intermediate-Temperature Self-Fluxing Method. Crystal Growth and Design, 2018, 18, 1162-1167.	1.4	30
3764	A Member of Fluorooxoborates: Li₂Na_{0.9}K_{0.1}B₅O₈F₂ with the Fundamental Building Block B₅O₁₀F₂ and a Short Cutoff Edge. Inorganic Chemistry, 2018, 57, 873-878.	1.9	23
3765	Systematic studies on Yb_xBi_{1â^'x}VO₄:Tm³⁺solid solutions: experiments and DFT calculations on up-conversion photoluminescence properties. RSC Advances, 2018, 8, 596-605.	1.7	5

#	Article	IF	Citations
3766	Fundamental principles that govern the copper doping behavior in complex clinker system. Journal of the American Ceramic Society, 2018, 101, 2527-2536.	1.9	29
3767	The functionalization effect of benzoic acid and anisole on the photocatalytic activity of monolayer MoS2. Applied Surface Science, 2018, 437, 314-320.	3.1	13
3768	Properties of a predicted tetragonal carbon allotrope: First principles study. Diamond and Related Materials, 2018, 82, 50-55.	1.8	17
3769	Refining Crystal Structures with Quadrupolar NMR and Dispersion-Corrected Density Functional Theory. Journal of Physical Chemistry C, 2018, 122, 1809-1820.	1.5	35
3770	Interactions of Oxygen and Water Molecules with Pyrite Surface: A New Insight. Langmuir, 2018, 34, 1941-1952.	1.6	39
3771	Strong hybridization between Bi-6s and O-2p orbitals in SillÃ©nâ€“Aurivillius perovskite Bi₄MO₈X (M = Nb, Ta; X = Cl, Br), visible light photocatalysts enabling stable water oxidation. Journal of Materials Chemistry A, 2018, 6, 3100-3107.	5.2	106
3772	A Novel Bioresidue to Compatibilize Sodium Montmorillonite and Linear Low Density Polyethylene. Industrial & Engineering Chemistry Research, 2018, 57, 1213-1224.	1.8	11
3773	High Yield Exfoliation of WS₂ Crystals into 1â€“2 Layer Semiconducting Nanosheets and Efficient Photocatalytic Hydrogen Evolution from WS₂/CdS Nanorod Composites. ACS Applied Materials & Interfaces, 2018, 10, 2810-2818.	4.0	112
3774	Structural stability, elastic and thermodynamic properties of Auâ€“Cu alloys from first-principles calculations. Physica B: Condensed Matter, 2018, 533, 58-62.	1.3	27
3775	Enhancement of catalytic activity of Pd-PVP colloid for direct H₂O₂synthesis from H₂and O₂in water with addition of 0.5 atom% Pt or Ir. Catalysis Science and Technology, 2018, 8, 1002-1015.	2.1	15
3776	A Combined 25 Mg Solidâ€State NMR and Ab Initio DFT Approach to Probe the Local Structural Differences in Magnesium Acetate Phases Mg(CH 3 COO) 2 â€‰â‹…â€‰nH 2 O (n=0,â€‰1,â€‰4). ChemPhysChem, 2018, 19, 1722-1732.	1.0	8
3777	Interfacial micro-structure and properties of TiO 2 /SnO 2 heterostructures with rutile phase: A DFT calculation investigation. Applied Surface Science, 2018, 451, 258-271.	3.1	19
3778	DFT study into the reaction mechanism of CO methanation over pure MoS₂. International Journal of Quantum Chemistry, 2018, 118, e25643.	1.0	12
3779	Mechanochemical syntheses and³⁵Cl solid-state NMR characterization of fluoxetine HCl cocrystals. CrystEngComm, 2018, 20, 2780-2792.	1.3	21
3780	Electrical and material properties of hydrothermally grown single crystal (111) UO2. European Physical Journal B, 2018, 91, 1.	0.6	6
3781	Impermeability of boron nitride defect-sensitive monolayer with atomic-oxygen-healing ability. Ceramics International, 2018, 44, 13888-13893.	2.3	12
3782	Promotion of the bifunctional electrocatalytic oxygen activity of manganese oxides with dual-affinity phosphate. Electrochimica Acta, 2018, 277, 143-150.	2.6	14
3783	Inelastic Neutron Scattering Study of the Aluminum and BrÃ¸nsted Site Location in Aluminosilicate LTA Zeolites. Journal of Physical Chemistry C, 2018, 122, 11450-11454.	1.5	9

#	Article	IF	Citations
3784	Determining the Crystal Structures of Peptide Analogs of Boronic Acid in the Absence of Single Crystals: Intricate Motifs of Ixazomib Citrate Revealed by XRPD Guided by ss-NMR. Crystal Growth and Design, 2018, 18, 3616-3625.	1.4	22
3785	Transforming Nickel Hydroxide into 3D Prussian Blue Analogue Array to Obtain Ni₂P/Fe₂P for Efficient Hydrogen Evolution Reaction. Advanced Energy Materials, 2018, 8, 1800484.	10.2	186
3786	Lithiation Products of a Silicon Anode Based on Soft X-ray Emission Spectroscopy: A Theoretical Study. Journal of Physical Chemistry C, 2018, 122, 11096-11108.	1.5	8
3787	Adsorption of alcohols and hydrocarbons on nonstoichiometric cementite{010} surfaces. Physical Chemistry Chemical Physics, 2018, 20, 14133-14144.	1.3	3
3788	Inside PEF: Chain Conformation and Dynamics in Crystalline and Amorphous Domains. Macromolecules, 2018, 51, 3515-3526.	2.2	110
3789	Gaussian basis implementation of the charge patching method. Journal of Computational Physics, 2018, 368, 196-209.	1.9	0
3790	Comparative study on mechanical properties of three different SiC polytypes (3C, 4H and 6H) under high pressure: First-principle calculations. Vacuum, 2018, 154, 37-43.	1.6	23
3791	Molecular Modeling of Univalent Cation Exchange in Zeolite N. Journal of Physical Chemistry C, 2018, 122, 10801-10810.	1.5	9
3792	Theoretical investigation on MgV₂O₆: ab-initio study. Philosophical Magazine, 2018, 98, 2077-2093.	0.7	6
3793	Work function and quantum efficiency study of metal oxide thin films on Ag(100). Physical Review B, 2018, 97, .	1.1	7
3794	Theoretical exploring the mechanical and electrical properties of tI12-B6C4O2. Computational Materials Science, 2018, 150, 259-264.	1.4	4
3795	Insight into the effect of maleic acid on the preparation of Î±-hemihydrate gypsum from phosphogypsum in Na2SO4 solution. Journal of Crystal Growth, 2018, 493, 34-40.	0.7	45
3796	The relationship between covalent bonds and the optical response in a nonpolar family ATeMoO 6 (A=Mg, Zn, Cd): A Berry-phase investigation. Journal of Solid State Chemistry, 2018, 264, 22-28.	1.4	13
3797	Insight into lead-free organic-inorganic hybrid perovskites for photovoltaics and optoelectronics: A first-principles study. Organic Electronics, 2018, 59, 99-106.	1.4	123
3798	Negative electron affinity from aluminium on the diamond (1â€‰0â€‰0) surface: a theoretical study. Journal of Physics Condensed Matter, 2018, 30, 235002.	0.7	15
3799	Syntheses, structures and efficient visible light-driven photocatalytic properties of layered cuprous halides based on two types of building units. Dalton Transactions, 2018, 47, 6965-6972.	1.6	32
3800	Lattice dynamical probe of phase transformations in niobium oxyfluoride Nb2O2F3. Physical Review B, 2018, 97, .	1.1	0
3801	Learning models for electron densities with Bayesian regression. Computational Materials Science, 2018, 149, 250-258.	1.4	10

#	Article	IF	Citations
3802	Periodic Density Functional Theory Study of the Structure, Raman Spectrum, and Mechanical Properties of Schoepite Mineral. Inorganic Chemistry, 2018, 57, 4470-4481.	1.9	51
3803	Influence of the core-hole effect on optical properties of magnesium oxide (MgO) near the MgL-edge region. Journal of Synchrotron Radiation, 2018, 25, 771-776.	1.0	5
3804	First principles investigation of structural, vibrational and thermal properties of black and blue phosphorene. International Journal of Modern Physics B, 2018, 32, 1850151.	1.0	12
3805	Possible Martensitic Transformation in Heusler Alloy Pt 2 MnSn from First Principles. Chinese Physics Letters, 2018, 35, 038101.	1.3	2
3806	Crystal structures and theoretical studies of polyphosphate LiZnP3O9 for nonlinear optical applications. Journal of Solid State Chemistry, 2018, 262, 313-319.	1.4	14
3807	[C₆H₁₄N]PbBr₃: An ABX₃â€Type Semiconducting Perovskite Hybrid with Aboveâ€Roomâ€Temperature Phase Transition. Chemistry - an Asian Journal, 2018, 13, 982-988.	1.7	20
3808	Can we predict the structure and stability of molecular crystals under increased pressure? Firstâ€principles study of glycine phase transitions. Journal of Computational Chemistry, 2018, 39, 1300-1306.	1.5	19
3809	Investigation of the Water Adsorption Properties and Structural Stability of MIL-100(Fe) with Different Anions. Langmuir, 2018, 34, 4180-4187.	1.6	33
3810	Theoretical investigations of Ge1â^'xSn x alloys (xâ€‰=â€‰0, 0.333, 0.667, 1) in P42/ncm phase. Journal of Materials Science, 2018, 53, 9611-9626.	1.7	26
3811	Tunable electronic and optical properties of GaS/GaSe van der Waals heterostructure. Current Applied Physics, 2018, 18, 673-680.	1.1	51
3812	DFT Study on Sulfur-Doped g-C₃N₄ Nanosheets as a Photocatalyst for CO₂ Reduction Reaction. Journal of Physical Chemistry C, 2018, 122, 7712-7719.	1.5	200
3813	2D/2D FeOCl/graphite oxide heterojunction with enhanced catalytic performance as a photo-Fenton catalyst. New Journal of Chemistry, 2018, 42, 6896-6902.	1.4	28
3814	First-principles analysis of ferroelectric transition in MnSnO3 and MnTiO3 perovskites. Journal of Solid State Chemistry, 2018, 262, 251-255.	1.4	7
3815	First-principles investigation of mechanical and electronic properties of tetragonal NbAl 3 under tension. Physica B: Condensed Matter, 2018, 538, 47-53.	1.3	7
3816	Predicting the ground-state structure of sodium boride. Physical Review B, 2018, 97, .	1.1	26
3817	Carbon nanotube-carbyne composite: A nanoreactor in a quasi-1D liquid state. Computational Materials Science, 2018, 149, 409-415.	1.4	6
3818	Hittorf's violet phosphorene as a promising candidate for optoelectronic and photocatalytic applications: first-principles characterization. Physical Chemistry Chemical Physics, 2018, 20, 11967-11975.	1.3	45
3819	Large spontaneous polarization in polar perovskites of PbTiO₃â€“Bi(Zn_{1/2}Ti_{1/2})O₃. Inorganic Chemistry Frontiers, 2018, 5, 1277-1281.	3.0	15

#	Article	IF	Citations
3820	Investigation of the physical properties of two Laves phase compounds HRh₂ (H = Ca and) Tj ETQq0 0 0 rgBT /Overlock 10	1.0	15
3821	The role of electric field in enhancing separation of gas molecules (H 2 S, CO 2 , H 2 O) on VIB modified g-C 3 N 4 (0â€¯0â€¯1). Applied Surface Science, 2018, 445, 568-574.	3.1	17
3822	DFT study of structural, electronic and elastic properties of two polymorphs of monoclinic CsGaQ2 (Qâ€¯=â€¯S, Se). Chinese Journal of Physics, 2018, 56, 1345-1352.	2.0	4
3823	â€œPop-On and Pop-Offâ€•Surface Chemistry of Alanine on Ni{111} under Elevated Hydrogen Pressures. Journal of Physical Chemistry C, 2018, 122, 7720-7730.	1.5	5
3824	CaP₃: A New Two-Dimensional Functional Material with Desirable Band Gap and Ultrahigh Carrier Mobility. Journal of Physical Chemistry Letters, 2018, 9, 1728-1733.	2.1	112
3825	The electronic and optical properties of Cs adsorbed GaAs nanowires via first-principles study. Physica E: Low-Dimensional Systems and Nanostructures, 2018, 101, 5-10.	1.3	10
3826	Hydrogen Bond Dynamics of Cellulose through Inelastic Neutron Scattering Spectroscopy. Biomacromolecules, 2018, 19, 1305-1313.	2.6	28
3827	Crystal Structures, Local Atomic Environments, and Ion Diffusion Mechanisms of Scandium-Substituted Sodium Superionic Conductor (NASICON) Solid Electrolytes. Chemistry of Materials, 2018, 30, 2618-2630.	3.2	109
3828	Towards the systematic crystallisation of molecular ionic cocrystals: insights from computed crystal form landscapes. Faraday Discussions, 2018, 211, 401-424.	1.6	20
3829	Monolayer group-III monochalcogenides by oxygen functionalization: a promising class of two-dimensional topological insulators. Npj Quantum Materials, 2018, 3, .	1.8	58
3830	Healable Structure Triggered by Thermal/Electrochemical Force in Layered GeSe₂ for High Performance Liâ€ion Batteries. Advanced Energy Materials, 2018, 8, 1703635.	10.2	59
3831	The promise of piezoelectric polymers. Polymer International, 2018, 67, 790-798.	1.6	43
3832	Adhesion, stability and electronic properties of Ti 2 AlN(0001)/TiAl(111) coherent interface from first-principles calculation. Intermetallics, 2018, 96, 49-57.	1.8	36
3833	Effect of annealing on the structure and magnetic properties of Co2FeAl0.5Si0.5 thin films on Ge(111). Journal of Alloys and Compounds, 2018, 748, 323-327.	2.8	10
3834	Terahertz optical properties of nonlinear optical CdSe crystals. Optical Materials, 2018, 78, 484-489.	1.7	7
3835	Investigation of the Linker Swing Motion in the Zeolitic Imidazolate Framework ZIF-90. Journal of Physical Chemistry C, 2018, 122, 7203-7209.	1.5	19
3836	Exploring Optical and Vibrational Properties of the Uranium Carbonate Andersonite with Spectroscopy and First-Principles Calculations. Journal of Physical Chemistry C, 2018, 122, 7410-7420.	1.5	18
3837	Negative thermal expansion and electronic structure variation of chalcopyrite type LiGaTe₂. RSC Advances, 2018, 8, 9946-9955.	1.7	35

#	Article	IF	Citations
3838	Intermolecular hydrogen bond stretching vibrations observed in terahertz spectra of crystalline vitamins. CrystEngComm, 2018, 20, 1960-1969.	1.3	20
3839	Structural, Optical, and Electronic Characterization of Fe-Doped Alumina Nanoparticles. Journal of Electronic Materials, 2018, 47, 711-720.	1.0	25
3840	ELSI: A unified software interface for Kohnâ€“Sham electronic structure solvers. Computer Physics Communications, 2018, 222, 267-285.	3.0	78
3841	Pressurized calcium looping in the presence of steam in a spout-fluidized-bed reactor with DFT analysis. Fuel Processing Technology, 2018, 169, 24-41.	3.7	32
3842	An insight into a novel cubic phase SnSe for prospective applications in optoelectronics and clean energy devices. Journal of Alloys and Compounds, 2018, 733, 22-32.	2.8	33
3843	Progress in Our Understanding of 19F Chemical Shifts. Annual Reports on NMR Spectroscopy, 2018, , 281-365.	0.7	16
3844	Pb 10 V 6 O 25 : A new lead vanadate with apatite structure. Journal of Molecular Structure, 2018, 1151, 223-229.	1.8	3
3845	Narrow Band Deep Red Photoluminescence of Y₂Mg₃Ge₃O₁₂:Mn⁴⁺,Li⁺Inverse Garnet for High Power Phosphor Converted LEDs. ECS Journal of Solid State Science and Technology, 2018, 7, R3086-R3092.	0.9	53
3846	Pressure-dependent structural, elastic, electronic and vibrational studies of Ba2InMO6 (M = Ta, Nb) from first principles. Computational Materials Science, 2018, 142, 99-107.	1.4	6
3847	Elastic, dynamical, and electronic properties of LiHg and Li3Hg: First-principles study. Frontiers of Physics, 2018, 13, 1.	2.4	3
3848	Theoretical investigations of group IV alloys in the Lonsdaleite phase. Journal of Materials Science, 2018, 53, 2785-2801.	1.7	31
3849	Synergistic combination of graphitic C3N4 and polyoxometalate-based phase-transfer catalyst for highly efficient reductant-free aerobic hydroxylation of benzene. Chemical Engineering Journal, 2018, 334, 873-881.	6.6	29
3850	Ultrafast molecular transport on carbon surfaces: The diffusion of ammonia on graphite. Carbon, 2018, 126, 23-30.	5.4	9
3851	Density Functional Theory Study on Electronic Structures and Magnetism for Nitrogen-Doped ZnS. Journal of Superconductivity and Novel Magnetism, 2018, 31, 1443-1448.	0.8	2
3852	The effect of metal transition dopant on electronic and mechanical properties of titanium nitride: First principle method. Computational Materials Science, 2018, 141, 82-90.	1.4	10
3853	DFT study on structural, electronic, and optical properties of cubic and monoclinic CuO. Journal of Computational Electronics, 2018, 17, 21-28.	1.3	29
3854	GeAs and SiAs monolayers: Novel 2D semiconductors with suitable band structures. Physica E: Low-Dimensional Systems and Nanostructures, 2018, 95, 149-153.	1.3	70
3855	Theoretical investigation on the adsorption and dissociation behaviors of TiCl4 on pyrolytic carbon surface. Applied Surface Science, 2018, 427, 156-165.	3.1	0

#	Article	IF	Citations
3856	Structural, electronic, elastic and lattice dynamical properties of CdIn₂Te₄ under pressure from first principle. International Journal of Modern Physics B, 2018, 32, 1850026.	1.0	4
3857	Bi3TeBO9: electronic structure, optical properties and photoinduced phenomena. Journal of Materials Science, 2018, 53, 1217-1226.	1.7	20
3858	Tight binding simulation study on zigzag single-walled carbon nanotubes. International Journal of Modern Physics B, 2018, 32, 1850020.	1.0	2
3859	A reactive force field molecular dynamics simulation of nickel oxidation in supercritical water. Journal of Supercritical Fluids, 2018, 133, 421-428.	1.6	21
3860	First-principles study of ternary Li-Al-Te compounds under high pressure. Solid State Communications, 2018, 270, 58-64.	0.9	6
3861	Interfacial Interactions in Monolayer and Fewâ€Layer SnS/CH₃NH₃PbI₃ Perovskite van der Waals Heterostructures and Their Effects on Electronic and Optical Properties. ChemPhysChem, 2018, 19, 291-299.	1.0	12
3862	Pressure effect of magnetic and electronic properties of Mn 2 PtGa Heusler alloy. Physics Letters, Section A: General, Atomic and Solid State Physics, 2018, 382, 224-230.	0.9	9
3863	Elucidating the Crystal Structure of dl-Arginine by Combined Powder X-ray Diffraction Data Analysis and Periodic DFT-D Calculations. Crystal Growth and Design, 2018, 18, 42-46.	1.4	11
3864	MBaYB6O12(M = Rb, Cs): two new rare-earth borates with large birefringence and short ultraviolet cutoff edges. Dalton Transactions, 2018, 47, 750-757.	1.6	28
3865	Vibrational and reorientational dynamics and thermal properties in [Mg(H2O)4](ReO4)2 supported by periodic DFT study. Vibrational Spectroscopy, 2018, 94, 49-60.	1.2	5
3866	Luminescence of Bi3+ in the double perovskite, La2MgTiO6. Optical Materials, 2018, 75, 809-813.	1.7	21
3867	Evaluating the Energetic Driving Force for Cocrystal Formation. Crystal Growth and Design, 2018, 18, 892-904.	1.4	145
3868	Noncentrosymmetric Cubic Cyanurate K₆Cd₃(C₃N₃O₃)₄ Containing Isolated Planar Ï€-Conjugated (C₃N₃O₃)^{3â€“} Groups. Inorganic Chemistry, 2018, 57, 32-36.	1.9	48
3869	Exploring the low friction of diamond-like carbon films in carbon dioxide atmosphere by experiments and first-principles calculations. Applied Surface Science, 2018, 436, 893-899.	3.1	31
3870	Impact of Coinage Metal Insertion on the Thermoelectric Properties of GeTe Solid-State Solutions. Journal of Physical Chemistry C, 2018, 122, 227-235.	1.5	49
3871	Labile Low-Valent Tin Azides: Syntheses, Structural Characterization, and Thermal Properties. Inorganic Chemistry, 2018, 57, 400-411.	1.9	6
3872	Theoretical Analysis of the Electrical and Optical Properties of ZnS. Lecture Notes in Electrical Engineering, 2018, , 9-19.	0.3	5
3873	Thermodynamics of disordering in Au3Cu. Journal of Alloys and Compounds, 2018, 735, 1344-1349.	2.8	5

#	Article	IF	Citations
3874	First principle study of structural, elastic and electronic properties of APt3 (A=Mg, Sc, Y and Zr). Philosophical Magazine, 2018, 98, 408-421.	0.7	5
3875	Weakly spin-dependent band structures of antiferromagnetic perovskite LaMO₃(Mâ€‰â€‰=â€‰â€‰Cr, Mn) Tj ETQ	0.7	10
3876	Synthesis, X-ray powder diffraction and DFT-D studies of indole-based compounds. Zeitschrift Fur Kristallographie - Crystalline Materials, 2018, 233, 421-427.	0.4	1
3877	A Maze of Solid Solutions of Pimobendan Enantiomers: An Extraordinary Case of Polymorph and Solvate Diversity. Crystal Growth and Design, 2018, 18, 264-273.	1.4	17
3878	Robust fully-compensated ferrimagnetism and semiconductivity in inverse Heusler compounds: Ti2VZ (Zâ€¯=â€¯P, As, Sb, Bi). Journal of Magnetism and Magnetic Materials, 2018, 449, 515-521.	1.0	8
3879	DFT analysis on the Pt with nano-carbon frames for low temperature fuel cell applications. Electrochimica Acta, 2018, 259, 598-605.	2.6	7
3880	A theoretical NMR study of selected benzazoles: Comparison of GIPAW and GIAOâ€PCM (DMSO) calculations. Magnetic Resonance in Chemistry, 2018, 56, 164-171.	1.1	14
3881	Enhanced works of separation for (0â€¯0â€¯0â€¯1)ZnO∣(1â€¯1â€¯1)ZrO2 interfaces via ion-doping in ZnO: Data-mining and density function theory study. Computational Materials Science, 2018, 142, 410-416.	1.4	7
3882	Nonlinear Optical Crystal Rb₄Sn₃Cl₂Br₈: Synthesis, Structure, and Characterization. Crystal Growth and Design, 2018, 18, 380-385.	1.4	22
3883	Kinetically Controlled Coprecipitation for General Fast Synthesis of Sandwiched Metal Hydroxide Nanosheets/Graphene Composites toward Efficient Water Splitting. Advanced Functional Materials, 2018, 28, 1704594.	7.8	91
3884	Structural Insights from ⁵⁹Co Solidâ€State NMR Experiments on Organocobalt(I) Catalysts. ChemPhysChem, 2018, 19, 227-236.	1.0	8
3885	A reinvestigation of a superhard phase Cm-carbon. Computational Materials Science, 2018, 143, 32-42.	1.4	18
3886	Theoretical study on Pb2VO2F5: large birefringence derived from optical anisotropies of VO2F4 groups. Journal of Materials Science, 2018, 53, 3483-3492.	1.7	8
3887	Improvement on thermal stability of TiAlSiN coatings deposited by IBAD. Surface Engineering, 2018, 34, 504-510.	1.1	8
3888	Novel GaN-based nanocomposites: Effective band structure and optical property tuning by tensile strain or external field. Applied Surface Science, 2018, 427, 554-562.	3.1	9
3889	Electronic, magnetic and optical properties of charge-compensated (Nb, TMâ€‰=â€‰Fe, Cr)-codoped SrTiO₃from first principles. Ferroelectrics, 2018, 537, 68-78.	0.3	4
3890	Revisiting the crystal structure of dickite: X-ray diffraction, solid-state NMR, and DFT calculations study. American Mineralogist, 2018, 103, 812-818.	0.9	4
3891	Mass-selective neutron spectroscopy of glassy versus polycrystalline structures in binary mixtures of beryllium and zirconium. Journal of Physics: Conference Series, 2018, 1055, 012004.	0.3	10

#	Article	IF	Citations
3892	Strain Tunable Bandgap and High Carrier Mobility in SiAs and SiAs2 Monolayers from First-Principles Studies. Nanoscale Research Letters, 2018, 13, 404.	3.1	17
3893	Structural, electronic and vibrational properties of DL-histidine. , 2018, , .		1
3894	Ultra-broadband THz spectroscopy for sensing and identification for security applications. , 2018, , .		2
3895	Structure and vibrational spectroscopy of methanesulfonic acid. Royal Society Open Science, 2018, 5, 181363.	1.1	27
3896	NMR Crystallography of the Polymorphs of Metergoline. Crystals, 2018, 8, 378.	1.0	15
3897	Theoretical Study of Hydrogen on LaFeO3 (010) Surface Adsorption and Subsurface Diffusion. Materials, 2018, 11, 2347.	1.3	0
3898	Physical properties of ThCr₂Si₂-type Rh-based compounds ARh₂Ge₂(A = Ca, Sr, Y and Ba): DFT based first-principles investigation. International Journal of Modern Physics B, 2018, 32, 1850357.	1.0	15
3899	Cation-tuned synthesis of the A₂SO₄Â·SbF₃(A = Na⁺,) Tj ETQq1 1 0.784314 rgBT properties. Dalton Transactions, 2018, 47, 17486-17492.	1.6	60
3900	A molecular roundabout: triple cyclically arranged hydrogen bonds in light of experiment and theory. New Journal of Chemistry, 2018, 42, 19467-19477.	1.4	10
3901	Computational and analytical approaches for investigating hydrates: the neat and hydrated solid-state forms of 3-(3-methylimidazolium-1-yl)propanoate. CrystEngComm, 2018, 20, 7826-7837.	1.3	6
3902	Diversity of methyl group dynamics in felodipine: a DFT supported NMR and QENS study. CrystEngComm, 2018, 20, 7371-7385.	1.3	8
3903	Reactive molecular dynamics simulation of thermal decomposition for nano-aluminized explosives. Physical Chemistry Chemical Physics, 2018, 20, 29341-29350.	1.3	55
3904	Theoretical investigation of conversion between different C₂H_xspecies over Pdâ€“Ag/Pd(100) surface alloys: influence on the selectivity and transformation of carbonaceous species. New Journal of Chemistry, 2018, 42, 19827-19836.	1.4	4
3905	Self-assembly of an oligo(p-phenylenevinylene)-based molecule on an HOPG surface: insights from multi-scale simulation and STM observation. RSC Advances, 2018, 8, 31868-31873.	1.7	3
3906	Enhanced visible light absorption performance of SnS₂and SnSe₂viasurface charge transfer doping. RSC Advances, 2018, 8, 40464-40470.	1.7	10
3907	Transition from antiferromagnetic ground state to robust ferrimagnetic order with Curie temperatures above 420 K in manganese-based antiperovskite-type structures. Journal of Materials Chemistry C, 2018, 6, 13336-13344.	2.7	5
3908	Vibrationally induced metallisation of the energetic azide Î±-NaN₃. Physical Chemistry Chemical Physics, 2018, 20, 29061-29069.	1.3	21
3909	Na₃Ca₄(TeO₃)(PO₄)₃: a new noncentrosymmetric tellurite phosphate with fascinating multimember-ring architectures and intriguing nonlinear optical performance. Dalton Transactions, 2018, 47, 17198-17201.	1.6	22

#	Article	IF	Citations
3910	3D to 2D reorganization of silverâ€“thiol nanostructures, triggered by solvent vapor annealing. Nanoscale, 2018, 10, 23018-23026.	2.8	3
3911	Transition metal attenuated mechanism for protective alumina formation from first principles. RSC Advances, 2018, 8, 41255-41269.	1.7	4
3912	Structural insights into T₂-cluster-containing chalcogenides with vertex-, edge- and face-sharing connection modes of NaQ₆ligands: Na₃ZnM^{III}Q₄(M^{III}= In, Ga; Q = S, Se). Dalton Transactions, 2018, 47, 15538-15544.	1.6	12
3913	A highly efficient Z-scheme B-doped g-C₃N₄/SnS₂photocatalyst for CO₂reduction reaction: a computational study. Journal of Materials Chemistry A, 2018, 6, 21056-21063.	5.2	134
3914	Li₈NaRb₃(SO₄)₆Â·2H₂O as a new sulfate deep-ultraviolet nonlinear optical material. Journal of Materials Chemistry C, 2018, 6, 12240-12244.	2.7	66
3915	Low-Cost Flexible ZnO Microwires Array Ultraviolet Photodetector Embedded in PAVL Substrate. Nanoscale Research Letters, 2018, 13, 277.	3.1	8
3916	Hydrogen dynamics in solid formic acid: insights from simulations with quantum colored-noise thermostats. Journal of Physics: Conference Series, 2018, 1055, 012003.	0.3	8
3917	Control of Uniaxial Negative Thermal Expansion in Layered Perovskites by Tuning Layer Thickness. Frontiers in Chemistry, 2018, 6, 455.	1.8	12
3918	Designing an Excellent Deep-Ultraviolet Birefringent Material for Light Polarization. Journal of the American Chemical Society, 2018, 140, 16311-16319.	6.6	350
3919	The accuracy of standard enthalpies and entropies for phases of petrological interest derived from density-functional calculations. Contributions To Mineralogy and Petrology, 2018, 173, 90.	1.2	22
3920	Temperature Dependent Micro-Structure of KAlF4 from Solid to Molten States. Materials, 2018, 11, 1846.	1.3	4
3921	The physical properties of ThCr₂Si₂-type superconductors MPd₂P₂ (M = Y, La): A theoretical investigation. International Journal of Modern Physics B, 2018, 32, 1850312.	1.0	3
3922	Open-Science Platform for Computational Materials Science: AiiDA and the Materials Cloud. , 2018, , 1-24.		1
3923	Targeted Deposition of Platinum onto Gold Nanorods by Plasmonic Hot Electrons. Journal of Physical Chemistry C, 2018, 122, 28901-28909.	1.5	49
3924	Stability of intrinsic and extrinsic co-decorated boron sheets with Li and Mg. Computational Condensed Matter, 2018, 17, e00345.	0.9	0
3925	Exotic Spectra and Lattice Vibrations of Ice X Using the DFT Method. Molecules, 2018, 23, 2780.	1.7	9
3926	Insight into the Crystalline Structure of ThF4 with the Combined Use of Neutron Diffraction, 19F Magic-Angle Spinning-NMR, and Density Functional Theory Calculations. Inorganic Chemistry, 2018, 57, 15350-15360.	1.9	12
3927	Theory-Driven Heterojunction Photocatalyst Design with Continuously Adjustable Band Gap Materials. Journal of Physical Chemistry C, 2018, 122, 28065-28074.	1.5	20

#	Article	IF	Citations
3928	Accurate ab initio determination of ballistic electron emission spectroscopy: Application to Au/Ge. Physical Review B, 2018, 98, .	1.1	4
3929	Cyano-Based Materials with Giant Optical Anisotropy and Second Harmonic-Generation Effect. Inorganic Chemistry, 2018, 57, 15001-15008.	1.9	16
3930	Light Absorption Properties and Electronic Band Structures of Lead Titanium Oxyfluoride Photocatalysts Pb₂Ti₄O₉F₂ and Pb₂Ti₂O_{5.4}F_{1.2}. Journal of Physical Chemistry C, 2018, 122, 26506-26511.	1.5	31
3931	Two Lanthanide Borate Chlorides LnB₄O₆(OH)₂Cl (Ln = La, Ce) with Wide Ultraviolet Transmission Windows and Large Second-Harmonic Generation Responses. Inorganic Chemistry, 2018, 57, 14953-14960.	1.9	14
3932	Electronic Structures of Ge₂Sb₂Te₅/Co₂FeX (X: Al,) Tj ETQq0 0 0 rgBT /Overlock 10	1.6	1
3933	A DFT-D study on influences of molecular vacancy, water and ethylenediamine substitutions on structural and electronic properties of nitromethane. Chinese Journal of Physics, 2018, 56, 3033-3038.	2.0	2
3934	Mechanical, Electronic and Optical Properties of Two Phases of NbB4: First-Principles Calculations. Zeitschrift Fur Naturforschung - Section A Journal of Physical Sciences, 2018, 73, 453-460.	0.7	3
3935	Quantum magnetism in molecular spin ladders probed with muon-spin spectroscopy. New Journal of Physics, 2018, 20, 103002.	1.2	12
3936	Machine Learning a General-Purpose Interatomic Potential for Silicon. Physical Review X, 2018, 8, .	2.8	222
3937	Extraction Difficulty of Lithium Ions from Various Crystal Planes of Lithium Titanate. Journal Wuhan University of Technology, Materials Science Edition, 2018, 33, 1086-1091.	0.4	8
3938	The ideal commensurate value of Sc and the superconducting phase under high pressure. Journal of Applied Physics, 2018, 124, 225901.	1.1	23
3939	Silicon Oxycarbide-Derived Carbon as Potential NO₂ Gas Sensor: A First Principlesâ€™ Study. IEEE Electron Device Letters, 2018, 39, 1760-1763.	2.2	37
3940	High-pressure <mml:math xmlns:mml="http://www.w3.org/1998/Math/MathML"><mml:msub><mml:mrow><mml:mi>CaF</mml:mi></mml:mrow><mml:mn>2</m revisited: A new high-temperature phase and the role of phonons in the search for superionic conductivity. Physical Review B, 2018, 98, .	1.1	7
3941	Novel electronic structures and enhanced optical properties of boron phosphide/blue phosphorene and F4TCNQ/blue phosphorene heterostructures: a DFT + NEGF study. Physical Chemistry Chemical Physics, 2018, 20, 28777-28785.	1.3	15
3942	Synthesis, structural and antimicrobial studies of binary and ternary complexes of a new tridentate thiosemicarbazone. Future Medicinal Chemistry, 2018, 10, 2507-2519.	1.1	7
3943	First principles study on ferromagnetism of diluted magnetic semiconductor Li(Zn, Mn)N. Journal of Applied Physics, 2018, 124, 203901.	1.1	2
3944	Structure and Chemical Order in Sâ€“Se Binary Glasses. Journal of Physical Chemistry B, 2018, 122, 12219-12226.	1.2	12
3945	First-principles thermodynamic theory of Seebeck coefficients. Physical Review B, 2018, 98, .	1.1	25

#	Article	IF	Citations
3946	Na4Yb(CO3)3F: A New UV Nonlinear Optical Material with a Large Second Harmonic Generation Response. Crystals, 2018, 8, 381.	1.0	5
3947	Vibrational spectroscopy of metal methanesulfonates: Mâ€‰=â€‰Na, Cs, Cu, Ag, Cd. Royal Society Open Science, 2018, 5, 171574.	1.1	15
3948	Electronic properties of defects inWeyl semimetal tantalum arsenide. Chinese Physics B, 2018, 27, 097101.	0.7	2
3949	Gd3Li3Te2O12:U6+,Eu3+: A Tunable Red Emitting Garnet Showing Efficient U6+ to Eu3+ Energy Transfer at Room Temperature. Inorganics, 2018, 6, 84.	1.2	3
3950	Theoretical Investigations of the Hexagonal Germanium Carbonitride. Materials, 2018, 11, 655.	1.3	3
3951	Ion-induced structural and optical performance evolution in LBO-like crystals: experimental and theoretical investigation. Inorganic Chemistry Frontiers, 2018, 5, 2955-2963.	3.0	8
3952	High-pressure vibrational properties of dense rubidium. Physical Review B, 2018, 98, .	1.1	2
3953	Nanocrystallization of Rare Tolbutamide Form V in Mesoporous MCM-41 Silica. Molecular Pharmaceutics, 2018, 15, 4926-4932.	2.3	16
3954	Towards hybrid density functional calculations of molecular crystals via fragment-based methods. Journal of Chemical Physics, 2018, 149, 124104.	1.2	13
3955	Selective Adsorption of Toluene on Perovskite-type Oxide. Journal of the Japan Petroleum Institute, 2018, 61, 272-281.	0.4	3
3956	Urchin-like CoP with Controlled Manganese Doping toward Efficient Hydrogen Evolution Reaction in Both Acid and Alkaline Solution. ACS Sustainable Chemistry and Engineering, 2018, 6, 15162-15169.	3.2	31
3957	On the structural aspects of solid solutions of enantiomers: an intriguing case study of enantiomer recognition in the solid state. CrystEngComm, 2018, 20, 6909-6918.	1.3	16
3958	First principles study on lattice vibration and electrical properties of layered perovskite Sr₂ M ₂O₇ (M = Nb, Ta). Chinese Physics B, 2018, 27, 086104.	0.7	1
3959	Spectroscopy of metal hexaborides: Phonon dispersion models. Journal of Raman Spectroscopy, 2018, 49, 1985-1998.	1.2	8
3960	Application of density functional theory in studying CO2 capture with TiO2-supported K2CO3 being an example. Applied Energy, 2018, 231, 167-178.	5.1	18
3961	Mechanical and electromechanical properties of functionalized hexagonal boron nitride nanosheet: A density functional theory study. Journal of Chemical Physics, 2018, 149, 114701.	1.2	23
3962	Exploring Local Disorder within CAU-1 Frameworks Using Hyperpolarized ¹²⁹Xe NMR Spectroscopy. Langmuir, 2018, 34, 12538-12548.	1.6	17
3963	NMR Crystallography, Hydrogen Bonding and Optical Properties of the Novel 2D Hybrid Oxyfluorotitanate [H₂taz]₂Â·(Ti₅O₅F₁₂). Crystal Growth and Design, 2018, 18, 6873-6884.	1.4	3

#	Article	IF	Citations
3964	High-Throughput Pressure-Dependent Density Functional Theory Investigation of Herringbone Polycyclic Aromatic Hydrocarbons: Part 2. Pressure-Dependent Electronic Properties. Journal of Physical Chemistry C, 2018, 122, 23828-23844.	1.5	11
3965	DNP NMR Studies of Crystalline Polymer Domains by Copolymerization with Nitroxide Radical Monomers. Macromolecules, 2018, 51, 8046-8053.	2.2	10
3966	PyDEF 2.0: An Easy to Use Postâ€treatment Software for Publishable Charts Featuring a Graphical User Interface. Journal of Computational Chemistry, 2018, 39, 2251-2261.	1.5	27
3967	Effect of the Processing Route on the Thermoelectric Performance of Nanostructured CuPb₁₈SbTe₂₀. Inorganic Chemistry, 2018, 57, 12976-12986.	1.9	29
3968	Modelling of structure and dynamics of molten NaF using first principles molecular dynamics. AIP Conference Proceedings, 2018, , .	0.3	7
3969	DFT modeling of metallic nanoparticles. Frontiers of Nanoscience, 2018, 12, 239-293.	0.3	8
3970	Understanding of the Elastic Constants, Energetics, and Bonding in Dicalcium Silicate Using First-Principles Calculations. Journal of Physical Chemistry C, 2018, 122, 24235-24245.	1.5	14
3971	Metal ion coordination enhancing quantum efficiency of ligand phosphorescence in a double-stranded helical chain coordination polymer of Pb²⁺with nicotinic acid. Dalton Transactions, 2018, 47, 14636-14643.	1.6	11
3972	Structural and Superconducting Properties of Tungsten Hydrides Under High Pressure. Frontiers in Physics, 2018, 6, .	1.0	8
3973	Multicolor Tuning and Temperature-Triggered Anomalous Eu³⁺-Related Photoemission Enhancement via Interplay of Accelerated Energy Transfer and Release of Defect-Trapped Electrons in the Tb³⁺,Eu³⁺-Doped Strontiumâ€“Aluminum Chlorites. ACS Applied Materials & Interfaces, 2018, 10, 36157-36170.	4.0	47
3974	Competing structural instabilities in<mml:math xmlns:mml="http://www.w3.org/1998/Math/MathML"><mml:mrow><mml:msub><mml:mi>Bi</mml:mi><mml:mn>21</mml:mn></mml:msub></mml:mrow></mml:math> Physical Review B, 2018, 98, .	1.1	19
3975	A Langbeinite-Type Yttrium Phosphate LiCs₂Y₂(PO₄)₃. Inorganic Chemistry, 2018, 57, 13087-13091.	1.9	26
3976	High-Throughput Pressure-Dependent Density Functional Theory Investigation of Herringbone Polycyclic Aromatic Hydrocarbons: Part 1. Pressure-Dependent Structure Trends. Journal of Physical Chemistry C, 2018, 122, 23815-23827.	1.5	9
3977	Roomâ€Temperature Ultrabroadband Photodetection with MoS₂ by Electronicâ€Structure Engineering Strategy. Advanced Materials, 2018, 30, e1804858.	11.1	66
3978	The Rubidium Barium Borate Resulting from B₇O₁₅ Fundamental Building Block Exhibits DUV Cutoff Edge. Inorganic Chemistry, 2018, 57, 13380-13385.	1.9	16
3979	Ca_xBa_{1â€“x}Nb₂O₆ Ferroelectric Nanopowders for Ultrahigh-Density Optical Data Storage. ACS Applied Nano Materials, 2018, 1, 6289-6300.	2.4	7
3980	Density-Functional and Tight-Binding Theory of Silicene and Silicane. Nanoscience and Technology, 2018, , 23-41.	1.5	0
3981	Synthesis, Crystal Structure, and Liquid Exfoliation of Layered Lanthanide Sulfides KLn₂CuS₆ (Ln = La, Ce, Pr, Nd, Sm). Inorganic Chemistry, 2018, 57, 13594-13605.	1.9	6

#	Article	IF	Citations
3982	Oxo- and Oxofluoroaluminates in the RbFâ€“Al₂O₃ System: Synthesis and Structural Characterization. Inorganic Chemistry, 2018, 57, 13702-13712.	1.9	5
3983	In Situ Formation of Graphene Stabilizes Zero-Valent Copper Nanoparticles and Significantly Enhances the Efficiency of Photocatalytic Water Splitting. ACS Sustainable Chemistry and Engineering, 2018, 6, 16876-16885.	3.2	30
3984	DFT Simulations of the Vibrational Spectrum and Hydrogen Bonds of Ice XIV. Molecules, 2018, 23, 1781.	1.7	15
3985	Simultaneous Control over Lattice Doping and Nanocluster Modification of a Hybrid CuO_x/TiO₂ Photocatalyst during Flame Synthesis for Enhancing Hydrogen Evolution. Solar Rrl, 2018, 2, 1800215.	3.1	17
3986	Chemical shift reference scale for Li solid state NMR derived by first-principles DFT calculations. Journal of Magnetic Resonance, 2018, 297, 33-41.	1.2	14
3987	Cubic Perovskite Pb(Mg_{1/3}Nb_{2/3})O₃: A Damage Tolerant, Machinable, and Thermal barrier coating material. Zeitschrift Fur Naturforschung - Section A Journal of Physical Sciences, 2018, 74, 71-81.	0.7	33
3988	Quantum Chemical Description of Solids: DFT Approach. Astrophysics and Space Science Library, 2018, , 87-94.	1.0	0
3989	BaB₂S₄: An Efficient and Air-Stable Thioborate as Infrared Nonlinear Optical Material with High Laser Damage Threshold. Chemistry of Materials, 2018, 30, 7428-7432.	3.2	67
3990	Electronic and Magnetic Properties of Bulk and Monolayer CrSi2: A First-Principle Study. Applied Sciences (Switzerland), 2018, 8, 1885.	1.3	8
3991	Raman spectra and structural peculiarities of TeO₂â€“TeO₃mixed oxides. Journal of Physics Condensed Matter, 2018, 30, 475403.	0.7	12
3992	Optical absorption driven by dynamical symmetry breaking in indium oxide. Physical Review B, 2018, 98, .	1.1	13
3993	Chemical shifts in molecular solids by machine learning. Nature Communications, 2018, 9, 4501.	5.8	170
3994	Atomistic simulation study of favored compositions of Ni-Nb-Al metallic glasses. Science China Technological Sciences, 2018, 61, 1829-1838.	2.0	6
3995	Efficient Nanoclay-Based Composite Photocatalyst: The Role of Nanoclay in Photogenerated Charge Separation. Journal of Physical Chemistry C, 2018, 122, 25900-25908.	1.5	24
3996	Multiscale in modelling and validation for solar photovoltaics. EPJ Photovoltaics, 2018, 9, 10.	0.8	6
3997	First Principle Calculation of NbC Precipitation Competition between TiC Particle and Ferrite Matrix. Journal Wuhan University of Technology, Materials Science Edition, 2018, 33, 1076-1081.	0.4	7
3998	Equation of state of the<mml:math xmlns:mml="http://www.w3.org/1998/Math/MathML"><mml:mrow><mml:mi>Î±</mml:mi><mml:mtext>â€²</mml:mtext><mml:mi>Pb</mml:mi></mml:mrow></mml:math>-<mml:math xmlns:mml="http://www.w3.org/1998/Math/MathML" mathvariant="normal">O</mml:math>and<mml:math xmlns:mml="http://www.w3.org/1998/Math/MathML"><mml:mrow><mml:mi>P</mml:mi><mml:mi>a</mml:mi><mml:mover accent="true"><mml:mn>3</mml:mn><mml:mo>Â¯</mml:mo></mml:mover></mml:mrow></mml:math>-type phases of<mml:math xmlns:mml="http://www.w3.org/1998/. Physical Review B, 2018, 98, .	1.1	7
3999	A Density Functional Theory Study on the Diffusion of Fission Gas Atoms in Uranium Dioxide. Journal of Nuclear Engineering and Radiation Science, 2018, 4, .	0.2	1

#	Article	IF	Citations
4000	A High-Throughput Study of the Electronic Structure and Physical Properties of Short-Period (GaAs)m(AlAs)n (m, n â‰¤ 10) Superlattices Based on Density Functional Theory Calculations. Nanomaterials, 2018, 8, 709.	1.9	4
4001	Understanding Phase Behavior of Nearly Energetically Equivalent Polymorphs To Achieve Controlled Crystallization for a Nav1.7 Pain Inhibitor Compound. Molecular Pharmaceutics, 2018, 15, 5072-5080.	2.3	3
4002	First-principles studies on mechanical, electronic, magnetic and optical properties of new multiferroic members BiLaFe2O6 and Bi2FeMnO6: Originated from BiFeO3. Current Applied Physics, 2018, 18, 1473-1479.	1.1	3
4003	Molybdenum-based double perovskites A2CrMoO6â^' (AÂ= Ca, Sr, Ba) as anode materials for solid oxide fuel cells. Electrochimica Acta, 2018, 290, 440-450.	2.6	29
4004	Correlation between spin transport signal and Heusler/semiconductor interface quality in lateral spin-valve devices. Physical Review B, 2018, 98, .	1.1	15
4005	Realizing Shallow Acceptor Levels in Delafossite CuAlO 2 () Surfaces by Chalcogen Doping. Physica Status Solidi - Rapid Research Letters, 2018, 12, 1800381.	1.2	2
4006	Bare and functionalized nanodiamonds in aqueous media: A theoretical study. Diamond and Related Materials, 2018, 89, 301-311.	1.8	6
4007	Modeling the Adsorption of NO and NH₃ on Fe-SSZ-13 from First-Principles: A DFT Study. Industrial & Engineering Chemistry Research, 2018, 57, 13396-13405.	1.8	16
4008	A honeycomb-like monolayer of HfO₂ and the calculation of static dielectric constant eliminating the effect of vacuum spacing. Physical Chemistry Chemical Physics, 2018, 20, 26453-26462.	1.3	29
4009	Periodic DFT study of structural transformations of cocrystal NTO/TZTN under high pressure. RSC Advances, 2018, 8, 32241-32251.	1.7	7
4010	Anionic Structure in Molten Cryoliteâ€“Alumina Systems. Journal of Physical Chemistry C, 2018, 122, 21807-21816.	1.5	11
4011	Tunable band gap of graphyne-based homo- and hetero-structures by stacking sequences, strain and electric field. Physical Chemistry Chemical Physics, 2018, 20, 26934-26946.	1.3	16
4012	Narrow-band red-emitting KZnF₃:Mn⁴⁺fluoroperovskites: insights into electronic/vibronic transition and thermal quenching behavior. Journal of Materials Chemistry C, 2018, 6, 10845-10854.	2.7	39
4013	Computational Surface Chemistry of Tetrahedral Amorphous Carbon by Combining Machine Learning and Density Functional Theory. Chemistry of Materials, 2018, 30, 7438-7445.	3.2	69
4014	Band structure interpolation using optimized local orbitals from linear-scaling density functional theory. Physical Review B, 2018, 98, .	1.1	6
4015	Rational Design of a LiNbO₃-like Nonlinear Optical Crystal, Li₂ZrTeO₆, with High Laser-Damage Threshold and Wide Mid-IR Transparency Window. Journal of the American Chemical Society, 2018, 140, 13089-13096.	6.6	108
4016	Centrosymmetric (NH₄)₂SbCl(SO₄)₂ and Non-centrosymmetric (NH₄)SbCl₂(SO₄): Synergistic Effect of Hydrogen-Bonding Interactions and Lone-Pair Cations on the Framework Structures and Macroscopic Centricities. Crystal Growth and Design, 2018, 18, 6239-6247.	1.4	71
4017	Second-order nonlinear optical properties of CuGa In1-Se2 (x = 0.54): Experimental and theoretical investigations. Solid State Sciences, 2018, 85, 1-8.	1.5	1

#	Article	IF	Citations
4018	Phonon fingerprints of CsPb₂Br₅. Journal of Physics Condensed Matter, 2018, 30, 405703.	0.7	12
4019	PbTeGeO₆: polar rosiaite-type germanate featuring a two dimensional layered structure. Dalton Transactions, 2018, 47, 16388-16392.	1.6	15
4020	A theoretical study of substitutional boronâ€“nitrogen clusters in diamond. Journal of Physics Condensed Matter, 2018, 30, 425501.	0.7	10
4021	Influence of Tm, Ho and Er dopants on the properties of Yb activated ZnTiO₃perovskite: a density functional theory insight. Materials Research Express, 2018, 5, 106202.	0.8	17
4022	Phase Modulators Based on High Mobility Ambipolar ReSe2 Field-Effect Transistors. Scientific Reports, 2018, 8, 12745.	1.6	19
4023	Thermal properties of 2:1 bismuth borate: Temperatureâ€dependent characterizations of lone electron pairs. Journal of the American Ceramic Society, 2018, 102, 2154.	1.9	2
4024	Effects of heteroatom doping on the performance of graphene in sodium-ion batteries: A density functional theory investigation. Carbon, 2018, 140, 276-285.	5.4	106
4025	Understanding SO₂ Poisoning over Different Copper Species of Cu-SAPO-34 Catalyst: A Periodic DFT Study. Journal of Physical Chemistry C, 2018, 122, 21468-21477.	1.5	26
4026	Long-Term Stability of Perovskite Solar Cells under Different Growth Conditions: A Defect-Controlled Water Diffusion Mechanism. Journal of Physical Chemistry Letters, 2018, 9, 5386-5391.	2.1	17
4027	Morphology Control Studies of MnTiO3 Nanostructures with Exposed {0001} Facets as a High-Performance Catalyst for Water Purification. ACS Applied Materials & Interfaces, 2018, 10, 31631-31640.	4.0	20
4028	n- and p-type ohmic contacts at monolayer gallium nitrideâ€“metal interfaces. Physical Chemistry Chemical Physics, 2018, 20, 24239-24249.	1.3	13
4029	Doubling the photocatalytic performance of SnO₂ by carbon coating mixed-phase particles. RSC Advances, 2018, 8, 30366-30373.	1.7	7
4030	First-principles calculations of nitrogen-doped antimony triselenide: A prospective material for solar cells and infrared optoelectronic devices. Frontiers of Physics, 2018, 13, 1.	2.4	9
4031	Exploring novel phase of tin sulfide for photon/energy harvesting materials. Solar Energy, 2018, 169, 648-657.	2.9	38
4032	Structural differences between single crystal and polycrystalline UBe13. Philosophical Magazine, 2018, 98, 2003-2017.	0.7	4
4033	Crystal structures and characterizations of two new selenite chlorides: 1D Ba2Zn(SeO3)2Cl2 and 2D BaZn2(SeO3)2Cl2. Journal of Solid State Chemistry, 2018, 265, 117-122.	1.4	4
4034	Strong Infrared Nonlinear Optical Efficiency and High Laser Damage Threshold Realized in Quaternary Alkali Metal Sulfides Na₂Ga₂MS₆ (M = Ge, Sn) Containing Mixed Nonlinear Optically Active Motifs. Inorganic Chemistry, 2018, 57, 6783-6786.	1.9	40
4035	A Cocatalyst that Stabilizes a Hydride Intermediate during Photocatalytic Hydrogen Evolution over a Rhodiumâ€Doped TiO₂ Nanosheet. Angewandte Chemie - International Edition, 2018, 57, 9073-9077.	7.2	62

#	Article	IF	Citations
4036	The simplest supramolecular helix. Chemical Communications, 2018, 54, 6012-6015.	2.2	6
4037	Assessment of conversion efficiency of Cr⁴⁺ ions by aliovalent cation additives in Cr:<scp>YAG</scp> ceramic for edge cladding. Journal of the American Ceramic Society, 2018, 101, 5098-5109.	1.9	13
4038	Exploration of new UV nonlinear optical materials in the sodiumâ€“zinc fluoride carbonate system with the discovery of a new regulation mechanism for the arrangement of [CO₃]^{2â¯} groups. Journal of Materials Chemistry C, 2018, 6, 6526-6533.	2.7	19
4039	Electronic Structure Control of Sub-nanometer 1D SnTe via Nanostructuring within Single-Walled Carbon Nanotubes. ACS Nano, 2018, 12, 6023-6031.	7.3	42
4040	Narrow Gap Semiconducting Germanium Allotrope from the Oxidation of a Layered Zintl Phase in Ionic Liquids. Journal of the American Chemical Society, 2018, 140, 6785-6788.	6.6	16
4041	First-principles investigations of crystal structures and physical properties of jadeite under various pressures. Physica B: Condensed Matter, 2018, 543, 32-37.	1.3	3
4042	New strategy for designing promising mid-infrared nonlinear optical materials: narrowing the band gap for large nonlinear optical efficiencies and reducing the thermal effect for a high laser-induced damage threshold. Chemical Science, 2018, 9, 5700-5708.	3.7	104
4043	Developing descriptors for CO₂methanation and CO₂reforming of CH₄over Al₂O₃supported Ni and low-cost Ni based alloy catalysts. Physical Chemistry Chemical Physics, 2018, 20, 15939-15950.	1.3	26
4044	Adventures in boron chemistry â€“ the prediction of novel ultra-flexible boron oxide frameworks. Faraday Discussions, 2018, 211, 569-591.	1.6	5
4045	The electronic and optical properties of carbon nitride derivatives: A first principles study. Applied Surface Science, 2018, 453, 442-448.	3.1	28
4046	Balanced design for the feasible super rocket fuels: A first-principle study on gauche CHN7 and CHN3. Journal of Molecular Graphics and Modelling, 2018, 84, 10-17.	1.3	1
4047	Structural, elastic, electronic, phonon, dielectric and optical properties of Bi3TeBO9 from first-principles calculations. Journal of Physics and Chemistry of Solids, 2018, 121, 139-144.	1.9	17
4048	Quantum Monte Carlo calculations of van der Waals interactions between aromatic benzene rings. Physical Review B, 2018, 97, .	1.1	6
4049	Doping Cu Atoms Excel as the Functional Material to Tune the Wettability for TMeNs Hard Coating. Advanced Materials Interfaces, 2018, 5, 1800391.	1.9	4
4050	On the possibility of singlet fission in crystalline quaterrylene. Journal of Chemical Physics, 2018, 148, 184101.	1.2	21
4051	Property of mono-vacancy in MAX phase M₃AC₂ (M=Ti, A=Al, Si, or Ge): First-principles calculations. Modern Physics Letters B, 2018, 32, 1850160.	1.0	4
4052	An Iron Oxychloride/Reduced Graphene Oxide Heterojunction with Enhanced Catalytic Performance as a Photoâ€Fenton Catalyst. European Journal of Inorganic Chemistry, 2018, 2018, 3080-3087.	1.0	17
4053	Insight into the physical properties of two niobium based compounds, Nb3Be and Nb3Be2, via a first principles calculation. Chinese Journal of Physics, 2018, 56, 1386-1393.	2.0	6

#	Article	IF	Citations
	M^IM^{II}P₃O₉ (M^I = Rb, M^{II} = Cd,) Tj ETQq0 0 0 rgBT /Overlo		
4054	Substitution Application in Cyclophosphate Family and Nonlinear Optical Properties. Inorganic Chemistry, 2018, 57, 7372-7379.	1.9	26
4055	Quantification of Impact Sensitivity Based on Solid-State Derived Criteria. Journal of Physical Chemistry A, 2018, 122, 5455-5463.	1.1	32
4056	Serendipitous isolation of a disappearing conformational polymorph of succinic acid challenges computational polymorph prediction. CrystEngComm, 2018, 20, 3971-3977.	1.3	19
4057	Epitaxial Growth of Well-Aligned Single-Crystalline VO₂ Micro/Nanowires Assisted by Substrate Facet Confinement. Crystal Growth and Design, 2018, 18, 3896-3901.	1.4	10
4058	Triiodide-Induced Band-Edge Reconstruction of a Lead-Free Perovskite-Derivative Hybrid for Strong Light Absorption. Chemistry of Materials, 2018, 30, 4081-4088.	3.2	52
4059	A thermodynamic description for water, hydrogen fluoride and hydrogen dissolutions in cryolite-base molten salts. Physical Chemistry Chemical Physics, 2018, 20, 17324-17341.	1.3	6
4060	Comparative Study of Hydration Kinetics of Cement and Tricalcium Silicate Using Terahertz Spectroscopy and Density Functional Theory Simulations. Journal of Infrared, Millimeter, and Terahertz Waves, 2018, 39, 651-666.	1.2	6
4061	CaCO3 phase diagram studied with Raman spectroscopy at pressures up to 50â€¯GPa and high temperatures and DFT modeling. Physics of the Earth and Planetary Interiors, 2018, 281, 31-45.	0.7	83
4062	NiO nanoparticle surface energy studies using first principles calculations. New Journal of Chemistry, 2018, 42, 10791-10797.	1.4	16
4063	Probing the interaction of noble gases with pristine and nitrogen-doped graphene through Raman spectroscopy. Physical Review B, 2018, 97, .	1.1	7
4064	NH₄Be₂BO₃F₂ and Î³â€²Be₂BO₃F: Overcoming the Layering Habit in KBe₂BO₃F₂ for the Nextâ€Generation Deepâ€Ultraviolet Nonlinear Optical Materials. Angewandte Chemie, 2018, 130, 9106-9110.	1.6	63
4065	Spectroscopic Characterization of Model Compounds, Reactants, and Byproducts Connected with an Isocyanate Production Chain. Industrial & Engineering Chemistry Research, 2018, 57, 7355-7362.	1.8	4
4066	Computation-Guided Development of Platinum Alloy Catalyst for Carbon Monoxide Preferential Oxidation. ACS Catalysis, 2018, 8, 5777-5786.	5.5	22
4067	Low dimensional solids based on Mo₆cluster cyanides and Mn²⁺, Mn³⁺or Cd²⁺metal ions: crystal chemistry, magnetic and optical properties. CrystEngComm, 2018, 20, 3396-3408.	1.3	8
4068	A Cocatalyst that Stabilizes a Hydride Intermediate during Photocatalytic Hydrogen Evolution over a Rhodiumâ€Doped TiO₂ Nanosheet. Angewandte Chemie, 2018, 130, 9211-9215.	1.6	14
4069	Research on the formation of M1-type alite doped with MgO and SO3â€”A route to improve the quality of cement clinker with a high content of MgO. Construction and Building Materials, 2018, 182, 156-166.	3.2	31
4070	First-principle study on the oxidative leaching mechanism of sphalerite in Ammoniacal solution. Hydrometallurgy, 2018, 179, 198-206.	1.8	7
4071	Lattice dynamics and thermodynamic properties of alkaline earth metal nitrates M(NO3)2 (M = Sr, Ba): A first principles study. Journal of Physics and Chemistry of Solids, 2018, 122, 268-277.	1.9	4

#	Article	IF	Citations
4072	Phase Diagram of Methane Hydrates and Discovery of MH-VI Hydrate. Journal of Physical Chemistry A, 2018, 122, 6007-6013.	1.1	5
4073	A Bifunctional MOF Catalyst Containing Metalâ€“Phosphine and Lewis Acidic Active Sites. Chemistry - A European Journal, 2018, 24, 15309-15318.	1.7	40
4074	Direct Correlation between Adsorption Energetics and Nuclear Spin Relaxation in a Liquidâ€saturated Catalyst Material. ChemPhysChem, 2018, 19, 2472-2479.	1.0	40
4075	Facile fabrication of a BiOI/TiO2 p-n junction via a surface charge-induced electrostatic self-assembly method. Applied Surface Science, 2018, 457, 59-68.	3.1	42
4076	Remarkable multimember-ring configurations in a new family of Na7MIISb5S12 (MII = Zn, Cd, Hg) exhibiting various three-dimensional tunnel structures. Chemical Communications, 2018, 54, 8269-8272.	2.2	21
4077	Synergetic effect of H and He impurities in Ti₃AlC₂: first principles calculations. Physical Chemistry Chemical Physics, 2018, 20, 18766-18774.	1.3	6
4078	Theoretical study of mechanical, thermal and optical properties of (Ti1â^'xNb x)3AlC2 solid solutions. European Physical Journal B, 2018, 91, 1.	0.6	2
4079	Fabrication, characterization and simulation of Zn-doped PbS nanopowder. Physica B: Condensed Matter, 2018, 545, 245-249.	1.3	6
4080	Electronic structure, elasticity, Debye temperature and anisotropy of cubic WO ₃ from first-principles calculation. Royal Society Open Science, 2018, 5, 171921.	1.1	26
4081	Tuning Nuclear Quadrupole Resonance: A Novel Approach for the Design of Frequency-Selective MRI Contrast Agents. Physical Review X, 2018, 8, .	2.8	8
4082	Two Novel Deepâ€Ultraviolet Nonlinear Optical Crystals with Shorter Phaseâ€Matching Second Harmonic Generation than KBe₂BO₃F₂: A Firstâ€Principles Prediction. Physica Status Solidi - Rapid Research Letters, 2018, 12, 1800276.	1.2	15
4083	Facile conversion of levulinic acid to Î³-valerolactone using a high surface area magnetically separable Ni/NiO catalyst. Sustainable Energy and Fuels, 2018, 2, 1699-1706.	2.5	26
4084	Engineering an effective noble-metal-free photocatalyst for hydrogen evolution: hollow hexagonal porous micro-rods assembled from In₂O₃@carbon coreâ€“shell nanoparticles. Journal of Materials Chemistry A, 2018, 6, 15747-15754.	5.2	75
4085	Passivating the sulfur vacancy in monolayer MoS2. APL Materials, 2018, 6, .	2.2	53
4086	Designing Deepâ€UV Birefringent Crystals by Cation Regulation. Chemistry - A European Journal, 2018, 24, 11267-11272.	1.7	47
4087	A stable C2/m phase of H₂S at 150â€“175 GPa. Japanese Journal of Applied Physics, 2018, 57, 083101.	0.8	1
4088	Covalency is Frustrating: La₂Sn₂O₇ and the Nature of Bonding in Pyrochlores under High Pressureâ€“Temperature Conditions. Inorganic Chemistry, 2018, 57, 15051-15061.	1.9	10
4089	Accurate quasiparticle calculation of x-ray photoelectron spectra of solids. Journal of Physics Condensed Matter, 2018, 30, 21LT01.	0.7	19

#	Article	IF	Citations
4090	Understanding the role of Ni-Sn interaction to design highly effective CO2 conversion catalysts for dry reforming of methane. Journal of CO2 Utilization, 2018, 27, 1-10.	3.3	68
4091	Elucidating the Structure of Ranitidine Hydrochloride Form II: Insights from Solid-State Spectroscopy and Ab Initio Simulations. Crystal Growth and Design, 2018, 18, 4671-4681.	1.4	10
4092	Two-Dimensional-Layered Perovskite ALaTa₂O₇:Bi³⁺ (A = K and Na) Phosphors with Versatile Structures and Tunable Photoluminescence. ACS Applied Materials & Interfaces, 2018, 10, 24648-24655.	4.0	91
4093	Experimental and computational investigations of the photosensitive Schottky barrier diode property of an azobenzene based small organic molecule. New Journal of Chemistry, 2018, 42, 13430-13441.	1.4	8
4094	Crystal structure and elasticity of Al-bearing phase H under high pressure. AIP Advances, 2018, 8, .	0.6	2
4095	Helium-Iron Compounds at Terapascal Pressures. Physical Review Letters, 2018, 121, 015301.	2.9	24
4096	First-principles study on the helium migration energies in B12X2 (X=O, Si, P, As) crystals for neutron absorber use. Journal of Asian Ceramic Societies, 2018, 6, 139-144.	1.0	0
4097	Mnâ€“graphene single-atom catalyst evaluated for CO oxidation by computational screening. Theoretical Chemistry Accounts, 2018, 137, 1.	0.5	42
4098	Density functional theory study of Al/NbB2 heterogeneous nucleation interface. Applied Surface Science, 2018, 456, 37-42.	3.1	39
4099	K₂TeP₂O₈: a new telluro-phosphate with a pentagonal Teâ€“Pâ€“O layer structure. Dalton Transactions, 2018, 47, 9453-9458.	1.6	20
4100	First-Principles Study of Lithium Intercalation and Diffusion in Oxygen-Defective Titanium Dioxide. Journal of Physical Chemistry C, 2018, 122, 19447-19454.	1.5	30
4101	Medium-sized ${m Si}_{n}^{-}$ (nâ€‰â€‰=â€‰â€‰14â€“20) clusters: a combined study of photoelectron spectroscopy and DFT calculations. Journal of Physics Condensed Matter, 2018, 30, 354002.	0.7	13
4102	Two-dimensional zigzag-shaped Cd₂C monolayer with a desirable bandgap and high carrier mobility. Journal of Materials Chemistry C, 2018, 6, 9175-9180.	2.7	19
4103	Tailoring nonlinear optical crystal borophosphate through the introduction of transition metal d orbitals for improving optical anisotropy and SHG response: a first-principles investigation. Materials Research Express, 2018, 5, 096204.	0.8	0
4104	Structural, elastic, mechanical and thermodynamic properties of HfB 4 under high pressure. Royal Society Open Science, 2018, 5, 180701.	1.1	10
4105	The First Examples of Lithiumâ€Containing Mixedâ€Alkali Strontium Borates with Different Dimensional Anionic Architectures and Short Cutoff Edges. Chemistry - A European Journal, 2018, 24, 15355-15364.	1.7	14
4106	Successful Computationally Directed Templating of Metastable Pharmaceutical Polymorphs. Crystal Growth and Design, 2018, 18, 5322-5331.	1.4	52
4107	High-Pressure Synthesis of Î²-Ir₄B₅ and Determination of the Compressibility of Various Iridium Borides. Inorganic Chemistry, 2018, 57, 10341-10351.	1.9	10

#	Article	IF	Citations
4108	Elasticity of high-entropy alloys from ab initio theory. Journal of Materials Research, 2018, 33, 2938-2953.	1.2	38
4109	Atomic-level insight into super-efficient electrocatalytic oxygen evolution on iron and vanadium co-doped nickel (oxy)hydroxide. Nature Communications, 2018, 9, 2885.	5.8	669
4110	(1,4-Butyldiammonium)CdBr₄: a layered organicâ€“inorganic hybrid perovskite with a visible-blind ultraviolet photoelectric response. Inorganic Chemistry Frontiers, 2018, 5, 2450-2455.	3.0	17
4111	First-principles calculations of structural, electronic, magnetic and elastic properties of Mo₂FeB₂under high pressure. Royal Society Open Science, 2018, 5, 172247.	1.1	7
4112	Investigations of Uranyl Fluoride Sesquihydrate (UO2F2·1.57H2O): Combining 19F Solid-State MAS NMR Spectroscopy and GIPAW Chemical Shift Calculations. Journal of Physical Chemistry A, 2018, 122, 6873-6878.	1.1	11
4113	Module-Guided Design Scheme for Deep-Ultraviolet Nonlinear Optical Materials. Journal of the American Chemical Society, 2018, 140, 10726-10733.	6.6	127
4114	Hierarchical tandem assembly of planar [3—3] building units into {3—[3—3]} oligomers: mixed-valency, electrical conductivity and magnetism. Chemical Science, 2018, 9, 7498-7504.	3.7	23
4115	Can an element form a two-dimensional nanosheet of type 15 pentagons?. Computational Materials Science, 2018, 154, 37-40.	1.4	34
4116	High-Performance Silicon-Compatible Large-Area UV-to-Visible Broadband Photodetector Based on Integrated Lattice-Matched Type II Se/n-Si Heterojunctions. Nano Letters, 2018, 18, 4697-4703.	4.5	212
4117	First principles calculation of the nonhydrostatic effects on structure and Raman frequency of 3C-SiC. Scientific Reports, 2018, 8, 11279.	1.6	4
4118	Electronic and mechanical properties of C/Si phases with sp2 and sp3 hybridization: A first-principles study. AIP Advances, 2018, 8, 075326.	0.6	0
4119	Shallow electron traps formed by Gd2+ ions adjacent to oxygen vacancies in cerium-doped Gd3Al2Ga3O12 crystals. Applied Physics Letters, 2018, 113, 041906.	1.5	11
4120	First-principles hydrogen adsorption properties of Li-decorated ThMoB4-type graphene. International Journal of Hydrogen Energy, 2018, 43, 16117-16127.	3.8	10
4121	Scaleâ€Up Biomass Pathway to Cobalt Singleâ€Site Catalysts Anchored on Nâ€Doped Porous Carbon Nanobelt with Ultrahigh Surface Area. Advanced Functional Materials, 2018, 28, 1802167.	7.8	112
4122	Roads to pentazolate anion: a theoretical insight. Royal Society Open Science, 2018, 5, 172269.	1.1	10
4123	Structural, Mechanical, Anisotropic, and Thermal Properties of AlAs in oC12 and hP6 Phases under Pressure. Materials, 2018, 11, 740.	1.3	12
4124	A Pathway to the Athermal Impact Initiation of Energetic Azides. Journal of Physical Chemistry C, 2018, 122, 19395-19408.	1.5	26
4125	Becquerelite mineral phase: crystal structure and thermodynamic and mechanical stability by using periodic DFT. RSC Advances, 2018, 8, 24599-24616.	1.7	36

#	Article	IF	Citations
4126	Native point defects of semiconducting layered Bi2O2Se. Scientific Reports, 2018, 8, 10920.	1.6	31
4127	Introducing Magnetism into 2D Nonmagnetic Inorganic Layered Crystals: A Brief Review from First-Principles Aspects. Crystals, 2018, 8, 24.	1.0	17
4128	Synthesis, Crystal Structures, Optical Properties and Theoretical Calculations of Two Metal Chalcogenides Ba2AlSbS5 and Ba2GaBiSe5. Crystals, 2018, 8, 165.	1.0	8
4129	Investigation of the Preferential Doping Site and Regulating on the Visible Light Response and Redox Performance for Fe- and/or La-Doped InNbO₄. Inorganic Chemistry, 2018, 57, 8558-8567.	1.9	10
4130	Plasmonic gold deposited on mesoporous Ti Si1â^'O2 with isolated silica in lattice: An excellent photocatalyst for photocatalytic conversion of CO2 into methanol under visible light irradiation. Journal of CO2 Utilization, 2018, 27, 11-21.	3.3	28
4131	A two-phase Hessian approach improves the DFT relaxation of slabs. Journal of Physics Condensed Matter, 2018, 30, 315901.	0.7	0
4132	DFT Insights into the Role of Relative Positions of Fe and N Dopants on the Structure and Properties of TiO2. Materials, 2018, 11, 313.	1.3	8
4133	Structural, Electronic, and Thermodynamic Properties of Tetragonal t-SixGe3â^'xN4. Materials, 2018, 11, 397.	1.3	7
4134	Anisotropic-Cyclicgraphene: A New Two-Dimensional Semiconducting Carbon Allotrope. Materials, 2018, 11, 432.	1.3	11
4135	Atomistic Simulations to Predict Favored Glass-Formation Composition and Ion-Beam-Mixing of Nano-Multiple-Metal-Layers to Produce Ternary Amorphous Films. Metals, 2018, 8, 129.	1.0	2
4136	Structural and Electronic Properties of Different Terminations for Quartz (001) Surfaces as Well as Water Molecule Adsorption on It: A First-Principles Study. Minerals (Basel, Switzerland), 2018, 8, 58.	0.8	27
4137	Understanding Cationic Polymer Adsorption on Mineral Surfaces: Kaolinite in Cement Aggregates. Minerals (Basel, Switzerland), 2018, 8, 130.	0.8	14
4138	Charged Si₉ Clusters in Neat Solids and the Detection of [H₂Si₉]^{2â^'} in Solution: A Combined NMR, Raman, Mass Spectrometric, and Quantum Chemical Investigation. Angewandte Chemie - International Edition, 2018, 57, 12950-12955.	7.2	28
4139	Interfacial stability, electronic property, and surface reactivity of Î±-MoO3/Î³-Al2O3 composites: DFT and DFTâ€ +â€U calculations. Computational Materials Science, 2018, 153, 217-227.	1.4	8
4140	Two noncentrosymmetric polyphosphates featuring infinite one-dimensional (PO3)â^ž chain, LiMP2O6 (M = Rb, Cs): Synthesis, structure and optical properties. Journal of Solid State Chemistry, 2018, 266, 150-154.	1.4	6
4141	Effect of aromatic nitrogen heterocycle treatment on the performance of perovskite solar cells. Japanese Journal of Applied Physics, 2018, 57, 08RE08.	0.8	3
4142	Theoretical investigation of sodium capture mechanism on kaolinite surfaces. Fuel, 2018, 234, 318-325.	3.4	29
4143	Inâ€situ highâ€temperature Raman spectroscopic studies of the vibrational characteristics and microstructure evolution of sodium tungstate dihydrate crystal during heating and melting. Journal of Raman Spectroscopy, 2018, 49, 1693-1705.	1.2	15

#	Article	IF	Citations
4144	Surface Segregation of NbAl3 Alloys by Boron Doping. Physica Status Solidi - Rapid Research Letters, 2018, 12, 1800168.	1.2	3
4145	Vibrational entropy of disorder in Cu₃Au with different degrees of short-range order. Physical Chemistry Chemical Physics, 2018, 20, 19441-19446.	1.3	5
4146	Structure and Optical Properties of the Li₂In₂GeSe₆ Crystal. Journal of Physical Chemistry C, 2018, 122, 17413-17422.	1.5	11
4147	Efficient Strategy for Determining the Atomic-Resolution Structure of Micro- and Nanocrystalline Solids within Polymeric Microbeads: Domain-Edited NMR Crystallography. Macromolecules, 2018, 51, 5364-5374.	2.2	18
4148	Advantageous Units in Antimony Sulfides: Exploration and Design of Infrared Nonlinear Optical Materials. ACS Applied Materials & Interfaces, 2018, 10, 26413-26421.	4.0	77
4149	Molecular Layer Deposition Using Ring-Opening Reactions: Molecular Modeling of the Film Growth and the Effects of Hydrogen Peroxide. ACS Omega, 2018, 3, 7141-7149.	1.6	10
4150	K₂ZnGe₃S₈: A Congruent-Melting Infrared Nonlinear-Optical Material with a Large Band Gap. Inorganic Chemistry, 2018, 57, 9446-9452.	1.9	31
4151	Relation between image charge and potential alignment corrections for charged defects in periodic boundary conditions. Journal of Chemical Physics, 2018, 149, 024103.	1.2	57
4152	Expanding Frontiers of Ultraviolet Nonlinear Optical Materials with Fluorophosphates. Chemistry of Materials, 2018, 30, 5397-5403.	3.2	193
4153	Open-Resonance-Assisted Hydrogen Bonds and Competing Quasiaromaticity. Journal of Organic Chemistry, 2018, 83, 9850-9857.	1.7	13
4154	Achieving Large Volumetric Gas Storage Capacity in Metalâ€“Organic Frameworks by Kinetic Trapping: A Case Study of Xenon Loading in MFU-4. Journal of the American Chemical Society, 2018, 140, 10191-10197.	6.6	46
4155	On the mechanical properties of novamene: A fully atomistic molecular dynamics and DFT investigation. Carbon, 2018, 139, 782-788.	5.4	18
4156	Development of persistent phosphor of Eu2+ doped Ba2SiO4 by Er3+ codoping based on vacuum referred binding energy diagram. Optical Materials, 2018, 84, 436-441.	1.7	14
4157	Vibrational assignments and thermodynamic properties of triclinic TATB. Physica B: Condensed Matter, 2018, 546, 1-9.	1.3	5
4158	Simultaneous dispersive and covalent monolayer MoS2/TiO2 cluster heterostructures: Insights into their enhanced photocatalytic activity. Superlattices and Microstructures, 2018, 121, 64-74.	1.4	0
4159	Mo⁶⁺ Cation Enrichment of the Structure Chemistry of Iodates: Syntheses, Structures, and Calculations of Ba(MoO₂)₂(IO₃)₄O, Ba₃[(MoO₂)₂(IO₃)₄O(OH)₄]Â·2H₂O, and Sr[(MoO₂)₆(IO₄)₂O₄]Â·H₂O. Inorganic Chemistry, 2018, 57, 9376-9387.	1.9	21
4160	Molecular Deformation, Charge Flow, and Spongelike Behavior in Anionâ€“Ï€ {[M(CN)₄]^{2â^’};[HAT(CN)₆]}_{â^ž} (M=Ni, Pd, Pt) Supramolecular Stacks. Chemistry - A European Journal, 2018, 24, 16302-16314.	1.7	10
4161	Complete assignment of the vibrational spectra of borazine: the inorganic benzene. RSC Advances, 2018, 8, 23875-23880.	1.7	6

#	Article	IF	Citations
4162	Supramolecular Organization of Nonstoichiometric Drug Hydrates: Dapsone. Frontiers in Chemistry, 2018, 6, 31.	1.8	23
4163	The Anisotropic Thermal Expansion of Non-linear Optical Crystal BaAlBO3F2 Below Room Temperature. Frontiers in Chemistry, 2018, 6, 252.	1.8	1
4164	Proton transfer in guanineâ€“cytosine base pair analogues studied by NMR spectroscopy and PIMD simulations. Faraday Discussions, 2018, 212, 331-344.	1.6	28
4165	The structure and elasticity of phase B silicates under high pressure by first principles simulation. Chinese Physics B, 2018, 27, 047402.	0.7	2
4166	First-principles study of Cu adsorption on vacancy-defected/Au-doped graphene. Modern Physics Letters B, 2018, 32, 1850139.	1.0	14
4167	Ag-Nb nanoscale multilayer study by global energy minimization. Computational Materials Science, 2018, 150, 96-101.	1.4	1
4168	An Integrated Design with new Metalâ€Functionalized Covalent Organic Frameworks for the Effective Electroreduction of CO₂. Chemistry - A European Journal, 2018, 24, 11051-11058.	1.7	45
4169	A Stable, Narrow-Gap Oxyfluoride Photocatalyst for Visible-Light Hydrogen Evolution and Carbon Dioxide Reduction. Journal of the American Chemical Society, 2018, 140, 6648-6655.	6.6	139
4170	Exfoliation of a non-van der Waals material from iron ore hematite. Nature Nanotechnology, 2018, 13, 602-609.	15.6	295
4171	Evolutionary structure prediction of two-dimensional IrB₁₄: a promising gas sensor material. Journal of Materials Chemistry C, 2018, 6, 5803-5811.	2.7	13
4172	Four alkali metal molybdates with two types of Moâ€“O chains, ABMo₃O₁₀ (A =) Tj ETQq0 0 0 rgBT /Overlock Chemistry, 2018, 42, 10879-10884.	1.4	6
4173	Lithium effect on the electronic properties of porous silicon for energy storage applications: a DFT study. Dalton Transactions, 2018, 47, 7505-7514.	1.6	12
4174	X-ray absorption spectroscopy study on SiC-side interface structure of SiO₂â€“SiC formed by thermal oxidation in dry oxygen. Japanese Journal of Applied Physics, 2018, 57, 060308.	0.8	8
4175	NH₄Be₂BO₃F₂ and Î³â€Be₂BO₃F: Overcoming the Layering Habit in KBe₂BO₃F₂ for the Nextâ€Generation Deepâ€Ultraviolet Nonlinear Optical Materials. Angewandte Chemie - International Edition, 2018, 57, 8968-8972.	7.2	200
4176	Synthesis, characterization and use of highly stable trimethyl sulfonium tin(IV) halide defect perovskites in dye sensitized solar cells. Polyhedron, 2018, 150, 83-91.	1.0	31
4177	Structural and electronic properties of low-index stoichiometric Cu2ZnSnS4 surfaces. Materials Research Express, 2018, 5, 055902.	0.8	4
4178	Interfacial properties and band alignment of noble-metal/anatase TiO2(1â€¯0â€¯1) hetero-structures. Computational Materials Science, 2018, 151, 160-173.	1.4	9
4179	Novel pK_a/DFT-Based Theoretical Model for Predicting the Drug Loading and Release of a pH-Responsive Drug Delivery System. Journal of Physical Chemistry C, 2018, 122, 12279-12290.	1.5	11

#	Article	IF	Citations
4180	Extending lead-free hybrid photovoltaic materials to new structures: thiazolium, aminothiazolium and imidazolium iodobismuthates. Dalton Transactions, 2018, 47, 7050-7058.	1.6	34
4181	Conformational Space of (1R,2S)-Dimethyl-Ephedrinium and (1S,2S)-Dimethyl-Pseudoephedrinium in the Synthesis of Nanoporous Aluminophosphates. Journal of Physical Chemistry C, 2018, 122, 20377-20390.	1.5	9
4182	Structural, mechanical and Raman spectroscopic characterization of the layered uranyl silicate mineral, uranophane-Î±, by density functional theory methods. Clay Minerals, 2018, 53, 377-392.	0.2	20
4183	High-pressure behavior and Hirshfeld surface analysis of nitrogen-rich materials: triazido-s-triazine (TAT) and triazido-s-heptazine (TAH). Journal of Materials Science, 2018, 53, 15977-15985.	1.7	6
4184	Bulk Crystal Growth, First-Principles Calculations, and Mid-Infrared Spectral Properties of Dy3+ Doped and Dy3+/Nd3+ Codoped LaF3 Single Crystals. Crystal Growth and Design, 2018, 18, 5981-5990.	1.4	16
4185	Applicability of Molybdite as an Electrode Material in Calcium Batteries: A Structural Study of Layer-type Ca_xMoO₃. Chemistry of Materials, 2018, 30, 5853-5861.	3.2	63
4186	Enhanced Photosensitive Schottky Diode Behavior of Pyrazine over 2-Aminopyrimidine Ligand in Copper(II)-Phthalate MOFs: Experimental and Theoretical Rationalization. ACS Omega, 2018, 3, 9160-9171.	1.6	26
4187	Improving coloration time and moisture stability of photochromic viologenâ€“carboxylate zwitterions. New Journal of Chemistry, 2018, 42, 15466-15471.	1.4	18
4188	Stability and superconductivity properties of metal substituted aluminum diborides (M0.5Al0.5B2). Computational Materials Science, 2018, 154, 234-242.	1.4	6
4189	Lead Bismuth Oxyhalides PbBiO₂X (X = Cl, Br) as Visible-Light-Responsive Photocatalysts for Water Oxidation: Role of Lone-Pair Electrons in Valence Band Engineering. Chemistry of Materials, 2018, 30, 5862-5869.	3.2	82
4190	Design and Development of a Bluish-Green Luminescent Material (K₂HfSi₃O₉:Eu²⁺) with Robust Thermal Stability for White Light-Emitting Diodes. ACS Photonics, 2018, 5, 3801-3813.	3.2	87
4191	Greater diffusion rate of carbon atoms from nonlinear migration in micro-cell and spatially heterogeneous stable states in FCC iron. Journal of Materials Science, 2018, 53, 15952-15968.	1.7	2
4192	Benchmarking of GGA density functionals for modeling structures of nanoporous, rigid and flexible MOFs. Journal of Chemical Physics, 2018, 149, 064110.	1.2	23
4193	Quantum Monte Carlo calculations of energy gaps from first principles. Physical Review B, 2018, 98, .	1.1	35
4194	Adduct-Type IR Nonlinear-Optical Crystal SbI₃Â·(S₈)₃ with a Large Second-Harmonic Generation and a High Laser-Induced Damage Threshold. Inorganic Chemistry, 2018, 57, 11282-11288.	1.9	39
4195	Achieving superior cycling stability byin situforming NdH₂â€“Mgâ€“Mg₂Ni nanocomposites. Journal of Materials Chemistry A, 2018, 6, 23308-23317.	5.2	67
4196	Charged Si₉ Clusters in Neat Solids and the Detection of [H₂Si₉]^{2â^'} in Solution: A Combined NMR, Raman, Mass Spectrometric, and Quantum Chemical Investigation. Angewandte Chemie, 2018, 130, 13132-13137.	1.6	12
4197	Exploring Multifunctional Applications of Hexagonal Boron Arsenide Sheet: A DFT Study. ACS Omega, 2018, 3, 9533-9543.	1.6	35

#	Article	IF	Citations
4198	Significance of crystal habit sphericity in the determination of the impact sensitivity of bistetrazole-based energetic salts. CrystEngComm, 2018, 20, 5718-5725.	1.3	16
4199	Magnetic phases of skyrmion-hosting 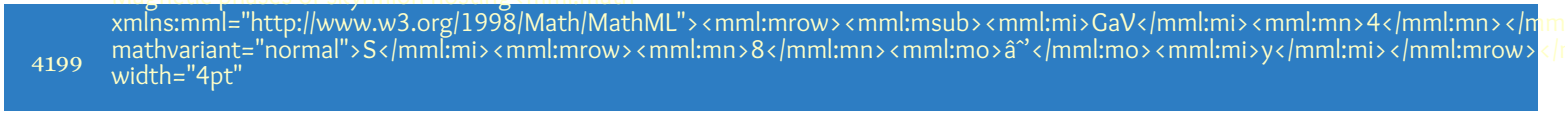		

#	Article	IF	Citations
4216	Low temperature synthesis of BiFeO₃nanoparticles with enhanced magnetization and promising photocatalytic performance in dye degradation and hydrogen evolution. RSC Advances, 2018, 8, 29613-29627.	1.7	57
4217	Experimental and theoretical study of Raman scattering spectra of ternary chalcogenides Tl₄HgI₆, Tl₄HgBr₆, and TlHgCl₃. Journal of Raman Spectroscopy, 2018, 49, 1840-1848.	1.2	7
4218	Watermelonâ€Like Structured SiO_xâ€“TiO₂@C Nanocomposite as a Highâ€Performance Lithiumâ€Ion Battery Anode. Advanced Functional Materials, 2018, 28, 1605711.	7.8	175
4219	From LiB₃O₅ to NaRbB₆O₉F₂: Fluorineâ€Directed Evolution of Structural Chemistry. Chemistry - A European Journal, 2018, 24, 10022-10027.	1.7	30
4220	Enhancing the Sensitivity of Solid-State NMR Experiments with Very Low Gyromagnetic Ratio Nuclei with Fast Magic Angle Spinning and Proton Detection. Journal of Physical Chemistry A, 2018, 122, 5635-5643.	1.1	26
4221	A Fluorooxosilicophosphate with an Unprecedented SiO₂F₄ Species. Angewandte Chemie - International Edition, 2018, 57, 9828-9832.	7.2	40
4222	Structural, electronic and optical properties of model silicon quantum dots: A computational study. Physica E: Low-Dimensional Systems and Nanostructures, 2018, 103, 194-200.	1.3	1
4223	New Phase of Ca(BH₄)₂ at Near Ambient Conditions. Journal of Physical Chemistry C, 2018, 122, 14272-14276.	1.5	5
4224	First-principles investigation of neutron-irradiation-induced point defects in B4C, a neutron absorber for sodium-cooled fast nuclear reactors. Japanese Journal of Applied Physics, 2018, 57, 055801.	0.8	14
4225	Copolymerization of CO and N₂ to Extended CON₂ Framework Solid at High Pressures. Journal of Physical Chemistry C, 2018, 122, 13054-13060.	1.5	18
4226	Mapping uncharted territory in iceÂfrom zeolite networks to ice structures. Nature Communications, 2018, 9, 2173.	5.8	57
4227	Oxygen vacancy induces self-doping effect and metalloid LSPR in non-stoichiometric tungsten suboxide synergistically contributing to the enhanced photoelectrocatalytic performance of WO_{3â^'x}/TiO_{2â^'x}heterojunction. Physical Chemistry Chemical Physics, 2018, 20, 17268-17278.	1.3	44
4228	Porous aluminophosphates as adsorbents for the separation of CO₂/CH₄and CH₄/N₂mixtures â€“ a Monte Carlo simulation study. Sustainable Energy and Fuels, 2018, 2, 1749-1763.	2.5	14
4229	Structural, electronic and vibrational properties of LaF₃ according to density functional theory and Raman spectroscopy. Journal of Physics Condensed Matter, 2018, 30, 255901.	0.7	5
4230	Nitrogenâ€Doped Grapheneâ€Supported Mixed Transitionâ€Metal Oxide Porous Particles to Confine Polysulfides for Lithiumâ€“Sulfur Batteries. Advanced Energy Materials, 2018, 8, 1800595.	10.2	151
4231	Micro-structure studies of the molten binary K₃AlF₆â€“Al₂O₃system byin situhigh temperature Raman spectroscopy and theoretical simulation. Inorganic Chemistry Frontiers, 2018, 5, 1861-1868.	3.0	37
4232	Hydrogen Evolution Catalyzed by a Molybdenum Sulfide Two-Dimensional Structure with Active Basal Planes. ACS Applied Materials & Interfaces, 2018, 10, 22042-22049.	4.0	22
4233	A Facetâ€Dependent Schottkyâ€Junction Electron Shuttle in a BiVO₄{010}â€“Auâ€“Cu₂O Zâ€Scheme Photocatalyst for Efficient Charge Separation. Advanced Functional Materials, 2018, 28, 1801214.	7.8	193

#	Article	IF	Citations
4234	Optical Properties of Cu₂ZnSn(S_xSe_{1â€x})₄ by Firstâ€Principles Calculations. Physica Status Solidi (A) Applications and Materials Science, 2018, 215, 1700945.	0.8	4
4235	Nanoscale momentum-resolved vibrational spectroscopy. Science Advances, 2018, 4, eaar7495.	4.7	111
4236	Density Functional Theory â€“ Machine Learning Approach to Analyze the Bandgap of Elemental Halide Perovskites and Ruddlesdenâ€Popper Phases. ChemPhysChem, 2018, 19, 2559-2565.	1.0	27
4237	Structure and Metallicity of Phase V of Hydrogen. Physical Review Letters, 2018, 120, 255701.	2.9	54
4238	A Fluorooxosilicophosphate with an Unprecedented SiO₂F₄ Species. Angewandte Chemie, 2018, 130, 9976-9980.	1.6	5
4239	Sodiation and Desodiation via Helical Phosphorus Intermediates in High-Capacity Anodes for Sodium-Ion Batteries. Journal of the American Chemical Society, 2018, 140, 7994-8004.	6.6	85
4240	Optical properties of Cs adsorbed wurtzite GaAs nanowires by first-principles study. Materials Research Express, 2018, 5, 065047.	0.8	4
4241	Pressure and Strain Effects on the Structural, Electronic, and Optical Properties of K4 Phosphorus. Zeitschrift Fur Naturforschung - Section A Journal of Physical Sciences, 2018, 73, 661-668.	0.7	3
4242	Investigations on ferromagnetism of Li and Mn codoped LiZnN by firstâ€principles calculations. Journal of the American Ceramic Society, 2019, 102, 303-309.	1.9	2
4243	The use of variable temperature <scp>¹³C</scp> solidâ€state <scp>MAS NMR</scp> and <scp>GIPAW DFT</scp> calculations to explore the dynamics of diethylcarbamazine citrate. Magnetic Resonance in Chemistry, 2019, 57, 200-210.	1.1	9
4244	Effect of Fe and Ti Substitution Doping on Magnetic Property of Monolayer CrSi2: a First-Principle Investigation. Journal of Superconductivity and Novel Magnetism, 2019, 32, 1341-1346.	0.8	4
4245	Formation energy and diffusion barrier of point defects in three uranium compounds as nuclear fuels. Nuclear Instruments & Methods in Physics Research B, 2019, 450, 114-117.	0.6	2
4246	Enhancing temperature stability in potassium-sodium niobate ceramics through phase boundary and composition design. Journal of the European Ceramic Society, 2019, 39, 305-315.	2.8	43
4247	Novel fluorescent label based on YVO4: Bi3+, Eu3+ for latent fingerprint detection. Dyes and Pigments, 2019, 160, 555-562.	2.0	48
4248	Comparative study of polytype 2H-MoS2 and 3R-MoS2 systems by employing DFT. Physica E: Low-Dimensional Systems and Nanostructures, 2019, 106, 338-345.	1.3	30
4249	Sr[B(OH)₄](IO₃) and Li₄Sr₅[B₁₂O₂₂(OH)₄](IO₃)₂: two unprecedented metal borate-iodates showing a subtle balance of enlarged band gap and birefringence. Chemical Communications, 2019, 55, 11139-11142.	2.2	29
4250	Structure-property correlation studies of alkaline-earth metalâ€”azides M(N₃)₂(Mâ€‰â€‰=â€‰â€‰Sr, Ba). Journal of Physics Condensed Matter, 2019, 31, 475402.	0.7	1
4251	DFT + U studies of the electronic and optical properties of ReS₂ mono-layer doped with lanthanide atoms. Materials Research Express, 2019, 6, 106307.	0.8	10

#	Article	IF	Citations
4252	Brownmillerite-Type Sr₂ScGaO₅ Oxide Ion Conductor: Local Structure, Phase Transition, and Dynamics. Chemistry of Materials, 2019, 31, 7395-7404.	3.2	16
4253	Chemisorption of NO₂ on V-Based SCR Catalysts: A Fundamental Study toward the Mechanism of â€œFast SCRâ€•Reaction. Journal of Physical Chemistry C, 2019, 123, 20451-20458.	1.5	24
4254	Pressure effects on mechanical and electronic properties of metallic C14 by first-principles calculation. International Journal of Modern Physics B, 2019, 33, 1950193.	1.0	0
4255	A Prolific Solvate Former, Galunisertib, under the Pressure of Crystal Structure Prediction, Produces Ten Diverse Polymorphs. Journal of the American Chemical Society, 2019, 141, 13887-13897.	6.6	109
4256	Effect of Phase Transition on Optical Properties and Photovoltaic Performance in Cesium Lead Bromine Perovskite: A Theoretical Study. Journal of Physical Chemistry C, 2019, 123, 20764-20768.	1.5	2
4257	Fast Ionic Conductivity in the Most Lithium-Rich Phosphidosilicate Li₁₄SiP₆. Journal of the American Chemical Society, 2019, 141, 14200-14209.	6.6	49
4258	Experimental and first-principles DFT studies on the band gap behaviours of microsized and nanosized Zn_(1â^'x)Mn_xO materials. Physical Chemistry Chemical Physics, 2019, 21, 19126-19146.	1.3	5
4259	Pb₇F₁₂Cl₂: a promising infrared nonlinear optical material with high laser damage threshold. Dalton Transactions, 2019, 48, 13529-13535.	1.6	13
4260	Step-wise transitions of electrons between valence and conduction bands: a tri-doped TiO2 approach. Materials Research Express, 2019, 6, 105515.	0.8	0
4261	Influence of Anion Charge on Li Ion Diffusion in a New Solid-State Electrolyte, Li₃LaI₆. Chemistry of Materials, 2019, 31, 7425-7433.	3.2	71
4262	First principles study of interactions of oxygenâ€“carbonâ€“vacancy in bcc Fe*. Chinese Physics B, 2019, 28, 106102.	0.7	0
4263	Effects of non-stoichiometry on electronic structure of Cu_xS_y compounds studied by first-principle calculations. Materials Research Express, 2019, 6, 105513.	0.8	14
4264	Emergence of magnetism in bulk amorphous palladium. Physical Review B, 2019, 100, .	1.1	7
4265	Development of Alâ€“Nbâ€“B master alloy with high Nb/B ratio for grain refinement of hypoeutectic Alâ€“Si cast alloys. Journal of Materials Science, 2019, 54, 14561-14576.	1.7	55
4266	Localized exciton emission in CsPbBr₃nanocrystals synthesized with excess bromide ions. Journal of Materials Chemistry C, 2019, 7, 10783-10788.	2.7	8
4267	Facile Growth of an Ultraviolet Hydroisocyanurate Crystal with Strong Nonlinearity and a Wide Phase-Matching Region from Ï€-Conjugated (HC₃N₃O₃)^{2â“} Groups. Inorganic Chemistry, 2019, 58, 11289-11293.	1.9	34
4268	The partial dehydrogenation of aluminium dihydrides. Chemical Science, 2019, 10, 8083-8093.	3.7	11
4269	Alkaline Earth Metalâ€“Organic Frameworks with Tailorable Ion Release: A Path for Supporting Biomineralization. ACS Applied Materials & Interfaces, 2019, 11, 32739-32745.	4.0	30

#	Article	IF	Citations
4270	Experimental and computational approaches to produce and characterise isostructural solvates. CrystEngComm, 2019, 21, 5533-5545.	1.3	18
4271	Phenethylammonium bismuth halides: from single crystals to bulky-organic cation promoted thin-film deposition for potential optoelectronic applications. Journal of Materials Chemistry A, 2019, 7, 20733-20741.	5.2	38
4272	Structural, elastic, thermal and lattice dynamic properties of new 321 MAX phases. Computational Materials Science, 2019, 170, 109144.	1.4	34
4273	Physical Properties of Group 14 in P6₂22 Phase: First-Principles Calculations*. Communications in Theoretical Physics, 2019, 71, 1036.	1.1	11
4274	From Electronic Structure to Design Principles for Photocathodes: <mml:math xmlns:mml="http://www.w3.org/1998/Math/MathML" display="inline" overflow="scroll"><mml:mi>Cu</mml:mi></mml:math> - <mml:math xmlns:mml="http://www.w3.org/1998/Math/MathML" display="inline" overflow="scroll"><mml:mi>Ba</mml:mi></mml:math> Alloys. Physical Review Applied, 2019, 11, .	1.5	2
4275	Structural and Optoelectronic Properties of the Î±-, Î²-, and Î³-Glycine Polymorphs and the Glycine Dihydrate Crystal: A DFT Study. Crystal Growth and Design, 2019, 19, 5204-5217.	1.4	13
4276	Strong-field nonlinear optical properties of monolayer black phosphorus. Nanoscale, 2019, 11, 16377-16383.	2.8	18
4277	Extended layer-by-layer Madelung potential analysis of layered oxyhalide photocatalysts and other layered systems. Journal of Materials Chemistry A, 2019, 7, 19846-19851.	5.2	13
4278	Continuous-time quantum Monte Carlo solver for dynamical mean field theory in the compact Legendre representation. Physical Review B, 2019, 99, .	1.1	9
4279	First-principles study of the structural, electronic, magnetic, elastic and optical properties of CoFeZrSi1â^'xGex(x = 0.00, 0.25, 0.50, 0.75, 1.00). International Journal of Modern Physics B, 2019, 33, 1950158.	1.0	4
4280	First-principles calculations of structural, mechanical and electronic properties of TiNi-X (X=C, Si, Ge,) Tj ETQq0 0 0 rgBT /Overlock 10 Tf	1.0	8
4281	Intermetallic M Pt₃ (M = Ti, Zr, Hf): Elastic, electronic, optical and thermal properties. International Journal of Modern Physics B, 2019, 33, 1950189.	1.0	10
4282	Effects of Strain on the Half-Metallic and Elastic Properties of FeCrTe and CoCrSi with Cl_b Structure. Spin, 2019, 09, .	0.6	7
4283	The Zn accumulation behavior, phase evolution and void formation in Sn-xZn/Cu systems by considering trace Zn: a combined experimental and theoretical study. Journal of Materials Research and Technology, 2019, 8, 4141-4150.	2.6	43
4284	MgH₂/Cu_xO Hydrogen Storage Composite with Defect-Rich Surfaces for Carbon Dioxide Hydrogenation. ACS Applied Materials & Interfaces, 2019, 11, 31009-31017.	4.0	37
4285	Chemical Bonding Construction of Reduced Graphene Oxide-Anchored Few-Layer Bismuth Oxychloride for Synergistically Improving Sodium-Ion Storage. Chemistry of Materials, 2019, 31, 7311-7319.	3.2	44
4286	Comparative study of negative electron affinity GaAs nanowire photocathodes with Cs/O and with Cs/NF 3 from firstâ€principles. International Journal of Energy Research, 2019, 43, 7477.	2.2	3
4287	Structural phase transitions in malononitrile, CH2(CN)2: crystal structure of the Î´ phase by neutron powder diffraction, and ab initio calculations of the structures and phonons of the Î± and Î´ phases. Journal of Physics Condensed Matter, 2019, 31, 255401.	0.7	0

#	Article	IF	Citations
4288	Insight into silicon-carbon multilayer films as anode materials for lithium-ion batteries: A combined experimental and first principles study. Acta Materialia, 2019, 178, 173-178.	3.8	29
4289	First-principles studies on electronic structures of superatomic compounds [Co6Se8(PMe3)6][C60] in several cubic structures. Results in Physics, 2019, 15, 102595.	2.0	0
4290	A red-emitting Sr₃La_(1â^'x)Eu_x(AlO)₃(BO₃)₄ phosphor with high thermal stability and color purity for near-UV-excited wLEDs. RSC Advances, 2019, 9, 26364-26372.	1.7	15
4291	Spontaneous proton transfer in a series of amphoteric molecules under hydrostatic pressure. Physical Chemistry Chemical Physics, 2019, 21, 17696-17702.	1.3	10
4292	The (Current) Acridine Solid Form Landscape: Eight Polymorphs and a Hydrate. Crystal Growth and Design, 2019, 19, 4884-4893.	1.4	16
4293	Computational Design of Novel Hydrogen-Doped, Oxygen-Deficient Monoclinic Zirconia with Excellent Optical Absorption and Electronic Properties. Scientific Reports, 2019, 9, 10159.	1.6	26
4294	Synthesis and structure of a new mixed metal iodate Ba₃Ga₂(IO₃)₁₂. CrystEngComm, 2019, 21, 4981-4986.	1.3	14
4295	Electron affinity of boron-terminated diamond (001) surfaces: a density functional theory study. Journal of Materials Chemistry C, 2019, 7, 9756-9765.	2.7	24
4296	Computing the self-consistent field in Kohnâ€“Sham density functional theory. Journal of Physics Condensed Matter, 2019, 31, 453001.	0.7	38
4297	Two-Dimensional Cobaltporphyrin-based Cobaltâ€“Organic Framework as an Efficient Photocatalyst for CO₂ Reduction Reaction: A Computational Study. ACS Sustainable Chemistry and Engineering, 2019, 7, 14102-14110.	3.2	48
4298	Computational Modeling for Biomimetic Sensors. Methods in Molecular Biology, 2019, 2027, 195-210.	0.4	4
4299	Polymorphic Transformation of Drugs Induced by Glycopolymeric Vesicles Designed for Anticancer Therapy Probed by Solid-State NMR Spectroscopy. ACS Applied Materials & Interfaces, 2019, 11, 28278-28288.	4.0	17
4300	A₂Bi₂(SO₄)₂Cl₄(A = NH₄, K,) Tj ETQq0 0 0 rgBT /Overloc birefringence in sulfate nonlinear optical materials. Journal of Materials Chemistry C, 2019, 7, 9900-9907.	2.7	63
4301	Interstitial Oxide Ion Conductivity in the Langasite Structure: Carrier Trapping by Formation of (Ga,Ge)₂O₈ Units in La₃Ga_{5â€“x}Ge_{1+x}O_{14+x/2} (0 <) Tj ETQq1 1 0.784314 rg	3.2	9
4302	First-principles calculations of the structural, elastic, vibrational and electronic properties of YB6 compound under pressure. European Physical Journal B, 2019, 92, 1.	0.6	10
4303	Theoretical prediction on the stability, electronic structure, room and elevated temperature properties of a new MAB phase Mo2AlB2. Journal of Materials Science and Technology, 2019, 35, 2926-2934.	5.6	16
4304	Successful Strategy for High Degree of Freedom Crystal Structure Determination from Powder X-Ray Diffraction Data: A Case Study for Selexipag Form I with 38 DOF. Crystal Growth and Design, 2019, 19, 4625-4631.	1.4	11
4305	Graphene oxide in ceramic-based layered structure: Nanosheet optimization. Construction and Building Materials, 2019, 224, 266-275.	3.2	15

#	Article	IF	Citations
4306	Schottky barrier height at metal/ZnO interface: A first-principles study. Microelectronic Engineering, 2019, 216, 111056.	1.1	13
4307	Phosphorous doped carbon nitride nanobelts for photodegradation of emerging contaminants and hydrogen evolution. Applied Catalysis B: Environmental, 2019, 257, 117931.	10.8	170
4308	Highly fluorescent Ti₃C₂ MXene quantum dots for macrophage labeling and Cu²⁺ ion sensing. Nanoscale, 2019, 11, 14123-14133.	2.8	140
4309	Effect of extended alkyl auxiliary groups on optical and electronic properties of Benzo[2,1-b:3,4-bâ€²:5,6-câ€³]trithiophene derivatives at bulk level: a first-principles study. Materials Research Express, 2019, 6, 095102.	0.8	2
4310	First-principles investigation of the vacancy-related properties of Ta₂AlC. Modern Physics Letters B, 2019, 33, 1950209.	1.0	1
4311	Understanding the electronic structure, mechanical properties, and thermodynamic stability of (TiZrHfNbTa)C combined experiments and first-principles simulation. Journal of Applied Physics, 2019, 126, .	1.1	19
4312	Interfacial properties of Cu7S4/MnS heterostructure from first-principles calculations. Journal of Physics and Chemistry of Solids, 2019, 134, 141-148.	1.9	7
4313	Broadband terahertz recognizing conformational characteristics of a significant neurotransmitter Î³-aminobutyric acid. RSC Advances, 2019, 9, 20240-20247.	1.7	17
4314	Density Functional Theory Studies of the Metalâ€“Insulator Transition in Vanadium Dioxide Alloys. Physica Status Solidi (B): Basic Research, 2019, 256, 1900210.	0.7	7
4315	Atomistic investigation on lithiation mechanism of silicon incorporated with amorphous carbon layer as anode material for lithium-ion battery. Applied Surface Science, 2019, 494, 111-115.	3.1	2
4316	Experimental and simulation studies of strontium/fluoride-codoped hydroxyapatite nanoparticles with osteogenic and antibacterial activities. Colloids and Surfaces B: Biointerfaces, 2019, 182, 110359.	2.5	43
4317	Mechanical, electronic, optical, and thermodynamic properties of orthorhonmbic LiCuBiO4 crystal: a firstâ€“priciples study. Journal of Materials Research and Technology, 2019, 8, 3783-3794.	2.6	41
4318	Syntheses, crystal structures, and characterizations of three new pyrophosphates CsNaZnP2O7, RbNaZnP2O7, and RbLiMgP2O7. Solid State Sciences, 2019, 95, 105940.	1.5	4
4319	Single-Atom-Thick Active Layers Realized in Nanolaminated Ti₃(Al_xCu_{1â€“x})C₂ and Its Artificial Enzyme Behavior. ACS Nano, 2019, 13, 9198-9205.	7.3	59
4320	Oxygen Vacancy Ordering in Aluminous Bridgmanite in the Earth's Lower Mantle. Geophysical Research Letters, 2019, 46, 8731-8740.	1.5	12
4321	Structure and magnetism of collapsed lanthanide elements. Physical Review B, 2019, 100, .	1.1	16
4322	Effect of high pressure on the typical 2D hydrogen-bonded crystal azodicarbonamide. Journal of Physics and Chemistry of Solids, 2019, 135, 109096.	1.9	1
4323	Electronic and vibrational properties of the two-dimensional Mott insulator<mml:math xmlns:mml="http://www.w3.org/1998/Math/MathML"><mml:mrow><mml:msub><mml:mi mathvariant="normal">V</mml:mi><mml:mrow><mml:mn>0.9</mml:mn></mml:mrow></mml:msub><mml:msub><mml:mi>PS</mml:mi> pressure. Physical Review B, 2019, 100, .	1.1	7

#	Article	IF	Citations
4324	Electronic Bands and Dielectric Functions of In0.5Tl0.5I Solid State Solution with Structural Defects. Journal of Electronic Materials, 2019, 48, 5586-5594.	1.0	12
4325	Environmental Effects on the Molecular Mobility of Ranitidine Hydrochloride: Crystalline State versus Drug Loaded into the Silica Matrix. Journal of Physical Chemistry C, 2019, 123, 18364-18375.	1.5	10
4326	AHgSnQ₄ (A = Sr, Ba; Q = S, Se): A Series of Hg-Based Infrared Nonlinear-Optical Materials with Strong Second-Harmonic-Generation Response and Good Phase Matchability. Inorganic Chemistry, 2019, 58, 10390-10398.	1.9	49
4327	RE(H2C3N3O3)2Â·(OH)Â·xH2O (RE = La, Y and Gd): potential UV birefringent materials with strong optical anisotropy originating from the (H2C3N3O3)â^' group. Dalton Transactions, 2019, 48, 12296-12302.	1.6	24
4328	Evidence of nanostructuring and reduced thermal conductivity in n-type Sb-alloyed SnSe thermoelectric polycrystals. Journal of Applied Physics, 2019, 126, .	1.1	28
4329	Firstâ€principles study of the atomic structures, electronic properties, and surface stability of BaTiO3(001) and (011) surfaces. Surface and Interface Analysis, 2019, 51, 1021-1032.	0.8	16
4330	Experimental and computational approaches to rationalise multicomponent supramolecular assemblies: dapsone monosolvates. Physical Chemistry Chemical Physics, 2019, 21, 17288-17305.	1.3	13
4331	Ta₃N₅nanorods encapsulated into 3D hydrangea-like MoS₂for enhanced photocatalytic hydrogen evolution under visible light irradiation. Dalton Transactions, 2019, 48, 13176-13183.	1.6	27
4332	Off-the-shelf DFT-DISPersion methods: Are they now â€œon-trendâ€•for organic molecular crystals?. Journal of Chemical Physics, 2019, 151, 044106.	1.2	11
4333	Effect of sulfur doping on fluorescence and quantum yield of graphene quantum dots: an experimental and theoretical investigation. Nanotechnology, 2019, 30, 435704.	1.3	88
4334	Interfacial coupling promoting hydrogen sulfide splitting on the staggered type II g-C3N4/r-TiO2 heterojunction. Journal of Catalysis, 2019, 377, 122-132.	3.1	42
4335	Enhancement of light emission in Bragg monolayer-thick quantum well structures. Scientific Reports, 2019, 9, 10162.	1.6	0
4336	Molecules with dipoles in periodic boundary conditions in a tetragonal cell. Journal of Physics Condensed Matter, 2019, 31, 335901.	0.7	2
4337	Ionic Liquid-Assisted Hydrothermal Synthesis of a Biocompatible Filler for Photo-Curable Dental Composite: From Theory to Experiment. Materials, 2019, 12, 2339.	1.3	2
4338	Experiment and First-Principles Calculations of A₂Mg₂TeB₂O₁₀ (A = Pb, Ba): Influences of the Cosubstitution on the Structure Transformation and Optical Properties. Inorganic Chemistry, 2019, 58, 11127-11132.	1.9	17
4339	Organometallic MFU-4l(arge) Metalâ€“Organic Frameworks. Organometallics, 2019, 38, 3444-3452.	1.1	27
4340	Highly active nanostructured CoS2/CoS heterojunction electrocatalysts for aqueous polysulfide/iodide redox flow batteries. Nature Communications, 2019, 10, 3367.	5.8	212
4341	Refinement of massive Î³ phase with enhanced properties in a Ta containing Î³-TiAl-based alloys. Scripta Materialia, 2019, 172, 113-118.	2.6	42

#	Article	IF	Citations
4342	Corrosion of Gold by a Nanoscale Gold and Copper Beltlike Structure. Journal of Physical Chemistry C, 2019, 123, 19920-19926.	1.5	2
4343	Novel Insights into the Hydroxylation Behaviors of Î±-Quartz (101) Surface and its Effects on the Adsorption of Sodium Oleate. Minerals (Basel, Switzerland), 2019, 9, 450.	0.8	50
4344	Atomistic View of Mercury Cycling in Polar Snowpacks: Probing the Role of Hg2+ Adsorption Using Ab Initio Calculations. Minerals (Basel, Switzerland), 2019, 9, 459.	0.8	2
4345	Prediction of Fluorooxoborates with Colossal Second Harmonic Generation (SHG) Coefficients and Extremely Wide Band Gaps: Towards Modulating Properties by Tuning the BO₃/BO₃F Ratio in Layers. Angewandte Chemie, 2019, 131, 11852-11856.	1.6	16
4346	Photo-electrochemical hydrogen evolution over FTO/Ni0.98Si0.02O2-Ni electrode induced by visible and UV light irradiation. Journal of Applied Electrochemistry, 2019, 49, 991-1002.	1.5	1
4347	Azobenzene-based lustrous golden thin films fabricated by electrophoretic deposition. Colloids and Surfaces A: Physicochemical and Engineering Aspects, 2019, 579, 123705.	2.3	5
4348	Structural modulation induced by MIIIA metals in Ba3MQ4X (M = Al, Ga, In; Q = S, Se; X = Cl, Br): an experimental and computational analysis. Dalton Transactions, 2019, 48, 12713-12719.	1.6	4
4349	Physical properties of group 14 semiconductor alloys in orthorhombic phase. Journal of Applied Physics, 2019, 126, 045709.	1.1	24
4350	A structural exploration of anisole accessed through extreme crystallisation conditions. CrystEngComm, 2019, 21, 4422-4426.	1.3	4
4351	Prediction of Fluorooxoborates with Colossal Second Harmonic Generation (SHG) Coefficients and Extremely Wide Band Gaps: Towards Modulating Properties by Tuning the BO₃/BO₃F Ratio in Layers. Angewandte Chemie - International Edition, 2019, 58, 11726-11730.	7.2	66
4352	Discovery of a new crystal structure of LiBeF3 and its thermodynamic and optical properties. Computational Materials Science, 2019, 169, 109077.	1.4	1
4353	Direct observation of reversible conversion and alloying reactions in a Bi₂(MoO₄)₃-based lithium-ion battery anode. Journal of Materials Chemistry A, 2019, 7, 17906-17913.	5.2	9
4354	Methylammonium Chloride Induces Intermediate Phase Stabilization for Efficient Perovskite Solar Cells. Joule, 2019, 3, 2179-2192.	11.7	1,228
4355	Multiple superionic states in heliumâ€“water compounds. Nature Physics, 2019, 15, 1065-1070.	6.5	69
4356	Ba₃B₁₀O₁₇F₂Â·0.1KF: the first mixed alkali/alkaline-earth metal fluorooxoborate with unprecedented double-layered Bâ€“O/F anionic arrangement. Chemical Communications, 2019, 55, 8923-8926.	2.2	14
4357	Investigation on photocatalytic mechanism of graphitic SiC (g-SiC)/MoS₂ van der Waals heterostructured photocatalysts for overall water splitting. Physical Chemistry Chemical Physics, 2019, 21, 15372-15379.	1.3	30
4358	Bimetallic palladium-supported halloysite nanotubes for low temperature CO oxidation: Experimental and DFT insights. Applied Surface Science, 2019, 493, 70-80.	3.1	16
4359	Electronic band structure, thermodynamics and optical characteristics of BeO1âˆ’A (Aâ€“=â€“S, Se, Te) alloys: Insights from ab initio study. Chemical Physics, 2019, 526, 110414.	0.9	39

#	Article	IF	Citations
4360	Effect of Fe doping on the structural, optical and electronic properties of BaTiO3: DFT based calculation. Chinese Journal of Physics, 2019, 60, 731-738.	2.0	13
4361	Equilibrium ground-state properties of the ternary alkali metal coinage metal phosphides K2CuP and K2AgP: New insights from first principles calculations. Journal of Alloys and Compounds, 2019, 804, 128-138.	2.8	8
4362	Structure of Na₃[Al(L-Lactate)₃]₂Â·6H₂O Crystallized from Lohtragon AL 250â€"A Commercial Cement Adjuvant. Crystal Growth and Design, 2019, 19, 4557-4563.	1.4	1
4363	An interfacial electron transfer relay center for accelerating the hydrogen evolution reaction. Journal of Materials Chemistry A, 2019, 7, 18304-18310.	5.2	19
4364	Two new derivatives of scandium borohydride, MSc(BH₄)₄, M = Rb, Cs, preparedviaa one-pot solvent-mediated method. Dalton Transactions, 2019, 48, 11829-11837.	1.6	7
4365	Carbon content and layers number controlling electronic properties of hybridized graphene and boron nitride. Ceramics International, 2019, 45, 19380-19387.	2.3	5
4366	Band alignment calculation of dielectric films on VO2. Microelectronic Engineering, 2019, 216, 111057.	1.1	2
4367	Determining interface structures in vertically aligned nanocomposite films. APL Materials, 2019, 7, .	2.2	19
4368	Computationally Guided Discovery of the Sulfide Li₃AlS₃ in the Liâ€"Alâ€"S Phase Field: Structure and Lithium Conductivity. Chemistry of Materials, 2019, 31, 9699-9714.	3.2	17
4369	Large-Scale Phonon Calculations Using the Real-Space Multigrid Method. Journal of Chemical Theory and Computation, 2019, 15, 6859-6864.	2.3	9
4370	Distinguishing between Structural Models of Î²â€²-Sialons Using a Combined Solid-State NMR, Powder XRD, and Computational Approach. Journal of Physical Chemistry A, 2019, 123, 9729-9736.	1.1	4
4371	Remote epitaxy using graphene enables growth of stress-free GaN. Nanotechnology, 2019, 30, 505603.	1.3	38
4372	Determining the anisotropy and exchange parameters of polycrystalline spin-1 magnets. New Journal of Physics, 2019, 21, 093025.	1.2	7
4373	First-principles calculation on the structural, elastic and thermodynamic properties of Ti-Al intermetallics. Materials Research Express, 2019, 6, 1065a4.	0.8	18
4374	Systematics of the allotrope formation in elemental gallium films. Materials Research Express, 2019, 6, 116401.	0.8	9
4375	A combined deep inelastic neutron scattering and ab initio lattice dynamics study of the hydride anion dynamics and bonding in La₂LiHO₃ oxyhydride. Journal of Physics Communications, 2019, 3, 103002.	0.5	11
4376	First-Principles Delimitation of the Boundary between Intralayer and Interlayer in Two-Dimensional Structures. Journal of Physical Chemistry C, 2019, 123, 26912-26920.	1.5	19
4377	Structural changes during the switching transition of chalcogenide selector devices. Applied Physics Letters, 2019, 115, .	1.5	13

#	Article	IF	Citations
4378	Synergistically Tuning Water and Hydrogen Binding Abilities Over Co₄N by Cr Doping for Exceptional Alkaline Hydrogen Evolution Electrocatalysis. Advanced Energy Materials, 2019, 9, 1902449.	10.2	205
4379	Waterâ€Mediated Synthesis of a Superionic Halide Solid Electrolyte. Angewandte Chemie, 2019, 131, 16579-16584.	1.6	92
4380	Waterâ€Mediated Synthesis of a Superionic Halide Solid Electrolyte. Angewandte Chemie - International Edition, 2019, 58, 16427-16432.	7.2	232
4381	Unraveling Polymorphic Pyrrhotite Electrochemical Oxidation by Underlying Electronic Structures. Journal of Physical Chemistry C, 2019, 123, 26442-26449.	1.5	9
4382	Platinum Porous Nanosheets with High Surface Distortion and Pt Utilization for Enhanced Oxygen Reduction Catalysis. Advanced Functional Materials, 2019, 29, 1904429.	7.8	96
4383	Biaxial strain and external electric field effects on the electronic structure of hydrogenated GaN monolayer. Superlattices and Microstructures, 2019, 136, 106270.	1.4	13
4384	Electronic Structure of In_{3â€“x}Se₄ Electron Transport Layer for Chalcogenide/p-Si Heterojunction Solar Cells. ACS Omega, 2019, 4, 17762-17772.	1.6	23
4385	The Influence of B, N and Si Doping on the CH3 Adsorption on the Diamond Surface Based on DFT Calculations. Crystals, 2019, 9, 427.	1.0	4
4386	Simultaneous Prediction of the Magnetic and Crystal Structure of Materials Using a Genetic Algorithm. Crystals, 2019, 9, 439.	1.0	8
4387	First-Principles Calculations of Structural, Mechanical, and Electronic Properties of the B2-Phase NiTi Shape-Memory Alloy Under High Pressure. Computation, 2019, 7, 57.	1.0	11
4388	Ensemble-Based Modeling of the NMR Spectra of Solid Solutions: Cation Disorder in Y₂(Sn,Ti)₂O₇. Journal of the American Chemical Society, 2019, 141, 17838-17846.	6.6	29
4389	Mapping Microstructural Dynamics up to the Nanosecond of the Conjugated Polymer P3HT in the Solid State. Chemistry of Materials, 2019, 31, 9635-9651.	3.2	10
4390	Rb₁₀Zn₄Sn₄S₁₇: A Chalcogenide with Large Laser Damage Threshold Improved from the Mn-Based Analogue. Inorganic Chemistry, 2019, 58, 15029-15033.	1.9	21
4391	Transition from Gas-like to Liquid-like Behavior in Supercritical N₂. Journal of Physical Chemistry Letters, 2019, 10, 6584-6589.	2.1	26
4392	LiCsPbP2O7: A new alkali metal lead pyrophosphate featuring two dimensional [LiP2O7]â^ž layer. Journal of Solid State Chemistry, 2019, 280, 120823.	1.4	0
4393	In Situ Characterization of Waters of Hydration in a Variable-Hydrate Active Pharmaceutical Ingredient Using ³⁵Cl Solid-State NMR and X-ray Diffraction. Crystal Growth and Design, 2019, 19, 7349-7362.	1.4	16
4394	Relation between O8 cluster shape and vibrational spectra in the Îµ-phase of solid oxygen. Japanese Journal of Applied Physics, 2019, 58, 095502.	0.8	1
4395	Designing excellent mid-infrared nonlinear optical materials with fluorooxo-functional group of d0 transition metal oxyfluorides. Science China Materials, 2019, 62, 1798-1806.	3.5	49

#	Article	IF	Citations
4396	Exploring mechanochemical parameters using a DoE approach: Crystal structure solution from synchrotron XRPD and characterization of a new praziquantel polymorph. European Journal of Pharmaceutical Sciences, 2019, 140, 105084.	1.9	21
4397	Nesting Co₃Mo Binary Alloy Nanoparticles onto Molybdenum Oxide Nanosheet Arrays for Superior Hydrogen Evolution Reaction. ACS Applied Materials & Interfaces, 2019, 11, 9002-9010.	4.0	74
4398	The Application of Periodic Density Functional Theory to the Study of Uranyl-Containing Materials: Thermodynamic Properties and Stability. , 2019, , .		0
4399	Moleculeâ€“Metal Bond of Alternant versus Nonalternant Aromatic Systems on Coinage Metal Surfaces: Naphthalene versus Azulene on Ag(111) and Cu(111). Journal of Physical Chemistry C, 2019, 123, 29219-29230.	1.5	20
4400	On the calculation of the bandgap of periodic solids with MGGA functionals using the total energy. Journal of Chemical Physics, 2019, 151, 161102.	1.2	10
4401	Dissociating stable nitrogen molecules under mild conditions by cyclic strain engineering. Science Advances, 2019, 5, eaax8275.	4.7	9
4402	Tuning Electronic Structure and Lattice Diffusion Barrier of Ternary Ptâ€“Inâ€“Ni for Both Improved Activity and Stability Properties in Oxygen Reduction Electrocatalysis. ACS Catalysis, 2019, 9, 11431-11437.	5.5	36
4403	Multiscale Evaluation of Moisture Susceptibility of Biomodified Bitumen. ACS Applied Bio Materials, 2019, 2, 5779-5789.	2.3	32
4404	In Situ Observation of the Effect of Accelerating Voltage on Electron Beam Damage of Layered Cathode Materials for Lithium-Ion Batteries. ACS Applied Materials & Interfaces, 2019, 11, 44293-44299.	4.0	15
4405	First-Principles Investigation on the Fully Compensated Ferrimagnetic Behavior in Ti2NbSb and TiZrNbSb. Chinese Physics Letters, 2019, 36, 067101.	1.3	0
4406	Synthesis and Electronic Structure of a 3D Crystalline Stack of MXene-Like Sheets. Chemistry of Materials, 2019, 31, 9788-9796.	3.2	34
4407	XBi₄S₇ (X = Mn, Fe): New Costâ€Efficient Layered nâ€Type Thermoelectric Sulfides with Ultralow Thermal Conductivity. Advanced Functional Materials, 2019, 29, 1904112.	7.8	24
4408	Heavy Mn²⁺ Doped MgAl₂O₄ Phosphor for Highâ€Efficient Nearâ€Infrared Lightâ€Emitting Diode and the Nightâ€Vision Application. Advanced Optical Materials, 2019, 7, 1901105.	3.6	167
4409	Nontoxic KBBF Family Member Zn₂BO₃(OH): Balance between Beneficial Layered Structure and Layer Tendency. Advanced Science, 2019, 6, 1901679.	5.6	56
4410	Cobalt Phosphide Ultrathin and Freestanding Sheets Prepared through Microwave Chemical Vapor Deposition: A Highly Efficient Oxygen Evolution Reaction Catalyst. ChemElectroChem, 2019, 6, 5469-5478.	1.7	16
4411	Giant Photoinduced Chirality in Thin Film Ge 2 Sb 2 Te 5. Physica Status Solidi - Rapid Research Letters, 2019, 13, 1900449.	1.2	2
4412	Uniform Ag Nanocubes Prepared by AgCl Particleâ€“Mediated Heterogeneous Nucleation and Disassembly and Their Mechanism Study by DFT Calculation. Small, 2019, 15, 1904031.	5.2	2
4413	Non-stoichiometry in Ca2Al2SiO7 enabling mixed-valent europium toward ratiometric temperature sensing. Science China Materials, 2019, 62, 1807-1814.	3.5	48

#	Article	IF	Citations
4414	Using first principles density functional theory approach to model the thermal conductivity of diamond-like materials. Materials Today: Proceedings, 2019, 19, 2109-2111.	0.9	1
4415	Effects of biaxial strain and functional groups on SiC/ti₃C₂ heterostructure: a first principle calculation. Materials Research Express, 2019, 6, 125070.	0.8	1
4416	Doping site identification in 112 iron pnictides through a first-principles core-electron spectroscopic study. Journal of Synchrotron Radiation, 2019, 26, 1367-1373.	1.0	10
4417	Structural, Spectroscopic, and Excitonic Dynamic Characterization in Atomically Thin Yb³⁺â€Doped MoS₂, Fabricated by Femtosecond Pulsed Laser Deposition. Advanced Optical Materials, 2019, 7, 1900753.	3.6	17
4418	Precursorâ€Transformation Strategy Preparation of CuP x Nanodotsâ€“Decorated CoP 3 Nanowires Hybrid Catalysts for Boosting pHâ€Universal Electrocatalytic Hydrogen Evolution. Small, 2019, 15, 1904681.	5.2	25
4419	First-principles study of electronic and optical properties of sulfur doped tin monoxide: A potential applicant for optoelectronic devices. Ceramics International, 2019, 45, 7495-7503.	2.3	7
4420	Mechanical behaviors, lattice thermal conductivity and vibrational properties of a new MAX phase Lu2SnC. Journal of Physics and Chemistry of Solids, 2019, 129, 162-171.	1.9	83
4421	Evaluation of Force-Field Calculations of Lattice Energies on a Large Public Dataset, Assessment of Pharmaceutical Relevance, and Comparison to Density Functional Theory. Journal of Chemical Information and Modeling, 2019, 59, 4778-4792.	2.5	20
4422	Monte Carlo simulation of transport properties in wide gap Hg3Se2I2. Semiconductor Science and Technology, 2019, 34, 115003.	1.0	1
4423	Recent progress on the prediction of two-dimensional materials using CALYPSO. Chinese Physics B, 2019, 28, 107306.	0.7	24
4424	Improving the photo-response of TiO₂ by tri-doping: a DFT based atomistic study. Materials Research Express, 2019, 6, 115510.	0.8	5
4425	The first principle study: electronic, optical and elastic properties of HfTe₅metal pentatelluride. Materials Research Express, 2019, 6, 116315.	0.8	3
4426	Elastic anisotropy and thermal conductivity of silicon allotropes. Results in Physics, 2019, 15, 102580.	2.0	16
4427	Sn₂Ga₂S₅: A Type of IR Nonlinear-Optical Material. Inorganic Chemistry, 2019, 58, 12002-12006.	1.9	18
4428	Pressure-induced isosymmetric phase transition in biurea. CrystEngComm, 2019, 21, 5872-5881.	1.3	3
4429	A new activity model for Mgâ€“Al biotites determined through an integrated approach. Contributions To Mineralogy and Petrology, 2019, 174, 76.	1.2	5
4430	Solid-State ¹⁷O NMR Study of Carboxylic Acid Dimers: Simultaneously Accessing Spectral Properties of Low- and High-Energy Tautomers. Journal of Physical Chemistry A, 2019, 123, 8243-8253.	1.1	11
4431	Electronic structure properties of transition metal dichalcogenide nanotubes: a DFT benchmark. Journal of Molecular Modeling, 2019, 25, 290.	0.8	8

#	Article	IF	Citations
4432	Proton Acidity and Proton Mobility in ECRâ€40, a Silicoaluminophosphate that Violates LÃ¶wenstein's Rule. Chemistry - A European Journal, 2019, 25, 13579-13590.	1.7	6
4433	Structural, elastic and electronic properties of new superhard orthorhombic C28. International Journal of Modern Physics B, 2019, 33, 1950227.	1.0	1
4434	Tuning the electronic structure of 2D materials by strain and external electric field: Case of GeI2 monolayer. Chemical Physics, 2019, 527, 110499.	0.9	53
4435	Mechanistic Insights into Selective CO₂ Conversion via RWGS on Transition Metal Phosphides: A DFT Study. Journal of Physical Chemistry C, 2019, 123, 22918-22931.	1.5	25
4436	Tuning Pressure-Induced Phase Transitions, Amorphization, and Excitonic Emissions of 2D Hybrid Perovskites via Varying Organic Amine Cations. Journal of Physical Chemistry C, 2019, 123, 22491-22498.	1.5	19
4437	Cation Disorder and Lithium Insertion Mechanism of Wadsleyâ€"Roth Crystallographic Shear Phases from First Principles. Journal of the American Chemical Society, 2019, 141, 15121-15134.	6.6	69
4438	Hydrogen in Î±-iron: role of phonons in the diffusion of interstitials at high temperature. Scientific Reports, 2019, 9, 12127.	1.6	5
4439	Comparison of structural, mechanical and optical properties of tantalum hemicarbide with tantalum monocarbide: ab initio calculations. Journal of Physics Communications, 2019, 3, 055017.	0.5	16
4440	Characterisation of fac-tris [2-phenylpyridinato-C², N]iridium(III) by inelastic neutron scattering spectroscopy and periodic density functional theory. Journal of Physics Communications, 2019, 3, 065010.	0.5	3
4441	Atom-projected and angular momentum resolved density of states in the ONETEP code. Electronic Structure, 2019, 1, 035002.	1.0	7
4442	Tuning Electronic Properties of Blue Phosphorene/Graphene-Like GaN van der Waals Heterostructures by Vertical External Electric Field. Nanoscale Research Letters, 2019, 14, 174.	3.1	16
4443	DFT Investigations of the Vibrational Spectra and Translational Modes of Ice II. Molecules, 2019, 24, 3135.	1.7	8
4444	Computational Analysis of Exotic Molecular and Atomic Vibrations in Ice XV. Molecules, 2019, 24, 3115.	1.7	11
4445	First-principles simulations on the structural, mechanical and thermodynamic properties of Î±, Î², and h-CuGaO2. Philosophical Magazine, 2019, 99, 3078-3095.	0.7	1
4446	Significant enhancement of cathode-ray scintillation for a conductive Bi-SMOF via in situ partial rare earth ion replacement. Journal of Materials Chemistry C, 2019, 7, 11099-11103.	2.7	27
4447	High thermal stability and colour saturation red-emitting Ba2AGe2O7: Eu3+ (A = Mg, Zn) phosphors for WLEDs. Journal of Luminescence, 2019, 216, 116734.	1.5	25
4448	Highly dispersed PtPd on graphitic nanofibers and its heavy d-Ï€ effect. Applied Catalysis B: Environmental, 2019, 259, 118080.	10.8	46
4449	Band structures, effective masses and exciton binding energies of perovskite polymorphs of CH3NH3PbI3. Solar Energy, 2019, 190, 617-621.	2.9	19

#	Article	IF	Citations
4450	Structure Model and Toxicity of the Product of Biodissolution of Chrysotile Asbestos in the Lungs. Chemical Research in Toxicology, 2019, 32, 2063-2077.	1.7	17
4451	DFT Calculations of the Structural, Mechanical, and Electronic Properties of TiV Alloy Under High Pressure. Symmetry, 2019, 11, 972.	1.1	8
4452	Second harmonic generation in Janus MoSSe a monolayer and stacked bulk with vertical asymmetry. Physical Chemistry Chemical Physics, 2019, 21, 21022-21029.	1.3	42
4453	Trifunctional Fishbone-like PtCo/Ir Enables High-Performance Zincâ€“Air Batteries to Drive the Water-Splitting Catalysis. Chemistry of Materials, 2019, 31, 8136-8144.	3.2	55
4454	Synthesis, Characterization, and Crystal Structure Determination of a New Lithium Zinc Iodate Polymorph LiZn(IO3)3. Crystals, 2019, 9, 464.	1.0	12
4455	Lead-Free Hybrid Metal Halides with a Green-Emissive [MnBr₄] Unit as a Selective Turn-On Fluorescent Sensor for Acetone. Inorganic Chemistry, 2019, 58, 13464-13470.	1.9	112
4456	Centrosymmetric K₂SO₄Â·(SbF₃)₂and noncentrosymmetric Rb₂SO₄Â·(SbF₃)₂resulting from cooperative effects of lone pair and cation size. Inorganic Chemistry Frontiers, 2019, 6, 3125-3132.	3.0	48
4458	Rb₃SbF₃(NO₃)₃: an excellent antimony nitrate nonlinear optical material with a strong second harmonic generation response fabricated by a rational multi-component design. Dalton Transactions, 2019, 48, 15144-15150.	1.6	33
4459	CO(NH₂)₂Â·NH₄Cl: an ultraviolet birefringent material with conjugated Cî€€O groups. CrystEngComm, 2019, 21, 6072-6079.	1.3	10
4460	Two new tin(iv)-containing phosphate fluorides with two types of Sn(iv)â€“Pâ€“Oâ€“F frameworks and short cutoff edges. New Journal of Chemistry, 2019, 43, 16127-16130.	1.4	0
4461	Electronic and magnetic properties of single-layer boron phosphide associated with materials processing defects. Computational Materials Science, 2019, 170, 109201.	1.4	63
4462	Cation Modulation on the Crystal Structure and Band Gap of Fluorooxoborates A₃B₃O₃F₆ (A = Alkali and Mixed Alkali Metal). Inorganic Chemistry, 2019, 58, 13411-13417.	1.9	16
4463	Rational Modification of Small Molecules with High Device Reproducibility Induced by Improved Interfacial Contact through Intermolecular Hydrogen Bonds. ACS Applied Materials & Interfaces, 2019, 11, 37973-37980.	4.0	4
4464	Structure and spectroscopy of the supercapacitor material hydrous ruthenium oxide, RuO₂Â·xH₂o, by neutron scattering*. Molecular Physics, 2019, 117, 3417-3423.	0.8	9
4465	LiBa₂M^{III}Q₄ (M^{III} = Al, Ga, In; Q = S, Se): A Series of Metal Chalcogenides with a Structural Transition. Inorganic Chemistry, 2019, 58, 12859-12866.	1.9	10
4466	On a new nitrogen sX hydrate from ice XVII. Journal of Chemical Physics, 2019, 151, 104305.	1.2	8
4467	Thermodynamic Properties of Hexagonal Molybdenum Disulfide Calculated from First Principles. Powder Metallurgy and Metal Ceramics, 2019, 58, 230-236.	0.4	1
4468	Mechanistic Insights into the Pathways of Phenol Hydrogenation on Pd Nanostructures. ACS Sustainable Chemistry and Engineering, 2019, 7, 17126-17136.	3.2	57

#	Article	IF	Citations
4469	Co-segregation behavior of Sc and Zr solutes and their effect on the Al Î£5 (210) [110] symmetrical tilt grain boundary: a first-principles study. Physical Chemistry Chemical Physics, 2019, 21, 19437-19446.	1.3	14
4470	Electronic and structural properties of low-index L12â€“Al3Zr surfaces by first-principle calculations. Calphad: Computer Coupling of Phase Diagrams and Thermochemistry, 2019, 66, 101645.	0.7	16
4471	Surface Induced Phenytoin Polymorph. 1. Full Structure Solution by Combining Grazing Incidence X-ray Diffraction and Crystal Structure Prediction. Crystal Growth and Design, 2019, 19, 6058-6066.	1.4	5
4472	Phenanthroline: A New Electron Acceptor Model for the Design and Syntheses of Photochromic Compounds. Crystal Growth and Design, 2019, 19, 6023-6027.	1.4	13
4473	â€œInvertingâ€•X-ray Absorption Spectra of Catalysts by Machine Learning in Search for Activity Descriptors. ACS Catalysis, 2019, 9, 10192-10211.	5.5	105
4474	Toward a better understanding of the enhancing/embrittling effects of impurities in Nickel grain boundaries. Scientific Reports, 2019, 9, 14024.	1.6	6
4475	Site discrimination and size effect of B-doping in Si nanocrystals by second-neighbor atom consideration. Journal of Applied Physics, 2019, 126, .	1.1	1
4476	Synthesis of MAX phases Nb₂CuC and Ti₂(Al_{0.1}Cu_{0.9})N by A-site replacement reaction in molten salts. Materials Research Letters, 2019, 7, 510-516.	4.1	58
4477	Novel Energetic Coordination Polymers Based on 1,5-Di(nitramino)tetrazole With High Oxygen Content and Outstanding Properties: Syntheses, Crystal Structures, and Detonation Properties. Frontiers in Chemistry, 2019, 7, 672.	1.8	6
4478	High-Pressure Study of Two Polymorphs of 2,4,6-Trinitrotoluene Using Neutron Powder Diffraction and Density Functional Theory Methods. Journal of Physical Chemistry C, 2019, 123, 26095-26105.	1.5	16
4479	Cs₂NaVCl₆: A Pb-Free Halide Double Perovskite with Strong Visible and Near-Infrared Light Absorption. ACS Applied Materials & Interfaces, 2019, 11, 38648-38653.	4.0	39
4480	Ab Initio Study of Ternary W5Si3 Type TM5Sn2X Compounds (TM = Nb, Ti and X = Al, Si). Materials, 2019, 12, 3217.	1.3	5
4481	Molecular insights into the activity and stability of popular methane reforming catalysts using quantum mechanical tools. Current Opinion in Chemical Engineering, 2019, 26, 38-45.	3.8	9
4482	SrI3O9H: A new alkaline earth metal iodate with two different anionic units using mild aqua-solution method. Solid State Sciences, 2019, 97, 105982.	1.5	5
4483	First-principles study of structural, electronic, elastic, thermodynamic and optical properties of LuPdBi half-Heusler compound. Modern Physics Letters B, 2019, 33, 1950378.	1.0	23
4484	Temperature-dependent gas sensing properties of porous silicon oxycarbide: Insight from first principles. Applied Surface Science, 2019, 493, 1286-1290.	3.1	10
4485	Molecular speciation of phosphorus in phosphogypsum waste by solid-state nuclear magnetic resonance spectroscopy. Science of the Total Environment, 2019, 696, 133958.	3.9	17
4486	Modification of O and CO binding on Pt nanoparticles due to electronic and structural effects of titania supports. Journal of Chemical Physics, 2019, 151, 114702.	1.2	11

#	Article	IF	Citations
4487	Exploring the electronic, mechanical, and anisotropy properties of novel tetragonal B₂CO phase. Journal of Materials Research, 2019, 34, 3617-3626.	1.2	5
4488	Insight into the factors influencing NMR parameters in crystalline materials from the KFâ€“YF3binary system. Dalton Transactions, 2019, 48, 587-601.	1.6	8
4489	Strongly coloured thiocyanate frameworks with perovskite-analogue structures. Chemical Science, 2019, 10, 793-801.	3.7	30
4490	First-principles calculations and high thermoelectric performance of Laâ€“Nb doped SrTiO₃ceramics. Journal of Materials Chemistry A, 2019, 7, 236-247.	5.2	40
4491	Unique SchrÃ¶dinger semimetal state in ternary Be₂P₃N honeycomb lattice. Journal of Materials Chemistry C, 2019, 7, 4118-4123.	2.7	8
4492	Nitrogen-Doped Biomass Carbons Meet with Polyoxometalates: Synergistic Catalytic Reductant-Free Aerobic Hydroxylation of Benzene to Phenol. ACS Sustainable Chemistry and Engineering, 2019, 7, 4230-4238.	3.2	20
4493	Characteristic fingerprint spectrum of neurotransmitter norepinephrine with broadband terahertz time-domain spectroscopy. Analyst, The, 2019, 144, 2504-2510.	1.7	35
4494	Mechanical properties of anhydrous oxalic acid and oxalic acid dihydrate. Physical Chemistry Chemical Physics, 2019, 21, 2673-2690.	1.3	43
4495	Efficient X-ray scintillating lead(<scp>ii</scp>)-based MOFs derived from rigid luminescent naphthalene motifs. Dalton Transactions, 2019, 48, 1722-1731.	1.6	45
4496	A unified model of impact sensitivity of metal azides. New Journal of Chemistry, 2019, 43, 1459-1468.	1.4	18
4497	From one-dimensional to two-dimensional wurtzite CuGaS₂nanocrystals: non-injection synthesis and photocatalytic evolution. Nanoscale, 2019, 11, 158-169.	2.8	38
4498	Experimental characterization and first principles calculations of linear and nonlinear optical properties of two orthophosphates A₃Al₂(PO₄)₃(A =) Tj ETQq1 1 0.784314 rgBT /O	1.1	31
4499	First principles study of surface properties and oxygen adsorption on the surface of Al₃Ti intermetallic alloys. RSC Advances, 2019, 9, 1752-1758.	1.7	15
4500	Visualization of the effect of additives on the nanostructures of individual bio-inspired calcite crystals. Chemical Science, 2019, 10, 1176-1185.	3.7	26
4501	First-principles investigation of the ground state, structural phase transition, and magnetic ordering of strained BiVO₃. Journal of Applied Physics, 2019, 125, 082532.	1.1	4
4502	Optical properties and lattice dynamics of a novel allotrope of orthorhombic elemental germanium. Journal of Physics Condensed Matter, 2019, 31, 135401.	0.7	3
4503	Theoretical study on nanostructural modifications of the Si(111) surface. Journal of Theoretical and Computational Chemistry, 2019, 18, 1950005.	1.8	0
4504	Crystallographic Investigations into the Polar Polymorphism of BaTeW₂O₉: Phase Transformation, Controlled Crystallization, and Linear and Nonlinear Optical Properties. Crystal Growth and Design, 2019, 19, 1767-1777.	1.4	17

#	Article	IF	Citations
4505	Soft X-ray Li-K and Si-L2, 3 Emission from Crystalline and Amorphous Lithium Silicides in Lithium-Ion Batteries Anode. Journal of the Electrochemical Society, 2019, 166, A5362-A5368.	1.3	3
4506	Investigations of the Hydrogen Bonds and Vibrational Spectra of Clathrate Ice XVI. Materials, 2019, 12, 246.	1.3	16
4507	Effect of V and Y doping on the structural, optical and electronic properties of CdS (hexagonal and) Tj ETQq0 0 0 rgBT /Overlock 10 Tf 5	1.1	32
4508	Raman Scattering Spectra of Î²-LiNH4SO4 Crystals. Journal of Applied Spectroscopy, 2019, 85, 1022-1028.	0.3	5
4509	Two-Dimensional Anti-Vanâ€™t Hoff/Le Bel Array AlB₆ with High Stability, Unique Motif, Triple Dirac Cones, and Superconductivity. Journal of the American Chemical Society, 2019, 141, 3630-3640.	6.6	154
4510	The role of sp²and sp³hybridized bonds on the structural, mechanical, and electronic properties in a hard BN framework. RSC Advances, 2019, 9, 2657-2665.	1.7	17
4511	Eu3+ doped (Li, Na, K) LaMgWO6 red emission phosphors: An example to rational design with theoretical and experimental investigation. Journal of Alloys and Compounds, 2019, 785, 651-659.	2.8	36
4512	Efficient Visibleâ€Lightâ€Induced Photocatalytic Activity of SrTiO₃ Coâ€Doped With Os and N: A GGAâ€‰+â€‰U Investigation. Physica Status Solidi (B): Basic Research, 2019, 256, 1800574.	0.7	5
4513	Electronic Structure Tunability of Diamonds by Surface Functionalization. Journal of Physical Chemistry C, 2019, 123, 4168-4177.	1.5	20
4514	Solvent driven phase transitions of acyclovir â€“ the role of water and solvent polarity. CrystEngComm, 2019, 21, 2180-2192.	1.3	8
4515	A New Cadmiumâ€Based Pb₂Cd₃(PO₄)₂(P₂O₇) with Two Types of Isolated Pâ€“O Groups. European Journal of Inorganic Chemistry, 2019, 2019, 1273-1278.	1.0	14
4516	Enhancing catalytic H2 generation by surface electronic tuning of systematically controlled Pt-Pb nanocrystals. Nano Research, 2019, 12, 2335-2340.	5.8	3
4517	Lone pair effects on ternary infrared nonlinear optical materials. Physical Chemistry Chemical Physics, 2019, 21, 5142-5147.	1.3	16
4518	Unexpected calcium polyhydride CaH4: A possible route to dissociation of hydrogen molecules. Journal of Chemical Physics, 2019, 150, 044507.	1.2	17
4519	Outstanding Piezoelectric Performance in Leadâ€Free 0.95(K,Na)(Sb,Nb)O₃â€0.05(Bi,Na,K)ZrO₃ Thick Films with Oriented Nanophase Coexistence. Advanced Electronic Materials, 2019, 5, 1800691.	2.6	18
4520	First-principles calculations of magnetism and half-metallic properties of CsYO2 (Yâ€¯=â€¯V, Cr, Mn, Fe, Co,) Tj ETQq1 1 0.784314 rgB	1.0	11
4521	Boosting the cycling stability of hydrated vanadium pentoxide by Y3+ pillaring for sodium-ion batteries. Materials Today Energy, 2019, 11, 218-227.	2.5	38
4522	Imaging the local electronic and magnetic properties of intrinsically phase separated Rb x Fe2â€“y Se2 superconductor using scanning microscopy techniques. Superconductor Science and Technology, 2019, 32, 044005.	1.8	6

#	Article	IF	Citations
4523	Structural and vibrational properties of lithium under ambient conditions within density functional theory. Physical Review B, 2019, 99, .	1.1	14
4524	Reactive molecular dynamics simulation of thermal decomposition for nano-AlH3/TNT and nano-AlH3/CL-20 composites. Journal of Materials Science, 2019, 54, 7016-7027.	1.7	26
4525	ASbF3Cl (A = Rb, Cs): Structural Evolution from Centrosymmetry to Noncentrosymmetry. Crystal Growth and Design, 2019, 19, 1874-1879.	1.4	8
4526	A Picture of Disorder in Hydrous Wadsleyiteâ€"Under the Combined Microscope of Solid-State NMR Spectroscopy and Ab Initio Random Structure Searching. Journal of the American Chemical Society, 2019, 141, 3024-3036.	6.6	13
4527	Structural, Dynamic, and Thermodynamic Study of KFâ€“AlF₃ Melts by Combining High-Temperature NMR and Molecular Dynamics Simulations. Journal of Physical Chemistry C, 2019, 123, 2147-2156.	1.5	8
4528	Structures, Elasticity, and Sensitivity Characteristics of É›â€CLâ€20 under High Pressure from Firstâ€Principles Calculations. Physica Status Solidi (B): Basic Research, 2019, 256, 1800440.	0.7	4
4529	Negative linear compressibility in uranyl squarate monohydrate. Journal of Physics Condensed Matter, 2019, 31, 175701.	0.7	11
4530	Effects of Electronic Delocalization and Hydrostatic Compression on Structure and Properties of Cage Compound 4â€Trinitroethylâ€2,6,8,10,12â€pentanitrohexaazaisowurtzitane. ChemistrySelect, 2019, 4, 1567-1575.	0.7	2
4531	DFT Simulation on Interaction of H₂O Molecules with ZnS and Cu-Activated Surfaces. Journal of Physical Chemistry C, 2019, 123, 3048-3057.	1.5	36
4532	Tunable, Multifunctional Ceramic Composites via Intercalation of Fused Graphene Boron Nitride Nanosheets. ACS Applied Materials & Interfaces, 2019, 11, 8635-8644.	4.0	25
4533	Multifunctional property exploration: Bi₄O₅I₂ with high visible light photocatalytic performance and a large nonlinear optical effect. RSC Advances, 2019, 9, 4539-4544.	1.7	22
4534	Effects of Impurity Doping on the Luminescence Performance of Mn4+-Doped Aluminates with the Magnetoplumbite-Type Structure for Plant Cultivation. Materials, 2019, 12, 86.	1.3	17
4535	Al80Cr20N-layer thickness-dependent microstructure and mechanical properties of Al50Cr50N/Al80Cr20N nanomultilayered films. Vacuum, 2019, 162, 1-7.	1.6	5
4536	Enhanced deep-red emission from Mn⁴⁺/Mg²⁺co-doped CaGdAlO₄phosphors for plant cultivation. Dalton Transactions, 2019, 48, 2455-2466.	1.6	50
4537	Molecular-scale structures of uranyl surface complexes on hematite facets. Environmental Science: Nano, 2019, 6, 892-903.	2.2	19
4538	Investigation on two new antimony-based quaternary chalcogenides: Na₆CdSb₄S₁₀ and Na₃CdSbSe₄. New Journal of Chemistry, 2019, 43, 3350-3356.	1.4	0
4539	BaB8O12F2: a promising deep-UV birefringent material. Inorganic Chemistry Frontiers, 2019, 6, 546-549.	3.0	45
4540	Crystal structure analysis and evidence of mixed anion coordination at the Ce³⁺ site in Y₃Al₂(Al,Si)₃(O,N)₁₂ oxynitride garnet phosphor. Journal of Materials Chemistry C, 2019, 7, 1330-1336.	2.7	19

#	Article	IF	Citations
4541	The first lithium difluorophosphate LiPO₂F₂with a neutral polytetrahedral microporous architecture. Chemical Communications, 2019, 55, 1817-1820.	2.2	20
4542	Explaining crystallization preferences of two polyphenolic diastereoisomers by crystal structure prediction. CrystEngComm, 2019, 21, 2067-2079.	1.3	18
4543	Structural behaviour of OP-ROY at extreme conditions. CrystEngComm, 2019, 21, 4473-4483.	1.3	21
4544	High-pressure polymorphism in l-threonine between ambient pressure and 22 GPa. CrystEngComm, 2019, 21, 4444-4456.	1.3	27
4545	Crystal structure, hydrogen bonding, mechanical properties and Raman spectrum of the lead uranyl silicate monohydrate mineral kasolite. RSC Advances, 2019, 9, 15323-15334.	1.7	24
4546	Effect of layer and stacking sequence in simultaneously grown 2H and 3R WS₂ atomic layers. Nanotechnology, 2019, 30, 345203.	1.3	16
4547	Hydrogen Diffusion Guided Design of Ptâ€Based Alloys for Inhibition of Butadiene Overâ€Hydrogenation. ChemPhysChem, 2019, 20, 1804-1811.	1.0	6
4548	Hydrochromic full-color MXene quantum dots through hydrogen bonding toward ultrahigh-efficiency white light-emitting diodes. Applied Materials Today, 2019, 16, 90-101.	2.3	86
4549	Exploring the novel structure, elastic and thermodynamic properties of W3Si silicides from first-principles calculations. Ceramics International, 2019, 45, 15649-15653.	2.3	73
4550	High-Throughput Screening Delafossite CuMO₂ (M = IIIA, 3d, 4d, 5d, and RE) Optoelectronic Functional Materials Based on First-Principles Calculations. Journal of Physical Chemistry C, 2019, 123, 14292-14302.	1.5	27
4551	Tuneable single-molecule electronic conductance of C₆₀by encapsulation. Physical Chemistry Chemical Physics, 2019, 21, 12606-12610.	1.3	14
4552	Molecular Modeling of Interactions between N-(Carboxymethyl)-N-tetradecylglycine and Fluorapatite. Minerals (Basel, Switzerland), 2019, 9, 278.	0.8	7
4553	Predicting three-dimensional icosahedron-based boron <mml:math xmlns:mml="http://www.w3.org/1998/Math/MathML"><mml:msub><mml:mi mathvariant="normal">B</mml:mi><mml:mn>60</mml:mn></mml:msub></mml:math>. Physical Review B, 2019, 99, .	1.1	21
4554	Native filament-to-dielectric interfaces in phase change superlattice memories. Microelectronic Engineering, 2019, 215, 111007.	1.1	5
4555	Î²â€CsB 9 O 14 : A Tripleâ€Layered Borate with Edgeâ€Sharing BO 4 Tetrahedra Exhibiting a Short Cutoff Edge and a Large Birefringence. Chemistry - A European Journal, 2019, 25, 11614-11619.	1.7	29
4556	Synthesis and microstructure characterization of tetragonal Zr1â€“xTixO2 (xâ€‰=â€‰0â€“1) solid solutions. Journal of Materials Science and Technology, 2019, 35, 1966-1976.	5.6	9
4557	Band structures and optical properties of Ag and Al co-doped ZnO by experimental and theoretic calculation. Physica E: Low-Dimensional Systems and Nanostructures, 2019, 114, 113602.	1.3	19
4558	K2[B4O5(OH)4]Â·H2O and K2[B4O5(OH)4]: two new hydrated potassium borates with isolated [B4O5(OH)4]2â¯ units and different structural frameworks. New Journal of Chemistry, 2019, 43, 11660-11665.	1.4	3

#	Article	IF	Citations
4559	Optoelectronic and thermal properties of LiXH3(X =Ba, Sr and Cs) for hydrogen storage materials: A first principle study. Solid State Communications, 2019, 299, 113659.	0.9	42
4560	Improving the accuracy of solid-state nuclear magnetic resonance chemical shift prediction with a simple molecular correction. Physical Chemistry Chemical Physics, 2019, 21, 14992-15000.	1.3	38
4561	Effects of strain on electronic and optical properties of LiNbO₃: a first principles study. Materials Research Express, 2019, 6, 114002.	0.8	10
4562	Excellent carrier mobility and opto/electronics performance material prediction: Focusing on single layer X2Te3 (Xâ€¯=â€¯Sb, Bi). Applied Surface Science, 2019, 491, 690-697.	3.1	0
4563	Unique crystal structures and their applications as materials for Li1+-M1–3Ti+4O3 (Mâ€¯=â€¯Nb or Ta,) Tj ETQq0 0 0 rgBT /Overlock 10 T	2.0	4
4564	Ge-vacancy improved the optical and electronic properties of GeAs2 semiconductor. Ceramics International, 2019, 45, 19534-19537.	2.3	63
4565	Structure and Electrical Performance of Na₂C₆O₆ under High Pressure. Journal of Physical Chemistry C, 2019, 123, 17163-17169.	1.5	3
4566	Single-Crystal NMR Characterization of Halogen Bonds. Journal of Physical Chemistry A, 2019, 123, 6194-6209.	1.1	17
4567	Electronic structures, bonding natures and defect processes in Sn-based 211 MAX phases. Computational Materials Science, 2019, 168, 203-212.	1.4	17
4568	Kinetics of antigorite dehydration: Rapid dehydration as a trigger for lower-plane seismicity in subduction zones. American Mineralogist, 2019, 104, 282-290.	0.9	16
4569	Molecular level investigation of methane and carbon dioxide adsorption on SiO2 surface. Computational Materials Science, 2019, 168, 213-220.	1.4	18
4570	Structural and magnetic properties of transition-metal doped scandium nitride (ScN): Spin density functional theory. Physica B: Condensed Matter, 2019, 570, 236-240.	1.3	6
4571	New two-dimensional carbon nitride allotrope with 1â€‰:â€‰1 stoichiometry featuring spine-like structures: a structural and electronic DFT-D study. Physical Chemistry Chemical Physics, 2019, 21, 15282-15285.	1.3	7
4572	Optically Modulated Ultra-Broad-Band Warm White Emission in Mn²⁺-Doped (C₆H₁₈N₂O₂)PbBr₄ Hybrid Metal Halide Phosphor. Chemistry of Materials, 2019, 31, 5788-5795.	3.2	131
4573	A theoretical approach of the ethanol adsorption on Au(100), Au(110) and Au(111) surfaces. Surface Science, 2019, 689, 121458.	0.8	5
4574	Whether Corrugated or Planar Vacancy Graphene-like Carbon Nitride (g-C₃N₄) Is More Effective for Nitrogen Reduction Reaction?. Journal of Physical Chemistry C, 2019, 123, 17296-17305.	1.5	46
4575	Effect of non-hydrostatic stress on the structure and elasticity of NaCl by first-principles calculation. AIP Advances, 2019, 9, 055014.	0.6	4
4576	KBiCl₂SO₄: The First Bismuth Chloride Sulfate Being Second-Order Nonlinear Optical Active. Crystal Growth and Design, 2019, 19, 3843-3850.	1.4	36

#	Article	IF	Citations
4577	Planar, Energetic, Ï€â€“Ï€-Stacked Compound with Weak Interactions Resulting in a High-Impact- and Low-Friction-Sensitive, Safer, Primary Explosive. Inorganic Chemistry, 2019, 58, 7653-7656.	1.9	32
4578	Tunable electronic and optical properties of the WS₂/IGZO heterostructureviaan external electric field and strain: a theoretical study. Physical Chemistry Chemical Physics, 2019, 21, 14713-14721.	1.3	4
4579	Ferroelastic lattice rotation and band-gap engineering in quasi 2D layered-structure PdSe₂under uniaxial stress. Nanoscale, 2019, 11, 12317-12325.	2.8	32
4580	First-principles study on the electronic and optical properties of the ZnTe/InP heterojunction. Journal of Computational Electronics, 2019, 18, 749-757.	1.3	16
4581	A comparative study of the vibrational and thermodynamic properties of Î±-RDX and Î³-RDX under ambient conditions. Journal of Molecular Modeling, 2019, 25, 182.	0.8	7
4582	An efficient ultrathin PtFeNi Nanowire/Ionic liquid conjugate electrocatalyst. Applied Catalysis B: Environmental, 2019, 256, 117828.	10.8	40
4583	Atomic structure and band alignment at Al2O3/GaN, Sc2O3/GaN and La2O3/GaN interfaces: A first-principles study. Microelectronic Engineering, 2019, 216, 111039.	1.1	12
4584	Two-dimensional ZnO for the selective photoreduction of CO₂. Journal of Materials Chemistry A, 2019, 7, 16294-16303.	5.2	62
4585	Modeling of surface gap state passivation and Fermi level de-pinning in solar cells. Applied Physics Letters, 2019, 114, .	1.5	20
4586	Synthesis and microstructure evolution of WCoB based cermets during spark plasma sintering. Ceramics International, 2019, 45, 17536-17544.	2.3	16
4587	Electronic band structures and optical properties of atomically thin AuSe: first-principle calculations. Journal of Semiconductors, 2019, 40, 062004.	2.0	7
4588	Terahertz spectroscopy from air plasmas created by two-color femtosecond laser pulses: The ALTESSE project. Europhysics Letters, 2019, 126, 24001.	0.7	39
4589	Mechanism of Sensitivity Enhancement of a ZnO Nanofilm Gas Sensor by UV Light Illumination. ACS Sensors, 2019, 4, 1577-1585.	4.0	51
4590	KNa₄B₂P₃O₁₃: A Deep-Ultraviolet Transparent Borophosphate Exhibiting Second-Harmonic Generation Response. Inorganic Chemistry, 2019, 58, 8918-8921.	1.9	19
4591	Comparative Analysis of Hydrogen Bond Vibrations in Ice VIII and VII. Journal of Physical Chemistry C, 2019, 123, 14880-14883.	1.5	14
4592	Bulk Inclusions of Double Pyridazine Molecular Rotors in Hexagonal Tris(o-phenylene)cyclotriphosphazene. Journal of Organic Chemistry, 2019, 84, 8449-8467.	1.7	18
4593	Enhanced tetragonality and large negative thermal expansion in a new Pb/Bi-based perovskite ferroelectric of (1 â^’) Tj ETQq0 0 0 rgBT /Overlock 10 Tf 50 102 Td (x)PbTiO₃â€“xBi(Zn_{1/2}V<su Chemistry Frontiers, 2019, 6, 1990-1995.	3.0	8
4594	The Effect of Pressure on Halogen Bonding in 4-Iodobenzonitrile. Molecules, 2019, 24, 2018.	1.7	11

#	Article	IF	Citations
4595	Structural, Elastic, Mechanical and Electronic Properties of NbWâ€Based Intermetallic Compounds: Firstâ€Principles Calculations. Physica Status Solidi (B): Basic Research, 2019, 256, 1800570.	0.7	1
4596	Physical Fingerprints of the 2O-tÎ±P Phase in Phosphorene Stacking. Journal of Physical Chemistry Letters, 2019, 10, 3190-3196.	2.1	4
4597	Comparative Study on Surface Structure, Electronic Properties of Sulfide and Oxide Minerals: A First-Principles Perspective. Minerals (Basel, Switzerland), 2019, 9, 329.	0.8	5
4598	Degradation of organic pollutants by peroxymonosulfate activated by MnO2 with different crystalline structures: Catalytic performances and mechanisms. Chemical Engineering Journal, 2019, 374, 170-180.	6.6	145
4599	Conformational sieving effect of organic structure-directing agents during the synthesis of zeolitic materials. Microporous and Mesoporous Materials, 2019, 287, 56-64.	2.2	5
4600	Influence of secondary phases on crack initiation and propagation during fracture process of as-cast Mg-Al-Zn-Nd alloy. Materials Science & Engineering A: Structural Materials: Properties, Microstructure and Processing, 2019, 759, 708-714.	2.6	21
4601	Poly(difluorophosphazene) as the First Deepâ€Ultraviolet Nonlinear Optical Polymer: A Firstâ€Principles Prediction. Angewandte Chemie - International Edition, 2019, 58, 10250-10254.	7.2	23
4602	Poly(difluorophosphazene) as the First Deepâ€Ultraviolet Nonlinear Optical Polymer: A Firstâ€Principles Prediction. Angewandte Chemie, 2019, 131, 10356-10360.	1.6	11
4603	Influence of Oxygen Vacancies on the Electronic and Optical Properties of Zirconium Dioxide from First-Principles Calculations. Journal of Electronic Materials, 2019, 48, 5154-5160.	1.0	66
4604	Role of a Hydroxide Layer on Cu Electrodes in Electrochemical CO₂ Reduction. ACS Catalysis, 2019, 9, 6305-6319.	5.5	109
4605	First Principle Study of the Attachment of Graphene onto Different Terminated Diamond (111) Surfaces. Advances in Condensed Matter Physics, 2019, 2019, 1-9.	0.4	7
4606	An energy band engineering design to enlarge the band gap of KTiOPO₄(KTP)-type sulfatesviaaliovalent substitution. Journal of Materials Chemistry C, 2019, 7, 8131-8138.	2.7	46
4607	Electronic, Elastic, and Vibrational Properties of ZrBeSi via First Principles. Physica Status Solidi (B): Basic Research, 2019, 256, 1900118.	0.7	3
4608	In Situ X-ray Absorption Spectroscopy Studies of Nanoscale Electrocatalysts. Nano-Micro Letters, 2019, 11, 47.	14.4	181
4609	Electronic structure, chemical bonding, optical, elastic and dynamical properties of MeB2 compounds: Effect of transition metal Meâ€¯=â€¯Sc, Ti and Zr. Computational Condensed Matter, 2019, 21, e00406.	0.9	12
4610	Bonding in 2D Donorâ€“Acceptor Heterostructures. Journal of the American Chemical Society, 2019, 141, 10300-10308.	6.6	42
4611	Electronic structures and elastic properties of a family of metal-free perovskites. Materials Chemistry Frontiers, 2019, 3, 1678-1685.	3.2	46
4612	17O NMR studies of organic and biological molecules in aqueous solution and in the solid state. Progress in Nuclear Magnetic Resonance Spectroscopy, 2019, 114-115, 135-191.	3.9	47

#	Article	IF	Citations
4613	Theory and practice of modeling van der Waals interactions in electronic-structure calculations. Chemical Society Reviews, 2019, 48, 4118-4154.	18.7	114
4614	Ultrasoft pseudopotentials with kinetic energy density support: Implementing the Tran-Blaha potential. Physical Review B, 2019, 99, .	1.1	10
4615	Structure and Morphology of Light-Reflecting Synthetic and Biogenic Polymorphs of Isoxanthopterin: A Comparison. Chemistry of Materials, 2019, 31, 4479-4489.	3.2	12
4616	Underlying Molecular Interactions between Sodium Montmorillonite Clay and Acidic Bitumen. Journal of Physical Chemistry C, 2019, 123, 15513-15522.	1.5	21
4617	Micro-Kinetic Modelling of CO-TPD from Fe(100)â€"Incorporating Lateral Interactions. Catalysts, 2019, 9, 310.	1.6	10
4618	Quantum Mechanical Modeling of the Vibrational Spectra of Minerals with a Focus on Clays. Minerals (Basel, Switzerland), 2019, 9, 141.	0.8	18
4619	Intrinsic phonon-mediated superconductivity in graphene-like BSi lattice. Journal of Physics Condensed Matter, 2019, 31, 345401.	0.7	5
4620	Crystal structures and decomposing of Bâ€“P compounds under pressure*. Chinese Physics B, 2019, 28, 056101.	0.7	5
4621	A new BaCa(CO₃)₂polymorph. Acta Crystallographica Section B: Structural Science, Crystal Engineering and Materials, 2019, 75, 291-300.	0.5	5
4622	Electronic Structure and Ferromagnetic Transition Temperature of Ga1â€“ xMnxAs in the Nonempirical Local Exchange Method. Inorganic Materials, 2019, 55, 1-8.	0.2	5
4623	A hybrid niobium-based oxide with bio-based porous carbon as an efficient electrocatalyst in photovoltaics: a general strategy for understanding the catalytic mechanism. Journal of Materials Chemistry A, 2019, 7, 14864-14875.	5.2	74
4624	Be₂CO₃F₂ Monolayer: A Flexible Ultraviolet Nonlinear Optical Material via Rational Design. Inorganic Chemistry, 2019, 58, 7715-7721.	1.9	2
4625	Combining Pseudopotential and All Electron Density Functional Theory for the Efficient Calculation of Core Spectra Using a Multiresolution Approach. Journal of Physical Chemistry A, 2019, 123, 4465-4474.	1.1	5
4626	Modulation of perovskite-related frameworks induced by alkaline earth metals in phosphate fluorides A₂MPO₄F (A = K, Rb; M = Ba, Ca). New Journal of Chemistry, 2019, 43, 7839-7845.	1.4	6
4627	Precisely-controlled, a few layers of iron titanate inverse opal structure for enhanced photoelectrochemical water splitting. Nano Energy, 2019, 62, 20-29.	8.2	24
4628	Structural and electrical properties of Gaâ€“Te systems under high pressure. Chinese Physics B, 2019, 28, 056104.	0.7	6
4629	Three new phosphates, Cs8Pb4(P2O7)4, CsLi7(P2O7)2 and LiCa(PO3)3: structural comparison, characterization and theoretical calculation. Dalton Transactions, 2019, 48, 8948-8954.	1.6	17
4630	Two alkali calcium borates exhibiting second harmonic generation and deep-UV cutoff edges. New Journal of Chemistry, 2019, 43, 9354-9363.	1.4	2

#	Article	IF	Citations
4631	Regularized SCAN functional. Journal of Chemical Physics, 2019, 150, 161101.	1.2	124
4632	Computational analysis of vibrational spectrum and hydrogen bonds of ice XVII. New Journal of Physics, 2019, 21, 043054.	1.2	15
4633	Cubic Germanium monochalcogenides (Ï€-GeS and Ï€-GeSe): Emerging materials for optoelectronic and energy harvesting devices. Solar Energy, 2019, 185, 211-221.	2.9	19
4634	Large optical gaps in the half-metallic ferromagnet xmlns:mml="http://www.w3.org/1998/Math/MathML"><mml:mi>M</mml:mi><mml:msub><mml:mrow><mml:mi mathvariant="normal">N</mml:mi></mml:mrow><mml:mn>4</mml:mn></mml:msub></mml:math> () Tj ETQq1 1 0.784314 rgBT /Ov xmlns:mml="http://www.w3.org/1998/Math/MathML"><mml:msub><mml:mrow><mml:mi mathvariant="n	1.1	10
4635	Predicting properties of MgOÂ·nAl₂O₃ by firstâ€principles calculation combined with bond valence models. Journal of the American Ceramic Society, 2019, 102, 6913-6924.	1.9	6
4636	Strontium and Zinc Substitution in Î²-Tricalcium Phosphate: An X-ray Diffraction, Solid State NMR and ATR-FTIR Study. Journal of Functional Biomaterials, 2019, 10, 20.	1.8	45
4637	Complex twin interfaces in M6C carbides. Materials Letters, 2019, 250, 167-169.	1.3	3
4638	High-Pressure Polymorphs of LaHO with Anion Coordination Reversal. Journal of the American Chemical Society, 2019, 141, 8717-8720.	6.6	19
4639	An XRD and NMR crystallographic investigation of the structure of 2,6-lutidinium hydrogen fumarate. CrystEngComm, 2019, 21, 3502-3516.	1.3	16
4640	Adsorption site, orientation and alignment of NO adsorbed on Au(100) using 3D-velocity map imaging, X-ray photoelectron spectroscopy and density functional theory. Physical Chemistry Chemical Physics, 2019, 21, 10939-10946.	1.3	11
4641	High Pressure Hydrocarbons Revisited: From van der Waals Compounds to Diamond. Geosciences (Switzerland), 2019, 9, 227.	1.0	18
4642	Exploring Accuracy Limits of Predictions of the 1H NMR Chemical Shielding Anisotropy in the Solid State. Molecules, 2019, 24, 1731.	1.7	11
4643	A systematic study of the surface structures and energetics of CH3NO2 surfaces by first-principles calculations. Journal of Molecular Modeling, 2019, 25, 164.	0.8	4
4644	Structural and electronic properties of Nb-Cr-Si based alloys: First-principles calculations. Physica B: Condensed Matter, 2019, 568, 1-5.	1.3	2
4645	Utilizing Crystal Structures for Predicting Impact of Mechanical and Surface Properties on Particle Fracture. Crystal Growth and Design, 2019, 19, 3670-3680.	1.4	25
4646	Epitaxial highly ordered Sb:SnO2 nanowires grown by the vapor liquid solid mechanism on m-, r- and a-Al2O3. Nanoscale Advances, 2019, 1, 1980-1990.	2.2	8
4647	Selecting substituent elements for LiMnPO4 cathode materials combined with density functional theory (DFT) calculations and experiments. Journal of Alloys and Compounds, 2019, 793, 360-368.	2.8	31
4648	Electronic structure, mechanical and physical properties of Ag alloyed Î±-Nb5Si3: First-principles calculations. Physica B: Condensed Matter, 2019, 564, 80-90.	1.3	6

#	Article	IF	Citations
4649	Discoloration Effect and One-Step Synthesis of Hydrogen Tungsten and Molybdenum Bronze (H_xMO₃) using Liquid Metal at Room Temperature. ACS Omega, 2019, 4, 7428-7435.	1.6	28
4650	Confined annealing-induced transformation of tin oxide into sulfide for sodium storage applications. Journal of Materials Chemistry A, 2019, 7, 11877-11885.	5.2	18
4651	A full additive QM/MM scheme for the computation of molecular crystals with extension to many-body expansions. Journal of Chemical Physics, 2019, 150, 154118.	1.2	6
4652	Soft-phonon driven hexagonal-orthorhombic phase transition in BaVS3. Physical Review B, 2019, 99, .	1.1	4
4653	Luminescence Properties of Undoped Langasite Crystals. Physics of the Solid State, 2019, 61, 307-314.	0.2	2
4654	Structural, electronic, optical and elastic properties of layered rhombohedral compounds ALaSe₂(A=K, Rb): Insights from an ab initio study. International Journal of Modern Physics B, 2019, 33, 1950084.	1.0	9
4655	Silver Oxalate: Mechanical Properties and Extreme Negative Mechanical Phenomena. Advanced Theory and Simulations, 2019, 2, 1900040.	1.3	23
4656	MoS2-Based Photodetectors Powered by Asymmetric Contact Structure with Large Work Function Difference. Nano-Micro Letters, 2019, 11, 34.	14.4	49
4657	The crystal structure of visible light absorbing piezoelectric semiconductor SrNb₂V₂O₁₁revisited: high-resolution X-ray diffraction, vibrational spectroscopy and computational study. Journal of Materials Chemistry C, 2019, 7, 5497-5505.	2.7	2
4658	Huge power factor in p-type half-Heusler alloys NbFeSb and TaFeSb. JPhys Materials, 2019, 2, 035002.	1.8	33
4659	Highly efficient and very robust blue-excitable yellow phosphors built on multiple-stranded one-dimensional inorganicâ€“organic hybrid chains. Chemical Science, 2019, 10, 5363-5372.	3.7	38
4660	Photovoltaic Performance of Phase-Pure Orthorhombic BiSI Thin-Films. ACS Applied Energy Materials, 2019, 2, 3878-3885.	2.5	50
4661	First-Principles Study on the Mechanical Properties and Electronic Structure of V Doped WCoB and W2CoB2 Ternary Borides. Materials, 2019, 12, 967.	1.3	17
4662	From Nonluminescent to Blueâ€Emitting Cs₄PbBr₆ Nanocrystals: Tailoring the Insulator Bandgap of 0D Perovskite through Sn Cation Doping. Advanced Materials, 2019, 31, e1900606.	11.1	61
4663	Tunable electronic and optical properties of new two-dimensional GaN/BAs van der Waals heterostructures with the potential for photovoltaic applications. Chemical Physics Letters, 2019, 728, 124-131.	1.2	63
4664	Alkaline-earth and aminonicotinate based coordination polymers with combined fluorescence/long-lasting phosphorescence and metal ion sensing response. Journal of Materials Chemistry C, 2019, 7, 6997-7012.	2.7	21
4665	First-principles studies of superhard BC8N structures. Journal of Applied Physics, 2019, 125, .	1.1	14
4666	Structureâ€“Property-Performance Relationship of Ultrathin Pdâ€“Au Alloy Catalyst Layers for Low-Temperature Ethanol Oxidation in Alkaline Media. ACS Applied Materials & Interfaces, 2019, 11, 24919-24932.	4.0	27

#	Article	IF	Citations
4667	Ultrathin MoS₂ Nanosheets Decorated Hollow CoP Heterostructures for Enhanced Hydrogen Evolution Reaction. ACS Sustainable Chemistry and Engineering, 2019, 7, 10105-10111.	3.2	50
4668	Observation of an oxonium ion intermediate in ethanol dehydration to ethene on zeolite. Nature Communications, 2019, 10, 1961.	5.8	40
4669	Electronic Structures of Alkaline Rare Earth Fluoride-Based Upconversion Nanomaterials. , 2019, , 447-467.		0
4670	Anomalous pressure dependence of the electronic properties of molecular crystals explained by changes in intermolecular electronic coupling. Synthetic Metals, 2019, 253, 9-19.	2.1	4
4671	Elastic and hydrostatic behaviour of a zinc dietary supplement, zinc glycinate hydrate. RSC Advances, 2019, 9, 13153-13158.	1.7	6
4672	Comparison between density functional theory and density functional tight binding approaches for finding the muon stopping site in organic molecular crystals. Journal of Chemical Physics, 2019, 150, 154301.	1.2	6
4673	Tungsten Nitride/Carbon Cloth as Bifunctional Electrode for Effective Polysulfide Recycling. ACS Applied Energy Materials, 2019, 2, 3314-3322.	2.5	35
4674	Synthesis, crystal structures and nonlinear optical properties of Î²-RbCdI3Â·H2O and CsCdI3Â·H2O. Dalton Transactions, 2019, 48, 6787-6793.	1.6	1
4675	From centrosymmetric to noncentrosymmetric: cation-directed structural evolution in X₃ZnB₅O₁₀(X = Na, K, Rb) and Cs₁₂Zn₄(B₅O₁₀)₄crystals. Inorganic Chemistry Frontiers, 2019, 6, 1461-1467.	3.0	14
4676	Deep-ultraviolet nonlinear optical crystal NaBe2BO3F2â€"Structure, growth and optical properties. Journal of Crystal Growth, 2019, 518, 45-50.	0.7	17
4677	DFT study the adsorption of ethyl xanthate on the S-site of Cu-activated sphalerite (1â€¯1â€¯0) surface in the presence of water molecule. Results in Physics, 2019, 13, 102271.	2.0	19
4678	Theoretical Prediction and Experimental Evaluation of Topological Landscape and Thermodynamic Stability of a Fluorinated Zeolitic Imidazolate Framework. Chemistry of Materials, 2019, 31, 3777-3783.	3.2	31
4679	Thermodynamic, Raman Spectroscopic, and UVâ€"Visible Optical Characterization of the Deltic, Squaric, and Croconic Cyclic Oxocarbon Acids. Journal of Physical Chemistry A, 2019, 123, 4241-4261.	1.1	13
4680	Structural, electronic, and optical properties of inhomogeneous Ca1â^'x Mg x O alloys. Journal of Applied Physics, 2019, 125, 155102.	1.1	5
4681	Rechargeable ultrahigh-capacity telluriumâ€"aluminum batteries. Energy and Environmental Science, 2019, 12, 1918-1927.	15.6	172
4682	Thermallyâ€Induced Reactions of Aromatic Crystalline Nitroso Compounds. ChemistrySelect, 2019, 4, 4709-4717.	0.7	5
4683	Synthesis, optical properties, and band structures of a series of layered mixed-anion compounds. Journal of Materials Science: Materials in Electronics, 2019, 30, 16827-16832.	1.1	3
4684	A spin density functional calculations in electronic structures and magnetic properties of transition metal doped GaP. Chemical Physics, 2019, 523, 57-62.	0.9	4

#	Article	IF	Citations
4685	Chemical bonding and band alignment at X2O3/GaN (Xâ€‰=â€‰Al, Sc) interfaces. Applied Physics Letters, 2019, 114, .	1.5	36
4686	Alternative Friction Mechanism for Amorphous Carbon Films Sliding against Alumina. Industrial & Engineering Chemistry Research, 2019, 58, 4810-4817.	1.8	16
4687	Silicene catalysts for CO₂hydrogenation: the number of layers controls selectivity. Nanoscale, 2019, 11, 7734-7743.	2.8	28
4688	Theoretical study of the oxidation of formic acid on a PtPd(111) surface. Progress in Reaction Kinetics and Mechanism, 2019, 44, 67-73.	1.1	5
4689	Periodic density functional theory study of the Raman spectrum of the hydrated uranyl oxyhydroxide mineral becquerelite. Theoretical Chemistry Accounts, 2019, 138, 1.	0.5	12
4690	Metal-free N, S co-doped graphene for efficient and durable nitrogen reduction reaction. Journal of Materials Science, 2019, 54, 9088-9097.	1.7	79
4691	Study of Structural, Electronic and Vibrational Properties of Porous Silicon with Different Porosity. Silicon, 2019, 11, 2505-2515.	1.8	4
4692	One-pot synthesis of porous 1T-phase MoS2 integrated with single-atom Cu doping for enhancing electrocatalytic hydrogen evolution reaction. Applied Catalysis B: Environmental, 2019, 251, 87-93.	10.8	160
4693	Thermodynamics and kinetics of an oxygen adatom on pristine and functionalized graphene: insight gained into their anticorrosion properties. Physical Chemistry Chemical Physics, 2019, 21, 12121-12129.	1.3	11
4694	Pressure and temperature effect of hexagonal phase FeN2: A first-principle study. Ceramics International, 2019, 45, 11776-11783.	2.3	15
4695	Advances in Sustainable Catalysis: A Computational Perspective. Frontiers in Chemistry, 2019, 7, 182.	1.8	36
4696	Distinguishing nitrogen-containing sites in the m face of 4H-SiC after nitric oxide annealing by X-ray absorption spectroscopy. Japanese Journal of Applied Physics, 2019, 58, 051007.	0.8	4
4697	Experimental and Computational Design of Highly Active Ceâ€“ZrO2â€“GO Photocatalyst for Eosin Yellow Dye Degradation: The Role of Interface and Ce3+ Ion. Catalysis Letters, 2019, 149, 1633-1650.	1.4	18
4698	Modulation of piezochromic fluorescence behavior by subtle structural change. Dyes and Pigments, 2019, 166, 301-306.	2.0	6
4699	Molecular Switch by Adsorbing the Au₆ Cluster on Single-Walled Carbon Nanotubes: Role of Many-Body Effects of vdW Forces. Journal of Physical Chemistry C, 2019, 123, 9217-9222.	1.5	6
4700	Module-Analysis-Assisted Design of Deep Ultraviolet Fluorooxoborates with Extremely Large Gap and High Structural Stability. Chemistry of Materials, 2019, 31, 2807-2813.	3.2	87
4701	(C₆H₁₃NH₃)₂(NH₂CHNH₂)Pb₂I<sub>7</su A Twoâ€dimensional Bilayer Inorganicâ€“Organic Hybrid Perovskite Showing Photodetecting Behavior. Chemistry - an Asian Journal, 2019, 14, 1530-1534.	1.7	18
4702	Palladium-loaded tantalum oxide modified Pt electrode toward electrochemical oxidation of ethylene glycol. Journal of Electroanalytical Chemistry, 2019, 839, 166-172.	1.9	3

#	Article	IF	Citations
4703	A first-principles study on magnetic properties of the intrinsic defects in wurtzite ZnO. Journal of Chemical Physics, 2019, 150, 094704.	1.2	16
4704	Theoretical insight into the hydrogen adsorption on MoS2 (MoSe2) monolayer as a function of biaxial strain/external electric field. Applied Surface Science, 2019, 478, 857-865.	3.1	38
4705	A first-principles study of novel cubic AlN phases. Journal of Physics and Chemistry of Solids, 2019, 130, 58-66.	1.9	5
4706	Bulk crystal growth and characterization of the bismuth ferrite-based material Bi₃FeO₄(MoO₄)₂. CrystEngComm, 2019, 21, 2508-2516.	1.3	10
4707	The physical properties of ThCr2Si2- type nickel-based superconductors BaNi2T2 (Tâ€¯=â€¯P, As): An ab-initio study. Chinese Journal of Physics, 2019, 59, 58-69.	2.0	11
4708	Phenylated Acene Derivatives as Candidates for Intermolecular Singlet Fission. Journal of Physical Chemistry C, 2019, 123, 5890-5899.	1.5	20
4709	High-pressure compressibility and electronic properties of bismuth silicate Bi2SiO5 from synchrotron experiments and first-principles calculations. Physical Review B, 2019, 99, .	1.1	8
4710	First-principles study of localized and delocalized electronic states in crystallographic shear phases of niobium oxide. Physical Review B, 2019, 99, .	1.1	30
4711	Properties of phase transition and interfaces of Cu2ZnSnS4 with hetero-phase junctions. Applied Surface Science, 2019, 481, 1044-1052.	3.1	4
4712	Investigation of half-metallicity and magnetism of bulk and (111)-surfaces of Fe2MnP full Heusler alloy. Vacuum, 2019, 164, 336-342.	1.6	37
4713	Computational design of metal-supported molecular switches: transient ion formation during light- and electron-induced isomerisation of azobenzene. Journal of Physics Condensed Matter, 2019, 31, 044003.	0.7	2
4714	Addendum: anomalous mechanical behavior of the deltic, squaric and croconic cyclic oxocarbon acids. Materials Research Express, 2019, 6, 069401.	0.8	7
4715	Quantitative estimation of properties from core-loss spectrum via neural network. JPhys Materials, 2019, 2, 024003.	1.8	21
4716	A Preview of a Construction of a Crystal Lattice Based on Intermolecular Interactions. Crystals, 2019, 9, 159.	1.0	0
4717	Martensitic transformation and magnetic properties in Pd2MnGa Heusler alloy by DFT study. Modern Physics Letters B, 2019, 33, 1950074.	1.0	1
4718	Optimization of Electrical Properties of MoS 2 Fieldâ€Effect Transistors by Dipole Layer Coulombic Interaction With Trap States. Physica Status Solidi - Rapid Research Letters, 2019, 13, 1900007.	1.2	5
4719	Effects of transmutation elements in tungsten. Computational Materials Science, 2019, 162, 133-139.	1.4	11
4720	Uncertainty quantification for classical effective potentials: an extension to potfit. Modelling and Simulation in Materials Science and Engineering, 2019, 27, 044001.	0.8	12

#	Article	IF	Citations
4721	Managing uncertainty in data-derived densities to accelerate density functional theory. JPhys Materials, 2019, 2, 034001.	1.8	9
4722	Quantitative analysis of 14N quadrupolar coupling using 1H detected 14N solid-state NMR. Physical Chemistry Chemical Physics, 2019, 21, 5941-5949.	1.3	20
4723	Synergistic Mechanism of Rare-Earth Modification TiO2 and Photodegradation on Benzohydroxamic Acid. Applied Sciences (Switzerland), 2019, 9, 339.	1.3	13
4724	Multinuclear NMR spectra and GIAO/DFT calculations of N-benzylazoles and N-benzylbenzazoles. Structural Chemistry, 2019, 30, 1729-1735.	1.0	10
4725	Refractive Index Modulates Second-Harmonic Responses in RE₈O(CO₃)₃(OH)₁₅X (RE = Y, Lu; X = Cl, Br): Rare-Earth Halide Carbonates as Ultraviolet Nonlinear Optical Materials. Chemistry of Materials, 2019, 31, 2130-2137.	3.2	28
4726	Theory of momentum-resolved phonon spectroscopy in the electron microscope. Physical Review B, 2019, 99, .	1.1	20
4727	A study of the synergistic effects of Mn/steam on CO₂ capture performance of CaO by experiment and DFT calculation. , 2019, 9, 409-423.		14
4728	Itinerant ferromagnetism induced by electron doping in SrCo2As2. Inorganic Chemistry Communication, 2019, 103, 25-29.	1.8	6
4729	A theoretical investigation of ThCr2Si2-type Pd-based superconductors XPd2Ge2 (Xâ€¯=â€¯Ca, Sr, La, Nd). Physica C: Superconductivity and Its Applications, 2019, 561, 35-44.	0.6	9
4730	Theoretical Insights of Ni₂P (0001) Surface toward Its Potential Applicability in CO₂ Conversion via Dry Reforming of Methane. ACS Catalysis, 2019, 9, 3487-3497.	5.5	36
4731	A preconditioning scheme for minimum energy path finding methods. Journal of Chemical Physics, 2019, 150, 094109.	1.2	12
4732	The Lorentz sphere visualised. Journal of Chemical Physics, 2019, 150, 094103.	1.2	1
4733	Electronic transport properties of boron and nitrogen pair co-doped 6,6,12-graphyne nanosheet from first principles. Physica Scripta, 2019, 94, 075801.	1.2	4
4734	Theoretical Study of As2O3 Adsorption Mechanisms on CaO surface. Materials, 2019, 12, 677.	1.3	29
4735	First-Principles Study of AlPO4-H3, a Hydrated Aluminophosphate Zeotype Containing Two Different Types of Adsorbed Water Molecules. Molecules, 2019, 24, 922.	1.7	9
4736	SrCdSnQ₄ (Q = S and Se): infrared nonlinear optical chalcogenides with mixed NLO-active and synergetic distorted motifs. Journal of Materials Chemistry C, 2019, 7, 4459-4465.	2.7	52
4737	Insight into C, Ge and Sn substitution on structural and electronic properties of Li2FeSiO4: Spin density functional theory. Materials Chemistry and Physics, 2019, 229, 467-473.	2.0	6
4738	Balanced Second-Order Nonlinear Optical Properties of Adducts CHI₃Â·(S₈)₃ and AsI₃Â·(S₈)₃: A Systematic Survey. Inorganic Chemistry, 2019, 58, 4619-4625.	1.9	40

#	Article	IF	Citations
4739	Rational design of a tubular, interlayer expanded MoS₂â€“N/O doped carbon composite for excellent potassium-ion storage. Journal of Materials Chemistry A, 2019, 7, 9305-9315.	5.2	97
4740	Cs2 Zn5 (PO4)4 and Cs3 La(PO4)2 : Two Cs-Containing Phosphates with Three-Dimensional Frameworks. European Journal of Inorganic Chemistry, 2019, 2019, 2462-2467.	1.0	10
4741	Bulk and surface properties of gypsum: A comparison between classical force fields and dispersion-corrected DFT calculations. Computational Materials Science, 2019, 164, 8-16.	1.4	10
4742	Short-Range Structure of Amorphous Calcium Hydrogen Phosphate. Crystal Growth and Design, 2019, 19, 3030-3038.	1.4	35
4743	Prediction of the near-IR spectra of ices by ab initio molecular dynamics. Physical Chemistry Chemical Physics, 2019, 21, 9433-9440.	1.3	2
4744	RbSbSO₄Cl₂: an excellent sulfate nonlinear optical material generated due to the synergistic effect of three asymmetric chromophores. Journal of Materials Chemistry C, 2019, 7, 5748-5754.	2.7	58
4745	Synthesis of large-scale few-layer PtS2 films by chemical vapor deposition. AIP Advances, 2019, 9, .	0.6	42
4746	The physical properties of ThCr2Si2-type Ru-based compounds SrRu2X2 (X = P, Ge, As): An ab-inito investigation. Physica C: Superconductivity and Its Applications, 2019, 562, 48-55.	0.6	4
4747	Systematic materials design for phase-change memory with small density changes for high-endurance non-volatile memory applications. Applied Physics Express, 2019, 12, 051008.	1.1	7
4748	Evaluation of the phase stability, and mechanical and thermal properties of Ba(Sr1/3Ta2/3)O3 as a potential ceramic material for thermal barrier coatings. Ceramics International, 2019, 45, 12989-12993.	2.3	5
4749	Phase stability and physical properties of (Zr1-Nb)2AlC MAX phases. Journal of Physics and Chemistry of Solids, 2019, 132, 38-47.	1.9	32
4750	MgCu2-type laves phases CaPt2, SrPd2 and SrPt2: A DFT based ab-initio investigation. Solid State Communications, 2019, 296, 1-7.	0.9	4
4751	Atomic investigation on reversible and irreversible lithium storage in silicon incorporated with multi-layered graphene. Materials Letters, 2019, 244, 108-110.	1.3	4
4752	Suppression of Defect-Induced Quenching via Chemical Potential Tuning: A Theoretical Solution for Enhancing Lanthanide Luminescence. Journal of Physical Chemistry C, 2019, 123, 11151-11161.	1.5	26
4753	Drastic photoluminescence modulation of an organic molecular crystal with high pressure. Materials Chemistry Frontiers, 2019, 3, 1510-1517.	3.2	17
4754	On the chain-melted phase of matter. Proceedings of the National Academy of Sciences of the United States of America, 2019, 116, 10297-10302.	3.3	19
4755	Two Polar Molybdenum(VI) Iodates(V) with Large Second-Harmonic Generation Responses. Chemistry of Materials, 2019, 31, 2992-3000.	3.2	60
4756	Ga-Doped and Pt-Loaded Porous TiO₂â€“SiO₂ for Photocatalytic Nonoxidative Coupling of Methane. Journal of the American Chemical Society, 2019, 141, 6592-6600.	6.6	218

#	Article	IF	Citations
4757	First-principles calculations of the effect of Ge content on the electronic, mechanical and acoustic properties of Li17Si4-xGex. Current Applied Physics, 2019, 19, 663-669.	1.1	1
4758	Structural and electronic properties of the Î±-GeSe surface. Surface Science, 2019, 686, 17-21.	0.8	4
4759	Solid state properties of hydroxyurea: Optical absorption measurement and DFT calculations. Journal of Applied Physics, 2019, 125, 134901.	1.1	4
4760	Nuclear Magnetic Resonance Spectroscopy as a Dynamical Structural Probe of Hydrogen under High Pressure. Physical Review Letters, 2019, 122, 135501.	2.9	9
4761	Bond characteristics, mechanical properties, and highâ€temperature thermal conductivity of (Hf_{1â^'x}Ta_x)C composites. Journal of the American Ceramic Society, 2019, 102, 6298-6308.	1.9	22
4762	Band Engineering of Double-Layered SillÃ©nâ€“Aurivillius Perovskite Oxychlorides for Visible-Light-Driven Water Splitting. Chemistry of Materials, 2019, 31, 3419-3429.	3.2	50
4763	BaHgGeSe₄ and SrHgGeSe₄: Two New Hg-Based Infrared Nonlinear Optical Materials. Chemistry of Materials, 2019, 31, 3034-3040.	3.2	104
4764	Origin of resistivity contrast in interfacial phase-change memory: The crucial role of Ge/Sb intermixing. Applied Physics Letters, 2019, 114, .	1.5	37
4765	Local magnetism, magnetic order and spin freezing in the â€˜nonmetallic metalâ€™ FeCrAs. Journal of Physics Condensed Matter, 2019, 31, 285803.	0.7	8
4766	Effects of Hydrostatic Pressure and Biaxial Strains on the Elastic, Electronic and Lattice Vibrational Properties of Trigonal Boron Nitride. Physica Status Solidi (B): Basic Research, 2019, 256, 1800699.	0.7	2
4767	Atomistic diffusion mechanism of rare earth carburizing/nitriding on iron-based alloy. Applied Surface Science, 2019, 484, 710-715.	3.1	17
4768	Nanorod CoFe2O4 modified activated carbon as an efficient electrocatalyst to improve the performance of air cathode microbial fuel cell. Journal of Electroanalytical Chemistry, 2019, 840, 134-143.	1.9	19
4769	Physical properties of ThCr2Si2-type Ni-based compounds SrNi2M2 (M= As and Ge): DFT based Ab-inito calculations. Physica C: Superconductivity and Its Applications, 2019, 560, 19-25.	0.6	2
4770	DFT calculations of energetic stability and geometry of O-terminated B- and N-doped diamond (1â€‰1â€‰1)-1â€‰â€‰Ã—â€‰â€‰ surfaces. Journal of Physics Condensed Matter, 2019, 31, 265002.	0.7	6
4771	Structural, electronic, optical and lattice dynamic properties of the different WO3 phases: First-principle calculation. Vacuum, 2019, 164, 411-420.	1.6	37
4772	Two Deep Ultraviolet Hydrated Borate Crystals: Centrosymmetric LiRbB₅O₈(OH)Â·H₂O and Non-Centrosymmetric K₂B₅O₈(OH)Â·2H₂O. Crystal Growth and Design, 2019, 19, 3052-3059.	1.4	5
4773	Structures, photoresponse properties and DNA binding abilities of 4-(4-pyridinyl)-2-pyridone salts. RSC Advances, 2019, 9, 9663-9677.	1.7	24
4774	Hypergolic zeolitic imidazolate frameworks (ZIFs) as next-generation solid fuels: Unlocking the latent energetic behavior of ZIFs. Science Advances, 2019, 5, eaav9044.	4.7	52

#	Article	IF	Citations
4775	Effect by Diamond Surface Modification on Biomolecular Adhesion. Materials, 2019, 12, 865.	1.3	3
4776	Effect of M elements (Mâ€‰â€‰=â€‰â€‰Ti, Zr, and Hf) on thermoelectric performance of the half-Heusler compounds MCoBi. Journal Physics D: Applied Physics, 2019, 52, 255501.	1.3	26
4777	Physical properties of Ima2-BN under pressure: First principles calculations. Chinese Journal of Physics, 2019, 59, 317-324.	2.0	22
4778	Insights into dynamic molecular intercalation mechanism for Al C battery by operando synchrotron X-ray techniques. Carbon, 2019, 146, 528-534.	5.4	42
4779	Multicomponent Crystal Forms of a Biologically Active Hydrazone with Some Dicarboxylic Acids: Salts or Cocrystals?. Crystal Growth and Design, 2019, 19, 2663-2678.	1.4	6
4780	Equation of State of Fluid Methane from First Principles with Machine Learning Potentials. Journal of Chemical Theory and Computation, 2019, 15, 2574-2586.	2.3	40
4781	Siliconâ€Compatible Photodetectors: Trends to Monolithically Integrate Photosensors with Chip Technology. Advanced Functional Materials, 2019, 29, 1808182.	7.8	198
4782	A Photostimulated BaSi₂O₅:Eu²⁺,Nd³⁺ Phosphorâ€inâ€Glass for Erasableâ€Rewritable Optical Storage Medium. Laser and Photonics Reviews, 2019, 13, 1900006.	4.4	55
4783	A DFT/ZORA Study of Cadmium Magnetic Shielding Tensors: Analysis of Relativistic Effects and Electronic-State Approximations. Journal of Chemical Theory and Computation, 2019, 15, 1785-1797.	2.3	5
4784	Effect of the Inherent Structure of Rh Nanocrystals on the Hydriding Behavior under Pressure. Journal of Physical Chemistry Letters, 2019, 10, 774-779.	2.1	5
4785	A novel porous C₄N₄monolayer as a potential anchoring material for lithiumâ€“sulfur battery design. Journal of Materials Chemistry A, 2019, 7, 4134-4144.	5.2	135
4786	Phonon-driven phase transitions in calcite, dolomite, and magnesite. Physical Review B, 2019, 99, .	1.1	7
4787	Hyperspatial optimization of structures. Physical Review B, 2019, 99, .	1.1	15
4788	First-principles anharmonic vibrational study of the structure of calcium silicate perovskite under lower mantle conditions. Physical Review B, 2019, 99, .	1.1	3
4789	Attractive In Situ Selfâ€Reconstructed Hierarchical Gradient Structure of Metallic Glass for High Efficiency and Remarkable Stability in Catalytic Performance. Advanced Functional Materials, 2019, 29, 1807857.	7.8	74
4790	Phononâ€“Glass and Heterogeneous Electrical Transport in A-Site-Deficient SrTiO₃. Journal of Physical Chemistry C, 2019, 123, 5198-5208.	1.5	17
4791	Molecular Topology and the Surface Chemical Bond: Alternant Versus Nonalternant Aromatic Systems as Functional Structural Elements. Physical Review X, 2019, 9, .	2.8	14
4792	First-principles molecular dynamics simulation of the ionic structure and electronic properties of Na3AlF6 molten salt. Chemical Physics Letters, 2019, 718, 63-68.	1.2	12

#	Article	IF	Citations
4793	An ab initio study of spectroscopic and thermodynamic characteristics of MgH2 and TiC systems. International Journal of Hydrogen Energy, 2019, 44, 6756-6762.	3.8	8
4794	Growth, Structure, and Optical Properties of Nonlinear LiGa_{0.55}In_{0.45}Te₂ Single Crystals. Crystal Growth and Design, 2019, 19, 1805-1814.	1.4	4
4795	Comprehensive investigation of methane conversion over Ni(111) surface under a consistent DFT framework: Implications for anti-coking of SOFC anodes. Applied Surface Science, 2019, 480, 243-255.	3.1	52
4796	Unveiling the origin of boosted photocatalytic hydrogen evolution in simultaneously (S, P,) Tj ETQq1 1 0.784314 rgBT /Overlock 10 Tf 5 84-94.	10.8	300
4797	On the mechanical properties of protomene: A theoretical investigation. Computational Materials Science, 2019, 161, 190-198.	1.4	11
4798	Simulation of Inelastic Neutron Scattering Spectra Using OCLIMAX. Journal of Chemical Theory and Computation, 2019, 15, 1974-1982.	2.3	95
4799	Ce³⁺self-doped CeO_x/FeOCl: an efficient Fenton catalyst for phenol degradation under mild conditions. Dalton Transactions, 2019, 48, 3476-3485.	1.6	31
4800	Crystal structures, dielectric properties and ferroelectricity in stuffed tridymite-type BaAl(2â^'2x)(Zn0.5Si0.5)2xO4 solid solutions. Dalton Transactions, 2019, 48, 3625-3634.	1.6	14
4801	Upconversion luminescence enhancement and lifetime based thermometry of Na(Gd/Lu)F₄solid solutions. New Journal of Chemistry, 2019, 43, 3848-3855.	1.4	13
4802	First-Principles Investigation of the Mechanical and Thermodynamic Properties of the Metal-Borohydrides as Electrolytes for Solid-State Batteries. Journal of the Electrochemical Society, 2019, 166, A493-A500.	1.3	10
4803	Predicting Hydration Reactivity of Cu-Doped Clinker Crystals by Capturing Electronic Structure Modification. ACS Sustainable Chemistry and Engineering, 2019, 7, 6412-6421.	3.2	20
4804	From DFT to machine learning: recent approaches to materials scienceâ€“a review. JPhys Materials, 2019, 2, 032001.	1.8	385
4805	First-Principles Investigation of Adsorption of Ag on Defected and Ce-doped Graphene. Materials, 2019, 12, 649.	1.3	9
4806	Density Functional Theory Study on Defect Behavior Related to the Bulk Lifetime of Silicon Crystals for Power Device Application. Physica Status Solidi (A) Applications and Materials Science, 2019, 216, 1800615.	0.8	6
4807	Thermoelastic properties of deuterated melamine, C₃N₆D₆, between 4.2â€“320â€…K at 5â€…kPa and between 0.1â€“5.0â€…GPa at 295â€…K from neutron powder diffraction and DFT calculations. High Pressure Research, 2019, 39, 160-178.	0.4	2
4808	Insight into Physical and Thermodynamic Properties of X3Ir (X = Ti, V, Cr, Nb and Mo) Compounds Influenced by Refractory Elements: A First-Principles Calculation. Crystals, 2019, 9, 104.	1.0	2
4809	The electronic, half-metallic, and magnetic properties of Ca1-Cr S ternary alloys: Insights from the first-principle calculations. Journal of Molecular Graphics and Modelling, 2019, 89, 22-32.	1.3	43
4810	Ba10In6Zn7S26-nZnS: An Inorganic Composite System with Interface Phase-Matching Tuned for High-Performance Infrared Nonlinear Optical Materials. Inorganic Chemistry, 2019, 58, 3990-3999.	1.9	8

#	Article	IF	Citations
4811	Element Replacement Approach by Reaction with Lewis Acidic Molten Salts to Synthesize Nanolaminated MAX Phases and MXenes. Journal of the American Chemical Society, 2019, 141, 4730-4737.	6.6	811
4812	Photoresponsive sulfone-based molecules: photoinduced electron transfer and heat/air-stable radicals in the solid state. New Journal of Chemistry, 2019, 43, 4506-4510.	1.4	3
4813	Spectroscopic characterisation of centropolyindanes. Physical Chemistry Chemical Physics, 2019, 21, 4568-4577.	1.3	2
4814	Investigation into the optimized growth, anisotropic properties and theoretical calculations of the polar material Cs₂TeW₃O₁₂. CrystEngComm, 2019, 21, 2345-2354.	1.3	5
4815	Effect of nitrogen-doping configuration in graphene on the oxygen reduction reaction. RSC Advances, 2019, 9, 6035-6041.	1.7	21
4816	Negative area compressibility in oxalic acid dihydrate. Materials Letters, 2019, 245, 25-28.	1.3	17
4817	Two Non-Ï€-Conjugated Deep-UV Nonlinear Optical Sulfates. Journal of the American Chemical Society, 2019, 141, 3833-3837.	6.6	183
4818	Negative thermal expansion in high pressure layered perovskite Ca₂GeO₄. Chemical Communications, 2019, 55, 2984-2987.	2.2	8
4819	LiGeBO₄: a nonlinear optical material with a balance between deep-ultraviolet cut-off edge and large SHG response induced by hand-in-hand tetrahedra. Inorganic Chemistry Frontiers, 2019, 6, 914-919.	3.0	17
4820	Insertion of an ultrathin Al₂O₃interfacial layer for Schottky barrier height reduction in WS₂field-effect transistors. Nanoscale, 2019, 11, 4811-4821.	2.8	24
4821	Coffee grounds-derived carbon as high performance anode materials for energy storage applications. Journal of the Taiwan Institute of Chemical Engineers, 2019, 97, 178-188.	2.7	32
4822	Zeolitic Open-Framework Borates with Noncentrosymmetric Structures and Nonlinear Optical Properties. Inorganic Chemistry, 2019, 58, 3527-3534.	1.9	20
4823	Band Offset Models of Three-Dimensionally Bonded Semiconductors and Insulators. Journal of Physical Chemistry C, 2019, 123, 5562-5570.	1.5	14
4824	Materials Selection and Mechanism of Non-linear Conduction in Chalcogenide Selector Devices. Scientific Reports, 2019, 9, 1867.	1.6	31
4825	Promoted reversible wettability transition by plasmonic effects at Ag/TiO2 heterointerface. Applied Physics Letters, 2019, 114, .	1.5	4
4826	Phonons in deformable microporous crystalline solids. Zeitschrift Fur Kristallographie - Crystalline Materials, 2019, 234, 513-527.	0.4	7
4827	Influences of pressure on structural and electronic properties of four types of HMX. Journal of Molecular Modeling, 2019, 25, 63.	0.8	3
4828	MnSiP₂: A New Mid-IR Ternary Phosphide with Strong SHG Effect and Ultrabroad Transparency Range. Chemistry of Materials, 2019, 31, 2010-2018.	3.2	47

#	Article	IF	Citations
4829	Simultaneous reduction of surface, bulk, and interface recombination for Au nanoparticle-embedded hematite nanorod photoanodes toward efficient water splitting. Journal of Materials Chemistry A, 2019, 7, 5258-5265.	5.2	17
4830	Terahertz Spectroscopic Investigation of Salicylic Acid and Sodium Salicylate. Journal of Applied Spectroscopy, 2019, 85, 1143-1150.	0.3	6
4831	First principle studies of ZnO1-xSx alloys under high pressure. Journal of Alloys and Compounds, 2019, 788, 905-911.	2.8	6
4832	The role of strontium deficiency and pressure on electron-phonon superconductivity in Sr3SnO. Physica C: Superconductivity and Its Applications, 2019, 559, 42-49.	0.6	0
4833	Theoretical Studies of the Structural, Mechanical and Raman Spectroscopic Properties of Uranyl-Containing Minerals. , 0, , .		0
4834	Investigation of NbC/TiC Heterogeneous Nucleation Interface by First-Principles and Experimental Methods. Metals, 2019, 9, 1265.	1.0	6
4835	Ab initio study of negative electron affinity from light metals on the oxygen-terminated diamond (1â€‰×â€‰1) surface. Journal of Physics Condensed Matter, 2019, 31, 295002.	0.7	10
4836	A Theoretical Study of the Energetic Stability and Geometry of Silicon-Vacancy Color Centers in Diamond (001) Surfaces. Applied Sciences (Switzerland), 2019, 9, 5471.	1.3	4
4837	First-Principles Investigations on Structural, Elastic, and Thermodynamic Properties of CaX (X = S, Se,) Tj ETQq0 0 0 rgBT /Overlock 10 Tf	0.1	7
4838	Synthesis, structure, and ferroelectricity of a kaolinite-p–aminobenzamide intercalation compound. Clays and Clay Minerals, 2019, 67, 461-470.	0.6	4
4839	Understanding the formation of apremilast cocrystals. Acta Crystallographica Section B: Structural Science, Crystal Engineering and Materials, 2019, 75, 803-814.	0.5	15
4840	New viewpoint about the persistent luminescence mechanism of Mn2+/Eu3+ co-doped Zn2GeO4. International Journal of Modern Physics B, 2019, 33, 1950389.	1.0	4
4841	Effect of trivalent manganese substitution in Î±-Al2O3 crystal on the absorption spectra based on first-principles calculations. Journal of Physics: Conference Series, 2019, 1402, 066004.	0.3	1
4842	Non-empirical study on pressure dependence of ruby bond length. Journal of Physics: Conference Series, 2019, 1402, 066005.	0.3	5
4843	Identification of normal modes responsible for ferroelectric properties in organic ferroelectric CBDC. Journal of Physics Communications, 2019, 3, 113001.	0.5	4
4844	Strain-dependent structure and Raman behaviours in the heavy-ion irradiated manganite at extreme low dose. Scientific Reports, 2019, 9, 19204.	1.6	4
4845	Surface Properties and Floatability Comparison of Aegirite and Specularite by Density Functional Theory Study and Experiment. Minerals (Basel, Switzerland), 2019, 9, 782.	0.8	10
4846	Sorption of selenium species onto phlogopite and calcite surfaces: DFT studies. Journal of Contaminant Hydrology, 2019, 227, 103553.	1.6	9

#	Article	IF	Citations
4847	A Comparative Computational Study of the Adsorption of TCNQ and F4-TCNQ on the Coinage Metal Surfaces. ACS Omega, 2019, 4, 16906-16915.	1.6	9
4848	Theoretical Insights on the High Pressure Behavior of Pentazolate Anion Complex [Co(H2O)4(N5)2]Â·4H2O. Scientific Reports, 2019, 9, 15648.	1.6	3
4849	Minimized lithium trapping by isovalent isomorphism for high initial Coulombic efficiency of silicon anodes. Science Advances, 2019, 5, eaax0651.	4.7	122
4850	Synthesis and support interaction effects on the palladium nanoparticle catalyst characteristics. Advances in Catalysis, 2019, , 1-120.	0.1	12
4851	Evidence for an Abrupt Transition between SiO₂ and SiC from EELS and <i>Ab Initio</i> Modelling. Materials Science Forum, 0, 963, 199-203.	0.3	1
4852	Beyond molecular nitrogen: revelation of two ambient-pressure metastable single- and double-bonded nitrogen allotropes built from three-membered rings. Physical Chemistry Chemical Physics, 2019, 21, 22930-22938.	1.3	8
4853	Mg(H2O)6B4O5(OH)4(H2O)3: a new hydrated borate with a short DUV cutoff edge. Dalton Transactions, 2019, 48, 17408-17413.	1.6	5
4854	FeOCl/Ln (Ln = La or Y): efficient photo-Fenton catalysts for ibuprofen degradation. New Journal of Chemistry, 2019, 43, 16273-16280.	1.4	13
4855	Vertical Alignment of Liquid-Crystal Molecules due to Unilateral Anchoring from Charge Accumulation at the Semiconductor Interface. Physical Review Applied, 2019, 12, .	1.5	5
4856	Theoretical Investigation of Arsenic and Selenium Species Adsorption Behavior on Different Mineral Adsorbents. Industrial & Engineering Chemistry Research, 2019, 58, 23559-23566.	1.8	15
4857	Computing Investigations of Molecular and Atomic Vibrations of Ice IX. ACS Omega, 2019, 4, 18936-18941.	1.6	4
4858	Influence of Ni doping in a lead-halide and a lead-free halide perovskites for optoelectronic applications. AIP Advances, 2019, 9, .	0.6	56
4859	A computational approach to study the optoelectronic properties of F-BODIPY derivatives at the bulk level for photovoltaic applications. Materials Research Express, 2019, 6, 125110.	0.8	2
4860	Natural abundance solid-state 33S NMR study of NbS3: applications for battery conversion electrodes. Chemical Communications, 2019, 55, 12687-12690.	2.2	11
4861	Partial substitution induced centrosymmetric to noncentrosymmetric structure transformation and promising second-order nonlinear optical properties of (K_{0.38}Ba_{0.81})Ga₂Se₄. Chemical Communications, 2019, 55, 13701-13704.	2.2	73
4862	A new criterion for the prediction of solid-state phase transition in TMDs. Physical Chemistry Chemical Physics, 2019, 21, 24070-24076.	1.3	4
4863	Assignment of the solid state spectra of the group VI hexacarbonyls by inelastic neutron scattering spectroscopy. Physical Chemistry Chemical Physics, 2019, 21, 24950-24955.	1.3	5
4864	Trends of the macroscopic behaviors of energetic compounds: insights from first-principles calculations. Physical Chemistry Chemical Physics, 2019, 21, 24034-24041.	1.3	3

#	Article	IF	Citations
4865	Theoretical study of the substrate and molecular density effects on molecular self-assembly. New Journal of Chemistry, 2019, 43, 17040-17045.	1.4	1
4866	The novel two-dimensional photocatalyst SnN₃with enhanced visible-light absorption for overall water splitting. Nanoscale, 2019, 11, 18628-18639.	2.8	25
4867	Density Functional Theory Analysis of the Adsorption Interactions of Carbon Impurities in Coal-associated Kaolinite. Processes, 2019, 7, 782.	1.3	3
4868	Possible enhancement of superconductivity by Sb doping in rare earth doped 112 compounds: an ab-initio study. International Journal of Environmental Analytical Chemistry, 2019, , 1-12.	1.8	1
4869	BaGe₂Pn₂ (Pn = P, As): Two Congruent-Melting Non-chalcopyrite Pnictides as Mid- and Far-Infrared Nonlinear Optical Materials Exhibiting Large Second Harmonic Generation Effects. Chemistry of Materials, 2019, 31, 10170-10177.	3.2	34
4870	Correlation of Morphology and In-Vitro Degradation Behavior of Spray Pyrolyzed Bioactive Glasses. Materials, 2019, 12, 3703.	1.3	8
4871	Calculating the Complex Permittivity of Powdered Crystalline Materials. , 2019, , .		0
4872	First-principle calculations of ternary compounds: Immm-BxTi3â^'xN2. International Journal of Modern Physics B, 2019, 33, 1950295.	1.0	0
4873	The structural, electronic, elastic and thermodynamic properties of V2AX (A = B, Al, Ga, In and Tl; X = C) Tj ETQq0 0 0 rgBT /Overlock 10	1.0	4
4874	Density functional theory study of the electronic and optical properties of Si incorporated SnO2. AIP Advances, 2019, 9, 115104.	0.6	2
4875	First-principle calculations of electronic, vibrational, and thermodynamic properties of 1,3-diamino-2,4,6-trinitrobenzene. Journal of Molecular Modeling, 2019, 25, 356.	0.8	4
4876	Quantum mechanics of proteins in explicit water: The role of plasmon-like solute-solvent interactions. Science Advances, 2019, 5, eaax0024.	4.7	39
4877	Amorphization activated ruthenium-tellurium nanorods for efficient waterÂsplitting. Nature Communications, 2019, 10, 5692.	5.8	312
4878	The Conundrum of Relaxation Volumes in First-Principles Calculations of Charged Defects in UO2. Applied Sciences (Switzerland), 2019, 9, 5276.	1.3	11
4879	Rb₃Na(H₂C₃N₃O₃)₄Â·3H₂O with Large Birefringence. ACS Omega, 2019, 4, 22197-22202.	1.6	18
4880	K₅(W₃O₉F₄)(IO₃): An Efficient Mid-Infrared Nonlinear Optical Compound with High Laser Damage Threshold. Chemistry of Materials, 2019, 31, 10100-10108.	3.2	92
4881	Integration of mesopores and crystal defects in metal-organic frameworks via templated electrosynthesis. Nature Communications, 2019, 10, 4466.	5.8	90
4882	Band gap, sorption properties and fluorescence sensing behaviour of a novel 1Dâ†'2D cathenane-like cobalt(II)â€"organic framework. Acta Crystallographica Section C, Structural Chemistry, 2019, 75, 1593-1604.	0.2	3

#	Article	IF	Citations
4883	Two basic vibrational modes of hydrogen bonds in ice XIII. AIP Advances, 2019, 9, 115118.	0.6	4
4884	Transformation of Optical Anisotropy Origins in Perovskite-Related Materials: A First-Principles Study. Journal of Physical Chemistry C, 2019, 123, 31167-31174.	1.5	14
4885	Spin density functional calculations of the electronic structures and magnetic properties of transition-metal doped BeO. Chinese Journal of Physics, 2019, 62, 335-341.	2.0	3
4886	Interfacial phenomena in nanocapacitors with multifunctional oxides. Physical Chemistry Chemical Physics, 2019, 21, 24643-24649.	1.3	0
4887	The layered uranyl silicate mineral uranophane-Î²: crystal structure, mechanical properties, Raman spectrum and comparison with the Î±-polymorph. Dalton Transactions, 2019, 48, 16722-16736.	1.6	20
4888	Two rare-earth-based quaternary chalcogenides EuCdGeQ₄(Q = S, Se) with strong second-harmonic generation. Dalton Transactions, 2019, 48, 17620-17625.	1.6	38
4889	Synthesis of a germanosilicate zeolite HPM-12 using a short imidazolium-based dication: structure-direction by charge-to-charge distance matching. Dalton Transactions, 2019, 48, 17752-17762.	1.6	9
4890	In situgrown Î±-Cos/Co heterostructures on nitrogen doped carbon polyhedra enabling the trapping and reaction-intensification of polysulfides towards high performance lithium sulfur batteries. Nanoscale, 2019, 11, 20579-20588.	2.8	16
4891	Theoretical predictions for low-temperature phases, softening of phonons and elastic stiffnesses, and electronic properties of sodium peroxide under high pressure. RSC Advances, 2019, 9, 30964-30975.	1.7	11
4892	Unraveling the effect of Gd doping on the structural, optical, and magnetic properties of ZnO based diluted magnetic semiconductor nanorods. RSC Advances, 2019, 9, 33207-33221.	1.7	123
4893	Structures and characteristics of atomically thin ZrO₂from monolayer to bilayer and two-dimensional ZrO₂â€“MoS₂heterojunction. RSC Advances, 2019, 9, 32984-32994.	1.7	25
4894	Atomic-level understanding of interface interactions in a halloysite nanotubesâ€“PLA nanocomposite. RSC Advances, 2019, 9, 39505-39514.	1.7	23
4895	Structural, mechanical, spectroscopic and thermodynamic characterization of the copper-uranyl tetrahydroxide mineral vandenbrandeite. RSC Advances, 2019, 9, 40708-40726.	1.7	10
4896	Theoretical investigation on the promotion of second harmonic generation from chalcopyrite family A^IGaS₂to A^{II}Ga₂S₄. RSC Advances, 2019, 9, 41861-41867.	1.7	5
4897	Suppression of thermal conductivity without impeding electron mobility in n-type XNiSn half-Heusler thermoelectrics. Journal of Materials Chemistry A, 2019, 7, 27124-27134.	5.2	18
4898	Photogalvanic Effect in Nitrogen-Doped Monolayer MoS2 from First Principles. Nanoscale Research Letters, 2019, 14, 380.	3.1	9
4899	A new diphosphate Li2Na2P2O7: Synthesis, crystal structure, electronic structure and luminescent properties. Journal of Solid State Chemistry, 2019, 269, 125-131.	1.4	15
4900	A dual approach to study the key features of nickel (II) and copper (II) coordination complexes: Synthesis, crystal structure, optical and nonlinear properties. Inorganica Chimica Acta, 2019, 484, 148-159.	1.2	39

#	Article	IF	Citations
4901	Influence of Heat Treatment Upon Microstructure of Casting Aluminum Alloys. , 2019, , 235-312.		2
4902	Lithiation behavior of graphene-silicon composite as high performance anode for lithium-ion battery: A first principles study. Applied Surface Science, 2019, 463, 610-615.	3.1	27
4903	Promoted effect of cobalt on surface (0â€¯1â€¯0) of MoS2 for CO methanation from a DFT study. Applied Surface Science, 2019, 463, 635-646.	3.1	5
4904	Chemisorption of metallic radionuclides on a monolayer MoS₂nanosheet. Nanoscale Advances, 2019, 1, 114-121.	2.2	10
4905	The electronic, elastic and thermodynamic properties of carbon-and nitrogen-doped Hf2PB: a theoretical approach. Materials Research Express, 2019, 6, 056507.	0.8	4
4906	Anomalous mechanical behavior of the deltic, squaric and croconic cyclic oxocarbon acids. Materials Research Express, 2019, 6, 045610.	0.8	23
4907	How does the NMR thermometer work? Application of combined quantum molecular dynamics and GIPAW calculations into the study of lead nitrate. Journal of Computational Chemistry, 2019, 40, 811-819.	1.5	1
4908	[C₅H₁₂N]SnCl₃: A Tin Halide Organicâ€“Inorganic Hybrid as an Aboveâ€Roomâ€Temperature Solidâ€State Nonlinear Optical Switch. Chemistry - A European Journal, 2019, 25, 2610-2615.	1.7	38
4909	Noncentrosymmetric cubic RbBSi2O6 polymorph with deep ultraviolet cut-off edge. Solid State Sciences, 2019, 91, 10-14.	1.5	1
4910	Ab initiocalculations of hardness, elastic, thermodynamic and electronic properties of metal nitrides (XN₂; X = Pd, Pt) under high-pressure. Materials Research Express, 2019, 6, 045904.	0.8	2
4911	Binding of hydrogen to phosphorus dopant in phosphorus-doped diamond surfaces: A density functional theory study. Applied Surface Science, 2019, 471, 309-317.	3.1	12
4912	Self-healing silicon-sodium alginate-polyaniline composites originated from the enhancement hydrogen bonding for lithium-ion battery: A combined simulation and experiment study. Journal of Power Sources, 2019, 412, 749-758.	4.0	38
4913	Emergence of glassy features in halomethane crystals. Physical Review B, 2019, 99, .	1.1	29
4914	First-principles study on the stability and properties of Î²-SiC/M+1AlC (M=Sc, Ti, V, Cr, Zr, Nb, Mo, Hf, Ta;) Tj ETQq1 1 0.784314 rgBT /Ov	1.9	5
4915	Prediction of MCO [M = S, (Cl₂B)₃B] Systems with Giant Optical Birefringence and Nonlinearity in the Deep-Ultraviolet Region. Inorganic Chemistry, 2019, 58, 77-80.	1.9	4
4916	Periodic DFT Study of the Thermodynamic Properties and Stability of Schoepite and Metaschoepite Mineral Phases. ACS Earth and Space Chemistry, 2019, 3, 17-28.	1.2	26
4917	First principles study on the electronic and magnetic properties in Zn doped BiFe0.9375Mg0.0625O3 with intrinsic defects. Materials Research Express, 2019, 6, 036104.	0.8	0
4918	Template effects on the pressure-dependent behavior of chabazite-type fluoroaluminophosphates: a computational approach. Physics and Chemistry of Minerals, 2019, 46, 385-401.	0.3	10

#	Article	IF	Citations
4919	Evolution of calcite surface reconstruction and interface adsorption of calcite-CO₂ with temperature. Materials Research Express, 2019, 6, 025035.	0.8	7
4920	Ce(IO₃)₂F₂â‹…H₂O: The First Rareâ€Earthâ€Metal Iodate Fluoride with Large Second Harmonic Generation Response. Chemistry - A European Journal, 2019, 25, 1221-1226.	1.7	46
4921	tâ€Si₆₄: A Novel Silicon Allotrope. ChemPhysChem, 2019, 20, 128-133.	1.0	45
4922	Firstâ€principles study: Structural, mechanical, electronic and thermodynamic properties of simpleâ€cubicâ€perovskite (Ba0.62K0.38)(Bi0.92Mg0.08)O3. Solid State Communications, 2019, 288, 22-27.	0.9	22
4923	Experimental and model studies about the lubrication of physisorbed isobutane molecules on hydrogenated diamond-like carbon films. Surface and Coatings Technology, 2019, 357, 759-767.	2.2	18
4924	Thermal Behavior and Detonation Characterization of 3,3â€Dinitroazetidinium Salicylate. Propellants, Explosives, Pyrotechnics, 2019, 44, 175-180.	1.0	3
4925	Exploring the effects of crystal facet in Bi2WO6/BiOCl heterostructures on photocatalytic properties: A first-principles theoretical study. Applied Surface Science, 2019, 469, 125-134.	3.1	49
4926	Bond length anomaly in TiB2 at high pressure: first principles calculations. Materials Research Express, 2019, 6, 026531.	0.8	4
4927	Structural, elastic and vibrational properties of celestite, SrSO₄, from synchrotron x-ray diffraction, thermal diffuse scattering and Raman scattering. Journal of Physics Condensed Matter, 2019, 31, 055703.	0.7	7
4928	Two-dimensional phosphorene/C3N p-n heterostructure: Effect of contact type on electronic and optical properties. Science China Technological Sciences, 2019, 62, 478-489.	2.0	2
4929	Synthesis of Pure Silica MWW Zeolite in Fluoride Medium by Using an Imidazoliumâ€Based Long Dication. Chemistry - A European Journal, 2019, 25, 1561-1572.	1.7	15
4930	First-principles study of structural, vibrational, and electronic properties of trigonally bonded II-IV-N2. Computational Materials Science, 2019, 158, 88-97.	1.4	6
4931	Magnetic properties of diluted magnetic semiconductors Li(Zn,TM)N with decoupled charge and spin doping (TM: V, Cr, Mn, Fe, Co and Ni). Computational Materials Science, 2019, 158, 260-264.	1.4	12
4932	Disassembly of 2D Vertical Heterostructures. Advanced Materials, 2019, 31, e1805976.	11.1	12
4933	Novel carbon-rich nitride C3N: A superhard phase in monoclinic symmetry. Computational Materials Science, 2019, 158, 170-177.	1.4	19
4934	Rational Band Design in Metal Chalcogenide Ba₆Zn₆HfS₁₄: Splitting Orbitals, Narrowing the Forbidden Gap, and Boosting Photocatalyst Properties. Crystal Growth and Design, 2019, 19, 193-199.	1.4	5
4935	Abrupt Structural Transformation in Asymmetric ABPO₄F (A = K, Rb, Cs). Inorganic Chemistry, 2019, 58, 1733-1737.	1.9	18
4936	A Eu ³⁺ -Eu ²⁺ ion redox shuttle imparts operational durability to Pb-I perovskite solar cells. Science, 2019, 363, 265-270.	6.0	793

#	Article	IF	Citations
4937	Adsorption of hazardous gases in nuclear islands on monolayer MoS2 sheet. Adsorption, 2019, 25, 159-171.	1.4	7
4938	Realizing High Thermoelectric Performance in BaCu_{2â€“x}Ag_xTe₂ through Enhanced Carrier Effective Mass and Point-Defect Scattering. ACS Applied Energy Materials, 2019, 2, 889-895.	2.5	26
4939	A theoretical NMR study of polymorphism in crystal structures of azoles and benzazoles. Magnetic Resonance in Chemistry, 2019, 57, 275-284.	1.1	9
4940	First-Principles Study of the Reaction between Fluorinated Graphene and Ethylenediamine. Molecules, 2019, 24, 284.	1.7	0
4941	Rational Design via Synergistic Combination Leads to an Outstanding Deep-Ultraviolet Birefringent Li₂Na₂B₂O₅ Material with an Unvalued B₂O₅ Functional Gene. Journal of the American Chemical Society, 2019, 141, 3258-3264.	6.6	177
4942	Mechanism research on surface hydration of kaolinite, insights from DFT and MD simulations. Applied Surface Science, 2019, 476, 6-15.	3.1	107
4943	The effect of high pressure on the structure and stability of sodium formate: Probed by in situ synchrotron X-ray diffraction technique. Solid State Communications, 2019, 289, 67-70.	0.9	2
4944	Broadening Frontiers of Infrared Nonlinear Optical Materials with Ï€-Conjugated Trigonal-Planar Groups. Chemistry of Materials, 2019, 31, 1110-1117.	3.2	56
4945	Artificial Second-Order Nonlinear Optics in a Centrosymmetric Optical Material BiVO₄: Breaking the Prerequisite for Nonlinear Optical Materials. ACS Omega, 2019, 4, 1045-1052.	1.6	6
4946	BaV2O6Â·H2O: A nonlinear optical crystal with a large bandgap. Optical Materials, 2019, 88, 642-647.	1.7	4
4947	The interactions between fine particles of coal and kaolinite in aqueous, insights from experiments and molecular simulations. Applied Surface Science, 2019, 467-468, 12-21.	3.1	46
4948	Tuning the electronic and structural properties of Gd-TiO2-GO nanocomposites for enhancing photodegradation of IC dye: The role of Gd3+ ion. Applied Catalysis B: Environmental, 2019, 243, 106-120.	10.8	60
4949	The linear and nonlinear optical response of CsGeX3 (X=Cl, Br, and I): The finite field and first-principles investigation. Optik, 2019, 179, 89-98.	1.4	20
4950	The effect of anti-site disorder and tetragonal distortion on the electronic structure of Ti2VSb. Physics Letters, Section A: General, Atomic and Solid State Physics, 2019, 383, 243-247.	0.9	2
4951	Tuning the electronic and optical properties of GaAs nanowire (10-10) surfaces by Zn doping: First-principles study. Solid State Communications, 2019, 288, 43-47.	0.9	7
4952	Exploration the p-type doping mechanism of GaAs nanowires from first-principles study. Physics Letters, Section A: General, Atomic and Solid State Physics, 2019, 383, 202-209.	0.9	26
4953	Synthesis, Computational Studies, Inelastic Neutron Scattering, Infrared and Raman Spectroscopy of Ruthenocene. European Journal of Inorganic Chemistry, 2019, 2019, 1142-1146.	1.0	7
4954	Theory prediction of the electronic structure, mechanical and thermodynamic properties of Ca5Pd6Ge6 under pressure. Philosophical Magazine, 2019, 99, 116-129.	0.7	0

#	Article	IF	Citations
4955	Phase transition, mechanical stability and optical response of MnSe: Pressure effect. Physica B: Condensed Matter, 2019, 553, 6-10.	1.3	4
4956	La6Ba4Si6O24F2:Sm3+ novel red-emitting phosphors: Synthesis, photoluminescence and theoretical calculations. Journal of Luminescence, 2019, 206, 417-425.	1.5	60
4957	Raman, infrared and NMR spectra, vibrational assignments and quantum mechanical calculations of centrosymmetric 3,6-Dicholoro-1,2,4,5-tetrazine. Journal of Molecular Structure, 2019, 1178, 298-304.	1.8	1
4958	Primitive and O-Functionalized R-Graphyne-like BN Sheet: Candidates for SO₂ Sensor with High Sensitivity and Selectivity at Room Temperature. ACS Applied Electronic Materials, 2019, 1, 34-43.	2.0	13
4959	FeOCl/POM Heterojunctions with Excellent Fenton Catalytic Performance via Different Mechanisms. Inorganic Chemistry, 2019, 58, 250-258.	1.9	28
4960	Topochemical Path in High Lithiation of MoS₂. Zeitschrift Fur Anorganische Und Allgemeine Chemie, 2019, 645, 309-316.	0.6	3
4961	Tripyridineâ€Derivativeâ€Derived Semiconducting Iodoâ€Argentate/Cuprate Hybrids with Excellent Visibleâ€Lightâ€Induced Photocatalytic Performance. Chemistry - an Asian Journal, 2019, 14, 269-277.	1.7	22
4962	First-principles study of elastic, electronic, optical and thermoelectric properties of newly synthesized K2Cu2GeS4 chalcogenide. Journal of Alloys and Compounds, 2019, 781, 37-46.	2.8	34
4963	Physical properties of spinel-type superconductors CuRh2S4 and CuRh2Se4: A DFT study. Results in Physics, 2019, 12, 73-82.	2.0	17
4964	Combined experimental and theoretical studies on adsorption mechanisms of gaseous mercury(II) by calcium-based sorbents: The effect of unsaturated oxygen sites. Science of the Total Environment, 2019, 656, 937-945.	3.9	27
4965	An NMR crystallography investigation of furosemide. Magnetic Resonance in Chemistry, 2019, 57, 191-199.	1.1	10
4966	Controlled synthesis of 3D porous structured cobalt-iron based nanosheets by electrodeposition as asymmetric electrodes for ultra-efficient water splitting. Applied Catalysis B: Environmental, 2019, 244, 583-593.	10.8	105
4967	Structural, electronic and optical properties of furan based materials at bulk level for photovoltaic applications: A first-principles study. Computational and Theoretical Chemistry, 2019, 1147, 20-28.	1.1	7
4968	First principle calculations of electronic, band structural, and optical properties of BixSr1-xTiO3 perovskite. Journal of Physics and Chemistry of Solids, 2019, 127, 107-114.	1.9	27
4969	Structural, spectroscopic, and thermodynamic characterization of ammonium oxalate monohydrate mineral using theoretical solid-state methods. Journal of Physics and Chemistry of Solids, 2019, 125, 31-42.	1.9	14
4970	Prediction of novel ground state and high pressure phases for W2N3: First-principles. Computational Materials Science, 2019, 156, 215-223.	1.4	1
4971	Elements (Si, Sn, and Mg) doped Î±-Ga2O3: First-principles investigations and predictions. Computational Materials Science, 2019, 156, 273-279.	1.4	38
4972	Insights Into Interfacial Interaction and Its Influence on the Electronic and Optical Properties of Twoâ€Dimensional WS₂/TX₂CO₂ (TXâ€‰=â€‰Ti, Zr) van der Waals Heterostructures. Physica Status Solidi (B): Basic Research, 2019, 256, 1800377.	0.7	2

#	Article	IF	Citations
4973	First-principles study of structural, elastic, and electronic properties of triclinic TATB under different pressures. Physica B: Condensed Matter, 2019, 552, 151-158.	1.3	22
4974	Effect of Sb substitution on structural and magnetic properties of MnBi based alloys. Physica B: Condensed Matter, 2019, 552, 190-194.	1.3	15
4975	Density Functional Theory Study of M_n₊₁AX_nPhases: A Review. Critical Reviews in Solid State and Materials Sciences, 2019, 44, 56-107.	6.8	46
4976	Thiadiazole-2-Thiol-5-Thione and 2,5-Dimercapto-1,3,4-Thiadiazol Tautomerism, Conformational Stability, Vibrational Assignments, Inhibitor Efficiency and Quantum Chemical Calculations. Zeitschrift Fur Physikalische Chemie, 2020, 234, 415-440.	1.4	8
4977	First-principles study on Sr-doped hydroxyapatite as a biocompatible filler for photo-cured dental composites. Journal of the Australian Ceramic Society, 2020, 56, 591-598.	1.1	16
4978	Structural, elastic, electronic, andoptical properties of layered TiNX (Xâ€‰=â€‰F,â€‰Cl,â€‰Br,â€‰I) compounds: a density functional theory study. Molecular Physics, 2020, 118, e1609706.	0.8	21
4979	Investigation of the Structural, Electronic and Mechanical Properties of Type-VIII Ba8Si46 Clathrate under High-Pressure through First-Principles. Silicon, 2020, 12, 381-391.	1.8	6
4980	First-principles study of NbC heterogeneous nucleation on TiC vs. TiN in microalloy steel. Ironmaking and Steelmaking, 2020, 47, 77-83.	1.1	6
4981	First-principle study and Hirshfeld surface analysis on the effect of H2O, NH3 and H2S on structural, electronic, elastic, optical and thermodynamic properties of a novel high-energy crystal 2,4,6-triamino-5-nitropyrimidine-1,3-dioxide. Journal of Materials Science, 2020, 55, 237-249.	1.7	8
4982	Study on the stability of organicâ€“inorganic perovskite solar cell materials based on first principle. Molecular Physics, 2020, 118, e1665200.	0.8	12
4983	Structural, electrical and optical properties of halogen doped phosphorene based on density functional theory. Journal of Alloys and Compounds, 2020, 812, 152125.	2.8	12
4984	Extreme negative mechanical phenomena in the zinc and cadmium anhydrous metal oxalates and lead oxalate dihydrate. Journal of Materials Science, 2020, 55, 218-236.	1.7	17
4985	Temperature dependence of the optical properties of MgO: Ab initio molecular dynamics calculations. Optik, 2020, 200, 163421.	1.4	4
4986	First-principles calculations on electronic structure and interfacial stability of Mg/NbB2 heterogeneous nucleation interface. Surface Science, 2020, 691, 121487.	0.8	13
4987	Superior sodium-storage behavior of flexible anatase TiO2 promoted by oxygen vacancies. Energy Storage Materials, 2020, 25, 903-911.	9.5	131
4988	Antiferromagnetic Slater insulator phase in copper tellurium oxide. Journal of Magnetism and Magnetic Materials, 2020, 495, 165861.	1.0	1
4989	Superconducting Hydrides Under Pressure. Annual Review of Condensed Matter Physics, 2020, 11, 57-76.	5.2	149
4990	Structural, optical and electronic properties of CuO and Zn doped CuO: DFT based First-principles calculations. Chemical Physics, 2020, 528, 110536.	0.9	34

#	Article	IF	Citations
4991	Modeling of alloying effect on elastic properties in BCC Nb-Ti-V-Zr solid solution: From unary to quaternary. Computational Materials Science, 2020, 172, 109289.	1.4	48
4992	Identifying Cu-oxo species in Cu-zeolites by XAS: A theoretical survey by DFT-assisted XANES simulation and EXAFS wavelet transform. Catalysis Today, 2020, 345, 125-135.	2.2	68
4993	Probing the 91Zr NMR parameters in the solid state by a combination of DFT calculations and experiments. Chemical Physics Letters, 2020, 738, 136855.	1.2	0
4994	A GGA+U study of electronic structure and the optical properties of different concentrations Tb doped ZnO. Physica B: Condensed Matter, 2020, 576, 411720.	1.3	9
4995	Chemical and structural stability of superconducting In5Bi3 driven by spinâ€“orbit coupling. JPhys Materials, 2020, 3, 015007.	1.8	1
4996	Li[LiCs₂Cl][Ga₃S₆]: A Nanoporous Framework of GaS₄ Tetrahedra with Excellent Nonlinear Optical Performance. Angewandte Chemie - International Edition, 2020, 59, 4856-4859.	7.2	117
4997	Surface-scale affinity and adsorption selectivity of alkaline earth metal oxides to H2O and CO2: Insight into SOFC anode modification. Applied Surface Science, 2020, 503, 144333.	3.1	10
4998	Surface engineering of hollow carbon nitride microspheres for efficient photoredox catalysis. Chemical Engineering Journal, 2020, 381, 122593.	6.6	49
4999	Chalcogenated-Ti3C2X2 MXene (Xâ€¯=â€¯O, S, Se and Te) as a high-performance anode material for Li-ion batteries. Applied Surface Science, 2020, 501, 144221.	3.1	77
5000	Uncovering the electrochemical mechanisms for hydrogen evolution reaction of heteroatom doped M2C MXene (Mâ€¯=â€¯Ti, Mo). Applied Surface Science, 2020, 500, 143987.	3.1	93
5001	First-principles study on structural stability and electronic properties of GaAs nanowire undergoing surface oxidization. Applied Surface Science, 2020, 501, 144231.	3.1	10
5002	Two-dimensional BiP3 with high carrier mobility and moderate band gap for hydrogen generation from water splitting. Applied Surface Science, 2020, 501, 144263.	3.1	59
5003	Formation mechanism of Î²-Sialon with different morphologies based on DFT calculation and its effect on the performance of refractory composites. Ceramics International, 2020, 46, 1836-1843.	2.3	0
5004	New candidate to reach Shockleyâ€“Queisser limit: The DFT study of orthorhombic silicon allotrope Si(oP32). Journal of Physics and Chemistry of Solids, 2020, 137, 109219.	1.9	15
5005	Preparation, Structure, and enhanced thermoelectric properties of Sm-doped BiCuSeO oxyselenide. Materials and Design, 2020, 185, 108263.	3.3	29
5006	Effects of Mn doping on the structural, morphological, electronic and optical properties of ZnO thin films by sol-gel spin coating method: An experimental and DFT+U study. Physica B: Condensed Matter, 2020, 577, 411766.	1.3	21
5007	Effect of potassium for cesium replacement in atomic level structure of potassium cobalt hexacyanoferrate(II). Radiochimica Acta, 2020, 108, 451-457.	0.5	5
5008	Ab-initio prediction of structure stability, electromagnetic, optical and thermoelectric behavior of orthorhombic LaXO3 (X= Cr, Mn, Fe): For device application. Journal of Molecular Graphics and Modelling, 2020, 94, 107482.	1.3	13

#	Article	IF	Citations
5009	First-principles investigation of the mechanical and thermodynamic properties of the antiperovskite centrosymmetric platinum-based superconductors APt3P (A=Ca, Sr, La and Ce). Physica B: Condensed Matter, 2020, 577, 411791.	1.3	1
5010	Non-PGM Iron Perovskite Three-Way Gasoline Emissions Control Catalysts: Kinetics, Reaction Mechanism and Catalyst Sizing Study. Topics in Catalysis, 2020, 63, 256-267.	1.3	4
5011	Far-infrared terahertz properties of L-cysteine and its hydrochloride monohydrate. Spectrochimica Acta - Part A: Molecular and Biomolecular Spectroscopy, 2020, 225, 117476.	2.0	13
5012	Electronic and thermoelectric properties of RbYSn half-Heusler compound with 8 valence electrons: Spin-orbit coupling effect. Chemical Physics, 2020, 528, 110510.	0.9	20
5013	The Origin of Optical Contrast in Sb 2 Te 3 â€Based Phaseâ€Change Materials. Physica Status Solidi (B): Basic Research, 2020, 257, 1900289.	0.7	12
5014	Orbital stability and homoclinic bifurcation in a parametrized deformable double-well potential. Chaos, Solitons and Fractals, 2020, 130, 109411.	2.5	3
5015	Electric field-modulated high sensitivity and selectivity for NH3 on Î±-C2N2 nanosheet: Insights from DFT calculations. Applied Surface Science, 2020, 505, 144619.	3.1	39
5016	Synthesis, crystal structure and optical properties of a new fluoroborate compound: Al7-xLi1+xB4O16+xF1-x (xÂ= 1/3). Journal of Molecular Structure, 2020, 1199, 126949.	1.8	0
5017	QuantumATK: an integrated platform of electronic and atomic-scale modelling tools. Journal of Physics Condensed Matter, 2020, 32, 015901.	0.7	771
5018	Transition from indirect to direct band gap in SiC monolayer by chemical functionalization: A first principles study. Superlattices and Microstructures, 2020, 137, 106320.	1.4	28
5019	The Spacer Cations Interplay for Efficient and Stable Layered 2D Perovskite Solar Cells. Advanced Energy Materials, 2020, 10, 1901566.	10.2	89
5020	Density Functional Theory Study of ZnIn₂S₄ and CdIn₂S₄ Polymorphs Using Fullâ€Potential Linearized Augmented Plane Wave Method and Modified Beckeâ€“Johnson Potential. Physica Status Solidi (B): Basic Research, 2020, 257, 1900485.	0.7	19
5021	Interface Engineered Roomâ€Temperature Ferromagnetic Insulating State in Ultrathin Manganite Films. Advanced Science, 2020, 7, 1901606.	5.6	24
5022	Li[LiCs₂Cl][Ga₃S₆]: A Nanoporous Framework of GaS₄ Tetrahedra with Excellent Nonlinear Optical Performance. Angewandte Chemie, 2020, 132, 4886-4889.	1.6	35
5023	Quantitative analysis on the microstructure of molten binary KFâ€AlF₃ system by in situ Raman spectroscopy assisted with first principles method. Journal of Raman Spectroscopy, 2020, 51, 187-192.	1.2	8
5024	First-principles investigation on the atomic structure, stability and electronic property of O(001)/B2(110) interface in Ti2AlNb alloys. Journal of Alloys and Compounds, 2020, 817, 152734.	2.8	12
5025	Substantial doping engineering in Na3V2-xFex(PO4)3 (0â‰¤xâ‰¤0.15) as high-rate cathode for sodium-ion battery. Materials and Design, 2020, 186, 108287.	3.3	48
5026	Physico-chemical properties of CrMoN coatings - combined experimental and computational studies. Thin Solid Films, 2020, 693, 137671.	0.8	13

#	Article	IF	Citations
5027	Novel Bi-based photocatalysts with unprecedented visible light-driven hydrogen production rate: Experimental and DFT insights. Chemical Engineering Journal, 2020, 384, 123351.	6.6	46
5028	Combined experimental and first-principles studies of a hydrated uranyl carbonate: Insight into phonon spectra for a core environmental class of uranium materials. Journal of Physics and Chemistry of Solids, 2020, 138, 109260.	1.9	3
5029	Silicene, Siloxene, or Silicane? Revealing the Structure and Optical Properties of Silicon Nanosheets Derived from Calcium Disilicide. Chemistry of Materials, 2020, 32, 795-804.	3.2	59
5030	Tuning electronic structure and optical properties of C3N by B doping. Physica B: Condensed Matter, 2020, 577, 411807.	1.3	2
5031	Solidâ€state 13 Câ€...NMR Evidence for Long Multicenter Intradimer Bonding in Zwitterionâ€like Structures. Chemistry - A European Journal, 2020, 26, 230-236.	1.7	2
5032	First-Principles Design and Simulations Promote the Development of Nonlinear Optical Crystals. Accounts of Chemical Research, 2020, 53, 209-217.	7.6	194
5033	Adsorption of different PAM structural units on kaolinite (0â€¯0â€¯1) surface: Density functional theory study. Applied Surface Science, 2020, 504, 144324.	3.1	32
5034	Rational Localization of Metal Nanoparticles in Yolkâ€“Shell MOFs for Enhancing Catalytic Performance in Selective Hydrogenation of Cinnamaldehyde. ChemSusChem, 2020, 13, 205-211.	3.6	22
5035	Structure and property study by first-principles calculations: Two-dimensional semi-hydrogenated-semi-oxidized bilayer BN (111)-oriented nanosheets. Diamond and Related Materials, 2020, 102, 107666.	1.8	8
5037	Integrating 2D/2D CdS/Î±-Fe2O3 ultrathin bilayer Z-scheme heterojunction with metallic Î²-NiS nanosheet-based ohmic-junction for efficient photocatalytic H2 evolution. Applied Catalysis B: Environmental, 2020, 266, 118619.	10.8	199
5038	Introduction to Carbon-Based Nanostructures. , 2020, , 1-10.		0
5039	The New Family of Two-Dimensional Materials and van der Waals Heterostructures. , 2020, , 70-91.		0
5040	Quantum Transport: General Concepts. , 2020, , 92-119.		0
5041	Klein Tunneling and Ballistic Transport in Graphene and Related Materials. , 2020, , 120-144.		0
5042	Quantum Transport in Disordered Graphene-Based Materials. , 2020, , 145-209.		0
5043	Identifying aspirin polymorphs from combined DFTâ€based crystal structure prediction and solidâ€state NMR. Magnetic Resonance in Chemistry, 2020, 58, 1018-1025.	1.1	6
5044	Vibrational Response of Felodipine in the THz Domain: Optical and Neutron Spectroscopy Versus Plane-Wave DFT Modeling. Journal of Infrared, Millimeter, and Terahertz Waves, 2020, 41, 1301-1336.	1.2	7
5045	Exploring the Reliability of DFT Calculations of the Infrared and Terahertz Spectra of Sodium Peroxodisulfate. Journal of Infrared, Millimeter, and Terahertz Waves, 2020, 41, 382-413.	1.2	14

#	Article	IF	Citations
5046	Frictionâ€“Load Relationship in the Adhesive Regime Revealing Potential Incapability of AFM Investigations. Tribology Letters, 2020, 68, 1.	1.2	8
5047	Evaluating Hellmannâ€“Feynman forces within non-local pseudopotentials. Computer Physics Communications, 2020, 250, 107034.	3.0	5
5048	The structural, electronic and dynamical investigations of NdMn2O5 and La2CoMnO6 for optoelectronic applications: A first principles study. Optik, 2020, 204, 164165.	1.4	11
5049	Detrimental effects of SO2 on gaseous mercury(II) adsorption and retention by CaO-based sorbent traps: Competition and heterogeneous reduction. Journal of Hazardous Materials, 2020, 387, 121679.	6.5	29
5050	K_{2.64}Cs_{0.36}SiF₇: a new fluorosilicate with atrans-perovskite structure. New Journal of Chemistry, 2020, 44, 2727-2732.	1.4	3
5051	Specific recognition of toxic allyl alcohol by pore-functionalized metalâ€“organic frameworks. Molecular Systems Design and Engineering, 2020, 5, 469-476.	1.7	8
5052	Pb₃Ba₃Zn₆(BO₃)₈and Î±-BaZn₂(BO₃)₂: new members of the zincoborates containing two different dimensional Znâ€“O units. Inorganic Chemistry Frontiers, 2020, 7, 101-107.	3.0	4
5053	Solution processed lead-free cesium titanium halide perovskites and their structural, thermal and optical characteristics. Journal of Materials Chemistry C, 2020, 8, 1591-1597.	2.7	67
5054	Câ€“Hâ€¦N hydrogen bonding in an overlayer of s-triazine physisorbed on a graphite surface. Molecular Physics, 2020, 118, e1706777.	0.8	4
5055	Investigations on p- and n-type diluted magnetic semiconductors X/Mn-codoped LiZnN (X= Li, Na and K). Journal of Alloys and Compounds, 2020, 821, 153235.	2.8	0
5056	Strain engineering and epitaxial stabilization of halide perovskites. Nature, 2020, 577, 209-215.	13.7	417
5057	In Situ Tuning of Defects and Phase Transition in Titanium Dioxide by Lithiothermic Reduction. ACS Applied Materials & Interfaces, 2020, 12, 5750-5758.	4.0	30
5058	The optical properties of Bi³⁺and Sb³⁺in YNbTiO₆analysed by means of DOS and semi-empirical calculations. Journal of Materials Chemistry C, 2020, 8, 2086-2093.	2.7	11
5061	Electronic Properties of Carbon-Based Nanostructures. , 2020, , 11-69.		0
5062	Quantum Hall Effects in Graphene. , 2020, , 210-236.		0
5063	Spin-Related Phenomena. , 2020, , 237-277.		0
5064	Ab Initio and Multiscale Quantum Transport in Graphene-Based Materials. , 2020, , 293-353.		0
5068	Oxygen reduction using a metal-free naphthalene diimide-based covalent organic framework electrocatalyst. Chemical Communications, 2020, 56, 1267-1270.	2.2	56

#	Article	IF	Citations
5069	Nature of the multicomponent crystal of salicylic acid and 1,2-phenylenediamine. CrystEngComm, 2020, 22, 708-719.	1.3	4
5070	Three metallic BN polymorphs: 1D multi-threaded conduction in a 3D network. Physical Chemistry Chemical Physics, 2020, 22, 489-496.	1.3	4
5071	Promoting effects of water on the NH3-SCR reaction over Cu-SAPO-34 catalysts: transient and permanent influences on Cu species. Dalton Transactions, 2020, 49, 764-773.	1.6	15
5072	Effect of anion dimensionality on optical properties: the _{âˆž}[B₇O₁₀(OH)₂] layer in CsB₇O₁₀(OH)₂vs. the _{âˆž}[B₇O₁₂] framework in CsBaB₇O₁₂. Dalton Transactions, 2020, 49, 1293-1299.	1.6	14
5073	Alkali-earth metal lead(ii) oxyhalide Ba27Pb8O8Cl54 exhibiting interesting [Pb4Ba4O4]8+ species. New Journal of Chemistry, 2020, 44, 1699-1702.	1.4	6
5074	Lone pair electron effect induced differences in linear and nonlinear optical properties of bismuth borates. New Journal of Chemistry, 2020, 44, 1228-1235.	1.4	9
5075	A phosphorene-like InP₃ monolayer: structure, stability, and catalytic properties toward the hydrogen evolution reaction. Journal of Materials Chemistry A, 2020, 8, 1307-1314.	5.2	31
5076	Effects of Li Confined Motion on NMR Quadrupolar Interactions: A Combined 7 Li NMR and DFTâ€MD Study of LiR 2 (PO 4) 3 (R=Ti or Zr) Phases. ChemSusChem, 2020, 13, 1027-1036.	3.6	4
5077	In2O3 nanoparticle-reduced graphene oxide hybrid for electrocatalytic nitrogen fixation: Computational and experimental studies. Journal of Materials Science, 2020, 55, 4624-4632.	1.7	41
5078	Syntheses, characterization, and theoretical calculation of Rb2Mg3(P2O7)2 polymorphs with deep-ultraviolet cutoff edges. Science China Materials, 2020, 63, 593-601.	3.5	16
5079	Phototherapy ablation of rabbit orthotopic tumors by non-stoichiometric BiPO4âˆ’x nanoparticles. Chemical Engineering Journal, 2020, 386, 123961.	6.6	14
5080	A new catalyst for urea oxidation: NiCo2S4 nanowires modified 3D carbon sponge. Journal of Energy Chemistry, 2020, 50, 195-205.	7.1	34
5081	Prediction of a novel carbon allotrope from first-principle calculations: A potential superhard material in monoclinic symmetry. Materials Chemistry and Physics, 2020, 242, 122480.	2.0	47
5082	Structural Diversity and Giant Birefringence in Cyanates BaCNOX (X = Cl, Br, I, and CNO) Containing Linear Ï€-Conjugated Units: A Combined Experimental and Theoretical Study. Crystal Growth and Design, 2020, 20, 1242-1247.	1.4	6
5083	Al₈(BO₃)₄(B₂O₅)F₈: A F-Containing Aluminum Borate Featuring Two Types of Isolated Bâ€“O Groups. Inorganic Chemistry, 2020, 59, 810-817.	1.9	5
5084	Nature of Interactions between Epoxides in Graphene Oxide. Journal of Physical Chemistry C, 2020, 124, 1695-1703.	1.5	5
5085	Coherent Epitaxial Semiconductorâ€“Ferromagnetic Insulator InAs/EuS Interfaces: Band Alignment and Magnetic Structure. ACS Applied Materials & Interfaces, 2020, 12, 8780-8787.	4.0	23
5086	Semiconductive Nature of Lead-Based Metalâ€“Organic Frameworks with Three-Dimensionally Extended Sulfur Secondary Building Units. Journal of the American Chemical Society, 2020, 142, 27-32.	6.6	51

#	Article	IF	Citations
5087	Breakdown of the electron delocalization in hexagonal borophene toward tunable energy gap. Applied Surface Science, 2020, 507, 144940.	3.1	1
5088	Multi-functional Mo-doping in MnO2 nanoflowers toward efficient and robust electrocatalytic nitrogen fixation. Applied Catalysis B: Environmental, 2020, 264, 118525.	10.8	211
5089	Influence of Au, Cu, Pd added in Ag alloy on stability and electronic structure of Ag/Al interface by first-principles calculations. Materials Today Communications, 2020, 22, 100670.	0.9	6
5090	The Effects of Fe and Si Elements on Structural, Mechanical, and Electronic Properties of an Feâ€“Siâ€“Ti System by Firstâ€Principles Calculations. Physica Status Solidi (B): Basic Research, 2020, 257, 1900479.	0.7	1
5091	On the piezotronic behaviours of wurtzite coreâ€“shell nanowires. Nanotechnology, 2020, 31, 095407.	1.3	6
5092	Judging the phase transition pressure of the unknown parent phase if the resulting state is known. Physical Chemistry Chemical Physics, 2020, 22, 624-627.	1.3	0
5093	RbNa(HC₃N₃O₃)Â·2H₂O exhibiting a strong second harmonic generation response and large birefringence as a new potential UV nonlinear optical material. Inorganic Chemistry Frontiers, 2020, 7, 150-156.	3.0	49
5094	Effects of interlayer interactions on the nanoindentation response of freely suspended multilayer gallium telluride. Nanotechnology, 2020, 31, 165706.	1.3	9
5095	Layered Cathode Materials for Lithium-Ion Batteries: Review of Computational Studies on LiNi_{1â€“xâ€“y}Co_xMn_yO₂ and LiNi_{1â€“xâ€“y}Co_xAl_yO₂. Chemistry of Materials, 2020, 32, 915-952.	3.2	196
5096	Designing Sulfide Borate as a Novel Type of Second-Order Nonlinear-Optical Material. Inorganic Chemistry, 2020, 59, 1547-1555.	1.9	57
5097	A modification of the electromigration device and modelling methods for diffusion and sorption studies of radionuclides in intact crystalline rocks. Journal of Contaminant Hydrology, 2020, 231, 103585.	1.6	4
5098	Photo-catalytic degradation of mixed gaseous HCHO and C6H6 in paper mills: Experimental and theoretical study on the adsorption behavior simulation and catalytic reaction mechanism. Journal of Hazardous Materials, 2020, 388, 121779.	6.5	16
5099	A theoretical prediction of a new silicon allotrope: tP36-Si. Computational Materials Science, 2020, 173, 109441.	1.4	10
5100	Generalised stacking fault energy of Ni-Al and Co-Al-W superalloys: Density-functional theory calculations. Materialia, 2020, 9, 100555.	1.3	20
5101	Tolerance Factor Control of Uniaxial Negative Thermal Expansion in a Layered Perovskite. Chemistry of Materials, 2020, 32, 605-610.	3.2	19
5102	DFT study on the electronic and magnetic properties of the Sr2FeNbO6 compound. Materials Today Communications, 2020, 23, 100844.	0.9	9
5103	Reducing the electronic band gap of BN monolayer by coexistence of P(As)-doping and external electric field. Superlattices and Microstructures, 2020, 137, 106357.	1.4	20
5104	Origin of Two Distinct Peaks of Ice in the THz Region and Its Application for Natural Gas Hydrate Dissociation. Journal of Physical Chemistry C, 2020, 124, 1165-1170.	1.5	12

#	Article	IF	Citations
5105	Promising zirconia-mixed Al-based nitrogen carriers for chemical looping of NH3: Reduced NH3 decomposition and improved NH3 yield. Fuel, 2020, 264, 116821.	3.4	24
5106	NaRb₃B₆O₉(OH)₃(HCO₃): A Borate-Bicarbonate Nonlinear Optical Material. Inorganic Chemistry, 2020, 59, 759-766.	1.9	13
5107	Properties of Si nanostructural modification on Si (111) surface. Chinese Journal of Physics, 2020, 67, 69-78.	2.0	0
5108	New apatiteâ€type phosphor Ca₉La(PO₄)₅(SiO₄)F₂:Tb³⁺,Dy³⁺ with improved color rendering index. Journal of the American Ceramic Society, 2020, 103, 2602-2609.	3.8	4
5109	Geometrical Frustration of B-H Bonds in Layered Hydrogen Borides Accessible by Soft Chemistry. CheM, 2020, 6, 406-418.	5.8	35
5110	CarNit4 â€“ A new polymeric energetic material based on poly(1,5-tetrazolediyl). Polymer, 2020, 186, 122048.	1.8	6
5111	Revealing the Sodium Storage Mechanism in High-Temperature-Synthesized Silicon Oxycarbides. Chemistry of Materials, 2020, 32, 410-423.	3.2	21
5112	A nonlocal continuum model for the piezopotential of two-dimensional semiconductors. Journal Physics D: Applied Physics, 2020, 53, 045303.	1.3	2
5113	Ag diffusion effect on the crystal structure, band structure, and optical property of Î±-CsPbI3 perovskite materials. Physica B: Condensed Matter, 2020, 579, 411917.	1.3	0
5114	Adsorption properties of formaldehyde on Î²12-borophene surfaces: A first-principles study. Chemical Physics Letters, 2020, 739, 137035.	1.2	9
5115	Multi-site surface complexation modelling of Se(IV) sorption on biotite. Chemical Geology, 2020, 533, 119433.	1.4	11
5116	Theoretical investigation the growth of Fe3Si on GaAs: Stability and electronic properties of Fe3Si/GaAs(0 0 1), (1 1 0) via DFT. Applied Surface Science, 2020, 506, 144691.	3.1	6
5117	Predicting gases sensing performance of Î±-MoO3 from nano-structural and electronic properties. Applied Surface Science, 2020, 509, 144913.	3.1	18
5118	Constructing 2D BiOIO3/MoS2 Z-scheme heterojunction wrapped by C500 as charge carriers transfer channel: Enhanced photocatalytic activity on gas-phase heavy metal oxidation. Journal of Colloid and Interface Science, 2020, 562, 429-443.	5.0	62
5119	Impact of the interface vacancy on Schottky barrier height for Au/AlN polar interfaces. Applied Surface Science, 2020, 505, 144650.	3.1	15
5120	High-pressure, high-temperature phase stability of iron-poor dolomite and the structures of dolomite-IIIc and dolomite-V. Physics of the Earth and Planetary Interiors, 2020, 299, 106403.	0.7	16
5121	Surface Nonlinear Optics on Centrosymmetric Dirac Nodalâ€Line Semimetal ZrSiS. Advanced Materials, 2020, 32, e1904498.	11.1	14
5122	Phase stability, elasticity, hardness and electronic structures for binary MnBm (Mâ€‰=â€‰Ni,) Tj ETQq1 1 0.784314 r Phase Transitions, 2020, 93, 158-174.	0.6	13

#	Article	IF	Citations
5123	Superconducting phases in a remarkable class of metallic ceramics. Journal of Physics and Chemistry of Solids, 2020, 138, 109275.	1.9	84
5124	Combining Embedded Mean-Field Theory with Linear-Scaling Density-Functional Theory. Journal of Chemical Theory and Computation, 2020, 16, 354-365.	2.3	3
5125	Effect of Ni substitution at Mn-site on structural and electronic properties of monovalent-dopedPr0.75Na0.25MnO3 manganite: Experimental and first principles LDA+U studies. Physica B: Condensed Matter, 2020, 579, 411904.	1.3	1
5126	Accuracy of Dispersion-Corrected Density Functional Theory Calculations of Elastic Tensors of Organic Molecular Structures. Crystal Growth and Design, 2020, 20, 206-213.	1.4	11
5127	Effective modelling of the Seebeck coefficient of Fe₂VAl. Journal of Physics Condensed Matter, 2020, 32, 125401.	0.7	4
5128	Structural and electronic properties of chemically functionalized SnC monolayer: a first principles study. Materials Research Express, 2020, 7, 015013.	0.8	16
5129	Insights on electronic structures, elastic features and optical properties of mixed-valence double perovskites Cs2Au2X6 (X=F, Cl, Br, I). Physics Letters, Section A: General, Atomic and Solid State Physics, 2020, 384, 126169.	0.9	32
5130	Effect of p-toluenesulfonyl hydrazide on copper corrosion in hydrochloric acid solution. Corrosion Science, 2020, 165, 108363.	3.0	27
5131	Strain-controllable ferromagnetism in Mn-doped AlP semiconductor with constant visible light absorption. Journal of Physics and Chemistry of Solids, 2020, 138, 109274.	1.9	1
5132	Electronic and optical properties of Tl4GeX3 (X = S, Se and Te) compounds for optoelectronics applications: insights from DFT-computations. Journal of Materials Research and Technology, 2020, 9, 413-420.	2.6	6
5133	Irregular influence of alkali metals on Cu-SAPO-34 catalyst for selective catalytic reduction of NOx with ammonia. Journal of Hazardous Materials, 2020, 387, 122007.	6.5	34
5134	Li2CdSiS4, a promising IR NLO material with a balanced Eg and SHG response originating from the effect of Cd with d10 configuration. Dalton Transactions, 2020, 49, 1975-1980.	1.6	25
5135	N-induced lattice contraction generally boosts the hydrogen evolution catalysis of P-rich metal phosphides. Science Advances, 2020, 6, eaaw8113.	4.7	211
5136	Double Linker Triphenylamine Dyes for Dye-Sensitized Solar Cells. Energies, 2020, 13, 4637.	1.6	8
5137	Electrochemical elucidation of Co_{0.5}M_{0.5}V₂O₄ (M =) Tj ETQq0 0 0 rgBT /Overlock 3349-3360.	3.2	9
5138	Transition metals doped borophene-graphene heterostructure for robust polysulfide anchoring: A first principle study. Applied Surface Science, 2020, 534, 147575.	3.1	18
5139	A type-II GaSe/HfS2 van der Waals heterostructure as promising photocatalyst with high carrier mobility. Applied Surface Science, 2020, 534, 147607.	3.1	97
5140	Hollow N-doped carbon @ O-vacancies NiCo2O4 nanocages with a built-in electric field as high-performance cathodes for hybrid supercapacitor. Electrochimica Acta, 2020, 364, 137260.	2.6	42

#	Article	IF	Citations
5141	Elastic behaviour and radiation tolerance in Nb-based 211 MAX phases. Materials Today Communications, 2020, 25, 101499.	0.9	10
5142	Photocatalytic Application of Two-dimensional Materials-based Heterostructure Based on Molybdenum and Tungsten Disulfides and Gallium Nitride: A Density-Functional Theory Study. Materials Today Communications, 2020, 25, 101646.	0.9	4
5143	Justification of crystal stability and origin of transport properties in ternary half-Heusler ScPtBi. RSC Advances, 2020, 10, 37482-37488.	1.7	10
5144	A₃BBi(P₂O₇)₂ (A = Rb, Cs; B = Pb, Ba): Isovalent Cation Substitution to Sustain Large Second-Harmonic Generation Responses. Chemistry of Materials, 2020, 32, 8713-8723.	3.2	73
5145	The 1H <mml:math xmlns:mml="http://www.w3.org/1998/Math/MathML" altimg="si1.svg"><mml:mrow><mml:msub><mml:mi>T</mml:mi><mml:mn>1</mml:mn></mml:msub></mml:mrow></mml:math> dispersion curve of fentanyl citrate to identify NQR parameters. Solid State Nuclear Magnetic Resonance, 2020, 110, 101697.	1.5	2
5146	Improved Understanding of Atomic Ordering in Y₄Si_xAl_{2â€“x}O_{9â€“x}N_x Materials Using a Combined Solid-State NMR and Computational Approach. Journal of Physical Chemistry C, 2020, 124, 23976-23987.	1.5	2
5147	Achievement of intrinsic white light emission by hybridization-deformable haloplumbates with rigid luminescent naphthalene motifs. Inorganic Chemistry Frontiers, 2020, 7, 4477-4487.	3.0	7
5148	New Salt and Cocrystal of Mequitazine: Impact of Coformer Flexibility and Hydrogen Bond Donors on Polymorphism. Crystal Growth and Design, 2020, 20, 7219-7229.	1.4	5
5149	Ba(MoO₂F)₂(XO₃)₂ (X = Se and Te): First Cases of Noncentrosymmetric Fluorinated Molybdenum Oxide Selenite/Tellurite Through Unary Substitution for Enlarging Band Gaps and Second Harmonic Generation. ACS Applied Materials & Interfaces, 2020, 12, 49812-49821.	4.0	25
5150	Pressure-Induced Polymerization of Polycyclic Areneâ€“Perfluoroarene Cocrystals: Single Crystal X-ray Diffraction Studies, Reaction Kinetics, and Design of Columnar Hydrofluorocarbons. Journal of the American Chemical Society, 2020, 142, 18907-18923.	6.6	47
5151	Novel benzothiazole half-squaraines: model chromophores to study dyeâ€“TiO₂interactions in dye-sensitized solar cells. Journal of Materials Chemistry A, 2020, 8, 22191-22205.	5.2	4
5152	Novel sulfur hydrides synthesized at extreme conditions. Physical Review B, 2020, 102, .	1.1	26
5153	The Reactivity of the Corrosion Mechanism in Transformers: A Computational Study. Journal of Bio- and Tribo-Corrosion, 2020, 6, 1.	1.2	2
5154	Influence of different ratios of Fe and N on the structural, mechanical, electronic properties of FexNy compounds: First-principles study. International Journal of Modern Physics B, 2020, 34, 2050256.	1.0	0
5155	Low-temperature synthesis of Ti3Al(Sn)C2 solid solution using replacement reaction. Journal of Materials Science: Materials in Electronics, 2020, 31, 20601-20610.	1.1	9
5156	Understanding high pressure molecular hydrogen with a hierarchical machine-learned potential. Nature Communications, 2020, 11, 5014.	5.8	5
5157	Explorations of Second-Order Nonlinear Optical Materials in the Alkaline Earth Barbiturate System: Noncentrosymmetric Ca(H₃C₄N₂O₃)₂Â·H₂O and Centrosymmetric Sr(H₅C₈N₄O₅)₂Â·4H₂O. Inorganic Chemistry, 2020, 59, 15962-15968.	1.9	11
5158	High pressure chemical reactivity and structural study of the Naâ€“P and Liâ€“P systems. Journal of Materials Chemistry A, 2020, 8, 21797-21803.	5.2	5

#	Article	IF	Citations
5159	Remarkable High Thermoelectric Conversion Efficiency Materials of BeMF₃ (M = Al, Y). Advanced Theory and Simulations, 2020, 3, 2000171.	1.3	9
5161	Improving electrocatalytic activity of 2H-MoS2 nanosheets obtained by liquid phase exfoliation: Covalent surface modification versus interlayer interaction. Journal of Catalysis, 2020, 391, 424-434.	3.1	25
5162	Graphene quantum dot modified Bi2WO6 with enhanced photocatalytic activity by reinforcing the charge separation. New Journal of Chemistry, 2020, 44, 19220-19226.	1.4	11
5163	The structural phase transition of ammonia borane under high pressure. International Journal of Hydrogen Energy, 2020, 45, 33047-33058.	3.8	6
5164	Solid-State 1H, 13C, and 17O NMR Characterization of the Two Uncommon Polymorphs of Curcumin. Crystal Growth and Design, 2020, 20, 7484-7491.	1.4	7
5165	Anisotropic dielectric behavior of layered perovskite-like Cs₃Bi₂I₉ crystals in the terahertz region. Physical Chemistry Chemical Physics, 2020, 22, 24555-24560.	1.3	6
5166	Combining phonon accuracy with high transferability in Gaussian approximation potential models. Journal of Chemical Physics, 2020, 153, 044104.	1.2	29
5167	A Theoretical Analysis on the Oxidation and Water Dissociation Resistance on Groupâ€IV Phosphide Monolayers. ChemPhysChem, 2020, 21, 2539-2549.	1.0	19
5168	Interactions of xanthate molecule with different mineral surfaces: A comparative study of Fe, Pb and Zn sulfide and oxide minerals with coordination chemistry. Minerals Engineering, 2020, 159, 106565.	1.8	21
5169	Band gap tuning of p-type al-doped tio2 thin films for gas sensing applications. Thin Solid Films, 2020, 714, 138382.	0.8	17
5170	Ultrahigh-Energy-Transfer Efficiency and Efficient Mn²⁺ Red Emission Realized by Structural Confinement in Ca₉LiMn(PO₄)₇:Eu²⁺,Tb³⁺ Phosphor. Inorganic Chemistry, 2020, 59, 15050-15060.	1.9	32
5171	Design and Precursor-based Solid-State Synthesis of Mixed-Linker Zr-MIL-140A. Inorganic Chemistry, 2020, 59, 15250-15261.	1.9	4
5172	Amine-Functionalized Zeolitic Imidazolate Framework-8 (ZIF-8) Nanocrystals for Adsorption of Radioactive Iodine. ACS Applied Nano Materials, 2020, 3, 9852-9861.	2.4	74
5173	Highly Efficient Reductive Catalytic Fractionation of Lignocellulosic Biomass over Extremely Low-Loaded Pd Catalysts. ACS Catalysis, 2020, 10, 12487-12506.	5.5	36
5174	Too Many Materials and Too Many Applications: An Experimental Problem Waiting for a Computational Solution. ACS Central Science, 2020, 6, 1890-1900.	5.3	63
5175	How PM2.5 Affects Pt-Catalyzed Oxygen Reduction Reaction. ACS Sustainable Chemistry and Engineering, 2020, 8, 9385-9392.	3.2	5
5176	Real-time in situ optical tracking of oxygen vacancy migration in memristors. Nature Electronics, 2020, 3, 687-693.	13.1	43
5177	Second-order nonlinear optical-active selenide borate Zn8Se2(BO2)12: Experimental and theoretical analysis. Journal of Solid State Chemistry, 2020, 290, 121572.	1.4	5

#	Article	IF	Citations
5178	Broadband terahertz spectroscopy of paper and banknotes. Optics Communications, 2020, 475, 126267.	1.0	8
5179	(NH₄)₃[B(OH)₃]₂(COOH)₃: a graphite-like UV nonlinear optical material with a large birefringenceviastructural optimization. Chemical Communications, 2020, 56, 9982-9985.	2.2	16
5180	Towards Accurate Predictions of Proton NMR Spectroscopic Parameters in Molecular Solids. ChemPhysChem, 2020, 21, 2075-2083.	1.0	14
5181	Extending the metal-induced gap state model of Schottky barriers. Journal of Vacuum Science and Technology B:Nanotechnology and Microelectronics, 2020, 38, .	0.6	14
5182	Broadband terahertz signatures and vibrations of dopamine. Analyst, The, 2020, 145, 6006-6013.	1.7	21
5183	Cost-effective composite methods for large-scale solid-state calculations. Faraday Discussions, 2020, 224, 292-308.	1.6	13
5184	High harmonic generation in grapheneâ€“boron nitride heterostructures. Journal of Materials Chemistry C, 2020, 8, 12085-12091.	2.7	14
5185	From first- to second-order phase transitions in hybrid improper ferroelectrics through entropy stabilization. Physical Review B, 2020, 102, .	1.1	14
5186	2D XBiSe3(XÂ=ÂAs, Sb) monolayers with high anisotropic mobility and enhanced optical absorption in visible light region. Applied Surface Science, 2020, 530, 147137.	3.1	13
5187	First-principle calculations on the Al/L12-Al3Zr heterogeneous nucleation interface. Calphad: Computer Coupling of Phase Diagrams and Thermochemistry, 2020, 69, 101768.	0.7	16
5188	Gypsum crystals pollutants: DFT and van der Waals interactions study on its surface deterioration. Computational and Theoretical Chemistry, 2020, 1187, 112921.	1.1	1
5189	Raman, DRIFT and ATR-IR spectra, corrosion inhibition, DFT and solid-state calculations of 4-amino-3-choloro-2,5,6-trifluoropyridine. Journal of Molecular Structure, 2020, 1207, 127837.	1.8	3
5190	Comprehensive first-principles calculations on physical properties of ScV2Ga4 and ZrV2Ga4 in comparison with superconducting HfV2Ga4. Materials Today Communications, 2020, 24, 100935.	0.9	23
5191	La₂SrB₁₀O₁₉: A Promising Ultraviolet Nonlinear Optical Crystal with an Enhanced Nonlinear Optical Effect and Shortened Cutoff Edge. Crystal Growth and Design, 2020, 20, 5626-5632.	1.4	6
5192	First-Principles High-Throughput Screening Pipeline for Nonlinear Optical Materials: Application to Borates. Chemistry of Materials, 2020, 32, 6772-6779.	3.2	59
5193	Pressureâ€“Temperature Phase Diagram of Lithium, Predicted by Embedded Atom Model Potentials. Journal of Physical Chemistry B, 2020, 124, 6015-6023.	1.2	11
5194	Na₂HeO: A possible helium compound from first-principles study. International Journal of Computational Materials Science and Engineering, 2020, 09, 2050001.	0.5	1
5195	CsZn 2 BO 3 X 2 (X 2 =F 2 , Cl 2 , and FCl): A Series of Berylliumâ€Free Deepâ€Ultraviolet Nonlinearâ€Optical Crystals with Excellent Properties. Angewandte Chemie, 2020, 132, 19168-19172.	1.6	28

#	Article	IF	Citations
5196	CsZn₂BO₃X₂ (X₂=F₂, Cl₂,) Tj ETQq0 0 0 rgBT /Overlock Properties. Angewandte Chemie - International Edition, 2020, 59, 19006-19010.	7.2	91
5197	Structure-property survey and computer-assisted screening of mid-infrared nonlinear optical chalcohalides. Coordination Chemistry Reviews, 2020, 421, 213379.	9.5	78
5198	Polymorphic Forms of Valinomycin Investigated by NMR Crystallography. International Journal of Molecular Sciences, 2020, 21, 4907.	1.8	8
5199	Predicting the structures and properties of few-layer two-dimensional (1Â1Â0)-oriented BN nanosheets: First-principles calculations. Chemical Physics, 2020, 534, 110765.	0.9	1
5200	Examining the half-metallicity and thermoelectric properties of new equiatomic quaternary Heusler compound CoVRhGe under pressure. Physica B: Condensed Matter, 2020, 583, 412058.	1.3	23
5201	Structural, electronic properties and boron stability of (001) surface of Nb5Si3 intermetallic by first-principles calculations. Vacuum, 2020, 179, 109558.	1.6	5
5202	Compressive behavior and electronic properties of ammonia ice: a first-principles study. RSC Advances, 2020, 10, 26579-26587.	1.7	4
5203	Crystal Structure, Infrared Spectrum and Elastic Anomalies in Tuperssuatsiaite. Scientific Reports, 2020, 10, 7510.	1.6	10
5204	Chemical Sensing with Atomically Thin Platinum Templated by a 2D Insulator. Advanced Materials Interfaces, 2020, 7, 1902104.	1.9	5
5205	Recent progress in solidâ€state nuclear magnetic resonance of halfâ€integer spin lowâ€Î³ quadrupolar nuclei applied to inorganic materials. Magnetic Resonance in Chemistry, 2021, 59, 864-907.	1.1	14
5206	Experimental and theoretical studies of the ternary thiophosphate PbPS₃ featuring ethane-like [P₂S₆]^{4â^’} units. Dalton Transactions, 2020, 49, 17221-17229.	1.6	8
5207	A₂BBi₂(PO₄)₂(P₂O₇) (A = K,) Tj ETQq1 1 0.784314 rgBT Chemistry, 2020, 2020, 4007-4014.	1.0	6
5208	Fast analytical evaluation of intermolecular electrostatic interaction energies using the pseudoatom representation of the electron density. III. Application to crystal structures via the Ewald and direct summation methods. Acta Crystallographica Section A: Foundations and Advances, 2020, 76, 630-651.	0.0	5
5209	Î±-CdP2: Large SHG Effect Originating from the Synergism of Parallel â^ž1[Pâ€“] Polyanion Chains and Distorted CdP4 Tetrahedra. Chemistry of Materials, 2020, 32, 10246-10253.	3.2	7
5210	Fluorine Triggered Surface and Lattice Regulation in Anatase TiO_{2â^’}_xF_x Nanocrystals for Ultrafast Pseudocapacitive Sodium Storage. Small, 2020, 16, e2006366.	5.2	31
5211	Electrospun hetero-CoP/FeP embedded in porous carbon nanofibers: enhanced Na⁺ kinetics and specific capacity. Nanoscale, 2020, 12, 24477-24487.	2.8	36
5212	EuHgGeSe₄ and EuHgSnS₄: Two Quaternary Eu-Based Infrared Nonlinear Optical Materials with Strong Second-Harmonic-Generation Responses. Inorganic Chemistry, 2020, 59, 18452-18460.	1.9	26
5213	Optical and Electronic Structural Properties of Cu₃N Thin Films: A First-Principles Study (LDA + U). ACS Omega, 2020, 5, 31918-31924.	1.6	10

#	Article	IF	Citations
5214	Electronic, elastic, vibrational and superconducting properties of a ternary superconductors LaIrP (P) Tj ETQq0 0 0 rgBT /Overlock 10 Tf 5	0.9	16
5215	Structures and optoelectronic properties of two-dimensional MC6 (Mâ€¯=â€¯Ti and Hf) predicted by computational approaches. Materials Today Communications, 2020, 25, 101606.	0.9	0
5216	Boosting Capacitive Sodium-Ion Storage in Electrochemically Exfoliated Graphite for Sodium-Ion Capacitors. ACS Applied Materials & Interfaces, 2020, 12, 52635-52642.	4.0	25
5217	Polarization consistent basis sets using the projector augmented wave method: a renovation brought by PAW into Gaussian basis sets. Physical Chemistry Chemical Physics, 2020, 22, 27037-27052.	1.3	2
5218	Eco-friendly, solution-processable and efficient low-energy lighting phosphors: copper halide based hybrid semiconductors Cu₄X₆(L)₂(X = Br, I) composed of covalent, ionic and coordinate bonds. Journal of Materials Chemistry C, 2020, 8, 16790-16797.	2.7	24
5219	First-principles investigation of the structure and electronic properties of graphene toward Li adsorption. Molecular Simulation, 2020, 46, 1522-1529.	0.9	5
5220	Exploiting Co Defects in CoFe-Layered Double Hydroxide (CoFe-LDH) Derivatives for Highly Efficient Photothermal Cancer Therapy. ACS Applied Materials & Interfaces, 2020, 12, 54916-54926.	4.0	43
5221	Dispersion-Corrected DFT Methods for Applications in Nuclear Magnetic Resonance Crystallography. Journal of Physical Chemistry A, 2020, 124, 10312-10323.	1.1	14
5222	Achieving Different Color Changes for Photochromic Compounds by Controlling Coordination Modes. Journal of Physical Chemistry C, 2020, 124, 27680-27686.	1.5	18
5223	AMnAs₃S₆ (A = Cs, Rb): Phase-Matchable Infrared Nonlinear Optical Functional Motif [As₃S₆]^{3â€“} Obtained via Surfactantâ€“Thermal Method. ACS Applied Materials & Interfaces, 2020, 12, 53950-53956.	4.0	25
5224	Radial Distribution Function from X-ray Absorption near Edge Structure with an Artificial Neural Network. Journal of the Physical Society of Japan, 2020, 89, 103001.	0.7	11
5225	Pressure-Induced Phase Transitions in Danburite-Type Borosilicates. Journal of Physical Chemistry C, 2020, 124, 26048-26061.	1.5	6
5226	Bi(III) Complexes Containing Dithiocarbamate Ligands: Synthesis, Structure Elucidation by Xâ€ray Diffraction, Solidâ€State 13 C/ 15 Nâ€‰NMR, and DFT Calculations. ChemistrySelect, 2020, 5, 8882-8891.	0.7	5
5227	Intrinsic Isotropic Near-Zero Thermal Expansion in Zn₄B₆O₁₂X (X) Tj ETQq1 1 0.784314 rgBT	4.0	16
5228	Enhanced optical anisotropyviadimensional control in alkali-metal chalcogenides. Physical Chemistry Chemical Physics, 2020, 22, 19697-19703.	1.3	14
5229	Highly efficient catalysts for oxygen reduction using well-dispersed iron carbide nanoparticles embedded in multichannel hollow nanofibers. Journal of Materials Chemistry A, 2020, 8, 18125-18131.	5.2	23
5230	Low defects density CsPbBr₃ single crystals grown by an additive assisted method for gamma-ray detection. Journal of Materials Chemistry C, 2020, 8, 11360-11368.	2.7	63
5231	Universal growth of ultra-thin IIIâ€“V semiconductor single crystals. Nature Communications, 2020, 11, 3979.	5.8	34

#	Article	IF	Citations
5232	Theoretically designed two-dimensional Î³-C₄O as an effective gas separation membrane for hydrogen purification. Physical Chemistry Chemical Physics, 2020, 22, 19492-19501.	1.3	8
5233	Inclusion of Neon into an Yttrium Borohydride Structure at Elevated Pressure â€“ An Experimental and Theoretical Study. European Journal of Inorganic Chemistry, 2020, 2020, 3846-3851.	1.0	2
5234	Effects of molecular vacancy and ethylenediamine on structural and electronic properties of CH3NO2 surfaces. Journal of Molecular Modeling, 2020, 26, 209.	0.8	0
5235	Atomic-scale investigations of enhanced hydrogen separation performance from doping boron and nitrogen in graphdiyne membrane. International Journal of Hydrogen Energy, 2020, 45, 28893-28902.	3.8	21
5236	Effects of triaxial strain on carrier activity, carrier lifetime, and absorption spectrum of (S, Se, Te) and 2ÂN Co-doped ZnO. Vacuum, 2020, 182, 109684.	1.6	14
5237	Influence of quantum dot shape on the formation energy of boron dopants in silicon. Journal of Applied Physics, 2020, 128, 055102.	1.1	2
5238	Structural, Electronic and Optical Characteristics of HgSiX2 (X=P, As) Chalcopyrite Materials: A DFT-Based Computer Simulation. Journal of the Korean Physical Society, 2020, 77, 72-77.	0.3	2
5239	Origin of Weaker Fermi Level Pinning and Localized Interface States at Metal Silicide Schottky Barriers. Journal of Physical Chemistry C, 2020, 124, 19698-19703.	1.5	11
5240	Insight into Si/SiCO thin films anodes for lithium-ion batteries with high capacity and cycling stability. Applied Materials Today, 2020, 20, 100773.	2.3	8
5241	Electronic, elastic, vibrational and dielectric properties of InPS4 by first principles. Materials Chemistry and Physics, 2020, 255, 123548.	2.0	1
5242	First-principles insights on the stability, linear and nonlinear optical properties of new potential thioborates AgBS2, CuBS2. Optical and Quantum Electronics, 2020, 52, 1.	1.5	1
5243	GeN3 monolayer: A promising 2D high-efficiency photo- hydrolytic catalyst with High carrier mobility transport anisotropy. Applied Catalysis B: Environmental, 2020, 279, 119368.	10.8	36
5244	Phase Distribution, Composition, and Disorder in Y₂(Hf,Sn)₂O₇ Ceramics: Insights from Solid-State NMR Spectroscopy and First-Principles Calculations. Journal of Physical Chemistry C, 2020, 124, 17073-17084.	1.5	7
5245	Ultrafine copper nanoclusters and single sites for Fenton-like reactions with high atom utilities. Environmental Science: Nano, 2020, 7, 2595-2606.	2.2	24
5246	Three non-centrosymmetric bismuth phosphates, Li₂ABi(PO₄)₂(A =) Tj ETQq0 0 0 rgBT /Overlock Frontiers, 2020, 7, 3364-3370.	3.0	17
5247	Mechanical and electronic properties of Ti-7333 alloy under tension: First-principles calculations. International Journal of Modern Physics B, 2020, 34, 2050150.	1.0	0
5248	Bending deformation regulates the electronic and optical properties of black phosphorene. International Journal of Modern Physics B, 2020, 34, 2050191.	1.0	6
5249	Computational Studies, NMR and Ir Spectral Analysis, Normal Coordinate Analysis, and Thermodynamic Properties of 2-Fluoro-4-Pyridineboronic Acid. Journal of Structural Chemistry, 2020, 61, 400-418.	0.3	1

#	Article	IF	Citations
5250	Theoretical prediction, synthesis, and crystal structure determination of new MAX phase compound V2SnC. Journal of Advanced Ceramics, 2020, 9, 481-492.	8.9	56
5251	Boosting Selective Adsorption of Xe over Kr by Double-Accessible Open-Metal Site in Metalâ€“Organic Framework: Experimental and Theoretical Research. Inorganic Chemistry, 2020, 59, 11793-11800.	1.9	34
5252	Structural stability, mechanical, electronic and optical behaviour of RbXS2 (XÂ= Y and La) under high pressure: A first-principle study. Journal of Alloys and Compounds, 2020, 848, 156401.	2.8	6
5253	Improving the oxidation resistance of WSi2 by boron doping: A DFT study. Materials Today Communications, 2020, 25, 101312.	0.9	3
5254	Effect of iodic acid concentration in preparation of zinc iodate: Experimental characterization of Zn(IO3)2, and its physical properties from density functional theory. Vacuum, 2020, 181, 109660.	1.6	14
5255	Neutron scattering study of tantalum dihydride. Physical Review B, 2020, 102, .	1.1	8
5256	Multifunctional zeolite nanorods as wax carriers and acid scavengers in asphalt binder. Construction and Building Materials, 2020, 264, 120249.	3.2	10
5257	Design and characterization of Eu2+-doped Ba4Si6O16 photostimulated phosphor for optical information storage. Journal of Luminescence, 2020, 227, 117556.	1.5	10
5258	Atomicâ€Scale Control of Electronic Structure and Ferromagnetic Insulating State in Perovskite Oxide Superlattices by Longâ€Range Tuning of BO₆ Octahedra. Advanced Functional Materials, 2020, 30, 2001984.	7.8	12
5259	Realizing Deep-Ultraviolet Second Harmonic Generation by First-Principles-Guided Materials Exploration in Hydroxyborates. Journal of the American Chemical Society, 2020, 142, 15157-15163.	6.6	66
5260	Mechanical Properties of a 2D Lead-Halide Perovskite, (C₆H₅CH₂NH₃)₂PbCl₄, by Nanoindentation and First-Principles Calculations. Journal of Physical Chemistry C, 2020, 124, 19204-19211.	1.5	25
5261	First-Principles Study on Electronic Structure, Elasticity, Debye Temperature and Anisotropy of Cubic KCaF₃. Materials Science Forum, 0, 999, 109-116.	0.3	4
5262	Photocatalytic mineralization of disperse red 167.1 by cubic Cu2O nanoparticles: Experimental and theoretical approach. Journal of Photochemistry and Photobiology A: Chemistry, 2020, 392, 112425.	2.0	6
5263	Crystal Structure Prediction Approach to Explore the Iron Carbide Phases: Novel Crystal Structures and Unexpected Magnetic Properties. Journal of Physical Chemistry C, 2020, 124, 17244-17254.	1.5	8
5264	Phase Transition and Negative Thermal Expansion in Guanidinium Magnesium-Hypophosphite Hybrid Perovskite. Chemistry of Materials, 2020, 32, 6886-6891.	3.2	19
5265	Ultrathin porphyrin and tetra-indole covalent organic frameworks for organic electronics applications. Journal of Chemical Physics, 2020, 153, 044702.	1.2	21
5266	Anisotropic mechanical properties and electronic structures of transition metal carbonitrides M2CN (Mâ€‰=â€‰V, Ti, Ta, Nb, Hf and Zr) by first-principles calculations. Applied Physics A: Materials Science and Processing, 2020, 126, 1.	1.1	4
5267	Voltage-gated multilayer graphene nanochannel for K+/Na+ separation: A molecular dynamics study. Journal of Molecular Liquids, 2020, 317, 114025.	2.3	10

#	Article	IF	Citations
5268	Challenging the Ostwald rule of stages in mechanochemical cocrystallisation. Chemical Science, 2020, 11, 10092-10100.	3.7	49
5269	Molecular simulation and microtextural characterization of quartz dissolution in sodium hydroxide. Journal of Petroleum Exploration and Production, 2020, 10, 2669-2684.	1.2	21
5270	A UV birefringent crystal: RbNH4(H2C3N3O3)2Â·2H2O. Inorganic Chemistry Communication, 2020, 120, 108149.	1.8	3
5271	Stable Silicene Wrapped by Graphene in Air. ACS Applied Materials & Interfaces, 2020, 12, 40620-40628.	4.0	11
5272	Co-crystals, Salts, and Ionic Co-crystals of Ethanol and Ammonia. ACS Earth and Space Chemistry, 2020, 4, 1612-1625.	1.2	0
5273	Optimal arrangement of Ï€-conjugated anionic groups in hydro-isocyanurates leads to large optical anisotropy and second-harmonic generation effect. Inorganic Chemistry Frontiers, 2020, 7, 3674-3686.	3.0	24
5274	Cu and Sb in tetragonal ZrO2 on fuel cladding. Journal of Applied Physics, 2020, 128, 135101.	1.1	0
5275	A non-empirical lattice-relaxation estimation of TM3+ doped Î±-Al2O3. IOP Conference Series: Materials Science and Engineering, 2020, 850, 012029.	0.3	1
5276	Evaluation of oxygen contribution on delithiation process of Li-rich layered 3d transition metal oxides. Materials Today Communications, 2020, 25, 101673.	0.9	4
5277	Two Mixed-Anion Units of [GeOSe₃] and [GeO₃S] Originating from Partial Isovalent Anion Substitution and Inducing Moderate Second Harmonic Generation Response and Large Birefringence. Inorganic Chemistry, 2020, 59, 16716-16724.	1.9	39
5278	High Interfacial Holeâ€Transfer Efficiency at GaFeO₃ Thin Film Photoanodes. Advanced Energy Materials, 2020, 10, 2002784.	10.2	20
5279	A curious case of dynamic disorder in pyrrolidine rings elucidated by NMR crystallography. Chemical Communications, 2020, 56, 14039-14042.	2.2	7
5280	Structural and electronic properties of non-metal doping in Li₂FePO₄F compound: spin density functional theory. Philosophical Magazine, 2020, 100, 3155-3164.	0.7	1
5281	Understanding the influences of Mg doping on the physical properties of SrMoO3 perovskite. Results in Physics, 2020, 19, 103337.	2.0	56
5282	Conformations in Solution and in Solid-State Polymorphs: Correlating Experimental and Calculated Nuclear Magnetic Resonance Chemical Shifts for Tolfenamic Acid. Journal of Physical Chemistry A, 2020, 124, 8959-8977.	1.1	5
5283	Raman study of 3.65â€…Ã…-phase MgSi(OH)₆under high pressure and the bands assignment. High Pressure Research, 2020, 40, 495-510.	0.4	4
5284	Intense d-p Hybridization Induced a Vast SHG Response Disparity between Tetrahedral Vanadates and Arsenates. Journal of Physical Chemistry C, 2020, 124, 24949-24956.	1.5	8
5285	Guest-Controlled Incommensurate Modulation in a Meta-Rigid Metalâ€“Organic Framework Material. Journal of the American Chemical Society, 2020, 142, 19189-19197.	6.6	24

#	Article	IF	Citations
5286	Fast site-to-site electron transfer of high-entropy alloy nanocatalyst driving redox electrocatalysis. Nature Communications, 2020, 11, 5437.	5.8	288
5287	Single-ion magnetism in the extended solid-state: insights from X-ray absorption and emission spectroscopy. Chemical Science, 2020, 11, 11801-11810.	3.7	8
5288	Strain effects in coreâ€“shell PtCo nanoparticles: a comparison of experimental observations and computational modelling. Physical Chemistry Chemical Physics, 2020, 22, 24784-24795.	1.3	15
5289	La₂Ga₃O_{7.5}: A Metastable Ternary Melilite with a Super-Excess of Interstitial Oxide Ions Synthesized by Direct Crystallization of the Melt. Chemistry of Materials, 2020, 32, 9016-9025.	3.2	18
5290	Experimental and Computational Determination of Optimal Boron Content in Layered Superconductor Sc₂₀C_{8â€“x}B_xC₂₀. Inorganic Chemistry, 2020, 59, 14290-14295.	1.9	1
5291	From magnetic order to quantum disorder in the Zn-barlowite series of Sâ€‰=â€‰1/2 kagomÃ© antiferromagnets. Npj Quantum Materials, 2020, 5, .	1.8	21
5292	Route to high-$$T_{c}$$ superconductivity of $$hbox {BC}_{{7}}$$ via strong bonding of boronâ€“carbon compound at high pressure. Scientific Reports, 2020, 10, 18090.	1.6	11
5293	First-principles investigation on the adsorption and dissociation of O2 and H2O molecules on the Ni-rich TiNi alloy surface. Applied Surface Science, 2020, 534, 147570.	3.1	19
5294	Bulk and Surface Chemistry of the Niobium MAX and MXene Phases from Multinuclear Solid-State NMR Spectroscopy. Journal of the American Chemical Society, 2020, 142, 18924-18935.	6.6	35
5295	The Structure of Molecular and Surface Platinum Sites Determined by DNP-SENS and Fast MAS¹⁹⁵Pt Solid-State NMR Spectroscopy. Journal of the American Chemical Society, 2020, 142, 18936-18945.	6.6	35
5296	Experimental and theoretical evidence of dihydrogen bonds in lithium amidoborane. Scientific Reports, 2020, 10, 17431.	1.6	5
5297	Application of NMR Crystallography to Highly Disordered Templated Materials: Extensive Local Structural Disorder in the Gallophosphate GaPO-34A. Inorganic Chemistry, 2020, 59, 11616-11626.	1.9	9
5298	2-Mercaptoimidazolium halides: structural diversity, stability and spontaneous racemisation. CrystEngComm, 2020, 22, 6034-6046.	1.3	2
5299	Raman signal from a hindered hydrogen rotor. Physical Review B, 2020, 102, .	1.1	7
5300	Hydrogen-Mediated Noncovalent Interactions in Solids: What Can NMR Crystallography Tell About?. Molecules, 2020, 25, 3757.	1.7	7
5301	Luminescent Thermochromic Silver Iodides as Wavelength-Dependent Thermometers. Inorganic Chemistry, 2020, 59, 13067-13077.	1.9	8
5302	Determination of Structural, Electronic, Optical and Mechanical Properties of Brookite TiO₂Using Various Exchange-Correlation. , 2020, , .		4
5303	Structure and vibrational spectroscopy of lithium and potassium methanesulfonates. Royal Society Open Science, 2020, 7, 200776.	1.1	3

#	Article	IF	Citations
5304	Strain-dependent electronic and optical properties of boron-phosphide and germanium-carbide hetero-bilayer: A first-principles study. AIP Advances, 2020, 10, 085128.	0.6	13
5305	Ultra-stable K metal anode enabled by oxygen-rich carbon cloth. Nano Research, 2020, 13, 3137-3141.	5.8	27
5306	Chlorine-35 Solid-State Nuclear Magnetic Resonance Spectroscopy as an Indirect Probe of the Oxidation Number of Tin in Tin Chlorides. Inorganic Chemistry, 2020, 59, 13651-13670.	1.9	11
5307	A Trifunctional Separator Based on a Blockage-Adsorption-Catalysis Synergistic Effect for Li-S Batteries. ACS Applied Materials & Interfaces, 2020, 12, 47599-47611.	4.0	23
5308	Thermodynamic properties of the uranyl carbonate minerals roubaultite, fontanite, widenmannite, grimselite, Äejkaite and bayleyite. Inorganic Chemistry Frontiers, 2020, 7, 4160-4179.	3.0	11
5309	Different mechanism of response of asymmetric lone pair electrons around ns2 cations to birefringence and second harmonic generation. Journal of Applied Physics, 2020, 128, 113104.	1.1	2
5310	Effects of lithium on the electronic properties of porous Ge as anode material for batteries. Journal of Computational Chemistry, 2020, 41, 2653-2662.	1.5	2
5311	Modulating the Electronic, Optical, and Transport Properties of CdTe and ZnTe Nanostructures with Organic Molecules: A Theoretical Investigation. ACS Omega, 2020, 5, 21922-21928.	1.6	2
5312	Ti3O5 and Al2TiO5 Crystals Flotation Characteristics from Ti-bearing Blast Furnace Slag: A Density Functional Theory and Experimental Study. Crystals, 2020, 10, 838.	1.0	4
5313	New possible candidate structure for phase IV of solid hydrogen. RSC Advances, 2020, 10, 26443-26450.	1.7	1
5314	Triple Interface Passivation Strategyâ€Enabled Efficient and Stable Inverted Perovskite Solar Cells. Small Methods, 2020, 4, 2000478.	4.6	44
5315	Inorganicâ€“Organic Hybrid Molecular Clusters with Cu2I2 Rhomboid Dimer Core as Light-Emitting Coating Materials. Journal of Cluster Science, 2021, 32, 1205-1211.	1.7	3
5316	AiiDA 1.0, a scalable computational infrastructure for automated reproducible workflows and data provenance. Scientific Data, 2020, 7, 300.	2.4	142
5317	Synthesis and structures of anionic rhenium polyhydride complexes of boronâ€“hydride ligands and their application in catalysis. Chemical Science, 2020, 11, 9994-9999.	3.7	15
5318	The crystal structure, morphology and mechanical properties of diaquabis(omeprazolate)magnesium dihydrate. Acta Crystallographica Section B: Structural Science, Crystal Engineering and Materials, 2020, 76, 275-284.	0.5	6
5319	Novel III-V Nitride Polymorphs in the P42/mnm and Pbca Phases. Materials, 2020, 13, 3743.	1.3	11
5320	Suppression of Oxidative Degradation of Tinâ€“Lead Hybrid Organometal Halide Perovskite Solar Cells by Ag Doping. ACS Energy Letters, 2020, 5, 3285-3294.	8.8	38
5321	First-Principles Study of the Elastic Properties of Nickel Sulfide Minerals under High Pressure. Minerals (Basel, Switzerland), 2020, 10, 737.	0.8	5

#	Article	IF	Citations
5322	CsHgNO₃Cl₂: A New Nitrate UV Birefringent Material Exhibiting an Optimized Layered Structure. Inorganic Chemistry, 2020, 59, 12578-12585.	1.9	32
5323	Bis-3,5-Diamino-1,2,4-Triazolyl-1,2,4,5-Tetrazine: From Insensitive High Energy Density Materials to Small Molecule Organic Semiconductors. Crystal Growth and Design, 2020, 20, 6510-6518.	1.4	3
5324	Structural Phase Transitions and Superconductivity Induced in Antiperovskite Phosphide CaPd3P. Inorganic Chemistry, 2020, 59, 12397-12403.	1.9	10
5325	Crystal Structure and Stoichiometric Composition of Potassium-Intercalated Tetracene. Inorganic Chemistry, 2020, 59, 12545-12551.	1.9	1
5326	Selenite bromide nonlinear optical materials Pb₂GaF₂(SeO₃)₂Br and Pb₂NbO₂(SeO₃)₂Br: synthesis and characterization. Dalton Transactions, 2020, 49, 14046-14051.	1.6	12
5327	New quaternary chalcogenide Ba4HgAs2S10 originating from the combination of linear [HgS2]2â^' and tetrahedral [AsS4]3â^' modules. Dalton Transactions, 2020, 49, 13060-13065.	1.6	4
5328	t₁-Noise eliminated dipolar heteronuclear multiple-quantum coherence solid-state NMR spectroscopy. Physical Chemistry Chemical Physics, 2020, 22, 20815-20828.	1.3	31
5329	Recently synthesized (Ti_{1â^'x}Mo_x)₂AlC (0 â‰¤ x â‰¤ 0.20) solid solutions: deciphering the structural, electronic, mechanical and thermodynamic properties via ab initio simulations. RSC Advances, 2020, 10, 31535-31546.	1.7	41
5330	Color Differences Highlight Concomitant Polymorphism of Chalcones. Crystal Growth and Design, 2020, 20, 6346-6355.	1.4	9
5331	Finding Optimal Mid-Infrared Nonlinear Optical Materials in Germanates by First-Principles High-Throughput Screening and Experimental Verification. ACS Applied Materials & Interfaces, 2020, 12, 45023-45035.	4.0	46
5332	Photocatalytic partial oxidation of methanol to methyl formate under visible light irradiation on Bi-doped TiO₂viatuning band structure and surface hydroxyls. RSC Advances, 2020, 10, 31442-31452.	1.7	7
5333	Application of Various Molecular Modelling Methods in the Study of Estrogens and Xenoestrogens. International Journal of Molecular Sciences, 2020, 21, 6411.	1.8	6
5334	Hierarchical Contribution of Anions to Second Harmonic Generation in A₂HgI₄ (A = Na, Ag, Cu) Regulated Dramatically by Metal Cations. Crystal Growth and Design, 2020, 20, 7470-7476.	1.4	2
5335	Gallium Species Incorporated into MOF Structure: Insight into the Formation of a 3D Polycrystalline Galliumâ€“Imidazole Framework. Inorganic Chemistry, 2020, 59, 13933-13941.	1.9	3
5336	Experimental and Density Functional Theory Study of the Adsorption Characteristics of CaO for SeO₂ in Simulated Flue Gas and the Effect of CO₂. Energy & Fuels, 2020, 34, 10872-10881.	2.5	23
5337	Crystalline Structures and Energetic Properties of Lithium Pentazolate under Ambient Conditions. ACS Omega, 2020, 5, 24946-24953.	1.6	7
5338	Physiological silicon incorporation into bone mineral requires orthosilicic acid metabolism to SiO ₄ ^{4â^'}. Journal of the Royal Society Interface, 2020, 17, 20200145.	1.5	16
5339	Multifunctional Quaternary Phosphorus/Bromoargentate Hybrids: The Achievement of Greenish Blue Luminescence, Repeatable Photocurrent Responses and Durable Antimicrobial Activities with Enhanced Water Stability . International Journal of Nanomedicine, 2020, Volume 15, 6225-6237.	3.3	4

#	Article	IF	Citations
5340	CeO₂(111) Surface with Oxygen Vacancy for Radical Scavenging: A Density Functional Theory Approach. Journal of Physical Chemistry C, 2020, 124, 20950-20959.	1.5	18
5341	From BiF₃to BiF₃Â·H₂O: diverse Bi(<scp>iii</scp>) coordination for structural transformation and birefringence regulation. CrystEngComm, 2020, 22, 6838-6846.	1.3	7
5342	Ba₃(BO₃)(CO₃)F: The First Borate Carbonate Fluoride Synthesized by the Highâ€Temperature Solution Method. Chemistry - A European Journal, 2020, 26, 16628-16632.	1.7	12
5343	Electron-beam irradiation of photopolymerized C60 film studied using in situ scanning tunneling microscope, in situ Fourier-transform infrared spectroscopy, and first-principles calculations. AIP Advances, 2020, 10, .	0.6	3
5344	Neutron Spin Resonance in a Quasi-Two-Dimensional Iron-Based Superconductor. Physical Review Letters, 2020, 125, 117002.	2.9	31
5345	Adsorption Mechanism of PbO/PbCl₂ on Kaolinite Surfaces during Coal Combustion Based on Frontier Orbital Theory. Energy & Fuels, 2020, 34, 11258-11269.	2.5	20
5346	Selective Control of Oxidation Resistance of Diamond by Dopings. ACS Applied Materials & Interfaces, 2020, 12, 42302-42313.	4.0	6
5347	Boosted Oxygen Evolution Reactivity via Atomic Iron Doping in Cobalt Carbonate Hydroxide Hydrate. ACS Applied Materials & Interfaces, 2020, 12, 40220-40228.	4.0	42
5348	Atomic PdAu Interlayer Sandwiched into Pd/Pt Core/Shell Nanowires Achieves Superstable Oxygen Reduction Catalysis. ACS Nano, 2020, 14, 11570-11578.	7.3	84
5349	Revealing the Structure and Oxygen Transport at Interfaces in Complex Oxide Heterostructures via ¹⁷O NMR Spectroscopy. Chemistry of Materials, 2020, 32, 7921-7931.	3.2	5
5350	A₂Bi₂(SeO₃)₃F₂ (A = K and Rb): Excellent Mid-Infrared Nonlinear Optical Materials with Both Strong SHG Responses and Large Band Gaps. Chemistry of Materials, 2020, 32, 7958-7964.	3.2	42
5351	Investigating Applications on the A64FX. , 2020, , .		14
5352	Hydration-Induced Disorder Lowers the Energy Barriers for Methyl Rotation in Drug Molecules. Journal of Physical Chemistry Letters, 2020, 11, 10256-10261.	2.1	7
5353	Electro-Optical Properties of Sputtered Calcium Lead Titanate Thin Films for Pyroelectric Detection. Micromachines, 2020, 11, 1073.	1.4	3
5354	Observation of the Griffiths phase in the ternary nitrides <mml:math xmlns:mml="http://www.w3.org/1998/Math/MathML"><mml:mrow><mml:msub><mml:mi>Sn</mml:mi><mml:mrow><mml:mn>1</mm mathvariant="normal">N</mml:mi><mml:msub><mml:mi>Fe</mml:mi><mml:mrow><mml:mn>3</mml:mn><mml:mo>+</mml:mo><m Physical Review B, 2020, 102, .	1.1	5
5355	Linker Substituents Control the Thermodynamic Stability in Metalâ€“Organic Frameworks. Journal of the American Chemical Society, 2020, 142, 21720-21729.	6.6	36
5356	The effective isotropy of the hydrogen local potential in biphenyl and other hydrocarbons. Journal of Chemical Physics, 2020, 153, 234306.	1.2	5
5357	Insight into the enhanced photocatalytic activity of Mo and P codoped SrTiO₃from first-principles prediction. RSC Advances, 2020, 10, 40117-40126.	1.7	12

#	Article	IF	Citations
5358	Chemically stable new MAX phase V₂SnC: a damage and radiation tolerant TBC material. RSC Advances, 2020, 10, 43783-43798.	1.7	34
5359	TeorÃa del Funcional de la Densidad en cristales de silicato de potasio. AplicaciÃ³n al cÃ¡lculo de propiedades mecÃ¡nicas y microdureza Vickers en vidrios. Boletin De La Sociedad Espanola De Ceramica Y Vidrio, 2022, 61, 107-120.	0.9	1
5360	Designing a sp3 nanoporous structure of carbon: A comprehensive study on the physical properties. Results in Physics, 2020, 19, 103473.	2.0	17
5361	Electronic and optical properties of Zn-S, Ag-C, Ag-N and Ag-S co-doped K2Ti6O13 with different doping concentrations. Optik, 2020, 223, 165547.	1.4	2
5362	Layered oxide <mml:math xmlns:mml="http://www.w3.org/1998/Math/MathML"><mml:mrow><mml:msub><mml:mi mathvariant="normal">B</mml:mi><mml:mn>2</mml:mn></mml:msub><mml:msub><mml:mi mathvariant="normal">S</mml:mi><mml:mn>2</mml:mn></mml:msub><mml:msub><mml:mi mathvariant="normal">O</mml:mi><mml:mn>9</mml:mn></mml:msub></mml:mrow></mml:math> with a deep-ultraviolet band gap and a strong and robust second-harmonic generation. Physical Review B, 2	1.1	25
5363	Role of the third metal oxide in Inâ€“Gaâ€“Znâ€“O4 amorphous oxide semiconductors: Alternatives to gallium. Journal of Applied Physics, 2020, 128, 215704.	1.1	6
5364	Creation of Gold Nanoparticles in ZnO by Ion Implantationâ€“DFT and Experimental Studies. Nanomaterials, 2020, 10, 2392.	1.9	10
5365	KLi₂RE(BO₃)₂ (RE = Dy, Ho, Er, Tm, Yb, and Y): Structural, Spectroscopic, And Thermogravimetric Studies on a Series of Mixed-Alkali Rare-Earth Orthoborates. Inorganic Chemistry, 2020, 59, 18214-18224.	1.9	5
5366	Anomalous mechanical materials squeezing three-dimensional volume compressibility into one dimension. Nature Communications, 2020, 11, 5593.	5.8	19
5367	Lattice Relaxation Effects on the Multiplet Energies of Ruby Under Pressure using One-Electron Calculations. IOP Conference Series: Materials Science and Engineering, 2020, 835, 012010.	0.3	4
5368	Phase Stability of Chloroform and Dichloromethane at High Pressure. Crystals, 2020, 10, 920.	1.0	7
5369	Parametrizing the Spatial Dependence of 1H NMR Chemical Shifts in Ï€-Stacked Molecular Fragments. International Journal of Molecular Sciences, 2020, 21, 7908.	1.8	5
5370	Infrared emitting material using infrared wavelength manipulation. Applied Materials Today, 2020, 21, 100811.	2.3	4
5371	Superhard and superconductive nondiamond-like BC structure. Diamond and Related Materials, 2020, 110, 108142.	1.8	0
5372	Thermal smearing in DFT calculations: How small is really small? A case of La and Lu atoms adsorbed on graphene. Materials Today Communications, 2020, 25, 101595.	0.9	18
5373	Effect of High Pressure on the Crystal Structures of Polymorphs of <scp>l</scp>-Histidine. Crystal Growth and Design, 2020, 20, 7788-7804.	1.4	15
5374	Catalytic NO Reduction by CO over Caâ€“Fe Oxides in the Presence of O₂ with Sintering Flue Gas Circulation. Industrial & Engineering Chemistry Research, 2020, 59, 20624-20629.	1.8	12
5375	Pentadiamond-like Metallic Hard Carbon Nitride. Journal of Physical Chemistry C, 2020, 124, 24978-24983.	1.5	12

#	Article	IF	Citations
5376	Lattice Stability and Elastic Properties of Zr-Ti-X Alloys (X = Al, V) by the First Principles Study. Metals, 2020, 10, 1317.	1.0	2
5377	Prediction of three-dimensional B3N5 with one-dimensional metallicity. Chemical Physics Letters, 2020, 760, 138002.	1.2	0
5378	Simulation of Inelastic Neutron Scattering Spectra Directly from Molecular Dynamics Trajectories. Journal of Chemical Theory and Computation, 2020, 16, 7702-7708.	2.3	14
5379	Highâ€Index Faceted RuCo Nanoscrews for Water Electrosplitting. Advanced Energy Materials, 2020, 10, 2002860.	10.2	58
5380	Theoretical and experimental study of FeSi on magnetic and phase properties. Applied Physics A: Materials Science and Processing, 2020, 126, 1.	1.1	7
5381	Influence of alloying elements on mechanical and electronic properties of NbMoTaWX (XÂ=ÂCr, Zr, V, Hf) Tj ETQq1 1 0.784314 rgBT	1.8	58
5382	Halogen bonding to the azulene Ï€-system: cocrystal design of pleochroism. Chemical Communications, 2020, 56, 15145-15148.	2.2	18
5383	Hexagonal Sr_{1â^'x/2}Al_{2â^'x}Si_xO₄:Eu²⁺,Dy³⁺transparent ceramics with tuneable persistent luminescence properties. Dalton Transactions, 2020, 49, 16849-16859.		13
5384	The micro-wear mechanism of diamond during diamond tool fly-cutting KDP (KH2PO4) from first principle calculations. Journal of Molecular Modeling, 2020, 26, 284.	0.8	5
5385	Influence of Y3+ ions on the optical properties of Dy3+-activated LaF3 single crystal. Journal of Luminescence, 2020, 224, 117264.	1.5	9
5386	An ab initio molecular dynamics exploration of associates in Ba-Bi liquid with strong ordering trends. Acta Materialia, 2020, 190, 81-92.	3.8	13
5387	Alloxan under pressureâ€“squeezing an extremely dense molecular crystal structure. Chemical Communications, 2020, 56, 6428-6431.	2.2	3
5388	Structural characterization of HPM-7, a more ordered than expected germanosilicate zeolite. Dalton Transactions, 2020, 49, 7037-7043.	1.6	7
5389	Thermally assisted photocatalytic conversion of CO₂â€“H₂O to C₂H₄over carbon doped In₂S₃nanosheets. Journal of Materials Chemistry A, 2020, 8, 10175-10179.	5.2	61
5390	Study on the Effect of Doping on Lattice Constant and Electronic Structure of Bulk AuCu by the Density Functional Theory. Journal of Multiscale Modeling, 2020, 11, 2030001.	1.0	21
5391	Optical, Electronic Properties and Anisotropy in Mechanical Properties of â€œXâ€•Type Carbon Allotropes. Materials, 2020, 13, 2079.	1.3	26
5392	Understanding magnetic relaxation in single-ion magnets with high blocking temperature. Physical Review B, 2020, 101, .	1.1	94
5393	Mechanical and electronic properties of van der Waals layered hcp PdH2. Scientific Reports, 2020, 10, 8037.	1.6	3

#	Article	IF	Citations
5394	Manganese-based layered double hydroxide nanoparticles as highly efficient ozone decomposition catalysts with tunable valence state. Nanoscale, 2020, 12, 12817-12823.	2.8	14
5395	Effects of cation size and concentration of cationic chlorides on the properties of formamidinium lead iodide based perovskite solar cells. Sustainable Energy and Fuels, 2020, 4, 3753-3763.	2.5	17
5396	Significant Improvement in Electrical Conductivity and Figure of Merit of Nanoarchitectured Porous SrTiO₃ by La Doping Optimization. ACS Applied Materials & Interfaces, 2020, 12, 28057-28064.	4.0	23
5397	Heat-resistant Pb(<scp>ii</scp>)-based X-ray scintillating metalâ€“organic frameworks for sensitive dosage detection via an aggregation-induced luminescent chromophore. Dalton Transactions, 2020, 49, 7309-7314.	1.6	30
5398	The <scp>ONETEP</scp> linear-scaling density functional theory program. Journal of Chemical Physics, 2020, 152, 174111.	1.2	94
5399	Siteâ€Specific Iron Substitution in STAâ€28, a Large Pore Aluminophosphate Zeotype Prepared by Using 1,10â€Phenanthrolines as Frameworkâ€Bound Templates. Angewandte Chemie - International Edition, 2020, 59, 15186-15190.	7.2	4
5400	LiIn₂SbO₆: A New Rutile-Related Structure Type with Unique Ion Channels. Chemistry of Materials, 2020, 32, 4785-4794.	3.2	10
5401	High pressure and elastic properties of a guanidinium-formate hybrid perovskite. Dalton Transactions, 2020, 49, 7228-7233.	1.6	11
5402	Impacts of Oxygen Vacancies on Zinc Ion Intercalation in VO₂. ACS Nano, 2020, 14, 5581-5589.	7.3	267
5403	First-principles calculations of electronic structure and optical and elastic properties of the novel ABX₃-type LaWN₃perovskite structure. RSC Advances, 2020, 10, 17317-17326.	1.7	27
5404	A highly distorted HgS₄ tetrahedron-induced moderate second-harmonic generation response of EuHgGeS₄. Inorganic Chemistry Frontiers, 2020, 7, 2451-2458.	3.0	39
5405	Diffusion quantum Monte Carlo and<mml:math xmlns:mml="http://www.w3.org/1998/Math/MathML"><mml:mrow><mml:mi>G</mml:mi><mml:mi>W</mml:mi></mml:mrow></mm of the electronic properties of monolayer and bulk hexagonal boron nitride. Physical Review B, 2020, 101, .	1.1	24
5406	Dimerization of Acetic Acid in the Gas Phaseâ€”NMR Experiments and Quantum-Chemical Calculations. Molecules, 2020, 25, 2150.	1.7	15
5407	Periodic DFT Calculationsâ€”Review of Applications in the Pharmaceutical Sciences. Pharmaceutics, 2020, 12, 415.	2.0	39
5408	Facetâ€Dependent, Fast Response, and Broadband Photodetector Based on Highly Stable Allâ€Inorganic CsCu₂I₃ Single Crystal with 1D Electronic Structure. Advanced Functional Materials, 2020, 30, 2002634.	7.8	126
5409	Hydrogen-Bond-Assisted Reinforcement of Interlayer Connections in Zn₂BO₃XÂ·H₂O (X = Cl, Br): Two UV Nonlinear Optical Crystals with KBBF-Type Structure. Inorganic Chemistry, 2020, 59, 7789-7794.	1.9	6
5410	Comparison of CH₄ and CO₂ Adsorptions onto Calcite(10.4), Aragonite(011)Ca, and Vaterite(010)CO₃ Surfaces: An MD and DFT Investigation. ACS Omega, 2020, 5, 11369-11377.	1.6	20
5411	Predictions of structural, electronic, mechanical, and thermodynamic properties of TMBCs (TMÂ=ÂTi, Zr,) Tj ETQq1 1 0.784314 rgBT /O	1.9	33

#	Article	IF	Citations
5412	Physical properties of a novel phase of boron nitride and its potential applications. Materials Chemistry and Physics, 2020, 252, 123245.	2.0	22
5413	Predicting the phase diagram of titanium dioxide with random search and pattern recognition. Physical Chemistry Chemical Physics, 2020, 22, 12697-12705.	1.3	22
5414	Reaction-driven transformation of Ni/NiO hybrid structure into Ni single atoms. Materials Today Energy, 2020, 17, 100436.	2.5	10
5415	Effects of H and He on the clustering behavior of transmutation elements in tungsten. Nuclear Instruments & Methods in Physics Research B, 2020, 470, 48-55.	0.6	4
5416	Ab Initio Prediction of Metal-Organic Framework Structures. Chemistry of Materials, 2020, 32, 5835-5844.	3.2	11
5417	Li₄Ca₂B₈O₁₆: A Borate with a Unique Fundamental Building Block and a Short Cutoff Edge. Inorganic Chemistry, 2020, 59, 8396-8403.	1.9	11
5418	Chemical Heterogeneities within the Disordered Mineral domains of Aragonite Platelets in Nacre from the European Abalone Haliotis tuberculata. Journal of Physical Chemistry C, 2020, 124, 14118-14130.	1.5	7
5419	Molecular packing of pharmaceuticals analyzed with paramagnetic relaxation enhancement and ultrafast magic angle pinning NMR. Physical Chemistry Chemical Physics, 2020, 22, 13160-13170.	1.3	22
5420	Study on the properties of perovskite materials under light and different temperatures and electric fields based on DFT. RSC Advances, 2020, 10, 20960-20971.	1.7	8
5421	IrO2 nanoparticle-decorated single-layer NiFe LDHs nanosheets with oxygen vacancies for the oxygen evolution reaction. Chemical Engineering Journal, 2020, 399, 125738.	6.6	60
5422	Understanding the photocatalytic mechanisms of the BiOI/Bi2MoO6 and BiOCl/Bi2MoO6 heterostructures: First-principles study. Journal of Physics and Chemistry of Solids, 2020, 146, 109577.	1.9	20
5423	Combined Molecular Dynamics and DFT Simulation Study of the Molecular and Polymer Properties of a Catechol-Based Cyclic Oligomer of Polyether Ether Ketone. Polymers, 2020, 12, 1054.	2.0	5
5424	Rational Design of Coâ€NiSe₂@Nâ€Doped Carbon Hollow Structure for Enhanced Liâ€“S Battery Performance. Energy Technology, 2020, 8, 2000302.	1.8	14
5425	Theoretical evaluation of hexazinane as a basic component of nitrogen-rich energetic onium salts. Molecular Systems Design and Engineering, 2020, 5, 1003-1011.	1.7	10
5426	Structural Refinement and Density Functional Theory Study of Synthetic Ge-AkaganÃ©ite (Î²-FeOOH). Crystals, 2020, 10, 239.	1.0	2
5427	Ab-Initio Study of the Electronic and Magnetic Properties of Boron- and Nitrogen-Doped Penta-Graphene. Nanomaterials, 2020, 10, 816.	1.9	11
5428	Sb³⁺ Dopant and Halogen Substitution Triggered Highly Efficient and Tunable Emission in Lead-Free Metal Halide Single Crystals. Chemistry of Materials, 2020, 32, 5327-5334.	3.2	215
5429	Functional Chalcogenide Na2HgSn2Se6 and K2MnGe2Se6 Exhibiting Flexible Chain Structure and Intriguing Birefringence Tunability. Inorganic Chemistry, 2020, 59, 7614-7621.	1.9	13

#	Article	IF	Citations
5430	MBenes: emerging 2D materials as efficient electrocatalysts for the nitrogen reduction reaction. Nanoscale Horizons, 2020, 5, 1106-1115.	4.1	114
5431	From BaAl2(BO3)2O to SnAl2(BO3)2F2: structure transformation based on ion regulation. New Journal of Chemistry, 2020, 44, 9852-9857.	1.4	2
5432	Effects of Lanthanum/Gadolinium Doping on Crystal Structures, Electronic Properties and Optical Characteristics of Bismuth Tungstate Photocatalyst: DFT Approach. Journal of the Physical Society of Japan, 2020, 89, 044707.	0.7	2
5433	Size effect on oxygen vacancy formation and gaseous adsorption in ZnO nanocrystallites for gas sensors: a first principle calculation study. Applied Physics A: Materials Science and Processing, 2020, 126, 1.	1.1	13
5434	A review on phase transition and structure-performance relationship of second-order nonlinear optical polymorphs. Coordination Chemistry Reviews, 2020, 418, 213380.	9.5	67
5435	Improvement of oxygen reduction capacity by activated carbon doped with broccoli-like Co-Ni2P in microbial fuel cells. Chemical Engineering Journal, 2020, 399, 125601.	6.6	16
5436	A dual-emitting inorganic-organic hybrid material with emission intensity enchanced via electron-transfer photochromism. Dyes and Pigments, 2020, 181, 108441.	2.0	16
5437	Adjustment of oxygen vacancy states in ZnO and its application in ppb-level NO2 gas sensor. Science Bulletin, 2020, 65, 1650-1658.	4.3	52
5438	Second-Order Nonlinear-Optical-Active Selenide Borate YSeBO₂: Featuring a [YSeBO₂]_n Planar Belt. Inorganic Chemistry, 2020, 59, 7905-7909.	1.9	22
5439	Structure and vibrational spectra of ReSe 2 nanoplates. Journal of Raman Spectroscopy, 2020, 51, 1305-1314.	1.2	6
5440	Rareâ€earth Metal Borosilicides R 9 Si 15â€“ x B 3 (R = Tb, Yb): New Ordered Structures Derived from the AlB 2 Structure Type. Zeitschrift Fur Anorganische Und Allgemeine Chemie, 2020, 646, 1168-1175.	0.6	2
5441	Controlling Î²Sn grain orientations in electronic interconnects with single-crystal Cobalt substrates. Acta Materialia, 2020, 194, 422-436.	3.8	9
5442	A computational insight of electronic and optical properties of Cd-doped BaZrO3. Chinese Journal of Physics, 2020, 66, 318-326.	2.0	15
5443	Vanadium (V) and Niobium (Nb) as the most promising co-catalysts for hydrogen sulfide splitting screened out from 3d and 4d transition metal single atoms. International Journal of Hydrogen Energy, 2020, 45, 17480-17492.	3.8	19
5444	Correlating Thermionic Emission with Specific Surface Reconstructions in a <100> Hydrogenated Single-Crystal Diamond. ACS Applied Materials & Interfaces, 2020, 12, 26534-26542.	4.0	4
5445	Rational Design of a Ni₃N_{0.85} Electrocatalyst to Accelerate Polysulfide Conversion in Lithiumâ€“Sulfur Batteries. ACS Nano, 2020, 14, 6673-6682.	7.3	212
5446	Abnormal bandgap enlargement resulted in a promising mid-infrared nonlinear optical material Rb₂CdBrI₃with an ultrahigh laser damage threshold. Journal of Materials Chemistry C, 2020, 8, 9005-9011.	2.7	5
5447	Structural transition, metallization, and superconductivity in quasi-two-dimensional layered <mml:math xmlns:mml="http://www.w3.org/1998/Math/MathML"><mml:mrow><mml:mi>Pd</mml:mi><mml:msub><mml:mi mathvariant="normal">S</mml:mi><mml:mn>2</mml:mn></mml:msub></mml:mrow></mml:math> under compression. Physical Review B, 2020, 101, .	1.1	22

#	Article	IF	Citations
5448	High-Pressure Polymeric Nitrogen Allotrope with the Black Phosphorus Structure. Physical Review Letters, 2020, 124, 216001.	2.9	119
5449	Insight into physicochemical properties of Nd₂CuO4Â±Î´ and the A-site cation deficient Nd1.9CuO4Â±Î´ layered oxides. Functional Materials Letters, 2020, 13, 2051034.	0.7	2
5450	A new non-centrosymmetric Gd-based borate crystal Rb₇SrGd₂(B₅O₁₀)₃: growth, structure, and nonlinear optical and magnetic properties. Dalton Transactions, 2020, 49, 9355-9361.	1.6	12
5451	Study on micro-structure and transport properties of KF-NaF-AlF3-Al2O3 system by first-principles molecular dynamics simulation. Journal of Fluorine Chemistry, 2020, 235, 109546.	0.9	11
5452	Neutron diffraction study of the Î±- to Î²-phase transition in BaD2 under high pressure. Solid State Communications, 2020, 318, 113965.	0.9	5
5453	Multimodal Structure Solution with 19F NMR Crystallography of Spin Singlet Molybdenum Oxyfluorides. Journal of the American Chemical Society, 2020, 142, 12288-12298.	6.6	11
5454	Mechanochemical reactions of cocrystals: comparing theory with experiment in the making and breaking of halogen bonds in the solid state. Chemical Communications, 2020, 56, 8293-8296.	2.2	18
5455	Modelling the enthalpy change and transition temperature dependence of the metalâ€“insulator transition in pure and doped vanadium dioxide. Physical Chemistry Chemical Physics, 2020, 22, 13474-13478.	1.3	12
5456	Criteria of active sites in nonradical persulfate activation process from integrated experimental and theoretical investigations: boronâ€“nitrogen-co-doped nanocarbon-mediated peroxydisulfate activation as an example. Environmental Science: Nano, 2020, 7, 1899-1911.	2.2	60
5457	Structural Phase Transitions, Electronic Properties, and Hardness of RuB₄ under High Pressure in Comparison with FeB₄ and OsB₄. Journal of Physical Chemistry C, 2020, 124, 14804-14810.	1.5	20
5458	Probing NaCl hydrate formation from aqueous solutions by terahertz time-domain spectroscopy. Physical Chemistry Chemical Physics, 2020, 22, 17791-17797.	1.3	11
5459	Borate Hydrides as a New Material Class: Structure, Computational Studies, and Spectroscopic Investigations on Sr₅(BO₃)₃H and Sr₅(¹¹BO₃)₃D. Chemistry - A European Journal, 2020, 26, 11742-11750.	1.7	14
5460	Formation of heterogeneous energetic materials to regulate sensitivity of TATB by 2D materials. Vacuum, 2020, 177, 109392.	1.6	1
5461	Cocrystals â€œDivorce and Marriageâ€: When a Binary System Meets an Active Multifunctional Synthon in a Ball Mill. Chemistry - A European Journal, 2020, 26, 13264-13273.	1.7	7
5462	Triple-layered SillÃ©nâ€“Aurivillius Perovskite Oxychloride Bi₅PbTi₃O₁₄Cl as a Visible-light-responsive Photocatalyst for Water Splitting. Chemistry Letters, 2020, 49, 978-981.	0.7	11
5463	AGa₃F₆(SeO₃)₂ (A = Rb, Cs): A New Type of Phase-Matchable Hexagonal Tungsten Oxide Material with Strong Second-Harmonic Generation Responses. Chemistry of Materials, 2020, 32, 6906-6915.	3.2	46
5464	Helix-constructed polar rare-earth iodate fluoride as a laser nonlinear optical multifunctional material. Chemical Science, 2020, 11, 7396-7400.	3.7	18
5465	Siteâ€Specific Iron Substitution in STAâ€28, a Large Pore Aluminophosphate Zeotype Prepared by Using 1,10â€Phenanthrolines as Frameworkâ€Bound Templates. Angewandte Chemie, 2020, 132, 15298-15302.	1.6	2

#	Article	IF	Citations
5466	Real-Space Mapping of Oxygen Coordination in Phase-Separated Aluminosilicate Glass: Implication for Glass Stability. ACS Applied Nano Materials, 2020, 3, 5053-5060.	2.4	14
5467	Two dimensional cubic boron nitride nanosheets converted from hexagonal boron nitride bilayers: electrical conductivity, magnetism and visible absorption properties. Chinese Journal of Physics, 2020, 66, 534-542.	2.0	0
5468	Inversely deducing the initiation mechanism of energetic materials under pressure from possible defect states in nitromethane. Chemical Physics Letters, 2020, 749, 137470.	1.2	7
5469	Influence of Lithium Vacancy Defects on Tritium Diffusion in Î²-Li₂TiO₃. Journal of Physical Chemistry C, 2020, 124, 12286-12294.	1.5	12
5470	Electronic properties and effective masses of hexagonal Bi9O7.5S6: First-principles calculations. Materials Science in Semiconductor Processing, 2020, 114, 105081.	1.9	4
5471	Adsorption and diffusion behaviors of H2, H2S, NH3, CO and H2O gases molecules on MoO3 monolayer: A DFT study. Physics Letters, Section A: General, Atomic and Solid State Physics, 2020, 384, 126533.	0.9	34
5472	Theoretical study on the effect of different surfaces on structure, excess energy, electronic structure and impact sensitivity in 1,3,5,7-tetranitro-1,3,5,7-tetraazacyclooctane. Surface Science, 2020, 700, 121650.	0.8	1
5473	Hydroxyl Defects and Oxide Vacancies within Ringwooditeâ€"toward Understanding the Defect Chemistry of Spinel-Type Oxides. Journal of Physical Chemistry C, 2020, 124, 12001-12009.	1.5	6
5474	Hierarchically Structured Allotropes of Phosphorus from Dataâ€Driven Exploration. Angewandte Chemie - International Edition, 2020, 59, 15880-15885.	7.2	26
5475	Deep-ultraviolet nonlinear optical crystals by design: A computer-aided modeling blueprint from first principles. Science China Materials, 2020, 63, 1597-1612.	3.5	33
5476	Synthesis and characterization of Pt(Cu0.67Sn0.33). Solid State Sciences, 2020, 105, 106282.	1.5	1
5477	tP40 carbon: A novel superhard carbon allotrope*. Chinese Physics B, 2020, 29, 106102.	0.7	23
5478	Band Structures, Magnetism, Half-metallicity and Elastic Properties of Full-Heusler Alloy Cr₂VSb. Journal of the Physical Society of Japan, 2020, 89, 064713.	0.7	21
5479	Investigating geometric structure, energies, electronic structure and impact sensitivity illustrated with surfaces of Îµ-CL-20. Applied Surface Science, 2020, 527, 146940.	3.1	4
5480	Doping Induced Hierarchical Lattice Expansion of Cobalt Diselenide/Carbon Nanosheet Hybrid for Fast and Stable Sodium Storage. Cell Reports Physical Science, 2020, 1, 100082.	2.8	7
5481	Nuclear dynamics in BaZr_{0.7}Ce_{0.2}Y_{0.1}O_{3âˆ'Î´} proton conductor as observed by neutron diffraction and Compton scattering. Journal of Physics Communications, 2020, 4, 045004.	0.5	6
5482	Density Functional Theory Study of Pd Aggregation on a Pyridineâ€Terminated Selfâ€Assembled Monolayer. Chemistry - A European Journal, 2020, 26, 10555-10563.	1.7	1
5483	Thermal quenching properties of narrow-band blue-emitting MBe₂(PO₄)₂:Eu²⁺(M = Ca, Sr) phosphors towards backlight display applications. Inorganic Chemistry Frontiers, 2020, 7, 2685-2691.	3.0	18

#	Article	IF	Citations
5484	Hierarchically Structured Allotropes of Phosphorus from Dataâ€Driven Exploration. Angewandte Chemie, 2020, 132, 16014-16019.	1.6	1
5485	A chondrule formation experiment aboard the ISS: Experimental set-up and test experiments. Icarus, 2020, 350, 113898.	1.1	7
5486	New Alkaline-Earth Metal Fluoroiodates Exhibiting Large Birefringence and Short Ultraviolet Cutoff Edge with Highly Polarizable (IO₃F)^{2â€“} Units. Chemistry of Materials, 2020, 32, 5723-5728.	3.2	44
5487	ONETEP + TOSCAM: Uniting Dynamical Mean Field Theory and Linear-Scaling Density Functional Theory. Journal of Chemical Theory and Computation, 2020, 16, 4899-4911.	2.3	5
5488	Te₃O₃(PO₄)₂: a phosphate crystal with large birefringence activated by the highly distorted [TeO₅] group and antiparallel [PO₄] pseudo-layer. Journal of Materials Chemistry C, 2020, 8, 9585-9592.	2.7	23
5489	First-Principles Calculations of High-Pressure Physical Properties of Ti0.5Ta0.5 Alloy. Symmetry, 2020, 12, 796.	1.1	1
5490	Measuring multiple 17Oâ€“13C J-couplings in naphthalaldehydic acid: a combined solid state NMR and density functional theory approach. Physical Chemistry Chemical Physics, 2020, 22, 3400-3413.	1.3	9
5491	Structure and Dynamics of the Superprotonic Conductor Caesium Hydrogen Sulfate, CsHSO4. Molecules, 2020, 25, 1271.	1.7	4
5492	Semiconducting few-layer PdSe₂ and Pd₂Se₃: native point defects and contacts with native metallic Pd₁₇Se₁₅. Physical Chemistry Chemical Physics, 2020, 22, 7365-7373.	1.3	8
5493	Mixed-metal thiophosphate CuCd₃PS₆: an infrared nonlinear optical material activated by its three-in-one tetrahedra-stacking architecture. Journal of Materials Chemistry C, 2020, 8, 5020-5024.	2.7	24
5494	Spin-glass behavior in Co-based antiperovskite compound SnNCo3. Applied Physics Letters, 2020, 116, .	1.5	10
5495	First-principles calculations of the structural, elastic, mechanical, electronic and optical properties of monoclinic Hf₄CuSi₄. International Journal of Modern Physics B, 2020, 34, 2050035.	1.0	4
5496	Electronic state analysis of Li2RuO3 positive electrode for lithium ion secondary battery. Modern Physics Letters B, 2020, 34, 2040024.	1.0	2
5497	ZnIO₃F: Zinc Iodate Fluoride with Large Birefringence and Wide Band Gap. Inorganic Chemistry, 2020, 59, 4172-4175.	1.9	40
5498	Clear evidence for element partitioning effects in a Tiâ€“6Alâ€“4V alloy by the first-principles phase field method. Journal of Physics Condensed Matter, 2020, 32, 264001.	0.7	8
5499	Fabrication of Silica/Sulfur@Polyaniline Spheres with Radial Mesochannels as Enhanced Cathode Materials for Highâ€Performance Lithiumâ^'Sulfur Batteries. ChemNanoMat, 2020, 6, 827-836.	1.5	2
5500	Regulating the electronic and optic properties of hexagonal boron nitride nanosheets via phosphorus doping. Europhysics Letters, 2020, 129, 37001.	0.7	5
5501	NMR Crystallography of Aluminum Carbide: Impurities in the Reagent and Improved ²⁷Al NMR Tensors. Journal of Physical Chemistry C, 2020, 124, 7238-7243.	1.5	2

#	Article	IF	Citations
5502	General synthesis of two-dimensional van der Waals heterostructure arrays. Nature, 2020, 579, 368-374.	13.7	393
5503	First-principles calculation on the structure stability, elastic properties and electronic structure of P-doped Mg₂Si. Materials Research Express, 2020, 7, 036533.	0.8	5
5504	First-principles prediction of enhancing graphene/Al interface bonding strength by graphene doping strategy. Applied Surface Science, 2020, 517, 146040.	3.1	31
5505	Cd₄SiQ₆ (Q = S, Se): Ternary Infrared Nonlinear Optical Materials with Mixed Functional Building Motifs. Crystal Growth and Design, 2020, 20, 2489-2496.	1.4	15
5506	Defective structures in FeCrAl alloys from first principles calculations. Japanese Journal of Applied Physics, 2020, 59, 046003.	0.8	6
5507	Oxygen adsorption on ideal ZrB2 and ZrC surfaces. Journal of Alloys and Compounds, 2020, 830, 154655.	2.8	11
5508	A comparative theoretical investigation of optoelectronic and mechanical properties of KYS2 and KLaS2. Materials Science in Semiconductor Processing, 2020, 113, 105048.	1.9	16
5509	The magnesium uranyl tricarbonate octadecahydrate mineral, bayleyite: Periodic DFT study of its crystal structure, hydrogen bonding, mechanical properties and infrared spectrum. Spectrochimica Acta - Part A: Molecular and Biomolecular Spectroscopy, 2020, 234, 118216.	2.0	6
5510	Chitosan and pectin coreâ€“shell beads encapsulating metforminâ€“clay intercalation compounds for controlled delivery. New Journal of Chemistry, 2020, 44, 10102-10110.	1.4	26
5511	Prediction of quasi-one-dimensional superconductivity in metastable two-dimensional boron. Physical Review B, 2020, 101, .	1.1	12
5512	M-SPARC: Matlab-Simulation Package for Ab-initio Real-space Calculations. SoftwareX, 2020, 11, 100423.	1.2	13
5513	Metal-Coordination Network vs Charge Transfer Complex: The Importance of the Surface. Journal of Physical Chemistry C, 2020, 124, 7922-7929.	1.5	5
5514	A novel C₆N₂monolayer as a potential material for charge-controlled CO₂capture. Journal of Materials Chemistry C, 2020, 8, 6542-6551.	2.7	23
5515	Structures of solid hydrogen at 300 K. Physical Review B, 2020, 101, .	1.1	13
5516	Secondary relaxation in the terahertz range in 2-adamantanone from theory and experiments. Physical Review B, 2020, 101, .	1.1	5
5517	Synergistic effect of hydrogen absorption on (TiÂ+ÂNi), (TiÂ+ÂV), (NiÂ+ÂV) doped Mg17Al12 (1Â1Â0) surfaces: A theoretical study. Applied Surface Science, 2020, 514, 145884.	3.1	6
5518	Modeling of explosives: 1,4,2,3,5,6-dioxatetrazinane as a new green energetic material with enhanced performance. Journal of Physics and Chemistry of Solids, 2020, 142, 109458.	1.9	15
5519	Designing a Deep-UV Nonlinear Optical Fluorooxosilicophosphate. Journal of the American Chemical Society, 2020, 142, 6472-6476.	6.6	89

#	Article	IF	Citations
5520	Vibrational Dynamics of Crystalline 4-Phenylbenzaldehyde from INS Spectra and Periodic DFT Calculations. Molecules, 2020, 25, 1374.	1.7	6
5521	5â€aminoâ€2â€methylpyridinium hydrogen fumarate: An XRD and NMR crystallography analysis. Magnetic Resonance in Chemistry, 2020, 58, 1026-1035.	1.1	4
5522	Molecular Packing-Dependent Thermal Expansion Behaviors in Metal Squarate Frameworks. Chemistry of Materials, 2020, 32, 2893-2898.	3.2	15
5523	Theoretical Exploration of Single-Layer Tl₂O as a Catalyst in Lithiumâ€"Oxygen Battery Cathodes. Journal of Physical Chemistry C, 2020, 124, 9089-9098.	1.5	31
5524	æ·±ç´«å–æ°ŸåŒ–ç¡¼é…¸ç›åŒæŠ˜å°„çŽ‡å’ŒæŠ˜å°„çŽ‡è‰²æ•£çš„æ€§èƒ½ å¢žç›Šç”¨ç©¶. Science China Materials, 2020, 63, 1480-14	8.5	75
5525	High-Performance UVâ€"Vis Photodetectors Based on a Lead-Free Hybrid Perovskite Crystal (MV)[SbI₃Cl₂]. Inorganic Chemistry, 2020, 59, 4349-4356.	1.9	22
5526	Introducing the crystalline phase of dicalcium phosphate monohydrate. Nature Communications, 2020, 11, 1546.	5.8	26
5527	Adsorption Behaviors of Different Water Structures on the Fluorapatite (001) Surface: A DFT Study. Frontiers in Materials, 2020, 7, .	1.2	11
5528	Synthesis of Meta Symmetric <scp>1T</scp>â€™â€<scp>WTe₂</scp> Using an <scp>Edgeâ€Induced</scp> Mechanism. Chinese Journal of Chemistry, 2020, 38, 709-713.	2.6	6
5529	Improved Chemical Stability of Organometal Halide Perovskite Solar Cells Against Moisture and Heat by Ag Doping. ChemSusChem, 2020, 13, 3261-3268.	3.6	11
5530	The Raman and IR vibration modes of metal pentazolate hydrates [Na(H2O)(N5)]Â·2H2O and [Mg(H2O)6(N5)2]Â·4H2O. Journal of Molecular Modeling, 2020, 26, 84.	0.8	3
5531	Visual color modulation and luminescence mechanism studies on Mn/Eu co-doped Znâ€"Mg-Ge-O long afterglow system. Ceramics International, 2020, 46, 14005-14018.	2.3	4
5532	Structural origin of physicochemical properties differences upon dehydration and polymorphic transformation of ciprofloxacin hydrochloride revealed by structure determination from powder X-ray diffraction data. CrystEngComm, 2020, 22, 7272-7279.	1.3	14
5533	Structure Solution of ACV-GLU Cocrystal by Combined XRD Refinement, 1D Solid State NMR and DFT Calculations. IOP Conference Series: Materials Science and Engineering, 2020, 774, 012036.	0.3	0
5534	Mechanochemical Formation of Racemic Praziquantel Hemihydrate with Improved Biopharmaceutical Properties. Pharmaceutics, 2020, 12, 289.	2.0	21
5535	Tuning the structure and intrinsic magnetic properties of Ce2Fe14B alloys by elimination of CeFe2 with La substitution. Journal of Magnetism and Magnetic Materials, 2020, 505, 166747.	1.0	23
5536	NMR crystallography of molecular organics. Progress in Nuclear Magnetic Resonance Spectroscopy, 2020, 118-119, 10-53.	3.9	95
5537	Electronic structures and optoelectronic properties of ATiOPO₄ (AÂ=ÂH, Li, Na, K, Rb, Cs, Fr,) Tj ETQq1 1 0.784314 rgBT and photo-degradation. Materials Research Express, 2020, 7, 045901.	0.8	6

#	Article	IF	Citations
5538	Gaussian Basis Sets for Crystalline Solids: All-Purpose Basis Set Libraries vs System-Specific Optimizations. Journal of Chemical Theory and Computation, 2020, 16, 2192-2201.	2.3	18
5539	K₂Na(IO₃)₂(I₃O₈) with Strong Second Harmonic Generation Response Activated by Two Types of Isolated Iodate Anions. Chemistry of Materials, 2020, 32, 3608-3614.	3.2	36
5540	Strong Second Harmonic Generation in a Tungsten Bronze Oxide by Enhancing Local Structural Distortion. Journal of the American Chemical Society, 2020, 142, 7480-7486.	6.6	33
5541	Approaching the activity limit of CoSe2 for oxygen evolution via Fe doping and Co vacancy. Nature Communications, 2020, 11, 1664.	5.8	191
5542	An investigation of the positive effects of doping an Al atom on the adsorption of CO₂ on BN nanosheets: a DFT study. Physical Chemistry Chemical Physics, 2020, 22, 9368-9374.	1.3	22
5543	The discontinuous effect of pressure on twin boundary strength in MgO. Physics and Chemistry of Minerals, 2020, 47, 1.	0.3	1
5544	Alignment of Polar Moieties Leading to Strong Second Harmonic Response in KCsMoP₂O₉. Chemistry of Materials, 2020, 32, 3297-3303.	3.2	31
5545	2D AlP₃ with high carrier mobility and tunable band structure. Journal of Physics Condensed Matter, 2020, 32, 055001.	0.7	19
5546	Physical Properties of XN (X = B, Al, Ga, In) in the Pmâ‾3n phase: First-Principles Calculations. Materials, 2020, 13, 1280.	1.3	25
5547	Toward an Understanding of the Formation and Desolvation of Methanol Solvate, and Structure of Methanolysis Product: A Case Study of Nicosulfuron. Crystals, 2020, 10, 157.	1.0	4
5548	First-principles studies of chalcopyrite-type (Cu, Li)GaS2 and (Cu, Li)InS2 systems. Japanese Journal of Applied Physics, 2020, 59, SCCB18.	0.8	0
5549	Directed self-assembly of viologen-based 2D semiconductors with intrinsic UVâ€“SWIR photoresponse after photo/thermo activation. Nature Communications, 2020, 11, 1179.	5.8	88
5550	Twoâ€Photon Absorption in Monolayer MXenes. Advanced Optical Materials, 2020, 8, 1902021.	3.6	50
5551	Excess enthalpy of mixing of mineral solid solutions derived from density-functional calculations. Physics and Chemistry of Minerals, 2020, 47, 15.	0.3	3
5552	Effects of phase, strain, pressure, vacancy, and doping on the adsorption of metallic radionuclides on monolayer 2H-MoS2. Adsorption, 2020, 26, 521-535.	1.4	4
5553	Tuning the electronic, optical and structural properties of GaS/C2N van der Waals heterostructure for photovoltaic application: first-principle calculations. SN Applied Sciences, 2020, 2, 1.	1.5	16
5554	First-principles investigation of interfacial stability, mechanical behavior and failure mechanism of Î²-SiC(1Â1Â1)/Al(1Â1Â1) interfaces. Computational Materials Science, 2020, 175, 109608.	1.4	17
5555	Rational Design of the Nonlinear Optical Response in a Tin Iodate Fluoride Sn(IO₃)₂F₂. Chemistry of Materials, 2020, 32, 2615-2620.	3.2	71

#	Article	IF	Citations
5556	Molecular Construction from AgGaS₂ to CuZnPS₄: Defect-Induced Second Harmonic Generation Enhancement and Cosubstitution-Driven Band Gap Enlargement. Chemistry of Materials, 2020, 32, 3288-3296.	3.2	63
5557	Evolution of Structural Transformation in Î³â€²-Fe₄N and GeNFe₃. Journal of Physical Chemistry C, 2020, 124, 6321-6327.	1.5	4
5558	Asymptotic Pairwise Dispersion Corrections Can Describe Layered Materials Accurately. Journal of Physical Chemistry Letters, 2020, 11, 2298-2302.	2.1	17
5559	A(H₃C₃N₃O₃)(NO₃) (A = K, Rb): Alkali-Metal Nitrate Isocyanurates with Strong Optical Anisotropy. Inorganic Chemistry, 2020, 59, 10361-10367.	1.9	30
5560	Determination of Zn-containing sites inÎ²-Ga₂O₃film grown through mist chemical vapor deposition via X-ray absorption spectroscopy. Japanese Journal of Applied Physics, 2020, 59, 070909.	0.8	4
5561	Systematic First-Principles Calculations of Charge Transfer Transitions of Transition Metal Ions (Sc3+, Ti3+, V3+, Cr3+, Mn3+, Fe3+) in Î±-Al2O3 with Structural Optimization. IOP Conference Series: Materials Science and Engineering, 2020, 835, 012005.	0.3	1
5562	Friction Performance and Mechanism of the Molybdenum Disulfide Film in Carbon Dioxide Atmosphere. ECS Journal of Solid State Science and Technology, 2020, 9, 055006.	0.9	0
5563	Local Distortions and Dynamics in Hydrated Y-Doped BaZrO₃. Journal of Physical Chemistry C, 2020, 124, 16689-16701.	1.5	12
5564	Polar polymorphism: Î±- and Î²-KCsWP₂O₉nonlinear optical materials with a strong second harmonic generation response. Journal of Materials Chemistry C, 2020, 8, 11441-11448.	2.7	19
5565	Theoretical Investigation of Electronic and Magnetic Optical Properties of CdS Doped and Co Doped With Transition Metals (Mn, Fe, and Cu): Spin Density Functional Theory. IEEE Transactions on Magnetics, 2020, 56, 1-6.	1.2	3
5566	Mechanical Properties of DO3 Based on First Principles. Crystals, 2020, 10, 488.	1.0	5
5567	Electronic, mechanical and vibrational properties of a tubular tetragonal carbon. Chemical Physics Letters, 2020, 751, 137565.	1.2	0
5568	Effects of C/Si ratios on structures and behaviors of NbSiCN nanocomposite films synthesized by reactive magnetron sputtering. Materials Characterization, 2020, 167, 110466.	1.9	3
5569	Nonlinear optical ASnX (A = Na, H; X = N, P) nanosheets with divalent tin lone electron pair effect by first-principles design. Nanoscale, 2020, 12, 14895-14902.	2.8	10
5570	Effects of Nb-vacancies and hydrostatic pressures on the electron density of states of Nb3Sn from first-principles calculations. Cryogenics, 2020, 108, 103073.	0.9	1
5571	Confinement Catalyst of Co₉S₈@N-Doped Carbon Derived from Intercalated Co(OH)₂ Precursor and Enhanced Electrocatalytic Oxygen Reduction Performance. ACS Applied Materials & Interfaces, 2020, 12, 33740-33750.	4.0	34
5572	Computational prediction of the spin-polarized semiconductor equiatomic quaternary Heusler compound MnVZrP as a spin-filter. RSC Advances, 2020, 10, 25609-25617.	1.7	4
5573	Origin of Magnetic Ordering in a Structurally Perfect Quantum Kagome Antiferromagnet. Physical Review Letters, 2020, 125, 027203.	2.9	21

#	Article	IF	Citations
5574	The structure and vibrational spectroscopy of cryolite, Na₃AlF₆. RSC Advances, 2020, 10, 25856-25863.	1.7	7
5575	Following the unusual breathing behaviour of¹⁷O-enriched mixed-metal (Al,Ga)-MIL-53 using NMR crystallography. Physical Chemistry Chemical Physics, 2020, 22, 14514-14526.	1.3	16
5576	Stability and superconductivity of lanthanum and yttrium decahydrides. Physical Review B, 2020, 101, .	1.1	19
5577	Cu-substituted sulfur in nano-ZnS: structural, optical and electronic properties study. Journal of Materials Science: Materials in Electronics, 2020, 31, 12696-12707.	1.1	9
5578	Computational Investigation of Copper Phosphides as Conversion Anodes for Lithium-Ion Batteries. Chemistry of Materials, 2020, 32, 6629-6639.	3.2	21
5579	Crystal structure determination of an elusive methanol solvate â€“ hydrate of catechin using crystal structure prediction and NMR crystallography. CrystEngComm, 2020, 22, 4969-4981.	1.3	19
5580	Termination-dependence of Fermi level pinning at rare-earth arsenide/GaAs interfaces. Applied Physics Letters, 2020, 116, .	1.5	6
5581	Flexible C₆BN Monolayers As Promising Anode Materials for High-Performance K-Ion Batteries. ACS Applied Materials & Interfaces, 2020, 12, 30731-30739.	4.0	69
5582	Experimental and theoretical study on the effect of different rare-earth oxides on the high-temperature stability of SiO2 glass at 1973K. Ceramics International, 2020, 46, 24371-24378.	2.3	19
5583	One-pot fabrication of porous nitrogen-deficient g-C3N4 with superior photocatalytic performance. Journal of Photochemistry and Photobiology A: Chemistry, 2020, 400, 112729.	2.0	17
5584	First-principles study on the thermodynamic, mechanical and magnetic properties of the Fe-N phases. International Journal of Modern Physics B, 2020, 34, 2050156.	1.0	2
5585	New refractory MAB phases and their 2D derivatives: insight into the effects of valence electron concentration and chemical composition. RSC Advances, 2020, 10, 25836-25847.	1.7	9
5586	Electronic structure and luminescent properties of undoped and Yb3+, Er3+ co-doped YSGG single crystals. Journal of Luminescence, 2020, 224, 117322.	1.5	4
5587	Microstructure and mechanical properties of Cr doped WCoB based cermets by spark plasma sintering and first principle calculation. Progress in Natural Science: Materials International, 2020, 30, 417-423.	1.8	8
5588	First-principle calculations of electronic structure and dielectric function of rutile TiO2 under hydrostatic pressure. Solid State Sciences, 2020, 106, 106330.	1.5	2
5589	Electronic and optical properties of polar intermetallic compound BaSn3: First principles study. Optik, 2020, 219, 165028.	1.4	3
5590	Optical properties of Co3+ doped in Î±-Al2O3 with Considering Lattice Relaxation Effect. IOP Conference Series: Materials Science and Engineering, 2020, 835, 012011.	0.3	0
5591	Synthesis, Crystal Structure and Green Luminescence in Zero-Dimensional Tin Halide (C₈H₁₄N₂)₂SnBr₆. Inorganic Chemistry, 2020, 59, 9962-9968.	1.9	69

#	Article	IF	Citations
5592	Effect of zinc substitution on crystal structure and magnetocaloric properties of ZnFe3N nitride. European Physical Journal Plus, 2020, 135, 1.	1.2	5
5593	Role of Rare Earth Ions in the Prevention of Dealumination of Zeolite Y for Fluid Cracking Catalysts. Journal of Physical Chemistry C, 2020, 124, 4626-4636.	1.5	29
5594	Silver-Modified Ba_{1â€“x}Co_{0.7}Fe_{0.2}Nb_{0.1}O_{3â^'Î´} Perovskite Performing as a Cathodic Catalyst of Intermediate-Temperature Solid Oxide Fuel Cells. ACS Applied Materials & Interfaces, 2020, 12, 9421-9433.	4.0	19
5595	Lithium migration pathways at the composite interface of LiBH₄and two-dimensional MoS₂enabling superior ionic conductivity at room temperature. Physical Chemistry Chemical Physics, 2020, 22, 4096-4105.	1.3	21
5596	Density Functional Theory Studies of Ruthenium Dye (N3) Adsorbed on a TiO2 Brookite Cluster for Application in Dye Sensitized Solar Cells. Progress in Theoretical Chemistry and Physics, 2020, , 143-155.	0.2	2
5597	Comparative study of the ReaxFF and potential models with density functional theory for simulating hexagonal ice. Computational Materials Science, 2020, 177, 109546.	1.4	4
5598	Off-stoichiometry effect on thermoelectric properties of the new p-type sulfides compounds Cu2CoGeS4. Journal of Alloys and Compounds, 2020, 826, 154240.	2.8	14
5599	In silico Raman spectroscopy of YAlO3 single-crystalline film. Spectrochimica Acta - Part A: Molecular and Biomolecular Spectroscopy, 2020, 231, 118111.	2.0	7
5600	Reversible photo/thermal stimuli-responsive electrical bistability performance in supramolecular co-crystals accompanied by crystalline-to-amorphous transformations. Journal of Materials Chemistry C, 2020, 8, 3258-3267.	2.7	14
5601	Noncentrosymmetric Fluorooxoborates A₁₀B₁₃O₁₅F₁₉ (A = K and Rb) with Unexpected [B₁₀O₁₂F₁₃]^{7â€“} Units and Deep-Ultraviolet Cutoff Edges. Inorganic Chemistry, 2020, 59, 3274-3280.	1.9	21
5602	Engineering of the Heterointerface of Porous Carbon Nanofiberâ€“Supported Nickel and Manganese Oxide Nanoparticle for Highly Efficient Bifunctional Oxygen Catalysis. Advanced Functional Materials, 2020, 30, 1910568.	7.8	92
5603	Active Electron Density Modulation of Co₃O₄â€Based Catalysts Enhances their Oxygen Evolution Performance. Angewandte Chemie - International Edition, 2020, 59, 6929-6935.	7.2	148
5604	Synthesis and Polymorphism of Mixed Aluminumâ€“Gallium Oxides. Inorganic Chemistry, 2020, 59, 3805-3816.	1.9	28
5605	Atomic-scale investigation of enhanced lithium, sodium and magnesium storage performance from defects in MoS₂/graphene heterostructures. Nanoscale, 2020, 12, 7098-7108.	2.8	29
5606	Band alignment control in a blue phosphorus/C₂N van der Waals heterojunction using an electric field. Physical Chemistry Chemical Physics, 2020, 22, 5873-5881.	1.3	29
5607	The tesseract in two dimensional materials, a DFT approach. RSC Advances, 2020, 10, 8618-8627.	1.7	3
5608	Active Electron Density Modulation of Co₃O₄â€Based Catalysts Enhances their Oxygen Evolution Performance. Angewandte Chemie, 2020, 132, 6996-7002.	1.6	34
5609	Nature of thermoelectric properties occurring in defected Sn₂P₂S₆chalcogenide crystals. CrystEngComm, 2020, 22, 2336-2349.	1.3	7

#	Article	IF	Citations
5610	Perovskite hetero-anionic-sublattice interfaces for optoelectronics and nonconventional electronics. Nanoscale, 2020, 12, 7263-7272.	2.8	5
5611	First-principles high pressure structure searching, longitudinal-transverse mode coupling and absence of simple cubic phase in sulfur. New Journal of Physics, 2020, 22, 023020.	1.2	5
5612	First-principles study of the surface structure and stability of BC5. Materials Research Express, 2020, 7, 015617.	0.8	1
5613	Elastic properties of single crystal Bi₁₂SiO₂₀ as a function of pressure and temperature and acoustic attenuation effects in Bi₁₂MO₂₀ (MÂ=ÂSi, Ge and Ti). Materials Research Express, 2020, 7, 025701.	0.8	7
5614	Mechanical, structural, and thermodynamic properties of TaC-ZrC ultra-high temperature ceramics using first principle methods. Materials Research Express, 2020, 7, 036502.	0.8	9
5615	First-principles study on the mechanical properties and thermodynamic properties of Moâ€“Ta alloys. Plasma Science and Technology, 2020, 22, 065601.	0.7	8
5616	Electronic and vibrational properties of pure MnPS3 crystal: Theoretical and experimental investigation. Computational Materials Science, 2020, 177, 109592.	1.4	9
5617	Influence of Cation on the Anion Frameworks and Properties of Four Lead Phosphates, A2PbBi2(PO4)2(P2O7) (A = Rb, Cs) and A2PbP2O7 (A = K, Rb). Inorganic Chemistry, 2020, 59, 2945-2951.	1.9	12
5618	Seed-mediated growth of heterostructured Cu_{1.94}Sâ€“MS (M = Zn, Cd, Mn) and alloyed CuNS₂(N = In, Ga) nanocrystals for use in structure- and composition-dependent photocatalytic hydrogen evolution. Nanoscale, 2020, 12, 6111-6120.	2.8	21
5619	Reorientational dynamics of trimethoxyboroxine: A molecular glass former studied by dielectric spectroscopy and 11B nuclear magnetic resonance. Journal of Chemical Physics, 2020, 152, 034503.	1.2	8
5620	Band structure, effective mass, and carrier mobility of few-layer h-AlN under layer and strain engineering. APL Materials, 2020, 8, .	2.2	28
5621	Na site doping a pathway for enhanced thermoelectric performance in Na_{1â^'x}CoO₂; the case of Gd and Yb dopants. Journal of Physics Condensed Matter, 2020, 32, 125502.	0.7	4
5622	Effect of transition metals doping on the structural and electronic properties of LiMnPO4: spin density functional investigation. Physica Scripta, 2020, 95, 045811.	1.2	12
5623	Invited Review: Modern Methods for Accurately Simulating the Terahertz Spectra of Solids. Journal of Infrared, Millimeter, and Terahertz Waves, 2020, 41, 491-528.	1.2	35
5624	Effect of urea additives on CuSO₄Â·5H₂O crystal habit: an experimental and theoretical study. CrystEngComm, 2020, 22, 2132-2137.	1.3	7
5625	P63/mmc-Ge and their Siâ€“Ge alloys with a mouldable direct band gap. Semiconductor Science and Technology, 2020, 35, 055012.	1.0	26
5626	Topological properties after light ion irradiation on Weyl semimetal niobium phosphide from first principles. Materials Today Communications, 2020, 24, 100939.	0.9	4
5627	Influence of Hydrogen/Fluorine Substitution on Structure, Thermal Phase Transitions, and Internal Molecular Motion of Aromatic Residues in the Crystal Lattice of Steroidal Rotors. Crystal Growth and Design, 2020, 20, 2202-2216.	1.4	8

#	Article	IF	Citations
5628	Molecular Modeling of Ammonia Gas Adsorption onto the Kaolinite Surface with DFT Study. Minerals (Basel, Switzerland), 2020, 10, 46.	0.8	10
5629	Theoretical and Experimental Study on the Electrochemical Behavior of Beta-Sodium Vanadate in Rechargeable Magnesium Batteries Using Several Electrolyte Solutions. Journal of the Electrochemical Society, 2020, 167, 070512.	1.3	9
5630	Synthesis, Crystal Structure, and Characterization of a Noncentrosymmetric Sulfate Cs₂Ca₂(SO₄)₃. European Journal of Inorganic Chemistry, 2020, 2020, 854-858.	1.0	16
5631	First-principles calculation of the mechanical properties of quartz under non-hydrostatic stress. Physics of the Earth and Planetary Interiors, 2020, 300, 106447.	0.7	1
5632	Synthesis, luminescence properties and theoretical calculations of La5BSi2O13:Dy3+ phosphor coatings for light-emitting diodes. Thin Solid Films, 2020, 698, 137865.	0.8	5
5633	A first-principles study of Mg/Ni induced magnetic properties of Zn0.95â^'xMgxNi0.05O. Journal of Magnetism and Magnetic Materials, 2020, 504, 166653.	1.0	9
5634	The Methyl Torsion in Unsaturated Compounds. ACS Omega, 2020, 5, 2755-2765.	1.6	11
5635	Na₃Sc₂(PO₄)₂F₃: rational design and synthesis of an alkali rare-earth phosphate fluoride as an ultraviolet nonlinear optical crystal with an enlarged birefringence. Journal of Materials Chemistry C, 2020, 8, 4965-4972.	2.7	34
5636	Superconducting praseodymium superhydrides. Science Advances, 2020, 6, eaax6849.	4.7	99
5637	Suppressing Voltage Fading of Liâ€Rich Oxide Cathode via Building a Wellâ€Protected and Partiallyâ€Protonated Surface by Polyacrylic Acid Binder for Cycleâ€Stable Liâ€Ion Batteries. Advanced Energy Materials, 2020, 10, 1904264.	10.2	101
5638	Negative Linear Compressibility and Auxeticity in Boron Arsenate. Annalen Der Physik, 2020, 532, 1900550.	0.9	14
5639	Highly disordered cobalt oxide nanostructure induced by sulfur incorporation for efficient overall water splitting. Nano Energy, 2020, 71, 104652.	8.2	105
5640	Identifying the Molecular Edge Termination of Exfoliated Hexagonal Boron Nitride Nanosheets with Solid-State NMR Spectroscopy and Plane-Wave DFT Calculations. Chemistry of Materials, 2020, 32, 3109-3121.	3.2	41
5641	Predicting Core Level Photoelectron Spectra of Amino Acids Using Density Functional Theory. Journal of Physical Chemistry Letters, 2020, 11, 2256-2262.	2.1	11
5642	Universal Phase Transitions of AlB₂-Type Transition-Metal Diborides. ACS Omega, 2020, 5, 4620-4625.	1.6	9
5643	The engineering of stilbazolium/iodocuprate hybrids with optical/electrical performances by modulating inter-molecular charge transfer among H-aggregated chromophores. Inorganic Chemistry Frontiers, 2020, 7, 1451-1466.	3.0	17
5644	Accelerating Atomic Catalyst Discovery by Theoretical Calculationsâ€Machine Learning Strategy. Advanced Energy Materials, 2020, 10, 1903949.	10.2	99
5645	Re-assessment of the Mgâ€“Znâ€“Ce system focusing on the phase equilibria in Mg-rich corner. Calphad: Computer Coupling of Phase Diagrams and Thermochemistry, 2020, 68, 101742.	0.7	22

#	Article	IF	Citations
5646	Large optical polarizability causing positive effects on the birefringence of planar-triangular BO₃groups in ternary borates. Dalton Transactions, 2020, 49, 3284-3292.	1.6	15
5647	An Unprecedented Antimony(III) Borate with Strong Linear and Nonlinear Optical Responses. Angewandte Chemie - International Edition, 2020, 59, 7793-7796.	7.2	143
5648	The investigation of optoelectronic, magnetic and dynamical properties of Ce and Ti doped 2D blue phosphorene: A dispersion corrected DFT study. Journal of Alloys and Compounds, 2020, 827, 154255.	2.8	28
5649	A unified mid-gap defect model for amorphous GeTe phase change material. Applied Physics Letters, 2020, 116, .	1.5	7
5650	An Unprecedented Antimony(III) Borate with Strong Linear and Nonlinear Optical Responses. Angewandte Chemie, 2020, 132, 7867-7870.	1.6	35
5651			

#	Article	IF	Citations
5664	Crystal and Electronic Structure of Bismuth Thiophosphate, BiPS₄: An Earth-Abundant Solar Absorber. Chemistry of Materials, 2020, 32, 1235-1242.	3.2	19
5665	Density Functional Theory Study of Steam Effect on SeO₂ Capture by CaO Adsorbents. Energy & Fuels, 2020, 34, 2074-2079.	2.5	9
5666	Telluriumâ€“oxygen group enhanced birefringence in tellurium phosphates: a first-principles investigation. RSC Advances, 2020, 10, 4087-4094.	1.7	2
5667	A Promising Fluorooxoborate Framework with Flexibile Capability for Diverse Cations to Enhance the Second Harmonic Generation. Chemistry - A European Journal, 2020, 26, 3723-3728.	1.7	10
5668	Al/Ga-Doped Li₇La₃Zr₂O₁₂ Garnets as Li-Ion Solid-State Battery Electrolytes: Atomistic Insights into Local Coordination Environments and Their Influence on ¹⁷O, ²⁷Al, and ⁷¹Ga NMR Spectra. Journal of the American Chemical Society, 2020, 142, 3132-3148.	6.6	51
5669	Exact orbital-free kinetic energy functional for general many-electron systems. Frontiers of Physics, 2020, 15, 1.	2.4	4
5670	First-principles calculations of the monoclinic transition-metal doped NaMnO₂cathode material. Philosophical Magazine, 2020, 100, 917-926.	0.7	2
5671	Atomic structures and electronic properties of Ni or N modified Cu/diamond interface. Journal of Physics Condensed Matter, 2020, 32, 225001.	0.7	9
5672	First-principle calculation of the band structure of Ge1â^'xSnx alloy by screened-exchange local-density approximation theory. Applied Physics A: Materials Science and Processing, 2020, 126, 1.	1.1	4
5673	Design of high-reflectance ceramic materials based on the first-principle calculation. Journal of Materials Science, 2020, 55, 5481-5487.	1.7	2
5674	First principles study of ferroelectric hexagonal compounds RInO3 (R = Dy, Er, and Ho): electronic structure, optical and dielectric properties. RSC Advances, 2020, 10, 4080-4086.	1.7	4
5675	A soft-chemistry assisted strong metalâ€“support interaction on a designed plasmonic coreâ€“shell photocatalyst for enhanced photocatalytic hydrogen production. Nanoscale, 2020, 12, 7011-7023.	2.8	23
5676	Structure, Properties, and Reactivity of Porphyrins on Surfaces and Nanostructures with Periodic DFT Calculations. Applied Sciences (Switzerland), 2020, 10, 740.	1.3	18
5677	A Versatile Snâ€Substituted Argyrodite Sulfide Electrolyte for Allâ€Solidâ€State Li Metal Batteries. Advanced Energy Materials, 2020, 10, 1903422.	10.2	183
5678	Exploring configurations and properties of boron carbide by first principle. Materials Research Express, 2020, 7, 015904.	0.8	4
5679	A novel T-C₃N and seawater desalination. Nanoscale, 2020, 12, 5055-5066.	2.8	26
5680	Systematic exploration of the interactions between Fe-doped kaolinite and coal based on DFT calculations. Fuel, 2020, 266, 117082.	3.4	32
5681	Calculation of Diamagnetic Susceptibility Tensors of Organic Crystals: From Coronene to Pharmaceutical Polymorphs. Journal of Physical Chemistry A, 2020, 124, 1409-1420.	1.1	8

#	Article	IF	Citations
5682	Two-Dimensional BAs/InTe: A Promising Tandem Solar Cell with High Power Conversion Efficiency. ACS Applied Materials & Interfaces, 2020, 12, 6074-6081.	4.0	32
5683	Black phosphorus-Au nanocomposite-based fluorescence immunochromatographic sensor for high-sensitive detection of zearalenone in cereals. Nanophotonics, 2020, 9, 2397-2406.	2.9	14
5684	Theoretical and experimental investigation on the intercalation of metformin into layered clay minerals. Applied Clay Science, 2020, 186, 105418.	2.6	15
5685	Nonlayered CdSe Flakes Homojunctions. Advanced Functional Materials, 2020, 30, 1908902.	7.8	28
5686	Superconducting atmospheric structure and pressure-induced novel phases of cobalt mononitride. Computational Materials Science, 2020, 174, 109464.	1.4	2
5687	Quantum Transport beyond DC. , 2020, , 278-292.		0
5689	Coordination assembly of 2D ordered organic metal chalcogenides with widely tunable electronic band gaps. Nature Communications, 2020, 11, 261.	5.8	52
5690	Exploring the high stability of NEA GaN nanowire photocathodes by activation methods: First principles. Applied Surface Science, 2020, 508, 145250.	3.1	22
5691	Theoretical study of the influence of hydrides on the performance of Mg and Y photocathodes. Journal of Applied Physics, 2020, 127, 025304.	1.1	0
5692	A first principle study of the structural, electronic, and temperature-dependent thermodynamic properties of graphene/MoS2 heterostructure. Journal of Molecular Modeling, 2020, 26, 40.	0.8	18
5693	Effects of boron doping on structural, electronic, elastic, and optical properties of energetic crystal 2,6-diamino-3,5-dinitropyrazine-1-oxide: a theoretical study using the first principles calculation and Hirshfeld surface analysis. Journal of Molecular Modeling, 2020, 26, 41.	0.8	1
5694	A Short Review of Current Computational Concepts for High-Pressure Phase Transition Studies in Molecular Crystals. Crystals, 2020, 10, 81.	1.0	19
5695	Transition-metal control of electronic and magnetic properties in GeC semiconductor: spin density functional calculations. Physica Scripta, 2020, 95, 035804.	1.2	1
5696	First-Principles Study on Structural, Mechanical, Anisotropic, Electronic and Thermal Properties of III-Phosphides: XP (X = Al, Ga, or In) in the P6422 Phase. Materials, 2020, 13, 686.	1.3	11
5697	The role of incoherent interface in evading strength-ductility trade-off dilemma of Ti2AlN/TiAl composite: A combined in-situ TEM and atomistic simulations. Composites Part B: Engineering, 2020, 185, 107794.	5.9	32
5698	Supramolecular organisation of sulphate salt hydrates exemplified with brucine sulphate. CrystEngComm, 2020, 22, 7204-7216.	1.3	4
5699	First-principles prediction of the native filament:dielectric interfaces for the possible filamentary switching mechanism in chalcogenide selector devices. Journal of Applied Physics, 2020, 127, 045105.	1.1	3
5700	Atomic insight into the interfacial bonding and role of carbon atoms on Î²-SiC(1Â1Â1)/Al2MgC2(0Â0Â0Â1): A first-principles study. Applied Surface Science, 2020, 511, 145633.	3.1	7

#	Article	IF	Citations
5701	Conductivity and mixed conductivity of a novel dense diffusion barrier and the sensing properties of limiting current oxygen sensors. Dalton Transactions, 2020, 49, 6682-6692.	1.6	59
5702	A systematic computational study of electronic, mechanical, and optical properties of Fe_{1â^'x}Co_x alloy. Journal of Physics Communications, 2020, 4, 045003.	0.5	6
5703	Synthesis, characterization, and DFT modeling of novel organic compound thin films derived from 2-amino-4-(2-hydroxy-3-methoxyphenyl)-4H-thiazolo[3,2-a][1,3,5]triazin-6(7H)-one. Optical Materials, 2020, 105, 109915.	1.7	59
5704	Integrating Density Functional Theory Modeling with Experimental Data to Understand and Predict Sorption Reactions: Exchange of Salicylate for Phosphate on Goethite. Soil Systems, 2020, 4, 27.	1.0	9
5705	Highly Graphitized Porous Carbonâ€FeNi₃ Fabricated from Oleic Acid for Advanced Lithiumâ€“Sulfur Batteries. Chemistry - A European Journal, 2020, 26, 8926-8934.	1.7	9
5706	Physical properties of a novel microporous carbon material. Diamond and Related Materials, 2020, 106, 107831.	1.8	31
5707	Impact of gas adsorption on the stability and electronic properties of negative electron affinity GaAs nanowire photocathodes. Journal of Colloid and Interface Science, 2020, 572, 297-305.	5.0	4
5708	Aliovalent-substituted synthesis for a non-centrosymmetric phosphate with enhanced nonlinear-optical response. Journal of Solid State Chemistry, 2020, 288, 121361.	1.4	2
5709	Catalytic reactivity of Co3O4 with different facets in the hydrogen abstraction of phenol by persulfate. Applied Catalysis B: Environmental, 2020, 270, 118819.	10.8	104
5710	Ab initio calculations on the Mg/TiN heterogeneous nucleation interface. Journal of Physics and Chemistry of Solids, 2020, 143, 109479.	1.9	9
5711	Control of framework Al distribution in ZSM-5 zeolite via post-synthetic TiCl4 treatment. Microporous and Mesoporous Materials, 2020, 302, 110223.	2.2	6
5712	Theoretical investigation of the structural, elastic, electronic, and optical properties of the ternary tetragonal tellurides KBTe2 (B = Al, In). Materials Science in Semiconductor Processing, 2020, 114, 105085.	1.9	29
5713	First-principles investigation of high pressure effect on structure, mechanical and electronic properties of Mo2ScAlC2. Physica B: Condensed Matter, 2020, 588, 412171.	1.3	1
5714	Functionalizing AlN monolayer with hydroxyl group: Effect on the structural and electronic properties. Physics Letters, Section A: General, Atomic and Solid State Physics, 2020, 384, 126444.	0.9	13
5715	LiBa₄Ga₅Q₁₂ (Q = S, Se): Noncentrosymmetric Metal Chalcogenides with a Cesium Chloride Topological Structure Displaying a Remarkable Laser Damage Threshold. Inorganic Chemistry, 2020, 59, 5674-5682.	1.9	25
5716	Chemical Shift Tensors of Cimetidine Form A Modeled with Density Functional Theory Calculations: Implications for NMR Crystallography. Journal of Physical Chemistry A, 2020, 124, 3109-3119.	1.1	26
5717	Hexagonal In₂Se₃: A Defect Wurtzite-Type Infrared Nonlinear Optical Material with Moderate Birefringence Contributed by Unique InSe₅ Unit. ACS Applied Materials & Interfaces, 2020, 12, 17699-17705.	4.0	43
5718	Role of point and line defects on the electronic structure of LaAlO3/SrTiO3 interfaces. APL Materials, 2020, 8, 041103.	2.2	3

#	Article	IF	Citations
5719	The Combined Influence of Dopant Species and Surface Termination on the Electronic Properties of Diamond Surfaces. Journal of Carbon Research, 2020, 6, 22.	1.4	11
5720	Monitoring the Site-Specific Solid-State NMR Data in Oligopeptides. International Journal of Molecular Sciences, 2020, 21, 2700.	1.8	4
5721	Computational and Spectroscopic Studies of Carbon Disulfide. Molecules, 2020, 25, 1901.	1.7	3
5722	Imparting Boron Nanosheets with Ambient Stability through Methyl Group Functionalization for Mechanistic Investigation of Their Lithiation Process. ACS Applied Materials & Interfaces, 2020, 12, 23370-23377.	4.0	15
5723	Controlling the electronic and optical properties of HfS₂ mono-layers via lanthanide substitutional doping: a DFT+U study. RSC Advances, 2020, 10, 15670-15676.	1.7	30
5724	Multiâ€Color Luminescence Transition of Upconversion Nanocrystals via Crystal Phase Control with SiO₂ for High Temperature Thermal Labels. Advanced Science, 2020, 7, 2000104.	5.6	14
5725	Optical properties of a hexagonal C/BN framework with sp2 and sp3 hybridized bonds. Scientific Reports, 2020, 10, 6808.	1.6	3
5726	Crystal structures and electronic properties of Sn₃N₄polymorphs synthesizedviahigh-pressure nitridation of tin. CrystEngComm, 2020, 22, 3531-3538.	1.3	1
5727	Predicting novel superconducting hydrides using machine learning approaches. Physical Review B, 2020, 101, .	1.1	29
5728	Penta-C20: A Superhard Direct Band Gap Carbon Allotrope Composed of Carbon Pentagon. Materials, 2020, 13, 1926.	1.3	31
5729	First-Principles Study of Nitrogen Adsorption and Dissociation on PuH2 (111) Surface. Molecules, 2020, 25, 1891.	1.7	2
5730	Long-range ferromagnetic ordering of Li(ZnMn)As induced by hole carrier. Journal of Magnetism and Magnetic Materials, 2020, 508, 166879.	1.0	2
5731	Theoretical study on compositionâ€•and pressureâ€dependent mechanical properties of AlON solid solution. Journal of the American Ceramic Society, 2020, 103, 4390-4401.	1.9	8
5732	Effect of Li interstitials on magnetic properties of V-doped LiZnAs. Modern Physics Letters B, 2020, 34, 2050160.	1.0	1
5733	Can We Predict the Pressure Induced Phase Transition of Urea? Application of Quantum Molecular Dynamics. Molecules, 2020, 25, 1584.	1.7	13
5734	The adsorption of NO onto an Al-doped ZnO monolayer and the effects of applied electric fields: A DFT study. Computational and Theoretical Chemistry, 2020, 1180, 112829.	1.1	26
5735	Hybrid band offset calculation for heterojunction interfaces between disparate semiconductors. Applied Physics Letters, 2020, 116, .	1.5	9
5736	Experimental and Theoretical Evidence of Spinâ€Orbit Heavy Atom on the Light Atom ¹Hâ€…NMR Chemical Shifts Induced through Hâ‹…â‹…â‹…I^{â˜} Hydrogen Bond. Chemistry - A European Journal, 2020, 26, 8698-8702.	1.7	9

#	Article	IF	Citations
5737	Tautomerism of azo dyes in the solid state studied by 15N, 14N, 13C and 1H NMR spectroscopy, X-ray diffraction and quantum-chemical calculations. Dyes and Pigments, 2020, 178, 108342.	2.0	13
5738	Mechanistic Study on Graphene Oxidation by KMnO₄ in Solution Phase and Resultant Carbonâ€“Carbon Unzipping. Journal of Physical Chemistry C, 2020, 124, 11165-11173.	1.5	5
5739	Volume Modulation of Nonlinear Optical Properties by Cation Substitution. Journal of Physical Chemistry C, 2020, 124, 10679-10686.	1.5	1
5740	Tailoring doping effect in olivine-type NaMnPO₄: insights from density functional theory. Physica Scripta, 2020, 95, 065804.	1.2	2
5741	Chlorine-mediated photocatalytic hydrogen production based on triazine covalent organic framework. Applied Catalysis B: Environmental, 2020, 272, 118989.	10.8	44
5742	Direct bandgap silicon through strain engineering of type-VIII silicon clathrate Si46: A first-principles study. Materials Chemistry and Physics, 2020, 250, 123021.	2.0	0
5743	LDA+U study of the electronic and magnetic properties of the Sr2FeMo1-xNbxO6 compound. Materials Today Communications, 2020, 23, 101155.	0.9	7
5744	Is the alumino-boron carbide Al3BC a promising thermoelectric material? A computational exploration. Solid State Sciences, 2020, 104, 106205.	1.5	2
5745	Tunable type-I/type-II transition in g-C3N4/graphyne heterostructure by BN-doping: A promising photocatalyst. Solar Energy Materials and Solar Cells, 2020, 210, 110516.	3.0	23
5746	KInSi_{1.32}Sn_{0.68}Se₆: An Infrared Nonlinear Optical Material Containing Three Types of Tetrahedral Units. Inorganic Chemistry, 2020, 59, 5823-5827.	1.9	16
5747	Increasing Energy Density with Capacity Preservation by Aluminum Substitution in Sodium Vanadium Phosphate. ACS Applied Materials & Interfaces, 2020, 12, 21651-21660.	4.0	26
5748	Integrated Dual-Functional ORMOSIL Coatings with AgNPs@rGO Nanocomposite for Corrosion Resistance and Antifouling Applications. ACS Sustainable Chemistry and Engineering, 2020, 8, 6786-6797.	3.2	34
5749	DFT study on Ag loaded 2H-MoS₂for understanding the mechanism of improved photocatalytic reduction of CO₂. Physical Chemistry Chemical Physics, 2020, 22, 10305-10313.	1.3	29
5750	Three diphosphates, Î±-Li₂Na₂P₂O₇, Li₈Pb₃Ba(P₂O₇)₄and Li₇Rb(P₂O₇)₂: influences of co-substitution on the crystal structure. Dalton Transactions, 2020, 49, 6744-6750.	1.6	5
5751	Phase dependence of Schottky barrier heights for Geâ€“Sbâ€“Te and related phase-change materials. Journal of Applied Physics, 2020, 127, .	1.1	7
5752	Plastic and Superionic Helium Ammonia Compounds under High Pressure and High Temperature. Physical Review X, 2020, 10, .	2.8	28
5753	Crystal structures of two furazidin polymorphs revealed by a joint effort of crystal structure prediction and NMR crystallography. Acta Crystallographica Section B: Structural Science, Crystal Engineering and Materials, 2020, 76, 322-335.	0.5	13
5754	Investigation on Mg3Sb2/Mg2Si Heterogeneous Nucleation Interface Using Density Functional Theory. Materials, 2020, 13, 1681.	1.3	1

#	Article	IF	Citations
5755	Five carbon allotropes from Squaroglitter structures. Computational Materials Science, 2020, 178, 109634.	1.4	49
5756	Growth and optical properties of a stoichiometric laser crystal Pr(BO2)3. Journal of Luminescence, 2020, 225, 117288.	1.5	5
5757	Soft X-ray Absorption Spectroscopy Probes OHÂ·Â·Â·Ï€ Interactions in Epoxy-Based Polymers. Journal of Physical Chemistry C, 2020, 124, 9622-9627.	1.5	9
5758	Zirconium trigallide polymorphs with tetragonal and cubic structures: optical and thermodynamic properties. Indian Journal of Physics, 2021, 95, 587-594.	0.9	5
5759	Theoretical analysis of borophene for lithium ion electrode. Materials Today: Proceedings, 2021, 38, 485-489.	0.9	4
5760	Rational design of porous carbon allotropes as anchoring materials for lithium sulfur batteries. Journal of Energy Chemistry, 2021, 52, 121-129.	7.1	76
5761	The vibrational, thermodynamic and mechanical properties of four types HMX based on the first-principles study. Journal of Energetic Materials, 2021, 39, 125-169.	1.0	12
5762	Adsorption and diffusion of oxygen on metal surfaces studied by first-principle study: A review. Journal of Materials Science and Technology, 2021, 62, 180-194.	5.6	78
5763	The integrated DL_POLY/DL_FIELD/DL_ANALYSER software platform for molecular dynamics simulations for exploration of the synthonic interactions in saturated benzoic acid/hexane solutions. Molecular Simulation, 2021, 47, 257-272.	0.9	5
5764	Reactive molecular dynamics simulation of oil shale combustion using the ReaxFF reactive force field. Energy Sources, Part A: Recovery, Utilization and Environmental Effects, 2021, 43, 349-360.	1.2	8
5765	Structural, mechanical, thermal, and optical properties of inverse-Heusler alloys Cr2CoZ (Z = Al, In): A first-principles investigation. Physics Letters, Section A: General, Atomic and Solid State Physics, 2021, 385, 126967.	0.9	39
5766	Consecutive removal of heavy metals and dyes by a fascinating method using titanate nanotubes. Journal of Environmental Chemical Engineering, 2021, 9, 104726.	3.3	17
5767	Ultra-incompressibility and high energy density of ReN8 with infinite nitrogen chains. Journal of Materials Science, 2021, 56, 3814-3826.	1.7	9
5768	The effective mass, vibration and electromagnetic properties of tetragonal iron aluminide FeAl2. Ceramics International, 2021, 47, 1766-1771.	2.3	1
5769	Emptyâ€State Band Mapping Using Momentumâ€Resolved Secondary Electron Emission. Advanced Functional Materials, 2021, 31, 2007319.	7.8	4
5770	Interaction between dispersant and coal slime added in semi-coke water slurry: An experimental and DFT study. Applied Surface Science, 2021, 540, 148327.	3.1	21
5771	Synthesis and photoluminescence properties of a novel red emitting Ba3ZnTa2O9: Eu3+ phosphor. Journal of Molecular Structure, 2021, 1224, 129075.	1.8	14
5772	Toxic volatile organic compounds sensing by Al2C monolayer: A first-principles outlook. Journal of Hazardous Materials, 2021, 403, 123600.	6.5	22

#	Article	IF	Citations
5773	Electronic theoretical study on the influence of shear deformation on the electronic structure and optical properties of Li absorbed silicene. Journal of Molecular Structure, 2021, 1223, 128968.	1.8	3
5774	Crystal face dependent intrinsic wettability of metal oxide surfaces. National Science Review, 2021, 8, nwaa166.	4.6	33
5775	Experimental and DFT study of BaLaCuS3: Direct band gap semiconductor. Journal of Physics and Chemistry of Solids, 2021, 148, 109670.	1.9	12
5776	Bi2WO6 doped with rare earth ions: Preparation, characterization and photocatalytic activity under simulated solar irradiation. Journal of Rare Earths, 2021, 39, 58-66.	2.5	31
5777	Iodine doped Z-scheme Bi2O2CO3/Bi2WO6 photocatalysts: Facile synthesis, efficient visible light photocatalysis, and photocatalytic mechanism. Chemical Engineering Journal, 2021, 403, 126327.	6.6	106
5778	Elemental mercury removal by Iâ^'-doped Bi2WO6 with remarkable visible-light-driven photocatalytic oxidation. Applied Catalysis B: Environmental, 2021, 282, 119534.	10.8	107
5779	Hunting the elusive shallow n-type donor â€“ An ab initio study of Li and N co-doped diamond. Carbon, 2021, 171, 857-868.	5.4	9
5780	Porous carbon-based MgAlF5Â·1.5H2O composites derived from carbon-coated clay presenting super high adsorption capacity for Congo Red. Chemical Engineering Journal, 2021, 406, 126784.	6.6	37
5781	Enhancing the degradation of carbamazepine by UVA-LED/WO3 process with peroxydisulfate: Effects of light wavelength and water matrix. Journal of Hazardous Materials, 2021, 404, 124126.	6.5	14
5782	Electronic structure of LiOsO3: Electron energy-loss spectroscopy and first-principles study. Solid State Communications, 2021, 323, 114099.	0.9	4
5783	Pyrite-activated persulfate for simultaneous 2,4-DCP oxidation and Cr(VI) reduction. Chemical Engineering Journal, 2021, 406, 126758.	6.6	123
5784	Negative area compressibility in silver oxalate. Journal of Materials Science, 2021, 56, 269-277.	1.7	11
5785	Evidence of low temperature phase transition in 2,6-dimethylpyrazine - picric acid cocrystal by means of temperature dependent investigations: X-ray, DSC and IR. Journal of Molecular Structure, 2021, 1228, 129432.	1.8	5
5786	Two-dimensional ZnI2 monolayer as a photocatalyst for water splitting and improvement its electronic and optical properties by strains. Physica E: Low-Dimensional Systems and Nanostructures, 2021, 126, 114487.	1.3	44
5787	Theoretical investigation of CoTa2O6/graphene heterojunctions for oxygen evolution reaction. Frontiers of Physics, 2021, 16, 1.	2.4	6
5788	Computational study of lattice dynamics and thermodynamic properties of energetic solid cyanuric triazide. Journal of Physics and Chemistry of Solids, 2021, 148, 109782.	1.9	5
5789	Improving the tribological properties of diamond-like carbon film applied under methane by tailoring sliding interface. International Journal of Refractory Metals and Hard Materials, 2021, 94, 105380.	1.7	8
5790	Structural, electronic and optical properties of lead-free antimony-copper based hybrid double perovskites for photovoltaics and optoelectronics by first principles calculations. Computational Materials Science, 2021, 186, 110009.	1.4	30

#	Article	IF	Citations
5791	Hydrophobic nano-layer on surface prevents H2O adsorption in moderately aluminum deficient Y zeolite crystals. Microporous and Mesoporous Materials, 2021, 310, 110621.	2.2	3
5792	Density functional characterization of Bi-based photocatalysts: BiTaO4, Bi4Ta2O11 and Bi7Ta3O18. Materials Science in Semiconductor Processing, 2021, 121, 105447.	1.9	33
5793	Insights into the physical properties of a new 211 MAX phase Nb2CuC. Journal of Physics and Chemistry of Solids, 2021, 149, 109759.	1.9	26
5794	Influence of the spin-orbit coupling effect on the electronic and thermoelectric properties of Cs2MI6 (M = Zr, Hf) variant perovskites. Materials Research Bulletin, 2021, 134, 111112.	2.7	11
5795	Effect of Transition Metal Impurities on the Adsorption of Flotation Reagents on Pyrite Surface. Mining, Metallurgy and Exploration, 2021, 38, 731-737.	0.4	0
5796	Thermodynamic modelling of magnetic laves phase in Feâ€“Ti system using first principle method. Intermetallics, 2021, 128, 106978.	1.8	5
5797	Highly active multivalent multielement catalysts derived from hierarchical porous TiNb2O7 nanospheres for the reversible hydrogen storage of MgH2. Nano Research, 2021, 14, 148-156.	5.8	68
5798	Selective methane sensing properties of VO2 at different temperatures: A first principles study. Applied Surface Science, 2021, 536, 147969.	3.1	20
5799	Interface engineering of Co3Fe7-Fe3C heterostructure as an efficient oxygen reduction reaction electrocatalyst for aluminum-air batteries. Chemical Engineering Journal, 2021, 404, 127124.	6.6	46
5800	Effect of the negative chemical pressure on physical properties of doped perovskite molybdates in the framework of DFT method. Journal of Alloys and Compounds, 2021, 854, 157088.	2.8	26
5801	Electric Fields and Interfacial Phaseâ€Change Memory Structures. Physica Status Solidi - Rapid Research Letters, 2021, 15, 2000412.	1.2	3
5802	Layer-dependent band gaps and dielectric constants of ultrathin fluorite crystals. Journal of Physics and Chemistry of Solids, 2021, 148, 109738.	1.9	8
5803	High capacity and mobility in germanium sulfide/graphene (GeS/Gr) van der Waals heterostructure as anode materials for sodiumâ€“ion batteries: A first-principles investigation. Applied Surface Science, 2021, 536, 147779.	3.1	15
5804	The role of Al and Co co-doping on the band gap tuning of TiO2 thin films for applications in photovoltaic and optoelectronic devices. Materials Science in Semiconductor Processing, 2021, 121, 105419.	1.9	27
5805	Elucidating the role of lattice thermal conductivity in<scp>Ï€â€phases</scp>of<scp>IVâ€VI</scp>monochalcogenides for highly efficient thermoelectric performance. International Journal of Energy Research, 2021, 45, 6369-6382.	2.2	6
5806	A selective and efficient precious metal-free electrocatalyst for chlorine evolution reaction: An experimental and computational study. Chemical Engineering Journal, 2021, 421, 127785.	6.6	18
5807	Construction of 3D porous CeO2 ceramic hosts with enhanced lithiophilicity for dendrite-free lithium metal anode. Journal of Power Sources, 2021, 484, 229253.	4.0	15
5808	Exploring the Optical, Structural and Electronic Properties of a Two-Dimensional GaSe/C2N van der Waals Heterostructure As a Photovoltaic Cell: A Computational Investigation. Journal of Electronic Materials, 2021, 50, 620-628.	1.0	5

#	Article	IF	Citations
5809	Structure of Ga-Sb-Se glasses by combination of 77Se NMR and neutron diffraction experiments with molecular dynamics. Journal of Non-Crystalline Solids, 2021, 557, 120574.	1.5	3
5810	K8Cd21Pb7(P2O7)16 and KCd2P3O10: Two new phosphates featuring special structure configurations. Journal of Solid State Chemistry, 2021, 294, 121834.	1.4	1
5811	Boosting carbonyl sulfide catalytic hydrolysis performance over N-doped Mg-Al oxide derived from MgAl-layered double hydroxide. Journal of Hazardous Materials, 2021, 407, 124546.	6.5	33
5812	Alkali metal adsorption on metal surfaces: new insights from new tools. Physical Chemistry Chemical Physics, 2021, 23, 7822-7829.	1.3	5
5813	A new nonlinear optical sulfate of layered structure: Cs2Zn2(SO4)3. Inorganic Chemistry Communication, 2021, 124, 108390.	1.8	13
5814	Reaction Mechanism and Structural Evolution of Fluorographite Cathodes in Solidâ€State K/Na/Li Batteries. Advanced Materials, 2021, 33, e2006118.	11.1	44
5815	The structural, mechanical and electronic properties of NbXSi (X=Fe, Co, Ni, Ru, Rh, Pd, Os, Ir and Pt) compounds from first-principles calculations. Materials Chemistry and Physics, 2021, 259, 124029.	2.0	11
5816	Atomically targeting NiFe LDH to create multivacancies for OER catalysis with a small organic anchor. Nano Energy, 2021, 81, 105606.	8.2	204
5817	Monolayer h-BN/C3B lateral heterostructures with promising electronic and optical properties: A first-principles study. Chemical Physics, 2021, 541, 111042.	0.9	2
5818	Interwoven scaffolded porous titanium oxide nanocubes/carbon nanotubes framework for high-performance sodium-ion battery. Journal of Energy Chemistry, 2021, 59, 38-46.	7.1	25
5819	Newly Synthesized Taâ€Based MAX Phase (Ta_{1â^'x}Hf_x)₄AlC₃ and (Ta_{1â^'x}Hf_x)₄Al_{0.5}Sn_{0.5}C₃ (0â€‰â‰€xâ€‰â‰€0.25) Solid Solutions: Unravelling the Mechanical, Electronic, and Thermodynamic Properties. Physica Status Solidi (B): Basic Research, 2021, 258, 2000307.	1.7	11
5820	Combination of solid-state NMR, molecular mechanics and DFT calculations for the molecular structure determination of methyl glycoside benzoates. Structural Chemistry, 2021, 32, 297-307.	1.0	0
5821	Adsorption of Mg2+ and K+ on the kaolinite (0 0 1) surface in aqueous system: A combined DFT and AIMD study with an experimental verification. Applied Surface Science, 2021, 538, 148158.	3.1	33
5822	Open versus Interpenetrated: Switchable Supramolecular Trajectories in Mechanosynthesis of a Halogen-Bonded Borromean Network. CheM, 2021, 7, 146-154.	5.8	17
5823	Mechanical, electronic and optical properties of K2TeX6 (X=Cl, Br, I) perovskite derivatives using density functional theory. Materials Science in Semiconductor Processing, 2021, 123, 105579.	1.9	6
5824	First-Principles study of structural, elastic and electronic properties for the KT-GaBP<mml:math xmlns:mml="http://www.w3.org/1998/Math/MathML" display="inline" id="d1e1334" altimg="si26.svg"><mml:msub><mml:mrow /><mml:mrow><mml:mn>2</mml:mn></mml:mrow></mml:msub></mml:math> semiconductor under pressure. Materials Science in Semiconductor Processing, 2021, 123, 105585.	1.9	0
5825	Structural stability, surface and photocatalytic properties of CdGeP2: A DFT study. Computational Materials Science, 2021, 187, 110099.	1.4	2
5826	Development and characterization of Alâ€“Al3Niâ€“Sn metal matrix composite. Materials Chemistry and Physics, 2021, 259, 124027.	2.0	15

#	Article	IF	Citations
5827	Bonding mechanism on TGDDM/CF and the influences of functional groups and interfacial water: An MD and DFT investigation. Applied Surface Science, 2021, 538, 148049.	3.1	3
5828	Role of TiC nanocrystalline and interface of TiC and amorphous carbon on corrosion mechanism of titanium doped diamond-like carbon films: Exploration by experimental and first principle calculation. Applied Surface Science, 2021, 542, 148740.	3.1	12
5829	Elastic3rd: A tool for calculating third-order elastic constants from first-principles calculations. Computer Physics Communications, 2021, 261, 107777.	3.0	22
5830	Electronic structure and optical properties in alkaline-earth metals (Aâ€‰=â€‰Mg, Ca, Ba) and Ir co-doped SrTiO3: A DFTâ€‰+â€‰U investigation. Optik, 2021, 228, 166128.	1.4	8
5831	A new lead-free SillÃ©nâ€“Aurivillius oxychloride Bi5SrTi3O14Cl with triple-perovskite layers for photocatalytic water splitting under visible light. Journal of Photochemistry and Photobiology A: Chemistry, 2021, 408, 113095.	2.0	8
5832	Effects of irradiation defects on the electronic structure and optical properties of LiI scintillator. Optical Materials, 2021, 112, 110727.	1.7	5
5833	Self-sacrificial templated formation of ZnO with decoration of catalysts for regulating CO and CH4 sensitive detection. Sensors and Actuators B: Chemical, 2021, 330, 129286.	4.0	16
5834	A novel vanadium-mediated MoS2 with metallic behavior for sodium ion batteries: Achieving fast Na+ diffusion to enhance electrochemical kinetics. Chemical Engineering Journal, 2021, 417, 128107.	6.6	27
5835	A predicted non-layered phase of In2Se3 by first principles. Solid State Communications, 2021, 325, 114159.	0.9	4
5836	Semiconducting properties of pyridyl appended linear dicarboxylate based coordination polymers: theoretical prediction via DFT study. Dalton Transactions, 2021, 50, 270-278.	1.6	8
5837	From AgGaS₂to AgHgPS₄: vacancy defects and highly distorted HgS₄tetrahedra double-induced remarkable second-harmonic generation response. Journal of Materials Chemistry C, 2021, 9, 1062-1068.	2.7	42
5838	From silicates to oxonitridosilicates: improving optical anisotropy for phase-matching as ultraviolet nonlinear optical materials. Chemical Communications, 2021, 57, 639-642.	2.2	32
5839	Elastic anisotropies and thermodynamic properties of metal dodecborides under high pressure. Journal of Chemical Thermodynamics, 2021, 154, 106346.	1.0	4
5840	The optical and elastic properties of strained ZnO by first principle calculations. Computational Condensed Matter, 2021, 26, e00525.	0.9	7
5841	Radical pair formation due to compression-induced electron transfer in crystals of energetic salts. Physical Chemistry Chemical Physics, 2021, 23, 1520-1526.	1.3	5
5842	Effect of substituted VIB transition metals on structural, electronic and magnetic properties of indium oxide: spin density functional calculations. Philosophical Magazine, 2021, 101, 468-478.	0.7	0
5843	Bi 2 O 2 Se:Bi 2 O 5 Se Highâ€K Stack as a 2D Analog of Si:SiO 2 : A Firstâ€Principles Study. Physica Status Solidi - Rapid Research Letters, 2021, 15, 2000465.	1.2	1
5844	A DFT study on pressure dependency of TiC and ZrC properties: Interconnecting elastic constants, thermodynamic, and mechanical properties. Ceramics International, 2021, 47, 9990-10005.	2.3	18

#	Article	IF	Citations
5845	The effects of fluorination and hydrogenation on the physical properties of two-dimensional (111)-oriented cubic boron nitride nanosheets. Thin Solid Films, 2021, 718, 138484.	0.8	2
5846	Nonlinear Optical Oxythiophosphate Approaching the Good Balance with Wide Ultraviolet Transparency, Strong Second Harmonic Effect, and Large Birefringence. Angewandte Chemie, 2021, 133, 6456-6460.	1.6	12
5847	Nonlinear Optical Oxythiophosphate Approaching the Good Balance with Wide Ultraviolet Transparency, Strong Second Harmonic Effect, and Large Birefringence. Angewandte Chemie - International Edition, 2021, 60, 6386-6390.	7.2	49
5848	Photoelectric properties of Sr2MgSi2O7: Eu2+ phosphors produced by co-precipitation method. Journal of Luminescence, 2021, 231, 117787.	1.5	13
5849	The electric memory properties of azo-chalcone derivatives based on different film forming processes. Journal of Molecular Structure, 2021, 1228, 129480.	1.8	2
5850	Chiral Switchable Low-Dimensional Perovskite Ferroelectrics. ACS Applied Materials & Interfaces, 2021, 13, 2044-2051.	4.0	66
5851	Acidity constant and DFT-based modelling of pH-responsive alendronate loading and releasing on propylamine-modified silica surface. Physical Chemistry Chemical Physics, 2021, 23, 2015-2024.	1.3	7
5852	Cr,Yb-codoped Ca₂LaHf₂Al₃O₁₂garnet phosphor: electronic structure, broadband NIR emission and energy transfer properties. Dalton Transactions, 2021, 50, 908-916.	1.6	38
5853	Nonlinear optical effects in two mercury cyanamide/guanidinium chlorides Hg3(NCN)2Cl2 and Hg2(C(NH2)3)Cl5. Journal of Materials Chemistry C, 2021, 9, 967-974.	2.7	3
5854	Characterization and luminescence sensing behaviour of a newly constructed hydrolytic stable Pb(II) coordination polymer. Inorganica Chimica Acta, 2021, 516, 120101.	1.2	3
5855	Titanium alloying enhancement of mechanical properties of NbTaMoW refractory high-Entropy alloy: First-principles and experiments perspective. Journal of Alloys and Compounds, 2021, 857, 157542.	2.8	24
5856	Three tetragonal superhard sp3 carbon allotropes. Solid State Communications, 2021, 323, 114095.	0.9	8
5857	Intriguing Dimensional Transition Inducing Variable Birefringence in K₂Na₂Sn₃S₈ and Rb₃NaSn₃Se₈. Inorganic Chemistry, 2021, 60, 1055-1061.	1.9	18
5858	A novel promising infrared nonlinear optical selenide KAg₃Ga₈Se₁₄ designed from benchmark AgGaQ₂ (Q =) Tj ETQq1 1 0.784314 rg	2.1	34
5859	A structural analysis of 2,5â€diarylâ€4 H â€2,4â€dihydroâ€3 H â€1,2,4â€triazolâ€3â€ones: NMR in the solid state, Xâ€ray crystallography, and GIPAW calculations. Magnetic Resonance in Chemistry, 2021, 59, 423-438.	1.1	4
5860	A novel approach to prepare Cu(I)Zn@MIL-100(Fe) adsorbent with high CO adsorption capacity, CO/CO2 selectivity and stability via controlled hostâ€“guest redox reaction. Chemical Engineering Journal, 2021, 404, 126492.	6.6	34
5861	Density functional theory study on a nitrogen-rich carbon nitride material C3N5 as photocatalyst for CO2 reduction to C1 and C2 products. Journal of Colloid and Interface Science, 2021, 585, 740-749.	5.0	51
5862	Phase transitions and elastic anisotropies of SiC polymorphs under high pressure. Ceramics International, 2021, 47, 6187-6200.	2.3	11

#	Article	IF	Citations
5863	New monomeric mixed-ligand complex of iron(III)-3-chloropyridine: Synthesis, structure, luminescence, electrochemical and magnetic properties. Journal of Molecular Structure, 2021, 1225, 129160.	1.8	4
5864	Negative thermal expansion in one-dimension of a new double sulfate AgHo(SO4)2 with isolated SO4 tetrahedra. Journal of Materials Science and Technology, 2021, 76, 111-121.	5.6	34
5865	The modulation of the TiAlSiN coating on the band gap of monolayer MoS₂. Surface Engineering, 2021, 37, 505-513.	1.1	0
5866	Investigation on composition-dependent properties of Mg5Al23â^'5O27+5N5â^'5 (0 â‰¤ x â‰¤ 1): Part I. optical properties via first-principles calculations. Journal of the European Ceramic Society, 2021, 41, 1543-1549.	2.8	4
5867	Electromagnetic wave absorbing properties of TMCs (TM=Ti, Zr, Hf, Nb and Ta) and high entropy (Ti0.2Zr0.2Hf0.2Nb0.2Ta0.2)C. Journal of Materials Science and Technology, 2021, 74, 105-118.	5.6	72
5868	Effects of Two Nearest V Substitution Doping on Magnetism of Monolayer CrSi2 via First-Principles Investigations. Journal of Superconductivity and Novel Magnetism, 2021, 34, 305-311.	0.8	2
5869	Modified g-C3N4/TiO2/CdS ternary heterojunction nanocomposite as highly visible light active photocatalyst originated from CdS as the electron source of TiO2 to accelerate Z-type heterojunction. Separation and Purification Technology, 2021, 257, 117976.	3.9	38
5870	Structural, mechanical and phonons properties of binary intermetallic compound BaSn3 under pressure. Solid State Communications, 2021, 323, 114110.	0.9	7
5871	Na3AMg7(PO4)6 (AÂ=ÂK, Rb and Cs): Structures, properties and theoretical studies of alkali metal magnesium orthophosphates. Journal of Molecular Structure, 2021, 1226, 129349.	1.8	9
5872	Structural, vibrational, mechanical, and optoelectronic properties of <scp>LiBH₄</scp> for hydrogen storage and optoelectronic devices: Firstâ€principles study. International Journal of Quantum Chemistry, 2021, 121, e26444.	1.0	8
5873	Energy profiles by DFT methods for CO and NO catalytic adsorption over ZnO surfaces. Catalysis Today, 2021, 360, 38-45.	2.2	16
5874	A comparison study of MnO₂ and Mn₂O₃ as zinc-ion battery cathodes: an experimental and computational investigation. RSC Advances, 2021, 11, 14408-14414.	1.7	12
5875	Code for nuclear materials. , 2021, , 483-494.		0
5876	Coexistence of metamagnetism and slow relaxation of magnetization in ammonium hexafluoridorhenate. RSC Advances, 2021, 11, 6353-6360.	1.7	6
5877	Anion-dependent structural variations and charge transport property analysis of 4â€²-(3-pyridyl)-4,2â€²:6â€²,4â€²â€²-terpyridinium salts. CrystEngComm, 2021, 23, 3569-3581.	1.3	5
5878	In situhydrothermal synthesis of polar second-order nonlinear optical selenate Na₅(SeO₄)(HSeO₄)₃(H₂O)₂. Inorganic Chemistry Frontiers, 2021, 8, 3141-3148.	3.0	11
5879	Carbon cluster formation and mobility degradation in 4H-SiC MOSFETs. Applied Physics Letters, 2021, 118, .	1.5	18
5880	Revisiting metal fluorides as lithium-ion battery cathodes. Nature Materials, 2021, 20, 841-850.	13.3	109

#	Article	IF	Citations
5881	Plasma-assisted defect engineering of N-doped NiCo₂O₄for efficient oxygen reduction. Physical Chemistry Chemical Physics, 2021, 23, 6591-6599.	1.3	22
5882	Structure and spectroscopy of methionyl-methionine for aquaculture. Scientific Reports, 2021, 11, 458.	1.6	2
5883	Computational techniques for characterisation of electrically conductive MOFs: quantum calculations and machine learning approaches. Journal of Materials Chemistry C, 2021, 9, 13584-13599.	2.7	14
5884	Pore control of Al-based MIL-53 isomorphs for the preferential capture of ethane in an ethane/ethylene mixture. Journal of Materials Chemistry A, 2021, 9, 14593-14600.	5.2	29
5885	Photothermal treatment of oropharyngeal cancer with carbon-defective silicon carbide. Journal of Materials Chemistry B, 2021, 9, 5284-5292.	2.9	3
5886	Insights into the physical properties and anisotropic nature of ErPdBi with an appearance of low minimum thermal conductivity. Chinese Physics B, 2021, 30, 016203.	0.7	16
5887	Unexpected aliovalent cation substitution between two NLO materials LiBa₃Bi₆(SeO₃)₇F₁₁and Ba₃Bi_{6.5}(SeO₃)₇F_{10.5}O_{0.5}. Chemical Communications, 2021, 57, 2982-2985.	2.2	11
5888	The crystal growth and properties of novel magnetic double molybdate RbFe₅(MoO₄)₇with mixed Fe³⁺/Fe²⁺states and 1D negative thermal expansion. CrystEngComm, 2021, 23, 3297-3307.	1.3	7
5889	Growth, crystal structure and theoretical studies of energy and optical properties of CdTe1â^'xSex thin films. Applied Nanoscience (Switzerland), 2022, 12, 335-342.	1.6	9
5890	First Principle Study on Mg2X (X = Si, Ge, Sn) Intermetallics by Bi Micro-Alloying. Crystals, 2021, 11, 142.	1.0	5
5891	Synergism of multiple functional chromophores significantly enhancing the birefringence in layered non-centrosymmetric chalcohalides. Inorganic Chemistry Frontiers, 2021, 8, 1588-1598.	3.0	12
5892	Taming the dynamics in a pharmaceutical by cocrystallization: investigating the impact of the coformer by solid-state NMR. CrystEngComm, 2021, 23, 6859-6870.	1.3	7
5893	Cubic, hexagonal and tetragonal FeGe_x phases (x = 1, 1.5, 2): Raman spectroscopy and magnetic properties. CrystEngComm, 2021, 23, 6506-6517.	1.3	1
5894	Cooperative B-site octahedral tilting, distortion and A-site conformational change induced phase transitions of a 2D lead halide perovskite. Materials Chemistry Frontiers, 2021, 5, 7587-7594.	3.2	10
5895	Room-Temperature NH₃ Sensors Based on Boron-Doped Graphene Oxide: Enhanced Sensing Performance by B-N Covalent Interaction. IEEE Nanotechnology Magazine, 2021, 20, 726-732.	1.1	6
5896	Modeling of plasmonic properties of nanostructures for next generation solar cells and beyond. Advances in Physics: X, 2021, 6, .	1.5	8
5897	Barium fluoroiodate crystals with a large band gap and birefringence. Inorganic Chemistry Frontiers, 2021, 8, 3127-3133.	3.0	16
5898	A newly-constructed hydrolytically stable Co(<scp>ii</scp>) coordination polymer showing dual responsive fluorescence sensing of pH and Cu²⁺. CrystEngComm, 2021, 23, 4370-4381.	1.3	24

#	Article	IF	Citations
5899	Calculation of the vibrational spectra of AgGaS₂ crystal with chalcopyrite structure. Journal of Physical Studies, 2021, 25, .	0.2	3
5900	First principles calculation of optical absorption and polarization properties of In doped <i>h</i>-LuFeO₃. Wuli Xuebao/Acta Physica Sinica, 2021, 70, 037101.	0.2	1
5901	Structureâ€“property correlations in piracetam polytypes. CrystEngComm, 2021, 23, 1226-1233.	1.3	6
5902	Mechanochemical reactivity inhibited, prohibited and reversed by liquid additives: examples from crystal-form screens. Chemical Science, 2021, 12, 3264-3269.	3.7	25
5904	Semiconductor to metallic transition under induced pressure in Cs₂AgBiBr₆ double halide perovskite: a theoretical DFT study for photovoltaic and optoelectronic applications. RSC Advances, 2021, 11, 24001-24012.	1.7	26
5905	Effect of doping of molybdenum on the optical properties of glasses of the Asâ€”S system. Physics of Complex Systems, 2021, 2, 115-121.	0.2	2
5906	First-Principles Study of Ag₃Sn, AgZn₃ and Ag₅Zn₈ Intermetallic Compounds. Key Engineering Materials, 0, 871, 254-263.	0.4	1
5907	The synthesis, characterization, and theoretical analysis of (NH4)3PbCl5. New Journal of Chemistry, 2021, 45, 2038-2043.	1.4	1
5908	Mononuclear copper(<scp>ii</scp>) Schiff base complex: synthesis, structure, electrical analysis and protein binding study. New Journal of Chemistry, 2021, 45, 2995-3006.	1.4	11
5909	Recent advances in NMR crystallography and polymorphism. Annual Reports on NMR Spectroscopy, 2021, 102, 1-80.	0.7	11
5910	Usage Scenarios for Byte-Addressable Persistent Memory in High-Performance and Data Intensive Computing. Journal of Computer Science and Technology, 2021, 36, 110-122.	0.9	2
5911	Computational insights into the formation driving force of CL-20 based solvates and their desolvation process. CrystEngComm, 2021, 23, 2150-2161.	1.3	7
5912	The high power conversion efficiency of a two-dimensional GeSe/AsP van der Waals heterostructure for solar energy cells. Physical Chemistry Chemical Physics, 2021, 23, 6042-6050.	1.3	22
5913	On the spectral features of dangling bonds in CH₄/H₂O amorphous ice mixtures. Physical Chemistry Chemical Physics, 2021, 23, 9532-9538.	1.3	6
5914	Structure-directing study of 1-methylimidazolium-based dication with tetramethylene as spacer length in the synthesis of microporous silicoaluminophosphates. New Journal of Chemistry, 2021, 45, 7185-7195.	1.4	1
5915	Design and host-involved in situ fabrication of La₄NiLiO₈ coating on Ni-rich cathode materials towards superior structural stability. Journal of Materials Chemistry A, 2021, 9, 3427-3440.	5.2	19
5916	Design and synthesis of Ba₃SiSe₅ with suitable birefringence modulated via M^{IV} atoms in the Baâ€“M^{IV}â€“Q (M^{IV} = Si, Ge; Q = S, Se) system. Dalton Transactions, 2021, 50, 11999-12005.	1.6	2
5917	B₃O₃ monolayer: an emerging 2D material for CO₂ capture. New Journal of Chemistry, 2021, 45, 15328-15335.	1.4	20

#	Article	IF	Citations
5918	Density functional theory predictions of the mechanical properties of crystalline materials. CrystEngComm, 2021, 23, 5697-5710.	1.3	41
5919	In situ illumination with inelastic neutron scattering: a study of the photochromic material cis-1,2-dicyano-1,2-bis(2,4,5-trimethyl-3-thienyl)ethene (CMTE). Physical Chemistry Chemical Physics, 2021, 23, 22324-22329.	1.3	2
5920	Electronic structure and elastic properties of Cd16Se15Te solid state solution: first principles study. Condensed Matter Physics, 2021, 24, 23702.	0.3	2
5921	Effects of AgTi3 intermetallic on suppression of Ag agglomeration: a theoretical study. Molecular Simulation, 2021, 47, 586-593.	0.9	3
5922	NaGaI₃O₉F: a new alkali metal gallium iodate combined with IO₃^{â˜’} and IO₃F^{2â˜’} units. Dalton Transactions, 2021, 50, 11562-11567.	1.6	13
5923	Exploring the optoelectronic and third-order nonlinear optical susceptibility of cross-shaped molecules: insights from molecule to material level. Journal of Molecular Modeling, 2021, 27, 12.	0.8	33
5924	The origins of charge separation in anisotropic facet photocatalysts investigated through first-principles calculations. RSC Advances, 2021, 11, 18500-18508.	1.7	5
5925	First chiral fluorinated lead vanadate selenite Pb₂(V₂O₄F)(VO₂)(SeO₃)₃with five asymmetric motifs and large optical properties. Dalton Transactions, 2021, 50, 7238-7245.	1.6	8
5926	Facile syntheses of silver thioantimonates exhibiting second-harmonic generation responses and large birefringence. Dalton Transactions, 2021, 50, 3568-3576.	1.6	7
5927	Interfacial properties of g-C3N4/TiO2 heterostructures studied by DFT calculations. Chinese Physics B, 2021, 30, 017101.	0.7	10
5928	Mechanistic insight into photocatalytic CO₂ reduction by a Z-scheme g-C₃N₄/TiO₂ heterostructure. New Journal of Chemistry, 2021, 45, 11474-11480.	1.4	16
5929	Elastically flexible molecular crystals. Chemical Society Reviews, 2021, 50, 11725-11740.	18.7	81
5930	Exploring the nature of the fergusoniteâ€“scheelite phase transition and ionic conductivity enhancement by Mo⁶⁺doping in LaNbO₄. Journal of Materials Chemistry A, 2021, 9, 4091-4102.	5.2	20
5931	Efficient electrochemical reduction of CO₂promoted by the electrospun Cu_{1.96}S/Cu tandem catalyst. Nanoscale, 2021, 13, 16986-16994.	2.8	8
5932	Stabilization of pentazolate anions in the high-pressure compounds Na₂N₅and NaN₅and in the sodium pentazolate framework NaN₅Â·N₂. Dalton Transactions, 2021, 50, 7229-7237.	1.6	20
5933	Electrocatalytic Site Activity Enhancement via Orbital Overlap in A₂MnRuO₇ (A = Dy³⁺, Ho³⁺, and Er³⁺) Pyrochlore Nanostructures. ACS Applied Energy Materials, 2021, 4, 176-185.	2.5	8
5934	K₂Pb(H₂C₃N₃O₃)₄(H₂O)₄: a potential UV nonlinear optical material with large birefringence. Inorganic Chemistry Frontiers, 2021, 8, 3547-3555.	3.0	27
5935	Theoretical study on the anisotropic photo-induced carrier mobilities in layered double hydroxide-based photocatalysts. Journal of Materials Chemistry A, 2021, 9, 20466-20482.	5.2	8

#	Article	IF	Citations
5936	RbPb8O4Cl9: the first alkali metal lead oxyhalide with distorted [PbO3Cl3] and [PbOCl5] mixed-anion groups. Dalton Transactions, 2021, 50, 14038-14043.	1.6	4
5937	SrTi(IO₃)₆Â·2H₂O and SrSn(IO₃)₆: distinct arrangements of lone pair electrons leading to large birefringences. RSC Advances, 2021, 11, 10309-10315.	1.7	5
5938	NaInX2 (Xâ€‰=â€‰S, Se) layered materials for energy harvesting applications: first-principles insights into optoelectronic and thermoelectric properties. Journal of Materials Science: Materials in Electronics, 2021, 32, 3878-3893.	1.1	9
5939	First-principles calculations on the deposition behavior of Li_xNa_y (x + y â‰¤ 5) clusters during the hybrid storage of Li and Na atoms on graphene. Physical Chemistry Chemical Physics, 2021, 23, 21817-21824.	1.3	2
5940	Amino acid-templated zinc phosphites: low-dimensional structures, fluorescence, and nonlinear optical properties. Dalton Transactions, 2021, 50, 5442-5445.	1.6	6
5941	Oxygen reduction reaction activity of an iron phthalocyanine/graphene oxide nanocomposite. RSC Advances, 2021, 11, 15927-15932.	1.7	10
5942	Dissecting the effects of water guest adsorption and framework breathing on the AlO₄(OH)₂ centres of metalâ€“organic framework MIL-53 (Al) by solid state NMR and structural analysis. Physical Chemistry Chemical Physics, 2021, 23, 18925-18929.	1.3	9
5943	Structural, Elastic and Electronic Properties of Nitride Ti₂CdN Phase in Comparison with the Carbide Ti₂CdC Phase from First-principles Study. Journal of Physics: Conference Series, 2021, 1718, 012019.	0.3	2
5944	The electronic and optical properties of SiO2â€“Alâ€“SiO2 withÂdensityÂfunctional theory. Modern Physics Letters B, 2021, 35, 2150136.	1.0	0
5945	Vacancy-mediated effects for simultaneously enhancing the Cu/graphene/Al interfacial bonding strength and thermal conductance: a first-principles study. Journal of Materials Science, 2021, 56, 5697-5707.	1.7	8
5946	Schottky barrier modification of GaSSe/graphene heterojunctions based on density functional theory. Journal Physics D: Applied Physics, 2021, 54, 155104.	1.3	6
5947	First-Principles study of structural stability and lithium storage property of Si_n clusters (n â‰¤ 6) adsorbed on graphene. Wuli Xuebao/Acta Physica Sinica, 2021, 70, 198101-198101.	0.2	1
5948	Ab initio molecular dynamics study of sodium NMR chemical shifts in the methylamine solution of [Na+ [2.2.2]cryptand Naâ^']. Physical Chemistry Chemical Physics, 2021, 23, 339-346.	1.3	4
5949	Molten Salt Synthesis of Nanolaminated Sc₂SnC MAX Phase. Wuji Cailiao Xuebao/Journal of Inorganic Materials, 2021, 36, 773.	0.6	15
5950	Iron-doping Enhanced Basic Nickel Carbonate for Moisture Resistance and Catalytic Performance of Ozone Decomposition. Wuji Cailiao Xuebao/Journal of Inorganic Materials, 2022, 37, 45.	0.6	1
5951	Potential Visible-Light Driven PtOâ„‚/GaN vdW Hetero-Bilayer Photocatalysts for Water Splitting Using First-Principles. IEEE Access, 2021, 9, 109510-109521.	2.6	10
5952	Relationship between Width and Height of Ï€* Peak in CK-XANES of Graphitic Carbons. Analytical Sciences, 2021, 37, 1617-1623.	0.8	3
5953	C2-Si: a novel silicon allotrope in the monoclinic phase. Chinese Journal of Chemical Physics, 0, , .	0.6	1

#	Article	IF	Citations
5954	On the structureâ€“property relationships of (Al, Ga, In)-doped spinel cobalt ferrite compounds: a combined experimental and DFT study. Physical Chemistry Chemical Physics, 2021, 23, 18112-18124.	1.3	6
5955	Co-crystal AXÂ·(H₃C₃N₃O₃) (A = Na, Rb, Cs; X = Br, I): a series of strongly anisotropic alkali halide cyanurates with a planar structural motif and large birefringence. Dalton Transactions, 2021, 50, 11555-11561.	1.6	7
5956	Halogen Bonding in Bicomponent Monolayers: Self-Assembly of a Homologous Series of Iodinated Perfluoroalkanes with Bipyridine. Langmuir, 2021, 37, 627-635.	1.6	3
5957	Megahertz dynamics in skyrmion systems probed with muon-spin relaxation. Physical Review B, 2021, 103, .	1.1	9
5958	Study of Ag precipitation and mechanical properties of Tiâ€“Taâ€“Ag ternary alloy. RSC Advances, 2021, 11, 2976-2984.	1.7	7
5959	Pressure-induced superconducting CS₂H₁₀ with an H₃S framework. Physical Chemistry Chemical Physics, 2021, 23, 22779-22784.	1.3	16
5960	Thermal Dehydrofluorination of GaPO-34 Revealed by NMR Crystallography. Journal of Physical Chemistry C, 2021, 125, 2537-2545.	1.5	5
5961	The uptake mechanism of palladium ions into Prussian-blue nanoparticles in a nitric acid solution toward application for the recycling of precious metals from electronic and nuclear wastes. RSC Advances, 2021, 11, 20701-20707.	1.7	4
5962	Negative linear compressibility in nanoporous metalâ€“organic frameworks rationalized by the empty channel structural mechanism. Physical Chemistry Chemical Physics, 2021, 23, 8508-8524.	1.3	9
5963	Metallic two-dimensional BP₂: a high-performance electrode material for Li- and Na-ion batteries. Physical Chemistry Chemical Physics, 2021, 23, 4386-4393.	1.3	13
5964	Formation of Lightweight Ternary Polyhydrides and Their Hydrogen Storage Mechanism. Journal of Physical Chemistry C, 2021, 125, 1723-1730.	1.5	19
5965	Zn(H2C3N3O3)2Â·3H2O: the first single-d10 transition metal based ultraviolet hydroisocyanurate crystal with large birefringence. Dalton Transactions, 2021, 50, 5617-5623.	1.6	6
5966	Operando Leaching of Pre-Incorporated Al and Mechanism in Transition Metal Hybrids for Elaborately Enhanced Charge Storage. SSRN Electronic Journal, 0, , .	0.4	0
5967	BaTi(BO₃)₂: an excellent birefringent material with highly coplanar isolated [BO₃] groups. New Journal of Chemistry, 2021, 45, 7065-7068.	1.4	7
5968	Na₂GaS₂Cl: a new sodium-rich chalcohalide with two-dimensional [GaS₂]_{âˆž} layers and wide interlayer space. Dalton Transactions, 2021, 50, 11167-11172.	1.6	12
5969	Flotation Behavior and Synergistic Mechanism of Benzohydroxamic Acid and Sodium Butyl-Xanthate as Combined Collectors for Malachite Beneficiation. Minerals (Basel, Switzerland), 2021, 11, 59.	0.8	6
5970	Shielded goethite catalyst that enables fast water dissociation in bipolar membranes. Nature Communications, 2021, 12, 9.	5.8	49
5971	A novel greenâ€emitting SrLaAlO4:Er3+ phosphor synthesized by coâ€precipitation method for w-LEDs and optical thermometry. Journal of Materials Science: Materials in Electronics, 2021, 32, 4228-4238.	1.1	4

#	Article	IF	Citations
5972	Synthesis, crystal structure and theoretical calculations of two rare-earth borates with DUV cut-off edges. New Journal of Chemistry, 2021, 45, 4823-4827.	1.4	3
5973	Heterovalent cations substitution to design asymmetric chalcogenides with promising nonlinear optical performances. Journal of Materials Chemistry C, 2021, 9, 8659-8665.	2.7	25
5974	Tunable band gaps and high carrier mobilities in stanene by small organic molecule adsorption under external electric fields. Physical Chemistry Chemical Physics, 2021, 23, 16023-16032.	1.3	5
5975	Energy storage mechanisms in vacancy-ordered Wadsleyâ€“Roth layered niobates. Journal of Materials Chemistry A, 2021, 9, 20006-20023.	5.2	12
5976	BaZnBe₂(BO₃)₂F₂: a novel zinc-beryllium borate with SBBO-type structure overcoming the polymorphism problem. Dalton Transactions, 2021, 50, 2138-2142.	1.6	8
5977	Daylight-White-Emitting and Abnormal Thermal Antiquenching Phosphors Based on a Layered Host SrIn₂(P₂O₇)₂. Inorganic Chemistry, 2021, 60, 2279-2293.	1.9	30
5978	First principles methods for solar energy harvesting materials. , 2021, , 101-128.		0
5979	Electronic band structure of cubic solid-state CdTe_{1ï¿½x}Se_x solutions. Ukrainian Journal of Physical Optics, 2021, 22, 101-109.	9.7	5
5980	CaCo_{0.05}Mn_{0.95}O_{3â^Î´}: A Promising Perovskite Solid Solution for Solar Thermochemical Energy Storage. ACS Applied Materials & Interfaces, 2021, 13, 3856-3866.	4.0	34
5981	Synthesis, characterization and theoretical investigation of a new chalcohalide, Ba₄GaS₄F₃. Dalton Transactions, 2021, 50, 6315-6320.	1.6	9
5982	Newly synthesized MAX phase Zr₂SeC: DFT insights into physical properties towards possible applications. RSC Advances, 2021, 11, 16892-16905.	1.7	25
5983	Templateâ€Free Selfâ€Caging Nanochemistry for Largeâ€Scale Synthesis of Sulfonatedâ€Graphene@Sulfur Nanocage for Longâ€Life Lithiumâ€Sulfur Batteries. Advanced Functional Materials, 2021, 31, 2008652.	7.8	37
5984	Order-disorder type of Peierls instability in <mml:math xmlns:mml="http://www.w3.org/1998/Math/MathML"><mml:msub><mml:mi>BaVS</mml:mi><mml:mn>3</mml:mn></mml:msub></mml:math> Physical Review B, 2021, 103, .	1.1	6
5985	Halogenated Ti₃C₂ MXenes with Electrochemically Active Terminals for High-Performance Zinc Ion Batteries. ACS Nano, 2021, 15, 1077-1085.	7.3	183
5986	Supertetrahedral polyanionic network in the first lithium phosphidoindate Li₃InP₂ â€“ structural similarity to Li₂SiP₂ and Li₂GeP₂ and dissimilarity to Li₃AlP₂ and Li₃GaP₂. Chemical Science, 2021, 12, 1278-1285.	3.7	8
5987	Three-dimensional metallic carbon allotropes with superhardness. Nanotechnology Reviews, 2021, 10, 1266-1276.	2.6	24
5988	High-pressure phase transition of AB3-type compounds: case of tellurium trioxide. RSC Advances, 2021, 11, 14316-14322.	1.7	0
5989	A new acentric borateâ€“nitrate Cs₃B₈O₁₃(NO₃) with interpenetrating porous 3D covalent and ionic lattices. Dalton Transactions, 2021, 50, 8676-8679.	1.6	4

#	Article	IF	Citations
5990	Pb₂TiFO(SeO₃)₂Br: a new polar compound with the strongest second harmonic generation in the selenite bromide family. Journal of Materials Chemistry C, 2021, 9, 6491-6497.	2.7	19
5991	Phase transition and chemical reactivity of 1H-tetrazole under high pressure up to 100 GPa. Physical Chemistry Chemical Physics, 2021, 23, 19503-19510.	1.3	3
5992	Synthesis, band structure and photocatalytic properties of SillÃ©nâ€“Aurivillius oxychlorides BaBi₅Ti₃O₁₄Cl, Ba₂Bi₅Ti₄O₁₇Cl and Ba₃Bi₅Ti₅O₂₀Cl with triple-, quadruple- and quintuple-perovskite layers. Journal of Materials Chemistry A, 2021, 9, 8332-8340.	5.2	22
5993	Terahertz Spectroscopy and Molecular Modeling of Barbituric Acid. Journal of Applied Spectroscopy, 2021, 87, 1000-1005.	0.3	1
5994	Synthesis, Electronic Structure, and Physical Properties of Layered Oxypnictides Sr₂ScCrAsO₃ and Ba₃Sc₂Cr₂As₂O₅. Inorganic Chemistry, 2021, 60, 1930-1936.	1.9	3
5995	A Theoretical Investigation on the Physical Properties of SrPd2Sb2 Superconductor. Journal of Superconductivity and Novel Magnetism, 2021, 34, 1133-1139.	0.8	16
5996	The electronic properties and structural stability of LaFeO3 oxide by niobium doping: A density functional theory study. International Journal of Hydrogen Energy, 2021, 46, 9193-9198.	3.8	10
5997	High-Temperature Magic-Angle Spin Nuclear Magnetic Resonance Reveals Sodium Ion-Doped Crystal-Phase Formation in FLiNaK Eutectic Salt Solidification. Journal of Physical Chemistry C, 2021, 125, 4704-4709.	1.5	4
5998	Effect of Crystal Orientation on Seebeck Coefficient and Electrical Conductivity of SrTiO3 Single Crystals. Crystal Growth and Design, 2021, 21, 1791-1799.	1.4	3
5999	Effects of Al substitution by Si in Ti3AlC2 nanolaminate. Scientific Reports, 2021, 11, 3410.	1.6	27
6000	Pressure dependence of structural, elastic, electronic, thermodynamic, and optical properties of van der Waals-type NaSn2P2 pnictide superconductor: Insights from DFT study. Results in Physics, 2021, 21, 103848.	2.0	48
6001	A Study on the Anti-thermal Dy³⁺/Eu³⁺ Co-doped BaLa₄Si₃O₁₃ Red Phosphors for White-Light-Emitting Diodes and Optical Thermometry Applications. Industrial & Engineering Chemistry Research, 2021, 60, 2931-2943.	1.8	21
6002	First Principles Study on Electronic and Optical Properties of Single Walled Carbon Nanotube for Photonics Application. IOP Conference Series: Materials Science and Engineering, 2021, 1051, 012089.	0.3	4
6003	A DFT based first-principles investigation of optoelectronic and structural properties of Bi₂Te₂Se. Physica Scripta, 2021, 96, 045810.	1.2	18
6004	Optoelectronic and solar cell applications of ZnO nanostructures. Results in Surfaces and Interfaces, 2021, 2, 100003.	1.0	15
6005	Studies of electrical and optical properties of cadmiumâ€doped zinc oxide for energy conversion devices. Fuel Cells, 2021, 21, 164-171.	1.5	3
6006	The nuts and bolts of core-hole constrained ab initio simulation for K-shell x-ray photoemission and absorption spectra. Journal of Physics Condensed Matter, 2021, 33, 154005.	0.7	20
6007	Halonitrides Zn₂NX (X=Cl,Br): Novel Mid-Infrared Nonlinear Optical Materials. Chemistry of Materials, 2021, 33, 1462-1470.	3.2	19

#	Article	IF	Citations
6008	Magnetic order and ballistic spin transport in a sine-Gordon spin chain. Physical Review B, 2021, 103, .	1.1	6
6009	First principles study of electronic, elastic, optical and magnetic properties of Rh 2 MnX (X = Ti, Hf, Sc,) Tj ETQq1 1 0.784314 rgBT /Ov	1.0	14
6010	Virtual Cocrystal Screening Methods as Tools to Understand the Formation of Pharmaceutical Cocrystalsâ€"A Case Study of Linezolid, a Wide-Range Antibacterial Drug. Crystal Growth and Design, 2021, 21, 2301-2314.	1.4	34
6011	Elastic stiffness coefficients of thiourea from thermal diffuse scattering. Journal of Applied Crystallography, 2021, 54, 287-294.	1.9	3
6012	Electronic and adsorption properties of the zigzagâ€edged triangle graphene nanosheets. International Journal of Quantum Chemistry, 2021, 121, e26607.	1.0	4
6013	Lithium enhancing electronic transport properties of monolayer 6,6,12-graphyne from first principles. Surfaces and Interfaces, 2021, 22, 100903.	1.5	2
6014	Observation of Dihydrogen Bonds in High-Pressure Phases of Ammonia Borane by X-ray and Neutron Diffraction Measurements. Inorganic Chemistry, 2021, 60, 3065-3073.	1.9	11
6015	First principles study of atmospheric pollutants adsorption on non-defect and monatomic defect graphene. Diamond and Related Materials, 2021, 112, 108252.	1.8	8
6016	Comprehensive study on the physical properties of tetragonal LaTGe3 (T = Rh, Ir, or Pd) compounds: An ab initio investigation. AIP Advances, 2021, 11, .	0.6	11
6017	Structural and electronic properties of the metal clusterâ€based compounds including high concentration of solvent molecules. Zeitschrift Fur Anorganische Und Allgemeine Chemie, 2021, 647, 751-758.	0.6	3
6018	Bi₂S₃ Nanowires: First-Principles Phonon Dynamics and Their Photocatalytic Environmental Remediation. Journal of Physical Chemistry C, 2021, 125, 4086-4091.	1.5	12
6019	Design of a Class of New sp ² â€" sp ³ Carbons Constructed by Graphite and Diamond Building Blocks. Chinese Physics Letters, 2021, 38, 028102.	1.3	15
6020	[C(NH2)3]3PO4Â·2H2O: A new metal-free ultraviolet nonlinear optical phosphate with large birefringence and second-harmonic generation response. Science China Materials, 2021, 64, 2008-2016.	3.5	28
6021	Effect of noble metal atoms on adsorption and electronic properties of graphene toward toxic gas. Computational and Theoretical Chemistry, 2021, 1196, 113115.	1.1	18
6022	Effects of Vacancy and Hydrogen on the Growth and Morphology of N-Type Phosphorus-Doped Diamond Surfaces. Applied Sciences (Switzerland), 2021, 11, 1896.	1.3	2
6023	Synthesis, structural and photoluminescence properties of novel red emitting Ba5(B2O5)2F2:xEu3+phosphors. Journal of Materials Science: Materials in Electronics, 2021, 32, 6379-6388.	1.1	1
6025	Random Structure Searching with Orbital-Free Density Functional Theory. Journal of Physical Chemistry A, 2021, 125, 1650-1660.	1.1	8
6026	Combined Experimental and DFT-TDDFT Characterization Studies of Crystalline Mesoporous-Assembled [ZrO2]NPs and [DPPPâ€‰+â€‰Gly/ZrO2]C Nanocomposite Thin Film. Electronic Materials Letters, 2021, 17, 188-206.	1.0	14

#	Article	IF	Citations
6027	Redox-active nanostructure electrode of Mn/Ni bimetal organic frameworks anchoring on multi-walled carbon nanotubes for advanced supercapacitor. Journal of Electroanalytical Chemistry, 2021, 882, 114993.	1.9	42
6028	Influences of Vacancy Concentration and Al Substitution on Structural, Electronic, and Elastic Properties of Nb₅Si₃ from Firstâ€Principles Calculations. Physica Status Solidi (B): Basic Research, 2021, 258, 2000591.	0.7	1
6029	The structural characteristics and electrical of MoS₂ and MoS₂/graphene: a first-principles study. IOP Conference Series: Earth and Environmental Science, 2021, 675, 012198.	0.2	2
6030	Predicting the impact sensitivities of energetic materials through zone-center phonon up-pumping. Journal of Chemical Physics, 2021, 154, 064105.	1.2	33
6031	Structural, elastic and mechanical properties of Tiâ€“15Nbâ€“xGe alloys: insight from DFT calculations. Bulletin of Materials Science, 2021, 44, 1.	0.8	6
6032	First principle studies on the structures, electronic propertiesÂandÂRaman spectrums of monolayer WX₂ (X = S, Se, Te) under strain condition. Modern Physics Letters B, 2021, 35, 2150135.	1.0	3
6033	Adsorption behaviors and crystal structure of AlN films on TiN (001) surfaces by first-principles study. Superlattices and Microstructures, 2021, 150, 106804.	1.4	1
6034	Exploring cation disorder in mixedâ€metal pyrochlore ceramics using ¹⁷O NMR spectroscopy and firstâ€principles calculations. Magnetic Resonance in Chemistry, 2021, 59, 961-974.	1.1	0
6035	First principles study of structural, elastic, mechanical and electronic properties of nitrogen-doped cubic diamond. Bulletin of Materials Science, 2021, 44, 1.	0.8	29
6036	Toward Large-Capacity and High-Stability Lithium Storages via Constructing Quinoneâ€“2D-MnO₂-Pillared Structures. Journal of Physical Chemistry C, 2021, 125, 3725-3732.	1.5	23
6037	Investigation on the Stability, Elastic Properties, and Electronic Structure of Mg₂Si Doped with Different Concentrations of Cu: A Firstâ€Principles Calculation. Physica Status Solidi (B): Basic Research, 2021, 258, 2000597.	0.7	7
6038	Boron coordination and B/Si ordering controls over equilibrium boron isotope fractionation among minerals, melts, and fluids. Chemical Geology, 2021, 561, 120030.	1.4	18
6039	A Series of Pentanary Salt-Inclusion Chalcogenoborates Containing a B₁₂Q₁₂ (Q = S, Se) Cluster Exhibiting a Kleinman-Forbidden Frequency-Doubling Effect. Inorganic Chemistry, 2021, 60, 3375-3383.	1.9	18
6040	The First Positive Uniaxial Cyanurate Crystals Containing a Crown-like Anionic Group Arrangement and Strengthened Optical Anisotropy. Crystal Growth and Design, 2021, 21, 2348-2354.	1.4	7
6041	Regulating Guanidinium-Based Hybrid Materials for Ultraviolet Nonlinear Optical Applications by Hybrid Strength and Hybrid Pattern. Inorganic Chemistry, 2021, 60, 3834-3842.	1.9	16
6042	Superhard B28N32 with three-dimensional metallicity: First-principles prediction. Computational Materials Science, 2021, 188, 110121.	1.4	1
6043	Insight into MoS₂â€“MoN Heterostructure to Accelerate Polysulfide Conversion toward Highâ€Energyâ€Density Lithiumâ€Sulfur Batteries. Advanced Energy Materials, 2021, 11, 2003314.	10.2	159
6044	Accelerating the development of new solar absorbers by photoemission characterization coupled with density functional theory. JPhys Energy, 2021, 3, 032001.	2.3	2

#	Article	IF	Citations
6045	Quantum Solvers for Plane-Wave Hamiltonians: Abridging Virtual Spaces Through the Optimization of Pairwise Correlations. Frontiers in Chemistry, 2021, 9, 603019.	1.8	10
6046	Population analysis with Wannier orbitals. Journal of Chemical Physics, 2021, 154, 104111.	1.2	3
6047	Recoverability of N₄^{xâ€“}Anions to Ambient Pressure: A First-Principles Study ofcyclo- andsyn-Tetranitrogen Units. Journal of Physical Chemistry C, 2021, 125, 7368-7377.	1.5	8
6048	Effect of Y-doped NbB_{2.5} on structural and superconducting properties. Physica Scripta, 2021, 96, 065805.	1.2	1
6049	Study on mechanical, electronic and optical properties of Pb-free double halide perovskites In2TiX6 (X) Tj ETQq0 0 0 rgBT /Overlock 10 T	0.9	3
6050	Temperature-Dependent Low-Frequency Vibrations of Thiamine Crystal Containing Hydrated Ions. Journal of Physical Chemistry A, 2021, 125, 1837-1844.	1.1	5
6051	Structure Determination of Multicomponent Crystalline Phases of (S)-Ibuprofen and l-Proline from Powder X-ray Diffraction Data, Augmented by Complementary Experimental and Computational Techniques. Crystal Growth and Design, 2021, 21, 2498-2507.	1.4	8
6052	Sodium Site Exchange and Migration in a Polar Stuffed-Cristobalite Framework Structure. Inorganic Chemistry, 2021, 60, 4322-4331.	1.9	2
6053	DFT investigation on highly selective NO2 sensing properties of MnPS3. Applied Surface Science, 2021, 543, 148846.	3.1	15
6054	Na₆MQ₄ (M=Zn, Cd; Q=S, Se): Promising New Ternary Infrared Nonlinear Optical Materials. Chemistry - A European Journal, 2021, 27, 6538-6544.	1.7	16
6055	An ab-initio study on structural, elastic, electronic, bonding, thermal, and optical properties of topological Weyl semimetal TaX (Xâ€‰=â€‰P, As). Scientific Reports, 2021, 11, 5592.	1.6	84
6056	Variation in electronic and optical responses due to phase transformation of SrZrO3 from cubic to orthorhombic under high pressure: a computational insight. Indian Journal of Physics, 2022, 96, 1-9.	0.9	10
6057	Detailed structural, mechanical, and electronic study of five structures for CaF2 under high pressure*. Chinese Physics B, 2021, 30, 030502.	0.7	2
6058	Effects of surface spatial structures and electronic properties of chalcopyrite and pyrite on Z-200 selectivity. Minerals Engineering, 2021, 163, 106803.	1.8	28
6059	Effects of Fe doping on the visible light absorption and bandgap tuning of lead-free (CsSnCl3) and lead halide (CsPbCl3) perovskites for optoelectronic applications. AIP Advances, 2021, 11, .	0.6	20
6060	A First-Principles Investigation on the Electronic and Mechanical Properties of 1T TiSe₂ Multilayers for Energy Storage. Journal of the Electrochemical Society, 2021, 168, 030531.	1.3	9
6061	Exploring the Size Effect of Pt Nanoparticles on the Photocatalytic Nonoxidative Coupling of Methane. ACS Catalysis, 2021, 11, 3352-3360.	5.5	66
6062	LaSiP₃ and LaSi₂P₆: Two Excellent Rareâ€Earth Pnictides with Strong SHG Responses as Midâ€and Farâ€Infrared Nonlinear Optical Crystals. Advanced Optical Materials, 2021, 9, 2002176.	3.6	9

#	Article	IF	Citations
6063	Structural modelling and mechanical behaviors of graphene/carbon nanotubes reinforced metal matrix composites via atomic-scale simulations: A review. Composites Part C: Open Access, 2021, 4, 100120.	1.5	11
6064	Ultra-Low Friction of Graphene/Honeycomb Borophene Heterojunction. Tribology Letters, 2021, 69, 1.	1.2	10
6065	Evaporation behavior of SiO₂ glass doped with various transition metal oxides. Journal of the American Ceramic Society, 2021, 104, 3130-3138.	1.9	21
6066	Understanding contact electrification at liquidâ€“solid interfaces from surface electronic structure. Nature Communications, 2021, 12, 1752.	5.8	56
6067	Theoretical study on compositionâ€dependent properties of ZnOÂ· n Al 2 O 3 spinels. Part I: Optical and dielectric. Journal of the American Ceramic Society, 2021, 104, 5099-5109.	1.9	5
6068	Unusual hydrogen implanted gold with lattice contraction at increased hydrogen content. Nature Communications, 2021, 12, 1560.	5.8	2
6069	New Salts and Cocrystals of Pymetrozine with Improvements on Solubility and Humidity Stability: Experimental and Theoretical Study. Crystal Growth and Design, 2021, 21, 2371-2388.	1.4	33
6070	Selfâ€Recoverable Mechanically Induced Instant Luminescence from Cr³⁺â€Doped LiGa₅O₈. Advanced Functional Materials, 2021, 31, 2010685.	7.8	84
6071	Physical properties of new MAX phase borides M2SB (M = Zr, Hf and Nb) in comparison with conventional MAX phase carbides M2SC (M = Zr, Hf and Nb): Comprehensive insights. Journal of Materials Research and Technology, 2021, 11, 1000-1018.	2.6	70
6072	Structures of bulk hexagonal post transition metal chalcogenides from dispersion-corrected density functional theory. Physical Review B, 2021, 103, .	1.1	6
6073	Current State-of-the-art In-house and Cloud-Based Applications of Virtual Polymorph Screening of Pharmaceutical Compounds: A Challenging Case ofAZD1305. Crystal Growth and Design, 2021, 21, 1972-1983.	1.4	17
6074	First-principles study on the geometric, electronic and thermodynamic properties of the CsPbI3 (001) surfaces. IOP Conference Series: Earth and Environmental Science, 2021, 692, 022020.	0.2	2
6075	Probing the tribological performances of hydrogenated amorphous carbon film in methane atmosphere based on Hertzian elastic contact model. Tribology International, 2021, 155, 106790.	3.0	10
6076	Advances in modelling electron energy loss spectra from first principles. JPhys Materials, 2021, 4, 024008.	1.8	1
6077	Ultra-incompressible High-Entropy Diborides. Journal of Physical Chemistry Letters, 2021, 12, 3106-3113.	2.1	17
6078	Investigating the Priorities of Youth for the Selection of Media for News Consumption. Global Mass Communication Review, 2021, VI, 161-171.	0.0	1
6079	2Dâ€HARECXS analysis of dopant and oxygen vacancy sites in Alâ€doped yttrium titanate. Journal of the American Ceramic Society, 2021, 104, 3760-3769.	1.9	3
6080	Atomic and electronic structure of two-dimensional Mo_{(1â^'} _x)W _x S₂ alloys. JPhys Materials, 2021, 4, 025004.	1.8	7

#	Article	IF	Citations
6081	Ï€-Conjugated Trigonal Planar [C(NH₂)₃]⁺ Cationic Group: A Superior Functional Unit for Ultraviolet Nonlinear Optical Materials. ACS Omega, 2021, 6, 9263-9268.	1.6	22
6082	Adsorption of Ca(II) and K(I) on the kaolinite surface: a DFT study with an experimental verification. Molecular Physics, 2021, 119, e1896047.	0.8	5
6083	Introduction of Li into Ag-Based Noncentrosymmetric Sulfides for High-Performance Infrared Nonlinear Optical Materials. Inorganic Chemistry, 2021, 60, 5198-5205.	1.9	26
6084	Localized Electron Density Engineering for Stabilized B-Î³ CsSnI₃-Based Perovskite Solar Cells with Efficiencies >10%. ACS Energy Letters, 0, , 1480-1489.	8.8	125
6085	A new activity model for Feâ€“Mgâ€“Al biotites: Iâ€”Derivation and calibration of mixing parameters. Contributions To Mineralogy and Petrology, 2021, 176, 1.	1.2	0
6086	Buckling of boron nanotubes under axial compression: Insights from molecular mechanics and continuum mechanics. Physica E: Low-Dimensional Systems and Nanostructures, 2021, 127, 114520.	1.3	3
6087	High-energy ball-milling preparation and characterization of Ln2O3â^'graphite nanocomposites. Materials Today Communications, 2021, 26, 102030.	0.9	7
6088	Flotation separation of molybdenite from chalcopyrite using rhodanine-3-acetic acid as a novel and effective depressant. Minerals Engineering, 2021, 162, 106747.	1.8	40
6089	Significant Reduction in Thermal Conductivity and Improved Thermopower of Electronâ€Doped Ba 1â€“ x La x TiO 3 with Nanostructured Rectangular Pores. Advanced Electronic Materials, 2021, 7, 2001044.	2.6	1
6090	DFT study on the controllable electronic and optical properties of GaSb/InAs heterostructure. Journal of Materials Research, 0, , 1.	1.2	2
6091	2-aminooxazole in Astrophysical Environments: IR Spectra and Destruction Cross Sections for Energetic Processing. Astrophysical Journal, 2021, 909, 123.	1.6	6
6092	FeMoO4 Revisited: Crosslike 90Â° Noncollinear Antiferromagnetic Structure Caused by Dzyaloshinskiiâ€“Moriya Interaction. Journal of Physical Chemistry C, 2021, 125, 5947-5956.	1.5	4
6093	Nano-GeTe Embedded in a Three-Dimensional Carbon Sponge for Flexible Li-Ion and Na-Ion Battery Anodes. ACS Applied Materials & Interfaces, 2021, 13, 15178-15189.	4.0	11
6094	Enhanced electrocatalytic activity of urchin-like Nb2O5 microspheres by synergistic effects with Pd toward electrooxidation of ethylene glycol in an alkaline medium. Molecular Catalysis, 2021, 504, 111436.	1.0	2
6095	An ab initio study of structural, elastic and electronic properties of hexagonal MAuGe (M = Lu, Sc) compounds. Condensed Matter Physics, 2021, 24, 13706.	0.3	3
6096	Synthesis of the scandium chloride hydrates ScCl₃Â·3H₂O and Sc₂Cl₄(OH)₂Â·12H₂O and their characterisation by X-ray diffraction, ⁴⁵Sc NMR spectroscopy and DFT calculations. Zeitschrift Fur Naturforschung - Section B Journal of Chemical Sciences, 2021, 76, 217-225.	0.3	3
6097	Charged surfaces and slabs in periodic boundary conditions. Electronic Structure, 2021, 3, 015002.	1.0	8
6098	Raman and theoretical studies on structural evolution of Li2BeF4 and binary LiF-BeF2 melts. Journal of Molecular Liquids, 2021, 325, 115208.	2.3	7

#	Article	IF	Citations
6099	2D constraint modifies packing behaviour: a halobenzene monolayer with X3 halogen-bonding motif. Molecular Physics, 2021, 119, e1900940.	0.8	2
6100	TiO2 as a Photocatalyst for Water Splittingâ€"An Experimental and Theoretical Review. Molecules, 2021, 26, 1687.	1.7	114
6101	Polymorphism of dimethylaminoborane N(CH₃)₂-BH₂. Acta Crystallographica Section B: Structural Science, Crystal Engineering and Materials, 2021, 77, 299-306.	0.5	1
6102	Typeâ€Ⅱ C 2 N/ZnTe Van Der Waals Heterostructure: A Promising Photocatalyst for Water Splitting. Advanced Materials Interfaces, 2021, 8, 2002068.	1.9	17
6103	Polytypism in semi-disordered lizardite and amesite by low-dose HAADF-STEM. American Mineralogist, 2022, 107, 221-232.	0.9	1
6104	Exfoliation of Quasi-Two-Dimensional Nanosheets of Metal Diborides. Journal of Physical Chemistry C, 2021, 125, 6787-6799.	1.5	32
6105	Tracing the main elements and electron orbitals that induce superconducting phase transition. Europhysics Letters, 2021, 133, 67004.	0.7	0
6106	Insights into the physical properties of inverse-Heusler alloy Cr₂CoGa via density functional theory. Physica Scripta, 2021, 96, 055704.	1.2	8
6107	From NWChem to NWChemEx: Evolving with the Computational Chemistry Landscape. Chemical Reviews, 2021, 121, 4962-4998.	23.0	39
6108	Comparative study of single-atom gold and iridium on CeO2{111}. Journal of Chemical Physics, 2021, 154, 164703.	1.2	2
6109	Rules of formation of Hâ€"Câ€"Nâ€"O compounds at high pressure and the fates of planetary ices. Proceedings of the National Academy of Sciences of the United States of America, 2021, 118, .	3.3	11
6110	The First Principles Calculation on the Raman Spectrum and Optical Properties of the Defect Monolayer MoS2. Brazilian Journal of Physics, 2021, 51, 493-498.	0.7	6
6111	High Pressure In Situ Singleâ€Crystal Xâ€Ray Diffraction Reveals Turnstile Linker Rotation Upon Roomâ€Temperature Stepped Uptake of Alkanes. Angewandte Chemie - International Edition, 2021, 60, 13430-13435.	7.2	18
6112	Phase transition-induced contact electric potential. Phase Transitions, 2021, 94, 270-279.	0.6	0
6113	Modeling and experimental studies of quartz and stishovite and the effects of metal dopants on the quartz-to-stishovite pressure-phase transition. MRS Communications, 2021, 11, 317-321.	0.8	1
6114	The mechanical and electronic properties of o-Fe2C, h-Fe3C, t-Fe5C2, m-Fe5C2 and h-Fe7C3 compounds: First-principles calculations. Physica B: Condensed Matter, 2021, 606, 412825.	1.3	4
6115	Cooperative evolution of polar distortion and nonpolar rotation of oxygen octahedra in oxide heterostructures. Science Advances, 2021, 7, .	4.7	20
6116	A Review on Combination of Ab Initio Molecular Dynamics and NMR Parameters Calculations. International Journal of Molecular Sciences, 2021, 22, 4378.	1.8	17

#	Article	IF	Citations
6117	Energetic stability and geometrical structure of variously terminated and N-doped diamond (111) surfaces â€“ A theoretical DFT study. Materials Chemistry and Physics, 2021, 262, 124283.	2.0	4
6118	Large Magnetocaloric Effect in Li₃K₉Gd₃(BO₃)₇ Crystal Featuring Sandwich-Like Three-Dimensional Framework. Inorganic Chemistry, 2021, 60, 6796-6803.	1.9	13
6119	FTIR Measurement of the Hydrogenated Si(100) Surface: The Structure-Vibrational Interpretation by Means of Periodic DFT Calculation. Journal of Physical Chemistry C, 2021, 125, 9219-9228.	1.5	2
6120	A Deepâ€UV Nonlinear Optical Borosulfate with Incommensurate Modulations. Angewandte Chemie, 2021, 133, 11558-11564.	1.6	11
6121	Structure and New Substructure of Î±-Ti2O3: X-ray Diffraction and Theoretical Study. Journal of Modern Materials, 2021, 8, 3-11.	0.8	2
6122	Nitrogen Vacancyâ€Induced Deposition of Pd Nanoparticles onto gâ€C₃N₄ with Greatly Improved Photocatalytic Activity in H₂ Evolution. Solar Rrl, 2021, 5, 2100145.	3.1	22
6123	Flat Zigzag Silicene Nanoribbon with Be Bridge. ACS Omega, 2021, 6, 12099-12104.	1.6	4
6124	Molecular Engineering toward an Enlarged Optical Band Gap in a Bismuth Sulfate via Homovalent Cation Substitution. Inorganic Chemistry, 2021, 60, 5851-5859.	1.9	12
6125	Cd₃(IO₃)(IO₄)F₂Â·0.1CdO: A Nonlinear-Optical Crystal with the Introduction of Fluoride into Iodate Containing Both [IO₃]^â and [IO₄]^{3â€} Groups. Inorganic Chemistry, 2021, 60, 6040-6046.	1.9	11
6126	Efficient DFT Solver for Nanoscale Simulations and Beyond. Journal of Physical Chemistry Letters, 2021, 12, 4134-4139.	2.1	13
6127	A Strategy for the Analysis of the Far-Infrared Vibrational Modes of Hydrogen-Disordered Ice V. Journal of Physical Chemistry C, 2021, 125, 7913-7918.	1.5	4
6128	First-principles study of mechanical and thermodynamic properties of W-V alloys. Physica Scripta, 2021, 96, 065706.	1.2	2
6129	Firstâ€Principles Study of the Effects of Interstitial H and Point Vacancies on the pâ€Type of Conductive Properties of Be/Mg/Caâ€Doped GaN. Physica Status Solidi (B): Basic Research, 2021, 258, 2100023.	0.7	4
6130	Improvement of Photocatalytic Activity of Bi2WO6 by Doping Ag and Y: A DFT Study. Journal of Electronic Materials, 2021, 50, 4027-4033.	1.0	7
6131	High Pressure In Situ Singleâ€Crystal Xâ€Ray Diffraction Reveals Turnstile Linker Rotation Upon Roomâ€Temperature Stepped Uptake of Alkanes. Angewandte Chemie, 2021, 133, 13542-13547.	1.6	0
6132	First-principles predictions of the structural, electronic, optical and elastic properties of the zintl-phases AE3GaAs3 (AE = Sr, Ba). Solid State Sciences, 2021, 114, 106563.	1.5	118
6133	First-principles study on the structural, electronic and optical properties of vacancy-ordered double perovskites Cs2PtI6 and Rb2PtI6. Optical Materials, 2021, 114, 110952.	1.7	34
6134	Pristine and Janus monolayers of vanadium dichalcogenides: potential materials for overall water splitting and solar energy conversion. Journal of Materials Science, 2021, 56, 12270-12284.	1.7	6

#	Article	IF	Citations
6135	Influence of pressure on the structure, mechanical and dynamic properties of boron-rich Na2B30. Journal of Solid State Chemistry, 2021, 296, 121962.	1.4	4
6136	Electron energy loss spectroscopy and first-principles study of GaN via Zn doping. Micron, 2021, 143, 103012.	1.1	0
6137	Enhanced Vis-NIR light absorption and thickness effect of Mo-modified SnO2 thin films: A first principle calculation study. Results in Physics, 2021, 23, 103997.	2.0	9
6138	Synthesis, crystal structure and physical properties of a new chalcogenides Rb3Ga3Ge7S20. Journal of Solid State Chemistry, 2021, 296, 121945.	1.4	5
6139	Synthesis of calcium orthocarbonate, Ca2CO4-Pnma at P-T conditions of Earthâ€™s transition zone and lower mantle. American Mineralogist, 2022, 107, 336-342.	0.9	23
6140	Cation Dynamics and Structural Stabilization in Formamidinium Lead Iodide Perovskites. Journal of Physical Chemistry Letters, 2021, 12, 3503-3508.	2.1	22
6141	Polymorphs of Rb3ScF6: X-ray and Neutron Diffraction, Solid-State NMR, and Density Functional Theory Calculations Study. Inorganic Chemistry, 2021, 60, 6016-6026.	1.9	0
6142	Study on the mechanism of water transport near the surface of pristine and nitrogen-doped Î²-graphyne. International Journal of Modern Physics B, 2021, 35, 2150152.	1.0	2
6143	DFT Simulations as Valuable Tool to Support NMR Characterization of Halide Perovskites: the Case of Pure and Mixed Halide Perovskites. Helvetica Chimica Acta, 2021, 104, e2000231.	1.0	8
6144	A Deepâ€UV Nonlinear Optical Borosulfate with Incommensurate Modulations. Angewandte Chemie - International Edition, 2021, 60, 11457-11463.	7.2	37
6145	Cation Substitution of Hexagonal Triple Perovskites: A Case in Trimetallic Tellurates A2Aâ€²BTe2O9. Inorganic Chemistry, 2021, 60, 6099-6106.	1.9	6
6146	Computational NMR of Carbohydrates: Theoretical Background, Applications, and Perspectives. Molecules, 2021, 26, 2450.	1.7	21
6147	Cobalt diselenide (001) surface with short-range Co-Co interaction triggering high-performance electrocatalytic oxygen evolution. Nano Research, 2021, 14, 4848-4856.	5.8	17
6148	Three-in-One Strategy Constructing a Series of Hybrid Tetrahedral Motif-Based Selenides with Balanced Second-Order Nonlinear Optical Performance. Inorganic Chemistry, 2021, 60, 6641-6648.	1.9	12
6149	Strengthen metal-oxygen covalency of CoFe-layered double hydroxide for efficient mild oxygen evolution. Nano Research, 2022, 15, 162-169.	5.8	29
6150	Dynamics & Spectroscopy with Neutronsâ€”Recent Developments & Emerging Opportunities. Polymers, 2021, 13, 1440.	2.0	8
6151	Boosting Creation of Oxygen Vacancies in Co-Co3O4 Homogeneous Hybrids for Aerobic Oxidation of Cyclohexane. Catalysis Letters, 2022, 152, 282-298.	1.4	19
6152	ANNNI model descriptions on structural energetics for a wide variety of metallic polytypes composed of close-packed layers. MRS Advances, 2021, 6, 163-169.	0.5	3

#	Article	IF	Citations
6153	Origin of the Band Gap Reduction of In-Doped Î²-Ga2O3. Journal of Electronic Materials, 2021, 50, 3856-3861.	1.0	11
6154	Pressure-Induced In Situ Construction of P-CO/HNIW Explosive Composites with Excellent Laser Initiation and Detonation Performance. ACS Applied Materials & Interfaces, 2021, 13, 20718-20727.	4.0	4
6155	First-principles calculations to investigate mechanical, optoelectronic and thermoelectric properties of half-Heusler p-type semiconductor BaAgP. Results in Physics, 2021, 23, 104068.	2.0	25
6156	Study on Ni-Ti alloys around equiatomic composition by the first-principles phase field method. Computational Materials Science, 2021, 191, 110284.	1.4	7
6157	Surface Chirality Influences Molecular Rotation upon Desorption. Physical Review Letters, 2021, 126, 166101.	2.9	3
6158	Formation of one-dimensional quantum crystals of molecular deuterium inside carbon nanotubes. Carbon, 2021, 175, 141-154.	5.4	5
6159	Electronic band structures of NdFe3(BO3)4 and NdGa3(BO3)4 crystals: ab initio calculations. Ferroelectrics, 2021, 575, 11-17.	0.3	1
6160	Computational Investigation of MgH₂/NbOx for Hydrogen Storage. Journal of Physical Chemistry C, 2021, 125, 8862-8868.	1.5	9
6161	Influence of Trimethylphosphine Oxide Loading on the Measurement of Zeolite Acidity by Solid-State NMR Spectroscopy. Journal of Physical Chemistry C, 2021, 125, 9497-9506.	1.5	15
6162	Influence of Nâ€vacancy on the electronic and optical properties of bulk <scp>GaN</scp> from firstâ€principles investigations. International Journal of Energy Research, 2021, 45, 15512-15520.	2.2	50
6163	The Electronic States and metallic character of Carbide Co/MoS2 Catalytic Interface. Electronic Structure, 0, , .	1.0	1
6164	First-principles Investigation on the Electrical and Structural Characteristics of VO₂ (M) and VO₂ (R). Materials Science Forum, 0, 1027, 64-68.	0.3	1
6165	The improved CO adsorption/sensing performance of Stone-Wales defected graphene doped with Fe: A DFT study. Physica E: Low-Dimensional Systems and Nanostructures, 2021, 128, 114603.	1.3	10
6166	Strain engineering on the electrical properties and photocatalytic activity in gold sulfide monolayer. Applied Surface Science, 2021, 546, 149066.	3.1	23
6167	Cd-doped ZnO nanoparticles: An experimental and first-principles DFT studies. Journal of Alloys and Compounds, 2021, 861, 158620.	2.8	21
6168	Probing tribological performances of hydrogenated amorphous carbon film applied in methane by structural modification with boron. Wear, 2021, 470-471, 203610.	1.5	8
6169	First-principles calculations of effects of pressure on paramagnetic, ferromagnetic, and antiferromagnetic spin-web Cu3TeO6. Journal of Molecular Modeling, 2021, 27, 129.	0.8	1
6170	Featureâ€rich structural, electronic, magnetic and optical properties of the fluorineâ€and nitrogenâ€incorporated CaF 2 compound. International Journal of Quantum Chemistry, 2021, 121, e26672.	1.0	0

#	Article	IF	Citations
6171	Structural and Electronic Properties of Ag-Doped in Ba-Site of YBa_{2-x}Ag_xCu₃O_{Î´} Using Density Functional Theory via First Principle Study. Solid State Phenomena, 0, 317, 549-555.	0.3	0
6172	Atomic-Scale Investigations of the Interaction Between Oxygen and (Fe3O4) (1 1 1) Surface. Transactions of the Indian Institute of Metals, 2021, 74, 1713.	0.7	0
6173	A Computational Validation of Water Molecules Adsorption on an NaCl Surface. Crystals, 2021, 11, 610.	1.0	4
6174	The Internal Field in a Ferromagnetic Crystal with Chiral Molecular Packing of Achiral Organic Radicals. Magnetochemistry, 2021, 7, 71.	1.0	3
6175	First-principles calculation of electronic, vibrational, and thermodynamic properties of triaminoguanidinium nitrate. Journal of Molecular Modeling, 2021, 27, 187.	0.8	0
6176	Crystal Structure Optimization Method for Evaluation of Mechanical Properties of Soft Crystals. Nihon Kessho Gakkaishi, 2021, 63, 63-68.	0.0	1
6177	Toward Physics-Based Solubility Computation for Pharmaceuticals to Rival Informatics. Journal of Chemical Theory and Computation, 2021, 17, 3700-3709.	2.3	15
6178	Self-Assembly of N,Nâ€²-Di(n-butyl)-1,3,8,10-tetramethylquinacridone Governed by Metallic Surface Features of a Ag(110) Substrate. Journal of Physical Chemistry C, 2021, 125, 10151-10158.	1.5	2
6179	Origin of high hardness and optoelectronic and thermo-physical properties of boron-rich compounds B6X (Xâ€‰=â€‰S, Se): A comprehensive study via DFT approach. Journal of Applied Physics, 2021, 129, .	1.1	28
6180	From Centrosymmetry to Noncentrosymmetry: Tailoring the Structural Arrangements of Carbonates with Strong Nonlinear Optical Response through Partial Anion Substitution. Advanced Optical Materials, 2021, 9, 2100594.	3.6	18
6181	Schottky barrier heights of defect-free metal/ZnO, CdO, MgO, and SrO interfaces. Journal of Applied Physics, 2021, 129, .	1.1	14
6182	<i>Ab Initio</i> Study on Structural Properties of NaFeSO₄OH Cathode Material for Rechargeable Sodium Ion Battery. Solid State Phenomena, 0, 317, 400-405.	0.3	1
6183	Different mechanism of stereochemical activity and birefringence in post-transition metal halides: A first-principles investigation. Journal of Solid State Chemistry, 2021, 297, 122038.	1.4	0
6184	RbMT₃(BO₃)₂O₃ (M=Ba, Sr; T=Al, Ga): New Doubleâ€Layered Oxyborates Constructed from [BO₃] Triangles and [TO₄] Tetrahedra. Chemistry - A European Journal, 2021, 27, 8698-8703.	1.7	6
6185	Microâ€Raman study of cesanite (Ca₂Na₃ (OH)(SO₄)₃) in chloride segregations from Udachnayaâ€East kimberlites. Journal of Raman Spectroscopy, 2022, 53, 497-507.	1.2	5
6186	First Principles Calculation of Band Structure and Physical Properties of Ferroelectric (NH4)2BeF4 Crystal. , 2021, , .		0
6187	Ab initio Calculations of Electronic Band Structure, Optical and Elastic Parameters of Solid-state CdTe-CdSe Solutions. , 2021, , .		0
6188	Thermal neutron cross sections of amino acids from average contributions of functional groups. Journal of Physics Condensed Matter, 2021, 33, 285901.	0.7	7

#	Article	IF	Citations
6189	Density functional theory investigation on the stability, adhesion strength, tensile properties and fracture behavior of Î³-Fe/Cu heterogeneous nucleation interface. Results in Physics, 2021, 24, 104143.	2.0	5
6190	K₅Mg₂La₃(BO₃)₆: An Efficient, Deep-Ultraviolet Nonlinear Optical Material. Chemistry of Materials, 2021, 33, 4240-4246.	3.2	33
6191	Layered Perovskite Oxyiodide with Narrow Band Gap and Long Lifetime Carriers for Water Splitting Photocatalysis. Journal of the American Chemical Society, 2021, 143, 8446-8453.	6.6	46
6192	Compound-tunable embedding potential method and its application to calcium niobate crystal <mml:math xmlns:mml="http://www.w3.org/1998/Math/MathML"><mml:mrow><mml:msub><mml:mi>CaNb</mml:mi><mml:mn>2</mml:mn></ mathvariant="normal">O</mml:mi><mml:mn>6</mml:mn></mml:msub></mml:mrow></mml:math> with point defects containing tantalum and uranium. Physical Review B, 2021, 103, .	1.1	7
6193	High-temperature phase transitions in dense germanium. Journal of Chemical Physics, 2021, 154, 174702.	1.2	6
6194	Phonon, Electronic Structure and Mechanical Properties of Superhard Material BC2N from First-Principles Calculations. Brazilian Journal of Physics, 2021, 51, 1199-1206.	0.7	2
6195	Second harmonic generation of <mml:math xmlns:mml="http://www.w3.org/1998/Math/MathML"><mml:mrow><mml:mi>Mo</mml:mi><mml:msub><mml:mi>Si</mml:mi><mml:m mathvariant="normal">N</mml:mi><mml:mn>4</mml:mn></mml:msub></mml:mrow></mml:math> -type layers. Physical Review B, 2021, 103, .	1.1	20
6196	Shearing Deformations of Î²-Cristobalite-Like Boron Arsenate. Symmetry, 2021, 13, 977.	1.1	8
6197	Motion of water monomers reveals a kinetic barrier to ice nucleation on graphene. Nature Communications, 2021, 12, 3120.	5.8	20
6198	Synergy of Solid-State NMR, Single-Crystal X-ray Diffraction, and Crystal Structure Prediction Methods: A Case Study of Teriflunomide (TFM). Crystal Growth and Design, 2021, 21, 3328-3343.	1.4	10
6199	Synthesis and characterization of a novel nickel pillaredâ€“clay catalyst: In-situ carbon nanotubeâ€“clay hybrid nanofiller from Ni-PILC. Applied Clay Science, 2021, 205, 106064.	2.6	11
6200	First-Principles Evaluation of Volatile Organic Compounds Degradation in Z-Scheme Photocatalytic Systems: MXene and Graphitic-CN Heterostructures. ACS Applied Materials & Interfaces, 2021, 13, 23843-23852.	4.0	47
6201	Mapping of Guest Localization in Mesoporous Silica Particles by Solid-State NMR and Ab Initio Modeling: New Insights into Benzoic Acid and p-Fluorobenzoic Acid Embedded in MCM-41 via Ball Milling. Journal of Physical Chemistry C, 2021, 125, 10096-10109.	1.5	16
6202	Influence of noble metals on the electronic and optical properties of the monoclinic ZrO2: A first-principles study. Vacuum, 2021, 187, 110112.	1.6	65
6203	High pressure core electron spectroscopy in 111 Fe-based superconducting materials: A first principles study. Computational Materials Science, 2021, 192, 110316.	1.4	7
6204	Crystal Structure Prediction and Dehydrogenation Mechanism of LiMg(BH₄)₃(NH₃)₂. Journal of Physical Chemistry C, 2021, 125, 10235-10242.	1.5	4
6205	Effect of M (Ni, Cu, Zn) doping on the structural, electronic, optical, and thermal properties of CdI2: DFT based theoretical studies. AIP Advances, 2021, 11, .	0.6	4
6206	Nano Sn 2 S 3 Embedded in Nitrogenousâ€Carbon Compounds for Longâ€Life and Highâ€Rate Cycling Sodiumâ€Ion Batteries. ChemSusChem, 2021, 14, 2383-2392.	3.6	11

#	Article	IF	Citations
6207	First Principles Study on Properties of Monolayer MoS2 Under Different Strains. Brazilian Journal of Physics, 2021, 51, 1230-1236.	0.7	5
6209	Ammonium fluorideâ€™s analogy to ice: Possibilities and limitations. Journal of Chemical Physics, 2021, 154, 204501.	1.2	4
6210	Structural phase instability, mixed-phase, and energy band gap change in BiFeO3 under lattice strain effect from first-principles investigation. Ceramics International, 2021, 47, 12592-12599.	2.3	8
6211	Nanoporous MoS₂ Membrane for Water Desalination: A Molecular Dynamics Study. Langmuir, 2021, 37, 7127-7137.	1.6	24
6212	Synthesis of Weaireâ€“Phelan Barium Polyhydride. Journal of Physical Chemistry Letters, 2021, 12, 4910-4916.	2.1	13
6213	Solvates of New Arylpiperazine Salicylamide Derivative-a Multi-Technique Approach to the Description of 5 HTR Ligand Structure and Interactions. International Journal of Molecular Sciences, 2021, 22, 4992.	1.8	3
6214	Structural, electronic, magnetic and optical properties of CaO induced by oxygen incorporation effects: A first-principles study. Physics Letters, Section A: General, Atomic and Solid State Physics, 2021, 397, 127241.	0.9	12
6215	Electron Transfer Facilitated by Ï€â€“Ï€ Stacking during the Nitrobenzene Recognition Process of an MOF Sensor. Journal of Physical Chemistry C, 2021, 125, 12433-12440.	1.5	21
6216	Density Functional Theory Investigation of the Conversion of 5-(Hydroxymethyl)furfural into 2,5-Dimethylfuran over the Pd(111), Cu(111), and Cu₃Pd(111) Surfaces. Journal of Physical Chemistry C, 2021, 125, 10295-10317.	1.5	18
6217	Comparative Analysis of Hydrogen-Bonding Vibrations of Ice VI. ACS Omega, 2021, 6, 14442-14446.	1.6	3
6218	Local atomic structure analysis around Mg atom doped in GaN by X-ray absorption spectroscopy and spectrum simulations. Journal of Synchrotron Radiation, 2021, 28, 1114-1118.	1.0	2
6219	Nanoâ€Scale Complexions Facilitate Li Dendriteâ€Free Operation in LATP Solidâ€State Electrolyte. Advanced Energy Materials, 2021, 11, 2100707.	10.2	36
6220	A Theoretical Study of Vibrational and Optical Properties of Isatin. Brazilian Journal of Physics, 2021, 51, 1207-1214.	0.7	7
6221	A two-dimensional SiGeO monolayer with high electron mobility and negative Poissonâ€™s ratio. Journal of Physics: Conference Series, 2021, 1906, 012004.	0.3	0
6222	Topology Effects in Molecular Organic Electronic Materials: Pyrene and Azupyrene**. ChemPhysChem, 2021, 22, 1065-1073.	1.0	15
6223	Ab initio random structure searching for battery cathode materials. Journal of Chemical Physics, 2021, 154, 174111.	1.2	19
6224	Materials Design and Optimization for Next-Generation Solar Cell and Light-Emitting Technologies. Journal of Physical Chemistry Letters, 2021, 12, 4638-4657.	2.1	12
6225	Mechanical anomalies in mercury oxalate and the deformation of the mercury cube coordination environment under pressure. Applied Physics A: Materials Science and Processing, 2021, 127, 1.	1.1	1

#	Article	IF	Citations
6226	Effects of pressure on the structural, mechanical, anisotropic, and electronic properties of $$hbox {MgTi}_{2}hbox {O}_{4}$$ via density functional theory. European Physical Journal B, 2021, 94, 1.	0.6	4
6227	CsZrF₄(IO₃): The First Polar Zirconium Iodate with cis-[ZrO₂F₆] Polyhedra Inducing Optimized Balance of Large Band Gap and Second Harmonic Generation. Chemistry of Materials, 2021, 33, 5555-5562.	3.2	29
6228	Zinc Complex-Based Multifunctional Reactive Lithium Polysulfide Trapper Approaching Its Theoretical Efficiency. ACS Applied Materials & Interfaces, 2021, 13, 23936-23944.	4.0	12
6229	Hydrogenated Anatase and Rutile TiO₂ for Sodium-Ion Battery Anodes. ACS Applied Energy Materials, 2021, 4, 5738-5746.	2.5	22
6230	Tin Chloride Sulfates A₃Sn₂(SO₄)_{3â€“x}Cl_{1+2x} (A =) Tj ETQq0 0 0 rgBT /Overl	1.4	22
6231	First-principles study of the effects of interstitial H and point vacancies on the photocatalytic performance of Be/Mg/Ca-doped GaN. Vacuum, 2021, 187, 110119.	1.6	14
6232	Ab-initio study of the structural, electronic, elastic and thermodynamic properties of Sc3XB (X=Sn, Al,) Tj ETQq0 0 0 rgBT /Overlock 10 T	0.9	8
6233	Î±-Ca₂CdP₂ and Î²-Ca₂CdP₂: Two Polymorphic Phosphide-Based Infrared Nonlinear Crystals with Distorted NLO-Active Tetrahedral Motifs Realizing Large Second Harmonic Generation Effects and Suitable Band Gaps. Inorganic Chemistry, 2021, 60, 7553-7560.	1.9	14
6234	LiB₂O₃F: A Beryllium-Free Deep-Ultraviolet Nonlinear Optical Material Designed Based on a Boron-Rich Strategy. Chemistry of Materials, 2021, 33, 4783-4791.	3.2	39
6235	A₂MoO₂F₃(IO₂F₂) (A = Rb,) Tj ETQq1 1 0.784314 rgBT Chemistry of Materials, 2021, 33, 5700-5708.	3.2	30
6236	Câ€“H Borylation Catalysis of Heteroaromatics by a Rhenium Boryl Polyhydride. ACS Catalysis, 2021, 11, 7394-7400.	5.5	11
6237	Effective degradation of sulfur mustard simulant using novel sulfur-doped mesoporous zinc oxide under ambient conditions. Journal of Hazardous Materials, 2021, 411, 125144.	6.5	17
6238	The effect of progressive aging on the bond strength of bitumen to siliceous stones. Applied Surface Science, 2021, 550, 149324.	3.1	22
6239	First-principles study of solid-state properties of adrenergic neurotransmitters, orthorhombic noradrenaline, and monoclinic adrenaline. Journal of Applied Physics, 2021, 129, 234702.	1.1	1
6240	Structural Features of Y2O2SO4 via DFT Calculations of Electronic and Vibrational Properties. Materials, 2021, 14, 3246.	1.3	4
6241	Theoretical study of novel Bâ€“Câ€“O compounds with non-diamond isoelectronic. Chinese Physics B, 2022, 31, 026201.	0.7	26
6242	Nitrogen doping and oxygen vacancy effects on the fundamental properties of BeO monolayer: a DFT study. Journal of Physics Condensed Matter, 2021, 33, 325305.	0.7	9
6243	Resolving Site-Specific Energy Levels of Small-Molecule Donor-Acceptor Heterostructures Close to Metal Contacts. Nanomaterials, 2021, 11, 1618.	1.9	0

#	Article	IF	Citations
6244	Structural, Thermal, and Vibrational Properties of N,N-Dimethylglycineâ€“Chloranilic Acidâ€”A New Co-Crystal Based on an Aliphatic Amino Acid. Materials, 2021, 14, 3292.	1.3	1
6245	Performant implementation of the atomic cluster expansion (PACE) and application to copper and silicon. Npj Computational Materials, 2021, 7, .	3.5	76
6246	BaYOBO3: A deep-ultraviolet rare-earth oxy-borate with a large second harmonic generation response. Science China Chemistry, 2021, 64, 1184-1191.	4.2	22
6247	Tuning optical and electronic properties of 2D ZnI2/CdS heterostructure by biaxial strains for optical nanodevices: A first-principles study. Journal of Applied Physics, 2021, 129, .	1.1	44
6248	Ethylene oxidation on unpromoted silver catalysts: Reaction pathway and selectivity analysis using DFT calculations. Surface Science, 2021, 708, 121834.	0.8	6
6249	Strong in-plane anisotropy in the electronic properties of doped transition metal dichalcogenides exhibited in W1â^'xNbxS2. Physical Review B, 2021, 103, .	1.1	7
6250	Accurate frozen core approximation for all-electron density-functional theory. Journal of Chemical Physics, 2021, 154, 224107.	1.2	1
6251	Missing Piece in the Crystal Chemistry of Znâ€“Sb Secondary Phases in ZnOâ€“Sb₂O₃â€“Bi₂O₃ Varistor Ceramics: Orthorhombic Î²-Zn₇Sb₂O₁₂. An Experimental and Theoretical Study of the Crystal Structure and Its Thermal and Vibrational Spectroscopic Characterization. Inorganic Chemistry, 2021, 60, 8648-8658.	1.9	3
6252	SrAlB3O6F2: A Fluoroaluminoborate with [Al2B6O14F4] Units and Large Birefringence. Inorganic Chemistry, 2021, 60, 10006-10011.	1.9	10
6253	Explanation of the microscopic mechanism of h-BN isostructural transformation under biaxial strain. Materials Today Communications, 2021, 27, 102391.	0.9	3
6254	Spectral proxies for bonding transitions in <mml:math xmlns:mml="http://www.w3.org/1998/Math/MathML"><mml:mrow><mml:msub><mml:mi>SiO</mml:mi><mml:mn>2</mml:mn></mml and <mml:math xmlns:mml="http://www.w3.org/1998/Math/MathML"><mml:mrow><mml:msub><mml:mi>MgSiO</mml:mi><mml:mn>3</mml:mn></m polymorphs at high pressure up to 270 GPa by O <mml:math xmlns:mml="http://www.w3.org/1998/Math/MathML"><mml:mi>K</mml:mi></mml:math> -edge x-ray Rama	1.1	7
6255	Na₂Rb₂Sr₁₈O₃₀ with [B₉O₁₉]^{11â^'} fundamental building block consisting of three [B₃O₇]^{5â^'} groups. Zeitschrift Fur Anorganische Und Allgemeine Chemie, 2021, 647, 1578-1582.	0.6	2
6256	Corrosion inhibition properties of small peptides: DFT and Monte Carlo simulation studies. Journal of Molecular Liquids, 2021, 331, 115782.	2.3	27
6257	DFT investigation on direct Z-scheme photocatalyst for overall water splitting: MoTe2/BAs van der Waals heterostructure. Applied Surface Science, 2021, 551, 149364.	3.1	59
6258	Preparation of MoS2â€“Ag/g-C3N4 Composite for Rhodamine B Degradation. Nano, 2021, 16, 2150078.	0.5	1
6259	Studies of Hydrogen Bond Vibrations of Hydrogen-Disordered Ice Ic. Crystals, 2021, 11, 668.	1.0	4
6260	Two orthorhombic superhard carbon allotropes: C16 and C24. Diamond and Related Materials, 2021, 116, 108426.	1.8	35
6261	Adsorption mechanism of water molecules on hematite (1 0 4) surface and the hydration microstructure. Applied Surface Science, 2021, 550, 149328.	3.1	28

#	Article	IF	Citations
6263	Analyzing Discrepancies in Chemical-Shift Predictions of Solid Pyridinium Fumarates. Molecules, 2021, 26, 3857.	1.7	3
6264	Effect of shear deformation on aluminum adsorption on silicene. Journal of Molecular Structure, 2021, 1234, 130172.	1.8	4
6265	Thickness effect on the properties of Mn-doped ZnO thin films synthesis by sol-gel and comparison to first-principles calculations. Ceramics International, 2021, 47, 17276-17285.	2.3	25
6266	Designed Synthesis of STA-30: A Small-Pore Zeolite Catalyst with Topology Type SWY. Chemistry of Materials, 2021, 33, 5242-5256.	3.2	6
6267	Quasi-four-component method with numeric atom-centered orbitals for relativistic density functional simulations of molecules and solids. Physical Review B, 2021, 103, .	1.1	7
6268	Raman and X-ray Photoelectron Spectroscopic Study of Aqueous Thiol-Capped Ag-Zn-Sn-S Nanocrystals. Materials, 2021, 14, 3593.	1.3	9
6269	Reversible Multi-Electron Storage Enabled by Na5V(PO4)2F2 for Rechargeable Magnesium Batteries. Energy Storage Materials, 2021, 38, 462-472.	9.5	21
6270	Stepping Out of Transition Metals: Activating the Dual Atomic Catalyst through Main Group Elements. Advanced Energy Materials, 2021, 11, 2101404.	10.2	33
6271	Fine structures and their impacts on the characteristic Raman spectra of molten binary alkali tungstates. Journal of Raman Spectroscopy, 2021, 52, 1452-1461.	1.2	3
6272	Mere Anarchy is Loosed: Structural Disorder in Cu₂Zn_{1â€“x}Cd_xSnS₄. Chemistry of Materials, 2021, 33, 4709-4722.	3.2	8
6273	Solidâ€state nuclear magnetic resonance of spinâ€9/2 nuclei ¹¹⁵In and ²⁰⁹Bi in functional inorganic complex oxides. Magnetic Resonance in Chemistry, 2021, 59, 1077-1088.	1.1	4
6274	Direct Electrochemical Protonation of Metal Oxide Particles. Journal of the American Chemical Society, 2021, 143, 9236-9243.	6.6	25
6275	Surface metallization from ab initio theory and subwavelength coupling via surface plasmon polaritons in Cu-doped lithium niobate/tantalate owing to charge accumulation. Applied Surface Science, 2021, 551, 149294.	3.1	8
6276	Hydrogen-Bonded Cyclic Dimers at Large Compression: The Case of 1H-pyrrolo[3,2-h]quinoline and 2-(2â€²-pyridyl)pyrrole. Molecules, 2021, 26, 3802.	1.7	1
6277	A catalytic reaction scheme for NO reduction by CO over Mn-terminated LaMnO3 perovskite: A DFT study. Fuel Processing Technology, 2021, 216, 106798.	3.7	26
6278	Chlorine isotope mantle heterogeneity: Constraints from theoretical first-principles calculations. Chemical Geology, 2021, 572, 120193.	1.4	7
6279	Accelerating water dissociation kinetics of Ni3N by tuning interfacial orbital coupling. Nano Research, 2021, 14, 3458-3465.	5.8	16
6280	The study of spectroscopy and vibrational assignments of high nitrogen material 1,1â€²-azobis-1,2,3-triazole. Journal of Molecular Modeling, 2021, 27, 205.	0.8	0

#	Article	IF	Citations
6281	Fast, efficient, and accurate dielectric screening using a local real-space approach. Physical Review B, 2021, 103, .	1.1	9
6282	New developments in the <scp>GDIS</scp> simulation package: Integration of <scp>VASP</scp> and <scp>USPEX</scp>. Journal of Computational Chemistry, 2021, 42, 1602-1626.	1.5	3
6283	The metalâ€“insulator phase change in vanadium dioxide and its applications. Journal of Applied Physics, 2021, 129, .	1.1	25
6284	Opening the germanene monolayer band gap using halogen atoms: An efficient approach studied by first-principles calculations. Applied Surface Science, 2021, 551, 149318.	3.1	30
6285	Second-order nonlinear optical and photoelectric properties of Zn4B6O12S. Journal of Alloys and Compounds, 2021, 867, 158879.	2.8	10
6286	Adsorption of DTC-CTS on sphalerite (1 1 0) and Cu-activated sphalerite (1 1 0) surfaces: A DFT study. Applied Surface Science, 2021, 551, 149466.	3.1	19
6287	Fluorineâ€Ðriven Enhancement of Birefringence in the Fluorooxosulfate: A Deep Evaluation from a Joint Experimental and Computational Study. Advanced Science, 2021, 8, e2003594.	5.6	83
6288	Be₂(BO₃)(IO₃): The First Anionâ€mixed Van der Waals Member in the KBe₂BO₃F₂ Family with a Very Strong Second Harmonic Generation Response. Angewandte Chemie - International Edition, 2021, 60, 17415-17418.	7.2	59
6289	Group 14 semiconductor alloys in the P41212 phase: A comprehensive study. Results in Physics, 2021, 25, 104254.	2.0	10
6290	Experimental methods in chemical engineering: Density functional theory. Canadian Journal of Chemical Engineering, 2021, 99, 1885-1911.	0.9	19
6291	Aliovalent substitution in phosphideâ€based materials â€“ Crystal structures of Na 10 AlTaP 6 and Na 3 GaP 2 featuring edgeâ€sharing E P 4 tetrahedra (E =Al/Ta and Ga). Zeitschrift Fur Anorganische Und Allgemeine Chemie, 2021, 647, 1804-1814.	0.6	1
6292	Electron-Beam Irradiation Induced Regulation of Surface Defects in Lead Halide Perovskite Thin Films. Research, 2021, 2021, 9797058.	2.8	9
6293	Sn₃C₂ monolayer with transition metal adatom for gas sensing: a density functional theory studies. Nanotechnology, 2021, 32, 355502.	1.3	11
6294	Germanether: a two-dimensional auxetic semiconductor with tunable direct-band-gap and high electron mobility. Journal of Physics Condensed Matter, 2021, 33, 315301.	0.7	1
6295	Intercalation voltages for spinel LixMn2O4 (0â‰xâ‰2) cathode materials: Calibration of calculations with the ONETEP linear-scaling DFT code. Materials Today Communications, 2021, 27, 102380.	0.9	0
6296	Study on a stress-magnetic relationship of DO3 based on first principles. Materials Today Communications, 2021, 27, 102196.	0.9	5
6297	Be 2 (BO 3)(IO 3): The First Anionâ€mixed Van der Waals Member in the KBe 2 BO 3 F 2 Family with a Very Strong Second Harmonic Generation Response. Angewandte Chemie, 2021, 133, 17555-17558.	1.6	7
6298	Revealing the Configuration and Conformation of Surface Organometallic Catalysts with DNP-Enhanced NMR. Journal of Physical Chemistry C, 2021, 125, 13433-13442.	1.5	11

#	Article	IF	Citations
6299	Structural Investigation of Silver Vanadium Phosphorus Oxide (Ag2VO2PO4) and Its Reduction Products. Chemistry of Materials, 2021, 33, 4425-4434.	3.2	0
6300	Unveiling the role of carbon defects in the exceptional narrowing of m-ZrO2 wide-bandgap for enhanced photoelectrochemical water splitting. International Journal of Hydrogen Energy, 2021, 46, 21499-21511.	3.8	5
6301	Mechanical and dynamic properties of stable two-dimensional boron-substituted ThMoB4â€“type graphene: First-Principles Study. Materials Today Communications, 2021, 27, 102322.	0.9	3
6302	Highly enhanced NH3-sensing performance of BC6N monolayer with single vacancy and Stone-Wales defects: A DFT study. Applied Surface Science, 2021, 551, 149383.	3.1	45
6303	Investigation of Unusual Conductivity Behavior and Ion Dynamics in Hexamethylguanidinium Bis(fluorosulfonyl)imide-Based Electrolytes for Sodium Batteries. Journal of Physical Chemistry C, 2021, 125, 12518-12530.	1.5	15
6304	Insights from Systematic DFT Calculations on Superconductors. , 0, , .		2
6305	First principle study on the mechanical response of ZrC and ZrN at high-pressure conditions: anisotropy perspective. Molecular Simulation, 2021, 47, 1135-1148.	0.9	6
6306	First principles study in the electronic structures and optical properties of chalcogenide-doped AgInS2. Optical and Quantum Electronics, 2021, 53, 1.	1.5	0
6307	SPARC: Simulation Package for Ab-initio Real-space Calculations. SoftwareX, 2021, 15, 100709.	1.2	27
6308	Synthesis of Oxygen Deficient TiO2 for Improved Photocatalytic Efficiency in Solar Radiation. Catalysts, 2021, 11, 904.	1.6	7
6309	Nontrivial topological states in new two-dimensional CdAs. Journal of Physics Condensed Matter, 2021, 33, 365701.	0.7	2
6310	Evidence of room-temperature ferromagnetism in vertically aligned Biâ€“Co co-doped ZnO nanowires. Journal Physics D: Applied Physics, 2021, 54, 415301.	1.3	9
6311	Two Tellurium(IV)-Based Sulfates Exhibiting Strong Second Harmonic Generation and Moderate Birefringence as Promising Ultraviolet Nonlinear Optical Materials. Inorganic Chemistry, 2021, 60, 11412-11418.	1.9	20
6312	Electrochemical reduction of SnO2 to Sn from the Bottom: In-Situ formation of SnO2/Sn heterostructure for highly efficient electrochemical reduction of carbon dioxide to formate. Journal of Catalysis, 2021, 399, 67-74.	3.1	33
6313	Unraveling the anomalous mechanoluminescence intensity change and pressure-induced red-shift for manganese-doped zinc sulfide. Nano Energy, 2021, 85, 106005.	8.2	19
6314	Photopolymerization effects on the external quantum efficiency of fullerene/zinc phthalocyanine heterojunction solar cells. AIP Advances, 2021, 11, .	0.6	3
6315	Stepwise Li Substitution Induced Structure Evolution and Improved Nonlinear Optical Performance for Diamond-like Sulfides. Inorganic Chemistry, 2021, 60, 12536-12544.	1.9	21
6316	Li₃La₂(BO₃)₃ and Li_{1.75}Na_{1.25}La₂(BO₃)₃: A Great Enhancement in Birefringence Induced by Optimal Arrangement of ï€-Conjugated [BO₃] Units. Inorganic Chemistry, 2021, 60, 12565-12572.	1.9	11

#	Article	IF	Citations
6317	Bond length controlling opto-structural properties of Mn doped CuO thin films: An experimental and theoretical study. Materials Science in Semiconductor Processing, 2021, 129, 105798.	1.9	15
6318	Toward a Mechanistic Understanding of Pellet Cladding Interaction Using Advanced 3D Characterization and Atomistic Simulation. , 2021, , 904-926.		0
6319	Accurate and Efficient Computation of Optical Absorption Spectra of Molecular Crystals: The Case of the Polymorphs of ROY. Journal of Chemical Theory and Computation, 2021, 17, 5214-5224.	2.3	4
6320	Comparative Studies on VS₂ Bilayer and VS₂/Graphene Heterostructure as the Anodes of Li Ion Battery. Key Engineering Materials, 0, 894, 61-66.	0.4	1
6321	³⁵Clâ€“¹H Heteronuclear correlation magicâ€angle spinning nuclear magnetic resonance experiments for probing pharmaceutical salts. Magnetic Resonance in Chemistry, 2021, 59, 1089-1100.	1.1	11
6322	Twinning enhanced electrical conductivity and surface activity of nanostructured CuCrO2 gas sensor. Sensors and Actuators B: Chemical, 2021, 338, 129845.	4.0	4
6323	Selective Oxidation of Various Phenolic Contaminants by Activated Persulfate via the Hydrogen Abstraction Pathway. ACS ES&T Engineering, 2021, 1, 1275-1286.	3.7	30
6324	Effects of pressure on narrowing the band gap, visible light absorption, and semi-metallic transition of lead-free perovskite CsSnBr3 for optoelectronic applications. Journal of Physics and Chemistry of Solids, 2021, 154, 110083.	1.9	33
6325	Preparation of Multifunctional Metal Oxynitride 2D Crystals and Oriented Transparent Free-Standing Oxynitride Films. Chemistry of Materials, 2021, 33, 6068-6077.	3.2	11
6326	Theoretical study on compositionâ€dependent properties of ZnOÂ·nAl₂O₃ spinels. Part II: Mechanical and thermophysical. Journal of the American Ceramic Society, 2021, 104, 6455-6466.	1.9	10
6327	Out-of-Plane Dielectric Susceptibility of Graphene in Twistronic and Bernal Bilayers. Nano Letters, 2021, 21, 6678-6683.	4.5	24
6328	Investigation of physical and superconducting properties of newly synthesized CaPd2P2 and SrPd2P2. Journal of Alloys and Compounds, 2021, 868, 159199.	2.8	18
6329	Ternary rare-earth sulfides RE3GaS6 (REâ€‰=â€‰Ho, Er): Crystal chemistry, second-order nonlinear optical properties and theoretical investigation. Journal of Alloys and Compounds, 2021, 868, 159112.	2.8	8
6330	Enhanced Photovoltaic Performance of BiSCl Solar Cells Through Nanorod Array. ChemSusChem, 2021, 14, 3351-3358.	3.6	11
6332	Revised Huang-Carter nonlocal kinetic energy functional for semiconductors and their surfaces. Physical Review B, 2021, 104, .	1.1	15
6333	Magnesium Deintercalation From the Spinelâ€Type MgMn 2â€y Fe y O 4 (0.4â‰yâ‰2.0) by Acidâ€Treatment and Electrochemistry. Chemistry - A European Journal, 2021, 27, 12599-12609.	1.7	5
6334	BiOBr/MoS2 catalyst as heterogenous peroxymonosulfate activator toward organic pollutant removal: Energy band alignment and mechanism insight. Journal of Colloid and Interface Science, 2021, 594, 635-649.	5.0	51
6335	First-principle study of the effects of biaxial strain on the photocatalytic and magnetic mechanisms of ZnO with Sm doping and point defects (VZn, Hi). Vacuum, 2021, 189, 110225.	1.6	6

#	Article	IF	Citations
6336	Adsorption of hydrated [Y(OH)2]+ on kaolinite (001) surface: Insight from DFT simulation. Powder Technology, 2021, 387, 80-87.	2.1	20
6337	Bimetal single-molecule magnets supported on benzene with large magnetic anisotropy and unquenched orbital moment. Physical Review Research, 2021, 3, .	1.3	3
6338	Beyond the Limit of Goldschmidt Tolerance Factor: Crystal Surface Engineering to Boost the Î±â€Phase Stability of Formamidiniumâ€Only Hybrid Inorganicâ€“Organic Perovskites. Solar Rrl, 2021, 5, 2100188.	3.1	8
6339	Effects of different Cu and N ratios on electronic and magnetic properties of (Cu, N) co-doped ZnO. Modern Physics Letters B, 0, , 2150379.	1.0	0
6340	Tuning the electronic properties of Stone-Wales defected graphene using uniaxial longitudinal and horizontal strain: A first-principles study. Fullerenes Nanotubes and Carbon Nanostructures, 2022, 30, 428-437.	1.0	3
6341	DFT study of the adsorption of 2,3-epoxypropyltrimethylammonium chloride on montmorillonite surfaces. Journal of Molecular Liquids, 2021, 334, 116145.	2.3	14
6342	Towards Computational Screening for New Energetic Molecules: Calculation of Heat of Formation and Determination of Bond Strengths by Local Mode Analysis. Frontiers in Chemistry, 2021, 9, 726357.	1.8	4
6343	Is Mg17Al12 ductile or brittle? A theoretical insight. Journal of Magnesium and Alloys, 2023, 11, 936-944.	5.5	12
6344	Direct and quasi-direct band gap of novel Si-Ge alloys in P-3m1 phase. Journal of Physics Condensed Matter, 2021, 33, 385702.	0.7	6
6345	Highly efficient and selectivity removal of heavy metal ions using single-layer Na K MnO2 nanosheet: A combination of experimental and theoretical study. Chemosphere, 2021, 275, 130068.	4.2	6
6346	Density functional theory calculations of copperâ€doped rutile crystals: Local structural, electronic, optical, and electron paramagnetic resonance properties. Magnetic Resonance in Chemistry, 2022, 60, 104-112.	1.1	1
6347	<scp>2â€Hydroxyâ€5â€nitropyridine and 5â€nitroâ€2â€pyridone: Tautomerism, infrared, Raman, and NMR spectral interpretations, normal coordinate analysis, and DFT calculations</scp>. Journal of the Chinese Chemical Society, 2021, 68, 1863-1879.	0.8	5
6348	The Advantage of Nanowire Configuration in Band Structure Determination. Advanced Functional Materials, 2021, 31, 2105426.	7.8	4
6349	Structural Transformation and Second-Harmonic-Generation Activity in Rare-Earth and d⁰ Transition-Metal Oxysulfides RE₃NbS₃O₄ (RE = Ce,) Tj ETQq1 1 0.784314 rgB	4.3	23
6350	MAX phase Zr2SeC and its thermal conduction behavior. Journal of the European Ceramic Society, 2021, 41, 4447-4451.	2.8	33
6351	Supramolecular Anchoring Strategy for Facile Production of Ruthenium Nanoparticles Embedded in N-Doped Mesoporous Carbon Nanospheres for Efficient Hydrogen Generation. ACS Applied Materials & Interfaces, 2021, 13, 32997-33005.	4.0	11
6352	Adsorption mechanism of polyacrylamide on kaolinite surface in the presence of Ca2+: Insights from DFT calculation. Chemical Physics Letters, 2021, 776, 138672.	1.2	15
6353	Structural, Physical, and Thermodynamic Properties of Aragonitic CaxSr1â€“xCO3 Solid Solutions. Journal of Physical Chemistry C, 2021, 125, 17474-17481.	1.5	4

#	Article	IF	Citations
6354	MoS₂/Graphene Heterostructure Anode for Li-Ion Battery Application: A First-Principles Study. Key Engineering Materials, 0, 896, 53-59.	0.4	0
6355	Cold Atmospheric Plasma (CAP) Technology and Applications. Synthesis Lectures on Mechanical Engineering, 2021, 6, i-191.	0.1	3
6356	Ptâ€“Cu Interaction Induced Construction of Single Pt Sites for Synchronous Electron Capture and Transfer in Photocatalysis. Advanced Functional Materials, 2021, 31, 2104343.	7.8	50
6357	Theoretical and Experimental Research on Ammonia Sensing Properties of Sulfur-Doped Graphene Oxide. Chemosensors, 2021, 9, 220.	1.8	8
6358	New Insights on the Vibrational Dynamics of 2-Methoxy-, 4-Methoxy- and 4-Ethoxy-Benzaldehyde from INS Spectra and Periodic DFT Calculations. Materials, 2021, 14, 4561.	1.3	4
6359	Effect of the Pt concentration on microstructures of Ti-Pt alloys using the first-principles phase field method. Acta Materialia, 2021, 215, 117050.	3.8	5
6360	The high Curie temperature and long-range ferromagnetism in Mn-doped 3C-SiC: a study using first-principles calculation. Journal of the Korean Physical Society, 2021, 79, 546-551.	0.3	1
6361	Hg₃P₂S₈: A New Promising Infrared Nonlinear Optical Material with a Large Second-Harmonic Generation and a High Laser-Induced Damage Threshold. Chemistry of Materials, 2021, 33, 6514-6521.	3.2	74
6362	After 200 Years: The Structure of Bleach and Characterization of Hypohalite Ions by Singleâ€Crystal Xâ€Ray Diffraction**. Angewandte Chemie - International Edition, 2021, 60, 24400-24405.	7.2	2
6363	Revisiting the third-order elastic constants of diamond: The higher-order effect. Diamond and Related Materials, 2021, 117, 108490.	1.8	9
6364	P2₁3 BN: a novel large-cell boron nitride polymorph. Communications in Theoretical Physics, 2021, 73, 125701.	1.1	18
6365	Observation of a molecular muonium polaron and its application to probing magnetic and electronic states. Physical Review B, 2021, 104, .	1.1	0
6366	Single-Atom Catalysts as Promising Cathode Materials for Lithiumâ€“Sulfur Batteries. Journal of Physical Chemistry C, 2021, 125, 18108-18118.	1.5	41
6367	A short-range disordered defect in the double layer ice. Journal of Molecular Liquids, 2021, 336, 116356.	2.3	1
6368	Influence of (Li/Na/K) doping and point defect (VAl, Hi) on the magnetic and photocatalytic performance of AlN: A first-principles study. Materials Chemistry and Physics, 2021, 268, 124706.	2.0	4
6369	High-temperature oxidation behavior of C/C composites in wet oxygen: Experiment and first-principle calculations. Corrosion Science, 2021, 189, 109577.	3.0	2
6370	The PtSe2/GaN van der Waals heterostructure photocatalyst with type II alignment: A first-principles study. Applied Catalysis A: General, 2021, 624, 118332.	2.2	34
6371	Predictive Mixing for Density Functional Theory (and Other Fixed-Point Problems). Journal of Chemical Theory and Computation, 2021, 17, 5715-5732.	2.3	10

#	Article	IF	Citations
6372	After 200 Years: The Structure of Bleach and Characterization of Hypohalite Ions by Singleâ€Crystal Xâ€Ray Diffraction**. Angewandte Chemie, 0, , .	1.6	0
6373	First-principles study of bipolar resistive memories based on monolayer Î±-GeTe. Nanotechnology, 2021, 32, 475701.	1.3	2
6374	Investigating lithium intercalation and diffusion in Nb-doped TiO2 by first principles calculations. Journal of the Taiwan Institute of Chemical Engineers, 2021, 125, 314-322.	2.7	11
6375	Kinetic Molecular Sieving of Cyclopentane/Neohexane Mixtures by the MFI Zeolite with Intersecting 10-Ring Channels. Industrial & Engineering Chemistry Research, 2021, 60, 13293-13300.	1.8	2
6376	Orthorhombic C36: a sp2â€“sp3 carbon with pressure-induced metallization and superconductivity. Journal of Materials Science, 2021, 56, 17665-17673.	1.7	7
6377	HMX/NMP cocrystal explosive: first-principles calculations. Journal of Molecular Modeling, 2021, 27, 254.	0.8	2
6378	First-principles calculations of the electronic, vibrational, and thermodynamic properties of 2,6-diamino-3,5-dinitropyrazine-1-oxide (LLM-105). Chemical Physics, 2021, 548, 111232.	0.9	3
6379	Redox-Active Tin Metalâ€“Organic Framework with a Thiolate-Based Ligand. Inorganic Chemistry, 2021, 60, 12691-12695.	1.9	10
6380	Highâ€Throughput Electronic Structures and Ferroelectric Interfaces of HfO 2 by GGA+ U (d,p) Calculations. Physica Status Solidi - Rapid Research Letters, 2021, 15, 2100295.	1.2	5
6381	Engineering cobalt sulfide/oxide heterostructure with atomically mixed interfaces for synergistic electrocatalytic water splitting. Nano Research, 2022, 15, 1246-1253.	5.8	43
6382	Changes in the physical properties of Mg2Ir3Si compared to Li2IrSi3 due to the substitution of Li by Mg and the exchange of positions between Ir and Si. Solid State Communications, 2021, 334-335, 114361.	0.9	0
6383	Firstâ€Principles Investigation of the Effect of Vanadium Doping on Hydrogen Incorporation in Tungsten. Crystal Research and Technology, 2021, 56, 2100115.	0.6	2
6384	Designing highly incompressible transition metal nitrides: A new class of W0.5Al0.5N phases. Journal of Applied Physics, 2021, 130, 065105.	1.1	1
6385	Influence on structural, electronic and optical properties of Fe doped <scp>ZnS</scp> quantum dot: A density functional theory based study. International Journal of Quantum Chemistry, 2021, 121, e26786.	1.0	4
6386	Type-II GeC/ZnTe heterostructure with high-efficiency of photoelectrochemical water splitting. Applied Physics Letters, 2021, 119, .	1.5	17
6387	Common workflows for computing material properties using different quantum engines. Npj Computational Materials, 2021, 7, .	3.5	10
6388	Electrochemically-Matched and Nonflammable Janus Solid Electrolyte for Lithiumâ€“Metal Batteries. ACS Applied Materials & Interfaces, 2021, 13, 39271-39281.	4.0	16
6389	Dynamical Immiscibility of Aqueous Carbonate Fluid in the Shortiteâ€“Water System at High-Pressureâ€“Temperature Conditions. Journal of Physical Chemistry C, 2021, 125, 18501-18509.	1.5	5

#	Article	IF	Citations
6390	NaRbB 3 O 4 F 3 : A New Fluorooxoborate with a Short UV Cutoff Edge Enriching the Structural Chemistry of Borate. Chemistry - an Asian Journal, 2021, 16, 3082-3085.	1.7	5
6391	Near edge absorption studies of pure and impure $$hbox {NbSe}_{2}$$; theory and experiment. Journal of Materials Science, 2021, 56, 17062-17079.	1.7	2
6392	Fundamental properties of octalithium plumbate ceramic breeder material. Journal of Nuclear Materials, 2021, 552, 152982.	1.3	3
6393	Theoretical study on structural, excitonic and electronic properties of Nb2O5 with five crystal structures. Materials Science in Semiconductor Processing, 2021, 130, 105831.	1.9	3
6394	Vanadium based zinc spinel oxides: Potential materials as photoanode for water oxidation and optoelectronic devices. International Journal of Hydrogen Energy, 2021, 46, 28110-28120.	3.8	1
6395	Comparative Studies on Monolayer and Bilayer Phosphorous as the Anodes of Li Ion Battery. Key Engineering Materials, 0, 896, 61-66.	0.4	0
6396	Moderately Concentrated Acetonitrileâ€•containing Electrolytes with High Ionic Conductivity for Durabilityâ€•oriented Lithiumâ€•Ion Batteries. ChemElectroChem, 2021, 8, 3095-3104.	1.7	6
6397	Investigation on composition-dependent properties of Mg5Al23â¯5O27+5N5â¯5 (0 â‰¤ x â‰¤ 1): Part II. Mechanical properties via first-principles calculations combined with bond valence models. Journal of the European Ceramic Society, 2021, 41, 4942-4950.	2.8	5
6398	Two-Dimensional Boron-Rich Monolayer B_xN as High Capacity for Lithium-Ion Batteries: A First-Principles Study. ACS Applied Materials & Interfaces, 2021, 13, 41169-41181.	4.0	20
6399	Two-state model for critical points and the negative slope of the melting curve. Physical Review B, 2021, 104, .	1.1	2
6400	Electronic, optical, and vibrational properties of B3N3H6 from first-principles calculations. Journal of Molecular Modeling, 2021, 27, 241.	0.8	0
6401	Robust cleaning mechanism permanently detaches hydrocarbon species from silicate surfaces by amphiphiles. Applied Surface Science, 2021, 558, 149954.	3.1	6
6402	Evolution of Structural, Thermal, Optical, and Vibrational Properties of Sc₂S₃, ScCuS₂, and BaScCuS₃ Semiconductors. European Journal of Inorganic Chemistry, 2021, 2021, 3355-3366.	1.0	2
6403	Impact of anionic system modification on the desired properties for CuGa(S1â¯Se)2 solid solutions. Computational Materials Science, 2021, 196, 110553.	1.4	5
6404	Crystal Structure, Vibrational, Spectroscopic and Thermochemical Properties of Double Sulfate Crystalline Hydrate [CsEu(H2O)3(SO4)2]Â·H2O and Its Thermal Dehydration Product CsEu(SO4)2. Crystals, 2021, 11, 1027.	1.0	43
6406	Embedding Cobalt Atom Clusters in CNTâ€•Wired MoS₂ Tubeâ€•inâ€•Tube Nanostructures with Enhanced Sulfur Immobilization and Catalyzation for Liâ€“S Batteries. Small, 2021, 17, e2102710.	5.2	52
6407	Two intermediate incommensurate phases in the molecular dissociation process of solid iodine under high pressure. Physical Review Research, 2021, 3, .	1.3	4
6408	Modulated electronic and optical properties of bilayer/trilayer Blue Phosphorene/MoX2 (X=S, Se) van der Waals heterostructures. Surfaces and Interfaces, 2021, 25, 101228.	1.5	5

#	Article	IF	Citations
6409	DFT Electronic Properties and Synthesis Thermodynamics of Li_xLa_{1â^'x}TiO₃ Electrolytes for Li-Ion Batteries. Journal of the Electrochemical Society, 2021, 168, 080516.	1.3	7
6410	Revisiting the Structure of Calcined and Hydrated AlPOâ€11 with DFTâ€Based Molecular Dynamics Simulations**. ChemPhysChem, 2021, 22, 2063-2077.	1.0	8
6411	Davis Computational Spectroscopy Workflowâ€"From Structure to Spectra. Journal of Chemical Information and Modeling, 2021, 61, 4486-4496.	2.5	4
6412	Density functional theory study on the electronic structure and optical properties of Li absorbed borophene. Molecular Physics, 0, , e1966114.	0.8	2
6413	First-principles calculations to investigate structural and elastic properties of Y2C3 under external pressure. Computational and Theoretical Chemistry, 2021, 1202, 113320.	1.1	0
6414	Structural and Electronic Effects of X-ray Irradiation on Prototypical [M(COD)Cl]₂Catalysts. Journal of Physical Chemistry A, 2021, 125, 7473-7488.	1.1	11
6415	High-throughput discovery of high-temperature conventional superconductors. Physical Review B, 2021, 104, .	1.1	45
6416	Enhancing air-stability and reproducibility of lead-free formamidinium-based tin perovskite solar cell by chlorine doping. Solar Energy Materials and Solar Cells, 2021, 227, 111072.	3.0	15
6417	Linear and Helical Cesium Iodide Atomic Chains in Ultranarrow Single-Walled Carbon Nanotubes: Impact on Optical Properties. ACS Nano, 2021, 15, 13389-13398.	7.3	20
6418	First-principles of Be/Mg/Ca doping and point defects of VZn and Hi in the magnetic and optical properties of ZnO. Materials Science in Semiconductor Processing, 2021, 131, 105857.	1.9	13
6419	Crystal and Electronic Structure of U₇Te₁₂-Type Tungsten Nitride Synthesized under High Pressure. Inorganic Chemistry, 2021, 60, 13278-13283.	1.9	8
6420	Ab initio exploration of the structural, elastic, electronic and optical properties of a new layered perovskite-type oxyï¬‚uoride: CsSrNb2O6F. Materials Science in Semiconductor Processing, 2021, 131, 105890.	1.9	47
6421	High-temperature oxidation behavior of CVD-SiC ceramic coating in wet oxygen and structural evolution of oxidation product: Experiment and first-principle calculations. Applied Surface Science, 2021, 556, 149808.	3.1	27
6422	Adsorption, sensing and optical properties of molecules on BC3 monolayer: First-principles calculations. Materials Science and Engineering B: Solid-State Materials for Advanced Technology, 2021, 271, 115266.	1.7	16
6423	Effect of sulfur deficiency on the structural, optical and electronic properties of MnS nanostructures. Chemical Physics Letters, 2021, 779, 138877.	1.2	20
6424	Density Functional Theory Study on the Interfacial Properties of CuS/Bi₂S₃ Heterostructure. Physica Status Solidi (B): Basic Research, 2021, 258, 2100268.	0.7	6
6425	TiN inducing ferrite nucleation based on the bcc-Fe/TiN interfaces formation at atomic scale by first-principles calculation. Computational Materials Science, 2021, 197, 110570.	1.4	16
6426	First-principles calculations to investigate structural, elastic, electronic and optical properties of lead-free perovskite derivatives Cs2SeX6 (X=Cl, Br, I). Optical Materials, 2021, 119, 111316.	1.7	29

#	Article	IF	Citations
6427	Operando leaching of pre-incorporated Al and mechanism in transition-metal hybrids on carbon substrates for enhanced charge storage. Matter, 2021, 4, 2902-2918.	5.0	22
6428	Structure enhancement of energetic materials: A theoretical study of the arylamines to arylpentazoles transformation. FirePhysChem, 2021, 1, 190-197.	1.5	7
6429	Regulating adsorption ability toward polysulfides in a porous carbon/Cu₃P hybrid for an ultrastable highâ€temperature lithiumâ€“sulfur battery. , 2021, 3, 841-855.		41
6430	Effects of p-type conductive properties of triaxial strain-regulated ZnO (S, Se, Te) system. Physica Scripta, 2021, 96, 125815.	1.2	3
6431	Effect of Ag alloying and trace precipitation on corrosion resistance of Ti-Ta-Ag ternary alloy. Royal Society Open Science, 2021, 8, 210243.	1.1	0
6432	A Congruentâ€Melting Midâ€Infrared Nonlinear Optical Vanadate Exhibiting Strong Secondâ€Harmonic Generation. Angewandte Chemie, 2021, 133, 22621-22627.	1.6	11
6433	Ab-Initio Predictions of the Energy Harvesting Performance of L-Arginine and L-Valine Single Crystals. Frontiers in Mechanical Engineering, 2021, 7, .	0.8	5
6434	Machineâ€Learningâ€Assisted Selective Synthesis of a Semiconductive Silver Thiolate Coordination Polymer with Segregated Paths for Holes and Electrons. Angewandte Chemie, 2021, 133, 23405.	1.6	0
6435	Electro-optical and charge transport properties of chalcone derivatives using a dual approach from molecule to material level simulations. Computational and Theoretical Chemistry, 2021, 1203, 113349.	1.1	10
6436	The Crystal Structure of 5â€Aminouracil and the Ambiguity of Alternative Polymorphs #. Israel Journal of Chemistry, 2021, 61, 590.	1.0	1
6437	On the Application of Strong Magnetic Fields during Organic Crystal Growth. Crystal Growth and Design, 2021, 21, 6254-6265.	1.4	2
6438	Computational study of TbMn2O5 and Tb2MnCoO6 to probe the structural, vibrational and optoelectronic properties using PBEÂ+ÂU functional. Optik, 2021, 241, 166835.	1.4	2
6439	OPTICS: Operant Probability Theory in Crystal Solutions, Application of ssNMR, and Probability Theory in Polymorph Identification. Crystal Growth and Design, 2021, 21, 5904-5913.	1.4	1
6440	Density Functional Theory Study of the Highâ€Pressure Characterization of Nitrogenâ€Rich Energetic Materials: Bisâ€Triaminoguanidinium Azotetrazolate (TAGzT). Physica Status Solidi (B): Basic Research, 0, , 2100365.	0.7	1
6441	A porous nanotube network structure of metallic carbon. Results in Physics, 2021, 28, 104579.	2.0	17
6442	Aluminum to germanium inversion in mulliteâ€type RAlGeO₅: Characterization of a rare phenomenon for RÂ=ÂY, Smâ€“Lu. Journal of the American Ceramic Society, 2022, 105, 728-741.	1.9	4
6443	First-principles study on the structural, elastic, electronic and optical properties of lead-free double perovskites Cs2CuBiX6 (X I, Br, Cl). Materials Today Communications, 2021, 29, 102842.	0.9	16
6444	Polymorphism of CdTe in the Fewâ€Monolayer Limit. Physica Status Solidi - Rapid Research Letters, 2021, 15, 2100358.	1.2	3

#	Article	IF	Citations
6445	The influence of N-vacancy on the electronic and optical properties of bulk InN nitrides. Materials Science and Engineering B: Solid-State Materials for Advanced Technology, 2021, 271, 115265.	1.7	57
6446	Engineering Co3+-rich crystal planes on Co3O4 hexagonal nanosheets for CO and hydrocarbons oxidation with enhanced catalytic activity and water resistance. Chemical Engineering Journal, 2021, 420, 130448.	6.6	34
6447	Controllable drilling by corrosive Cu1Ox to access highly accessible single-site catalysts for bacterial disinfection. Applied Catalysis B: Environmental, 2021, 293, 120228.	10.8	11
6448	A comprehensive study of the thermophysical and optoelectronic properties of Nb2P5 via ab-initio technique. Results in Physics, 2021, 28, 104623.	2.0	20
6449	Effect of hydrostatic compression on physical properties of Li2TmSi3 (Tm = Ir, Pt, Rh, Os) with ground-state optical features. Journal of Physics and Chemistry of Solids, 2021, 156, 110124.	1.9	5
6450	Investigations on magnetic properties of p-type ferromagnetic (Ca, Na)(Zn, Mn)2As2. Materials Science and Engineering B: Solid-State Materials for Advanced Technology, 2021, 271, 115282.	1.7	2
6451	A member of p-type TCO family: Sn2TaxNb2-xO7 with a tunable band gap and controllable hole mobility. Materials Science and Engineering B: Solid-State Materials for Advanced Technology, 2021, 271, 115255.	1.7	0
6452	Ab Initio Study of Hexagonal Boron Nitride as the Tunnel Barrier in Magnetic Tunnel Junctions. ACS Applied Materials & Interfaces, 2021, 13, 47226-47235.	4.0	6
6453	Surface and subsurface damage in 14â€‰MeV Au ion-irradiated diamond. Journal of Applied Physics, 2021, 130, 105303.	1.1	0
6455	The crystal structure of LiSc2SbO6. Journal of Solid State Chemistry, 2021, 304, 122615.	1.4	2
6456	Computational investigation on interaction mechanism of sulfur mustard adsorption by zeolitic imidazolate frameworks ZIF-8 and ZIF-67: Insights from periodic and cluster DFT calculations. Journal of Molecular Liquids, 2021, 344, 117705.	2.3	13
6457	First-principles study of the structural phase transition process of solid nitrogen under pressure. Journal of Molecular Modeling, 2021, 27, 307.	0.8	0
6458	Finding a Series of BaBOF₃ Fluorooxoborate Polymorphs with Tunable Symmetries: A Simple but Flexible Case. Chemistry of Materials, 2021, 33, 7905-7913.	3.2	22
6459	Exploring the electronic properties of Si-doped AlN (0001) surface with Cs adsorption layer for solar cell anode applications. Materials Science in Semiconductor Processing, 2021, 132, 105899.	1.9	2
6460	Exploring space-energy matching via quantum-molecular mechanics modeling and breakage dynamics-energy dissipation via microhydrodynamic modeling to improve the screening efficiency of nanosuspension prepared by wet media milling. Expert Opinion on Drug Delivery, 2021, 18, 1643-1657.	2.4	1
6461	Studies on the Performance of Two Dimensional AlSi as the Anodes of Li Ion Battery. Solid State Phenomena, 0, 324, 109-115.	0.3	0
6462	Boosting Potassium Storage Performance of Red Phosphorous via Modifying the Nickel Foam Substrate. ACS Applied Energy Materials, 2021, 4, 9682-9691.	2.5	4
6463	A periodic DFT study of IR spectra of amino acids: An approach toward a better understanding of the N-H and O-H stretching regions. Vibrational Spectroscopy, 2021, 116, 103280.	1.2	20

#	Article	IF	Citations
6464	Pristine and Janus chromium dichalcogenides: Potential photocatalysts for overall water splitting in wide solar spectrum under strain and electric field. Solar Energy Materials and Solar Cells, 2021, 230, 111258.	3.0	20
6465	2D van der Waals Layered [C(NH₂)₃]₂SO₃S Exhibits Desirable UV Nonlinear-Optical Trade-Off. Inorganic Chemistry, 2021, 60, 14544-14549.	1.9	18
6466	Synthesis and Characterizations of Two Tellurides Î²-BaGa₂Te₄ and Ba₅Ga₂Ge₃Te₁₂ with Flexible Chain Structure. Inorganic Chemistry, 2021, 60, 14793-14802.	1.9	12
6467	First-principles DFT investigations of the vibrational spectra of chloro-quine and hydroxychloroquine. Journal of Physics Communications, 2021, 5, 105009.	0.5	0
6468	Machineâ€Learningâ€Assisted Selective Synthesis of a Semiconductive Silver Thiolate Coordination Polymer with Segregated Paths for Holes and Electrons. Angewandte Chemie - International Edition, 2021, 60, 23217-23224.	7.2	12
6469	Ba₄GeSb₂Se₁₁: An Infrared Nonlinear Optical Crystal with a V-Shaped Se₃^{2â€“} Group Possessing a Large Contribution to the SHG Response. Inorganic Chemistry, 2021, 60, 15593-15598.	1.9	5
6470	In situ synthesis of 2D/2D MXene-COF heterostructure anchored with Ag nanoparticles for enhancing Schottky photocatalytic antibacterial efficiency under visible light. Journal of Colloid and Interface Science, 2022, 608, 735-748.	5.0	39
6471	Amelioration of sintering and multi-frequency dielectric properties of Mg3B2O6: A mechanism study of nickel substitution using DFT calculation. Journal of Advanced Ceramics, 2021, 10, 1398-1407.	8.9	27
6472	Theoretical Studies of Electronic and Optical Properties of Bixbyite and Fluorite Polymorphs of Sb-Doped Y2O3. Journal of Electronic Materials, 2021, 50, 6784-6794.	1.0	1
6473	Enabling highly efficient and broadband electromagnetic wave absorption by tuning impedance match in high-entropy transition metal diborides (HE TMB2). Journal of Advanced Ceramics, 2021, 10, 1299-1316.	8.9	46
6474	Enhanced interface interaction in Cu2S@Ni core-shell nanorod arrays as hydrogen evolution reaction electrode for alkaline seawater electrolysis. Journal of Power Sources, 2021, 506, 230235.	4.0	40
6475	Unified and ultimate high-pressure phase of several nanolaminate Mn+1AXn (nâ€¯=â€¯1, 2, 3, etc.) ceramics from first principles. Results in Physics, 2021, 28, 104681.	2.0	2
6476	Stimulated band structure by external isotropic static pressure and its impact on optoelectronic properties of PbZrO3: An ab-initio calculation. Optik, 2021, 241, 167024.	1.4	3
6477	Behavior of Li-ion on the surface of Ti3C2â€“T (T = O, S, Se, F, Cl, Br) MXene: Diffusion barrier and conductive pathways. Journal of Applied Physics, 2021, 130, .	1.1	14
6478	Electronic and optical properties of pristine and Li/Na/K/Mg/Ca decorated net-Y: First-principles calculations. Materials Science and Engineering B: Solid-State Materials for Advanced Technology, 2021, 271, 115269.	1.7	2
6479	Flux growth synthesis, single crystal and electronic structure of the new intermetallic compound Pt2Ga17Ta3. Computational Materials Science, 2021, 197, 110591.	1.4	0
6480	Phase diagrams and superconductivity of ternary Na-Al-H compounds at high pressure. Physical Review B, 2021, 104, .	1.1	5
6481	Raman spectroscopic and theoretical studies on the structure of Ta (V) fluoro and oxofluoro complexes in molten FLiNaK. Journal of Molecular Liquids, 2021, 337, 116409.	2.3	5

#	Article	IF	Citations
6482	Effects of Oxygenated Acids on Graphene Oxide: The Source of Oxygen-Containing Functional Group. Frontiers in Chemistry, 2021, 9, 736954.	1.8	3
6483	Lattice mismatch, mechanical properties and lattice-compensation effect in Si1-xGex alloys by using first-principles calculations combined with virtual crystal approximation. Physics Letters, Section A: General, Atomic and Solid State Physics, 2021, 411, 127528.	0.9	6
6484	First-principles and experiment investigation of Bi2O3/Bi2WO6 heterojunctions. Colloids and Interface Science Communications, 2021, 44, 100502.	2.0	4
6485	A first-principles prediction of electronic, mechanical and thermodynamic properties of Î±-LuAlB4 and Î²-LuAlB4 ceramics. Vacuum, 2021, 191, 110375.	1.6	5
6486	Refined Structures of O-Phospho-l-serine and Its Calcium Salt by New Multinuclear Solid-State NMR Crystallography Methods. Journal of Physical Chemistry B, 2021, 125, 10985-11004.	1.2	2
6487	High harmonic studies of structural phase transitions in silicon. Computational Materials Science, 2021, 197, 110621.	1.4	2
6488	Can We Predict the Isosymmetric Phase Transition? Application of DFT Calculations to Study the Pressure Induced Transformation of Chlorothiazide. International Journal of Molecular Sciences, 2021, 22, 10100.	1.8	4
6489	A Congruentâ€Melting Midâ€Infrared Nonlinear Optical Vanadate Exhibiting Strong Secondâ€Harmonic Generation. Angewandte Chemie - International Edition, 2021, 60, 22447-22453.	7.2	37
6490	Durable superlubricity of hydrogenated diamond-like carbon film against different friction pairs depending on their interfacial interaction. Applied Surface Science, 2021, 560, 150023.	3.1	33
6491	A comprehensive DFT based insights into the physical properties of tetragonal superconducting Mo5PB2. Results in Physics, 2021, 28, 104612.	2.0	24
6492	Tribological behaviour of microalloyed Cu50Zr50 alloy. Journal of Tribology, 0, , 1-22.	1.0	0
6493	Uncovering the Promotion of CeO₂/CoS_{1.97} Heterostructure with Specific Spatial Architectures on Oxygen Evolution Reaction. Advanced Materials, 2021, 33, e2102593.	11.1	118
6494	Controlled Morphology Synthesis of Nanostructured Î²-AlF_{3â€“x}(OH)_x with Tunable Specific Surface Area. Crystal Growth and Design, 2021, 21, 5914-5927.	1.4	2
6495	Effect of Mo substitution on the structure and electrical properties of Gd2Ru2O7 pyrochlore. Physica B: Condensed Matter, 2021, 619, 413227.	1.3	0
6496	First-principles investigation of the structural stability of TKX-50 under high pressure. Physica B: Condensed Matter, 2021, 619, 413229.	1.3	4
6497	First principles study of the electronic, elastic and vibrational properties of BiOI. Solid State Communications, 2021, 336, 114419.	0.9	3
6498	Chemical and computational strategy for design of â€œswitchableâ€•sorbent based on hydroxyapatite nanoparticles for dispersive micro-solid phase extraction of tetracyclines. Journal of Hazardous Materials, 2021, 419, 126504.	6.5	13
6499	Adsorption mechanism of sulphide gas molecules on Î³-Fe(1Â1Â1) surface: A density functional theory study. Applied Surface Science, 2021, 563, 150376.	3.1	5

#	Article	IF	Citations
6500	A (110) Facet-Dominated Vanadium Dioxide Enabling Bidirectional Electrocatalysis for Lithiumâ€“Sulfur Batteries. ACS Nano, 2021, 15, 16878-16886.	7.3	29
6501	Corrosion-induced CaCO3 fouling in steel tube of oilfield wastewater treatment and the interfacial bonding mechanism: An experimental and theoretical investigation. Journal of Petroleum Science and Engineering, 2021, 205, 108759.	2.1	0
6502	MechElastic: A Python library for analysis of mechanical and elastic properties of bulk and 2D materials. Computer Physics Communications, 2021, 267, 108068.	3.0	54
6503	High-temperature Mo-based bulk metallic glasses. Scripta Materialia, 2021, 203, 114095.	2.6	16
6504	Superhard carbon-rich Câ€“N compounds hidden in compression of the mixture of carbon black and tetracyanoethylene. Carbon, 2021, 184, 846-854.	5.4	5
6505	Alleviating mechanical degradation of hexacyanoferrate via strain locking during Na+ insertion/extraction for full sodium ion battery. Nano Research, 2022, 15, 2123-2129.	5.8	21
6506	Unveiling substitution preference of chromium ions in sulphoaluminate cement clinker phases. Composites Part B: Engineering, 2021, 222, 109092.	5.9	40
6507	Chlorine isotope fractionation during serpentinization and hydrothermal mineralization: A density functional theory study. Chemical Geology, 2021, 581, 120406.	1.4	6
6508	Reduction of NO on chemically doped, metal-free graphene. Carbon Trends, 2021, 5, 100111.	1.4	6
6509	Band gap Engineering of ZnO via transition metal Doping: An ab initio study. Chemical Physics Letters, 2021, 781, 138979.	1.2	12
6510	Tensile strain induced surface reactions for co-adsorption of H2O and OHâ^' on vacancy Al (111) surface. Vacuum, 2021, 192, 110459.	1.6	2
6511	Ternary Feâ€“Wâ€“B bulk metallic glasses with ultrahigh thermal stabilities. Materials Science & Engineering A: Structural Materials: Properties, Microstructure and Processing, 2021, 826, 142034.	2.6	2
6512	Plasmon-enhanced Hydrogen evolution reaction kinetics through the strong coupling of Au-O Bond on Au-MoO2 heterostructure nanosheets. Nano Energy, 2021, 88, 106302.	8.2	31
6513	Degradation of carbamazepine by UVA/WO3/hypochlorite process: Kinetic modelling, water matrix effects, and density functional theory calculations. Environmental Research, 2021, 201, 111569.	3.7	6
6514	VASPKIT: A user-friendly interface facilitating high-throughput computing and analysis using VASP code. Computer Physics Communications, 2021, 267, 108033.	3.0	2,308
6515	Bi4AO6Cl2 (A = Ba, Sr, Ca) with Double and Triple Fluorite Layers for Visible-Light Water Splitting. Inorganic Chemistry, 2021, 60, 15667-15674.	1.9	4
6516	Theory prediction of band structures, densities of states, mechanical and thermodynamic properties of solid solutions BaxK1-xBi0.92Mg0.08O3. Physica B: Condensed Matter, 2021, 618, 413163.	1.3	2
6517	Electronic structures, effective masses and optical properties of B6Ch (Ch=O, S, Se, Te) based on DFT study. Solid State Communications, 2021, 336, 114423.	0.9	2

#	Article	IF	Citations
6518	Atomic level insights into the Ti2AlC oxidation mechanism by the combination of density functional theory and ab initio molecular dynamics calculations. Corrosion Science, 2021, 191, 109756.	3.0	16
6519	Charge transfer channels of silver @ cuprous oxide heterostructure core-shell nanoparticles strengthen high photocatalytic antibacterial activity. Journal of Colloid and Interface Science, 2021, 601, 531-543.	5.0	28
6520	The first-principles prediction of two-dimensional indium-arsenide bilayers. Materials Science in Semiconductor Processing, 2021, 134, 106041.	1.9	3
6521	Physical properties of MAX phase Zr2PbC under pressure: Investigation via DFT scheme. Physica B: Condensed Matter, 2021, 620, 413258.	1.3	8
6522	Theoretical research for oxidation mechanism of <mml:math xmlns:mml="http://www.w3.org/1998/Math/MathML" altimg="si1.svg"><mml:mrow><mml:mi mathvariant="bold">Î±</mml:mi></mml:mrow></mml:math>-Ti: A combination of DFT and ab initio molecular dynamics study. Vacuum, 2021, 193, 110522.	1.6	16
6523	Molecular structure and ammonia gas adsorption capacity of a Cu(II)-1,10-phenanthroline complex intercalated in montmorillonite by DFT simulations. Microporous and Mesoporous Materials, 2021, 327, 111408.	2.2	2
6524	Optoelectronic properties exploration of native point defects on GaN nanowires. Applied Surface Science, 2021, 565, 150600.	3.1	3
6525	Construction of a ternary spatial junction in yolkâ€“shell nanoreactor for efficient photo-thermal catalytic hydrogen generation. Chemical Engineering Journal, 2021, 423, 130188.	6.6	54
6526	Selective synthesis of Ni12P5 and Ni2P nanoparticles: Electronic structures, magnetic and optical properties. Materials Science and Engineering B: Solid-State Materials for Advanced Technology, 2021, 273, 115389.	1.7	7
6527	Theoretical study of thiophene-inserted COF as high performance anode material for Li-ion battery. Chemical Physics Letters, 2021, 783, 139042.	1.2	6
6528	Influence of oxygen vacancy compensation on the structure, electronic and mechanical properties of yttrium stabilized tetragonal zirconia. Materials Science in Semiconductor Processing, 2021, 135, 106082.	1.9	5
6529	Effects of external electric field on adsorption behavior of organic molecules on stanene: Highly sensitive sensor devices. Solid State Communications, 2021, 338, 114459.	0.9	8
6530	First-principles analysis of desired inherent photovoltaic functionalities of tetragonal CuAlX2 (X=O,) Tj ETQq0 0 0 rgBT /Overlock 10 Tf 5	1.4	3
6531	Chemisorption mechanism of defluorinated fluorine on bcc Fe surface during formation of PTFE transfer film. Applied Surface Science, 2021, 567, 150777.	3.1	4
6532	Insight into the structure-capacity relationship in biomass derived carbon for high-performance sodium-ion batteries. Journal of Energy Chemistry, 2021, 62, 497-504.	7.1	34
6533	Engineering the electronic and magnetic properties of nitrogene monolayer and bilayer by doping: A first-principles study. Applied Surface Science, 2021, 566, 150711.	3.1	10
6534	The effect of heterocyclization of 2-mercaptobenzimidazole on its strength of coordination to iron: A dispersion-corrected DFT study. Applied Surface Science, 2021, 567, 150819.	3.1	10
6535	Theoretical investigation of hydrated [Lu(OH)2]+ adsorption on kaolinite(0Â0Â1) surface with DFT calculations. Applied Surface Science, 2021, 565, 150473.	3.1	20

#	Article	IF	Citations
6536	2D CoGeSe3 monolayer as a visible-light photocatalyst with high carrier mobility: Theoretical prediction. Applied Surface Science, 2021, 565, 150588.	3.1	6
6537	The influence of Ag and Cu on the electronic and optical properties of ZrO from first-principles calculations. Materials Science in Semiconductor Processing, 2021, 135, 106084.	1.9	61
6538	Novel BCN2 and CN compounds in C2/m phase: First-principle calculations. Journal of Physics and Chemistry of Solids, 2021, 158, 110231.	1.9	7
6539	Two-dimensional SiMI4(MÂ=ÂGe, Sn) monolayers as visible-light-driven photocatalyst of hydrogen production. Spectrochimica Acta - Part A: Molecular and Biomolecular Spectroscopy, 2021, 261, 120013.	2.0	8
6540	Experimental and theoretical studies on structural, morphological, electronic, optical and magnetic properties of Zn1-xCuxO thin films (0â‰¤xâ‰¤0.125). Materials Science in Semiconductor Processing, 2021, 134, 106012.	1.9	7
6541	Multifunctional triphenylbenzene-based polyimide covalent organic framework with absolute eclipsed stacking models for fluorescence detecting of Fe3+ and electrochemical detecting of Pb2+. Microchemical Journal, 2021, 170, 106663.	2.3	11
6542	A comparative study of Ag doping effects on the electronic, optical, carrier conversion, photocatalytic and electrical properties of MoS2. Materials Science and Engineering B: Solid-State Materials for Advanced Technology, 2021, 273, 115442.	1.7	7
6543	Investigation on phase structure and magnetic properties of high-temperature Ni-Pt-Co-Mn-Sn magnetic shape memory alloys by first-principles calculations. Computational Materials Science, 2021, 199, 110748.	1.4	5
6544	Press dependent electronic structure and optical property of Ba2Mg(PO4)2:Eu2+. Journal of Alloys and Compounds, 2021, 883, 160870.	2.8	1
6545	First-principles calculation of the electronic properties and external force modulation of a new tetragonal structure C3N2 crystal. Solid State Communications, 2021, 338, 114455.	0.9	3
6546	Dual-metallic single Ru and Ni atoms decoration of MoS2 for high-efficiency hydrogen production. Applied Catalysis B: Environmental, 2021, 298, 120557.	10.8	99
6547	Fabrication of Z-scheme VO-Bi2WO6/g-C3N4 heterojunction composite with visible-light-driven photocatalytic performance for elemental mercury removal. Chemical Engineering Journal, 2021, 425, 131537.	6.6	28
6548	Confining nano FeSb2S4 in carbon nanotube/oxide graphene 3D porous networks for high-capacity sodium ion battery anode. Journal of Alloys and Compounds, 2021, 884, 161116.	2.8	10
6549	Synthesis, structure, linear and nonlinear optical properties of noncentrosymmetric quaternary diamond-like semiconductors, Cu2ZnGeSe4 (CZGSe) and the novel Cu4ZnGe2Se7. Journal of Alloys and Compounds, 2021, 888, 161499.	2.8	13
6550	Nature of electronic topological transition and superconductivity in bismuth under high pressure from ab initio random structure searching. Computational Materials Science, 2021, 200, 110806.	1.4	5
6551	Revealing the atomic-scale structure and the fracture mechanism of the Î±-Al2O3/Î³-Fe ceramic-metal interface. Journal of Alloys and Compounds, 2021, 885, 161163.	2.8	11
6552	Tailoring electronic properties and polarization relaxation behavior of MoS2 monolayers for electromagnetic energy dissipation and wireless pressure micro-sensor. Chemical Engineering Journal, 2021, 425, 131700.	6.6	35
6553	Exploring reaction mechanism of CO oxidation over SrCoO3 catalyst: A DFT study. Applied Surface Science, 2021, 570, 151234.	3.1	11

#	Article	IF	Citations
6554	Revealing the adhesion strength and electronic properties of Ti3SiC2/Cu interface in Ti3SiC2 reinforced Cu-based composite by a first-principles study. Surfaces and Interfaces, 2021, 27, 101467.	1.5	11
6555	A temperature-dependent Raman scattering and X-ray diffraction study of K2Mo2O7Â·H2O and ab initio calculations of K2Mo2O7. Spectrochimica Acta - Part A: Molecular and Biomolecular Spectroscopy, 2021, 263, 120184.	2.0	5
6556	Photoinduced linkage isomers in a model ruthenium nitrosyl complex: Identification and assignment of vibrational modes. Spectrochimica Acta - Part A: Molecular and Biomolecular Spectroscopy, 2021, 263, 120217.	2.0	10
6557	Role of water on ozonation of cinnamaldehyde to benzaldehyde under Ca(OH)2 catalysis: A combined in situ DRIFTS and DFT study. Applied Surface Science, 2021, 569, 151071.	3.1	11
6558	Electronic, magnetic, and optical properties of bulk and (1 1 1)-surfaces of CoMnZnSi quaternary Heusler alloy. Journal of Magnetism and Magnetic Materials, 2021, 539, 168425.	1.0	7
6559	Adsorption of NO and O2 on MnO2 and (MnO2)3/Al2O3. Applied Surface Science, 2021, 569, 150994.	3.1	3
6560	Electronic and elastic properties of two new B-C-N superhard materials from first principles. Solid State Communications, 2021, 340, 114520.	0.9	2
6561	Deep understanding the effect of annealing temperature on fluorescence and persistent luminescence properties of Mn doped Zn2GeO4 films deposited by RF magnetron sputtering. Applied Surface Science, 2021, 570, 151192.	3.1	5
6562	Fluorine-substituted cyclobutenes in the solid state: Crystal structures, vibrational spectra and mechanical and thermodynamic properties. Journal of Physics and Chemistry of Solids, 2022, 160, 110337.	1.9	1
6563	N-containing silane coupling agent-assisted synthesis of highly dispersed and stable PdC phase for semi-hydrogenation of acetylene. Chemical Engineering Science, 2022, 247, 116939.	1.9	5
6564	Photo- and thermo-catalytic mechanisms for elemental mercury removal by Ce doped commercial selective catalytic reduction catalyst (V2O5/TiO2). Chemosphere, 2022, 287, 132336.	4.2	15
6565	Understanding lithium, sodium, and potassium storage mechanisms in silicon oxycarbide. Chemical Engineering Journal, 2022, 428, 131072.	6.6	20
6566	Exploration of the toxic target gas molecules for layered and tubular g-C3N4: Density functional theory. Applied Surface Science, 2022, 571, 151230.	3.1	5
6567	Dual-functional Co5.47N/Fe3N heterostructure interconnected 3D N-doped carbon nanotube-graphene hybrids for accelerating polysulfide conversion in Li-S batteries. Chemical Engineering Journal, 2022, 427, 131774.	6.6	38
6568	Fabrication of Al2O3/CaO with anti-sintering for efficient removal of As2O3 in simulated flue gas: Experimental and DFT study. Fuel, 2022, 307, 121812.	3.4	32
6569	Infrared spectra of the Î² and Î³ phases of oleic acid under high pressure. Spectrochimica Acta - Part A: Molecular and Biomolecular Spectroscopy, 2022, 265, 120290.	2.0	5
6570	Improved thermal stability and infrared emissivity of high-entropy REMgAl11O19 and LaMAl11O19 (RE=La,) Tj ETQq0 0 0 rgBT /Overlock	5.6	25
6571	Effect of oxygen atoms adsorption and doping on hexagonal boron nitride. Physica E: Low-Dimensional Systems and Nanostructures, 2022, 135, 114977.	1.3	10

#	Article	IF	Citations
6572	Accurate prediction of band gap of materials using stacking machine learning model. Computational Materials Science, 2022, 201, 110899.	1.4	21
6573	High-temperature superconductivity in transition metallic hydrides MH₁₁(M = Mo, W, Nb,) Tj ETQq1 1 0.784314 rgBT /Ove	1.3	15
6574	Effects of Mg substitution on electronic properties of CaF2. Journal of Physics: Conference Series, 2021, 1719, 012027.	0.3	0
6575	Native O and Se Vacancy Defects in Bi₂O₅Se, Bi₂O₉Se₃, and Bi₂O₁₀Se₃ Dielectrics for Nanoelectronics. Physica Status Solidi - Rapid Research Letters, 2021, 15, 2000540.	1.2	1
6576	The low energy phonon modes of the hydrogenated and deuterated Ï€-conjugated system 7,7,8,8-tetracyanoquinodimethane: an inelastic neutron scattering study. Physical Chemistry Chemical Physics, 2021, 23, 2899-2905.	1.3	1
6577	Barium-based scintillating MOFs for X-ray dosage detection with intrinsic energy resolution via luminescent multidentate naphthalene disulfonate moieties. Journal of Materials Chemistry C, 2021, 9, 5615-5620.	2.7	18
6578	First-Principles Studies for Electronic Structure and Optical Properties of p-Type Calcium Doped Î±-Ga2O3. Materials, 2021, 14, 604.	1.3	22
6579	1T-CrO₂monolayer: a high-temperature Dirac half-metal for high-speed spintronics. Nanoscale Advances, 2021, 3, 3093-3099.	2.2	15
6580	Observing the three-dimensional dynamics of supported metal complexes. Inorganic Chemistry Frontiers, 2021, 8, 1416-1431.	3.0	9
6581	Electrochemical reduction of CO₂ and N₂ to synthesize urea on metalâ€“nitrogen-doped carbon catalysts: a theoretical study. Dalton Transactions, 2021, 50, 11158-11166.	1.6	23
6582	Structural diversity, large interlayer spacing and switchable electronic properties of graphitic systems. Journal of Materials Science, 2021, 56, 5509-5519.	1.7	3
6583	From Ce(IO₃)₄ to CeF₂(IO₃)₂: fluorinated homovalent substitution simultaneously enhances SHG response and bandgap for mid-infrared nonlinear optics. Journal of Materials Chemistry C, 0, , .	2.7	11
6584	Dynamic effects in crystalline coordination polymers. CrystEngComm, 2021, 23, 5738-5752.	1.3	22
6585	Advances in the computation of NMR parameters for inorganic nuclides. , 2021, , .		0
6586	First-principles study on the electronic and optical properties of the orthorhombic CsPbBr₃ and CsPbI₃ with Cmcm space group. New Journal of Chemistry, 2021, 45, 15857-15862.	1.4	16
6587	Distinctive modulation of optical anisotropy by halogens in Î±/Î²-Cdâ€“Pâ€“X (X = Cl, Br, and I). Dalton Transactions, 2021, 50, 12006-12015.	1.6	0
6588	Mechanical study of a copper dietary supplement, copper glycinate hydrate. CrystEngComm, 2021, 23, 1815-1820.	1.3	1
6589	Ultraviolet nonlinear optical crystals A₃SrBi(P₂O₇)₂(A = K, Rb) with large second harmonic generation responses. Inorganic Chemistry Frontiers, 2021, 8, 2061-2067.	3.0	9

#	Article	IF	Citations
6590	Evaluating the crystalline orbital hierarchy and high-pressure structureâ€“property response of an extended-ligand platinum(<scp>ii</scp>) bis(1,2-dioximato) complex. CrystEngComm, 2021, 23, 6359-6364.	1.3	0
6591	Infrared spectra of amorphous and crystalline urea ices. Physical Chemistry Chemical Physics, 2021, 23, 22344-22351.	1.3	14
6592	Understanding the anchoring and catalytic effect of the Co@C₂N monolayer in lithiumâ€“selenium batteries: a first-principles study. Nanoscale, 2021, 13, 16316-16323.	2.8	10
6593	Ionic Phases of Ammonia-Rich Hydrate at High Densities. Physical Review Letters, 2021, 126, 015702.	2.9	5
6594	Explanation for the conductivity difference of half-Heusler transparent conductors via ionization energy. Physical Chemistry Chemical Physics, 2021, 23, 9285-9293.	1.3	5
6595	Defects in H/He neutral beam irradiated potassium doped tungsten alloy by positron annihilation technique. Wuli Xuebao/Acta Physica Sinica, 2021, 70, 167803.	0.2	3
6596	Laser-induced crystallization and phase transitions of <mml:math xmlns:mml="http://www.w3.org/1998/Math/MathML"><mml:mrow><mml:msub><mml:mi>As</mml:mi><mml:mn>12</mml:mn></mml:m under high pressure. Physical Review B, 2021, 103, .	1.1	0
6597	A first-principles study of a new ternary silicide superconductor Li2IrSi3â€. Journal of Physics: Conference Series, 2021, 1718, 012018.	0.3	0
6598	In situ construction of MoS2@CoS2 spherical hydrangea-shaped clusters for enhanced visible-light photocatalytic degradation of sulfamethoxazole. New Journal of Chemistry, 2021, 45, 5645-5653.	1.4	8
6599	Adsorption of Transition Metal Catalysts on Carbon Supports: A Theoretical Perspective. Johnson Matthey Technology Review, 2022, 66, 4-20.	0.5	1
6600	Earth-abundant iron(<scp>iii</scp>) species serves as a cocatalyst boosting the multielectron reduction of IO₃^{â^'}/I^{â^'}redox shuttle in Z-scheme photocatalytic water splitting. Journal of Materials Chemistry A, 2021, 9, 11718-11725.	5.2	8
6601	Structural Determination of a Graphite/Hexagonal Boron Nitride Superlattice Observed in the Experiment. Inorganic Chemistry, 2021, 60, 2598-2603.	1.9	6
6602	Hexamorphism of Dantrolene: Insight into the Crystal Structures, Stability, and Phase Transformations. Crystal Growth and Design, 2021, 21, 1190-1201.	1.4	16
6603	Narrowing bandgap and enhanced mechanical and optoelectronic properties of perovskite halides: Effects of metal doping. AIP Advances, 2021, 11, .	0.6	37
6604	Influence of molybdenum and technetium doping on visible light absorption, optical and electronic properties of lead-free perovskite CsSnBr₃for optoelectronic applications. RSC Advances, 2021, 11, 2405-2414.	1.7	23
6605	Investigation of vanadiaâ€“alumina catalysts with solid-state NMR spectroscopy and DFT. Physical Chemistry Chemical Physics, 2021, 23, 19352-19363.	1.3	1
6606	Electro-optic modulation in a non-centrosymmetric antiferroelectric crystal. Journal of Materials Chemistry C, 2021, 9, 9431-9435.	2.7	2
6607	A Robust Flow-Through Platform for Organic Contaminant Removal. Cell Reports Physical Science, 2021, 2, 100296.	2.8	8

#	Article	IF	Citations
6608	A series of oxysulfides RE₂M₂S₃O₄(RE = Y, Tm; M = Zr,) Tj ETQq0 0 0 rgBT /Overloc {[M₂S₃O₄]^{8â^'}}_{â^ž}wrinkle layer. Chemical Communications, 2021, 57, 3500-3503.	2.2	9
6609	Mn²⁺/Mn⁴⁺co-doped LaM_{1â^'x}Al_{11â^'y}O₁₉(M) Tj ETQq1 1 0.7843 properties. Dalton Transactions, 2021, 50, 4651-4662.	1.6	19
6610	The modulation effect of electron-rich solvents on the supramolecular networks and photochromic properties of naphthalene diimide molecules. CrystEngComm, 2021, 23, 3356-3363.	1.3	14
6611	Conjugated-Polypyridine-Derivative-Derived Semiconductive Iodoplumbates with Tunable Architectures and Efficient Visible-Light-Induced Photocatalytic Property. Inorganic Chemistry, 2021, 60, 2105-2111.	1.9	10
6612	Theoretical evaluation of the corrosion inhibition performance of aliphatic dipeptides. New Journal of Chemistry, 2021, 45, 3610-3629.	1.4	11
6613	Quantitative insights into the phase behaviour and miscibility of organic photovoltaic active layers from the perspective of neutron spectroscopy. Journal of Materials Chemistry C, 2021, 9, 11873-11881.	2.7	2
6614	Rb₃In(SO₄)₃: a defluorinated mixed main-group metal sulfate for ultraviolet transparent nonlinear optical materials with a large optical band gap. Journal of Materials Chemistry C, 2021, 9, 5124-5131.	2.7	16
6615	Experimental ¹³C and ¹H Solid-State NMR Response in Weakly Tetrel-Bonded Methyl Groups. Journal of Physical Chemistry C, 2021, 125, 2111-2123.	1.5	10
6616	Decoupling the Voltage Hysteresis of Liâ€Rich Cathodes: Electrochemical Monitoring, Modulation Anionic Redox Chemistry and Theoretical Verifying. Advanced Functional Materials, 2021, 31, .	7.8	59
6617	Firstâ€Principles Computational Screening of Dopants to Improve the Deacon Process over RuO₂. ChemCatChem, 2018, 10, 465-469.	1.8	11
6618	Boronâ€“Nitrogenâ€Doped Nanographenes: A Synthetic Tale from Borazine Precursors. Chemistry - A European Journal, 2020, 26, 6608-6621.	1.7	20
6619	Perspectives of fast magicâ€angle spinning ⁸⁷Rb NMR of organic solids at high magnetic fields. Magnetic Resonance in Chemistry, 2021, 59, 162-171.	1.1	1
6620	Rings in Network Glasses: The $$mathrm{B_2O_3}$$ Case. Springer Series in Materials Science, 2015, , 367-414.	0.4	4
6621	A Proposal for Intermediate Band Solar Cells with Optimized Transition Energy in Cr Doped 3C-SiC. Springer Proceedings in Energy, 2015, , 69-76.	0.2	2
6622	EELS modelling using a pseudopotential DFT code. , 2008, , 437-438.		1
6623	Interatomic Potentials. Springer Theses, 2010, , 33-49.	0.0	3
6624	Hydrogen Bonding in Minerals at High Pressures. NATO Science for Peace and Security Series B: Physics and Biophysics, 2010, , 493-501.	0.2	2
6626	Eu3+-doped SrGe4O9 red emitting phosphors: structural, luminescence properties, theoretical calculation and applications. Applied Physics A: Materials Science and Processing, 2020, 126, 1.	1.1	1

#	Article	IF	Citations
6627	Study on phonon spectra and heat capacities of CL-20/MTNP cocrystal and co-formers by density functional theory method. Journal of Molecular Modeling, 2020, 26, 148.	0.8	11
6628	Enhanced Cr(VI) reduction by direct transfer of photo-generated electrons to Cr 3d orbitals in CrO42–intercalated BiOBr with exposed (110) facets. Applied Catalysis B: Environmental, 2020, 277, 119065.	10.8	55
6629	Thermodynamics of the solid solution - Aqueous solution system (Ba,Sr,Ra)SO4 + H2O: I. The effect of strontium content on radium uptake by barite. Applied Geochemistry, 2018, 89, 59-74.	1.4	45
6630	Potential high-T superconductivity in ZrB2 polymorph under pressure. Computational Materials Science, 2020, 176, 109517.	1.4	5
6631	Newly synthesized A-site ordered cubic-perovskite superconductor (Ba0.54K0.46)4Bi4O12: A DFT investigation. Physica C: Superconductivity and Its Applications, 2020, 574, 1353669.	0.6	23
6632	Designing a sp3 structure of carbon T-C9: First-principles calculations. Results in Physics, 2020, 19, 103690.	2.0	16
6633	Electron spin mediated distortion in metallic systems. Scripta Materialia, 2020, 185, 159-164.	2.6	3
6634	Crystal structures and stabilities of AlxGa1-xN and P-Type AlxGa1-xN with different Al compositions: A density functional study. Vacuum, 2020, 173, 109170.	1.6	1
6636	A₆Sb₄F₁₂(SO₄)₃ (A = Rb, Cs): Two Novel Antimony Fluoride Sulfates with Unique Crown-like Clusters. Inorganic Chemistry, 2020, 59, 8345-8352.	1.9	35
6637	Sn₃B₈O₁₅: A Ternary Tin(II) Borate with Flexible [B₈O₁₈]^{12â€“} Fundamental Building Block Formed by [B₇O₁₆]^{11â€“} and [BO₃]^{3â€“} Groups. Inorganic Chemistry, 2021, 60, 883-891.	1.9	8
6638	Size and Crystal Orientation-Dependent Thermal Behaviors of ZnO Nanobelts. Journal of Physical Chemistry C, 2020, 124, 27222-27229.	1.5	2
6639	Structure and Vibrational Spectra of 2,5-Diiodothiophene: A Model for Polythiophene. Journal of Physical Chemistry C, 2017, 121, 12636-12642.	1.5	11
6640	A Muon Spectroscopic and Computational Study of the Microscopic Electronic Structure in Thermoelectric Hybrid Silicon Nanostructures. Journal of Physical Chemistry C, 2020, 124, 9656-9664.	1.5	4
6641	Unoccupied Interface and Molecular States in Thiol and Dithiol Monolayers. Langmuir, 2017, 33, 12056-12064.	1.6	12
6642	Atomic Scale Mechanisms of Multimode Oxide Growth on Nickelâ€“Chromium Alloy: Direct In Situ Observation of the Initial Oxide Nucleation and Growth. ACS Applied Materials & Interfaces, 2021, 13, 1903-1913.	4.0	8
6643	Computationally Directed Discovery of MoBi₂. Journal of the American Chemical Society, 2021, 143, 214-222.	6.6	17
6644	Insights of BO3â€“PO4 replacement for the design and synthesis of a new borateâ€“phosphate with unique 1âˆž[Zn4BO11] chains and two new phosphates. Inorganic Chemistry Frontiers, 2018, 5, 327-334.	3.0	11
6645	The role of hydrogen coverage and location in 1,3-butadiene hydrogenation over Pt/SiO₂. Reaction Chemistry and Engineering, 2020, 5, 87-100.	1.9	18

#	Article	IF	Citations
6646	The crystal structures and mechanical properties of the uranyl carbonate minerals roubaultite, fontanite, sharpite, widenmannite, grimselite and Äejkaite. Inorganic Chemistry Frontiers, 2020, 7, 4197-4221.	3.0	9
6647	The thermal stability of FAPbBr₃nanocrystals from temperature-dependent photoluminescence and first-principles calculations. RSC Advances, 2020, 10, 44373-44381.	1.7	13
6648	Effects of Cr- and Mn-alloying on the band gap tuning, and optical and electronic properties of lead-free CsSnBr₃perovskites for optoelectronic applications. RSC Advances, 2020, 10, 43660-43669.	1.7	26
6649	Theoretical investigations of structural, electronic, and physical properties of Rb2BX6 (Bâ€‰=â€‰Ti, Se, Pd;) Tj ETQq1 1 0.784314 rgB	1.1	11
6650	Accelerating the convergence of auxiliary-field quantum Monte Carlo in solids with optimized Gaussian basis sets. Journal of Chemical Physics, 2020, 153, 194111.	1.2	12
6651	Adsorption of CO, H₂S and CH₄ molecules on SnS₂ monolayer: a first-principles study. Molecular Physics, 2021, 119, .	0.8	9
6652	f90wrap: an automated tool for constructing deep Python interfaces to modern Fortran codes. Journal of Physics Condensed Matter, 2020, 32, 305901.	0.7	27
6653	Phase transformation and its effect on the piezopotential in a bent zinc oxide nanowire. Nanotechnology, 2021, 32, 075404.	1.3	1
6654	Raman spectroscopy and lattice dynamics calculations of tetragonally-structured single crystal zinc phosphide (Zn₃P₂) nanowires. Nanotechnology, 2021, 32, 085704.	1.3	10
6655	Pressure dependent elastic, electronic, superconducting, and optical properties of ternary barium phosphides (BaM ₂P₂; M = Ni, Rh): DFT based insights. Physica Scripta, 2020, 95, 105809.	1.2	27
6656	LDA+U study of hydrostatic pressure effect on double perovskite Sr₂FeNbO₆: crystal structure, mechanical and electronic properties. Physica Scripta, 2020, 95, 115704.	1.2	5
6657	Pressure-dependent physical properties of cubic SrBO3 (B = Cr, Fe) perovskites investigated by density functional theory. Chinese Physics B, 2020, 29, 123101.	0.7	17
6658	Electronic structure and optical properties of Ge- and F-doped Î±-Ga₂O₃: First-principles investigations*. Chinese Physics B, 2020, 29, 126301.	0.7	7
6659	Parameters setup for first-principles on well-formedness and thermodynamic properties of bulk and habit surfaces of Mg2Si. Materials Research Express, 2020, 7, 076513.	0.8	2
6660	Molecular-scale descriptions and experimental characterizations of nitrocellulose soaked in pure liquid ethanol or diethyl ether respectively at room temperature. Materials Research Express, 2020, 7, 105101.	0.8	4
6661	Study of a new layered ternary chalcogenide CuZnTe₂ and its potassium intercalation effect. Materials Research Express, 2020, 7, 105904.	0.8	5
6662	First-principles calculation of the effect of Ti content on the structure and properties of TiVNbMo refractory high-entropy alloy. Materials Research Express, 2020, 7, 106516.	0.8	18
6663	Effect of pressure on the geometric, electronic structure, elastic, and optical properties of the normal spinel MgFe₂O₄: a first-principles study. Materials Research Express, 2020, 7, 106101.	0.8	23

#	Article	IF	Citations
6664	Zero-point energies prevent a trigonal to simple cubic transition in high-pressure sulfur. Electronic Structure, 2020, 2, 045003.	1.0	1
6665	A combined density functional theory and x-ray photoelectron spectroscopy study of the aromatic amino acids. Electronic Structure, 2020, 2, 044005.	1.0	11
6666	Regularised atomic body-ordered permutation-invariant polynomials for the construction of interatomic potentials. Machine Learning: Science and Technology, 2020, 1, 015004.	2.4	46
6667	Position-dependent stability and lifetime of the skyrmion state in nickel-substituted <mml:math xmlns:mml="http://www.w3.org/1998/Math/MathML"><mml:mrow><mml:msub><mml:mi>Cu</mml:mi><mml:mn>1</mml:mn></mml:msub></mml:mrow></mml:math> Physical Review B, 2020, 102, .	1.1	4
6668	Local lattice distortion in high-entropy alloys. Physical Review Materials, 2017, 1, .	0.9	144
6669	Using forces to accelerate first-principles anharmonic vibrational calculations. Physical Review Materials, 2017, 1, .	0.9	5
6670	First-principles prediction of the morphology of <mml:math xmlns:mml="http://www.w3.org/1998/Math/MathML"><mml:mrow><mml:mi>L</mml:mi><mml:msub><mml:mn>1</mml:mn></mml:msub></mml:mrow></mml:math> FePt nanoparticles supported on Mg(Ti)O for heat-assisted magnetic recording applications. Physical Review Materials, 2017, 1, .	0.9	9
6671	Structure of naturally hydrated ferrihydrite revealed through neutron diffraction and first-principles modeling. Physical Review Materials, 2017, 1, .	0.9	11
6672	Band structure, band offsets, substitutional doping, and Schottky barriers of bulk and monolayer InSe. Physical Review Materials, 2017, 1, .	0.9	39
6673	Towards diluted magnetism in TaAs. Physical Review Materials, 2017, 1, .	0.9	3
6674	Defects at the <mml:math xmlns:mml="http://www.w3.org/1998/Math/MathML"><mml:mrow><mml:mtext>Si</mml:mtext><mml:mo>(</mml:mo><mml:mn>001</mml:mn></mml:mrow></mml:math> interface: Analysis of structures generated with classical force fields and density functional theory. Physical Review Materials, 2017, 1, .	0.9	6
6675	Hyperhoneycomb boron nitride with anisotropic mechanical, electronic, and optical properties. Physical Review Materials, 2017, 1, .	0.9	3
6676	Phase diagram of germanium telluride encapsulated in carbon nanotubes from first-principles searches. Physical Review Materials, 2017, 1, .	0.9	10
6677	Postaragonite phases of <mml:math xmlns:mml="http://www.w3.org/1998/Math/MathML"><mml:msub><mml:mi>CaCO</mml:mi><mml:mn>3</mml:mn></mml:msub></mml:math> at lower mantle pressures. Physical Review Materials, 2018, 2, .	0.9	31
6678	Real-space pairwise electrostatic summation in a uniform neutralizing background. Physical Review Materials, 2018, 2, .	0.9	3
6679	Phase transitions of titanite <mml:math xmlns:mml="http://www.w3.org/1998/Math/MathML"><mml:msub><mml:mi>CaTiSiO</mml:mi><mml:mn>5</mml:mn></mml:msub></mml:math> from density functional perturbation theory. Physical Review Materials, 2018, 2, .	0.9	6
6680	Structural and electronic properties of the alkali metal incommensurate phases. Physical Review Materials, 2018, 2, .	0.9	20
6681	Oxygen vacancies and hydrogen in amorphous In-Ga-Zn-O and ZnO. Physical Review Materials, 2018, 2, .	0.9	21

#	Article	IF	Citations
6682	Prediction of pressure-induced stabilization of noble-gas-atom compounds with alkali oxides and alkali sulfides. Physical Review Materials, 2019, 3, .	0.9	20
6683	First-principles calculations of solute transport in zirconium: Vacancy-mediated diffusion with metastable states and interstitial diffusion. Physical Review Materials, 2019, 3, .	0.9	12
6684	van der Waals forces stabilize low-energy polymorphism in <mml:math xmlns:mml="http://www.w3.org/1998/Math/MathML"><mml:mrow><mml:msub><mml:mi mathvariant="normal">B</mml:mi><mml:mn>2</mml:mn></mml:msub><mml:msub><mml:mi mathvariant="normal">O</mml:mi><mml:mn>3</mml:mn></mml:msub></mml:mrow></mml:math> : Implications for the crystallization anomaly. Physical Review Materials, 2019, 3, .	0.9	9
6685	Electronic structure of metallic and insulating phases of vanadium dioxide and its oxide alloys. Physical Review Materials, 2019, 3, .	0.9	11
6686	Stability and electronic properties of GaN phases with inversion symmetry to inherently inhibit polarization. Physical Review Materials, 2019, 3, .	0.9	11
6687	Solubility of deuterium and hydrogen in fcc iron at high pressures and temperatures. Physical Review Materials, 2019, 3, .	0.9	9
6688	Disorder-driven glasslike thermal conductivity in colusite <mml:math xmlns:mml="http://www.w3.org/1998/Math/MathML"><mml:mrow><mml:mi mathvariant="normal">C</mml:mi><mml:msub><mml:mi mathvariant="normal">u</mml:mi><mml:mn>26</mml:mn></mml:msub><mml:msub><mml:mi mathvariant="normal">V</mml:mi><mml:mn>2</mml:mn></mml:msub><mml:mi mathvariant="normal">S</mml:mi><mml:msub><mml:mi mathvariant="normal">n</mml:mi><mml:mn>6	0.9	24
6689	Systematic development of ab initio tight-binding models for hexagonal metals. Physical Review Materials, 2020, 4, .	0.9	3
6690	Electronic structure of amorphous copper iodide: A <mml:math xmlns:mml="http://www.w3.org/1998/Math/MathML"><mml:mi>p</mml:mi></mml:math> -type transparent semiconductor. Physical Review Materials, 2020, 4, .	0.9	10
6691	Phase stabilities of <mml:math xmlns:mml="http://www.w3.org/1998/Math/MathML"><mml:msub><mml:mi>MgCO</mml:mi><mml:mn>3</mml:mn></mml:msub> xmlns:mml="http://www.w3.org/1998/Math/MathML"><mml:msub><mml:mi>MgCO</mml:mi><mml:mn>3</mml:mn></mml:msub> studied by Raman spectroscopy, x-ray diffraction, and density functional theory calculations. Physical	1.9	28
6692	Stability, electronic structures, and band alignment of two-dimensional <mml:math xmlns:mml="http://www.w3.org/1998/Math/MathML"><mml:msub><mml:mi>II</mml:mi><mml:mi>A</mml:mi></mml:msub></mml:ma -IV- <mml:math xmlns:mml="http://www.w3.org/1998/Math/MathML"><mml:msub><mml:mi mathvariant="normal">N</mml:mi><mml:mn>2</mml:mn></mml:msub></mml:math> materials. Physical Review Materials, 2020, 4, .	0.9	8
6693	High-pressure transformations in liquid rubidium. Physical Review Materials, 2020, 4, .	0.9	10
6694	Beryllium polyhydride <mml:math xmlns:mml="http://www.w3.org/1998/Math/MathML"><mml:mrow><mml:msub><mml:mi>Be</mml:mi><mml:mn>4</mml:mn></mml:msub><mml:msub><mml:mi mathvariant="normal">H</mml:mi><mml:mn>8</mml:mn></mml:msub><mml:msub><mml:mrow><mml:mo>(synthesized at high pressure and temperature. Physical Review Materials, 2020, 4, .	0.9	8
6695	Magnetism and NÃ©el skyrmion dynamics in <mml:math xmlns:mml="http://www.w3.org/1998/Math/MathML"><mml:mrow><mml:msub><mml:mi>GaV</mml:mi><mml:mn>4</mml:mn></mml:msub><mml:msub><mml:mi mathvariant="normal">S</mml:mi><mml:mrow><mml:mn>8</mml:mn><mml:mtext>â€“</mml:mtext><mml:mi>y</mml:mi></mml:mrow></mml:msub></mml:mrow></mml:math>. Physical Review Research, 2020, 2, .	1.3	9
6696	Computation of diffuse scattering arising from one-phonon excitations in a neutron time-of-flight single-crystal Laue diffraction experiment. Journal of Applied Crystallography, 2015, 48, 1122-1129.	1.9	6
6697	Investigation of high-pressure planetary ices by cryo-recovery. II. High-pressure apparatus, examples and a new high-pressure phase of MgSO₄Â·5H₂O. Journal of Applied Crystallography, 2018, 51, 692-705.	1.9	14
6698	A new diffractometer for diffuse scattering studies on the ID28 beamline at the ESRF. Journal of Synchrotron Radiation, 2019, 26, 272-279.	1.0	25
6699	Distinguishing nitrogen-containing sites in SiO₂/4H-SiC(0001) after nitric oxide annealing by X-ray absorption spectroscopy. Journal of Synchrotron Radiation, 2019, 26, 462-466.	1.0	10

#	Article	IF	Citations
6700	X-ray diffraction data as a source of the vibrational free-energy contribution in polymorphic systems. IUCrJ, 2019, 6, 558-571.	1.0	10
6701	High-pressure polymorphism in pyridine. IUCrJ, 2020, 7, 58-70.	1.0	12
6702	The structure of kaliophilite KAlSiO₄, a long-lasting crystallographic problem. IUCrJ, 2020, 7, 1070-1083.	1.0	9
6703	The modulated low-temperature structure of malayaite, CaSnOSiO₄. Acta Crystallographica Section B: Structural Science, Crystal Engineering and Materials, 2020, 76, 316-321.	0.5	1
6704	Structural variety of heterosynthons in linezolid cocrystals with modified thermal properties. Acta Crystallographica Section B: Structural Science, Crystal Engineering and Materials, 2020, 76, 892-912.	0.5	4
6705	The ambient hydration of the aluminophosphate JDF-2 to AlPO-53(A): insights from NMR crystallography. Acta Crystallographica Section C, Structural Chemistry, 2017, 73, 191-201.	0.2	6
6706	Intermolecular interactions and disorder in six isostructural celecoxib solvates. Acta Crystallographica Section C, Structural Chemistry, 2020, 76, 632-638.	0.2	6
6707	Phenol hemihydrate: redetermination of the crystal structure by neutron powder diffraction, Hirshfeld surface analysis and characterization of the thermal expansion. Acta Crystallographica Section E: Crystallographic Communications, 2020, 76, 1062-1069.	0.2	1
6708	First-principle calculations of crystal structures, electronic structures, and optical properties of RETaO4 (RE = Y, La, Sm, Eu, Dy, Er). Optical Engineering, 2018, 57, 1.	0.5	6
6709	First-principles calculations of crystal structure, electronic structure and optical properties of RETaO4(RE= Y, La, Sm, Eu, Dy, Er). , 2017, , .		1
6710	Directed assembly of bimetallic nanoarchitectures by interfacial photocatalysis with plasmonic hot electrons. , 2018, , .		3
6711	The view from the high end fortran, parallelism and the HECToR service. ACM SIGPLAN Fortran Forum, 2010, 29, 3-10.	0.5	1
6712	An early evaluation of Intel's optane DC persistent memory module and its impact on high-performance scientific applications. , 2019, , .		35
6713	Application of Vibrational Spectroscopy to the Characterization of Phyllosilicates and other Industrial Minerals. , 0, , 171-226.		7
6714	The Elastic Anisotropic and Thermodynamic Properties of I4mm-B₃C. Acta Physica Polonica A, 2016, 129, 103-107.	0.2	10
6715	Elastic Anisotropic and Thermodynamic Properties of I-4m2-BCN. Acta Physica Polonica A, 2016, 129, 1124-1130.	0.2	13
6716	Hot Compression Test of Heat Resistant Steel. Acta Physica Polonica A, 2017, 131, 1340-1344.	0.2	1
6717	Specific Features of Content Dependences for Energy Gap in In_xTl_{1-x}I Solid State Crystalline Alloys. Acta Physica Polonica A, 2018, 133, 68-75.	0.2	16

#	Article	IF	Citations
6718	Terahertz time-domain spectroscopy of zone-folded acoustic phonons in 4H and 6H silicon carbide. Optics Express, 2019, 27, 3618.	1.7	29
6719	Extrinsic photoluminescence properties of individual micro-particle of Cs₄PbBr₆ perovskite with â€œdefectâ€•structure. Optics Express, 2019, 27, 31207.	1.7	13
6720	Nonlinear optical properties of anisotropic two-dimensional layered materials for ultrafast photonics. Nanophotonics, 2020, 9, 1651-1673.	2.9	26
6721	Studies of the Electronic, Optical, and Thermodynamic Properties for Metal-Doped LiH Crystals by First Principle Calculations. Zeitschrift Fur Naturforschung - Section A Journal of Physical Sciences, 2020, 75, 575-586.	0.7	2
6722	Toward a Comprehensive Mechanistic Understanding of Hydrogen Uptake in Zirconium Alloys by Combining Atom Probe Analysis With Electronic Structure Calculations. , 2015, , 515-539.		3
6723	Structure determination from powder data: Mogul and CASTEP. Zeitschrift FÃ¼r Kristallographie, Supplement, 2009, 2009, 215-220.	0.5	34
6724	Elastic properties of CdTe1â€“xSex(x = 1/16) solid solution: First principles study. Semiconductor Physics, Quantum Electronics and Optoelectronics, 2020, 23, 355-360.	0.3	3
6725	matador: a Python library for analysing, curating and performing high-throughput density-functional theory calculations. Journal of Open Source Software, 2020, 5, 2563.	2.0	7
6726	Theoretical and Spectroscopic Characterization of API-Related Azoles in Solution and in Solid State. Current Pharmaceutical Design, 2020, 26, 4847-4857.	0.9	2
6727	A Possible Pairing Mechanism in Fe-Based High Temperature Superconductors. The Open Condensed Matter Physics Journal, 2008, 1, 13-18.	0.2	2
6728	Electronic Properties of Bulk and Single-Layer MoS2 Using ab Initio DFT: Application of Spin-Orbit Coupling (SOC) Parameters. East European Journal of Physics, 2020, , .	0.1	3
6729	The First Principles Investigation of Structural, Electronic, Mechanical and Lattice Dynamical Properties of the B and N Doped M2AX Type MAX Phases Ti2AlB0.5C0.5 and Ti2AlN0.5C0.5 Compounds. Journal of Boron, 0, , .	0.0	7
6730	First-Principles Forecast of Gapless Half-Metallic and Spin-Gapless Semiconducting Materials: Case Study of Inverse Ti2CoSi-Based Compounds. Applied Sciences (Switzerland), 2020, 10, 782.	1.3	3
6731	Comparative Computational Study of L-Amino Acids as Green Corrosion Inhibitors for Mild Steel. Computation, 2021, 9, 1.	1.0	21
6732	Atomic-Approach to Predict the Energetically Favored Composition Region and to Characterize the Short-, Medium-, and Extended-Range Structures of the Ti-Nb-Al Ternary Metallic Glasses. Materials, 2019, 12, 432.	1.3	1
6733	Insights on Substitution Preference of Pb Ions in Sulfoaluminate Cement Clinker Phases. Materials, 2021, 14, 44.	1.3	10
6734	Removal Mechanism Investigation of Ultraviolet Induced Nanoparticle Colloid Jet Machining. Molecules, 2021, 26, 68.	1.7	7
6735	First Principles Study on the Structural, Elastic, Electronic and Optical Properties of Cubic â€˜Half-Heuslerâ€™ Alloy RuVAs Under Pressure. International Journal of Material and Mathematical Sciences, 2020, , 51-63.	0.2	4

#	Article	IF	Citations
6736	High-Pressure Transformations and Ionic Conductivity in Low-Z Complex Hydride LiBH4. Review of High Pressure Science and Technology/Koatsuryoku No Kagaku To Gijutsu, 2011, 21, 213-220.	0.1	7
6737	Comparison of Functionals for Metal Hexaboride Band Structure Calculations. Modeling and Numerical Simulation of Material Science, 2014, 04, 53-69.	0.5	7
6738	Electron Density Response to Phonon Dynamics in MgB₂: An Indicator of Superconducting Properties. Modeling and Numerical Simulation of Material Science, 2018, 08, 21-46.	0.5	6
6739	The electronic structure and optical properties of P-doped silicon nanotubes. Wuli Xuebao/Acta Physica Sinica, 2014, 63, 067102.	0.2	4
6740	Terahertz study of L-asparagine and its monohydrate. Wuli Xuebao/Acta Physica Sinica, 2014, 63, 133203.	0.2	5
6741	First-principle study of the effects of oxygen vacancy on the electronic structure and the absorption spectrum of ZnO. Wuli Xuebao/Acta Physica Sinica, 2014, 63, 147101.	0.2	7
6742	First-principles investigations on tetragonal distortion, electronic structure, magnetism, and phonon dispersion of Ga2XCr (X = Mn, Fe, Co, Ni, Cu) Heusler alloys. Wuli Xuebao/Acta Physica Sinica, 2015, 64, 077104.	0.2	2
6743	Density functional theory study of structure stability and electronic structures of graphyne derivatives. Wuli Xuebao/Acta Physica Sinica, 2016, 65, 133101.	0.2	2
6744	Terahertz spectrum study of organic electro-optic crystal 4-N, N-dimethylamino-4'-N'-methyl-stilbazolium tosylate. Wuli Xuebao/Acta Physica Sinica, 2017, 66, 244211.	0.2	3
6745	Electronic structures and ferroelectric properties of Ba-doped ZnO. Wuli Xuebao/Acta Physica Sinica, 2018, 67, 107701.	0.2	2
6746	First principle study of nonlinear optical crystals. Wuli Xuebao/Acta Physica Sinica, 2018, 67, 114203.	0.2	9
6747	First principle study of influence of transition metal (Cr, Mn, Fe, Co) doping on magnetism of TiO₂. Wuli Xuebao/Acta Physica Sinica, 2020, 69, 197101.	0.2	2
6748	Exploring the Temperature Dependent Solid-State ALC Spectrum of the C₆H₆Mu^{â€¢}Radical with Ab-Initio Simulation Techniques. , 2018, , .		1
6749	Phase Stability and Electronic Structure of In-Free Photovoltaic Materials Cu₂IISnSe₄(II: Zn, Cd, Hg). Japanese Journal of Applied Physics, 2011, 50, 05FF01.	0.8	25
6750	On the Excess Shear Modulus in Relating to Martensitic Transformation in Steel. Journal of Smart Processing, 2013, 2, 128-133.	0.0	1
6751	Effects of Fe Substitution on Lithium Incorporation into Muscovite. Journal of the Mineralogical Society of Korea, 2015, 28, 127-133.	0.2	2
6752	Sol-Gel Synthesis, Crystal Structure and Electronic Properties in Bi2+xAlxNi4-3xO7+Î´ (0.0 â‰¤ x â‰¤ 0.75) Composite Oxides. International Research Journal of Pure and Applied Chemistry, 2011, 1, 30-41.	0.2	1
6753	A new rare-earth borate birefringent crystal with quasi-two-dimensional [BO₃] layers. Journal of Materials Chemistry C, 2021, 9, 15886-15890.	2.7	11

#	Article	IF	Citations
6754	Ab initio molecular dynamics with enhanced sampling in heterogeneous catalysis. Catalysis Science and Technology, 2022, 12, 12-37.	2.1	29
6755	K₂ZnMoP₂O₁₀: a novel nonlinear optical molybdophosphate with a strong second harmonic generation response and moderate birefringence. Journal of Materials Chemistry C, 2021, 9, 15321-15328.	2.7	14
6756	The crystalline sponge method: quantum chemical in silico derivation and analysis of guest binding energies. CrystEngComm, 2021, 23, 7570-7575.	1.3	2
6757	Tuning the Electronic Structure of Monolayer MgI2 by Biaxial Strain and External Electric Field. Modern Physics, 2021, 11, 99-108.	0.1	1
6758	Structural, optical, dielectric and electrical transport properties of a [Mg(H2O)6]2+-templated proton conducting, semiconducting and photoresponsive 3D hydrogen bonded supramolecular framework. New Journal of Chemistry, 0, , .	1.4	1
6759	THz/Far infrared synchrotron observations of superlattice frequencies in MgB₂. Physical Chemistry Chemical Physics, 2021, 23, 23922-23932.	1.3	2
6760	Studies on activation factors for oxidative coupling of methane over lithium-based silicate/germanate catalysts. Catalysis Science and Technology, 2022, 12, 75-83.	2.1	1
6761	First-Principles study on the mechanical properties of Cu3Si compound. , 2021, , .		0
6762	Achieving Shortâ€Wavelength Phaseâ€Matching Second Harmonic Generation in Boronâ€Rich Borosulfate with Planar [BO₃] Units. Angewandte Chemie - International Edition, 2022, 61, .	7.2	50
6763	Quantifying Mechanical Properties of Molecular Crystals: A Critical Overview of Experimental Elastic Tensors. Angewandte Chemie, 2022, 134, .	1.6	7
6764	Gramâ€Scale Synthesis of Nanosized Li₃HoBr₆ Solid Electrolyte for Allâ€Solidâ€State Liâ€Se Battery. Small Methods, 2021, 5, e2101002.	4.6	22
6765	Metal-Free Z-Scheme aza-CMP/C₂N Heterostructure to Facilitate Photocatalytic CO₂ Reduction: A Computational Study. Journal of Physical Chemistry C, 2021, 125, 23133-23141.	1.5	4
6766	Refractive indexÂof graphene AA and AB stacked bilayers under the influence of relative planar twisting. Journal of Physics Condensed Matter, 2022, 34, 015302.	0.7	3
6767	Molecular Mechanism of Gas Diffusion in Ice-Ih. ACS Earth and Space Chemistry, 2021, 5, 3258-3267.	1.2	1
6768	Nonexistence of the sâ˜f volume-collapse transition in solid gadolinium at pressure. Physical Review B, 2021, 104, .	1.1	1
6769	Diamond Coating Reduces Nuclear Fuel Rod Corrosion at Accidental Temperatures: The Role of Surface Electrochemistry and Semiconductivity. Materials, 2021, 14, 6315.	1.3	3
6770	Strong SHG Responses in a Berylliumâ€Free Deepâ€UVâ€Transparent Hydroxyborate via Covalent Bond Modification. Angewandte Chemie - International Edition, 2021, 60, 27151-27157.	7.2	50
6771	Firstâ€Principles Calculations of Electronic Structure and Optical Properties of Siâ€Doped and VacancyÂÎ²â€Ga₂O₃. Crystal Research and Technology, 2022, 57, .	0.6	7

#	Article	IF	Citations
6772	Mechanochemical Synthesis and Physicochemical Characterization of Previously Unreported Praziquantel Solvates with 2-Pyrrolidone and Acetic Acid. Pharmaceutics, 2021, 13, 1606.	2.0	10
6773	Crystal engineering of supramolecular 1,4â€benzene bisamides by side chain modification â€towards tuneable anisotropic morphologies and surfaces. ChemPhysChem, 2021, 22, 2585.	1.0	2
6774	Excitonic effect in black phosphorus oxides. 2D Materials, 2022, 9, 015007.	2.0	2
6775	Experimental and Theoretical Investigations of Terahertz Spectra of the Structural Isomers: Mannose and Galactose. Journal of Spectroscopy, 2021, 2021, 1-9.	0.6	3
6776	Propiedades MecÃ¡nicas del Î²-MnO2 por DFT. Revista De Ciencias TecnolÃ“gicas, 2021, 4, 224-233.	0.0	0
6777	Tailoring the morphology of BiNbO4 of polymorph in 2D nanosheets for enhancement of photocatalytic activity in the visible range. Physica E: Low-Dimensional Systems and Nanostructures, 2022, 136, 115009.	1.3	4
6778	Hybrid Metalâ€Halide Infrared Nonlinear Optical Crystals of (TMEDA)MI₅ (M = Sb, Bi) with High Stability. Advanced Optical Materials, 2021, 9, 2101333.	3.6	20
6779	Reconstructing Reliable Powder Patterns from Spikelets (Q)CPMG NMR Spectra: Simplification of UWNMR Crystallography Analysis. Molecules, 2021, 26, 6051.	1.7	3
6780	Density Functional Theoryâ€Based Prediction of the Pressureâ€Dependent Magnetic Properties of CaRuO₃. Physica Status Solidi (B): Basic Research, 2022, 259, 2100290.	0.7	1
6781	High-Pressure Synthesis of Bulk Cobalt Cementite, Co₃C. Chemistry of Materials, 2021, 33, 9601-9607.	3.2	2
6782	Quantifying Mechanical Properties of Molecular Crystals: A Critical Overview of Experimental Elastic Tensors. Angewandte Chemie - International Edition, 2022, 61, .	7.2	18
6783	Significant enhancement of electrical conductivity by incorporating carbon fiber into CoSb3 thermoelectric skutterudite fabricated by spark plasma sintering method. Journal of Materials Science, 2021, 56, 20138-20153.	1.7	1
6784	Fast and Accurate Electric Field Gradient Calculations in Molecular Solids With Density Functional Theory. Frontiers in Chemistry, 2021, 9, 751711.	1.8	4
6785	Phosphorus Substitution Preference in Yeâ€™elimite: Experiments and Density Functional Theory Simulations. Materials, 2021, 14, 5874.	1.3	3
6786	Strong SHG Responses in a Berylliumâ€Free Deepâ€UVâ€Transparent Hydroxyborate via Covalent Bond Modification. Angewandte Chemie, 2021, 133, 27357.	1.6	9
6787	Modeling the Structure of Crystalline Alamethicin and Its NMR Chemical Shift Tensors. Antibiotics, 2021, 10, 1265.	1.5	0
6788	First-principles investigations of the geometric structures and electronic properties of pristine and Ag/Au-doped Janus MoSSe/C60 and WSSe/C60 heterostructures. Applied Surface Science, 2022, 575, 151660.	3.1	5
6789	Adhesion strength, stability and electronic properties of TiB2 reinforced copper matrix composites: A first principles study. Physica B: Condensed Matter, 2021, , 413457.	1.3	1

#	Article	IF	Citations
6790	Metal-catalyst-free gas-phase synthesis of long-chain hydrocarbons. Nature Communications, 2021, 12, 5937.	5.8	7
6791	Influence of anharmonicity and interlayer interaction on Raman spectra in mono- and few-layer MoS2: A computational study. Physica E: Low-Dimensional Systems and Nanostructures, 2022, 136, 114999.	1.3	9
6792	Compensating Electronic Effect Enables Fast Siteâ€toâ€Site Electron Transfer over Ultrathin RuMn Nanosheet Branches toward Highly Electroactive and Stable Water Splitting. Advanced Materials, 2021, 33, e2105308.	11.1	73
6793	Interpolation between W Dopant and Co Vacancy in CoOOH for Enhanced Oxygen Evolution Catalysis. Advanced Materials, 2022, 34, e2104667.	11.1	45
6794	Syntheses, Structures and Properties of Alkali and Alkaline Earth Metal Diamond-Like Compounds Li2MgMSe4 (M = Ge, Sn). Materials, 2021, 14, 6166.	1.3	6
6795	GaSeCl₅O: A Molecular Compound with Very Strong SHG Effect. Inorganic Chemistry, 2021, 60, 15653-15658.	1.9	11
6796	Computational Study of A15 Ru-Based Alloys for High-Temperature Structural Applications. , 0, , .		0
6797	Effective Repeatable Mechanoluminescence in Heterostructured Li_{1â^'}_xNa_xNbO₃: Pr³⁺. Small, 2021, 17, e2103441.	5.2	26
6798	Adsorption performance and mechanism of the commonly used collectors with Oxygen-containing functional group on the ilmenite surface: A DFT study. Journal of Molecular Liquids, 2022, 346, 117829.	2.3	20
6799	Interplay between Local Structure and Nuclear Dynamics in Tungstic Acid: A Neutron Scattering Study. Journal of Physical Chemistry C, 2021, 125, 23864-23879.	1.5	4
6800	Copper(I) iodide-based organicâ€“inorganic hybrid compounds as phosphor materials. Zeitschrift Fur Naturforschung - Section B Journal of Chemical Sciences, 2021, 76, 759-764.	0.3	6
6801	A Novel BN Polymorph in P4/mbm Phase with a (4,4) Nanotube. Physica Status Solidi (B): Basic Research, 2022, 259, 2100333.	0.7	7
6802	Achieving Shortâ€Wavelength Phaseâ€Matching Second Harmonic Generation in Boronâ€Rich Borosulfate with Planar [BO₃] Units. Angewandte Chemie, 2022, 134, e202112844.	1.6	3
6803	Quantification of the Properties of Organic Molecules Using Coreâ€Loss Spectra as Neural Network Descriptors. Advanced Intelligent Systems, 0, , 2100103.	3.3	1
6804	Interfacial charge transfer and enhanced photocatalytic mechanisms for Pt nanoparticles loaded onto sulfur-doped g-C3N4 in H2 evolution. Materials Today Energy, 2021, 22, 100881.	2.5	9
6805	A comprehensive study of the structural, elastic, electronic, and optical properties of the tetragonal sodium chalcogenides NaAlX₂ (Xâ€‰=â€‰O, S, Se, Te). Philosophical Magazine, 2022, 102, 69-94.	0.7	0
6806	New Covalent Triazine Framework Rich in Nitrogen and Oxygen as a Host Material for Lithiumâ€“Sulfur Batteries. ACS Applied Materials & Interfaces, 2021, 13, 50258-50269.	4.0	16
6807	Intrinsic mechanical and interfacial characteristics of precipitates contributing to the room and elevated temperature strength in Mgâ€“Snâ€“Y alloys. Journal of Materials Research and Technology, 2021, 15, 3928-3941.	2.6	7

#	Article	IF	Citations
6808	Atomically dispersed Ta and Co dual activity sites for synergetic electroreduction I3â˜. Solar Energy, 2021, 228, 486-494.	2.9	1
6809	Developing feature-rich electronic and magnetic properties in the Î²-As monolayer for spintronic and optoelectronic applications by C and Si doping: A first-principles study. Surfaces and Interfaces, 2021, 27, 101534.	1.5	1
6810	Promotion of oxidation pretreatment on sulfidation of cuprite surface and its contribution to flotation. Minerals Engineering, 2021, 174, 107256.	1.8	7
6811	Potential valorization of granitic waste material as microproppant for induced unpropped microfractures in shale. Journal of Natural Gas Science and Engineering, 2021, 96, 104281.	2.1	4
6812	Electronic and optical properties of adsorbed of Zr-atom on vacancy-defective graphene: First principles calculations. Computational and Theoretical Chemistry, 2021, 1206, 113468.	1.1	1
6814	Ab Initio Quantum Chemistry and Semi-Empirical Description of Solid State Phases Under High Pressure: Chemical Applications. NATO Science for Peace and Security Series B: Physics and Biophysics, 2010, , 325-339.	0.2	0
6816	Synthesis and Structureâ€“Property Relations of Binary Transition Metal Carbides at Extreme Conditions. NATO Science for Peace and Security Series B: Physics and Biophysics, 2010, , 397-406.	0.2	0
6817	Simulation of surface segregation of in to Al(001) surface. Wuli Xuebao/Acta Physica Sinica, 2010, 59, 5641.	0.2	2
6819	A Combined Bond-Valence and Periodic DFT Study of the Active Sites in M1 Phase of MoVTeNbO Composite Oxide Catalyst. Chinese Journal of Catalysis, 2010, 31, 1286-1292.	6.9	0
6820	Ab initio calculation of pressure-induced phase transition of TiN polytypes. Wuli Xuebao/Acta Physica Sinica, 2011, 60, 057102.	0.2	1
6821	Electronic structure and magnetism of Cr-doped ZnO nanowires. Wuli Xuebao/Acta Physica Sinica, 2011, 60, 127503.	0.2	1
6822	Influence of natural impurity on electronic structure and catalytic activity of pyrite. Wuli Xuebao/Acta Physica Sinica, 2011, 60, 097801.	0.2	1
6823	Projector Self-Consistent DFT+U Using Nonorthogonal Generalised Wannier Functions. , 2012, , 65-88.		0
6824	Electronic structure and optical properties of 0.5NdAlO3-0.5CaTiO3 from first-principles calculation. Wuli Xuebao/Acta Physica Sinica, 2012, 61, 077702.	0.2	3
6825	First-principles study on the effects of high Al doped on the band gap and absorption spectrum of ZnO. Wuli Xuebao/Acta Physica Sinica, 2012, 61, 167102.	0.2	3
6826	The Alloying of Ti, C, N in Bulk -Fe and Their Effects on Bond Characters. Wuli Xuebao/Acta Physica Sinica, 2012, 61, 127101.	0.2	5
6827	A First Principles Simulation Framework for the Interactions between a Si(001) Surface and a Scanning Probe. Journal of Surface Engineered Materials and Advanced Technology, 2012, 02, 194-202.	0.2	0
6828	New insights into oxidation properties and band structure of fluorescein dyes from ab initio calculations. Highlights in Theoretical Chemistry, 2013, , 11-19.	0.0	0

#	Article	IF	Citations
6830	Lightwave Refraction and Its Consequences: A Viewpoint of Microscopic Quantum Scatterings by Electric and Magnetic Dipoles. , 0, , .		0
6831	Linear-Scaling Methods. Springer Theses, 2013, , 23-44.	0.0	0
6832	First-principle study on the effect of high Ga doping on the optical band gap and the band-edge of optical absorption of ZnO. Wuli Xuebao/Acta Physica Sinica, 2013, 62, 157101.	0.2	6
6833	Theoretical Spectroscopy. Springer Theses, 2013, , 45-58.	0.0	1
6834	First-principles study on the effect of high Mn doped on the band gap and absorption spectrum of ZnO. Wuli Xuebao/Acta Physica Sinica, 2013, 62, 037101.	0.2	0
6835	First-Principles Study of Electronic Structure and Optical Properties of (Zr-Al) Codoped ZnO. , 2013, , .		0
6836	Effect of concentration of heavy oxygen vacancy in rutile and anatase (TiO2) on electric conductivity performance studied by simulation and calculation. Wuli Xuebao/Acta Physica Sinica, 2013, 62, 237101.	0.2	5
6837	First-principles study on the electronic structure and optical properties of RDX. Wuli Xuebao/Acta Physica Sinica, 2013, 62, 163102.	0.2	4
6838	First principles calculations of solid phase transition of nitromethane. Wuli Xuebao/Acta Physica Sinica, 2014, 63, 098105.	0.2	3
6839	Impact of (Al, Ga, In) and 2N preferred orientation heavy co-doping on conducting property of ZnO. Wuli Xuebao/Acta Physica Sinica, 2014, 63, 057101.	0.2	3
6840	The Dynamics of Cyclopentadienyl on Cu(111). Springer Theses, 2014, , 71-104.	0.0	0
6841	Electronic structures and phase instabilities of cubic Na1/2Bi1/2TiO3 and K1/2Bi1/2TiO3ï¼š a first-principles comparative study. Wuli Xuebao/Acta Physica Sinica, 2014, 63, 167101.	0.2	0
6842	First-principle study on the effects of Tl doping on the band gap and the band-edge of optical absorption of InI. Wuli Xuebao/Acta Physica Sinica, 2014, 63, 147102.	0.2	3
6843	Theoretical Assessment of the Mechanical, Electronic, and Vibrational Properties of the Paramagnetic Insulating Cerium Dioxide and Investigation of Intrinsic Defects. Advances in Chemical and Materials Engineering Book Series, 2014, , 431-446.	0.2	0
6844	The Atomic-Scale Motion of Thiophene on Cu(111). Springer Theses, 2014, , 143-168.	0.0	0
6845	Quantum Influences in the Diffusive Motion of Pyrrole on Cu(111). Springer Theses, 2014, , 105-141.	0.0	0
6846	Application of Computational Mineralogy to Studies of Hydroxyls in Clay Minerals. Journal of the Mineralogical Society of Korea, 2014, 27, 271-281.	0.2	1
6847	Molecular Dynamics Simulation: From â€œAb Initioâ€•to â€œCoarse Grainedâ€• , 2015, , 1-61.		0

#	Article	IF	Citations
6848	10.3 Introduction to surface phonons. , 2015, , 586-615.		0
6849	First-Principles Methods. Springer Theses, 2015, , 39-61.	0.0	0
6850	Local Structure Analysis of Graphitic Carbon Particles by Using Soft X-ray Absorption Spectroscopy and the First-principle Calculations. Journal of the Society of Powder Technology, Japan, 2015, 52, 515-522.	0.0	0
6852	Linear Finite Element Analysis of Nanotubes. Engineering Materials, 2016, , 63-106.	0.3	0
6854	The Singlet-Triplet Splitting of Ethylene Interacting with the Cu(100) Surface and with Small Copper Clusters. Himia, Fizika Ta Tehnologia Poverhni, 2015, 6, 42-55.	0.2	0
6856	Theoretical Predication of the Synthesis of ReNCl. , 2016, , .		0
6857	Site preference in isoelectronic Heusler alloy Fe2RuSi. Wuli Xuebao/Acta Physica Sinica, 2016, 65, 147102.	0.2	5
6858	Development and Validation of High-Throughput Crystallisation and Analysis (HTCAA) Methodology for Physical Form Screening. Springer Theses, 2016, , 39-75.	0.0	0
6859	Nanocluster-Assembled Materials. , 2016, , 127-162.		0
6860	Chapter 2 Manganese Dioxide Absorbents. , 2016, , 31-78.		0
6861	Chapter 5 Other Absorbents. , 2016, , 163-188.		0
6862	Gas Detection in Humid Atmosphere Using In2O3- and SnO2-Based Sensors. Ukrainian Journal of Physics, 2017, 62, 249-255.	0.1	0
6863	A Comparative Study of the Effect of Strain on the Electronic and Optical Properties of Filled and Unfilled Ba₈Si₄₆ Type I-clathrate. Acta Physica Polonica A, 2017, 132, 836-838.	0.2	0
6864	Elastic Anisotropic and Thermodynamic Properties of Two BC7 Phases. Acta Physica Polonica A, 2017, 132, 1340-1346.	0.2	1
6865	First-Principles Investigation of Magnesium Ion Adsorptions and Diffusions on 1H-Monolayer MoS2 for Energy Storages. , 2018, , 313-321.		0
6866	Future. Springer Series in Surface Sciences, 2018, , 549-562.	0.3	0
6867	Theoretical Methods of Surface Dynamics. Springer Series in Surface Sciences, 2018, , 117-142.	0.3	0
6868	Modeling of Non-Covalent Interactions of Vat Dyes with Carbon Nitride Fragments. Bulletin of the South Ural State University Series Chemistry, 2018, 10, 37-42.	0.3	0

#	Article	IF	Citations
6869	Lityum Bor KarbÃ¼r (LiBC) BileÅŸiÄŸinin YapÄ±sal, Elektronik ve Mekanik Ã–zelliklerinin BasÄ±nÃ§ AltÄ±nda DeÄŸiÅŸimi. Journal of the Faculty of Engineering and Architecture of Gazi University, 2018, 33, .	0.3	0
6870	A Computational Mineralogy Study of the Crystal Structure and Stability of Aluminum Silicate (Al₂SiO₅) Minerals. Journal of the Mineralogical Society of Korea, 2018, 31, 13-22.	0.2	0
6871	Icosahedral (H2)13 supermolecule. Physical Review Materials, 2018, 2, .	0.9	0
6873	Effects of Si and Y co-doping on stability and oxidation resistance of <i>Î³</i>-TiAl based alloys. Wuli Xuebao/Acta Physica Sinica, 2019, 68, 196101.	0.2	3
6874	Competitive adsorption of CO and H₂ on strained Fe(110) surface. Wuli Xuebao/Acta Physica Sinica, 2019, 68, 217103.	0.2	2
6875	First-principles study of five isomers of two-dimensional GeSe under in-plane strain. Wuli Xuebao/Acta Physica Sinica, 2019, 68, 113103.	0.2	5
6876	Electronic and optical properties of n-pr co-doped anatase TiO₂ from first-principles. Wuli Xuebao/Acta Physica Sinica, 2019, 68, 017401.	0.2	13
6877	First-Principles to Study the Electronic Structure of CuAlO₂ Materials. Material Sciences, 2019, 09, 447-457.	0.0	0
6878	Prediction of the fundamental properties of novel Be-B-Ta-based ternary compounds from first-principles calculations. Physical Review Materials, 2019, 3, .	0.9	3
6880	Simulation Studies for Black Phosphorus: From Theory to Experiment. Engineering Materials, 2020, , 101-115.	0.3	0
6882	Polymorphism and phase transformation in the dimethyl sulfoxide solvate of 2,3,5,6-tetrafluoro-1,4-diiodobenzene. Acta Crystallographica Section C, Structural Chemistry, 2020, 76, 524-529.	0.2	0
6883	Syntheses, characterization and calculations of LimAnM6O15 (A=Rb, Cs; M=Si, Ge; m+n=6). Science China Materials, 2020, 63, 1769-1778.	3.5	14
6885	Exploration of optoelectronic, nonlinear and charge transport properties of hydroquinoline derivatives by DFT approach. Materials Science-Poland, 2020, 38, 284-295.	0.4	0
6886	Electron localisation descriptors in ONETEP: a tool for interpreting localisation and bonding in large-scale DFT calculations. Electronic Structure, 2020, 2, 027001.	1.0	10
6887	Raman and infrared phonons in tetragonal ZnP₂and CdP₂crystals: a density functional study. Journal of Physics Condensed Matter, 2020, 32, 445401.	0.7	2
6888	Research on the anisotropic mechanical behavior of microscale Sn58Bi solder matrix via finite element simulation. , 2020, , .		0
6889	Density functional theory studies of hydrogen bonding vibrations in sI gas hydrates. New Journal of Physics, 2020, 22, 093066.	1.2	6
6891	Computational Auxiliary for the Progress of Sodium-Ion Solid-State Electrolytes. ACS Nano, 2021, 15, 17232-17246.	7.3	42

#	Article	IF	Citations
6892	Trifluoromethylâ€Group Bearing, Hydrophobic Bulky Cations as Defect Passivators for Highly Efficient, Stable Perovskite Solar Cells. Solar Rrl, 2021, 5, 2100712.	3.1	11
6893	Experimental and Theoretical Solid-State ²⁹Si NMR Studies on Defect Structures in La_{9.33+x}(SiO₄)₆O_{2+1.5x} Apatite Oxide Ion Conductors. Inorganic Chemistry, 2021, 60, 16817-16825.	1.9	5
6894	Excess heat capacity and entropy of mixing along the hydroxyapatite-chlorapatite and hydroxyapatite-fluorapatite binaries. Physics and Chemistry of Minerals, 2021, 48, 44.	0.3	2
6895	Orbital Mapping of Semiconducting Perylenes on Cu(111). Journal of Physical Chemistry C, 2021, 125, 24477-24486.	1.5	2
6896	Colloidal Cu-Zn-Sn-Te Nanocrystals: Aqueous Synthesis and Raman Spectroscopy Study. Nanomaterials, 2021, 11, 2923.	1.9	7
6897	Lithium Storage Performance Boosted via Delocalizing Charge in Zn_xCo_{1â”}_xPS₃/CoS₂ of 2D/3D Heterostructure. Small, 2022, 18, e2104295.	5.2	13
6898	Reductive Adsorption of Atmospheric Oxidized Mercury on Ice: Insights from Density Functional Calculations. ACS Earth and Space Chemistry, 0, , .	1.2	1
6899	Theoretical prediction of the structural, electronic and optical properties of vacancy-ordered double perovskites Tl2TiX6 (X = Cl, Br, I). Journal of Solid State Chemistry, 2022, 305, 122684.	1.4	10
6900	Spectroscopic Signatures of Hydrogen-Bonding Motifs in Protonic Ionic Liquid Systems: Insights from Diethylammonium Nitrate in the Solid State. Journal of Physical Chemistry C, 2021, 125, 24463-24476.	1.5	4
6901	Examination of proline, hydroxyproline and pyroglutamic acid with different polar groups by terahertz spectroscopy. Spectrochimica Acta - Part A: Molecular and Biomolecular Spectroscopy, 2022, 267, 120539.	2.0	8
6902	Subnanometer high-entropy alloy nanowires enable remarkable hydrogen oxidation catalysis. Nature Communications, 2021, 12, 6261.	5.8	169
6903	Photoinduced electron transfer properties of 4-phenyl-Pyridine-N-Oxide and its coordination compound. Dyes and Pigments, 2022, 197, 109917.	2.0	2
6904	A first-principle investigate about the different response of birefringence and SHG from AB3O6 (A= Bi,) Tj ETQq0 0 0 rgBT /Overlock 10 T	1.2	0
6905	Properties of RbHgF3 fluoro-perovskite under growing hydrostatic pressure from first-principles calculations. AIP Advances, 2021, 11, .	0.6	9
6906	Adsorption of La on kaolinite (0 0 1) surface in aqueous system: A combined simulation with an experimental verification. Journal of Molecular Liquids, 2022, 347, 117956.	2.3	12
6907	211-MAX borides: The stable boron-substituted 211-MAX compounds by first-principles. Materials Today Communications, 2020, 25, 101689.	0.9	2
6909	New Spiral Form of Carbon Nitride with Ultrasoftness and Tunable Electronic Structures. ACS Omega, 2021, 6, 516-522.	1.6	3
6910	New insight of Ca element refining grain structure in commercial purity Mg based on the first-principle calculation. International Journal of Cast Metals Research, 2021, 34, 6-13.	0.5	2

#	Article	IF	Citations
6911	Analysis of the effects of alloying with Si and Cr on the properties of manganese austenite based on AB INITIO modelling. Eastern-European Journal of Enterprise Technologies, 2020, 6, 28-36.	0.3	3
6912	First principles study of structural, electronic and optical properties of orthorhombic phase Ni-doped Bi2Se3 using density functional theory. Computational Condensed Matter, 2020, 25, e00510.	0.9	8
6914	Diabat method for polymorph free energies: Extension to molecular crystals. Journal of Chemical Physics, 2020, 153, 244105.	1.2	1
6915	High-Pressure Neutron Powder Diffraction Study of Îµ-CL-20: A Gentler Way to Study Energetic Materials. Journal of Physical Chemistry C, 2020, 124, 27985-27995.	1.5	9
6916	An investigation of vacancy defects on electronic and magnetic properties of TlN nanosheet: By density function calculation. Solid State Communications, 2022, 341, 114576.	0.9	1
6917	Oxidation mechanism of the arsenopyrite surface by oxygen with and without water: Experimental and theoretical analysis. Applied Surface Science, 2022, 573, 151574.	3.1	14
6918	DIMS: A tool for setting up defects and impurities CASTEP calculations. Computational Materials Science, 2022, 202, 110976.	1.4	6
6919	Rare earth La single atoms supported MoO3-x for efficient photocatalytic nitrogen fixation. Applied Catalysis B: Environmental, 2022, 301, 120766.	10.8	76
6920	Enhanced photocatalytic Hg0 oxidation activity of iodine doped bismuth molybdate (Bi2MoO6) under visible light. Journal of Colloid and Interface Science, 2022, 607, 1864-1875.	5.0	18
6921	Regulation of impedance matching feature and electronic structure of nitrogen-doped carbon nanotubes for high-performance electromagnetic wave absorption. Journal of Materials Science and Technology, 2022, 108, 1-9.	5.6	5
6922	Enhanced photoelectrocatalytic performance of Î±-MnO₂ by Sb and N charge compensation. New Journal of Chemistry, 2021, 45, 22261-22268.	1.4	0
6923	Tuning MoSO monolayer properties for optoelectronic and spintronic applications: effect of external strain, vacancies and doping. RSC Advances, 2021, 11, 35614-35623.	1.7	6
6924	Uncovering the missing piece of unsaturated two-dimensional phosphorus: a theoretical approach. Journal of Materials Chemistry C, 2021, 9, 16771-16777.	2.7	1
6925	Surface Phonons: Theoretical Methods and Results. Springer Handbooks, 2020, , 737-782.	0.3	2
6926	Application IO Analysis with Lustre Monitoring Using LASSi for ARCHER. Lecture Notes in Computer Science, 2020, , 255-266.	1.0	0
6927	Topotactic desolvation and condensation reactions of 3D Zn3TiF7(H2O)2(taz)3Â·S (S = 3H2O or C2H5OH). Dalton Transactions, 2020, 49, 17758-17771.	1.6	1
6928	Open-Science Platform for Computational Materials Science: AiiDA and the Materials Cloud. , 2020, , 1813-1835.		1
6929	Effects of Defects and Doping on an Al Atom Adsorbed on Graphene: A First-Principles Investigation. Coatings, 2020, 10, 131.	1.2	1

#	Article	IF	Citations
6930	Revealing the crystal structures and relative dielectric constants of fluorinated silicon oxides. Journal of Materials Chemistry C, 2021, 9, 15983-15989.	2.7	3
6931	The crystal structures of Fe-bearing MgCO₃sp²- andsp³-carbonates at 98â€...GPa from single-crystal X-ray diffraction using synchrotron radiation. Acta Crystallographica Section E: Crystallographic Communications, 2020, 76, 715-719.	0.2	7
6932	First Principles Study of Structural, Elastic, Electronic and Optical Features of the Non-centrosymmetric Superconductors SrMGe3 (Where M= Ir, Pt, and Pd). International Journal of Material and Mathematical Sciences, 2020, , 16-28.	0.2	3
6933	Modification of the Surface Structure and Electronic Properties of Diamond (100) with Tin as a Surface Termination: A Density Functional Theory Study. Journal of Physical Chemistry C, 2021, 125, 25165-25174.	1.5	3
6934	Density Functional Theory Study on the Adsorption Mechanism of Sulphide Gas Molecules on Î±-Fe2O3(001) Surface. Inorganics, 2021, 9, 80.	1.2	13
6935	Ca₃(TeO₃)₂(MO₄) (M = Mo, W): Mid-Infrared Nonlinear Optical Tellurates with Ultrawide Transparency Ranges and Superhigh Laser-Induced Damage Thresholds. Inorganic Chemistry, 2021, 60, 18512-18520.	1.9	16
6936	Evaluation of the structural, electronic, optical, elastic, mechanical, and vibrational properties of graphene-like g-GaN using density functional theory. AIP Advances, 2021, 11, .	0.6	5
6937	Ab initio calculations of the elastic, vibrational, electronic properties, and electron-phonon constant of superconducting YB₆ compound under low pressure. Physica Scripta, 2021, 96, 125850.	1.2	2
6938	Study on the Strengthening Mechanism of Rare Earth Ce in Magnesium Alloys, Based on First-Principle Calculations and Electronegativity Theory. Materials, 2021, 14, 6681.	1.3	4
6939	Effect of Mn-doped CaO on NO removal by CO in carbonation of calcium looping for CO2 capture in a fluidized bed reactor. Fuel, 2022, 310, 122395.	3.4	10
6940	A New Corner-Shared 1D Hybrid Lead Halide: Broad-Band Photoluminescence and Semiconductive Properties. Inorganic Chemistry Communication, 2021, , 109042.	1.8	3
6941	First-principles study of the effect of H on elastic properties of Al2Cu. Materials Letters, 2022, 308, 131191.	1.3	6
6942	Rational design of a novel two-dimensional porous metal-organic framework material for efficient benzene sensor. Chinese Chemical Letters, 2022, 33, 3726-3732.	4.8	9
6943	Pressure Dependence of Structural Behavior and Electronic Properties in Double Perovskite Ba₂SmSbO₆. Journal of Physical Chemistry C, 2021, 125, 25253-25260.	1.5	4
6944	Atomistic modelling of iodine-oxygen interactions in strained sub-oxides of zirconium. Journal of Nuclear Materials, 2022, 558, 153394.	1.3	1
6945	Structural and vibrational properties of methane up to 71 GPa. Physical Review B, 2021, 104, .	1.1	2
6946	Site-Selective Eu³⁺ Luminescence in the Monoclinic Phase of YSiO₂N. Chemistry of Materials, 2021, 33, 8873-8885.	3.2	20
6947	First-principles studies on two-dimensional B3O3 adsorbent as a potential drug delivery platform for TEPA anticancer drug. Journal of Molecular Modeling, 2021, 27, 347.	0.8	16

#	Article	IF	Citations
6948	Superior Infrared Nonlinear Optical Performance Achieved by Synergetic Functional Motif and Vacancy Site Modulations. Chemistry of Materials, 2021, 33, 8831-8837.	3.2	23
6949	Rational Design of a Two-Dimensional Janus CuFeO_{2+Î´} Single Layer as a Photocatalyst and Photoelectrode. Journal of Physical Chemistry Letters, 2021, 12, 10863-10873.	2.1	7
6950	<mml:math xmlns:mml="http://www.w3.org/1998/Math/MathML"><mml:mi>Na</mml:mi><mml:mi>Zn</mml:mi><mml:msub><mml:mi mathvariant="normal">F</mml:mi><mml:mn>3</mml:mn></mml:msub></mml:math> as a low-pressure analog of <mml:math xmlns:mml="http://www.w3.org/1998/Math/MathML"><mml:mi>Mg</mml:mi><mml:mi>Si</mml:mi><mml:msub><mml:mi mathvariant="normal">O</mml:mi><mml:mn>3</mml:mn></mml:msub></mml:math>. Physical Review Ma	0.9	1
6951	A closer look into the contribution of atmospheric gas-phase pathways in the formation of perfluorocarboxylic acids. Atmospheric Pollution Research, 2021, 12, 101255.	1.8	8
6952	Asymmetrical 1st reflection trend owing to metallization difference atâ€‰Â±â€‰Z-faces in indium tin oxide coated Fe-doped lithium niobate. Optics Express, 2020, 28, 32042.	1.7	1
6953	Negative thermal expansion of cubic silicon dicarbodiimide, Si(NCN)₂, studied by ab initio lattice dynamics. Journal of Physics Condensed Matter, 2020, 32, 465402.	0.7	5
6954	First principles study of post-boron carbide phases with icosahedra broken. Chinese Physics B, 2020, 29, 103102.	0.7	1
6955	OPTOELECTRONIC STUDY OF DOUBLE PEROVSKITE Rb2SnBr6: A FIRST PRINCIPLES CALCULATIONS. , 2020, , 1-5.		3
6956	STRUCTURAL, MECHANICAL AND OPTOELECTRONIC STUDY OF DOUBLE PEROVSKITE Cs2SnBr6 USING FIRST PRINCIPLES CALCULATION. , 2020, , 6-9.		3
6957	Role of hydrogen co-doping on opto-electronic behaviors of Na-H co-doped zinc oxide: a first principle study. Journal of Physics Communications, 2020, 4, 115002.	0.5	2
6958	A point defect model for YBa2Cu3O7 from density functional theory. Journal of Physics Communications, 2020, 4, 115003.	0.5	7
6959	Regulating electronic properties of <scp>BiOBr</scp> to enhance visible light response via 3d transition metals doping: <scp>DFT</scp> +â€‰U calculations. International Journal of Quantum Chemistry, 2021, 121, .	1.0	6
6960	Beyond two-center tight binding: Models for Mg and Zr. Physical Review Materials, 2020, 4, .	0.9	0
6961	Pressure-induced Pbâ€“Pb bonding and phase transition in Pb₂SnO₄. Acta Crystallographica Section B: Structural Science, Crystal Engineering and Materials, 2020, 76, 979-991.	0.5	8
6962	Valence mediation of samarium towards polysulfides as a redox mediator for high performance Liâ€“S batteries. Materials Today Energy, 2020, 17, 100484.	2.5	5
6963	Quantum transport: general concepts. , 0, , 91-117.		1
6964	RbMo2P3O14 with large birefringence mainly induced by highly distorted [MoO6] in uncommon [Mo2P3O14]â^ž layers. Dalton Transactions, 2021, 50, 17559-17565.	1.6	3
6965	Bi particles with exposed (012) facet on 3D substrate as highly active and durable electrode for CO2 reduction to formate. Journal of CO2 Utilization, 2022, 55, 101797.	3.3	10

#	Article	IF	Citations
6966	First-principles calculation to investigate the influence of shear deformation on the electronic structure and optical properties of hydrogenated silicene. Computational and Theoretical Chemistry, 2022, 1207, 113506.	1.1	0
6967	First principle study and Hirshfeld surface analysis on the effect of type, number, and position of small molecules on the structural stability and optical property of a powerful energetic crystal 6-nitro-7-azido-pyrazol[3,4-d][1,2,3]triazine-2-oxide. Materials Advances, 2022, 3, 1035-1046.	2.6	1
6968	Separation of ethane/ethylene gas mixture by ethane-selective CAU-3-NDCA adsorbent. Microporous and Mesoporous Materials, 2022, 330, 111572.	2.2	9
6969	First-principles calculations to investigate the structural, electronic and optical properties of lead-free double perovskites Rb2SeI6 and K2SeI6. Solar Energy, 2022, 231, 236-242.	2.9	27
6970	Exploring graphene quantum dots@TiO2 rutile (0 1 1) interface for visible-driven hydrogen production in photoelectrochemical cell: Density functional theory and experimental study. Applied Surface Science, 2022, 576, 151871.	3.1	10
6971	Noncentrosymmetric chalcohalide K2Ba3Ge3S9Cl2: A new nonlinear optical material with remarkable laser-induced damage threshold. Journal of Alloys and Compounds, 2022, 895, 162602.	2.8	11
6972	Computational materials design: Composition optimization to develop novel Ni-based single crystal superalloys. Computational Materials Science, 2022, 202, 111021.	1.4	6
6973	Novel 2D HfTeS4 for water splitting with high visible-light absorption. Applied Surface Science, 2022, 578, 151992.	3.1	11
6974	First-principles calculations of electronic and optical properties of orthorhombic Bi2Se3 nano thin film. Computational Condensed Matter, 2022, 30, e00618.	0.9	3
6975	DFT aspects of the elastic, mechanical, magnetic, thermodynamic and optical properties of Ce3XY perovskites. Philosophical Magazine, 0, , 1-20.	0.7	7
6976	KSSOLV-GPU: An efficient GPU-enabled MATLAB toolbox for solving the Kohn-Sham equations within density functional theory in plane-wave basis set. Chinese Journal of Chemical Physics, 2021, 34, 552-564.	0.6	9
6977	Electronic and optical properties of nitrogen and sulfur doped strontium titanate as eï¬cient photocatalyst for water splitting: A DFT study. International Journal of Hydrogen Energy, 2022, 47, 1605-1612.	3.8	22
6978	From CeF₂(SO₄)Â·H₂O to Ce(IO₃)₂(SO₄): Defluorinated Homovalent Substitution for Strong Second-Harmonic-Generation Effect and Sufficient Birefringence. Chemistry of Materials, 2021, 33, 9317-9325.	3.2	23
6979	Solid-State Structural Properties of Alloxazine Determined from Powder XRD Data in Conjunction with DFT-D Calculations and Solid-State NMR Spectroscopy: Unraveling the Tautomeric Identity and Pathways for Tautomeric Interconversion. Crystal Growth and Design, 2022, 22, 524-534.	1.4	8
6980	Synthesis and Characterization of New-Type Ionic Cocrystals with Cyanuric Acid and Alkali Halides: AXÂ·(H3C3N3O3)2 (A = Rb, Cs; X = Cl, Br). Crystal Growth and Design, 2021, 21, 7194-7200.	1.4	0
6981	Adsorption of Cr(OH)n(3â^'n)+ (n = 1â€“3) on Illite (001) and (010) Surfaces: A DFT Study. Processes, 2021, 9, 2048.	1.3	2
6982	Tunable CO/H ₂ ratios of electrochemical reduction of CO ₂ through the Zn-Ln dual atomic catalysts. Science Advances, 2021, 7, eabl4915.	4.7	82
6983	Nâ€Doped and Pâ€Doped Graphene on MgO (111): A Firstâ€Principles Study. Advanced Engineering Materials, 0, , 2100762.	1.6	0

#	Article	IF	Citations
6984	Hydrogen adsorption on TaSe2 monolayer doped with light metals: A DFT study. Vacuum, 2022, 196, 110775.	1.6	7
6985	Light doping effects of rare-earth elements: Sc, Y, La and Lu in rockSalt AlNâ€”first-principles study. Applied Physics A: Materials Science and Processing, 2021, 127, 1.	1.1	8
6986	Firstâ€principles study of structural, electronic and elastic properties of Sb 2 S 3 under pressure. Physica Status Solidi (B): Basic Research, 0, , 2100234.	0.7	1
6987	The ferroelastic phase transition in hydrogen cyanide studied by density functional theory. Journal of Physics Condensed Matter, 2021, , .	0.7	1
6988	Expanding the Solid Form Landscape of Bipyridines. Crystal Growth and Design, 2021, 21, 7201-7217.	1.4	5
6989	Screening criteria for high-performance p-type transparent conducting materials and their applications. Materials Today Physics, 2022, 22, 100583.	2.9	17
6990	Microscopic processes during ultrafast laser generation of Frenkel defects in diamond. Physical Review B, 2021, 104, .	1.1	9
6991	Single-Crystal X-ray and Solid-State NMR Characterisation of AND-1184 and Its Hydrochloride Form. Materials, 2021, 14, 7175.	1.3	0
6992	An electrochemically switched ion exchange Î±-ZrP/PPy film as a synergistically catalytic and anchoring material towards lithium-sulfur battery design. Electrochimica Acta, 2022, 403, 139609.	2.6	6
6993	The Electronic Structural and Defect-Induced Absorption Properties of a Ca2B10O14F6 Crystal. Crystals, 2021, 11, 1430.	1.0	0
6994	Atomic-level insights into the steric hindrance effect of single-atom Pd catalyst to boost the synthesis of dimethyl carbonate. Applied Catalysis B: Environmental, 2022, 304, 120922.	10.8	22
6995	Prediction of three-dimensional stretchable boron nitride nanoribbons. Diamond and Related Materials, 2021, 121, 108740.	1.8	1
6996	A 3D C@TiO2 multishell nanoframe for simultaneous photothermal catalytic hydrogen generation and organic pollutant degradation. Journal of Colloid and Interface Science, 2022, 609, 535-546.	5.0	13
6997	Phonons and low thermal expansion in sodalite zinc borate <mml:math xmlns:mml="http://www.w3.org/1998/Math/MathML"><mml:mrow><mml:msub><mml:mi>Zn</mml:mi><mml:mn>4</mml:mn></mml:msub><mml:msub><mml:mi mathvariant="normal">B</mml:mi><mml:mn>6</mml:mn></mml:msub><mml:msub><mml:mi		

#	Article	IF	Citations
7002	Crystal Structures of Two Titanium Phosphate-Based Proton Conductors: Ab Initio Structure Solution and Materials Properties. Inorganic Chemistry, 2022, 61, 2379-2390.	1.9	7
7003	Limbic Inducted and Delocalized Effects of Diazole in Carbon Nitride Skeleton for Propelling Photocatalytic Hydrogen Evolution. ACS Applied Materials & Interfaces, 2021, 13, 56273-56284.	4.0	29
7004	Effect of Yb concentration on the structural, magnetic and optoelectronic properties of Yb doped ZnO: first principles calculation. Optical and Quantum Electronics, 2021, 53, 1.	1.5	10
7005	AAl3P6O20 (A = Rb, Cs): Two deep-ultraviolet transparent nonlinear optical materials designed by aliovalent substitution. Journal of Alloys and Compounds, 2022, 902, 162608.	2.8	4
7006	First-Principles Approach to Extracting Chemical Information from X-ray Absorption Near-Edge Spectra of Ga-Containing Materials. Journal of Physical Chemistry C, 2021, 125, 27901-27908.	1.5	5
7007	Polymorphic Pb14O8I12 and Pb7O4I6 oxyhalides featuring unprecedented [O8Pb14] clusters with broad IR transparency. Science China Materials, 2022, 65, 773-779.	3.5	7
7008	Fatigue and its effect on the piezopotential properties of gallium nitride nanowires. Nanotechnology, 2022, 33, 095401.	1.3	0
7009	Origin of the Enhanced Piezoelectricity of Vanadium-Doped La₂Ti₂O₇ Ceramics. Journal of Physical Chemistry C, 2021, 125, 26180-26187.	1.5	3
7010	A novel BN polymorph with ductile manner. Journal of Solid State Chemistry, 2022, 306, 122794.	1.4	13
7011	Experimental and theoretical investigation of crystal structure of formamidiniumâ€“copperâ€“iodide single crystals grown from aqueous solution. Journal of Solid State Chemistry, 2021, 306, 122778.	1.4	2
7012	Anion Control of the Electrolyte Na_{3â€“x}SbS_{4â€“x}Br_x Extends Cycle Life in Solid-State Sodium Batteries. Chemistry of Materials, 2021, 33, 9184-9193.	3.2	13
7013	Contrasting Photochemical Activity of Two Sub-layers for Natural 2D Nanoclay with an Asymmetric Layer Structure. ACS Applied Materials & Interfaces, 2021, 13, 59431-59439.	4.0	6
7014	Solid-State Study of the Structure, Dynamics, and Thermal Processes of Safinamide Mesylateâ”€A New Generation Drug for the Treatment of Neurodegenerative Diseases. Molecular Pharmaceutics, 2021, , .	2.3	2
7015	Multifunctional ZnCo₂O₄ Quantum Dots Encapsulated In Carbon Carrier for Anchoring/Catalyzing Polysulfides and Selfâ€Repairing Lithium Metal Anode in Lithiumâ€Sulfur Batteries. Advanced Functional Materials, 2022, 32, 2109462.	7.8	44
7016	Post-Synthetic and In Situ Vacancy Repairing of Iron Hexacyanoferrate Toward Highly Stable Cathodes for Sodium-Ion Batteries. Nano-Micro Letters, 2022, 14, 9.	14.4	32
7017	Exploring failure mode and enhancement mechanism of doped rare-earth elements iron-based/alumina-ceramic interface. Ceramics International, 2022, 48, 7827-7835.	2.3	3
7018	Intrinsic Nature of Spontaneous Magnetic Fields in Superconductors with Time-Reversal Symmetry Breaking. Physical Review Letters, 2021, 127, 237002.	2.9	13
7019	Cd₇SiAs₆, a Nonchalcopyrite Arsenide with a Strong Nonlinear-Optical Response. Inorganic Chemistry, 2021, 60, 18634-18638.	1.9	4

#	Article	IF	Citations
7020	Newly Synthesized Three-Dimensional Boron-Rich Chalcogenides B₁₂X (X = S and Se): Theoretical Characterization of the Physical Properties for Optoelectronic and Mechanical Applications. ACS Omega, 2021, 6, 33899-33913.	1.6	17
7021	Structural, elastic, electronic and optical properties of the half-Heusler ScPtSb and YPtSb compounds under pressure. Condensed Matter Physics, 2021, 24, 43702.	0.3	9
7022	Enhancement of band gap and birefringence induced via Ï€-conjugated chromophore with â€œtail effectâ€• Inorganic Chemistry Frontiers, 2022, 9, 1224-1232.	3.0	11
7023	Pressure effects on the metallization and dielectric properties of GaP. Physical Chemistry Chemical Physics, 2021, 23, 26829-26836.	1.3	7
7024	Modeling Methods for Plasmonic Effects in Halide Perovskite Based Systems for Photonics Applications. , 2021, , 1-52.		0
7025	The effect of pressure on the structural, electronic and vibrational properties of solid carbon dioxide phases. Physical Chemistry Chemical Physics, 2022, 24, 4462-4474.	1.3	1
7026	Hubbardâ€™s Modified Density Functional Theory Calculations for the Electronic Structure and Optical Properties of Carbon Doped Anatase TiO2. Springer Proceedings in Complexity, 2021, , 371-381.	0.2	2
7027	Unraveling the superior anchoring of lithium polyselenides to the confinement bilayer C₂N: an efficient host material for lithiumâ€“selenium batteries. Physical Chemistry Chemical Physics, 2021, 23, 26981-26989.	1.3	7
7028	Enhanced catalytic performance of pillared Î´-MnO₂ with enlarged layer spaces for lithiumâ€“ and sodiumâ€“oxygen batteries: a theoretical investigation. Nanoscale, 2021, 13, 20637-20648.	2.8	15
7029	Designing sp3 networks of two novel carbon allotropes in the P4/mmm phase. Chinese Journal of Physics, 2022, 75, 90-103.	2.0	23
7030	Lithium Intercalation Mechanism and Critical Role of Structural Water in Layered H₂V₃O₈ High-Capacity Cathode Material for Lithium-Ion Batteries. Chemistry of Materials, 2022, 34, 694-705.	3.2	11
7031	Hydrogenation of CO₂ into aromatics over ZnZrOâ€“Zn/HZSM-5 composite catalysts derived from ZIF-8. Catalysis Science and Technology, 2022, 12, 799-811.	2.1	17
7032	HgSO4: An excellent mid-infrared sulfate nonlinear optical crystal with wide band gap and strong second harmonic generation response. Journal of Alloys and Compounds, 2022, 902, 163727.	2.8	6
7033	Large dielectric switch effects induced by an orderâ€“disorder transformation in cyclopropylamine perchlorate crystals. Nanoscale, 2022, 14, 675-679.	2.8	2
7034	Highly sensitive and selective room-temperature gas sensors based on B6N6H6 monolayer for sensing SO2 and NH3: A first-principles study. Results in Physics, 2022, 33, 105208.	2.0	32
7035	A Reentrant Phase Transition and a Novel Polymorph Revealed in High-Pressure Investigations of CF4 up to 46.5 GPa. Journal of Chemical Physics, 2022, 156, 044503.	1.2	2
7036	First-principles study of structural, electronic, elastic, and optical properties of the tetragonal AInS2 (A=K, Rb, Cs) chalcogenides. Computational Condensed Matter, 2022, 30, e00644.	0.9	2
7037	Unraveling the importance between electronic intensity and oxygen vacancy on photothermocatalytic toluene oxidation over CeO2. Chemical Engineering Journal, 2022, 433, 134619.	6.6	31

#	Article	IF	Citations
7038	A first-principles study on D022 precipitation phases of Ni-based superalloys with loading stress and high temperature. Solid State Communications, 2022, 342, 114632.	0.9	4
7039	Effects and mechanism of (Be/Mg/Ca) doping and point defects (VZn, Hi) on the p-type conductivity of ZnO: A first-principles study. Solid State Communications, 2022, 343, 114653.	0.9	0
7040	First-principles study of electronic and optical properties of defective sawtooth penta-graphene nanoribbons. Computational Materials Science, 2022, 203, 111065.	1.4	11
7041	Electronic, elastic, mechanical and anisotropic response of W3XC2 (X: Si, Ge and Al) alloys via first-principles. Solid State Communications, 2022, 343, 114648.	0.9	2
7042	Strain engineered electronic structures and optical response of InS single crystal with negative Poisson's ratio. Computational Materials Science, 2022, 203, 111091.	1.4	2
7043	Interlayer water structure of phyllomanganates: Insights from MD simulations of chalcophanite-group oxide dehydration. Geochimica Et Cosmochimica Acta, 2022, 318, 495-509.	1.6	3
7044	Effects of thickness and orientation on electromechanical properties of gallium nitride nanofilm: A multiscale insight. Computational Materials Science, 2022, 203, 111122.	1.4	8
7045	Adsorption of toxic gases on metal doped C3N monolayer: A theoretical study. Computational and Theoretical Chemistry, 2022, 1208, 113559.	1.1	1
7046	Ba2B13O19(OH)5Â·5H2O: A promising nonlinear optical material with a unique 2[B13O19(OH)5]âˆž two-dimensional layer. Journal of Alloys and Compounds, 2022, 897, 163194.	2.8	3
7047	Exploring the structural, electronic and optical properties of vacancy-ordered double perovskites Cs2TlAsX6 (X = I, Br, Cl) based on first-principles. Physics Letters, Section A: General, Atomic and Solid State Physics, 2022, 427, 127917.	0.9	18
7048	Na+/Ag+ substitution induced birefringence enhancement from AgGaS2 to NaGaS2. Journal of Alloys and Compounds, 2022, 896, 163093.	2.8	10
7049	DFT study on the crystal structure, optoelectronic, and thermoelectric properties of lead-free inorganic A2PdBr6 (A = K, Rb, and Cs) perovskites. Materials Today Communications, 2022, 30, 103061.	0.9	11
7050	First-principles calculations on electronic, optical and photocatalytic properties of BiNbO4. Materials Science in Semiconductor Processing, 2022, 140, 106391.	1.9	6
7051	Enhancing stability of Co9S8 by iron incorporation for oxygen evolution reaction and supercapacitor electrodes. Chemical Engineering Journal, 2022, 431, 133980.	6.6	13
7052	Tuning the electronic and optical properties of two-dimensional hydrogenated c-BN nanosheets by Be and C dopants and vacancy defects. Chemical Physics, 2022, 555, 111441.	0.9	1
7053	Temperature-dependent structure of 3.5 wt.% NaCl aqueous solution: Theoretical and Raman investigation. Journal of Molecular Structure, 2022, 1253, 132279.	1.8	5
7054	Noncentrosymmetric (KBa0.5)In2Se4 and (K0.58Ba0.71)(Ga0.89In1.11)Se4 derived from centrosymmetric BaIn2Se4 via partial cation substitution: structural chemistry and nonlinear optical activity. Journal of Alloys and Compounds, 2022, 899, 163255.	2.8	4
7055	Optoelectronic and thermodynamic properties, infrared and Raman spectra of NbO2 and Nb2O5 from DFT formalism. Journal of Physics and Chemistry of Solids, 2022, 163, 110549.	1.9	11

#	Article	IF	Citations
7056	Computational design of materials for metal-ion batteries. , 2023, , 404-429.		4
7057	Ammonia Mono Hydrate IV: An Attempted Structure Solution. Crystals, 2022, 12, 135.	1.0	0
7058	Ba₆(Cu_xZ_y)Sn₄S₁₆ (Z = Mg,) Tj ETQq0 0 0 rgBT /Overlo Inorganic Chemistry, 2022, 61, 2640-2651.	1.9	7
7059	Pb₄SeBr₆: A Congruently Melting Midâ€Infrared Nonlinear Optical Material with Excellent Comprehensive Performance. Advanced Optical Materials, 2022, 10, .	3.6	21
7060	Building a stabilized structure from surface to bulk of Ni-rich cathode for enhanced electrochemical performance. Energy Storage Materials, 2022, 47, 87-97.	9.5	22
7061	Crystal Structure and Theoretical Analysis of Cs2Ca3(SO4)4. Crystals, 2022, 12, 126.	1.0	2
7062	Double echo symmetry-based REDOR and RESPDOR pulse sequences for proton detected measurements of heteronuclear dipolar coupling constants. Journal of Magnetic Resonance, 2022, 336, 107147.	1.2	9
7063	Interfacial Adsorption and Electron Properties of Water Molecule/Cluster on Anatase TiO₂(101) Surface: Raman and DFT Investigation. Langmuir, 2022, 38, 1057-1066.	1.6	10
7064	Raman tensor of zinc-phosphide (Zn₃P₂): from polarization measurements to simulation of Raman spectra. Physical Chemistry Chemical Physics, 2021, 24, 63-72.	1.3	3
7065	Solid-state ¹⁷O NMR study of Î±-<scp>d</scp>-glucose: exploring new frontiers in isotopic labeling, sensitivity enhancement, and NMR crystallography. Chemical Science, 2022, 13, 2591-2603.	3.7	13
7066	Enantiotropy of Simvastatin as a Result of Weakened Interactions in the Crystal Lattice: Entropy-Driven Double Transitions and the Transient Modulated Phase as Seen by Solid-State NMR Spectroscopy. Molecules, 2022, 27, 679.	1.7	2
7067	Predicting Lithium Iron Oxysulfides for Battery Cathodes. ACS Applied Energy Materials, 2022, 5, 575-584.	2.5	6
7068	A Dual-Surface Mechanism of Oxidant-Free Pyrrole Polymerization in the Two-Dimensional Titanium Carbide (MXene) Interlayer Nanospace. Journal of Physical Chemistry C, 2022, 126, 1316-1325.	1.5	5
7069	Evaluation of Olivine LiFePO₄ Polyanionic Cathode Material Using Density Functional Theory. Key Engineering Materials, 0, 908, 293-298.	0.4	1
7070	Coordination units of Mn²⁺ modulation toward tunable emission in zero-dimensional bromides for white light-emitting diodes. Journal of Materials Chemistry C, 2022, 10, 2095-2102.	2.7	35
7071	Excitonic Effects in Fe/As K â€Edge Absorption for Iron Based Superconductors: A Combined DFT and BSE Analysis. Advanced Theory and Simulations, 0, , 2100525.	1.3	0
7072	A strategy of combination reaction to improve electrochemical performance in two-dimensional Mo1-W Se2 battery-type electrode materials. Ceramics International, 2023, 49, 7196-7207.	2.3	3
7073	Bandgap evolution of Mg₃N₂ under pressure: Experimental and theoretical studies. Chinese Physics B, 2022, 31, 066205.	0.7	2

#	Article	IF	Citations
7074	First-principles Study on the Influence of Electric Field on Electronic Structure and Optical Properties of GaN/g-C3N4 Heterojunction. Wuli Xuebao/Acta Physica Sinica, 2022, .	0.2	0
7075	Theoretical study on the controllable preparation of superhard BC₂N under high pressure. Journal of Materials Chemistry C, 2022, 10, 1660-1665.	2.7	6
7076	Mercury LÎ±1 High Energy Resolution Fluorescence Detected X-ray Absorption Spectroscopy: A Versatile Speciation Probe for Mercury. Inorganic Chemistry, 2022, 61, 5201-5214.	1.9	7
7077	Variable dimensionality of the anion framework in four new borophosphates and fluoroborophosphates with short cutoff edges. Dalton Transactions, 2022, 51, 2840-2845.	1.6	7
7078	Adsorption of Inorganic Anions on Anatase TiO ₂ (101) Surface: A First-Principles Study. SSRN Electronic Journal, 0, , .	0.4	0
7079	Bromination mechanisms of aromatic pollutants: formation of Br2 and bromine transfer from metallic oxybromides. Environmental Science and Pollution Research, 2022, , 1.	2.7	2
7080	Suppressing electrolyte-lithium metal reactivity via Li+-desolvation in uniform nano-porous separator. Nature Communications, 2022, 13, 172.	5.8	83
7081	High-Temperature Superconductivity in the Lanthanide Hydrides at Extreme Pressures. Applied Sciences (Switzerland), 2022, 12, 874.	1.3	4
7082	Crystal Structures of Ironâ€Based Oxides and Their Catalytic Efficiencies for the Oxygen Evolution Reaction: A Trend in Alkaline Media. ChemElectroChem, 2022, 9, .	1.7	3
7083	Structural, optical, and magnetic properties of a new complex (1â^'x)Bi1/2Na1/2TiO3â€‰+â€‰xMgNiO3â^'Î´ solid solution system. Applied Physics A: Materials Science and Processing, 2022, 128, 1.	1.1	5
7084	Electronic and catalytic properties of carbon nitride derivatives tuned by building blocks and linkages. International Journal of Hydrogen Energy, 2022, 47, 8761-8775.	3.8	5
7085	Comparative Analysis of the Hydrogen Bond Vibrations of Ice XII. ACS Omega, 2022, 7, 2970-2974.	1.6	2
7086	High-pressure phase behaviors of titanium dioxide revealed by a Î”-learning potential. Journal of Chemical Physics, 2022, 156, 074106.	1.2	2
7087	Manipulation of charge carrier flow in Bi₄NbO₈Cl nanoplate photocatalyst with metal loading. Chemical Science, 2022, 13, 3118-3128.	3.7	17
7088	Ferroelectric properties in metal-coordinated complex tris(2-hydroxyethyl) ammonium trichloro cadmium(<scp>ii</scp>). Journal of Materials Chemistry C, 2022, 10, 2255-2262.	2.7	1
7089	Directing Crystallization Outcomes of Conformationally Flexible Molecules: Polymorphs, Solvates, and Desolvation Pathways of Fluconazole. Molecular Pharmaceutics, 2022, 19, 456-471.	2.3	13
7090	Terahertz frequency shifts due to multiphonon scattering in thiamin crystals containing hydrated ions. Applied Physics Letters, 2022, 120, .	1.5	3
7091	Portable Acceleration of Materials Modeling Software: CASTEP, GPUs, and OpenACC. Computing in Science and Engineering, 2022, 24, 46-55.	1.2	4

#	Article	IF	Citations
7092	Alleviating Interfacial Recombination of Heterojunction Electron Transport Layer via Oxygen Vacancy Engineering for Efficient Perovskite Solar Cells Over 23%. Energy and Environmental Materials, 2023, 6, .	7.3	4
7093	Relationship between the Crystal Structure and Tuberculostatic Activity of Some 2-Amidinothiosemicarbazone Derivatives of Pyridine. Materials, 2022, 15, 349.	1.3	1
7094	Novel Calcium sp³ Carbonate CaC₂O₅-I4Ì...2d May Be a Carbon Host in Earthâ€™s Lower Mantle. ACS Earth and Space Chemistry, 2022, 6, 73-80.	1.2	13
7095	Molecular dynamics simulations of radiation damage in YBa₂Cu₃O₇. Superconductor Science and Technology, 2022, 35, 035010.	1.8	6
7096	Ferroelectric-HfO2/oxide interfaces, oxygen distribution effects, and implications for device performance. Applied Physics Letters, 2022, 120, .	1.5	6
7097	Pressure-induced coupled structuralâ€“electronic transition in SnS₂ under different hydrostatic environments up to 39.7 GPa. RSC Advances, 2022, 12, 2454-2461.	1.7	12
7098	Critical assessment of machine-learned repulsive potentials for the density functional based tight-binding method: A case study for pure silicon. Journal of Chemical Physics, 2022, 156, 064101.	1.2	4
7099	Multicomponent (Hf0.25Zr0.25Ti0.25Cr0.25)B2 ceramic modified SiCâ€“Si composite coatings: In-situ synthesis and high-temperature oxidation behavior. Ceramics International, 2022, 48, 12608-12624.	2.3	13
7100	First-Principles Study of Ti-Deficient Ti₃C₂ MXene Nanosheets as NH₃ Gas Sensors. ACS Applied Nano Materials, 2022, 5, 2470-2475.	2.4	26
7101	A6Mo2P4O19 (A = Rb, Cs) and Rb2MoP2O9: new molybdophosphates with distinct polyanionic configurations. Dalton Transactions, 2022, 51, 1481-1488.	1.6	1
7102	Compressed superhydrides: the road to room temperature superconductivity. Journal of Physics Condensed Matter, 2022, 34, 173001.	0.7	12
7103	Theoretical investigations on the nitro-explosive sensing process of a MOF sensor: Roles of hydrogen bond and Ï€-Ï€ stacking. Chemical Physics Letters, 2022, 793, 139393.	1.2	8
7104	Controlling magnetic-semiconductor properties of the Si- and Al-doped blue phosphorene monolayer. Journal Physics D: Applied Physics, 2022, 55, 165302.	1.3	3
7105	Ba₂B₅O₈(OH)₂(NO₃)Â·3H₂O: the design of an alkaline earth metal borate-nitrate optimized from a hydroxylic borate. Dalton Transactions, 2022, 51, 1979-1984.	1.6	3
7106	Density functional theory investigation of the mechanical, electronic and optical properties of Pb-free vacancy-ordered double perovskites K2PdCl6 and K2PdBr6. Physica Scripta, 2022, 97, 015801.	1.2	3
7107	Vibrational Dynamics in crystalline 4-(dimethylamino) benzaldehyde: Inelastic Neutron Scattering and Periodic DFT Study. Materials, 2022, 15, 475.	1.3	2
7108	A novel 2D graphene oxide modified Î±-AgVO3 nanorods: Design, fabrication, and enhanced visible-light photocatalytic performance. Journal of Advanced Ceramics, 2022, 11, 308-320.	8.9	36
7109	A new I₃O₉^{3â^’} group constructed from IO₃^{â^’} and IO₅^{5â^’} anion units in Cs₃[Ga₂O(I₃O₉)(IO₃)₄(HIO₃)]. CrystEngComm, 2021, 24, 77-82.	1.3	2

#	Article	IF	Citations
7110	Probing the Lubrication of Shear-Induced Self-assembled Layer on Amorphous Carbon Films in Methane Atmosphere. Tribology Letters, 2022, 70, 1.	1.2	2
7111	Highly polarized [GeOTe₃] motif-driven structural order promotion and an enhanced second harmonic generation response in the new nonlinear optical oxytelluride Ba₃Ge₂O₄Te₃. Journal of Materials Chemistry C, 2021, 10, 150-159.	2.7	21
7112	Effect of Point Defects on Electronic Properties and Structure of Talc (001) Surface by First Principles. Minerals (Basel, Switzerland), 2022, 12, 69.	0.8	1
7113	Ni/CexZr1-xO2 catalyst prepared via one-step co-precipitation for CO2 reforming of CH4 to produce syngas: role of oxygen storage capacity (OSC) and oxygen vacancy formation energy (OVFE). Journal of Materials Science, 2022, 57, 2839-2856.	1.7	8
7114	Theoretical design of SnS2â€“graphene heterojunctions with vacancy and impurity defects for multi-purpose photoelectric devices. Physical Chemistry Chemical Physics, 2022, 24, 966-974.	1.3	1
7115	Interfacial coupling effects on adsorptive and photocatalytic performances for photoresponsive graphene-wrapped SrTiO3@Ag under UVâ€“visible light: experimental and DFT approach. Environmental Science and Pollution Research, 2022, 29, 28098-28114.	2.7	10
7116	Boronâ€Rich Boron Nitride Nanotubes as Highly Selective Adsorbents for Selected Diatomic Air Pollutants: A DFT Study. Advanced Theory and Simulations, 2022, 5, .	1.3	8
7117	Elucidation of the structural and optical properties of metal cation (Na⁺, K⁺,) Tj ETQq1 1 0.784314 rgBT /Ov nanocrystals. Journal of Materials Chemistry A, 2022, 10, 3562-3578.	5.2	18
7118	Coexistence of carbonyl and ether groups on oxygen-terminated (110)-oriented diamond surfaces. Communications Materials, 2022, 3, .	2.9	10
7119	The effect of both Pt decoration and the defects on the adsorption of graphene for SO 2. International Journal of Quantum Chemistry, 0, , .	1.0	1
7120	High-Pressure Synthesis of Light Lanthanide Dodecaborides (PrB₁₂ and CeB₁₂): Effects of Valence Fluctuation on Volume and Formation Pressure. Inorganic Chemistry, 2022, 61, 2568-2575.	1.9	3
7121	Two new tellurite halides with cationic layers: syntheses, structures, and characterizations of CdPb₂Te₃O₈Cl₂ and Cd₁₃Pb₈Te₁₄O₄₂Cl₁₄. Inorganic Chemistry Frontiers, 2022, 9, 1023-1030.	3.0	9
7122	Lattice solvent controlled photochromism of tripyridyl-triazine-based zinc bromide complexes. Inorganic Chemistry Frontiers, 2022, 9, 879-888.	3.0	12
7123	Pb₂Al₂B₃O₈F₃: structure and properties of a new fluoroaluminoborate with non-traditional chain-like B₃O₈ groups. Dalton Transactions, 2022, 51, 3964-3969.	1.6	2
7124	HgTeO₂F(OH): A Nonlinear Optical Oxyfluoride Constructed of Active [TeO₂F(OH)]^{2â€“} Pyramids and V-Shaped [HgO₂]^{2â€“} Groups. Inorganic Chemistry, 2022, 61, 2333-2339.	1.9	19
7125	Silver isotope fractionation in ore-forming hydrothermal systems. Geochimica Et Cosmochimica Acta, 2022, 322, 24-42.	1.6	5
7126	Polymorphism, polytypism and modular aspect of compounds with the general formula A ₂ M ₃(TO₄)₄ (A = Na, Rb, Cs, Ca;) Tj ETQq0 0 0 rgBT /Overlock orderâ€“disorder, topological description and DFT calculations. Acta Crystallographica Section B: Structural Science, Crystal Engineering and Materials, 2022, 78, 61-69.	0.5	3
7127	Hierarchical Modulation of Optical Anisotropy Driven by Metal Cation Polyhedra in Fluorooxoborates M II B 4 O 6 F 2 (M II =Be, Mg, Pb, Zn, Cd). Chemistry - A European Journal, 2022, 28, .	1.7	3

#	Article	IF	Citations
7128	Two-dimensional antimony selenide (Sb2Se3) nanosheets prepared by hydrothermal method for visible-light photodetectors. Solar Energy, 2022, 233, 213-220.	2.9	13
7129	Responses to comments on the paper â€œtwo-dimensional Sc2C: A reversible and high capacity hydrogen storage material predicted by first-principles calculationsâ€. International Journal of Hydrogen Energy, 2022, 47, 9829-9834.	3.8	0
7130	Hollow carbon nanospheres coated by Î´-MnO2 as S host to enhance the catalytic conversion of polysulfides in Li-S batteries. Applied Surface Science, 2022, 585, 152498.	3.1	15
7131	Theoretical Prediction of Rhenium Separation from Ammonium Perrhenate by Phononâ€“Photon Resonance Absorption. ACS Omega, 2022, 7, 5437-5441.	1.6	3
7132	2D-Nb₂CT_z-Supported, 3D-Carbon-Encapsulated, Oxygen-Deficient Nb₂O₅ for an Advanced Li-Ion Battery. ACS Applied Energy Materials, 2022, 5, 2121-2129.	2.5	11
7133	Electronic structure and structural stability of (Ba0.75Ae0.25)Fe2As2 (AeÂ=ÂLi, Na, Rb). Physica C: Superconductivity and Its Applications, 2022, 593, 1354013.	0.6	1
7134	The behavior of zeolites wairakite and phillipsite at high P-T parameters. Spectrochimica Acta - Part A: Molecular and Biomolecular Spectroscopy, 2022, 273, 120979.	2.0	3
7135	Multi-Level Structural Design Strategy toward Low-Sensitivity Energetic Materials: From Planar Molecule to Layered Packing Crystal. Crystal Growth and Design, 2022, 22, 1882-1891.	1.4	4
7136	gpaw-tools â€“ higher-level user interaction scripts for GPAW calculations and interatomic potential based structure optimization. Computational Materials Science, 2022, 204, 111201.	1.4	3
7137	Analysis of diamond tool wear mechanism in terms of stress for KDP Fly cutting. Materials Today Communications, 2022, 30, 103146.	0.9	0
7138	First-principles study of the influence of lone pair electrons and molecular groups on the birefringence of phosphate and fluorophosphate. Physica B: Condensed Matter, 2022, 630, 413676.	1.3	6
7139	Probing the mechanism of H2 production in water gas shift reaction over Ce-modified CaO: A DFT study. Journal of the Energy Institute, 2022, 101, 149-159.	2.7	12
7140	Effect of W on the thermal stability, mechanical properties and corrosion resistance of Fe-based bulk metallic glass. Intermetallics, 2022, 143, 107485.	1.8	16
7141	Empowering hydrogen storage performance of B4C3Âmonolayer through decoration with lithium: A DFT study. Surfaces and Interfaces, 2022, 29, 101723.	1.5	15
7142	Highly efficient As(III) removal through simultaneous oxidation and adsorption by N-CQDs modified MIL-53(Fe). Separation and Purification Technology, 2022, 286, 120409.	3.9	26
7143	P2221-C8: A novel carbon allotrope denser than diamond. Scripta Materialia, 2022, 212, 114549.	2.6	15
7144	A novel ultra-low friction heterostructure: Aluminum substrate-honeycomb borophene/graphene heterojunction. Computational Materials Science, 2022, 205, 111236.	1.4	5
7145	Two non-centrosymmetric scandium borate nonlinear optical crystals containing the B5O10 anion group. Journal of Alloys and Compounds, 2022, 902, 163832.	2.8	12

#	Article	IF	Citations
7146	DFT study of Cu-modified and Cu-embedded WSe2 monolayers for cohesive adsorption of NO2, SO2, CO2, and H2S. Applied Surface Science, 2022, 583, 152522.	3.1	26
7147	A new salt-inclusion chalcogenide exhibiting distinctive [Cd11In9S26]3â^' host framework and decent nonlinear optical performances. Journal of Alloys and Compounds, 2022, 902, 163656.	2.8	7
7148	Design of a diamond-like infrared nonlinear optical material LiBS2 with ultra-wide band gap. Journal of Alloys and Compounds, 2022, 902, 163839.	2.8	3
7149	Oxidative polymerization of bisphenol A (BPA) via H-abstraction by Bi2.15WO6 and persulfate: Importance of the surface complexes. Chemical Engineering Journal, 2022, 435, 134816.	6.6	30
7150	DFT-based study of the structural, optoelectronic, mechanical and magnetic properties of Ti₃AC₂ (A = P, As, Cd) for coating applications. RSC Advances, 2022, 12, 4395-4407.	1.7	11
7151	Role of van der Waals forces in the metalâ€“insulator transition of transition metal oxides. Physical Chemistry Chemical Physics, 2022, 24, 5455-5461.	1.3	0
7152	Mechanical anisotropy and tabletability of famotidine polymorphs. CrystEngComm, 2022, 24, 1795-1802.	1.3	2
7153	First-principles insights into mechanical, optoelectronic, and thermo-physical properties of transition metal dichalcogenides ZrX2 (X = S, Se, and Te). AIP Advances, 2022, 12, .	0.6	16
7154	Investigation of the fireside corrosion of a new wrought Ni-Fe-Cr-based alloy in advanced ultra-supercritical steam boilers. Corrosion Science, 2022, 199, 110152.	3.0	3
7155	Efficiently Computing Excitations of Complex Systems: Linear-Scaling Time-Dependent Embedded Mean-Field Theory in Implicit Solvent. Journal of Chemical Theory and Computation, 2022, , .	2.3	0
7156	Atomic-Level Structure of Mesoporous Hexagonal Boron Nitride Determined by High-Resolution Solid-State Multinuclear Magnetic Resonance Spectroscopy and Density Functional Theory Calculations. Chemistry of Materials, 0, , .	3.2	5
7157	All sp2 hybridization BN polymorphs with wide bandgap. Journal of Applied Physics, 2022, 131, .	1.1	24
7158	Affinityâ€Engineered Flexible Scaffold toward Energyâ€Dense, Highly Reversible Na Metal Batteries. Energy and Environmental Materials, 2023, 6, .	7.3	11
7159	Three orders of magnitude two-beam-coupling gain increase from Cu-doped (K0.5Na0.5)0.2(Sr0.75Ba0.25)0.9Nb2O6 crystal owing to huge depolarization field-induced surface metallization. European Physical Journal Plus, 2022, 137, 1.	1.2	0
7160	Two novel carbon allotropes with tetragonal symmetry: First-principles calculations. Journal of Solid State Chemistry, 2022, 309, 122971.	1.4	21
7161	Investigating the influence of nano film depositions on the metal surface on the solid-liquid interfacial work function. Surfaces and Interfaces, 2022, 29, 101789.	1.5	1
7162	A study on the electronic properties of A site and B site doped SrTiO₃ for thermoelectric applications using first-principles calculations. Physica Scripta, 2022, 97, 035808.	1.2	1
7163	First-Principles Study on the Half-Metallicity of New MXene Materials Nd2NT2 (T = OH, O, S, F, Cl, and) Tj ETQq1 1 0.784314 rgBT /Ov	1.8	4

#	Article	IF	Citations
7164	Superlubricity Enabled by Loadâ€Driven Redistribution of Electrons. Advanced Materials Interfaces, 2022, 9, .	1.9	9
7165	Understanding the ZIF-L to ZIF-8 transformation from fundamentals to fully costed kilogram-scale production. Communications Chemistry, 2022, 5, .	2.0	45
7166	Abrading bulk metal into single atoms. Nature Nanotechnology, 2022, 17, 403-407.	15.6	102
7167	Ultrafast charge transfer dynamics in 2D covalent organic frameworks/Re-complex hybrid photocatalyst. Nature Communications, 2022, 13, 845.	5.8	46
7168	Successful prediction of the elastic properties of multiphase high entropy alloys in the AlTiVCr-Si system through a novel computational approach. Materialia, 2022, 21, 101365.	1.3	1
7169	Graphene quantum dots/carbon nitride heterojunction with enhanced visible-light driven photocatalysis of nitric oxide: An experimental and DFT study. Carbon, 2022, 191, 502-514.	5.4	35
7170	Sliding Modulation in Nonlinear Optical Effect in Two-Dimensional van der Waals Cu₂MoS₄. ACS Applied Materials & Interfaces, 2022, 14, 9535-9543.	4.0	5
7171	Siâ€“C alloys with direct band gaps for photoelectric application. Vacuum, 2022, 199, 110952.	1.6	16
7172	The effects of active elements on adhesion strength of SiC/Cu interface in SiC reinforced Cu-based composite: A first-principles investigation. Materials Today Communications, 2022, 31, 103233.	0.9	4
7173	Study on Electronic, Mechanical and Optical Properties of Perovskite Cs₂AgGaX₆ (X = Cl, Br). Journal of Nanoelectronics and Optoelectronics, 2021, 16, 1521-1527.	0.1	3
7174	Guanidinium Fluorooxoborates as Efficient Metal-free Short-Wavelength Nonlinear Optical Crystals. Chemistry of Materials, 2022, 34, 440-450.	3.2	67
7175	NMR Response of the Tetrel Bond Donor. Journal of Physical Chemistry C, 2022, 126, 851-865.	1.5	10
7176	Hydration of TiO₂ Facets Regulates As(III) Adsorption: DFT and DRIFTS Study. Langmuir, 2022, 38, 275-281.	1.6	9
7177	Few-Layer WS₂â€“WSe₂ Lateral Heterostructures: Influence of the Gas Precursor Selenium/Tungsten Ratio on the Number of Layers. ACS Nano, 2022, 16, 1198-1207.	7.3	16
7178	Theoretical Investigations of a BN Polymorph with sp2 + sp3 Hybridizations. Crystals, 2021, 11, 1574.	1.0	6
7179	Interfacial Stabilities, Electronic Properties and Interfacial Fracture Mechanism of 6H-SiC Reinforced Copper Matrix Studied by the First Principles Method. Crystals, 2022, 12, 51.	1.0	2
7180	Ino-Chloridolithates from Ionothermal Synthesis. Inorganic Chemistry, 2021, 60, 19145-19151.	1.9	1
7181	Novel Hydrogen-Bonded Metal-Nucleobase Frameworks for Highly Selective Capture and Separation of Ethane/Propane and Nitrogen from Methane. SSRN Electronic Journal, 0, , .	0.4	0

#	Article	IF	Citations
7182	Investigation on Morphology of Primary Mg2si in Al-20%Mg2si Composite with Experiment and First-Principle Calculations. SSRN Electronic Journal, 0, , .	0.4	0
7183	Resolving alternative structure determinations of indapamide using ¹³C solid-state NMR. Chemical Communications, 2022, 58, 4767-4770.	2.2	2
7184	Structural, elastic and optoelectronic properties of inorganic cubic FrBX₃ (B = Ge, Sn; X =) Tj ETQq0 0 0 rgBT /Overlock 10	1.7	35
7185	A combination of proton spin diffusion NMR and molecular simulations to probe supramolecular assemblies of organic molecules in nanoporous materials. Dalton Transactions, 2022, 51, 5434-5440.	1.6	2
7186	Adsorption and solidification of cadmium by calcium sulfate dihydrate (gypsum) in an aqueous environment: a dispersion-corrected DFT and ab initio molecular dynamics study. Physical Chemistry Chemical Physics, 2022, 24, 9521-9533.	1.3	6
7187	Theoretical exploration of mechanical, electronic structure and optical properties of aluminium based double halide perovskite. RSC Advances, 2022, 12, 10209-10218.	1.7	11
7188	A structure determination protocol based on combined analysis of 3D-ED data, powder XRD data, solid-state NMR data and DFT-D calculations reveals the structure of a new polymorph of<scp>l</scp>-tyrosine. Chemical Science, 2022, 13, 5277-5288.	3.7	15
7189	Electronic and optical properties of a novel two-dimensional semiconductor material TlPt₂S₃: a first-principles study. Physical Chemistry Chemical Physics, 2022, 24, 7642-7652.	1.3	11
7190	Metalâ€“organic frameworks as hypergolic additives for hybrid rockets. Chemical Science, 2022, 13, 3424-3436.	3.7	14
7191	Infrared nonlinear optical sulfide CsCd₄In₅S₁₂ exhibiting large second harmonic generation response. Journal of Materials Chemistry C, 2022, 10, 5183-5189.	2.7	10
7192	Implementation of predictive models: Practical aspects. Theoretical and Computational Chemistry, 2022, , 405-433.	0.2	0
7193	Lattice Instability and Raman Spectra of Bao Under High Pressure: A First Principles Study. SSRN Electronic Journal, 0, , .	0.4	0
7194	Centrosymmetric Rb[Te₂O₄(OH)₅] and noncentrosymmetric K₂[Te₃O₈(OH)₄]: metal tellurates with corner and edge-sharing (Te₄O₁₈)^{12â^'} anion groups. Inorganic Chemistry Frontiers, 2022, 9, 2628-2636.	3.0	7
7195	Low-energy Ga₂O₃ polymorphs with low electron effective masses. Physical Chemistry Chemical Physics, 2022, 24, 7045-7049.	1.3	8
7196	KEu₂In₃B₁₂S₁₃: a novel type of thioborate featuring B₁₂S₁₂ cluster and unique In₆S₆ 12-membered ring. Dalton Transactions, 2022, 51, 4619-4622.	1.6	6
7197	Na₂SrB₁₆O₂₆: a new borate with independent interpenetrating Bâ€“O networks and deep-ultraviolet cutoff edge. Dalton Transactions, 2022, 51, 4097-4103.	1.6	2
7198	Electronic engineering of amorphous Feâ€“Coâ€“S sites in hetero-nanoframes for oxygen evolution and flexible Alâ€“air batteries. Journal of Materials Chemistry A, 2022, 10, 19757-19768.	5.2	11
7199	First Principles and Experimental Study on the Atomic Formation of MnSâ€“Al₂SiO₅ Inclusions in Steel. ISIJ International, 2022, 62, 1126-1135.	0.6	7

#	Article	IF	Citations
7200	Competitive nucleation and growth behavior in Liâ€“Se batteries. Energy and Environmental Science, 2022, 15, 1493-1502.	15.6	16
7201	Partial reduction of NO to N₂O on Cu{311}: role of intermediate N₂O₂. Catalysis Science and Technology, 2022, 12, 2793-2803.	2.1	2
7202	The First Principle Study: Electronic, Optical, Elastic, and Mechanical Properties of Sno. SSRN Electronic Journal, 0, , .	0.4	0
7203	The doping effects on antibonding states and carriers of two-dimensional PC6. Physical Chemistry Chemical Physics, 2022, , .	1.3	2
7204	Inducing large birefringence by enhancing asymmetric electron distribution of Yâ€“O polyhedra. Inorganic Chemistry Frontiers, 2022, 9, 1956-1963.	3.0	8
7205	Multi-component crystals containing urea: mechanochemical synthesis and characterization by ³⁵Cl solid-state NMR spectroscopy and DFT calculations. CrystEngComm, 2022, 24, 2626-2641.	1.3	7
7206	Novel hybrid monolayers Si_xGe_ySn_{1â^'xâ^'y}: first principles study of structural, electronic, optical, and electron transport properties with NH₃ sensing application. Physical Chemistry Chemical Physics, 2022, 24, 9475-9491.	1.3	2
7207	Understanding the role of solvent in regulating the crystal habit. CrystEngComm, 2022, 24, 2226-2240.	1.3	14
7208	Type-I/Type-Ii Transition of Mose2/G-Gan Van Der Waals Heterostructures Mediated by Biaxial StrainÂAnd Electric Field for Overall Water Splitting. SSRN Electronic Journal, 0, , .	0.4	0
7209	Mediation of water-soluble oligoaniline by phenol in the anilineâ€“persulfate system under alkaline conditions. Physical Chemistry Chemical Physics, 2022, 24, 10394-10407.	1.3	2
7210	The synthesis and structureâ€“property relation analysis of metal chalcohalide crystals Cs₂InPS₄X₂ (X = Cl, Br) with mixed anions. Dalton Transactions, 2022, 51, 4728-4733.	1.6	1
7211	Edge-sharing BO₄ tetrahedra and penta-coordinated silicon in the high-pressure modification of NaBSi₃O₈. Inorganic Chemistry Frontiers, 2022, 9, 1735-1742.	3.0	6
7212	Catalytic properties of the ferryl ion in the solid state: a computational review. Catalysis Science and Technology, 2022, 12, 3069-3087.	2.1	1
7213	Physical and Superconducting Properties of Chiral Noncentrosymmetric TaRh₂B₂ and NbRh₂B₂: A Comprehensive DFT Study. ACS Applied Electronic Materials, 2022, 4, 1143-1152.	2.0	8
7214	Spectroscopic Techniques and DFT Calculations to Highlight the Effect of Fe³⁺ on the Properties of FeNb₁₁O₂₉, Anode Material for Lithium-Ion Batteries. Journal of Physical Chemistry C, 2022, 126, 4698-4709.	1.5	3
7215	First principles study of structural, elastic, electronic, and optical properties of the cubic perovskites AVO3 (Aâ€‰=â€‰Ca and La). Emergent Materials, 2022, 5, 175-186.	3.2	2
7216	The comparative study of structural, electronic, and optical properties of hydrogen peroxide and its dihydrate under pressures: first-principle calculations. Journal of Molecular Modeling, 2022, 28, 72.	0.8	6
7217	The Structural, Electronic, Magnetic, and Optical Properties of CsTe Monolayer: Effects of the Biaxial Strain and Electrical Field. Journal of Electronic Materials, 2022, 51, 2346-2355.	1.0	0

#	Article	IF	Citations
7218	High-pressure <mml:math xmlns:mml="http://www.w3.org/1998/Math/MathML"><mml:mrow><mml:msub><mml:mi>Na</mml:mi><mml:mn>3</mml:mn></mml: <mml:math		

#	Article	IF	Citations
7236	Uncovering a Vital Band Gap Mechanism of Pnictides. Advanced Science, 2022, 9, e2105787.	5.6	15
7237	Europium (II) Sulfate EuSO₄: Synthesis Methods, Crystal and Electronic Structure, Luminescence Properties. European Journal of Inorganic Chemistry, 2022, 2022, .	1.0	5
7238	SI: Advances in Density Functional Theory (DFT) Studies of Solids. Materials, 2022, 15, 2099.	1.3	5
7239	Exploring the Effect of the Number of Hydrogen Atoms on the Properties of Lanthanide Hydrides by DMFT. Applied Sciences (Switzerland), 2022, 12, 3498.	1.3	0
7240	Solid-State Photo-NMR Study on Light-Induced Nitrosyl Linkage Isomers Uncovers Their Structural, Electronic, and Diamagnetic Nature. Analytical Chemistry, 2022, 94, 4474-4483.	3.2	10
7241	Effects of (Li/Na/K) doping and point defects (VAl, Hi) on the transmission performance and optical properties of AlN. Applied Physics A: Materials Science and Processing, 2022, 128, 1.	1.1	1
7242	Atomic Model of Gold Adsorption onto the Pyrite Surface with DFT Study. Minerals (Basel,) Tj ETQq0 0 0 rgBT /Overlock 10 Tf 50 502 Td	0.8	4
7243	A Hybrid Halide Perovskite Birefringent Crystal. Angewandte Chemie - International Edition, 2022, 61, .	7.2	37
7244	Solid Electrolyte Interface Regulated by Solventâ€inâ€Water Electrolyte Enables Highâ€Voltage and Stable Aqueous Mgâ€MnO₂ Batteries. Advanced Energy Materials, 2022, 12, .	10.2	14
7245	The uptake characteristics of Prussian-blue nanoparticles for rare metal ions for recycling of precious metals from nuclear and electronic wastes. Scientific Reports, 2022, 12, 5135.	1.6	6
7246	MARMOT: magnetism, anisotropy, and more, using the relativistic disordered local moment picture at finite temperature. Electronic Structure, 2022, 4, 017001.	1.0	5
7247	NaGa₃Se₅: An Infrared Nonlinear Optical Material with Balanced Performance Contributed by Complex {[Ga₃Se₅]^{â^'}}_{â^ž} Anionic Network. Inorganic Chemistry, 2022, 61, 5479-5483.	1.9	10
7248	Regulating the Pore Structure and Heteroatom Doping of Hollow Carbon Fiber Based on a Trifunctional Template Method for High-Performance Lithium-Ion Capacitors. ACS Applied Energy Materials, 2022, 5, 3034-3042.	2.5	5
7249	Firstâ€Principles Investigation About Different Sequence of Stereochemical Activity and Birefringence in Antimony Halides. Physica Status Solidi (B): Basic Research, 0, , 2100576.	0.7	1
7250	Novel Boron Nitride Polymorphs with Graphite-Diamond Hybrid Structure. Chinese Physics Letters, 2022, 39, 036301.	1.3	5
7251	Distinguishing Sb-containing sites in SnO₂ using spectrum simulation of X-ray absorption spectroscopy. Japanese Journal of Applied Physics, 2022, 61, 048001.	0.8	3
7252	Lattice Dynamics in Organic Ferroelectrics Using Neutron Spectroscopy and Ab-Initio Modeling. Frontiers in Physics, 2022, 10, .	1.0	0
7253	Selective and efficient hydrogen separation of Pdâ€“Auâ€“Ag ternary alloy membrane. International Journal of Hydrogen Energy, 2022, 47, 13054-13061.	3.8	12

#	Article	IF	Citations
7254	Ab initio studies of magnetism and topology in solid Pd-rich $${varvec{a}}$$-PdSi alloys. Scientific Reports, 2022, 12, 4624.	1.6	3
7255	Understanding the growth mechanism of SiO2 on the surface of FeSi clusters: an MD and DFT simulation study. Journal of Sol-Gel Science and Technology, 2022, 102, 335-342.	1.1	2
7256	Dramatic n-Type Doping of Monolayer Graphene with Ferroelectric LiNbO₃ Crystals and Bilayer Two-Dimensional Electron Gases. Journal of Physical Chemistry C, 2022, 126, 4534-4541.	1.5	1
7257	Finding the First Squarates Nonlinear Optical Crystal NaHC₄O₄Â·H₂O with Strong Second Harmonic Generation and Giant Birefringence. , 2022, 4, 572-576.		19
7258	How Much Structural Information Could Be Extracted from XANES Spectra for Palladium Hydride and Carbide Nanoparticles. Journal of Physical Chemistry C, 2022, 126, 4921-4928.	1.5	7
7259	How different are the surfaces of semiconductor Ag2Se quantum dots with various sizes?. Science Bulletin, 2022, 67, 619-625.	4.3	5
7260	Predicting the stability and electronic structure of alkali metal aurides. Journal of Physics Condensed Matter, 2022, , .	0.7	0
7261	Highly Efficient Supramolecular Nucleating Agents for Poly(3-hexylthiophene). Macromolecules, 2022, 55, 2861-2871.	2.2	4
7262	Firstâ€Principles Calculations of Pressure Effects on the Structural, Electronic, Elastic, and Thermodynamic Properties of Rb ₂ M F ₆ (M â€‰=â€‰Si, Ni, Pd) Crystals. Physica Status Solidi (B): Basic Research, 0, , 2100607.	0.7	0
7263	Optical Properties and Lattice Dynamics of Pure and Sâ€Alloyed Cuâ€“Znâ€“Snâ€“Te Semiconductors: Firstâ€Principles Calculations and Raman Scattering. Physica Status Solidi (B): Basic Research, 0, , 2100618.	0.7	0
7264	First-principles study of the elastic, thermal and optical properties of Î±-PbO2 and Î²-PbO2. Indian Journal of Physics, 2022, 96, 3449-3460.	0.9	1
7265	Structural, mechanical, electronic and bonding properties of TMB₂ (TMâ€‰=â€‰Y, Sc, Ti) under pressure: a DFT investigation. Philosophical Magazine, 0, , 1-16.	0.7	0
7266	Design and Fabrication of a 5Ti5Zr5Nb1Sn Highâ€Entropy Alloy as Metallic Biomedical Material. Advanced Engineering Materials, 2022, 24, .	1.6	1
7267	Preparation of Niobium Aluminium Alloy Based on Shock Compression Method. Crystals, 2022, 12, 381.	1.0	0
7268	Synthesis and Characterization of (1â^'x)Bi1/2Na1/2TiO3+xSrNiO3-Î´ Solid Solution System. Journal of Electronic Materials, 2022, 51, 2716-2731.	1.0	1
7269	First principles of Fe/Co/Ni doping and the coexistence of O vacancy in the magnetic and optical properties of rutile TiO₂(110) surface. Physica Scripta, 2022, 97, 045815.	1.2	1
7270	Synthesis and Crystal Structure of a New Chiral Hydrogen-Bonded Organic Framework ZIOC-2. Crystal Growth and Design, 2022, 22, 2547-2556.	1.4	1
7271	Structure determination from unindexed powder data from scratch by a global optimization approach using pattern comparison based on cross-correlation functions. Acta Crystallographica Section B: Structural Science, Crystal Engineering and Materials, 2022, 78, 195-213.	0.5	6

#	Article	IF	Citations
7272	Computational materials discovery for lanthanide hydrides at high pressure for high temperature superconductivity. Physical Review Research, 2022, 4, .	1.3	2
7273	Theoretical and experimental characterization of Sn-based hydroxyapatites doped with Bi. Journal of the Australian Ceramic Society, 2022, 58, 803-815.	1.1	8
7274	Structural, elastic, electronic and optical properties of the newly synthesized selenides Tl2CdXSe4 (Xâ€‰=â€‰Ge, Sn). European Physical Journal B, 2022, 95, 1.	0.6	6
7275	Investigation on morphology of primary Mg2Si in Al-20wt.%Mg2Si composite with experiment and first-principle calculations. Materials Characterization, 2022, 187, 111836.	1.9	4
7276	CsY(SO₄)₂Â·4H₂O: A Deep-Ultraviolet Birefringent Crystal Induced by an Edge-Sharing Connection. Inorganic Chemistry, 2022, 61, 4468-4475.	1.9	11
7277	Uncovering the Structural Diversity and Excellent Performance of a Deep Ultraviolet Nonlinear Optical System Li(B₂O₃)_nF (n = 1, 1.5, 2, and 3) by Multicomponent Prediction. Chemistry of Materials, 2022, 34, 3133-3139.	3.2	10
7278	A Hybrid Halide Perovskite Birefringent Crystal. Angewandte Chemie, 2022, 134, .	1.6	6
7279	Study on the structural, mechanical, and dynamical stabilities and properties of Nb₂AN (AÂ=ÂSi, Ge, and Sn) MAX phases by first principle. Journal of the American Ceramic Society, 2022, 105, 5285-5298.	1.9	4
7280	Stacking Faults Assist Lithium-Ion Conduction in a Halide-Based Superionic Conductor. Journal of the American Chemical Society, 2022, 144, 5795-5811.	6.6	50
7281	Behavior of Occupied and Void Space in Molecular Crystal Structures at High Pressure. Crystal Growth and Design, 2022, 22, 2328-2341.	1.4	7
7282	One-Side Capping in Two-Dimensional WO₃-Type Materials Leading to Strong Second-Harmonic Response. Chemistry of Materials, 2022, 34, 3501-3508.	3.2	14
7283	Effect of annealing temperature in carbon powder on thermoelectric properties of the SrTiO3â^Î´ single crystal in the [111] crystal orientation. Ceramics International, 2022, 48, 18876-18883.	2.3	2
7284	Atomically Thin TaSe₂ Film as a Highâ€Performance Substrate for Surfaceâ€Enhanced Raman Scattering. Small, 2022, 18, e2107027.	5.2	28
7285	A₂BeS₂O₈ (A = NH₄, K, Rb, Cs) Deep Ultraviolet Nonlinear Optical Crystals. Chemistry of Materials, 2022, 34, 3781-3788.	3.2	18
7286	An Experimental and Theoretical Study of the Optical Properties of (C2H7N4O)2BiCl5 for an Optoelectronic Application. Inorganics, 2022, 10, 48.	1.2	5
7287	2.5 V high performance aqueous and semiâ€solidâ€state symmetric supercapacitors enabled by 3 m sulfolaneâ€saturated aqueous electrolytes. Energy Technology, 0, , .	1.8	2
7288	Structure and disorder in MgSiO₃ glasses above megabar pressures via nuclear magnetic resonance: DFT calculations. Journal of the American Ceramic Society, 2022, 105, 5151-5166.	1.9	3
7289	High-precision atomic image reconstruction from photoelectron hologram of O on W(110) by SPEA-L1. Journal of Electron Spectroscopy and Related Phenomena, 2022, 256, 147177.	0.8	2

#	Article	IF	Citations
7291	Deep dive into machine learning density functional theory for materials science and chemistry. Physical Review Materials, 2022, 6, .	0.9	28
7292	Differences in Coformer Interactions of the 2,4-Diaminopyrimidines Pyrimethamine and Trimethoprim. Crystal Growth and Design, 2022, 22, 3163-3173.	1.4	4
7293	Solar-Light-Driven Ag9(SiO4)2NO3 for Efficient Photocatalytic Bactericidal Performance. Journal of Composites Science, 2022, 6, 108.	1.4	1
7294	Terahertz spectral properties of glucose and two disaccharides in solid and liquid states. IScience, 2022, 25, 104102.	1.9	4
7295	Adsorption of carboxyl-containing monomers on C₃S: a first-principle study. Petroleum Science and Technology, 2023, 41, 444-456.	0.7	2
7296	A DFT+U approach: Superior charge transfer characteristics and optoelectronic properties of GQD@TiO2Ârutile (110) surface for improved hydrogen evolution. Surfaces and Interfaces, 2022, 30, 101952.	1.5	4
7297	Assignment of the Vibrational Spectra of Diiron Nonacarbonyl, Fe2(CO)9. Physchem, 2022, 2, 108-115.	0.5	1
7298	Study of Two-Dimensional Janus WXY (Xâ‰Y= S, Se, and Te) Trilayer Homostructures for Photovoltaic Applications Using DFT Screening of Different Stacking Patterns. ACS Omega, 2022, 7, 12947-12955.	1.6	5
7299	Calculation of the vibrational spectra of CdSe and CdS crystals with zinc blende structure. Materials Today: Proceedings, 2022, 62, 5812-5818.	0.9	2
7300	Theoretical investigation of structural, topological, mechanical and thermal behavior of SrPtS and BaPtS Heusler alloys. Physica Scripta, 2022, 97, 055703.	1.2	2
7301	An experimental and theoretical study of the structural, optical, electrical, and dielectric properties of PrAsO4. Journal of Alloys and Compounds, 2022, 910, 164894.	2.8	6
7302	Structural, electronic and optoelectronic properties of asymmetric organic ligands in Dion-Jacobson phase perovskites. Solid State Communications, 2022, 350, 114761.	0.9	4
7303	Structural and optical properties of undoped and Sb-doped lead oxide thin films synthesized via the chemical bath deposition method. Optical Materials, 2022, 126, 112179.	1.7	10
7304	Highâ€Rate Performance of Fluorinated Carbon Material Doped by Phosphorus Species for Lithiumâ€Fluorinated Carbon Battery. Energy Technology, 2022, 10, .	1.8	10
7305	Vibrational Spectroscopy of Hexahalo Complexes. Inorganic Chemistry, 2022, , .	1.9	1
7306	First-principles study of the influence of Nb doping on the electronic structure and optoelectronic properties of Î²-Ga2O3. Physics Letters, Section A: General, Atomic and Solid State Physics, 2022, 433, 128025.	0.9	5
7307	Optical response, lithiation and charge transfer in Sn-based 211 MAX phases with electron localization function. Journal of Materials Research and Technology, 2022, 18, 2470-2479.	2.6	13
7308	B3O3 monolayer with dual application in sensing of COVID-19 biomarkers and drug delivery for treatment purposes: A periodic DFT study. Journal of Molecular Liquids, 2022, 354, 118855.	2.3	19

#	Article	IF	Citations
7309	The effect mechanism of Zn, Ni and Mn solute elements on the WC/Cu-based filler metal interfacial properties: first-principles calculations and experiments. Journal of Materials Research and Technology, 2022, 18, 2354-2362.	2.6	12
7310	Ni-induced photoabsorption and hydrogen desorption on the Liâ€“Mg hydrides using ab initio calculation. Solid State Communications, 2022, 347, 114736.	0.9	4
7311	Interfacial characterization and its influence on the corrosion behavior of Mg-SiO2 nanocomposites. Acta Materialia, 2022, 230, 117840.	3.8	13
7312	Photocatalytic hydrogen evolution reaction with high solar-to-hydrogen efficiency driven by the Sb2S3 monolayer and RuI2/Sb2S3 heterostructure with solar light. Journal of Power Sources, 2022, 532, 231352.	4.0	40
7313	First-principles calculations to investigate the polymorph effects of CuAlO2. Computational Materials Science, 2022, 209, 111403.	1.4	7
7314	Pressure modified structure, bandgap, and optical property of self-activated strontium chlorovanadate phosphors. Physica B: Condensed Matter, 2022, 635, 413845.	1.3	1
7315	A simulation study on the electromagnetic structure and optical properties of Co doped TiO2. Computational Materials Science, 2022, 209, 111404.	1.4	3
7316	Atomic structures and stability of finite-size extended interstitial defects in silicon: Large-scale molecular simulations with a neural-network potential. Scripta Materialia, 2022, 214, 114650.	2.6	2
7317	A Cubic Mg2MnO4 Cathode for non-aqueous Magnesium Batteries. Energy Storage Materials, 2022, 48, 12-19.	9.5	14
7318	NO2 capture on graphene/WSe2 heterostructure with high sensitivity and selectivity modulated by external electric field. Journal of Physics and Chemistry of Solids, 2022, 165, 110684.	1.9	7
7319	Influence of Nd concentrations on the structural, electronic and optical properties of anatase TiO2: A first-principles approach. Computational Condensed Matter, 2022, 31, e00672.	0.9	1
7320	Study on the most effective pressure application method to increase the critical temperature of MgB2. Materials Today Communications, 2022, 31, 103432.	0.9	0
7321	Exploring the elastic, mechanical and anisotropic response of Ti-5Al-XSn alloys through DFT calculations. Chinese Journal of Physics, 2022, 77, 151-160.	2.0	7
7322	Modulation effect of low-electronegativity non-metallic elements on the electronic structure of group-IVB transition metal oxides. Materials Science in Semiconductor Processing, 2022, 144, 106607.	1.9	0
7323	Ti0.85Eu3SiS7: The rare-earth/Ti based quaternary sulfide containing two variable valence elements. Journal of Solid State Chemistry, 2022, 311, 123082.	1.4	1
7324	Exploration of multifunctional gas Opto-sensing material of oxidic tubular g-C3N4: Density functional theory. Applied Surface Science, 2022, 591, 153211.	3.1	1
7325	Mg-ion diffusion on the surface of Ti3C2S2 MXene. Journal of Physics and Chemistry of Solids, 2022, 166, 110713.	1.9	7
7326	Size effect of PdC nanoparticles synthesized by S-containing silane coupling agents on semi-hydrogenation of acetylene. Applied Surface Science, 2022, 589, 153021.	3.1	2

#	Article	IF	Citations
7327	Effect of Fe2+/3+ doping on the new magnetic mechanism and itinerant electronic characteristics of ZnO. Journal of Magnetism and Magnetic Materials, 2022, 554, 169305.	1.0	2
7328	Exploring the origin of efficient adsorption of poly- and perfluoroalkyl substances in household point-of-use water purifiers: Deep insights from a joint experimental and computational study. Science of the Total Environment, 2022, 831, 154988.	3.9	16
7329	A silk sericin-confined in-situ synthesis strategy: Fe7S8 inserted N,S co-doped carbon nano-aggregates for high-performance sodium storage. Journal of Alloys and Compounds, 2022, 910, 164875.	2.8	6
7330	Ni, In co-doped ZnIn2S4 for efficient hydrogen evolution: Modulating charge flow and balancing H adsorption/desorption. Applied Catalysis B: Environmental, 2022, 310, 121337.	10.8	55
7331	The dehydrogenation of butane on metal-free graphene. Journal of Colloid and Interface Science, 2022, 619, 377-387.	5.0	8
7332	First-principles calculations to investigate the interfacial energy and electronic properties of Mg/AlN interface. Journal of Physics and Chemistry of Solids, 2022, 167, 110705.	1.9	15
7333	First-principles calculations of structural, electronic and elastic properties of carbon allotropes. Materials Science in Semiconductor Processing, 2022, 146, 106692.	1.9	3
7334	As2O3 capture from incineration flue gas by Fe2O3-modified porous carbon: Experimental and DFT insights. Fuel, 2022, 321, 124079.	3.4	15
7335	Lattice Matching and Halogen Regulation for Synergistically Induced Uniform Zinc Electrodeposition by Halogenated Ti₃C₂ MXenes. ACS Nano, 2022, 16, 813-822.	7.3	90
7336	Zn, O Co-doped 2D GaN for Visible Light-driven Photocatalytic Water Splitting using First-principles. , 2021, , .		0
7337	Pushing KTiOPO₄-like Nonlinear Optical Sulfates into the Deep-Ultraviolet Spectral Region. Inorganic Chemistry, 2021, 60, 18950-18956.	1.9	7
7338	Synthesis and Characterization of Novel Nanoparticles of Lithium Aluminum Iodate LiAl(IO3)4, and DFT Calculations of the Crystal Structure and Physical Properties. Nanomaterials, 2021, 11, 3289.	1.9	3
7339	Research on the Electronic Properties of Tyrosine Dipeptide Molecule: Evaluation of the First-principles Theory. Russian Journal of Physical Chemistry B, 2021, 15, S181-S188.	0.2	0
7340	The electronic states of ITOâ€“MoS2: Experiment and theory. MRS Communications, 2022, 12, 137-144.	0.8	3
7341	Surface functionalization of phosphorene via P-H bond for ambient protection and robust photocatalytic H2 evolution. Science China Materials, 2022, 65, 1245-1251.	3.5	2
7342	Study on the relationship between uniaxial strain and critical transition temperature of MgB₂ based on first-principles. Journal of Physics Condensed Matter, 2022, 34, 105601.	0.7	1
7343	A First-Principles Study of Gas Molecule Adsorption on Carbon-, Nitrogen-, and Oxygen-Doped Two-Dimensional Borophene. Advances in Condensed Matter Physics, 2021, 2021, 1-10.	0.4	5
7344	Plasmonic and Graphene-Functionalized High-Performance Broadband Quasi-Two-Dimensional Perovskite Hybrid Photodetectors. ACS Applied Materials & Interfaces, 2021, 13, 61496-61505.	4.0	11

#	Article	IF	Citations
7345	Preparation of CeO₂/CaO with Anti-sintering for Efficient Capture of As₂O₃ from Flue Gas at a High Temperature. Energy & Fuels, 2021, 35, 20197-20205.	2.5	18
7346	Structural Chemistry and Excellent Nonlinear Optical Properties of a Series of Ternary Selenides Ga_xIn_{2â€“x}Se₃. Inorganic Chemistry, 2022, 61, 431-438.	1.9	14
7347	Calculating dynamical mean-field theory forces in ab initio ultrasoft pseudopotential formalism. Physical Review B, 2021, 104, .	1.1	6
7348	PbBi₃O₄X₃ (X = Cl, Br) with Single/Double Halogen Layers as a Photocatalyst for Visible-Light-Driven Water Splitting: Impact of a Halogen Layer on the Band Structure and Stability. Chemistry of Materials, 2021, 33, 9580-9587.	3.2	11
7349	Effect of Lattice Substitution on Adsorption of Hexavalent Chromium by Montmorillonite, Nontronite, and Beidellite. Minerals (Basel, Switzerland), 2021, 11, 1407.	0.8	2
7350	Navigating the Ti-C-O and Al-C-O ternary systems through theory-driven discovery. Physical Review Materials, 2021, 5, .	0.9	2
7351	Pressure dependent structural, elastic and mechanical properties with ground state electronic and optical properties of half-metallic Heusler compounds Cr2YAl (Y=Mn, Co): first-principles study. Heliyon, 2021, 7, e08585.	1.4	9
7352	Determining the Three-Dimensional Structures of Silica-Supported Metal Complexes from the Ground Up. Inorganic Chemistry, 2022, 61, 1067-1078.	1.9	8
7353	Implicit Solvation Methods for Catalysis at Electrified Interfaces. Chemical Reviews, 2022, 122, 10777-10820.	23.0	82
7354	Anomalous magnetic exchange in a dimerized quantum magnet composed of unlike spin species. Physical Review B, 2021, 104, .	1.1	2
7355	Firstâ€principles investigation of the (HfSe ₂) _{4â^' n} â€“(HfSSe) _n (n Â=Â0, 1, 2, 3, 4) lateral heterostructures. International Journal of Quantum Chemistry, 2022, 122, .	1.0	2
7356	Posttreatment Effects on the Crystal Structure and Superconductivity of Ca-Free Double-Layered Cuprate Sr₂SrCu₂O_{4+y}F_{2â€“y}. Chemistry of Materials, 2021, 33, 9690-9697.	3.2	1
7357	Crystal structure of phenanthrenide salts stabilized by 15-crown-5 and 18-crown-6. Zeitschrift Fur Naturforschung - Section B Journal of Chemical Sciences, 2022, 77, 197-201.	0.3	1
7358	The first principle study of structural, mechanical, electronic and optical properties of double halide perovskite K₂BI₆ (Bâ€‰=â€‰Ti, Zr and Hf). Molecular Physics, 0, , .	0.8	3
7359	Rotational Dynamics of Desorption: Methane and Ethane at Stepped and Kinked Platinum Surfaces. Journal of Physical Chemistry C, 2021, 125, 27938-27948.	1.5	2
7360	Molecular Engineering of Thienyl Functionalized Ullazines as Holeâ€Transporting Materials for Perovskite Solar Cells. Solar Rrl, 2022, 6, .	3.1	5
7361	KNa0.78Eu0.27In3.80B12S12: A Novel Hexanary Thioborate Featuring B12S12 Cluster and Diverse InSx (x =) Tj ETQq0 0 0 rgBT /Overloc	3.0	3
7362	Computer simulation of hypothetical hydrogen ordered structure of ice XIX. Physical Chemistry Chemical Physics, 2022, 24, 11023-11029.	1.3	2

#	Article	IF	Citations
7363	Stoichiometry modulates the optoelectronic functionality of zinc phosphide (Zn_{3â[']x}P_{2+x}). Faraday Discussions, 0, 239, 202-218.	1.6	6
7364	Challenges of modeling nanostructured materials for photocatalytic water splitting. Chemical Society Reviews, 2022, 51, 3794-3818.	18.7	64
7365	The Effect of Vanadium Doping on Carbon Behavior in Tungsten: A Firstâ€Principle Study. Crystal Research and Technology, 0, , 2100182.	0.6	0
7366	Structural-Phase Ð¡hanges During the D1aâ†'A1 Phase Transition in the Ni4Mo Alloy. Izvestiya of Altai State University, 2022, , 36-43.	0.1	0
7367	Enriched dâ€Band Holes Enabling Fast Oxygen Evolution Kinetics on Atomicâ€Layered Defectâ€Rich Lithium Cobalt Oxide Nanosheets. Advanced Functional Materials, 2022, 32, .	7.8	24
7368	Electronic phase transition and enhanced optoelectronic performance of lead-free halide perovskites AGeI3 (A = Rb, K) under pressure. Materials Today Communications, 2022, 31, 103532.	0.9	13
7369	Indirect electrodeposition of a NiMo@Ni(OH)2MoO composite catalyst for superior hydrogen production in acidic and alkaline electrolytes. Renewable Energy, 2022, 191, 370-379.	4.3	4
7370	Sensing Material-Dependent Interference of Multiple Heavy Metal Ions: Experimental and Simulated Thermodynamics Study on Cu(II), Cd(II), and As(III) Electroanalysis. Analytical Chemistry, 2022, 94, 6225-6233.	3.2	12
7371	Suppression of the superconducting phase in new structures of elemental sulfur at terapascal pressures. Physical Review B, 2022, 105, .	1.1	2
7372	Two-Dimensional Negative Thermal Expansion in a Crystal of LiBO₂. Chemistry of Materials, 2022, 34, 4195-4201.	3.2	7
7373	Carbon and Silicon co-doping effect on microstructural and optoelectronic properties of ZnO: An ab initio study. Optik, 2022, , 169138.	1.4	0
7374	The fingerprints of nifedipine/isonicotinamide cocrystal polymorph studied by terahertz time-domain spectroscopy. International Journal of Pharmaceutics, 2022, 620, 121759.	2.6	7
7375	Size Effects of the Anions in the Ionothermal Synthesis of Carbon Nitride Materials. Chemistry - A European Journal, 2022, 28, .	1.7	18
7376	A novel superhard boron nitride polymorph with monoclinic symmetry. Communications in Theoretical Physics, 2022, 74, 065701.	1.1	7
7377	Surface spinel and interface oxygen vacancies enhanced lithium-rich layered oxides with excellent electrochemical performances. Chemical Engineering Journal, 2022, 443, 136434.	6.6	29
7378	Stability Trends in Mono-Metallic 3d Layered Double Hydroxides. Nanomaterials, 2022, 12, 1339.	1.9	4
7379	Crystalline C ₃ N ₃ H ₃ tube (3,0) nanothreads. Proceedings of the National Academy of Sciences of the United States of America, 2022, 119, e2201165119.	3.3	13
7380	Chloride Adsorption Capacity of Monocarbonate: The Importance of Iron Doping. ACS Sustainable Chemistry and Engineering, 2022, 10, 5621-5632.	3.2	3

#	Article	IF	Citations
7381	Exploring the Stability of Single-Atom Catalysts Using the Density Functional Theory-Based Global Optimization Method: H₂ Formation on VO_x/Î³-Al₂O₃(100). Journal of Physical Chemistry C, 2022, 126, 6973-6981.	1.5	7
7382	The Combination of Structure Prediction and Experiment for the Exploration of Alkaliâ€Earth Metalâ€Contained Chalcopyriteâ€Like IR Nonlinear Optical Material. Advanced Science, 2022, 9, e2106120.	5.6	44
7383	Possible applications of Mo2C in the orthorhombic and hexagonal phases explored via ab-initio investigations of elastic, bonding, optoelectronic and thermophysical properties. Results in Physics, 2022, 37, 105505.	2.0	30
7384	The self-complementary effect through strong orbital coupling in ultrathin high-entropy alloy nanowires boosting pH-universal multifunctional electrocatalysis. Applied Catalysis B: Environmental, 2022, 312, 121431.	10.8	40
7385	Spectral broadening mechanism of Yb³⁺-doped cubic Lu_xSc_{2-x}O₃ sesquioxide crystals for ultrafast lasers. Optical Materials Express, 2022, 12, 1963.	1.6	6
7386	First-principles insights into the mechanical, optoelectronic, thermophysical, and lattice dynamical properties of binary topological semimetal BaGa2. Results in Physics, 2022, 37, 105507.	2.0	14
7387	Effects of the cation ordering in Mg:Al and Zn:Al layered double hydroxides on crystallographic and spectroscopical properties by means of first principles calculations. Applied Clay Science, 2022, 223, 106496.	2.6	6
7388	Klein tunneling and ballistic transport in graphene and related materials. , 0, , 118-142.		0
7389	Quantum transport in disordered graphene-based materials. , 0, , 143-218.		0
7390	Ab initio and multiscale quantum transport in graphene-based materials. , 0, , 232-299.		0
7391	Electronic structure calculations: the density functional theory (DFT). , 0, , 314-331.		0
7392	Electronic structure calculations: the many-body perturbation theory (MBPT). , 0, , 332-337.		0
7393	Green's functions and ab initio quantum transport in the Landauerâ€“BÃ¼ttiker formalism. , 0, , 338-357.		0
7401	Computational vibrational spectroscopy of moleculeâ€“surface interactions: what is still difficult and what can be done about it. Physical Chemistry Chemical Physics, 2022, 24, 15158-15172.	1.3	12
7402	Stabilizing intermediate phases via the efficient confinement effects of the SnS₂-SPAN fibre composite for ultra-stable half/full sodium/potassium-ion batteries. Journal of Materials Chemistry A, 2022, 10, 11449-11457.	5.2	36
7403	Mg(H₂O)₆[(IO₂(OH))₂(IO₃)]₂: a new iodate with a very large band gap and optical anisotropy. Journal of Materials Chemistry C, 2022, 10, 8776-8782.	2.7	9
7405	Depolarization of Few-Layer III-V and II-VI Materials through Symmetric Rumpling. Physical Chemistry Chemical Physics, 2022, , .	1.3	0
7406	Nickel nanoparticle-activated MoS₂for efficient visible light photocatalytic hydrogen evolution. Nanoscale, 2022, 14, 8601-8610.	2.8	11

#	Article	IF	Citations
7407	High-T_p-triggered phase transition exhibiting switchable dielectricâ€“thermal responses and long photoluminescence lifetime in a novel inclusion luminophor. CrystEngComm, 2022, 24, 3630-3636.	1.3	3
7408	N-Coordinated Ir single atoms anchored on carbon octahedrons for catalytic oxidation of formaldehyde under ambient conditions. Catalysis Science and Technology, 2022, 12, 4001-4011.	2.1	6
7409	FIRST-PRINCIPLES SIMULATION: STUDY OF THE STRUCTURAL, ELECTRONIC, MECHANICAL AND OPTICAL PROPERTIES OF DISULFIDE XS₂ (X=Ta, Ti) COMPOUNDS FOR OPTOELECTRONIC APPLICATIONS. Surface Review and Letters, 2022, 29, .	0.5	3
7410	Muonâ€“Nitrogen Quadrupolar Level Crossing Resonance in a Charge Transfer Salt. Journal of Physical Chemistry C, 2022, 126, 7529-7534.	1.5	2
7411	Various Dimensional Culâ€“DPA Coordination Polymers Based on the Same Components for Different Electronic and Photothermal Properties. Small Structures, 2022, 3, .	6.9	3
7412	Four Carbon Allotropes Form COT Structures. ACS Applied Electronic Materials, 2022, 4, 2353-2363.	2.0	9
7413	Electronic Structure Calculation of Cr3+ and Fe3+ in Phosphor Host Materials Based on Relaxed Structures by Molecular Dynamics Simulation. Technologies, 2022, 10, 56.	3.0	2
7414	Maximizing the linear and nonlinear optical responses of alkaline tricyanomelaminate. Fundamental Research, 2022, , .	1.6	5
7415	Ab initio simulations of Î±- and Î²-ammonium carbamate (NH₄Â·NH₂CO₂), and the thermal expansivity of deuterated Î±-ammonium carbamate from 4.2 to 180â€…K by neutron powder diffraction. Acta Crystallographica Section B: Structural Science, Crystal Engineering and Materials, 2022, 78, 459-475.	0.5	2
7416	Lone Pair-Driven Enhancement of Birefringence in Polar Alkali Metal Antimony Phosphates. Chemistry of Materials, 2022, 34, 4224-4231.	3.2	19
7417	Lattice Dynamics in the NASICON NaZr₂(PO₄)₃ Solid Electrolyte from Temperature-Dependent Neutron Diffraction, NMR, and Ab Initio Computational Studies. Chemistry of Materials, 2022, 34, 4029-4038.	3.2	6
7418	A New BCN Compound with Monoclinic Symmetry: First-Principle Calculations. Materials, 2022, 15, 3186.	1.3	4
7419	N-Iodosaccharinâ€“pyridine co-crystal system under pressure: experimental evidence of reversible twinning. Acta Crystallographica Section B: Structural Science, Crystal Engineering and Materials, 2022, 78, 436-449.	0.5	2
7420	Edgeâ€Assisted Epitaxy of 2D TaSe₂â€MoSe₂ Metalâ€“Semiconductor Heterostructures and Application to Schottky Diodes. Advanced Functional Materials, 2022, 32, .	7.8	10
7421	An experimental and theoretical investigation of Co-containing hydroxyapatites prepared at different temperatures. Journal of the Australian Ceramic Society, 0, , .	1.1	0
7422	Hydrogenated Zinc Oxide as an Alternative Low-Loss Plasmonic Material with Fano Resonance in Near-IR. Journal of Physical Chemistry C, 2022, 126, 8190-8198.	1.5	2
7423	The spontaneous self-assembly of a molecular water pipe in 3D space. IUCrJ, 2022, 9, 364-369.	1.0	5
7424	High-Pressure Structural Behavior of para-Xylene. Crystal Growth and Design, 0, , .	1.4	2

#	Article	IF	Citations
7425	The Magnetic Suppression and Electronic Structure Evolution of K1-xFe2Se2 with Different K Vacancy Concentration. Journal of Superconductivity and Novel Magnetism, 0, , 1.	0.8	0
7426	Low-frequency lattice vibrations from atomic displacement parameters of Î±-FOX-7, a high energy density material. Acta Crystallographica Section B: Structural Science, Crystal Engineering and Materials, 2022, 78, 376-384.	0.5	2
7427	An Optimized KBe₂BO₃F₂â€Like Structure: The Unity of Deepâ€Ultraviolet Transparency, Nonlinear Optical Property, and Ferroelectricity. Advanced Optical Materials, 2022, 10, .	3.6	12
7428	Beam-driven dynamics of aluminium dopants in graphene. 2D Materials, 2022, 9, 035009.	2.0	8
7429	Hydrogen-bonded metal-nucleobase frameworks for highly selective capture of ethane/propane from methane and methane/nitrogen separation. Nano Research, 2022, 15, 7695-7702.	5.8	15
7430	New quaternary sulfide LiGaSiS4: Synthesis, structure and optical properties. Journal of Solid State Chemistry, 2022, , 123230.	1.4	0
7431	Small Organic Molecular-Based Hybrid Halides with High Photoluminescence Quenching Temperature. Inorganic Chemistry, 2022, 61, 7560-7567.	1.9	10
7432	Characterisation of Vandenbrandeite: A Potential Alteration Product of Spent Nuclear Fuel. American Mineralogist, 2022, , .	0.9	0
7433	High Ionâ€Selectivity of Garnet Solid Electrolyte Enabling Separation of Metallic Lithium. Energy and Environmental Materials, 2023, 6, .	7.3	1
7434	Stability, deformation, physical properties of novel hard B2CO phases. Journal of Materials Science, 2022, 57, 9231-9245.	1.7	3
7435	Selective Hydrogenation of 1,3-Butadiene over Ceria Catalyst: A Molecular Insight. Molecular Catalysis, 2022, 524, 112331.	1.0	3
7436	Structural, electronic, mechanical, and thermodynamic properties of Cuâ€“Ti intermetallic compounds: First-principles calculations. Solid State Communications, 2022, 352, 114814.	0.9	5
7437	Cooperative Enhancement of Second Harmonic Generation in an Organicâ€“Inorganic Hybrid Antimony Halide. Crystal Growth and Design, 2022, 22, 3875-3881.	1.4	22
7438	Quantitative Analysis of Nanorough Hydrogenated Si(111) Surfaces through Vibrational Spectral Assignment by Periodic DFT Calculations. Journal of Physical Chemistry C, 2022, 126, 8278-8286.	1.5	0
7439	Two-dimensional TeX(X=C, Si, Ge) monolayers with strong intrinsic electric field for efficiency hydrogen evolution reaction. Surfaces and Interfaces, 2022, 31, 102011.	1.5	4
7440	A Theoretical Perspective to Study the Optical Properties of Tetrafluoroborates. ChemPhysChem, 2022, 23, .	1.0	1
7441	Application of atomic simulation for studying hydrogen embrittlement phenomena and mechanism in iron-based alloys. International Journal of Hydrogen Energy, 2022, 47, 20288-20309.	3.8	24
7442	Systematic Comparison of Genetic Algorithm and Basin Hopping Approaches to the Global Optimization of Si(111) Surface Reconstructions. Journal of Physical Chemistry A, 2022, 126, 3043-3056.	1.1	5

#	Article	IF	Citations
7443	Force constant disorder in the Ni₄₄Nb₅₆ bulk metallic glass as observed by deep inelastic neutron scattering augmented by isotopic substitution. Physica Scripta, 2022, 97, 065702.	1.2	1
7444	Low-temperature magnetic crossover in the topological kagome magnet TbMn6Sn6. Communications Physics, 2022, 5, .	2.0	12
7445	Driving the active site incorporation in zeolitic materials via the organic structureâ€directing agent through development of Hâ€bonds with hydroxyl groups. Chemistry - A European Journal, 2022, , .	1.7	3
7446	First-principles study of structural, electronic, elastic and dielectric properties of RbLi₂(NH₂)₃, LiH and LiNH₂. International Journal of Modern Physics B, 2022, 36, .	1.0	1
7447	A transferable force-field for alkali metal nitrates. Journal of Physics Communications, 2022, 6, 055011.	0.5	3
7448	Inâ€situ separation and characterization of britholite crystals in REâ€bearing slag via superâ€gravity. Journal of the American Ceramic Society, 0, , .	1.9	1
7449	Realization of Enlarged Birefringence from BaCdBe₂(BO₃)₂F₂ to NaMgBe₂(BO₃)₂F via the Cation Size Effect as a Potential Deep-Ultraviolet Birefringent Material. Inorganic Chemistry, 2022, 61, 7624-7630.	1.9	8
7450	Colorimetric paper test strips based on cesium lead bromide perovskite nanocrystals for rapid detection of ciprofloxacin hydrochloride. Journal of Physics Condensed Matter, 2022, 34, 304002.	0.7	1
7451	Insight into the activation of CO2 and H2 on K2O-adsorbed Fe5C2(110) for olefins production: A density functional theory study. Molecular Catalysis, 2022, 524, 112323.	1.0	4
7452	Development of the new interatomic potentials for the wurtzite phase of ZnO. Applied Physics A: Materials Science and Processing, 2022, 128, .	1.1	2
7453	Elastic, electronic, optical and thermoelectric properties of the novel Zintl-phase Ba2ZnP2. Solid State Sciences, 2022, 128, 106893.	1.5	75
7454	Significant improvement of the Seebeck coefficient of Fe2VAlÂwith antisite defects. Materials Today Communications, 2022, 31, 103510.	0.9	2
7455	To what extent do bond length and angle govern the 13C and 1H NMR response to weak CHâ‹¯O hydrogen bonds? A case study of caffeine and theophylline cocrystals. Solid State Nuclear Magnetic Resonance, 2022, 119, 101795.	1.5	2
7456	Influence of heavy Hf doping in CeO2: Prediction on various physical properties. Results in Physics, 2022, 37, 105569.	2.0	5
7457	Pt accelerated coarsening of A15 precipitates in Cr-Si alloys. Materials and Design, 2022, 218, 110655.	3.3	0
7458	Spinel-type MgxMn2-yFeyO4 as a new electrode for sodium ion batteries. Electrochimica Acta, 2022, 421, 140492.	2.6	5
7459	Unraveling the adsorption behaviors of uranium and thorium on the hydroxylated titanium carbide MXene. Computational Materials Science, 2022, 210, 111460.	1.4	10
7460	Radial and axial vibration modes of graphyne nanotubes. Materials Today Communications, 2022, 31, 103610.	0.9	1

#	Article	IF	Citations
7461	Prediction of two-dimensional AlBrSe monolayer as a highly efficient photocatalytic for water splitting. Surfaces and Interfaces, 2022, 31, 102020.	1.5	18
7462	Synthesis, crystal structure and optical properties of the first bromine-containing iodate: Pb2IO3Br3. Solid State Sciences, 2022, 129, 106898.	1.5	0
7463	Oxidation mechanism of arsenopyrite under alkaline conditions: Experimental and theoretical analyses. Journal of Cleaner Production, 2022, 358, 131987.	4.6	9
7464	Ab initio study of negative electron affinity on the scandium-terminated diamond (100) surface for electron emission devices. Carbon, 2022, 196, 176-185.	5.4	6
7465	Insights on structural, elastic, electronic and optical properties of double-perovskite halides Rb2CuBiX6 (X=Br, Cl). Journal of Physics and Chemistry of Solids, 2022, 167, 110791.	1.9	14
7466	First principles study on optical and thermal properties of BaTiS3. Optik, 2022, 261, 169196.	1.4	4
7467	Locating the rate-limiting step of hydrogen conversion on Sr2Fe1.5Mo0.5O6 (0 0 1) surface: Implications for efficient SOFC anode design. Applied Surface Science, 2022, 595, 153513.	3.1	6
7468	Electronic and magnetic properties of iridium-based novel Heusler alloys. Journal of Magnetism and Magnetic Materials, 2022, 555, 169405.	1.0	0
7469	Investigation on the WC/Cu interfacial bonding properties: First-principles prediction and experimental verification. International Journal of Refractory Metals and Hard Materials, 2022, 106, 105872.	1.7	13
7470	Effects of surface microtopography on material removal and ultra-smooth surface creation processes in ultraviolet-induced nanoparticle colloid jet machining. Colloids and Surfaces A: Physicochemical and Engineering Aspects, 2022, 648, 129161.	2.3	2
7471	Efficient photothermal degradation on Bi12CoO20 sillenite with a strong internal electric field induced by the thermal effect. Applied Catalysis B: Environmental, 2022, 313, 121452.	10.8	8
7472	Computational molecular-level prediction of heterocyclic compoundâ€“metal surface interfacial behavior. Journal of Colloid and Interface Science, 2022, 622, 452-468.	5.0	16
7473	Growth and characterization of melem hydrate crystals with a hydrogen-bonded heptazine framework. Physical Chemistry Chemical Physics, 2022, 24, 13922-13934.	1.3	7
7474	High Open-Circuit Voltage in Double Perovskite Oxide A2NdSbO6 (A = Ba, Sr) Photoanode-Based Dye-Sensitized Solar Cells. Journal of Electronic Materials, 2022, 51, 4281-4287.	1.0	3
7475	Insights into the influence mechanism of Mg2+ doping on hydration activity of kaolinite surface: A DFT calculation. Chemical Physics, 2022, 560, 111576.	0.9	12
7476	Tailoring Oxygen Reduction Reaction Pathway on Spinel Oxides via Surficial Geometricalâ€Site Occupation Modification Driven by the Oxygen Evolution Reaction. Advanced Materials, 2022, 34, e2202874.	11.1	52
7477	The structural, mechanical, and electronic properties of LiAlB ₄ under pressure from first principles. Physica Status Solidi C: Current Topics in Solid State Physics, 2017, 14, 1700080.	0.8	0
7478	Rice husk-derived porous silicon dioxide fillers for enhancing ionic conductivity in a solid-state electrolyte of lithiumâ€“sulfur batteries under molecular dynamic calculation. Journal of Materials Chemistry A, 2022, 10, 12928-12937.	5.2	4

#	Article	IF	Citations
7479	Linear unit BN₂: a novel birefringence-enhanced fundamental module with sp orbital hybridization. RSC Advances, 2022, 12, 14757-14764.	1.7	1
7480	Significant photodegradation of carcinogenic organic dyes by a 1D supramolecular heteroleptic Cu(<scp>ii</scp>) complex under sunlight irradiation. New Journal of Chemistry, 2022, 46, 11804-11811.	1.4	3
7481	Mid-Infrared Nonlinear Optical Halides with Diamond-like Structures: A Theoretical and Experimental Study. Chemistry of Materials, 2022, 34, 5301-5310.	3.2	9
7482	Simulated carbon K edge spectral database of organic molecules. Scientific Data, 2022, 9, 214.	2.4	6
7483	Anatomy of Classical Boronâ€“Boron Bonding: Overlap and sp Dissonance. Journal of Physical Chemistry A, 2022, , .	1.1	4
7484	Structural, elastic and mechanical properties of Hf-doped TiAl2 and Î±-TiAl3 intermetallic compounds: first-principle calculations. European Physical Journal B, 2022, 95, .	0.6	5
7485	Ab-initio Study of structural, elastic, electronic and optical properties of hexahalometallate single crystals K2XBr6(Xâ€‰=â€‰Se, Pt). Scientific Reports, 2022, 12, 8345.	1.6	2
7486	Realizing high thermoelectric performance in GeTe by defect engineering on cation sites. Journal of Materials Chemistry C, 2022, 10, 9052-9061.	2.7	5
7487	Indirect to direct band gap transition through order to disorder transformation of Cs₂AgBiBr₆via creating antisite defects for optoelectronic and photovoltaic applications. RSC Advances, 2022, 12, 15461-15469.	1.7	21
7488	A flexible functional module to regulate ultraviolet optical nonlinearity for achieving a balance between a second-harmonic generation response and birefringence. Chemical Science, 2022, 13, 6990-6997.	3.7	14
7489	B/N co-doped carbon supported molybdenum carbide catalysts with oxygen vacancies for facile synthesis of flavones through oxidative dehydrogenation. Journal of Colloid and Interface Science, 2022, 623, 735-743.	5.0	4
7490	Monitoring Gases Content in Modern Agriculture: A Density Functional Theory Study of the Adsorption Behavior and Sensing Properties of CO2 on MoS2 Doped GeSe Monolayer. Sensors, 2022, 22, 3860.	2.1	10
7491	Pressure-induced electronic transitions in samarium monochalcogenides. Physical Review B, 2022, 105, .	1.1	2
7492	Boron Impurity Deposition on a Si(100) Surface in a SiHCl3-BCl3-H2 System for Electronic-Grade Polysilicon Production. Minerals (Basel, Switzerland), 2022, 12, 651.	0.8	1
7493	Exceptionally high work density of a ferroelectric dynamic organic crystal around room temperature. Nature Communications, 2022, 13, .	5.8	15
7494	Crystallographic Insights into the Crystal Structure and Intrinsic Properties of Ca₁₂Al₁₄O₃₃-Type Rb₃LiZn₂(MoO₄)₄ Single Crystals. Inorganic Chemistry, 0, . .	1.9	1
7495	Extremely Stable, Highly Conductive Boronâ€Hydrogen Complexes in Forsterite and Olivine. Journal of Geophysical Research: Solid Earth, 2022, 127, .	1.4	1
7496	Experimental and Theoretical Studies on the Intercalation of Naproxen into the Mg2Al and Zn2Al Layered Double Hydroxides by Ion Exchange Reaction. Journal of Pharmaceutical Sciences, 2022, 111, 2369-2377.	1.6	2

#	Article	IF	Citations
7497	Enhanced electroactivity of BiOCl/PPy hybrid film with anamnestic lattice site for synergistically efficient selective uptake/release of chloride ions. Electrochimica Acta, 2022, 422, 140508.	2.6	1
7498	Adsorption mechanism of aliphatic amino acids on kaolinite surfaces. Applied Clay Science, 2022, 226, 106566.	2.6	11
7499	Electronic structure, optical and elastic properties of AgAlS2 crystal under hydrostatic pressure. Materials Science in Semiconductor Processing, 2022, 148, 106814.	1.9	6
7500	Experimental and theoretical analysis of elemental mercury removal from syngas over Fe-Ti spinel. Fuel, 2022, 324, 124430.	3.4	10
7501	Integration of negative, zero and positive linear thermal expansion makes borate optical crystals light transmission temperature-independent. Materials Horizons, 2022, 9, 2207-2214.	6.4	3
7502	BaI3O9OH: A new alkaline-earth metal hydroxy iodates with two groups. New Journal of Chemistry, 0, , .	1.4	1
7503	Insight into the relationship of redox ability and separation efficiency via the case of Î±-Bi2O3/Bi5NO3O7. Inorganic Chemistry Frontiers, 0, , .	3.0	1
7504	Theoretical Prediction of the Carrier Mobilities for MII2MIIIâ€'Clâ€'Layered Double Hydroxides in the Three-Dimensional Directions. Journal of Materials Chemistry C, 0, , .	2.7	0
7505	Effect of Valence Floating on the Magnetic Properties of Caâ€“Sn Co-Doping Y_{3â^'x}Ca_xFe_{5â^'x}Sn_xO₁₂ (x = 0â€“0.25). IEEE Transactions on Magnetics, 2022, 58, 1-5.	1.2	2
7506	Alkali metal partial substitution-induced improved second-harmonic generation and enhanced laser-induced damage threshold for Ag-based sulfides. Inorganic Chemistry Frontiers, 2022, 9, 3779-3787.	3.0	11
7507	Controlling the Cation Exsolution of Perovskite to Customize Heterostructure Active Site for Oxygen Evolution Reaction. ACS Applied Materials & Interfaces, 2022, 14, 25638-25647.	4.0	26
7508	Theoretical study on S/Fe-doped hexagonal boron nitride (h-BN) sheet: Electronic and optical properties. Applied Surface Science, 2022, 598, 153719.	3.1	7
7509	Silver-Rich Hybrid Framework Iodide Based on [Ag₈I₆]²⁺ Clusters Displays Low-Temperature Dual Emission and Luminescence Thermochromism. Inorganic Chemistry, 2022, 61, 8662-8669.	1.9	2
7510	Formation and Stability of Dense Methane-Hydrogen Compounds. Physical Review Letters, 2022, 128, .	2.9	5
7511	ZnO _{1â^'} _x S _x Solid Solution as Potential Buffer Layer Materials for Cu ₂ ZnSnS ₄ â€Based Thin Film Solar Cells: Structural and Interfacial Properties. Advanced Materials Interfaces, 0, , 2200376.	1.9	1
7512	Crystal Structure and Twisted Aggregates of Oxcarbazepine Form III. Crystal Growth and Design, 2022, 22, 4146-4156.	1.4	2
7513	Selective Photocatalytic CO₂ Reduction to CH₄ on Tri-s-triazine-Based Carbon Nitride via Defects and Crystal Regulation: Synergistic Effect of Thermodynamics and Kinetics. ACS Applied Materials & Interfaces, 2022, 14, 25417-25426.	4.0	11
7514	Lattice dynamics and elastic properties of black phosphorus. Physical Review B, 2022, 105, .	1.1	8

#	Article	IF	Citations
7515	Boosting the Electrocatalytic Oxygen Evolution of Perovskite LaCo_{1â^'}_xFe_xO₃ by the Construction of Yolkâ€Shell Nanostructures and Electronic Modulation. Small, 2022, 18, .	5.2	31
7516	NaBaBS₃: A Promising Infrared Functional Material with Large Birefringence Induced by Ï€-Conjugated [BS₃] Units. Chemistry of Materials, 2022, 34, 5215-5223.	3.2	13
7517	Synthesis, Structure, and Electric Conductivity of Higher Hydrides of Ytterbium at High Pressure. Inorganic Chemistry, 2022, 61, 8694-8702.	1.9	3
7518	Modeling Interfacial Evolutions at Atomistic Scale in the Process of Titanium Oxide Inducing Ferrite Nucleation in Steels. Crystal Growth and Design, 2022, 22, 4059-4071.	1.4	5
7519	Point defect formation energies in graphene from diffusion quantum Monte Carlo and density functional theory. Physical Review B, 2022, 105, .	1.1	1
7520	Cation Regulation to Investigate the Chalcogenide Borate RE₆Nb₂MgSB₈O₂₆ (RE = Laâ€“Nd) Family. Inorganic Chemistry, 2022, 61, 8653-8661.	1.9	7
7521	Raman Spectroscopy of Janus MoSSe Monolayer Polymorph Modifications Using Density Functional Theory. Materials, 2022, 15, 3988.	1.3	6
7522	Electronic properties of CaF2 bulk and interfaces. Journal of Applied Physics, 2022, 131, .	1.1	8
7523	Phase Composition, Structure and Properties of the Spark Plasma Sintered Ceramics Obtained from the Al12Mg17-B-Si Powder Mixtures. Nanomaterials, 2022, 12, 1895.	1.9	3
7524	Theoretical Investigations of Electronic and Optical Properties of Vanadium Doped Wurtzite Zinc Oxide from First Principle Calculation Method. Iraqi Journal of Physics, 2022, 20, 38-52.	0.2	2
7525	BaSi₇P₁₀ and SrSi₇P₁₀: Two Infrared Nonlinear Optical Phosphides with T2 Supertetrahedra Exhibiting Strong Secondâ€Harmonic Generation Effects. Advanced Optical Materials, 2022, 10, .	3.6	4
7526	Investigation on the structural, electronic, elastic and mechanical properties of Ti2Al(C1-xOx) solid solutions: First-principles calculations. Current Applied Physics, 2022, , .	1.1	1
7527	Role of Titanium replacement with Pd atom on band gap reduction in the anatase Titanium Dioxide: First-Principles calculation approach. Results in Physics, 2022, 38, 105688.	2.0	8
7528	First-Principles Dynamics of Fluorine Adsorption on Clean and Monohydrogenated Si{001}. Langmuir, 2022, 38, 7256-7271.	1.6	1
7529	Terahertz Spectroscopy and Density Functional Theory Analysis of the Molecular Interactions in Crystalline Orotic Acid Monohydrate. Journal of Applied Spectroscopy, 0, , .	0.3	0
7530	Regulating electronic structure of hollow LaxCoyO4@NC by La incorporation for electrochemical oxygen evolution reaction. Journal of Electroanalytical Chemistry, 2022, 918, 116480.	1.9	3
7531	Exploration for the Optical Properties and Fluorescent Prediction of Nitrotriazole and Nitrofurazan: First-Principles and TD-DFT Calculations. ACS Omega, 0, , .	1.6	0
7532	Metallated porphyrinic metalâ^'organic frameworks for CO2 conversion to HCOOH: A computational screening and mechanistic study. Molecular Catalysis, 2022, 527, 112407.	1.0	9

#	Article	IF	Citations
7533	First-principles study on the effect of biaxial strain on the carrier lifetime and absorption spectrum redshift of (S, Se, Te) double-doped ZnO. Computational Materials Science, 2022, 211, 111552.	1.4	0
7534	Study to amino acid-based inhibitors as an effective anti-corrosion material. Journal of Molecular Liquids, 2022, 360, 119449.	2.3	7
7535	First-principles calculations to investigate variation in the bandgap of NaSrF3 Fluoro-Perovskite with external static isotropic pressure and its Impact on optical properties. Computational and Theoretical Chemistry, 2022, 1214, 113766.	1.1	21
7536	Advances in Structure Prediction of Lanthanides and Actinides with Genetic Algorithms. ACS Symposium Series, 0, , 157-171.	0.5	0
7537	Adsorption Selectivity of Ticl4 Precursor on Pt Surfaces for Atomic Layer Deposition by Density Functional Theory. SSRN Electronic Journal, 0, , .	0.4	0
7538	First Principle DFT + U Calculations for the Optoelectronic Properties of Cu and C-Cu co-doped TiO2 Anatase Model. Asian Journal of Chemistry, 2022, 34, 1863-1868.	0.1	1
7539	Liquid exfoliation of five-coordinate layered titanate K₂Ti₂O₅ single crystals in water. CrystEngComm, 2022, 24, 5112-5119.	1.3	1
7540	Phase diagram prediction of GaN and its high pressure melting characteristics. Wuli Xuebao/Acta Physica Sinica, 2022, .	0.2	0
7541	Controlling polymorphism in molecular cocrystals by variable temperature ball milling. Faraday Discussions, 0, 241, 178-193.	1.6	17
7542	AAg₃Ga₈Se₁₄ (A = Rb, Cs): second-harmonic generation responses realized through the parallel arrangement of AgSe₄ and GaSe₄ tetrahedrons. Dalton Transactions, 2022, 51, 11048-11053.	1.6	2
7543	Theoretical and experimental investigations of enhanced uranium(VI) adsorption by nitrogen doping strategy. Physical Chemistry Chemical Physics, 0, , .	1.3	1
7544	One-step construction of Y, C, and O tridoped g-C₃N₄ as a bifunctional photocatalyst for H₂ evolution and organic pollutant degradation under visible light irradiation. Sustainable Energy and Fuels, 2022, 6, 3858-3871.	2.5	9
7545	First-principles study of InxGa1-xAs1-yPy with different compositions. Optical Review, 0, , .	1.2	0
7546	Electronic Structure, Optical, and Elastic Properties of AgGaS ₂ Crystal: Theoretical Study. Advanced Theory and Simulations, 0, , 2200247.	1.3	1
7547	Effect of MgO on the structure of SiO₂â€poor/rich MgOâ€CaOâ€SiO₂ melts by in situ high temperature timeâ€gated Raman spectroscopy and theoretical calculation. Journal of Raman Spectroscopy, 2022, 53, 1635-1646.	1.2	2
7548	Large Conjugated Bis/Triimidazolium Derivatives Directed Iodobismuthates(III): Syntheses, Structures, and Visible-Light-Induced Photocatalytic Properties. Crystal Growth and Design, 2022, 22, 4601-4609.	1.4	4
7549	Accelerating the theoretical study of Liâ€polysulfide adsorption on singleâ€atom catalysts via machine learning approaches. International Journal of Quantum Chemistry, 0, , .	1.0	0
7550	Yinâ€“Yang Complementarity Strategy Achieving Giant Optical Anisotropy in a Metal-free Birefringent Material C(NH₂)₃(HC₄O₄). Crystal Growth and Design, 2022, 22, 4236-4242.	1.4	2

#	Article	IF	Citations
7551	Orientation-Controlled Anisotropy in Single Crystals of Quasi-1D BaTiS₃. Chemistry of Materials, 2022, 34, 5680-5689.	3.2	6
7552	Alkaline-Earth Metal Effects on Physical Properties of Ferromagnetic AVO₃ (A = Ba, Sr, Ca,) Tj ETQq1 1 0.784314 rgBT /O	1.6	16
7553	N-doped carbon-coated Cu2O nanowire arrays on copper foam for rapid and stable water disinfection. Journal of Colloid and Interface Science, 2022, 625, 761-773.	5.0	3
7554	Effect of Pressure on the Superconducting Transition Temperature and Physical Properties of CaPd₂P₂: A DFT Investigation. ACS Omega, 2022, 7, 21528-21536.	1.6	5
7555	First-principles prediction of outstanding mechanical and thermodynamic properties of YX2Si2 (XÂ=ÂPd) Tj ETQq0 0 0 rgBT /Overlock 10	0.9	5
7556	Manipulating resonances and absorptions of terahertz ferrite ceramics. Ceramics International, 2022, , .	2.3	0
7557	Partially Diffusive Helium-Silica Compound under High Pressure. Chinese Physics Letters, 0, , .	1.3	3
7558	Antimicrobial Properties of TiO2 Microparticles Coated with Ca- and Cu-Based Composite Layers. International Journal of Molecular Sciences, 2022, 23, 6888.	1.8	3
7559	Lone-Pair-Induced Intra- and Interlayer Polarizations in SillÃ©n-Aurivillius Layered Perovskite Bi₄NbO₈Br. Inorganic Chemistry, 2022, 61, 9816-9822.	1.9	7
7560	Strained Cs₂AgInCl₆ double perovskite material: band structure, optical spectra and mechanical stability. Physica Scripta, 2022, 97, 085801.	1.2	3
7561	Effects of halogen and hydrogen halide on graphene: Halogenation and exfoliation. Physica E: Low-Dimensional Systems and Nanostructures, 2022, 143, 115379.	1.3	1
7562	Experimental and Computational Studies on Octyl Hydroxamic Acid as an Environmentally Friendly Inhibitor of Cobalt Chemical Mechanical Polishing. ACS Applied Materials & Interfaces, 2022, 14, 28321-28336.	4.0	19
7563	Tailoring the Surface of Natural Graphite with Functional Metal Oxides via Facile Crystallization for Lithium-Ion Batteries. ACS Applied Materials & Interfaces, 2022, 14, 29797-29805.	4.0	6
7564	Adsorption of Lanthanide Atoms on Graphene: Similar, Yet Different. Journal of Physical Chemistry Letters, 2022, 13, 6042-6047.	2.1	5
7565	Inverse Relationship between Thickness and Wear of Fluorinated Graphene: â€œThinner Is Betterâ€• Nano Letters, 0, , .	4.5	10
7566	High-pressure study of hydrogen storage material ethylenediamine bisborane from first-principle calculations. Journal of Materials Research and Technology, 2022, , .	2.6	2
7567	Two Metal Phosphate Nonlinear Optical Materials Simultaneously Exhibiting Ultraviolet Transparence and a Large Birefringence. Chemistry of Materials, 2022, 34, 5919-5927.	3.2	16
7568	Enhanced Surface Passivation of Lead Sulfide Quantum Dots for Short-Wavelength Photodetectors. Chemistry of Materials, 2022, 34, 5433-5442.	3.2	13

#	Article	IF	Citations
7569	Compressing the Channels in the Crystal Structure of Copper Squarate Metal-Organic Framework. Solids, 2022, 3, 374-384.	1.1	2
7570	First-Principles Calculation of the Bonding Strength of the Al2O3-Fe Interface Enhanced by Amorphous Na2SiO3. Materials, 2022, 15, 4415.	1.3	2
7571	Prediction of the pressure-induced phase transition, mechanical properties, and electronic structures for ScB4 via first principle calculations. Applied Physics A: Materials Science and Processing, 2022, 128, .	1.1	0
7572	Nickel Nanoflowers with Controllable Cation Vacancy for Enhanced Electrochemical Nitrogen Reduction. ACS Applied Materials & Interfaces, 2022, 14, 28033-28043.	4.0	14
7573	All-proportional solid solution versus two-phase coexistence in the Tiâ€“V alloy by first-principles phase field and SQS methods. Scientific Reports, 2022, 12, .	1.6	2
7574	Efficient Screening of Coformers for Active Pharmaceutical Ingredient Cocrystallization. Crystal Growth and Design, 2022, 22, 4513-4527.	1.4	14
7575	First-principles study of point defects with different valences on the carrier activity, lifetime, absorption spectrum, and redox reaction of AlN (Li/Na/K) system. Philosophical Magazine, 2022, 102, 2003-2030.	0.7	0
7576	Design of New Borates with Deep Ultraviolet Transparency Inspired by the Flexibility of Unusual Triple-Layered Frameworks. Crystal Growth and Design, 0, , .	1.4	1
7577	Light-Driven Hydrogen Production from Steam Methane Reforming via Bimetallic PdNi Catalysts Derived from Layered Double Hydroxide Nanosheets. Energy & Fuels, 2022, 36, 11627-11635.	2.5	28
7578	First-principles study of electronic and optical properties of small edge-functionalized penta-graphene quantum dots. AIP Advances, 2022, 12, .	0.6	6
7579	Metal to semiconductor transition and figure of merit enhancement of Li2CuAs compound by Na substitution. Bulletin of Materials Science, 2022, 45, .	0.8	2
7580	Exploration of the Crystal Structure and Thermal and Spectroscopic Properties of Monoclinic Praseodymium Sulfate Pr2(SO4)3. Molecules, 2022, 27, 3966.	1.7	14
7581	Theoretical approach to the phonon modes of GaSb nanowires. Physica E: Low-Dimensional Systems and Nanostructures, 2022, 143, 115372.	1.3	1
7582	Energy Harvesting Using Cotton Fabric Embedded with 2D Hexagonal Boron Nitride. ACS Applied Materials & Interfaces, 2022, 14, 30343-30351.	4.0	6
7583	The effect of chloride atoms to induce organohalide perovskite intermediate crystal phase: a simulation rationale. Applied Physics Express, 2022, 15, 075504.	1.1	2
7584	Design of frustrated Lewis pair in defective TiO2 for photocatalytic non-oxidative methane coupling. Chem Catalysis, 2022, 2, 1775-1792.	2.9	12
7585	Vacancy induced magnetism and electronic structure modification in monolayer hexagonal boron arsenide: A first-principles study. Applied Surface Science, 2022, 600, 154053.	3.1	8
7586	Advanced prediction of organicâ€“metal interactions through DFT study and electrochemical displacement approach. Journal of Magnesium and Alloys, 2023, 11, 301-316.	5.5	6

#	Article	IF	Citations
7587	Adsorption mechanism of hydrated Lu(OH)2+ and Al(OH)2+ ions on the surface of kaolinite. Powder Technology, 2022, 407, 117611.	2.1	4
7588	Novel Two-Dimensional MC2N4 (MÂ=ÂCr, Mo, W) Monolayers for Overall Water Splitting with High Visible-Light Absorption. Solar Energy, 2022, 241, 416-427.	2.9	6
7589	Study the application of new type green corrosion inhibitors for iron metal. Inorganic Chemistry Communication, 2022, 142, 109650.	1.8	6
7590	AbstAb-initio insights into the elastic, bonding, phonon, optoelectronic and thermophysical properties of SnTaS2. Solid State Sciences, 2022, 131, 106947.	1.5	12
7591	Three new C N compounds in orthorhombic symmetry: Theoretical investigations. Diamond and Related Materials, 2022, 127, 109181.	1.8	4
7592	Density-functional theory study of magnetic and electronic properties of KFe2Se2 under pressure. Chemical Physics, 2022, 561, 111604.	0.9	2
7593	Improved flotation separation of sulfide minerals by synthesized surfactant based on para-position methyl effect. Separation and Purification Technology, 2022, 297, 121550.	3.9	11
7594	Band structure calculation and crystal field induced electronic properties illustration for spinel CuGa2O4*. Computational Materials Science, 2022, 212, 111579.	1.4	1
7595	Insight into highly efficient FeOx catalysts for the selective catalytic reduction of NOx by NH3: Experimental and DFT study. Applied Surface Science, 2022, 599, 153998.	3.1	16
7596	Understanding the mechanism of carbon deposition of Ni3Co catalysts for methane dry reforming. Applied Surface Science, 2022, 599, 154002.	3.1	14
7597	First principle studies revealing the effect of O2, CO2, and H2 adsorption on field emission behaviour of graphene. Applied Surface Science, 2022, 599, 153938.	3.1	3
7598	First principles on the structure and electronic properties of vertically regulated two-dimensional cubic boron nitride and diamond like carbon sandwich heterostructures. Surface Science, 2022, 724, 122146.	0.8	2
7599	Prussian blue analogue/KB-derived Ni/Co/KB composite as a superior adsorption-catalysis separator modification material for Li-S batteries. Journal of Colloid and Interface Science, 2022, 625, 425-434.	5.0	7
7600	Rb₂MGe₃S₈ (M=Zn, Cd): Non-Centrosymmetry Transformation Led by Structure Change of [MGe₃S₈]²⁻ Unit^{â€»}. Acta Chimica Sinica, 2022, 80, 633.	0.5	2
7601	KFÂ·B(OH)₃: a KBBF-type material with large birefringence and remarkable deep-ultraviolet transparency. Chemical Communications, 2022, 58, 8770-8773.	2.2	18
7602	High-pressure structural phase transitions and metallization in layered HfS₂ under different hydrostatic environments up to 42.1 GPa. Journal of Materials Chemistry C, 0, , .	2.7	10
7603	Determination of intrinsic defects of functional KDP crystals with flawed surfaces and their effect on the optical properties. Nanoscale, 2022, 14, 10041-10050.	2.8	18
7604	Construction of a fast Li-ion path in a MOF-derived Fe₃O₄@NC sulfur host enables high-rate lithiumâ€“sulfur batteries. Dalton Transactions, 0, , .	1.6	2

#	Article	IF	Citations
7605	Microstructure Tiâ€“Fe Phase Separation Mechanism in the Direct Reduction Process of Titanomagnetite with Coal by Microwave Heating. ISIJ International, 2022, 62, 1802-1815.	0.6	1
7606	New alkaline-earth amidosulfates and their unexpected decomposition to S₄N₄. Dalton Transactions, 2022, 51, 11737-11746.	1.6	4
7607	The interfacial effect induced by rare earth oxide in boosting the conversion of CO₂ to formate. Energy and Environmental Science, 2022, 15, 3494-3502.	15.6	25
7608	Electronic structure modification and N-doped carbon shell nanoarchitectonics of Ni₃FeN@NC for overall water splitting performance evaluation. Journal of Materials Chemistry A, 2022, 10, 16704-16713.	5.2	21
7609	Computational Analysis of Hydrogen Bond Vibrations of Ice III in the Far-Infrared Band. Crystals, 2022, 12, 910.	1.0	1
7610	Terahertz spectroscopy and lattice vibrational analysis of pararealgar and orpiment. Chinese Physics B, 2022, 31, 103302.	0.7	1
7611	Structural, electronics, magnetic, optical, mechanical and hydrogen storage properties of <scp>Gaâ€based hydrideâ€perovskites</scp> X <scp> GaH ₃ </scp> (X Â=ÂK, Li). International Journal of Energy Research, 2022, 46, 15617-15626.	2.2	34
7612	Investigation on the optical and electrical performance of aluminium doped gallium oxide thin films. Optical and Quantum Electronics, 2022, 54, .	1.5	5
7613	First-Principles Investigation of the Structural, Elastic and Thermodynamic Properties of CaRu2X2 (Xâ€‰=â€‰P, As) under Pressure. Journal of Superconductivity and Novel Magnetism, 0, , .	0.8	0
7614	Synthesis and Characterization of (FA)₃(HEA)₂Pb₃I₁₁: A Rare Example of <1 1 0>-Oriented Multilayered Halide Perovskites. Chemistry of Materials, 2022, 34, 5780-5790.	3.2	2
7615	Eu₂P₂S₆: The First Rareâ€Earth Chalcogenophosphate Exhibiting Large Secondâ€Harmonic Generation Response and High Laserâ€Induced Damage Threshold. Angewandte Chemie - International Edition, 2022, 61, .	7.2	64
7616	New Approach toward Dual-Emissive Organicâ€“Inorganic Hybrids by Integrating Mn(II) and Cu(I) Emission Centers in Ionic Crystals. ACS Applied Materials & Interfaces, 2022, 14, 31000-31009.	4.0	11
7617	Electronic and Magnetic Properties of 2D/3D MnB: An Ab-initio & Monte Carlo Study. Hittite Journal of Science & Engineering, 2022, 9, 103-110.	0.2	0
7618	Enhancement of spin-mixing conductance by <mml:math xmlns:mml="http://www.w3.org/1998/Math/MathML"><mml:mi>s</mml:mi><mml:mtext>â”</mml:mtext><mml:mi>d</mml:mi></mml:math> orbital hybridization in heavy metals. Physical Review B, 2022, 105, .	1.1	2
7619	Effect of Relaxations on the Conductivity of La_{1/2+1/2x}Li_{1/2â€“1/2x}Ti_{1â€“x}Al_xO₃ Fast Ion Conductors. Chemistry of Materials, 2022, 34, 5484-5499.	8.2	6
7620	Effects of Zn, Mg and Cu Doping on Oxidation Reaction of Al (111) Surface. Frontiers in Chemistry, 0, 10, .	1.8	2
7621	Experimental and firstâ€principles investigations on gâ€C ₃ N ₄ /ZnS heterostructures with enhanced photocatalyst capability. Micro and Nano Letters, 2022, 17, 259-271.	0.6	3
7622	Eu₂P₂S₆: The First Rareâ€Earth Chalcogenophosphate Exhibiting Large Secondâ€Harmonic Generation Response and High Laserâ€Induced Damage Threshold. Angewandte Chemie, 2022, 134, .	1.6	1

#	Article	IF	Citations
7623	High Tc superconductivity in layered hydrides XH15 (X = Ca, Sr, Y, La) under high pressures. Frontiers of Physics, 2022, 17, .	2.4	3
7624	Surface Redox Pseudocapacitance Boosting Vanadium Nitride for Highâ€Power and Ultraâ€Stable Potassiumâ€Ion Capacitors. Advanced Functional Materials, 2022, 32, .	7.8	15
7625	A DFT-Based Quantitative and Geometric Analysis of the Effect of Pressure on Boron Arsenate. Materials, 2022, 15, 4858.	1.3	4
7626	AgGaGeSe4: An Infrared Nonlinear Quaternary Selenide with Good Performance. Symmetry, 2022, 14, 1426.	1.1	1
7627	Rutin precursor for the synthesis of superparamagnetic ZnFe2O4 nanoparticles: experimental and density functional theory. Applied Physics A: Materials Science and Processing, 2022, 128, .	1.1	11
7628	Tower carbon: a new large-cell carbon allotrope. Journal of Physics Condensed Matter, 2022, 34, 365702.	0.7	5
7629	Defect engineering in wide-bandgap perovskites for efficient perovskiteâ€“silicon tandem solar cells. Nature Photonics, 2022, 16, 588-594.	15.6	112
7630	Catalytic dissociation of a water molecule on the (1 1 1) surfaces of Pt0.5Ni0.5 bimetal: Density functional theory (DFT) study. Applied Surface Science, 2022, 602, 154238.	3.1	2
7631	Design of Infrared Nonlinear Optical Compounds with Diamond-like Structures and Balanced Optical Performance. Inorganic Chemistry, 2022, 61, 11454-11462.	1.9	5
7632	Zero-Dimensional Molecular Ferroelectrics with Significant Nonlinear Effect and Giant Entropy. Chemistry of Materials, 2022, 34, 6323-6330.	3.2	12
7633	Dipolar Heteronuclear Correlation Solid-State NMR Experiments between Half-Integer Quadrupolar Nuclei: The Case of ¹¹Bâ€“¹⁷O. Journal of Physical Chemistry C, 2022, 126, 11652-11666.	1.5	3
7634	Directional Construction of New Nonlinear Optical Bifunctional Units through Molecular Engineering Design Inspired by the B₃O₇-Typed Configuration. ACS Applied Materials & Interfaces, 2022, 14, 32270-32278.	4.0	6
7635	Anion Redox in an Amorphous Titanium Polysulfide. ACS Applied Materials & Interfaces, 2022, 14, 33191-33199.	4.0	1
7636	Lattice deformation and phase transition of aluminum nitride studied by density functional theory calculations. Journal of the Ceramic Society of Japan, 2022, 130, 452-457.	0.5	2
7637	Selective Separation of Fluorite from Scheelite Using N-Decanoylsarcosine Sodium as a Novel Collector. Minerals (Basel, Switzerland), 2022, 12, 855.	0.8	5
7638	Localized Soft Vibrational Modes and Coherent Structural Phase Transformations in Rutile TiO₂ Nanoparticles under Negative Pressure. Nano Letters, 0, , .	4.5	0
7639	First Investigation of Nonlinear Optical Oxychalcogenide with <scp>Threeâ€Dimensional</scp> Anionic Framework and Special <scp>Windmillâ€Like</scp> Functional Motifs^{â€}. Chinese Journal of Chemistry, 2022, 40, 2407-2414.	2.6	12
7640	Highly response and humidity-resistant gas sensor based on polyaniline-functionalized Bi2MoO6 with UV activation. Electrochimica Acta, 2022, 427, 140863.	2.6	10

#	Article	IF	Citations
7641	Construction of Ultrafine Ag₂S NPs Anchored onto 3D Network Rodlike Bi₂SiO₅ and Insight into the Photocatalytic Mechanism. Inorganic Chemistry, 2022, 61, 11387-11398.	1.9	14
7642	Investigation of Photo(electro)catalytic water splitting to evolve H2 on Pt-g-C3N4 nanosheets. International Journal of Hydrogen Energy, 2022, 47, 28007-28018.	3.8	15
7643	Universal Principle for Large-Scale Production of a High-Quality Two-Dimensional Monolayer via Positive Charge-Driven Exfoliation. Journal of Physical Chemistry Letters, 2022, 13, 6597-6603.	2.1	6
7644	Anisotropic Band-Edge Absorption of Millimeter-Sized Zn(3-ptz)₂ Single-Crystal Metalâ€“Organic Frameworks. ACS Omega, 2022, 7, 24432-24437.	1.6	3
7645	Regulating the spin state of single-atom doped covalent triazine frameworks for efficient nitrogen fixation. Journal of Colloid and Interface Science, 2022, 627, 931-941.	5.0	4
7646	Alkaline-Earth Chalcogenide Nanocrystals: Solution-Phase Synthesis, Surface Chemistry, and Stability. ACS Nano, 2022, 16, 12024-12035.	7.3	8
7647	Ephemeral data derived potentials for random structure search. Physical Review B, 2022, 106, .	1.1	15
7648	Rashba Splitting and Electronic Valley Characteristics of Janus Sb and Bi Topological Monolayers. International Journal of Molecular Sciences, 2022, 23, 7629.	1.8	2
7649	A triatomic carbon and derived pentacarbides with superstrong mechanical properties. IScience, 2022, 25, 104712.	1.9	6
7650	Study on the strengthening mechanism of rare earth yttrium on magnesium alloys. Materials Science & Engineering A: Structural Materials: Properties, Microstructure and Processing, 2022, 850, 143513.	2.6	17
7651	First-principles probing of Au-doped WS2 monolayer as a superb CO sensor with high selectivity and fast diffusion. Materials Today Communications, 2022, 32, 103922.	0.9	5
7652	Hydrous SiO2 in subducted oceanic crust and H2O transport to the core-mantle boundary. Earth and Planetary Science Letters, 2022, 594, 117708.	1.8	10
7653	Opto-electro-mechanical properties of lead-free hybrid double perovskites Cs2AgSbX6 (X = Cl, Br, I) for solar cells: A first-principles study. Journal of Physics and Chemistry of Solids, 2022, 169, 110880.	1.9	16
7654	Analyzing the electronic and optical properties of bulk, unstrained, and strained monolayers of SrS2 by DFT. Physica E: Low-Dimensional Systems and Nanostructures, 2022, 143, 115403.	1.3	4
7655	Predicting impact sensitivity of energetic materials: insights from energy transfer of carriers. Acta Materialia, 2022, 236, 118137.	3.8	36
7656	Interactions between Mg2+-doped kaolinite and coal: Insights from DFT calculation and flotation. Applied Surface Science, 2022, 600, 154071.	3.1	18
7657	The <mml:math xmlns:mml="http://www.w3.org/1998/Math/MathML" altimg="si1.svg" display="inline"		

#	Article	IF	Citations
7659	MX (MÂ=ÂAu, Ag; XÂ=ÂS, Se, Te) monolayers: Promising photocatalysts for oxygen evolution reaction with excellent light capture capability. Applied Surface Science, 2022, 600, 154055.	3.1	9
7660	First principles study of the structural stability, lattice dynamics, optical and thermoelectric properties of NaSrX(X = As, Sb and Bi). Materials Science in Semiconductor Processing, 2022, 149, 106840.	1.9	6
7661	The effects of Zn/Fe co-dopants on the structural, thermal, magnetic, and in vitro biocompatibility properties of calcium pyrophosphate ceramics. Physica B: Condensed Matter, 2022, 643, 414123.	1.3	2
7662	First-principles study of anti-perovskites Ca4Pn2O (Pn = As, Sb, Bi) as a potential optical material. Materials Science in Semiconductor Processing, 2022, 150, 106920.	1.9	0
7663	Ab initio study of the optoelectronic properties of Î±-Ba2SnS4. Materials Science in Semiconductor Processing, 2022, 150, 106917.	1.9	3
7664	Light-Switchable Oxygen Vacancies Enhanced Nitrogen Fixation Performance on BiOBr: Mechanism of Formation, Reconversion and Function. Chemical Engineering Journal, 2022, 450, 138066.	6.6	13
7665	Intelligent coating based on metal-insulator transitional Ti3O5 towards fire sensing and protection. Chemical Engineering Journal, 2022, 450, 137910.	6.6	5
7666	Structural transition, mechanical properties and electronic structure of the ZnO under high pressure via first-principles investigations. Applied Physics A: Materials Science and Processing, 2022, 128, .	1.1	1
7667	Molecular and Electronic Structure of Isolated Platinum Sites Enabled by the Expedient Measurement of¹⁹⁵Pt Chemical Shift Anisotropy. Journal of the American Chemical Society, 2022, 144, 13511-13525.	6.6	14
7668	13C CP MAS NMR and DFT Studies of 6-Chromanyl Ethereal Derivatives. Molecules, 2022, 27, 4630.	1.7	0
7669	Electronic Structures and Electrical Properties of Cr²⁺-, Cu²⁺-, Ni²⁺-, and Zn²⁺-Doped Sodium Titanate Nanotubes. ACS Omega, 2022, 7, 27587-27601.	1.6	7
7670	NaBH₄-Assisted Synthesis of Bâ€“(Niâ€“Co)/MgAl₂O₄ Nanostructures for the Catalytic Dry Reforming of Methane. ACS Applied Nano Materials, 2022, 5, 10951-10961.	2.4	10
7671	Solution-processable copper(I) iodide-based inorganic-organic hybrid semiconductors composed of both coordinate and ionic bonds. Journal of Solid State Chemistry, 2022, 314, 123427.	1.4	8
7672	First-Principles Study of the Effect of Titanium Doping on Carbon Monoxide Poisoning Properties of Zirconium-Cobalt Alloys. Crystals, 2022, 12, 1015.	1.0	1
7673	DFTâ€“Assisted Structure Determination from Powder X-ray Diffraction Data of a New Zonisamide/Ïµ-Caprolactam Cocrystal. Crystals, 2022, 12, 1020.	1.0	1
7674	High-performance intermetallic PtCo oxygen reduction catalyst promoted by molybdenum. Applied Catalysis B: Environmental, 2022, 317, 121767.	10.8	7
7675	Catalytic Cleavage of the Câ€“O Bond in Lignin and Lignin-Derived Aryl Ethers over Ni/AlP_yO_x Catalysts. ACS Catalysis, 2022, 12, 9473-9485.	5.5	16
7676	Combining X-ray and NMR Crystallography to Explore the Crystallographic Disorder in Salbutamol Oxalate. Crystal Growth and Design, 2022, 22, 4696-4707.	1.4	1

#	Article	IF	Citations
7677	Coherent interfaces govern direct transformation from graphite to diamond. Nature, 2022, 607, 486-491.	13.7	60
7678	Sharp Enhancement of Birefringence in Antimony Oxalates Achieved by the Cationâ€“Anion Synergetic Interaction Strategy. Inorganic Chemistry, 2022, 61, 12481-12488.	1.9	12
7679	Existence of yttrium allotrope with incommensurate hostâ€“guest structure at moderate pressure: First evidence from computational approach. Computational Materials Science, 2022, 213, 111652.	1.4	2
7680	Optimizing electronic structure of porous Ni/MoO2 heterostructure to boost alkaline hydrogen evolution reaction. Journal of Colloid and Interface Science, 2022, 627, 862-871.	5.0	38
7681	Investigation of crystal field effects for the spectral broadening of Yb³⁺-doped Lu_xY_{2â^'x}O₃ sesquioxide crystals. RSC Advances, 2022, 12, 22555-22563.	1.7	2
7682	Molecular and Crystalline Vibration Characteristics of Baicalin Investigated By Terahertz Spectroscopy and Density Functional Theory. IEEE Transactions on Terahertz Science and Technology, 2022, 12, 611-618.	2.0	3
7683	Impact of Hole Transport Layers in Inorganic Lead-Free B-Î³-CsSnI3 Perovskite Solar Cells: A Numerical Analysis. , 0, , .		3
7684	Artificially steering electrocatalytic oxygen evolution reaction mechanism by regulating oxygen defect contents in perovskites. Science Advances, 2022, 8, .	4.7	54
7685	Toward Computational Screening of Bimetallic Alloys for Methane Activation: A Case Study of MgPt Alloy. ACS Catalysis, 2022, 12, 9458-9472.	5.5	9
7686	Fluoride Shuttle Battery Reactions of CuF₂: Intermediate Phase for Defluorination. Journal of Physical Chemistry C, 2022, 126, 12361-12369.	1.5	2
7687	Difluoro(oxalato)borates as Short-Wavelength Optical Crystals with Bifunctional [BF₂C₂O₄] Units. Chemistry of Materials, 2022, 34, 7516-7525.	3.2	15
7688	Highâ€Performance Flexible Sulfur Cathodes with Robust Electrode Skeletons Built by a Hierarchical Selfâ€Assembling Slurry. Advanced Science, 2022, 9, .	5.6	5
7689	Study of the Structural, Electronic and Optical Properties of 1T-ZrX₂ Materials (X=S, Se, Te). Solid State Phenomena, 0, 335, 3-13.	0.3	1
7690	Room-temperature epitaxial welding of 3D and 2D perovskites. Nature Materials, 2022, 21, 1042-1049.	13.3	32
7691	Temperature-dependent Raman spectra of KTaO3 crystal and melt along with its phonon and electronic properties. Journal of Molecular Liquids, 2022, , 120098.	2.3	1
7692	Experimental and theoretical characterization of Bi-based hydroxyapatites doped with Ce. Ceramics International, 2022, 48, 33440-33454.	2.3	9
7693	F-Doped Ni-Rich Layered Cathode Material with Improved Rate Performance for Lithium-Ion Batteries. Processes, 2022, 10, 1573.	1.3	3
7694	Exploiting Nanoscale Complexion in LATP Solid-State Electrolyte via Interfacial Mg2+ Doping. Nanomaterials, 2022, 12, 2912.	1.9	3

#	Article	IF	Citations
7695	Lightweight alkali-induced lattice-dynamical stability and energy storage mechanism of quaternary Mg-based hydrides under pressure effect. International Journal of Hydrogen Energy, 2022, 47, 30592-30601.	3.8	3
7696	â€œCrystal memoryâ€•Affects the Properties of Peptide Hydrogels â€“ The Case of the Cyclic Tyrâ€Tyr dipeptide. Chemistry - A European Journal, 2022, 28, .	1.7	2
7697	Firstâ€Principles Investigation of Phase Stability in Substoichiometric Zirconium Carbide under High Pressure. Advanced Theory and Simulations, 2022, 5, .	1.3	1
7698	Mechanism of improved crystallinity by defect-modification in proton-irradiated GaAsPN photovoltaics: Experimental and first-principle calculations approach. Journal of Applied Physics, 2022, 132, .	1.1	1
7699	Synthesis, structural, and DFT studies of Cu(II) dithiocarbamate complexes. Journal of Molecular Structure, 2023, 1271, 133988.	1.8	5
7700	Design of Cuâ€“Cr Alloys with High Strength and High Ductility Based on First-Principles Calculations. Metals, 2022, 12, 1406.	1.0	3
7701	An Optically Anisotropic Crystal with Large Birefringence Arising from Cooperative Ï€ Orbitals. Angewandte Chemie, 2022, 134, .	1.6	5
7702	Lanthanide-Doped MAPbI₃ Single Crystals: Fabrication, Optical and Electrical Properties, and Multi-mode Photodetection. Chemistry of Materials, 2022, 34, 7412-7423.	3.2	11
7703	Mechanical Characterization of Anhydrous Microporous Aluminophosphate Materials: Tridimensional Incompressibility, Ductility, Isotropy and Negative Linear Compressibility. Solids, 2022, 3, 457-499.	1.1	2
7704	Anisotropic Thermal Expansion and Electronic Structure of LiInSe2. Molecules, 2022, 27, 5078.	1.7	10
7705	Understanding irradiation damage in high-temperature superconductors for fusion reactors using high resolution X-ray absorption spectroscopy. Communications Materials, 2022, 3, .	2.9	5
7706	Robust Nickel Aspartate Framework for Shape Recognition of Hexane Isomers. ACS Sustainable Chemistry and Engineering, 2022, 10, 11330-11337.	3.2	5
7707	Study of the Crystallographic Distortion Mechanism during the Annealing of Kaolinite. Minerals (Basel, Switzerland), 2022, 12, 994.	0.8	1
7708	Graphene bandgap opening by constructing superlattices with BN or MoO₂ under pressure. Journal of Physics: Conference Series, 2022, 2331, 012001.	0.3	0
7709	Lattice instability, anharmonicity and Raman spectra of BaO under high pressure: A first principles study. Journal of Physics and Chemistry of Solids, 2022, 170, 110967.	1.9	2
7710	MOF-Transformed In2O3-x@C Nanocorn Electrocatalyst for Efficient CO2 Reduction to HCOOH. Nano-Micro Letters, 2022, 14, .	14.4	35
7712	Origin of the Large Entropy Change in the Molecular Caloric and Ferroelectric Ammonium Sulfate. Advanced Functional Materials, 2022, 32, .	7.8	4
7713	Laser damage mechanism and threshold improvement of nonlinear optical La₃Ga_{5.5}Nb_{0.5}O₁₄ crystal for a mid-infrared high-intensity laser. Optical Materials Express, 2022, 12, 3449.	1.6	3

#	Article	IF	Citations
7714	Vat Orange 7 as an organic electrode with ultrafast hydronium-ion storage and super-long life for rechargeable aqueous zinc batteries. Chemical Engineering Journal, 2023, 451, 138776.	6.6	10
7715	Asymmetric Coupled Dualâ€Atom Sites for Selective Photoreduction of Carbon Dioxide to Acetic Acid. Advanced Functional Materials, 2022, 32, .	7.8	46
7716	A superhard orthorhombic carbon allotrope. Chinese Journal of Physics, 2022, 79, 409-419.	2.0	10
7717	Pb₅(GeO₄)(Ge₂O₇) and Pb_{3.32}Ca_{1.68}(GeO₄)(Ge₂O₇): Two Nonlinear Optical Germanates Induced by Diverse PbOx Polyhedra. Inorganic Chemistry, 2022, 61, 13637-13643.	1.9	8
7718	Investigation of the electronic structural and optical properties of CH3NH3HgI3 crystal. Journal of Molecular Modeling, 2022, 28, .	0.8	3
7719	DFT study of the structural, electronic and optoelectronic properties of PDAPb(I_{1â^'x}Br) Tj ETQq1 1 0.784314 rgBT /Ove	1.0	4
7720	Superconductivity Versus Magnetism in the Amorphous Palladium â€œIdesâ€• Pd1â^'c(H/D/T)c. Journal of Low Temperature Physics, 0, , .	0.6	1
7721	Millimeter-scale semiconductive metal-organic framework single crystal for X-ray imaging. Cell Reports Physical Science, 2022, 3, 101004.	2.8	4
7722	Deep Ultraviolet-Transparent Materials with Strong Second-Harmonic Response. Chemistry of Materials, 2022, 34, 8004-8012.	3.2	14
7723	Solid-State Nuclear Magnetic Resonance Spectroscopy-Assisted Structure Determination of Coordination Polymers. Chemistry of Materials, 2022, 34, 7678-7691.	3.2	2
7724	Selective separation of light rare-earth elements by supramolecular encapsulation and precipitation. Nature Communications, 2022, 13, .	5.8	19
7725	A Hybrid Antiperovskite with Strong Linear and Secondâ€Order Nonlinear Optical Responses. Angewandte Chemie, 0, , .	1.6	0
7726	Activated Proton Storage in Molybdenum Selenide through Electronegativity Regulation. Advanced Functional Materials, 2022, 32, .	7.8	12
7727	First-principles calculations to investigate the effect of Cs-doping in BaTiO3 for water-splitting application. Solid State Communications, 2022, 355, 114920.	0.9	10
7728	Etude expÃ©rimentale et thÃ©orique dâ€™un nouveau composÃ© halogÃ¨ne pnicture Hg<mml:math xmlns:mml="http://www.w3.org/1998/Math/MathML"><mml:msub><mml:mrow /> <mml:mn>12</mml:mn></mml:msub></mml:math>Sb<mml:math xmlns:mml="http://www.w3.org/1998/Math/MathML"><mml:mrow><mml:msub><mml:mrow /> <mml:mn>6</mml:mn>		

#	Article	IF	Citations
7732	Structure of Zinc and Nickel Histidine Complexes in Solution Revealed by Molecular Dynamics and Raman Optical Activity. Chemistry - A European Journal, 2022, 28, .	1.7	3
7733	Conversion of n-type to p-type conductivity in ZnO by incorporation of Ag and Ag-Li. Materials Today Communications, 2022, 33, 104278.	0.9	1
7734	Room-Temperature Superconductivity in Yb/Lu Substituted Clathrate Hexahydrides under Moderate Pressure. Research, 2022, 2022, .	2.8	12
7735	Enhanced Rashba Splitting of Au(111) Surface States with Hydrogenâ€Bonded Melamineâ€Based Organic Framework. Advanced Materials Interfaces, 2022, 9, .	1.9	3
7736	From Phosphate Fluoride to Fluorophosphate: Design of Novel Ultraviolet/Deep-Ultraviolet Nonlinear Optical Materials for BePO₃F with Optical Property Enhancement. ACS Applied Materials & Interfaces, 2022, 14, 39081-39090.	4.0	13
7737	High-Temperature-Sensing Smart Bolt Based on Indium Tin Oxide/In2O3 Thin-Film Thermocouples with Nickel-Based Single-Crystal Superalloy via Screen Printing. Chemosensors, 2022, 10, 347.	1.8	2
7738	High-Pressure Structural Transformation Pathway and Electronic Properties of AgGaTe₂: Ab Initio Evolutionary Structural Searching. Journal of Physical Chemistry C, 2022, 126, 14236-14244.	1.5	1
7739	Topological Stoneâ€“Wales Defects Enhance Bonding and Electronic Coupling at the Graphene/Metal Interface. ACS Nano, 2022, 16, 11979-11987.	7.3	12
7740	Plasticity Improvement of Mg Alloys with Alloying Atoms (Gd, Y). Physica Status Solidi (B): Basic Research, 2022, 259, .	0.7	2
7741	Radio-Frequency Manipulation of State Populations in an Entangled Fluorine-Muon-Fluorine System. Physical Review Letters, 2022, 129, .	2.9	2
7742	Synergistic Lubrication Effect between Oxidized Black Phosphorus and Oil Molecules Triggers Superlubricity. Journal of Physical Chemistry Letters, 0, , 8245-8253.	2.1	4
7743	New insights into the interaction between monomers from acrylamide-based polymeric flocculants and montmorillonite: A DFT study. Journal of Molecular Liquids, 2022, 365, 120171.	2.3	6
7744	A Hybrid Antiperovskite with Strong Linear and Secondâ€Order Nonlinear Optical Responses. Angewandte Chemie - International Edition, 2022, 61, .	7.2	24
7745	Phase Transformations and Phase Segregation during Potassiation of Sn_xP_y Anodes. Chemistry of Materials, 2022, 34, 7460-7467.	3.2	4
7746	Band structural and absorption characteristics of antimonene/bismuthene monolayer heterojunction calculated by first-principles. Frontiers in Chemistry, 0, 10, .	1.8	0
7747	First-principles study of the structural, electronic and optical properties of two-dimensional PC6X and PX6 (X=N, As). Vacuum, 2022, 205, 111429.	1.6	5
7748	Spin dynamics, entanglement, and the nature of the spin liquid state in <mml:math xmlns:mml="http://www.w3.org/1998/Math/MathML"><mml:msub><mml:mi>YbZnGaO</mml:mi><mml:mn>4</mml:mn></mml:msub> Physical Review B, 2022, 106, .	1.1	4
7749	An excellent deep-ultraviolet birefringent material based on [BO2]â^ž infinite chains. Light: Science and Applications, 2022, 11, .	7.7	64

#	Article	IF	Citations
7750	Crystal Growth of K₂HCO₃FÂ·H₂O with a Very Short Cutoff Edge and Large Birefringence. Crystal Growth and Design, 2022, 22, 5639-5644.	1.4	9
7751	(Na_{0.74}Ag_{1.26})BaSnS₄: A New AgGaS₂â€Type Nonlinear Optical Sulfide with a Wide Band Gap and High Laser Induced Damage Threshold. Chemistry - A European Journal, 2022, 28, .	1.7	9
7752	Investigation of 2D material anodes with different anions for lithium ion batteries: comparison of MoO₂, MoS₂ and MoSe₂. Journal of Physics: Conference Series, 2022, 2331, 012005.	0.3	0
7753	NaB₃O₄F(OH): A Hydroxyfluorooxoborate with One-Dimensional Chain Featuring Large Birefringence and Short Ultraviolet Cutoff Edge. Inorganic Chemistry, 2022, 61, 13600-13607.	1.9	2
7754	DFT insights into the electronic structure, mechanical behaviour, lattice dynamics and defect processes in the first Sc-based MAX phase Sc2SnC. Scientific Reports, 2022, 12, .	1.6	14
7756	Investigations of cysteine isomers using Terahertz and Raman spectroscopies. Infrared Physics and Technology, 2022, 125, 104299.	1.3	4
7757	Towards a deeper understanding of superlubricity on graphite governed by interfacial adhesion. Carbon, 2022, 199, 479-485.	5.4	5
7758	Oxygen-vacancy-induced structural transition and enhanced magnetism in Sc, Fe-codoped SrTiO3: A theoretical study*. Chemical Physics Letters, 2022, 805, 139943.	1.2	2
7759	Equilibrium boron isotope fractionation during serpentinization and applications in understanding subduction zone processes. Chemical Geology, 2022, 609, 121047.	1.4	6
7760	Narrowing down the conformational space with solid-state NMR in crystal structure prediction of linezolid cocrystals. Solid State Nuclear Magnetic Resonance, 2022, 121, 101813.	1.5	5
7761	Investigation on time-dependent behavior of resistivity in high-resistivity silicon wafers. Materials Science in Semiconductor Processing, 2022, 151, 106995.	1.9	2
7762	CO2-ZrO2 interaction in CDRM: A combined experimental and theoretical study. Surface Science, 2022, 725, 122164.	0.8	2
7763	First-principles investigation of the effect of noble metals on the electronic and optical properties of GaN nitride. Materials Science in Semiconductor Processing, 2022, 151, 107051.	1.9	32
7764	Dimethyl fumarate molecule, crystal, and plane: Optical absorption measurement and structural/optoelectronic properties by density functional theory calculations. Journal of Physics and Chemistry of Solids, 2022, 170, 110958.	1.9	0
7765	DFT-FE 1.0: A massively parallel hybrid CPU-GPU density functional theory code using finite-element discretization. Computer Physics Communications, 2022, 280, 108473.	3.0	24
7766	MuFinder: A program to determine and analyse muon stopping sites. Computer Physics Communications, 2022, 280, 108488.	3.0	7
7767	Evolution of ferromagnetic stability with magnetic impurity and vacancies in Cr-doped CaZn2As2 system. Materials Science and Engineering B: Solid-State Materials for Advanced Technology, 2022, 285, 115955.	1.7	0
7768	A high-efficient strain-stress method for calculating higher-order elastic constants from first-principles. Computer Physics Communications, 2022, 280, 108478.	3.0	10

#	Article	IF	Citations
7769	A larger-cell tetragonal carbon allotrope tP176 carbon with superhardness. Materials Letters, 2022, 326, 132925.	1.3	9
7770	The roles of gold and silver nanoparticles on ZnIn2S4/silver (gold)/tetra(4-carboxyphenyl)porphyrin iron(III) chloride hybrids in carbon dioxide photoreduction. Journal of Colloid and Interface Science, 2022, 628, 831-839.	5.0	7
7771	Terahertz spectral identification and low-frequency vibrational analysis of dinitrotoluene isomers. Spectrochimica Acta - Part A: Molecular and Biomolecular Spectroscopy, 2022, 283, 121722.	2.0	0
7772	Temperature-dependent oxygen annealing effect on the properties of Ga2O3 thin film deposited by atomic layer deposition. Journal of Alloys and Compounds, 2022, 925, 166727.	2.8	12
7773	Roles of transfer layer and surface adhesion on superlubricity behaviors of diamond-like carbon film depending on rotating and reciprocating motion. Applied Surface Science, 2022, 604, 154538.	3.1	12
7774	Surface reconstruction and sulfur vacancies engineering in pentlandite for improving hydrogen evolution reaction. Applied Surface Science, 2022, 604, 154470.	3.1	6
7775	Solvent-mediated selectivity control of furfural hydrogenation over a N-doped carbon-nanotube-supported Co/CoOx catalyst. Applied Catalysis B: Environmental, 2022, 318, 121838.	10.8	22
7776	An ab-initio investigation of novel double halide perovskite Cs2InCoX6(X=F, Cl, Br) materials with direct band structure and broadband light absorption. Materials Science in Semiconductor Processing, 2022, 152, 107047.	1.9	6
7777	Two novel easily exfoliated quaternary chalcogenides with high performance of photocatalytic hydrogen production. Applied Surface Science, 2022, 604, 154555.	3.1	13
7778	Hierarchical Fe/ZSM-5 zeolites for efficient Hg0 removal from coal-fired flue gas. Chemical Engineering Journal, 2022, 450, 138180.	6.6	12
7779	First-principles study of the effect of point defects (Hi-VAl) on the magnetic and photocatalytic properties of monolayer AlN: Be/Mg/Ca. Applied Surface Science, 2022, 604, 154506.	3.1	3
7780	Pb₃SBrI₃: the first Pb-based chalcohalide with multiple halogens features a unique two-dimensional structure composed of diverse Pb-centered polyhedra. Dalton Transactions, 2022, 51, 12921-12927.	1.6	6
7781	Formation of Noble Metal Phases (Pt, Pd, Rh, Ru, Ir, Au, Ag) in the Process of Fractional Crystallization of the CuFeS2 Melt. Minerals (Basel, Switzerland), 2022, 12, 1136.	0.8	5
7782	NMR Crystallography as a Vital Tool in Assisting Crystal Structure Determination from Powder XRD Data. Crystals, 2022, 12, 1277.	1.0	3
7783	Indirect learning and physically guided validation of interatomic potential models. Journal of Chemical Physics, 2022, 157, .	1.2	3
7784	Interactions of xanthates of increasing chain length with pyrite surfaces: A DFT-D and microcalorimetry study. Applied Surface Science, 2023, 607, 154910.	3.1	11
7785	Understanding the synthesis and reactivity of ADORable zeolites using NMR spectroscopy. Current Opinion in Colloid and Interface Science, 2022, 61, 101634.	3.4	5
7786	Few-layer bismuthene enabled solid-state Li batteries. Energy Storage Materials, 2022, 52, 655-663.	9.5	10

#	Article	IF	Citations
7787	Revealing the electronic, optical, phonon and thermoelectrical characteristics of bulk and monolayered RbLiS and RbLiSe compounds by DFT. Journal of Physics and Chemistry of Solids, 2022, 170, 110972.	1.9	1
7788	An ab initio approach to understand the structural, thermophysical, electronic, and optical properties of binary silicide SrSi: A double Weyl semimetal. Results in Physics, 2022, 42, 105973.	2.0	3
7789	First-principles calculations to investigate structural, elastic, electronic, thermodynamic, and thermoelectric properties of CaPd3B4O12 (BÂ=ÂTi, V) perovskites. Results in Physics, 2022, 42, 105977.	2.0	54
7790	Design of a new ultraviolet nonlinear optical material KNO3SO3NH3 exhibiting an unexpected strong second harmonic generation response. Materials Today Physics, 2022, 28, 100849.	2.9	19
7791	Bio-grafted silica to make an asphalt road a sink for reactive environmental pollutants. Environmental Pollution, 2022, 313, 120142.	3.7	2
7792	Ab-initio-based interface modeling and statistical analysis for estimate of the water contact angle on a metallic Cu(111) surface. Surfaces and Interfaces, 2022, 34, 102342.	1.5	2
7793	Optical and electronic parameters of Rb2SO4 crystals. Optik, 2022, 269, 169875.	1.4	2
7794	Insight into synergistic corrosion inhibition of 3-amino-1,2,4-triazole-5-thiol (ATT) and NaF on magnesium alloy: Experimental and theoretical approaches. Corrosion Science, 2022, 208, 110618.	3.0	8
7795	First-principles calculations to investigate the structural, electronic, optical anisotropy, and bonding properties of a newly synthesized ThRhGe equiatomic ternary intermetallic superconductor. Results in Physics, 2022, 42, 106004.	2.0	6
7796	Influence of high pressure on Ce3+ luminescence in LuAlO3 and YAlO3 single crystals and single crystalline layers. Journal of Luminescence, 2022, 252, 119276.	1.5	1
7797	SnS2 monolayer as a promising candidate for NO2 sensor or capturer with high selectivity and sensitivity: A first-principles study. Materials Science in Semiconductor Processing, 2022, 152, 107073.	1.9	8
7798	Study on the influence of solution temperature on the synergistic effect of precipitation strengthening and fine grain strengthening of AA6061. Materials Today Communications, 2022, 33, 104312.	0.9	2
7799	Facile one-pot preparation and luminescence mechanism of stable Bi3+-doped Cs2AgInCl6 double perovskite nanocrystals. Journal of Luminescence, 2022, 252, 119246.	1.5	3
7800	Adsorption selectivity of TiCl4 precursor on Pt surfaces for atomic layer deposition via density functional theory. Applied Surface Science, 2022, 606, 154695.	3.1	1
7801	Ab-initio study of the electronic and photocatalytic performances of MoS2-xSex/SiC van der Waals heterostructures with asymmetric Se doping. Physica B: Condensed Matter, 2022, 646, 414350.	1.3	0
7802	Study on the structural, electronic and optical properties of double-perovskite halides Cs2AgSbX6 (X=I, Br, Cl) based on first-principles. Materials Science in Semiconductor Processing, 2022, 152, 107077.	1.9	16
7803	First principle study on the interactions of NH3, NOx and O2 with Fe3O4 (1 1 1) surfaces. Applied Surface Science, 2022, 605, 154645.	3.1	1
7804	First-principles study of the effect of N on the â^'5 (210) [001] grain boundary of Î³-Fe. Materials Today Communications, 2022, 33, 104496.	0.9	1

#	Article	IF	Citations
7805	Broad-band cyan emission induced by two-locations of Eu2+ activator for a new phosphor BaLa2Y2(SiO4)3O: Eu2+. Physica B: Condensed Matter, 2022, 646, 414304.	1.3	1
7806	New salts of teriflunomide (TFM) â€“ Single crystal X-ray and solid state NMR investigation. Solid State Nuclear Magnetic Resonance, 2022, 122, 101820.	1.5	1
7807	A comprehensive DFT study of physical and photocatalytic properties of Sr1-xCdxTiO3. Materials Today Communications, 2022, 33, 104495.	0.9	2
7808	TTDFT: A GPU accelerated Tucker tensor DFT code for large-scale Kohn-Sham DFT calculations. Computer Physics Communications, 2023, 282, 108516.	3.0	1
7809	Nanoscale surface modification to suppress capacity fade of Ni-Rich layered oxide material at high cut-off voltage. Chemical Engineering Journal, 2023, 451, 138911.	6.6	12
7810	Density-functional theory. , 2023, , 27-65.		0
7811	Oxygen vacancy-mediated amorphous GeOx assisted polysulfide redox kinetics for room-temperature sodium-sulfur batteries. Journal of Colloid and Interface Science, 2023, 629, 76-86.	5.0	3
7812	Wide band gap thiophosphates ASrPS₄ (A = Li, Na, K, Rb, Cs): cation size effect induced successive structural transformation. Dalton Transactions, 2022, 51, 15067-15073.	1.6	4
7813	Erbium ion implantation into LiNbO₃, Al₂O₃, ZnO and diamond â€“ measurement and modelling â€“ an overview. Physical Chemistry Chemical Physics, 2022, 24, 19052-19072.	1.3	2
7814	Probing the Low Friction Mechanism of Hydrogen-Free Dlc Film in Oxygen and Nitrogen Environments by First-Principles Calculations and Molecular Dynamics Simulation. SSRN Electronic Journal, 0, , .	0.4	0
7815	MXene/ZnO flexible freestanding film as a dendrite-free support in lithium metal batteries. Journal of Materials Chemistry A, 2022, 10, 17199-17207.	5.2	11
7816	First-principles study of lead-free Ge-based 2D Ruddlesdenâ€“Popper hybrid perovskites for solar cell applications. Physical Chemistry Chemical Physics, 2022, 24, 21052-21060.	1.3	2
7817	Characterization of the charge transfer luminescence of the [WO₆]^{6â^'} octahedron in Ca₃WO₆ and the [WO₅]^{4â^'} square pyramid in Ca₃WO₅Cl₂. Physical Chemistry Chemical Physics, 2022, 24, 24203-24211.	1.3	2
7818	Anisotropy, segmental dynamics and polymorphism of crystalline biogenic carboxylic acids. Physical Chemistry Chemical Physics, 2022, 24, 25904-25917.	1.3	2
7819	Mercurial possibilities: determining site distributions in Cu₂HgSnS₄ using ^{63/65}Cu, ¹¹⁹Sn, and ¹⁹⁹Hg solid-state NMR spectroscopy. Physical Chemistry Chemical Physics, 2022, 24, 24306-24316.	1.3	5
7820	A comparative study of the mechanical stability, electronic, optical and photocatalytic properties of CsPbX₃ (X = Cl, Br, I) by DFT calculations for optoelectronic applications. RSC Advances, 2022, 12, 23704-23717.	1.7	12
7821	Polymorphs and solid solutions: materials with new luminescent properties obtained through mechanochemical transformation of dicyanoaurate(I) salts. Faraday Discussions, 0, , .	1.6	3
7822	Ba₂HgTe₅: a Hg-based telluride with giant birefringence induced by linear [HgTe₂] units. Inorganic Chemistry Frontiers, 2022, 9, 5024-5031.	3.0	6

#	Article	IF	Citations
7823	Perovskite-structure TlBO₃ (B = Cr, Mn) for thermomechanical and optoelectronic applications: an investigation via a DFT scheme. RSC Advances, 2022, 12, 27492-27507.	1.7	6
7824	AAg₂PS₄(A = K, Na/K): the first-type of noncentrosymmetric alkali metal Ag-based thiophosphates exhibiting excellent second-order nonlinear optical performances. Inorganic Chemistry Frontiers, 2022, 9, 4990-4998.	3.0	13
7825	Comparative Study of the Mechanical, Optoelectronic and Photocatalytic Properties of the Defect-Free and Oxygen-Defected Tio2 Nanosheets Under Uniaxial Strain Conditions by Dft Simulations. SSRN Electronic Journal, 0, , .	0.4	0
7826	Lattice dynamic stability and electronic structures of ternary hydrides La_{1â^'x}Y_xH₃via first-principles cluster expansion. RSC Advances, 2022, 12, 26808-26814.	1.7	2
7827	[C(NH₂)₃]BiCl₂SO₄: an excellent birefringent material obtained by multifunctional group synergy. Inorganic Chemistry Frontiers, 2022, 9, 5572-5578.	3.0	13
7828	An anodeless, mechanically flexible and energy/power dense sodium battery prototype. Energy and Environmental Science, 2022, 15, 4686-4699.	15.6	15
7829	Manipulation of n â†' Ï€* electronic transitionsviaimplanting thiophene rings into two-dimensional carbon nitride nanosheets for efficient photocatalytic water purification. Journal of Materials Chemistry A, 2022, 10, 20559-20570.	5.2	17
7830	Hydroxamate based transition metalâ€“organic coordination polymers with semiconductive properties. Dalton Transactions, 2022, 51, 12709-12716.	1.6	5
7831	Three-dimensional porous platinumâ€“telluriumâ€“rhodium surface/interface achieve remarkable practical fuel cell catalysis. Energy and Environmental Science, 2022, 15, 3877-3890.	15.6	32
7832	Activity and selectivity of N₂ fixation on B doped g-C₉N₁₀: a density functional theory study. Journal of Materials Chemistry C, 2022, 10, 11791-11800.	2.7	2
7833	First-principles investigation on the electronic structures of CdSe_xS_{1â^'x} and simulation of CdTe solar cell with a CdSe_xS_{1â^'x} window layer by SCAPS. RSC Advances, 2022, 12, 22188-22196.	1.7	3
7834	The modulation mechanism of geometric and electronic structures of bimetallic catalysts: Pd_{13â^'m}Ag_m (m=0â€“13) clusters for acetylene semi-hydrogenation. Inorganic Chemistry Frontiers, 2022, 9, 5169-5180.	3.0	1
7835	Mechanism of high photoluminescence quantum yield of melem. Physical Chemistry Chemical Physics, 2022, 24, 23602-23611.	1.3	4
7836	Synthetic control of structure and conduction properties in Naâ€“Yâ€“Zrâ€“Cl solid electrolytes. Journal of Materials Chemistry A, 2022, 10, 21565-21578.	5.2	10
7837	[ASr₄Cl][Ge₃S₁₀] (A = Na, K) and [KBa₄Cl][Ge₃S₁₀]: new salt-inclusion infrared nonlinear optical crystals with zero-dimensional [Ge₃S₉] clusters. Inorganic Chemistry Frontiers, 2022, 9, 5932-5940.	3.0	16
7838	Sc₂F₂(B₂O₅): a deep ultraviolet scandium borate fluoride exhibiting large birefringence induced by the synergistic effect of B₂O₅and ScO_nF₂groups. Inorganic Chemistry Frontiers, 2022, 9, 5153-5160.	3.0	23
7839	Direct synthesis of a stable radical doped electrically conductive coordination polymer. Inorganic Chemistry Frontiers, 2022, 9, 5016-5023.	3.0	3
7840	Biaxial stress and functional groups (T = O, F, and Cl) tuning the structural, mechanical, and electronic properties of monolayer molybdenum carbide. Physical Chemistry Chemical Physics, 2022, 24, 17862-17869.	1.3	7

#	Article	IF	Citations
7841	The exploration of new infrared nonlinear optical crystals based on the polymorphism of BaGa₄S₇. Inorganic Chemistry Frontiers, 2022, 9, 4632-4641.	3.0	14
7842	BaSc₂(HPO₃)₄(H₂O)₂: a new nonlinear optical phosphite exhibiting a 3D {[Sc₂(HPO₃)₄]^{2â^'}}_{â^ž} anionic framework and phase-matchable SHG effect. Inorganic Chemistry Frontiers, 2022, 9, 5377-5385.	3.0	14
7843	Understanding the role of rare-earth metal doping on the electronic structure and optical characteristics of ZnO. Molecular Systems Design and Engineering, 2022, 7, 1516-1528.	1.7	5
7844	Density functional theory calculations for the electronic structure of carbon and copper co-doped TiO2 rutile model. AIP Conference Proceedings, 2022, , .	0.3	1
7845	Regulation of surface oxygen activity in Li-rich layered cathodes using band alignment of vanadium phosphate surface coatings. Journal of Materials Chemistry A, 2022, 10, 24487-24509.	5.2	2
7846	Monitoring MgCl₂ hydrate formation from aqueous solutions using terahertz time-domain spectroscopy. Physical Chemistry Chemical Physics, 2022, 24, 23490-23496.	1.3	0
7847	Theoretical Research of two-dimensional germanether in sodium-ion battery. Wuli Xuebao/Acta Physica Sinica, 2022, .	0.2	0
7848	Electrochemical behavior of Znâ€“Co layered double hydroxide in supercapacitor with the assistance of theoretical calculation models. Materials Express, 2022, 12, 564-569.	0.2	0
7849	AgNO3-preplanted Li metal powder electrode: Preliminary formation of lithiophilic Ag and a Li3N-rich solid electrolyte interphase. Chemical Engineering Journal, 2023, 452, 139409.	6.6	8
7850	Low-consumption with efficient capture and characteristics of heavy metals from coal combustion by modified kaolin: Experimental and simulation studies. Fuel, 2023, 332, 126094.	3.4	5
7851	Enhanced photocatalytic activity of MoS2 via NÂ+ÂF codoping and strain engineering: A first-principles investigation. Applied Surface Science, 2023, 607, 154881.	3.1	9
7852	First-principles insights into the electronic, optical, mechanical, and thermodynamic properties of lead-free cubic ABO3 [A = Ba, Ca, Sr; B = Ce, Ti, Zr] perovskites. AIP Advances, 2022, 12, .	0.6	29
7853	Simulation and Calculation for Predicting Structures and Properties of High-Entropy Alloys. , 0, , .		2
7854	Forced Disorder in the Solid Solution Li₃Pâ€“Li₂S: A New Class of Fully Reduced Solid Electrolytes for Lithium Metal Anodes. Journal of the American Chemical Society, 2022, 144, 16350-16365.	6.6	13
7855	Determining the THz and Infrared Spectral Properties of Single Crystals and Thin Crystalline Films from First Principles. , 2022, , .		0
7856	A DFT Study on the Adsorption of Carboxyl-Containing Monomers on CH (001) Surface. Russian Journal of Physical Chemistry B, 2022, 16, 804-808.	0.2	4
7857	Metallic Aluminum Suboxides with Ultrahigh Electrical Conductivity at High Pressure. Research, 2022, 2022, .	2.8	3
7858	Impact of structure on the vibrational properties of Ag8SnSe6 crystal: Experimental and theoretical studies. Optical Materials: X, 2022, 15, 100180.	0.3	2

#	Article	IF	Citations
7859	Mechanochemical bottom-up synthesis of phosphorus-linked, heptazine-based carbon nitrides using sodium phosphide. Beilstein Journal of Organic Chemistry, 0, 18, 1203-1209.	1.3	2
7860	KC₉H₅O₆(H₂O): A Promising UV Nonlinear-Optical Material with Large Birefringence Based on a Ï€-Conjugated (C₉H₅O₆)^{â^'}Group. Inorganic Chemistry, 2022, 61, 14880-14886.	1.9	4
7861	New insights into intrinsic point defects of delafossite CuAlO₂ as optoelectronic materials. Journal of the American Ceramic Society, 2022, 105, 7535-7547.	1.9	3
7862	Mechanical, tribological and electrochemical behavior of Zr-based ceramic thin films for dental implants. Ceramics International, 2023, 49, 2102-2114.	2.3	5
7863	Identification of Graphene Dispersion Agents through Molecular Fingerprints. ACS Nano, 2022, 16, 16109-16117.	7.3	2
7864	Boron arsenate and its pressure-dependent auxetic properties. APL Materials, 2022, 10, 091109.	2.2	2
7865	Synthesis and property investigation of Er-doped Bi4(Ge0.5Si0.5)3O12 (BGSO): a potential gain medium of C-band laser. Applied Physics A: Materials Science and Processing, 2022, 128, .	1.1	2
7866	Enhanced thermoelectric properties of Cu2Se via Sb doping: An experimental and computational study. Journal of the European Ceramic Society, 2023, 43, 401-406.	2.8	12
7867	VELAS: An open-source toolbox for visualization and analysis of elastic anisotropy. Computer Physics Communications, 2023, 283, 108540.	3.0	9
7868	Exploration of the structural, optoelectronic and vibrational behavior of Sb2S3 through the first principles approach for phenomenal applications in solar cells. Optical and Quantum Electronics, 2022, 54, .	1.5	4
7869	Effects of Vacancies on the Structural, Elastic, Electronic and Thermodynamic Properties of C11b-VSi2 by First-Principles Calculations. Metals, 2022, 12, 1625.	1.0	4
7870	The structural, mechanical and electronic properties of Tiâ€“Al-based compounds by first-principles calculations. Journal of Molecular Modeling, 2022, 28, .	0.8	0
7871	P212121-C16: An ultrawide bandgap and ultrahard carbon allotrope with the bandgap larger than diamond. Frontiers of Physics, 2022, 17, .	2.4	6
7872	Insights on modulating electronic and transport properties of the sawtoothâ€“sawtooth penta-SiC₂ nanoribbons under uniaxial small strain by first-principles calculations. AIP Advances, 2022, 12, 095318.	0.6	2
7873	Experimentally and Theoretically Revealing the Co-Doping Effects of Ceâ€“Sr in Gd₂Zr₂O₇. Langmuir, 2022, 38, 11529-11538.	1.6	2
7874	High-Performance Adsorbent for Ethane/Ethylene Separation Selected through the Computational Screening of Aluminum-Based Metalâ€“Organic Frameworks. ACS Applied Materials & Interfaces, 2022, 14, 43637-43645.	4.0	5
7875	The electronic and mechanical properties of Fe₁₆N₂ up to 150â€‰GPa: First-principles calculation. Journal of Applied Physics, 2022, 132, 095904.	1.1	1
7876	Mechanical, thermodynamic properties and phase transition in crystal CaZn₂ under high pressureÂâ€” a DFT study. International Journal of Modern Physics C, 0, , .	0.8	1

#	Article	IF	Citations
7877	Unraveling the Ordered Phase of the Quintessential Hybrid Perovskite MAPbI₃â”€Thermophysics to the Rescue. Journal of Physical Chemistry Letters, 2022, 13, 8422-8428.	2.1	2
7878	A nanodispersion-in-nanograins strategy for ultra-strong, ductile and stable metal nanocomposites. Nature Communications, 2022, 13, .	5.8	22
7879	Effect of hydrostatic pressure on the structural, elastic, and optoelectronic properties of vacancy-ordered double perovskite Cs2PdBr6. Journal of Molecular Modeling, 2022, 28, .	0.8	4
7880	Adhesion strength, interfacial bonding, and fracture mechanism of the Mg/Ti2AlC interface from first-principles calculation. Journal of Materials Research and Technology, 2022, 20, 3195-3207.	2.6	22
7881	PbBi(SeO₃)₂F and Pb₂Bi(SeO₃)₂Cl₃: Coexistence of Three Kinds of Stereochemically Active Lone-Pair Cations Exhibiting Excellent Nonlinear Optical Properties. Inorganic Chemistry, 2022, 61, 15368-15376.	1.9	19
7882	Ag₄SnGe₂S₇: A Noncentrosymmetric Chalcogenide in I₄â€“IIâ€“IV₂â€“VI₇ System with Non-Diamond-Like Structure Featuring 1D _{â^ž}[SnGe₂S₈]^{6â€“} Infinite Chain. Inorganic Chemistry, 2022, 61, 15303-15309.	1.9	0
7883	Concentration dependences of electronic band structure of CdSe1â€“xSx thin films. Applied Nanoscience (Switzerland), 0, , .	1.6	1
7884	Bandgap engineering in BP/PtO2 van der Waals (vdW) hetero-bilayer using first-principles study. AIP Advances, 2022, 12, .	0.6	1
7885	Ligand Engineering Triggered Efficiency Tunable Emission in Zero-Dimensional Manganese Hybrids for White Light-Emitting Diodes. Nanomaterials, 2022, 12, 3142.	1.9	3
7886	Reducing the Carbon Footprint of Bituminous Composites Using Amine-Impregnated Zeolite. ACS Sustainable Chemistry and Engineering, 2022, 10, 13004-13016.	3.2	1
7887	Comparison of CO2, N2, CO, H2S, CH4, and H2O adsorptions onto sI methane hydrate surface. Frontiers in Earth Science, 0, 10, .	0.8	0
7888	Effective Inhibition of Ethane Generation on Fe₅C₂ Nanoparticles Doped with ppm Level of Pd for Selective Hydrogenation of Acetylene. Industrial & Engineering Chemistry Research, 2022, 61, 13341-13353.	1.8	3
7889	First-Principles Calculations to Investigate the Effect of Van der Waals Interactions on the Crystal and Electronic Structures of Tin-Based 0D Hybrid Perovskites. Inorganics, 2022, 10, 155.	1.2	25
7890	Strain Effects on the Two-Dimensional Cr₂N MXene: An Ab Initio Study. ACS Omega, 2022, 7, 33884-33894.	1.6	6
7891	Structural, Electronic, and Vibrational Properties of N ₂ O ₄ under Pressure from Firstâ€Principles Study. Physica Status Solidi (B): Basic Research, 0, , 2200264.	0.7	0
7892	Building efficient interfacial property with graphene heterogeneous interface. International Journal of Mechanical Sciences, 2023, 237, 107782.	3.6	10
7893	Extension of MAX phases from ternary carbides and nitrides (XÂ=ÂC and N) to ternary borides (XÂ=ÂB, C,) Tj ETQq0 0 0 rgBT /Overlock	1.1	11
7894	Dual-Ligand-Oriented Design of Noncentrosymmetric Complexes with Nonlinear-Optical Activity. Inorganic Chemistry, 2022, 61, 16509-16514.	1.9	3

#	Article	IF	Citations
7895	Hydrogen storage capacity and reversibility of Li-decorated B4CN3 monolayer revealed by first-principles calculations. International Journal of Hydrogen Energy, 2022, 47, 38271-38281.	3.8	19
7896	BaSb(H2PO2)3Cl2: An excellent UV nonlinear optical hypophosphite exhibiting strong second-harmonic generation response. Materials Today Physics, 2022, 28, 100876.	2.9	10
7897	First-Principles Study of Structure and Optical Properties of Perovskite PbTiO₃ under Pressure. Integrated Ferroelectrics, 2022, 230, 210-224.	0.3	0
7898	Improving optical properties of wurtzite GaN with C and Fe co-doping: A DFT+U study. Journal of Physics Communications, 0, , .	0.5	0
7899	129Xe NMR analysis of pore structures and adsorption phenomena in rare-earth element phosphates. Microporous and Mesoporous Materials, 2022, 344, 112209.	2.2	1
7900	Nonuniform grids for Brillouin zone integration and interpolation. Physical Review B, 2022, 106, .	1.1	4
7901	Ab initio prediction of half-metallicity in the NaMnZ2 (Z = S, Se, Te) ternary layered compounds. Computational Condensed Matter, 2022, 33, e00754.	0.9	0
7902	Inelastic Neutron Scattering from Thin Film Biaxially Oriented Polyethylene Terephthalate. Journal of Physical Chemistry A, 2022, 126, 7491-7501.	1.1	2
7903	1,3-Butadiene on Titan: Crystal Structure, Thermal Expansivity, and Raman Signatures. ACS Earth and Space Chemistry, 2022, 6, 2274-2281.	1.2	3
7904	Siteâ€Preferences in the Mixedâ€Valent Series FeMo _{1â^'n} V _n O ₄ : Controlling the Formation of the Îµâ€Polymorph and the Charge Localization. Zeitschrift Fur Anorganische Und Allgemeine Chemie, 0, , .	0.6	0
7905	Exploring the Potential of Multinuclear Solidâ€state 1H, 13C, and 35Cl Magnetic Resonance to Characterize Static and Dynamic Disorder in Pharmaceutical hydrochlorides. ChemPhysChem, 0, , .	1.0	3
7906	Effect of Al modification on the adsorption of As2O3 on the CaSiO3(001) surface: A DFT study. Journal of Molecular Graphics and Modelling, 2023, 118, 108357.	1.3	11
7907	Modelling hydrogen mobility in forsterite as diffusion coupled to inter-site reaction. Contributions To Mineralogy and Petrology, 2022, 177, .	1.2	4
7908	Computational study of structural, electronic, elastic and vibrational properties of LiAlSi, NaAlSi, and KAlSi Half-Heusler alloys. Indian Journal of Physics, 2023, 97, 1389-1395.	0.9	2
7909	A green and sustainable strategy toward lithium resources recycling from spent batteries. Science Advances, 2022, 8, .	4.7	26
7910	Structural, Electronic, and Optical Properties of Cs₂SnX₄ (Xâ€‰=â€‰Cl, Br, and I) Multilayers: A Density Functional Theory Study. Physica Status Solidi (B): Basic Research, 2023, 260, .	0.7	2
7911	Design of novel deep-UV nonlinear optical materials with one-dimensional functional module [BO2]â^ž chain and fluorine-driven short phase-matching. Materials Today Physics, 2022, 28, 100852.	2.9	21
7912	Synthesis and Characterization of Mediumâ€Highâ€Entropy M₂SnC (M=Ti/V/Nb/Zr/Hf) MAX Phases. Small Structures, 2023, 4, .	6.9	15

#	Article	IF	Citations
7913	Systematic Mapping of Electrocatalytic Descriptors for Hybrid and Non-Hybrid Molybdenum Dichalcogenides with Graphene Support for Cathodic Hydrogen Generation. Journal of Physical Chemistry C, 2022, 126, 17011-17024.	1.5	6
7914	A DFT study of optical, elastic, mechanical, and overall water-splitting photocatalytic properties of pristine and Cd substituted BaZrO3: A lead free environment friendly material. Materials Science and Engineering B: Solid-State Materials for Advanced Technology, 2022, 286, 116041.	1.7	8
7915	A comparative DFT exploration on M- and A-site double transition metal MAX phase, Ti3ZnC2. Open Ceramics, 2022, 12, 100308.	1.0	13
7916	Improving the accuracy of GIPAW chemical shielding calculations with cluster and fragment corrections. Solid State Nuclear Magnetic Resonance, 2022, 122, 101832.	1.5	7
7917	Mo-doped Cr-Ti-Mo ternary o-MAX with ultra-low wear at elevated temperatures. Journal of the European Ceramic Society, 2022, 42, 7403-7413.	2.8	9
7918	FIRST-PRINCIPLES CALCULATIONS OF THE STRUCTURAL, ELECTRONIC AND ELASTIC PROPERTIES OF SrGeO3 AND SrZrO3 CUBIC PEROVSKITES.. , 2021, 6, 7-18.		0
7919	Computational Techniques for Nanostructured Materials. , 2022, , 459-480.		0
7920	Exploring the configurational space of amorphous graphene with machine-learned atomic energies. Chemical Science, 2022, 13, 13720-13731.	3.7	8
7921	Large optical anisotropy differentiation induced by the anion-directed regulation of structures. Inorganic Chemistry Frontiers, 2022, 9, 6441-6447.	3.0	10
7922	Argyrodite configuration determination for DFT and AIMD calculations using an integrated optimization strategy. RSC Advances, 2022, 12, 31156-31166.	1.7	2
7923	K₂(BeS)O₄F₂: a novel fluorosulfate with unprecedented 1D [(BeO₃F)â€“(SO₃F)]_{âˆž}chains exhibiting large birefringence. Inorganic Chemistry Frontiers, 2022, 9, 6490-6497.	3.0	4
7924	Functionalized ceriaâ€“niobium supported nickel catalysts for gas phase semi-hydrogenation of phenylacetylene to styrene. Catalysis Science and Technology, 2022, 12, 7133-7150.	2.1	6
7925	KSb(BeF₃)F₃: a totally fluorine strategy for achieving wide bandgap and large birefringence. Journal of Materials Chemistry C, 2022, 10, 17577-17582.	2.7	8
7926	Thermodynamic and dynamic stability in a new potential Cs₂AgAsCl₆ perovskite: insight from DFT study. Physical Chemistry Chemical Physics, 2022, 24, 26609-26621.	1.3	4
7927	Ce_{1âˆ’x}Sr_xO_{2âˆ’Î´} solid solution supports cobalt-based catalysts for hydrogen production via auto-thermal reforming of acetic acid. Catalysis Science and Technology, 2022, 12, 7457-7469.	2.1	4
7928	Optimal data generation for machine learned interatomic potentials. Machine Learning: Science and Technology, 2022, 3, 045031.	2.4	3
7929	Hydration behavior of MgO surface: A first-principles study. Applied Surface Science, 2023, 611, 155441.	3.1	7
7930	A Carboxylic Ester-Based Electrolyte with Additive to Improve Performance of Lithium Batteries at Ultra-Low Temperature. Journal of the Electrochemical Society, 2022, 169, 100539.	1.3	3

#	Article	IF	Citations
7931	Stabilizing Ti₃C₂T_x in a Water Medium under Multiple Environmental Conditions by Scavenging Oxidative Free Radicals. Chemistry of Materials, 2022, 34, 9517-9526.	3.2	7
7932	Revealing solid electrolyte interphase formation through interface-sensitive Operando X-ray absorption spectroscopy. Nature Communications, 2022, 13, .	5.8	11
7933	On the Tensile Strength of Spark Plasma Sintered AlMgB14 Ceramics. Nanomaterials, 2022, 12, 3805.	1.9	1
7934	Electronic and Optical Properties of $$V-Doped$$ ÂAlN Rock-salt Structure: A First-principles Study Within GGA and $$GGA+U$$ Method. Journal of Superconductivity and Novel Magnetism, 2022, 35, 3661-3669.	0.8	1
7935	Decentering the Symmetry via Docking B and F in the KBe₂BO₃F₂-Family Structure. Inorganic Chemistry, 2022, 61, 17855-17863.	1.9	0
7936	ZIF-75 under Pressure: Negative Linear Compressibility and Pressure-Induced Instability. Applied Sciences (Switzerland), 2022, 12, 10413.	1.3	5
7937	First-Principles Study on the Structural, Electronic, and Lithium Storage Properties of Ti₃C₂T₂ (T = O, F, H, OH) MXene. ACS Omega, 2022, 7, 40578-40585.	1.6	5
7938	Low-Pt-Based Sn Alloy for the Dehydrogenation of Methylcyclohexane to Toluene: A Density Functional Theory Study. Catalysts, 2022, 12, 1221.	1.6	3
7939	Li_xAg_{1â€“}_xGaSe₂: Interplay Between Lithium and Silver in Midâ€Infrared Nonlinear Optical Chalcogenides. Advanced Optical Materials, 2022, 10, .	3.6	14
7940	Roomâ€Temperature Solidâ€State Transformation of Na4SnS4Â·14H2O into Na4Sn2S6Â·5H2O: an Unusual Epitaxial Reaction Including Bond Formation, Mass Transport, and Ionic Conductivity. Chemistry - A European Journal, 0, , .	1.7	2
7941	Revealing the electronic, optical, elastic, mechanical, anisotropic, and thermoelectric responses of <scp> Sc ₂ NiZ </scp> (<scp>Z</scp> Â=Â <scp>Si</scp> , <scp>Ge</scp> , and <scp>Sn</scp>) <scp>Heusler</scp> alloys via <scp>DFT</scp> calculations. International Journal of Quantum Chemistry, 0, , .	1.0	1
7942	Pt Single Atoms on CrN Nanoparticles Deliver Outstanding Activity and CO Tolerance in the Hydrogen Oxidation Reaction. Advanced Materials, 2023, 35, .	11.1	33
7943	Finding a Deepâ€UV Borate BaZnB₄O₈ with Edgeâ€sharing [BO₄] Tetrahedra and Strong Optical Anisotropy. Chemistry - A European Journal, 2023, 29, .	1.7	6
7944	Mechanical and thermoelectric properties of the RbSnX3 (Xâ€‰=â€‰F, Cl) compounds. Applied Physics A: Materials Science and Processing, 2022, 128, .	1.1	0
7945	Engineering Nanoclay Edges to Enhance Antimicrobial Property against Gramâ€Negative Bacteria: Understanding the Membrane Destruction Mechanism by Contactâ€Kill. Advanced Functional Materials, 2023, 33, .	7.8	12
7946	Investigation of Electronic and Optical Properties of (Cs, Br, Cs-Br) Doped Mono-Layer Hexagonal Boron Nitride Using First Principles. Crystals, 2022, 12, 1406.	1.0	0
7947	Two-dimensional mineral hydrogel-derived single atoms-anchored heterostructures for ultrastable hydrogen evolution. Nature Communications, 2022, 13, .	5.8	25
7948	Phase Stability and Mechanical Properties Analysis of AlCoxCrFeNi HEAs Based on First Principles. Metals, 2022, 12, 1860.	1.0	4

#	Article	IF	Citations
7949	Effect of Si on Microstructure and Wear Resistance of Hypereutectic High-Chromium Cast Iron. Journal of Materials Engineering and Performance, 2023, 32, 5450-5465.	1.2	1
7950	Correlation between the activity of Fe@ (N, S, and P) doped graphene catalysts and the coordination environment: A density functional theory study. International Journal of Hydrogen Energy, 2023, 48, 171-179.	3.8	5
7951	The spontaneous polarization of In-doped Î²-Ga₂O₃ by first-principles calculation. AIP Advances, 2022, 12, 105115.	0.6	1
7952	Cs2B4O5(OH)4: A new hydrated borate with a short UV cutoff edge. Inorganica Chimica Acta, 2022, , 121252.	1.2	0
7953	Effects of Yttrium Doping on Erbium-Based Hydroxyapatites: Theoretical and Experimental Study. Materials, 2022, 15, 7211.	1.3	3
7954	Prediction of electronic and optical properties of monoclinic 1Tâ€™-phase OsSe2 monolayer using DFT principles. Materials Today Communications, 2022, 33, 104764.	0.9	5
7955	Comparative study of the mechanical, optoelectronic and photocatalytic properties of the defect-free and oxygen defect induced TiO2 nanosheets under uniaxial strain conditions by DFT simulations. Physica E: Low-Dimensional Systems and Nanostructures, 2023, 146, 115556.	1.3	2
7956	First-principle calculations of the structural, vibrational, mechanical, electronic, and optical properties of Îµ-O8 under pressure. Journal of Molecular Modeling, 2022, 28, .	0.8	1
7957	Mechanosynthesis of a Structurally Characterized, Wellâ€Đefined Graphitic Phosphorusâ€Linked Carbon Nitride (gâ€PCN) with Water Splitting Activity. Advanced Materials Interfaces, 2022, 9, .	1.9	1
7958	Upper limit of the transition temperature of superconducting materials. Patterns, 2022, 3, 100609.	3.1	2
7959	Complete Crystal Structures and Elastic Properties of the Uranyl Minerals Johannite, Pseudojohannite and Derriksite. Crystals, 2022, 12, 1503.	1.0	0
7960	Molecular Assembled Electrocatalyst for Highly Selective CO₂ Fixation to C₂₊ Products. ACS Nano, 2022, 16, 17021-17032.	7.3	10
7961	DFT Study on the Adsorption of Monomeric Hydroxyl Aluminum on Fe(II)/Mg Replacement Kaolinite (001) Surfaces. ACS Omega, 0, , .	1.6	0
7962	Design Principles to Maximize Nonâ€Bonding States for Highly Tribopositive Behavior. Advanced Functional Materials, 2023, 33, .	7.8	16
7963	Surface chemical heterogeneous distribution in over-lithiated Li1+xCoO2 electrodes. Nature Communications, 2022, 13, .	5.8	9
7964	Pressure Induced Clathrate Hydrogen-Rich Superconductors KH₂₀ and KH₃₀. Inorganic Chemistry, 2022, 61, 18112-18118.	1.9	1
7965	SbHPO₃F: 2D van der Waals Layered Phosphite Exhibiting Large Birefringence. Inorganic Chemistry, 2022, 61, 16997-17001.	1.9	10
7966	Photovoltaically top-performing perovskite crystal facets. Joule, 2022, 6, 2626-2643.	11.7	52

#	Article	IF	Citations
7967	Extended Analytic Embedded-Atom Model for BCC Tantalum and Its Application to Determination of Gibbs Free Energy and Thermal Equation of State. International Journal of Thermophysics, 2022, 43, .	1.0	0
7968	Predicting Diamond-like Nitrides as Infrared Nonlinear Optical Materials with High Thermal Conductivity. Chemistry of Materials, 2022, 34, 10059-10067.	3.2	8
7969	Spectroscopic and Simulation Insights into the Corrosion Mechanism of Sulfite on Titanium. Journal of Physical Chemistry B, 2022, 126, 9016-9025.	1.2	1
7970	First-principles study of physical, and superconducting properties of newly discovered full-Heusler compound MgPd ₂ Sb. Physica Scripta, 2022, 97, 125705.	1.2	6
7971	Interface characteristics of graphene/ZnS hybrid-dimensional heterostructures. Optics Express, 2022, 30, 42605.	1.7	1
7972	Hydrates of active pharmaceutical ingredients: A 35Cl and 2H solid-state NMR and DFT study. Solid State Nuclear Magnetic Resonance, 2022, 122, 101837.	1.5	6
7973	First-principles study on the mechanical, electronic and optical properties of double halide perovskite Cs₂TlSbX₆ (X = Cl, Br, I). Physica Scripta, 2022, 97, 125821.	1.2	3
7974	Improvement of the performance of graphene/Al(1 1 1) interface with defect mode and doped mode. Computational and Theoretical Chemistry, 2022, 1217, 113931.	1.1	2
7975	RE(OH)₂NO₃ (RE = Tb, Dy, Ho, and Er): Synthesis and Nonlinear Optical Properties of Water-Resistant Lanthanide Hydroxide Nitrates. Inorganic Chemistry, 2022, 61, 18162-18169.	1.9	5
7976	Thermal equation of states for body-centered cubic tungsten using extended analytic embedded-atom model. Modelling and Simulation in Materials Science and Engineering, 2022, 30, 085014.	0.8	1
7977	Theoretical insight into optical properties of ZnGa2O4 transparent ceramic. Materials Today Communications, 2023, 34, 104846.	0.9	1
7978	Mid-infrared nonlinear optical heptachlorodigallate AGa2Cl7 (A = Ga+, In+) with a unique second harmonic generation mechanism induced by monovalent cations. Materials Today Physics, 2022, 28, 100894.	2.9	4
7979	Sn₃B₁₀O₁₇Cl₂ Achieving Birefringence Enhancement by Stereochemical Activity Lone Pair. Inorganic Chemistry, 2022, 61, 18238-18244.	1.9	7
7980	Oriented Crystal Growth during Perovskite Surface Reconstruction. ACS Applied Materials & Interfaces, 2022, 14, 51149-51156.	4.0	2
7981	A DFT+U study of structural, electronic and optical properties of Ag- and Cu-doped ZnO. Microelectronics International, 2023, 40, 53-62.	0.4	0
7982	First principle studies of TiO₂-ZnO alloys under high pressure. Journal of Physics Condensed Matter, 2023, 35, 024003.	0.7	1
7983	Robust and Highly Conductive Water-Stable Copper Iodide-Based Hybrid Single Crystals. Chemistry of Materials, 2022, 34, 10040-10049.	3.2	7
7984	Effects of electric fields along different directions on the sensitivity and decomposition of TKX-50. Journal of Physics and Chemistry of Solids, 2022, 171, 111035.	1.9	1

#	Article	IF	Citations
7985	Glass-forming ability and structural features of melt-quenched and gel-derived SiO2-TiO2 glasses. Journal of Non-Crystalline Solids, 2022, 598, 121967.	1.5	7
7986	Response of the structure and vibrational modes of nitromethane to pressure. Materials Today Communications, 2022, 33, 104732.	0.9	0
7987	First principle studies on electronic and thermoelectric properties of Fe2TiSn based multinary Heusler alloys. Computational Materials Science, 2023, 216, 111856.	1.4	3
7988	Anomalous strain-dependent charge density in honeycomb borophene. Computational Materials Science, 2023, 216, 111838.	1.4	0
7989	First principles investigation on the boron-oxygen complexes in diamond. Computational Materials Science, 2023, 216, 111867.	1.4	2
7990	High-Throughput screening quaternary kesterite Cu2ABS4 (AÂ=ÂDivalent metals; BÂ=ÂTetravalent metals) photovoltaic materials. Computational Materials Science, 2023, 216, 111817.	1.4	0
7991	Insight into the role of atomic interaction and ionic radius in Al doped BiFeO3: Structural, electronic, and optical properties. Physica B: Condensed Matter, 2023, 648, 414417.	1.3	2
7992	A comprehensive DFT evaluation of catalytic and optoelectronic properties of BaTiO3 polymorphs. Physica B: Condensed Matter, 2023, 648, 414418.	1.3	16
7993	Excellent thermostability and blue light emitting properties of a new phosphor BaLa2Y2(SiO4)3:Tm3+. Physica B: Condensed Matter, 2023, 649, 414435.	1.3	2
7994	Influence of Mn2+ doping on refractive and electronic properties of Î²-LiNH4SO4 crystals. Physica B: Condensed Matter, 2023, 648, 414426.	1.3	0
7995	High-pressure induced structural changes of energetic ionic salts: Dihydroxylammonium 3,3â€²-dinitro-5,5â€²-bis-1,2,4-triazole-1,1â€²-diolate (MAD-X1). Chemical Physics, 2023, 564, 111727.	0.9	0
7996	The growth mechanism and intriguing optical and electronic properties of few-layered HfS₂. Nanoscale Advances, 2022, 5, 171-178.	2.2	2
7997	How does tuning the van der Waals bonding strength affect adsorbate structure?. Physical Chemistry Chemical Physics, 2022, 24, 29371-29380.	1.3	1
7998	Exploration of the physical properties of the newly synthesized kagome superconductor LaIr₃Ga₂ using different exchangeâ€“correlation functionals. Physical Chemistry Chemical Physics, 2022, 24, 29640-29654.	1.3	5
7999	Crystal structure of formamidiniumâ€“leadâ€“chlorideâ€“dimethyl sulfoxide and phase relationship of related crystalline systems. CrystEngComm, 0, , .	1.3	0
8000	¹H chemical shift anisotropy: a high sensitivity solid-state NMR dynamics probe for surface studies?. Physical Chemistry Chemical Physics, 2023, 25, 5348-5360.	1.3	4
8001	Optoelectronic investigation and spectroscopic characteristics of polyamide-66 polymer. E-Polymers, 2022, 22, 858-869.	1.3	2
8002	Ammonia Sensing Properties of SnSâ‚‚/SnOâ‚‚ Nanocomposite-Based Gas Sensor by SnSâ‚‚ Annealing. IEEE Sensors Journal, 2022, 22, 23456-23463.	2.4	1

#	Article	IF	Citations
8003	The bonding of H in Zr under strain. Journal of Nuclear Materials, 2023, 573, 154124.	1.3	0
8004	First-principles study on the hydrogen storage properties of MgH2(1 0 1) surface by CuNi co-doping. Chemical Physics, 2023, 565, 111760.	0.9	12
8005	Prediction of new 2D Hf2Br2N2 monolayer as a promising candidate for photovoltaic applications. Materials Chemistry and Physics, 2023, 294, 126979.	2.0	51
8006	Enwrapping g-C3N4 on In2O3 hollow hexagonal tubular for photocatalytic CO2 conversion: Construction, characterization, and Z-scheme mechanism insight. Journal of Colloid and Interface Science, 2023, 631, 122-132.	5.0	26
8007	Novel far-red emitting phosphor Mn4+-activated BaLaLiWO6 with excellent performance for indoor plant cultivation of light-emitting diodes. Journal of Alloys and Compounds, 2023, 934, 167927.	2.8	8
8008	Inverse spinel cobalt manganese oxide nanosphere materials as an electrode for high-performance asymmetric supercapacitor. Journal of Alloys and Compounds, 2023, 933, 167645.	2.8	6
8009	Ab initio Methods for Electronic Transport in Semiconductors and Nanostructures. Springer Handbooks, 2023, , 1515-1558.	0.3	0
8010	On the mechanical properties of CO ₂ â€Ⅱ with particular emphasis on its auxetic potential. Physica Status Solidi (B): Basic Research, 0, , .	0.7	1
8011	Mechanical Properties of a New Hybrid Inorganicâ€“Organic Framework: A Nanoindentation, High-Pressure X-ray Diffraction, and Computational Study. Crystal Growth and Design, 2022, 22, 6984-6994.	1.4	0
8012	Origin of the distinction in hardness of lower tungsten carbides: An experimental and ab initio theoretical study. Journal of the American Ceramic Society, 2023, 106, 2184-2195.	1.9	2
8013	Enhanced Oxygen Mobility in Undoped ZrO₂â€“CeO₂ Heterostructure. Physica Status Solidi (A) Applications and Materials Science, 2023, 220, .	0.8	1
8014	The hydrogen bond continuum in solid isonicotinic acid. Journal of Magnetic Resonance, 2022, , 107334.	1.2	0
8015	Li_{0.5}Na_{0.5}AlB₂O₄F₂: Fluoroaluminoborate with Aligned ¹_{âˆž}[BO₂] Chain Induced by Unprecedented [AlO₃F₃]^{6â^’} Species Features Enhanced Birefringence. Advanced Optical Materials, 2023, 11, .	3.6	5
8016	Exploring the effect of layer spacing of graphene for lithium single-atom diffusion using first principles calculations. Computational and Theoretical Chemistry, 2022, 1217, 113937.	1.1	0
8017	K₃C₆N₇O₃·2H₂O: A Multifunctional Nonlinear Optical Cyamelurate Crystal with Colossal Ï€-Conjugated Orbitals. ACS Applied Materials & Interfaces, 2022, 14, 53074-53080.	4.0	14
8018	Electronic properties of defects induced by hydrogen and helium radiation on semimetal <mml:math xmlns:mml="http://www.w3.org/1998/Math/MathML" display="inline" id="d1e607" altimg="si6.svg"><mml:msub><mml:mrow><mml:mi>M</mml:mi><mml:mi>o</mml:mi><mml:mi>T</mml:mi><mml:mi>e</mml:mi> Chemical Physics, 2022, , 111764.	0.9	0
8019	Conformational Flexibility-Controlled Piezochromic Behavior of Organic Fluorophores. Chemistry of Materials, 2022, 34, 10711-10720.	3.2	4
8020	Mechanochemical Synthesis and Study of the Local Structure of NaGaS₂ Glass and Glassâ€“Ceramics. Inorganic Chemistry, 2022, 61, 18476-18485.	1.9	2

#	Article	IF	Citations
8021	MAX phase forming mechanism of Mâ€“Alâ€“C (MÂ=ÂTi, V, Cr) coatings: In-situ X-ray diffraction and first-principle calculations. Journal of Materials Science and Technology, 2023, 143, 140-152.	5.6	8
8022	Electron-Deficient Zn-N6 Configuration Enabling Polymeric Carbon Nitride for Visible-Light Photocatalytic Overall Water Splitting. Nano-Micro Letters, 2022, 14, .	14.4	21
8023	Application of B3O3 monolayer as an electrical sensor for detection of formaldehyde gas: A DFT study. Computational and Theoretical Chemistry, 2023, 1219, 113941.	1.1	8
8024	Zr2SeB and Hf2SeB: Two new MAB phase compounds with the Cr2AlC-type MAX phase (211 phase) crystal structures. Journal of Advanced Ceramics, 2022, 11, 1764-1776.	8.9	18
8025	Xâ€•ray excited luminescence of highâ€•quality doped GaN single crystals. Physica Status Solidi (A) Applications and Materials Science, 0, , .	0.8	1
8026	Effect of Various Electron and Hole Transport Layers on the Performance of CsPbI₃-Based Perovskite Solar Cells: A Numerical Investigation in DFT, SCAPS-1D, and wxAMPS Frameworks. ACS Omega, 2022, 7, 43210-43230.	1.6	118
8027	LiAlS2: A promising infrared frequency-conversion material with ultrawide band gap and high laser-induced damage threshold. Science China Materials, 2023, 66, 1189-1196.	3.5	6
8028	Effect of Sr-Doping on the Photocatalytic Performance of LaNiO3â^Ïƒ. Catalysts, 2022, 12, 1434.	1.6	3
8029	Rational Design of Metal-Alkoxide-Functionalized Metalâ€“Organic Frameworks for Synergistic Dual Activation of CH₄ and CO₂ toward Acetic Acid Synthesis. ACS Applied Materials & Interfaces, 2022, 14, 52979-52992.	4.0	2
8030	Core-shell hollow nanostructures as highly efficient polysulfide conversion and adsorption cathode for shuttle-free lithium-sulfur batteries. Chemical Engineering Journal, 2023, 454, 140338.	6.6	14
8031	Investigation of electronic structure, optical properties, map of electrostatic potential, and toxicity of HfO2, Hf0.88Si0.12O2, Hf0.88Ge0.12O2 and Hf0.88Sn0.12O2 by computational and virtual screening. Journal of Computational Electronics, 0, , .	1.3	1
8032	CaBO2F: A novel deep-UV structural template with high nonlinear optical performance induced by electron delocalization. Science China Materials, 0, , .	3.5	10
8033	Zn₃GaB₆O₁₂As and Zn₄P₆N₁₂S: Isotropic Zero Thermal Expansion Materials Based on the â€œCage-Restrictingâ€•Model. Chemistry of Materials, 2022, 34, 9915-9922.	3.2	4
8034	Structure, electronic, optical and elastic properties of (NH4)2BeF4 crystal in paraelectric phase. Current Applied Physics, 2023, 45, 76-85.	1.1	3
8035	Li₂PbB₂O₅: A Pyroborate with Large Birefringence Induced by the Synergistic Effect of Stereochemical Active Lone Pair Cations and Ï€-Conjugated [B₂O₅] Groups. Inorganic Chemistry, 2022, 61, 18795-18801.	1.9	7
8036	Sub-micron grains and excellent mechanical properties of low-density Ti40Nb30Mo30-C refractory complex concentrated alloy reinforced with in-situ (Ti, Nb)C. Materials Science & Engineering A: Structural Materials: Properties, Microstructure and Processing, 2022, 860, 144335.	2.6	3
8037	Electron induced efficient dechlorination of trichlorethylene with S doped Fe2B: The enhancement mechanism of S. Environment International, 2022, 170, 107619.	4.8	4
8038	Two-dimensional hydrogenated/fluorinated graphyne/graphyne-like BN van der Waals heterostructures and their potential application in ultraviolet photodetection: a theoretical prediction. Applied Surface Science, 2022, , 155739.	3.1	0

#	Article	IF	Citations
8039	Group 14 elements in the Cmcm phase with a direct band structure for photoelectric application. Physica Scripta, 2023, 98, 015701.	1.2	11
8040	Growth, Structure, and Optical Properties of a Nonlinear Optical Niobium Borate Crystal CsNbOB₂O₅ with Distorted NbO₅ Square Pyramids. Inorganic Chemistry, 2022, 61, 19302-19308.	1.9	6
8041	Effect of Si on the oxidation behaviors of Ti3Al1â^'xSixC2 at 1000 Â°C. Chemistry - A European Journal, 0, , .	1.7	0
8042	Cellulose hydrogen bond detection using terahertz time-domain spectroscopy to indicate deterioration of oilâ€“paper insulation. Cellulose, 2023, 30, 727-740.	2.4	3
8043	Towards In Silico Mining for Superconductors â€“ Cutting the Gordian Knot. Physica C: Superconductivity and Its Applications, 2022, , 1354187.	0.6	0
8044	AIn₃Si₄P₉ (A = Ca, Sr): quaternary phosphides with double-helix structures exhibiting high laser-induced damage thresholds. Inorganic Chemistry Frontiers, 2023, 10, 1112-1118.	3.0	3
8045	First-principle study on the effect of point defects on the mechanical properties, thermal conductivity, and optical properties of wurtzite AlN. Vacuum, 2023, 207, 111694.	1.6	3
8046	Effect of alloying on the phase stability and elastic properties of L1₂ Cu₃Pt crystal structure. MATEC Web of Conferences, 2022, 370, 02002.	0.1	0
8047	High-pressure synthesis and crystal structures of molybdenum nitride Mo₃N₅ with anisotropic compressibility by a nitrogen dimer. Dalton Transactions, 2023, 52, 469-475.	1.6	4
8048	Improving the intrinsic conductivity of Î´-MnO₂ by indium doping for high-performance neutral aqueous sodium-ion supercapacitors with commercial-level mass-loading. Journal of Materials Chemistry A, 2023, 11, 2133-2144.	5.2	8
8049	The formation and stability of fluoxetine HCl cocrystals investigated by multicomponent milling. CrystEngComm, 2023, 25, 213-224.	1.3	3
8050	Halogenation as a Novel Scheme for Enhanced Photocatalytic Activity in AlSb Monolayer: A First-Principles Study. Catalysis Science and Technology, 0, , .	2.1	0
8051	Identification of structural changes in CaCu₃Ti₄O₁₂ on high energy ball milling and their effect on photocatalytic performance. Catalysis Science and Technology, 2023, 13, 1041-1058.	2.1	2
8052	Modelling amorphous materials via a joint solid-state NMR and X-ray absorption spectroscopy and DFT approach: application to alumina. Chemical Science, 2023, 14, 1155-1167.	3.7	5
8053	An orthorhombic carbon allotrope with a quasi-direct band gap and superhard. Diamond and Related Materials, 2023, 131, 109592.	1.8	15
8054	Cd(NH₂SO₃)₂Â·xH₂O (x= 0, 2): new sulfamates with a unique coordination environment and reversible phase transitions. Inorganic Chemistry Frontiers, 2023, 10, 1411-1420.	3.0	6
8055	Hot corrosion behavior of network structured TiBw/TA15 composite with Na2SO4 film at 800ÂÂ°C. Materials Characterization, 2023, 195, 112499.	1.9	3
8056	Physical properties of BaRu2X2 (XÂ=ÂP, As) superconducting compound sunder pressure effects: Ab initio study. Physica C: Superconductivity and Its Applications, 2023, 604, 1354176.	0.6	1

#	Article	IF	Citations
8057	Anomalous thermal expansion of strontium squarate trihydrate induced by hydrogen-bond weakening. Inorganic Chemistry Frontiers, 2023, 10, 552-557.	3.0	1
8058	Structural stability and lithium storage property of Sn clusters (xÂâ‰Â6) deposited on graphene based on first-principles calculation. Diamond and Related Materials, 2023, 131, 109567.	1.8	0
8059	First-principles calculations to investigate elastic, electronic, optical and thermodynamic properties of Pt3X (Xâ€¯=â€¯Ti, Cu). Results in Physics, 2023, 44, 106141.	2.0	7
8060	Improved first-principles electronic band structure for cubic (Pm <mml:math) Tj ETQq1 1 0.784314 rgBT /Overlock 10 Tf 50 642 Td (xml 111913	1.4	12
8061	Synthesis of platinum nanoparticles on strontium titanate nanocuboidsviasurface organometallic grafting for the catalytic hydrogenolysis of plastic waste. Journal of Materials Chemistry A, 2023, 11, 1216-1231.	5.2	10
8062	Nanoporous cyanuric acid nanosheets for semiconductors: Insights from chemical bonding. Chemical Physics Letters, 2023, 811, 140236.	1.2	0
8063	Two-dimensional silicether: A promising anode material for sodium-ion battery. Computational Materials Science, 2023, 218, 111920.	1.4	5
8064	Î³-P₄S₃I₂: a new metal-free infrared second-order nonlinear optical crystal designed by polymorphism strategy. Inorganic Chemistry Frontiers, 2023, 10, 1119-1126.	3.0	9
8065	NiFeO H with electron-deficient Ni2+ for oxygen evolution in mild media. Journal of Power Sources, 2023, 556, 232444.	4.0	0
8066	Type-I/Type-II Transition of MoSe2/g-GaN van der Waals heterostructures mediated by biaxial strain and electric field for overall water splitting. Materials Science and Engineering B: Solid-State Materials for Advanced Technology, 2023, 288, 116195.	1.7	4
8067	Understanding the photocatalytic mechanisms of the BiOBr/BiOCl heterostructures: First-principles study. Physica B: Condensed Matter, 2023, 651, 414582.	1.3	4
8068	A combined experimental and computational approach on La0.6Sr0.4MnO3 perovskite. Materials Chemistry and Physics, 2023, 295, 127163.	2.0	1
8069	Enhanced charge carrier density of a p-n BiOCl/BiVO4 heterostructure by Ni doping for photoelectrochemical applications. Journal of Alloys and Compounds, 2023, 937, 168434.	2.8	7
8070	Synthesis, crystal structure and 19F NMR parameters modelling of CaTiF6(H2O)2 yielding to a revision of the bond-valence parameters for the Ti4+/Fâ¯ ion pair. Journal of Solid State Chemistry, 2023, 319, 123793.	1.4	1
8071	Terahertz spectroscopy for quantitatively elucidating the crystal transformation of chiral histidine enantiomers to racemic compounds. Food Chemistry, 2023, 406, 135043.	4.2	4
8072	Insights into the effects of Al-ion implantation temperature on material properties of 4H-SiC. Applied Surface Science, 2023, 613, 156014.	3.1	3
8073	First principles study on the influence of multi-element doping on the mechanical properties of Î¸/Al interface in Al-Cu alloy. Materials Today Communications, 2023, 34, 105114.	0.9	0
8074	Single pot selective conversion of furfural into 2-methylfuran over a Co-CoOx/AC bifunctional catalyst. Applied Surface Science, 2023, 612, 155871.	3.1	5

#	Article	IF	Citations
8075	Functional group inhomogeneity in graphene oxide using correlative absorption spectroscopy. Applied Surface Science, 2023, 613, 155885.	3.1	2
8076	Metallic boro-carbides of A₂BC (A = Ti, Zr, Hf and W): a comprehensive theoretical study for thermo-mechanical and optoelectronic applications. RSC Advances, 2022, 12, 32994-33007.	1.7	6
8077	Ab initio methods for the computation of physical properties and performance parameters of electrochemical energy storage devices. Physical Chemistry Chemical Physics, 2023, 25, 1476-1503.	1.3	3
8078	Structural and electronic properties of Î²-MnO₂ nanoclusters. MATEC Web of Conferences, 2022, 370, 09004.	0.1	0
8079	Terahertz Spectroscopic Analysis of Co-Crystallized Mixtures in an L-threonine Diastereomer System. Spectroscopy (Santa Monica), 2022, , 36-44.	0.3	0
8080	Reconstruction of Cooperite (PtS) Surfaces: A DFT-D+U Study. ACS Omega, 2022, 7, 43390-43410.	1.6	4
8081	High-strength, self-initiated, wide pH range of underwater adhesive suitable for different severe environments. Chemical Engineering Journal, 2023, 455, 140640.	6.6	10
8082	Equiatomic binary phases of Copperâ€Rare Earth Elements. An overview of monocuprides from firstâ€principles calculations. ChemPhysChem, 2023, 24, .	1.0	1
8083	Reducing the Carbon Footprint of Air-Blown Bitumen Using Physisorption. ACS Sustainable Chemistry and Engineering, 2022, 10, 15767-15776.	3.2	0
8084	Computational Screening and Experimental Validation on Multicomponent Crystals of a New Class of Janus Kinase (JAK) Inhibitor Drug with Improved Solubility. Crystals, 2022, 12, 1722.	1.0	0
8085	Fast light-switchable polymeric carbon nitride membranes for tunable gas separation. Nature Communications, 2022, 13, .	5.8	12
8086	AeMg₆Ga₆S₁₆ (Ae = Ca, Sr, Ba): The First Double Alkalineâ€Earth Metal Chalcogenides with Excellent Performances. Advanced Optical Materials, 2023, 11, .	3.6	8
8087	A Comparative View of Alkaline and Alkaline-Earth Element Intercalation into Perovskite-Type A_xLa_yTiO₃ (A = Li, Na, or Mg) Based on Theoretical Calculations and Experiments. ACS Applied Energy Materials, 2022, 5, 15749-15757.	2.5	6
8088	Energy Level, Crystal Morphology and Fluorescence Emission Tuning in Cocrystals via Molecularâ€Level Engineering. Chemistry - A European Journal, 2023, 29, .	1.7	3
8089	Experimental and Theoretical Study of Ultra-Hard AlMgB14-TiB2 Composites: Structure, Hardness and Self-Lubricity. Materials, 2022, 15, 8450.	1.3	2
8090	Exploring the Optimal Alloy for Nitrogen Activation by Combining Bayesian Optimization with Density Functional Theory Calculations. ACS Omega, 2022, 7, 45403-45408.	1.6	4
8091	High-refractive index and mechanically cleavable non-van der Waals InGaS3. Npj 2D Materials and Applications, 2022, 6, .	3.9	9
8092	Experimental investigation and thermodynamic assessment of Laâ€“Yâ€“Ni ternary system in Ni-rich corner. Rare Metals, 0, , .	3.6	1

#	Article	IF	Citations
8093	Euphonic: inelastic neutron scattering simulations from force constants and visualization tools for phonon properties. Journal of Applied Crystallography, 2022, 55, 1689-1703.	1.9	5
8094	From Ba₃Nb₂O₂F₁₂(H₂O)₂ to Ba_{0.5}NbO₂F₂(H₂O): Achieving Balanced Nonlinear Optical Performance by O/F Ratio Regulation. Inorganic Chemistry, 2022, 61, 20709-20715.	1.9	7
8095	Effect of potential difference between nano-Al2O3 whisker and Mg matrix on the dispersion of Mg composites. International Journal of Minerals, Metallurgy and Materials, 2023, 30, 104-111.	2.4	1
8096	Selective and rapid extraction of trace amount of gold from complex liquids with silver(I)-organic frameworks. Nature Communications, 2022, 13, .	5.8	31
8097	Explorations of Second-Order Nonlinear Optical Materials in the Monovalent Trithiocyanurate System. Crystal Growth and Design, 2023, 23, 362-368.	1.4	2
8098	Ab initio study of pressure dependence of the structural, elastic and thermodynamic properties of AlXY₃ (Xâ€‰=â€‰B, C). Phase Transitions, 2023, 96, 1-15.	0.6	3
8099	An ab-initio perspective on the electronic and optical characteristics of MoSe2 nanosheet: Role of external electric field. Physica B: Condensed Matter, 2023, 651, 414574.	1.3	0
8100	Density Functional Simulation Study of Surface Wettability of Coal Molecules with Different Degrees of Defects. ACS Omega, 2022, 7, 47031-47039.	1.6	1
8101	Effects of Multiple Local Environments on Electron Energy Loss Spectra of Epitaxial Perovskite Interfaces. Journal of Physical Chemistry C, 2022, 126, 21453-21466.	1.5	0
8102	Benchmark accuracy of predicted NMR observables for quadrupolar ¹⁴N and ¹⁷O nuclei in molecular crystals. Magnetic Resonance in Chemistry, 2023, 61, 253-267.	1.1	4
8103	The Antiperovskiteâ€Type Oxychalcogenides Ae₃Q[GeOQ₃] (Ae = Ba, Sr; Q = S, Se) with Large Second Harmonic Generation Responses and Wide Band Gaps. Advanced Science, 2023, 10, .	5.6	23
8104	A combined solid-state NMR and quantum chemical calculation study of hydrogen bonding in two forms of Î±-d-glucose. Solid State Nuclear Magnetic Resonance, 2023, 123, 101848.	1.5	2
8105	First-Principles Investigation of Adsorption Behaviors and Electronic, Optical, and Gas-Sensing Properties of Pure and Pd-Decorated GeS₂ Monolayers. ACS Omega, 2022, 7, 46440-46451.	1.6	7
8106	On the photovoltaic effect asymmetry in ferroelectrics. Journal of Physics Condensed Matter, 2023, 35, 094001.	0.7	3
8107	Schwarz <scp>P</scp>â€surface via isolated <scp>sp²</scp> carbon heptagons: Design and properties. Journal of Computational Chemistry, 2023, 44, 954-961.	1.5	1
8108	The Rise of 212 MAX Phase Borides: DFT Insights into the Physical Properties of Ti₂PB₂, Zr₂PbB₂, and Nb₂AB₂ [A = P, S] for Thermomechanical Applications. ACS Omega, 2023, 8, 954-968.	1.6	9
8109	Biaxial strain and electrical field's effects on the structural, electronic, magnetic, and optical properties of monolayer CrTe. Physics Letters, Section A: General, Atomic and Solid State Physics, 2023, 458, 128594.	0.9	0
8110	Origin and Regulation of Selfâ€Discharge in MXene Supercapacitors. Advanced Functional Materials, 2023, 33, .	7.8	42

#	Article	IF	Citations
8111	A Crystalline Dimeric Steroidal Diboronate with Electronically Impeded Rotation. Journal of Organic Chemistry, 0, , .	1.7	2
8112	Revealing carbon capture chemistry with 17-oxygen NMR spectroscopy. Nature Communications, 2022, 13, .	5.8	4
8113	Influence of pressure-induced formation of dihydrogen bonds on lattice parameters, volume, and vibrational modes of ammonia borane. Journal of Chemical Physics, 2022, 157, .	1.2	2
8114	ShakeNBreak: Navigating the defect configurational landscape. Journal of Open Source Software, 2022, 7, 4817.	2.0	11
8115	Influence of High Pressure on the Pedal-like Motion and Photoreactivity in the Cocrystals of 1,2-Di(4-pyridyl)ethylene with trans-2-(4-Fluorophenyl)vinylboronic Acid. Crystal Growth and Design, 2023, 23, 246-255.	1.4	0
8116	Additive WO2 promotes Ni - based catalyst for hydrogen production from auto-thermal reforming of acetic acid. Fuel, 2023, 339, 126914.	3.4	4
8117	RbClÂ·(H₂SeO₃)₂: A Salt-Inclusion Selenite Featuring Short UV Cut-Off Edge and Large Birefringence. Inorganic Chemistry, 2023, 62, 557-564.	1.9	6
8118	Unexpected Factors Affecting the Kinetics of Guest Molecule Release from Investigation of Binary Chemical Systems Trapped in a Single Void of Mesoporous Silica Particles. ChemPhysChem, 2023, 24, .	1.0	2
8119	Dense Structure of Yttrium Nitride as a Post-Rock-Salt Phase: High-Pressure Experiments and Computations. Inorganic Chemistry, 2022, 61, 20906-20912.	1.9	1
8120	Trade-Off for Better Balanced Nonlinear Optical Performance with Disordered Si in ZnGeP₂. Chemistry of Materials, 2022, 34, 11007-11013.	3.2	3
8121	LiNaB₆O₉F₂: A Promising UV NLO Crystal Having Fluorineâ€Directed Optimal Performances and Double Interpenetrating ³[B₆O₉F₂]_{âˆž} Networks. Advanced Optical Materials, 2023, 11, .	3.6	11
8122	Illustrating the Key Role of Hydrogen Bonds in Fabricating Pure-Phase Two-Dimensional Perovskites. Journal of Physical Chemistry C, 2022, 126, 21857-21863.	1.5	0
8123	DFT Simulation-Based Design of 1T-MoS2 Cathode Hosts for Li-S Batteries and Experimental Evaluation. International Journal of Molecular Sciences, 2022, 23, 15608.	1.8	7
8124	First-principles investigation of TiC(001)/TiAl(100) interface: atomic structure, stability and electronic property. Journal of Materials Science, 2022, 57, 21339-21351.	1.7	3
8125	First-principles calculations to investigate adhesion strength, stability and electronic properties of Al(111)/TiAl3(112) interface. Indian Journal of Physics, 2023, 97, 1679-1685.	0.9	1
8126	From PEF to PBF: What difference does the longer alkyl chain make a computational spectroscopy study of poly(butylene 2,5-furandicarboxylate). Frontiers in Chemistry, 0, 10, .	1.8	4
8127	Enabling Efficient Photocatalytic Hydrogen Evolution via In Situ Loading of Ni Single Atomic Sites on Red Phosphorus Quantum Dots. Advanced Functional Materials, 2023, 33, .	7.8	7
8128	Ultrahigh Content Boron and Nitrogen Codoped Hierarchically Porous Carbon Obtained from Biomass Byproduct Okara for Capacitive Deionization. ACS Omega, 2022, 7, 48282-48290.	1.6	9

#	Article	IF	Citations
8129	Tribological behavior analysis of interaction strengths between different interfaces. Diamond and Related Materials, 2022, , 109666.	1.8	1
8130	Effect of adding Nb foil on joint properties of laser fusion welding for TC4 titanium and 7075 aluminum alloy. Chinese Journal of Aeronautics, 2023, 36, 508-521.	2.8	2
8131	Uniaxial pressureâ€induced 2Dâ€1D dimensionality change in GaSe and related materials. Physica Status Solidi - Rapid Research Letters, 0, , .	1.2	0
8132	Ternary superconducting hydrides stabilized via Th and Ce elements at mild pressures. Fundamental Research, 2022, , .	1.6	5
8133	Structure and Phase Composition of Natural Magnesite in 1173â€“6500 K Temperature Range. Russian Physics Journal, 2022, 65, 1142-1148.	0.2	1
8134	CRYSTAL23: A Program for Computational Solid State Physics and Chemistry. Journal of Chemical Theory and Computation, 2023, 19, 6891-6932.	2.3	43
8135	Clamping effect driven design and fabrication of new infrared birefringent materials with large optical anisotropy. Science China Chemistry, 2023, 66, 1086-1093.	4.2	13
8136	Olivineâ€Type MgMn_{0.5}Zn_{0.5}SiO₄ Cathode for Mgâ€Batteries: Experimental Studies and First Principles Calculations. Small, 2023, 19, .	5.2	6
8137	Metallic to half-metallic transition driven by pressure and anion composition in niobium oxyfluoride. Journal of Materials Chemistry C, 2023, 11, 1791-1797.	2.7	1
8138	Novel Janus 2D structures of XMoY (X, Y = O, S, Se, Te) composition for solar hydrogen production. International Journal of Hydrogen Energy, 2023, 48, 14226-14237.	3.8	5
8139	First-Principles Calculations with Six Structures of Alkaline Earth Metal Cyanide A(CN)₂ (A = Be, Mg, Ca, Sr, and Ba): Structural, Electrical, and Phonon Properties. ACS Omega, 0, , .	1.6	1
8140	Energy harvesting using two-dimensional (2D) d-silicates from abundant natural minerals. Journal of Materials Chemistry C, 2023, 11, 2098-2106.	2.7	8
8141	A Cation-Driven Approach toward Deep-Ultraviolet Nonlinear Optical Materials. Research, 2023, 6, .	2.8	5
8142	The Halogen Bond in Weakly Bonded Complexes and the Consequences for Aromaticity and Spin-Orbit Coupling. Molecules, 2023, 28, 772.	1.7	13
8143	Halogen-Doped Chevrel Phase Janus Monolayers for Photocatalytic Water Splitting. Nanomaterials, 2023, 13, 368.	1.9	1
8144	Low-Dimensional Metalâ€“Organic Magnets as a Route toward the S = 2 Haldane Phase. Journal of the American Chemical Society, 2023, 145, 1783-1792.	6.6	2
8145	Chlorination of Hydrogenated Silicon Nanosheets Revealed by Solid-State Nuclear Magnetic Resonance Spectroscopy. Chemistry of Materials, 2023, 35, 539-548.	3.2	3
8146	Mechanism of Selective Chlorination of Fe from Fe2SiO4 and FeV2O4 Based on Density Functional Theory. Metals, 2023, 13, 139.	1.0	1

#	Article	IF	Citations
8147	A first-principles study of the electronic, mechanical, vibrational, and optical properties of the zirconium carbide under high pressure. Physica Scripta, 2023, 98, 025817.	1.2	4
8148	<mml:math xmlns:mml="http://www.w3.org/1998/Math/MathML"><mml:mi>Î¼</mml:mi><mml:mi mathvariant="normal">SR</mml:mi></mml:math> investigation of magnetism in <mml:math xmlns:mml="http://www.w3.org/1998/Math/MathML"><mml:mi>Î²</mml:mi><mml:mtext>â€™</mml:mtext><mml:mrow><mml:msub><mml:mi></mml:mi></mml:msub></mml:mrow></mml:math> : Antiferromagnetism. Physical Review Research, 2023, 5, .	1.3	1
8149	Brillouin Scattering Study of Electro-Optic KTa1â€'xNbxO3 Crystals. Materials, 2023, 16, 652.	1.3	2
8150	First principles computation of insulatorâ€“semiconductorâ€“metal transition and its impact on structural, elastic, mechanical, anisotropic and optical properties of CsSrF₃ under systematic static isotropic pressure. Molecular Simulation, 2023, 49, 453-471.	0.9	2
8151	CuGaO₂/TiO₂ heterostructure nanosheets: Synthesis, enhanced photocatalytic performance, and underlying mechanism. Journal of the American Ceramic Society, 2023, 106, 3009-3023.	1.9	4
8152	Study on Room-Temperature Wet Oxidation of Silicon Catalyzed by Copper. Langmuir, 2023, 39, 750-755.	1.6	1
8153	Rational Design of the First Ammonium Magnesium Borate with Deep-Ultraviolet Cutoff Edge and Moderate Birefringence and Further Investigation into the Nature of Ammonium in the Borate System. Inorganic Chemistry, 2023, 62, 1697-1707.	1.9	5
8154	Discerning subtle high-pressure phase transitions in glyphosate. CrystEngComm, 0, , .	1.3	0
8155	Insights into the physical properties of newly synthesized AMn2P2 (A= Ca, Sr) via density functional theory. Physica B: Condensed Matter, 2023, 653, 414651.	1.3	1
8156	Mechanical and optoelectronic properties of ternary telluride NbFeTe2: A DFT approach. Computational Condensed Matter, 2023, , e00788.	0.9	2
8157	Raman- and Infrared-Active Phonons in Nonlinear Semiconductor AgGaGeS4. Crystals, 2023, 13, 148.	1.0	2
8158	Interface Engineering Enables High-Performance Sb Anode for Sodium Storage. Nanomaterials, 2023, 13, 254.	1.9	19
8159	First principle comparative study of transitional elements Co, Rh, Ir(III)-based double halide perovskites. Materials Today Communications, 2023, 34, 105431.	0.9	4
8160	Reaction Mechanisms and Kinetics of Nanozymes: Insights from Theory and Computation. Advanced Materials, 2024, 36, .	11.1	28
8161	Nuclear quantum dynamics in Hexamethylenetetramine and its deuterated counterpart: a DFT-augmented neutron study. Physica Scripta, 2023, 98, 025707.	1.2	2
8162	Synthesis, characterization, computational studies, and photocatalytic properties of Cu doped Bi2S3 nanorods. Materials Today Communications, 2023, 34, 105418.	0.9	0
8163	Electron energy loss spectroscopy of K0.7Fe1.7Se2 superconductor. EPJ Applied Physics, 0, , .	0.3	0
8164	The element occupation preference of Î¼ phase in ternary Ni-Cr-Mo model superalloy. Materials and Design, 2023, 225, 111569.	3.3	2

#	Article	IF	Citations
8165	Li/Na atoms' substitution effects on the structural, electronic, and mechanical properties of the CaSnO3 perovskite for battery applications. Computational Materials Science, 2023, 219, 112006.	1.4	4
8166	First-principles study on stability, electronic and mechanical properties of 4^3T175 carbon allotrope. Computational Materials Science, 2023, 219, 111956.	1.4	1
8167	High-entropy alloy metallene for highly efficient overall water splitting in acidic media. Chinese Journal of Catalysis, 2023, 45, 174-183.	6.9	14
8168	Effect of Mg-doping on the hydration reactivity of polycrystalline dicalcium silicate: A study explored by DFT simulation. Construction and Building Materials, 2023, 366, 130122.	3.2	3
8169	Terminal-dependent ion recognition of BiOBr/PPy hybrid film with befitting absorption function for rapidly selective bromine ions removal. Chemical Engineering Journal, 2023, 457, 141213.	6.6	3
8170	Computational study of Be doped LaAlO3 perovskite. Physica B: Condensed Matter, 2023, 652, 414631.	1.3	0
8171	Effects of Sm and VZn in different valence states on the magnetic property, carrier lifetime, electric dipole moment, visible light, and redox reaction of ZnO:Hi under biaxial strain. Materials Chemistry and Physics, 2023, 297, 127362.	2.0	1
8172	Mechanism of Pt3Co nanocatalysts to improve the performance for oxygen reduction reactions: DFT study on oxygen adsorption and durability of different facets. Materials Science and Engineering B: Solid-State Materials for Advanced Technology, 2023, 289, 116202.	1.7	0
8173	Experimental and computational studies on the formation of mixed amide-hydride solid solutions for CsNH2â€“CsH system. Results in Engineering, 2023, 17, 100895.	2.2	1
8174	Investigation of the crystal structure, electronic and optical properties of Cr-doped BaTiO3 on the Ti site using first principles calculations. Journal of Physics and Chemistry of Solids, 2023, 175, 111209.	1.9	10
8175	Density Functional Theory Study on the Adsorption of Fe(OH)2+ on Kaolinite Surface in Water Environment. Processes, 2023, 11, 38.	1.3	0
8176	Lowâ€Coordination Trimetallic PtFeCo Nanosaws for Practical Fuel Cells. Advanced Materials, 2023, 35, .	11.1	18
8177	First-Principles Calculations to Investigate Direct-Band Novel Cobalt-Based Double Perovskite Materials for Optoelectronic Applications. Energy & Fuels, 2023, 37, 1266-1274.	2.5	3
8178	Electronic structure, elastic and thermodynamic properties of SnS from theoretical study. , 2022, 19, 927-938.		0
8179	Structural, elastic, optical and thermodynamic properties of CdGeP2 from theoretical prediction. , 2022, 18, 781-796.		0
8180	Dynamic Diastereomerism on Chiral Surfaces. Journal of Physical Chemistry C, 2023, 127, 229-233.	1.5	1
8181	Towards hydrogen-rich ionic (NH₄)(BH₃NH₂BH₂NH₂BH₃) and related molecular NH₃BH₂NH₂BH₂NH₂BH₃. Dalton Transactions, 0, , .	1.6	2
8182	Optical and structural properties of 2D transition metal dichalcogenides semiconductor MoS2. Bulletin of Materials Science, 2023, 46, .	0.8	6

#	Article	IF	Citations
8183	Internal electric field enhanced photoelectrochemical water splitting in direct Z-scheme GeC/HfS2 heterostructure: A first-principles study. Applied Physics Letters, 2023, 122, .	1.5	13
8184	Atomic mean square displacement study of the bond breaking mechanism of energetic materials before explosive initiation. Physical Chemistry Chemical Physics, 2023, 25, 5613-5618.	1.3	4
8185	An effective pathway to design and synthesize UV birefringent crystalsviarational assembly of Ï€-conjugated [CO₃]^{2â¯}and [NO₃]^{â¯}triangles. Journal of Materials Chemistry C, 2023, 11, 3325-3333.	2.7	4
8186	Î²-(C₃H₇N₆)₂Cl₂Â·H₂O and (C₃H₇N₆)FÂ·H₂O: two UV birefringent crystals induced by uniformly aligned structural groups. Inorganic Chemistry Frontiers, 2023, 10, 2022-2029.	3.0	1
8187	Effect of heteroatom in conductive polymer coating of cathode materials on electrochemical performance of lithium sulfur batteries. Ionics, 2023, 29, 1019-1028.	1.2	4
8188	C(NH₂)₃(I₃O₈)(HI₃O₈)(H₂I₂C An Unprecedented Asymmetric Guanidinium Polyiodate with a Strong Second-Harmonic-Generation Response and a Wide Band Gap. Inorganic Chemistry, 2023, 62, 1323-1327.	1.9	7
8189	Tautomerism of Î²-Diketones and Î²-Thioxoketones. Encyclopedia, 2023, 3, 182-201.	2.4	0
8190	Magnetic Transition State Searching: Beyond the Static Ion Approximation. Magnetochemistry, 2023, 9, 42.	1.0	4
8191	Triggering the mechanism of the initial reaction of energetic materials under pressure based on Raman intensity analysis. Physical Chemistry Chemical Physics, 2023, 25, 5685-5693.	1.3	4
8192	A hybrid halide lead-free pseudo-perovskite with large birefringence. Inorganic Chemistry Frontiers, 2023, 10, 2039-2044.	3.0	6
8193	Effects of pressure on structural, electronic, optical, and mechanical properties of nitrogen-rich energetic material: 6-azido-8-nitrotetrazolo[1,5-b]pyridazine-7-amine (3at). Journal of Molecular Modeling, 2023, 29, .	0.8	0
8194	Two non-centrosymmetric mixed alkali metal and alkaline earth metal scandium borate nonlinear optical materials with short ultraviolet cutoff edges. Dalton Transactions, 2023, 52, 3344-3350.	1.6	5
8195	Single-Layer MoS2: A Two-Dimensional Material with Negative Poissonâ€™s Ratio. Coatings, 2023, 13, 283.	1.2	4
8196	Ab initio studies of the gas adsorption on the surface CdSe1â€“xSx ultra-thin films. Applied Nanoscience (Switzerland), 0, , .	1.6	0
8197	Crystallite Size Dependent Superparamagnetic Properties of Gold Doped Reduced Graphene Oxide Nanocomposite: An Experimental and Density Functional Theory Study. Journal of Inorganic and Organometallic Polymers and Materials, 2023, 33, 810-819.	1.9	2
8198	Tuning the optical properties of the metalâ€“organic framework UiO-66 via ligand functionalization. Physical Chemistry Chemical Physics, 2023, 25, 6333-6341.	1.3	5
8199	CO2 adsorption enhancement and charge transfer characteristics for composite graphene doped with atoms at defect sites. Journal of Molecular Modeling, 2023, 29, .	0.8	1
8200	Highly Nonstoichiometric YAG Ceramics with Modified Luminescence Properties. Advanced Functional Materials, 2023, 33, .	7.8	3

#	Article	IF	Citations
8201	RKKY Interaction in Spin Valve Structure with LaAlO₃ Spacer. Materials Science Forum, 0, 1080, 131-137.	0.3	1
8202	Tuning the Local Coordination of CoP_{1â€“x}S_x between NiAs- and MnP-Type Structures to Catalyze Lithiumâ€“Sulfur Batteries. ACS Nano, 2023, 17, 3143-3152.	7.3	19
8203	Structures of elemental potassium at terapascal pressures. Physical Review B, 2023, 107, .	1.1	1
8204	Effect of Varying Stiffness and Functionalization on the Interfacial Failure Behavior of Isotactic Polypropylene on Hydroxylated Î³-Al₂O₃ by MD Simulation. ACS Applied Materials & Interfaces, 2023, 15, 6133-6141.	4.0	0
8205	Ethanol Solvent Used in Constructing Ultra-Low-Temperature Zinc-Ion Capacitors with a Long Cycling Life. ACS Applied Materials & Interfaces, 2023, 15, 5180-5190.	4.0	7
8206	Preparing La-Doped LiAl₅O₈ from the Electrode Materials of Waste Lithium-Ion Batteries. ACS Sustainable Chemistry and Engineering, 2023, 11, 1386-1393.	3.2	0
8207	Revisiting the electronic and optical properties of SiO2 polymorphs by hybrid functional calculations. Journal of Applied Physics, 2023, 133, .	1.1	0
8208	Topological Impact of Delocalization on the Stability and Band Gap of Partially Oxidized Graphene. ACS Omega, 2023, 8, 5124-5135.	1.6	5
8209	A family of CuI-based 1D polymers showing colorful short-lived TADF and phosphorescence induced by photo- and X-ray irradiation. Dalton Transactions, 2023, 52, 4017-4027.	1.6	6
8210	Unexpected giant negative area compressibility in palladium diselenide. National Science Review, 2023, 10, .	4.6	3
8211	Characterizing Moleculeâ€“Metal Surface Chemistry with Ab Initio Simulation of X-ray Absorption and Photoemission Spectra. Journal of Physical Chemistry C, 2023, 127, 1870-1880.	1.5	2
8212	Structure and Characterization of K₂Na₃B₂P₃O₁₃, a New Nonlinear Optical Borophosphate with One-Dimensional Chain Structure and Short Ultraviolet Cutoff Edge. Inorganic Chemistry, 2023, 62, 2480-2488.	1.9	2
8213	Experimentally Validated Ab Initio Crystal Structure Prediction of Novel Metalâ€“Organic Framework Materials. Journal of the American Chemical Society, 2023, 145, 3515-3525.	6.6	3
8214	Highly soluble copper(<scp>i</scp>) iodide-based hybrid luminescent semiconductors containing molecular and one-dimensional coordinated anionic inorganic motifs. Journal of Materials Chemistry C, 2023, 11, 3086-3094.	2.7	4
8215	Photo-assisted thermal catalysis for methanol synthesis from methane oxidation on Cu-MOR/g-C3N4. Fuel, 2023, 340, 127525.	3.4	3
8216	Identification and low-frequency vibrational analysis of three free anthraquinones via terahertz spectroscopy. Spectrochimica Acta - Part A: Molecular and Biomolecular Spectroscopy, 2023, 293, 122439.	2.0	1
8217	Feature-rich electronic and magnetic properties in silicene monolayer induced by nitrogenation: A first-principles study. Chemical Physics, 2023, 568, 111844.	0.9	0
8218	Theoretical investigation of the structural, electronic, elastic and optical properties of the new layered ternary chalcogenide tetragonal compounds Cu2MX4 (M = W and Mo; X=S and Se). Journal of Solid State Chemistry, 2023, 321, 123880.	1.4	3

#	Article	IF	Citations
8219	LAVA 1.0: A general-purpose python toolkit for calculation of material properties with LAMMPS and VASP. Computer Physics Communications, 2023, 286, 108667.	3.0	4
8220	[illegible] properties of the Hf<mml:math xmlns:mml="http://www.w3.org/1998/Math/MathML" altimg="si98.svg" display="inline" id="d1e2137"><mml:msub><mml:mrow /><mml:mrow><mml:mn>2</mml:mn></mml:mrow></mml:msub></mml:math>Ge<mml:math xmlns:mml="http://www.w3.org/1998/Math/MathML" altimg="si99.svg" display="inline"		

#	Article	IF	Citations
8237	Structure, electronic and optical properties of B single- and double-doped graphene. Materials Science and Engineering B: Solid-State Materials for Advanced Technology, 2023, 290, 116336.	1.7	2
8238	Discovery of novel low modulus Nbâ€“Tiâ€“Zr biomedical alloys via combined machine learning and first principles approach. Materials Chemistry and Physics, 2023, 299, 127537.	2.0	5
8239	Tailoring the Electronic Structure of Ir Alloy Electrocatalysts through Lanthanide (La, Ce, Pr, and) Tj ETQq0 0 0 rgBT /Overlock 10 Tf 50 6	2.8	3
8240	Theoretical design of MoxW1â^'xS2/graphene heterojunction with adjustable band gap: potential candidate materials for next generation of optoelectronic devices. ChemPhysChem, 0, , .	1.0	0
8241	Phase transition and non-monotonic change in bandgap of Ca3N2 under pressure. Physica B: Condensed Matter, 2023, 660, 414883.	1.3	2
8242	Solution combustion synthesis of Mg-TiC@NiO nanocomposite and investigation on its metallurgical and biological properties. Journal of Molecular Liquids, 2023, 376, 121487.	2.3	1
8243	Interfacial Chemistry in the Electrocatalytic Hydrogenation of CO₂ over C-Supported Cu-Based Systems. ACS Catalysis, 2023, 13, 5876-5895.	5.5	3
8244	Amorphous <scp> BaTiO ₃ </scp> Electron Transport Layer for Thermal <scp> Equilibriumâ€Governed Î³â€CsPbI ₃ </scp> Perovskite Solar Cell with High Power Conversion Efficiency of 19.96%. Energy and Environmental Materials, 0, , .	7.3	1
8245	Mechanocatalysis: Simple and Rapid Mechanochemical Synthesis of Ammonia in Hydrogen, Nitrogen, and Water System. ChemCatChem, 2023, 15, .	1.8	1
8246	An Insight towards the Design of a Ruthenium-Containing Biomaterial. , 0, , .		0
8247	Experimental and theoretical characterization of Dy-doped hydroxyapatites. Journal of the Australian Ceramic Society, 2023, 59, 849-864.	1.1	3
8248	Phosphoric acid resistance PtCu/C oxygen reduction reaction electrocatalyst for HT-PEMFCs: A theoretical and experimental study. Applied Surface Science, 2023, 619, 156663.	3.1	7
8249	Determination of the relative orientation between 15N-1H dipolar coupling and 1H chemical shift anisotropy tensors under fast MAS solid-state NMR. Journal of Magnetic Resonance, 2023, 350, 107428.	1.2	1
8250	Four superhard tetragonal carbon allotropes: First-principles calculations. Diamond and Related Materials, 2023, 135, 109854.	1.8	7
8251	WOx nanowire supported ultra-fine Ir-IrOx nanocatalyst with compelling OER activity and durability. Chemical Engineering Journal, 2023, 464, 142613.	6.6	9
8252	Raman spectra and vibrational properties of FOX-7 under pressure and temperature: First-principles calculations. Spectrochimica Acta - Part A: Molecular and Biomolecular Spectroscopy, 2023, 293, 122489.	2.0	2
8253	Atomic-scale friction of black phosphorus/degraded Cu substrate: A route to robust superlubricity obtained by the critical load. Applied Surface Science, 2023, 619, 156749.	3.1	2
8254	Lithium-decorated SiB monolayer for reversible hydrogen storage: High-capacity realization through strain engineering. Applied Surface Science, 2023, 618, 156707.	3.1	9

#	Article	IF	Citations
8255	A new tetragonal superhard carbon allotrope with unusual stress-strain behavior. Solid State Communications, 2023, 366-367, 115153.	0.9	0
8256	A comparative study of cubic methylammonium lead iodide (CH3NH3PbI3) perovskite by using density functional theory. Materials Today Communications, 2023, 35, 105814.	0.9	1
8257	The mechanism of easier desorption of Fe atoms on the (1 0 0) surface of LiFePO4 and FePO4. Chemical Physics, 2023, 570, 111891.	0.9	1
8258	Properties of GdSF and phase diagram of the GdF3 - Gd2S3 system. Journal of Solid State Chemistry, 2023, 322, 123991.	1.4	3
8259	Structure and physical properties of predicted MAX phase V2SiC under pressure: A first principle calculation. Materials Today Communications, 2023, 35, 105907.	0.9	1
8260	Investigating the electronic, elastic, mechanical, anisotropic, and optical aspects of Sc2RuZ (Z: Al, Ga,) Tj ETQq1 1 0.784314 rgBT /Ov	1.3	2
8261	A theoretical benchmark for the electronic, optical, and thermoelectrical characteristics of bulk and monolayer BiS2. , 2023, 178, 207568.		2
8262	Synthesize, construction and enhanced performance of Bi2WO6/ZnS heterojunction under visible light: Experimental and DFT study. Arabian Journal of Chemistry, 2023, 16, 104760.	2.3	3
8263	Metal-free single atom catalysts towards efficient acetonitrile reduction to ethylamine. Applied Surface Science, 2023, 622, 156891.	3.1	1
8264	Boron-induced controlled synthesis of Co-nano particles over Bx(CN)y matrix for CO hydrogenation in aqueous media. Fuel Processing Technology, 2023, 244, 107719.	3.7	0
8265	Structural, mechanical and electronic properties of orthorhombic Nb2X4Si5 (X=V, Nb, Ta, Cr, Mo, W) compounds from first-principles calculations. Computational Condensed Matter, 2023, 35, e00792.	0.9	1
8266	Electronic and optical properties of Be, Ca, Ba and Eu adsorbed on Î²-Si3N4 (2 0 0) surface based on first-principles calculations. Materials Science in Semiconductor Processing, 2023, 160, 107406.	1.9	3
8267	Improved flotation of chalcopyrite from galena and pyrite by employing Cu-affinity phosphate collector. Minerals Engineering, 2023, 197, 108064.	1.8	10
8268	First-principles calculations to investigate structural, electronics, optical, and mechanical properties of Bi-based novel fluoroperovskites TBiF3 (T = Hg, Xe) for optoelectronic applications. Materials Science in Semiconductor Processing, 2023, 160, 107399.	1.9	13
8269	Unusual mechanical properties of CO2â€“V: Auxetic potential in a high-pressure polymorph of carbon dioxide. Journal of Physics and Chemistry of Solids, 2023, 178, 111349.	1.9	0
8270	Vanadium tunning amorphous iron phosphate encapsulated iron phosphide on phosphorous-doped graphene promoted oxygen reactions for flexible zinc air batteries. Applied Catalysis B: Environmental, 2023, 331, 122674.	10.8	11
8271	Low-temperature phase transitions and reorientational dynamics studied by 11B NMR in glassy crystal ortho-carborane. Journal of Non-Crystalline Solids: X, 2023, 18, 100180.	0.5	0
8272	High hydrogen production in two-dimensional GaTe/ZnI2 type-II heterostructure for water splitting. Journal of Physics and Chemistry of Solids, 2023, 178, 111317.	1.9	43

#	Article	IF	Citations
8273	Investigation of the structural, thermal, magnetic and cell viability properties of Ce/Sr co-doped hydroxyapatites. Journal of Molecular Structure, 2023, 1283, 135318.	1.8	7
8274	Recyclable Co3O4/NaF for hydrogen generation from ethyl acetate: The promoting effect between Co3O4 and NaF. Fuel, 2023, 343, 127942.	3.4	0
8275	The electronic, optical, and vibrational properties of Ag₃X (X = S, Se) with density functional theory. Modern Physics Letters B, 0, , .	1.0	0
8276	First-principles prediction of electronic, optical, and thermodynamic properties of c-TiAl3 with M doping (Mâ€‰=â€‰V, Nb, Ta). Indian Journal of Physics, 0, , .	0.9	0
8277	Comparison of adsorption capacity of water and hydroxide with collector reagents on geversite (PtSb2) mineral surface: A DFT-D insights. Computational Materials Science, 2023, 224, 112174.	1.4	3
8278	First-principles calculations to investigate Structural, Electronic, optical and mechanical properties of Cu-based fluoroperovskite XCuF3 (XÂ=ÂK, Ru). Computational and Theoretical Chemistry, 2023, 1224, 114115.	1.1	6
8279	The induced polarization enhanced birefringence in AlPS4 family: A first-principles investigation. Chemical Physics Letters, 2023, 822, 140496.	1.2	1
8280	Adsorption behaviors, electronic and gas-sensing properties of C3N4 monolayers and heterojunctions for SF6 decomposition products. Applied Surface Science, 2023, 626, 157090.	3.1	13
8281	Effect of dual improved electronic and cationic conductivity via W doping on cyclability and rate performance of LiNi0.90Co0.04Mn0.03Al0.03O2 cathode for rechargeable LiBs. Journal of Energy Storage, 2023, 63, 107088.	3.9	6
8282	Fabrication and characterization of PEG-In2O3 modified PbO2 anode for electrochemical degradation of metronidazole. Electrochimica Acta, 2023, 442, 141919.	2.6	1
8283	As <mml:math xmlns:mml="http://www.w3.org/1998/Math/MathML" altimg="si31.svg" display="inline" id="d1e1295"><mml:mi>K</mml:mi></mml:math>-edge absorption at high pressures in AFeAs (A=Na/Li): First principles results. Journal of Electron Spectroscopy and Related Phenomena, 2023, 263, 147286.	0.8	1
8284	A detailed experimental performance of 4-quinolone derivatives as corrosion inhibitors for mild steel in acid media combined with first-principles DFT simulations of bond breaking upon adsorption. Journal of Molecular Liquids, 2023, 375, 121299.	2.3	11
8285	First-Principles Microkinetic Modeling Unravelling the Performance of Edge-Decorated Nanocarbons for Hydrogen Production from Methane. ACS Applied Materials & Interfaces, 2023, 15, 6951-6962.	4.0	9
8286	Uniaxial Negative Thermal Expansion in an Orthorhombic Superconductor CoZr₃. Journal of the Physical Society of Japan, 2023, 92, .	0.7	2
8287	In-situ formation of onion-like carbon film by tribo-induced catalytic degradation of hydrocarbon: Effect of lubrication condition and load. Chemical Engineering Journal, 2023, 459, 141566.	6.6	7
8288	Chemisorption of Molybdenum Atom on Carbon Nanotube Using Density Functional Theory. Springer Proceedings in Materials, 2023, , 3-13.	0.1	0
8289	Computational investigation of Î±-SiO₂surfaces as a support for Pd. Physical Chemistry Chemical Physics, 2023, 25, 6121-6130.	1.3	2
8290	Structural, elastic, and electronic properties of BC12 carbon under pressure. Chemical Physics, 2023, 568, 111838.	0.9	3

#	Article	IF	Citations
8291	Compounds consisting of coplanar Ï€-conjugated B3O6-typed structures: An emerging source of ultraviolet nonlinear optical materials. , 2023, 42, 100019.		7
8292	DFT exploration of the electronic, optical, phonon and thermoelectrical performances of bulk and monolayered AuCN. Theoretical Chemistry Accounts, 2023, 142, .	0.5	2
8293	Layer-Dependent Nanowear of Graphene Oxide. ACS Nano, 2023, 17, 2497-2505.	7.3	4
8294	Halogenated and chalcogenated Ti2C MXenes: High capacity electrode materials for lithium-ion batteries. Chemical Physics Letters, 2023, 814, 140356.	1.2	3
8295	Determining Local Magnetic Susceptibility Tensors in Paramagnetic Lanthanide Crystalline Powders from Solid-State NMR Chemical Shift Anisotropies. Journal of Physical Chemistry A, 2023, 127, 1547-1554.	1.1	1
8296	Vibrational, thermodynamic and acoustic properties of AgAlS2 crystal. Physica B: Condensed Matter, 2023, 654, 414731.	1.3	0
8297	Electronic, mechanical, optical and thermodynamic properties of the quaternary semiconductors Sr3GeMgN4 and Ba3GeMgN4. Materials Science and Engineering B: Solid-State Materials for Advanced Technology, 2023, 290, 116292.	1.7	0
8298	Microporous melamine-formaldehyde networks loaded on rice husks for dynamic removal of organic micropollutants. Environmental Pollution, 2023, 322, 121200.	3.7	1
8299	Structural, Spectroscopic, Electric and Magnetic Properties of New Trigonal K5FeHf(MoO4)6 Orthomolybdate. Molecules, 2023, 28, 1629.	1.7	6
8300	Computational evaluation of halogen-bonded cocrystals enables prediction of their mechanochemical interconversion reactions. Chemical Science, 2023, 14, 3140-3146.	3.7	3
8301	Shortâ€Range Atomic Topology of Ab Initio Generated Amorphous PdSi Alloys. Advanced Theory and Simulations, 2023, 6, .	1.3	1
8302	Searching for Suitable Kojic Acid Coformers: From Cocrystals and Salt to Eutectics. Crystal Growth and Design, 2023, 23, 1874-1887.	1.4	1
8303	Thoriumâ€Ðoped Lithium Fluoride Single Crystal: A Potential Promising Candidate for Solid State Nuclear Optical Clock Materials. Advanced Optical Materials, 2023, 11, .	3.6	4
8304	Functionalization of Metalâ€“Organic Framework Nanochannels for Water Transport and Purification. ACS Applied Nano Materials, 2023, 6, 3003-3011.	2.4	3
8305	Solution-Processable Copper Halide Based Hybrid Materials Consisting of Cationic Ligands with Different Coordination Modes. Inorganic Chemistry, 2023, 62, 3660-3668.	1.9	3
8306	An extensive study on multiple ETL and HTL layers to design and simulation of high-performance lead-free CsSnCl3-based perovskite solar cells. Scientific Reports, 2023, 13, .	1.6	102
8307	Î±-BBO-like Ï€-Conjugated Crystal with Large Birefringence. Crystal Growth and Design, 2023, 23, 1330-1335.	1.4	2
8308	First-principles approach to the structural, electronic and intercalation voltage of Prussian blue (KxFe[Fe(CN)6]) (xâ€‰=â€‰1, 2) as potential cathode material for potassium ion batteries. Journal of Solid State Electrochemistry, 2023, 27, 1095-1106.	1.2	0

#	Article	IF	Citations
8309	Pseudopotential contributions to the quadrupole moment in charged periodic systems. Physical Review B, 2023, 107, .	1.1	0
8310	Study on low hydrostatic pressure-dependent optoelectronic, mechanical, and anisotropic properties of heavy thallium perovskites TlPbX3 (Xâ€‰=â€‰Cl, Br). Journal of Materials Research, 2023, 38, 2007-2017.	1.2	4
8311	In situ formation of cocatalytic sites boosts single-atom catalysts for nitrogen oxide reduction. Proceedings of the National Academy of Sciences of the United States of America, 2023, 120, .	3.3	7
8312	DFT insights into Nb-based 211 MAX phase carbides: Nb₂AC (A = Ga, Ge, Tl, Zn, P, In, and Cd). RSC Advances, 2023, 13, 5538-5556.	1.7	4
8313	Octahedral Distortion and Excitonic Behavior of Cs₃Bi₂Br₉ Halide Perovskite at Low Temperature. Journal of Physical Chemistry C, 2023, 127, 3523-3531.	1.5	2
8314	Hollow nanotube arrays of nickleâ€“cobalt metal sulfide for high energy density supercapacitors. RSC Advances, 2023, 13, 5557-5564.	1.7	8
8315	Elastic, electronic, optical, and thermodynamic properties of M₂SeC (M = Hf, Zr) under high pressure. AIP Advances, 2023, 13, 025154.	0.6	0
8316	Monolayer NbSe₂ Favors Ultralow Friction and Super Wear Resistance. Nano Letters, 2023, 23, 1865-1871.	4.5	4
8317	Composition Engineering Opens an Avenue Toward Efficient and Sustainable Nitrogen Fixation. Energy and Environmental Materials, 2024, 7, .	7.3	5
8318	Microwaveâ€Assisted Rapid Substitution of Ti for Zr to Produce Bimetallic (Zr/Ti)UiOâ€66â€NH₂ with Congenetic â€œShellâ€“Coreâ€•Structure for Enhancing Photocatalytic Removal of Nitric Oxide. Small, 2023, 19, .	5.2	9
8319	Phase Transitions, Mechanical and Dynamic Stability, and Electronic Properties of SnO Polymorphs under High Pressure. Physica Status Solidi (B): Basic Research, 2023, 260, .	0.7	1
8320	Formation of ibrutinib solvates: so similar, yet so different. IUCrJ, 2023, 10, 210-219.	1.0	1
8321	Facile synthesis of MgAl2O4 spinel matrix nanocomposite with TiC, AlTi3, and Al2O3 reinforcements by mechanical alloying. Journal of the Australian Ceramic Society, 2023, 59, 269-280.	1.1	1
8322	Regulation of the nature and sites of copper species in CuNaY zeolites for ethylene and ethane separation. New Journal of Chemistry, 2023, 47, 5650-5658.	1.4	0
8323	Structural and Spectroscopic Effects of Li+ Substitution for Na+ in LixNa1â^'xCaLa0.5Er0.05Yb0.45(MoO4)3 Upconversion Scheelite-Type Phosphors. Crystals, 2023, 13, 362.	1.0	7
8324	Study of Structural, optoelectronic and elastic properties of MAX phase of Ti2BrX (XÂ=ÂB, C and N) by density functional theory. Inorganic Chemistry Communication, 2023, 150, 110515.	1.8	1
8325	New insights about the intercalation of 5-Fluorouracil into 2D Mgâ€“Al layered double hydroxide nanosheets: A theoretical and experimental investigation. Journal of Drug Delivery Science and Technology, 2023, 81, 104294.	1.4	1
8326	Charge Density Evolution Governing Interfacial Friction. Journal of the American Chemical Society, 2023, 145, 5536-5544.	6.6	12

#	Article	IF	Citations
8327	Insertion of CO ₂ in metal ion-doped two-dimensional covalent organic frameworks. Proceedings of the National Academy of Sciences of the United States of America, 2023, 120, .	3.3	5
8328	Atomically dispersed indium and cerium sites for selectively electroreduction of CO2 to formate. Nano Research, 2023, 16, 8757-8764.	5.8	9
8329	Alignment of Î›-Shaped Basic Building Units to Construct One New KMoO₃(IO₃) Polar Polymorph. Inorganic Chemistry, 2023, 62, 3896-3903.	1.9	6
8330	Mechanistic Insight into Favorable Aldehyde Hydrogenation over Hydroxymethyl Hydrogenolysis in 5-Hydroxymethylfurfural by Formic Acid over Single-Atom Co-N₃/C. Journal of Physical Chemistry C, 2023, 127, 4535-4543.	1.5	4
8331	First-Principles Calculations on the Enhancing Effect of Zr on the Mechanical and Thermodynamic Properties of Irâ€“Rh Alloys. Transactions of the Indian Institute of Metals, 0, , .	0.7	1
8333	Effect of microstrain on the magnetic properties of reduced graphene oxide by Fe3O4 nanoparticles: insight from experimental and density functional theory. Applied Physics A: Materials Science and Processing, 2023, 129, .	1.1	1
8334	Amorphous As2S3 Doped with Transition Metals: An Ab Initio Study of Electronic Structure and Magnetic Properties. Nanomaterials, 2023, 13, 896.	1.9	1
8335	Peroxidase-like Nanozymes for Point-of-Care SERS Sensing and Wound Healing. ACS Applied Bio Materials, 2023, 6, 1272-1282.	2.3	3
8336	Rb₄Li₂TiOGe₄O₁₂: a novel high-performance titanyl germanate anode for Li-ion batteries. Journal of Materials Chemistry A, 2023, 11, 7170-7178.	5.2	0
8337	Interfacial electronic properties and tunable band offset in graphyne/MoSe₂ heterostructure with high carrier mobility. New Journal of Chemistry, 2023, 47, 7084-7092.	1.4	0
8338	Electronic properties of Y-247 ceramic via computational method. Materials Today: Proceedings, 2023, , .	0.9	0
8339	Discovering the Solid-State Secrets of Lorlatinib by NMR Crystallography: To Hydrogen Bond or not to Hydrogen Bond. Journal of Pharmaceutical Sciences, 2023, 112, 1915-1928.	1.6	5
8340	Atomic reconstruction and oxygen adsorption behavior of the pyrite (100) surface: a DFT study. Physical Chemistry Chemical Physics, 2023, 25, 8826-8835.	1.3	0
8341	Layered Heterostructures Based on MoS₂/MoSe₂ Nanosheets Deposited on GaN Substrates for Photodetector Applications. ACS Applied Nano Materials, 2023, 6, 4224-4235.	2.4	6
8342	Interface engineering of LDH-based material as efficient anti-corrosive system via synergetic performance of host, interlayers, and morphological features of nature-mimic architectures. Chemical Engineering Journal, 2023, 462, 142239.	6.6	17
8343	Strainâ€Ðriven Superlubricity of Graphene/Graphene in Commensurate Contact. Advanced Materials Interfaces, 2023, 10, .	1.9	5
8344	Efficient and Stable Perovskite Solar Cells by Tailoring of Interfaces. Advanced Materials, 2023, 35, .	11.1	21
8345	Decoding Supramolecular Packing Patterns from Computed Anisotropic Deformability Maps of Molecular Crystals. Journal of Physical Chemistry C, 2023, 127, 5533-5543.	1.5	1

#	Article	IF	Citations
8346	Millimeter-Sized Monoisotopic Cubic ¹⁰Boron Phosphide. Crystal Growth and Design, 2023, 23, 2812-2817.	1.4	1
8347	In Operando Optical Tracking of Oxygen Vacancy Migration and Phase Change in few Nanometers Ferroelectric HZO Memories. Advanced Functional Materials, 2023, 33, .	7.8	4
8348	An interlinked prediction-experiment paradigm discovering deep-ultraviolet fluorooxoborates with desired optical nonlinearity and birefringence. Matter, 2023, 6, 1188-1202.	5.0	24
8349	The structural and thermodynamic properties of CaLi₂ at high pressure. International Journal of Modern Physics C, 0, , .	0.8	0
8350	Is the impact sensitivity of RDX polymorph dependent?. Journal of Chemical Physics, 2023, 158, .	1.2	5
8351	Determining the Electronic Structure and Thermoelectric Properties of MoS₂/MoSe₂ Typeâ€Ⅱ Heterojunction by DFT and the Landauer Approach. Advanced Materials Interfaces, 2023, 10, .	1.9	2
8352	The boron-phosphorous co-doping scheme for possible n-type diamond from first principles. Computational Materials Science, 2023, 222, 112113.	1.4	2
8353	When Polymorphism in Metalâ€“Organic Frameworks Enables Water Sorption Profile Tunability for Enhancing Heat Allocation and Water Harvesting Performance. Advanced Materials, 2024, 36, .	11.1	8
8354	High stability and moderate second-order nonlinear optical properties of hybrid lead-free perovskite [(CH₃)₃NCH₂Cl]CdCl₃ bulk crystals. CrystEngComm, 2023, 25, 2264-2270.	1.3	2
8355	A Secondâ€Order Nonlinear Optical Material Consisting of Two Ï€â€Conjugated Groups. ChemPlusChem, 2023, 88, .	1.3	2
8356	Determination of conduction type in high-resistivity silicon by combining spreading resistance profiling (SRP) with hydrofluoric acid treatment. Applied Physics Letters, 2023, 122, .	1.5	0
8357	Stable all-solid-state Li-Te battery with Li3TbBr6 superionic conductor. Nano Research, 2023, 16, 9344-9351.	5.8	1
8358	Sulfur X-ray Absorption and Emission Spectroscopy of Organic Sulfones. Journal of Physical Chemistry A, 2023, 127, 3692-3704.	1.1	1
8359	Computational Analysis of Vibrational Spectra of Hydrogen Bonds in sII and sH Gas Hydrates. ACS Omega, 2023, 8, 11634-11639.	1.6	0
8360	[C(NH₂)₂NHNO₂][C(NH₂)₃](NO₃)₂: A Mixed Organic Cationic Hybrid Nitrate with an Unprecedented Nonlinear-Optical-Active Unit. Inorganic Chemistry, 2023, 62, 4757-4761.	1.9	7
8361	Magnetic Structure and Crystal Field States of <mml:math xmlns:mml="http://www.w3.org/1998/Math/MathML"><mml:msub><mml:mi mathvariant="normal">Pr</mml:mi><mml:mn>2</mml:mn></mml:msub><mml:msub><mml:mi mathvariant="normal">Pd</mml:mi><mml:mn>3</mml:mn></mml:msub><mml:msub><mml:mi mathvariant="normal">Ge</mml:mi><mml:mn>5</mml:mn></mml:msub></mml:math>: <mml:math	1.1	3
8362	Probing Local Environments of Oxygen Vacancies Responsible for Hydration in Sc-Doped Barium Zirconates at Elevated Temperatures: In Situ X-ray Absorption Spectroscopy, Thermogravimetry, and Active Learning Ab Initio Replica Exchange Monte Carlo Simulations. Chemistry of Materials, 2023, 35, 2289-2301.	3.2	3
8363	Selective Oxidation of Cyclohexane to Cyclohexanol/Cyclohexanone by Surface Peroxo Species on Cu-Mesoporous TiO₂. Inorganic Chemistry, 2023, 62, 4872-4882.	1.9	1

#	Article	IF	Citations
8364	Microstructures in Iron-rich FeSi Alloys by First-principles Phase Field and Special Quasirandom Structure Methods. ISIJ International, 2023, 63, 553-558.	0.6	0
8365	Stability and electronic properties of hydrogenated <scp>C₃B</scp> structure. International Journal of Quantum Chemistry, 2023, 123, .	1.0	0
8366	Crystal plane dependent dispersion of cobalt metal on metastable aluminas. Journal of Catalysis, 2023, 421, 210-220.	3.1	1
8367	A {Cu₂I₃^{â^'}}_{âˆž} chain hybrid with two-step phase transition, switchable dielectrics, thermochromism and piezochromism. Dalton Transactions, 0, , .	1.6	1
8368	Zn₂BS₃Br: An Infrared Nonlinear Optical Material with Significant Dual-Property Enhancements Designed through a Template Grafting Strategy. Chemistry of Materials, 2023, 35, 2647-2654.	3.2	7
8369	Na₂BaB₁₂O₁₈F₄: A Mixed Alkali/Alkaline-Earth Metal Fluorooxoborate with Two Unprecedented Interpenetrating Three-Dimensional Bâ€“O/F Anionic Networks and a Short Ultraviolet Cutoff Edge. Inorganic Chemistry, 2023, 62, 5008-5015.	1.9	3
8370	Temperature phase transitions in silver niobate and lithium tantalate-modified silver niobate ceramics. Physical Chemistry Chemical Physics, 2023, 25, 11410-11417.	1.3	1
8371	Targetâ€Driven Design of Deepâ€UV Nonlinear Optical Materials via Interpretable Machine Learning. Advanced Materials, 2023, 35, .	11.1	18
8372	Unique features of the structural phase transition in acetylene showing simultaneous characteristics of reconstructive, displacive and orderâ€“disorder. Physical Chemistry Chemical Physics, 2023, 25, 9909-9924.	1.3	0
8373	Elastic properties of SiO2 nanostructure in high-pressure conditions. Digest Journal of Nanomaterials and Biostructures, 2023, 18, 263-272.	0.3	0
8374	Do Models beyond Hybrid Density Functionals Increase the Agreement with Experiment for Predicted NMR Chemical Shifts or Electric Field Gradient Tensors in Organic Solids?. Journal of Physical Chemistry A, 2023, 127, 2846-2858.	1.1	8
8375	An effective strategy of indium half-doping to stabilize the structure and improve optoelectronic characteristics of Tl-Co based double perovskite: First principles study. Results in Physics, 2023, 47, 106375.	2.0	4
8376	Interface of Ni-MgCr₂O₄ Spinel Promotes the Autothermal Reforming of Acetic Acid through Accelerated Oxidation of Carbon-Containing Intermediate Species. ACS Catalysis, 2023, 13, 4560-4574.	5.5	9
8377	Vacancy defect influences on optoelectronic properties for In0.875Ga0.125As0.25P0.75: a first-principles study. Optical Review, 2023, 30, 166-173.	1.2	0
8378	Ab Initio Study of the Electronic Structure and Lattice Dynamics of Scheelite Type AgTcO₄. Physica Status Solidi (B): Basic Research, 2023, 260, .	0.7	0
8379	Simulation of Hafnium-Based FinFET and Ferroelectricity of Related 2-Dimensional Hafnium-Based Materials. , 0, 29, 69-76.		0
8380	CaB₂O₂F₄: A Novel [BOF₂]_{âˆž}-Based Structural Template with a Strong Second Harmonic Generation Response and Large Band Gap. Journal of Physical Chemistry C, 2023, 127, 6586-6592.	1.5	1
8381	Covalent organic framework@graphene composite as a high-performance electrode for Li-ion batteries. Molecular Simulation, 2023, 49, 729-741.	0.9	1

#	Article	IF	Citations
8382	Activation of NO₂ by Modifying the Porphyrin Unit with Oxygen in a MnN₄ Graphene Layer. ChemistrySelect, 2023, 8, .	0.7	0
8383	Automatic differentiation for orbital-free density functional theory. Journal of Chemical Physics, 2023, 158, .	1.2	2
8384	From ultra-low friction to superlubricity state of black phosphorus: Enabled by the critical oxidation and load. Friction, 2023, 11, 1829-1844.	3.4	3
8385	Structural, elastic, electronic, and optical properties of NaAlSi3O8 and Al4[Si4O10](OH)8 from first-principles calculations. Journal of Molecular Modeling, 2023, 29, .	0.8	1
8386	The contribution of phonons to the thermal expansion of some simple cubic hexaboride structures: SmB₆, CaB₆, SrB₆ and BaB₆. Physical Chemistry Chemical Physics, 2023, 25, 10749-10758.	1.3	1
8387	First principles calculations and analysis of electronic and optical structure of Ho-doped ZnO films. Journal of Materials Science: Materials in Electronics, 2023, 34, .	1.1	0
8388	Control of dynamic sp3-C stereochemistry. Nature Chemistry, 2023, 15, 615-624.	6.6	3
8389	Electronic band structure and density of state modulation of amphetamine and ABW typeâ€“zeolite adsorption system: DFT-CASTEP analysis. Journal of Molecular Modeling, 2023, 29, .	0.8	4
8390	Two-dimensional dichalcogenides of type XY$$_2$$ (X=Mo,W; Y=S,Se): A DFT study of the structural, optoelectronic, thermodynamic properties, infrared, and Raman spectra. Journal of Materials Research, 2023, 38, 2072-2083.	1.2	2
8391	Electronic band structure, mechanical and optical characteristics of new lead-free halide perovskites for solar cell applications based on DFT computation. Bulletin of Materials Science, 2023, 46, .	0.8	5
8392	A DFT study to investigate structural, electronic, optical, mechanical and magnetic properties of NaGeBr3 for photovoltaic and optoelectronic applications. Emergent Materials, 2023, 6, 699-709.	3.2	6
8393	Two UV optical crystals with strong optical anisotropy, large band gaps and an Î±-BBO type structure. Dalton Transactions, 0, , .	1.6	0
8394	Pressureâ€Induced Semiconductorâ€toâ€Metallic Transition of Monoclinic KCa₂Nb₃O₁₀ Layered Perovskite: A Theoretical DFT Insight. Crystal Research and Technology, 2023, 58, .	0.6	4
8395	The Site and High Field Î²NMR Properties of ⁸Li⁺ Implanted in Î±-Al₂O₃. Journal of Physics: Conference Series, 2023, 2462, 012009.	0.3	1
8396	é«˜å†å•¶æ°®å•‰é‡çš„æ°®æŽºæ‚èœ,çªçŠ¶ç¢³ä¿ƒè¿›å¯¹åšç¡«åŒ–ç‰©çš„ é™åˆ¶ä»¥å®žçŽ°é«˜æ€§èƒ½é”‚ç¡«ç”µæ±±Science China Mate		
8397	A simulation study on the phase transition behavior of solid nitrogen under extreme conditions. Physical Chemistry Chemical Physics, 0, , .	1.3	0
8398	MuSpinSim: spin dynamics calculations for muon science. Journal of Physics: Conference Series, 2023, 2462, 012017.	0.3	0
8399	Second-harmonic-generation of [(Se,Te)Cl₃]⁺[GaCl₄]^{â^'} with aligned ionic tetrahedra. Inorganic Chemistry Frontiers, 2023, 10, 2636-2644.	3.0	3

#	Article	IF	Citations
8400	Heteroatomâ€Driven Coordination Fields Altering Single Cerium Atom Sites for Efficient Oxygen Reduction Reaction. Advanced Materials, 2023, 35, .	11.1	39
8401	Room-temperature synthesis of lead-free copper(I)-antimony(III)-based double perovskite nanocrystals. APL Materials, 2023, 11, .	2.2	3
8402	Enhanced Cycling Performance of a Li-Excess Li₂CuO₂ Cathode Additive by Cosubstitution Nanoarchitectonics of Ni and Mn for Lithium-Ion Batteries. ACS Applied Materials & Interfaces, 2023, 15, 18790-18799.	4.0	3
8403	Structures and hydrogen storage properties of AeVH3 (Ae = Be, Mg, Ca, Sr) perovskite hydrides by DFT calculations. International Journal of Hydrogen Energy, 2023, 48, 24401-24411.	3.8	24
8404	Prediction of four Si₃N₄ compounds by first-principles calculations. AIP Advances, 2023, 13, 045310.	0.6	0
8405	Effect of acids on optical and dielectric properties of g-C3N4 and the DFT simulation. Optical and Quantum Electronics, 2023, 55, .	1.5	0
8406	High Strength Titanium with Fibrous Grain for Advanced Bone Regeneration. Advanced Science, 2023, 10, .	5.6	2
8407	Elucidating the Role of Noncovalent Interactions in Favipiravir, a Drug Active against Various Human RNA Viruses; a 1H-14N NQDR/Periodic DFT/QTAIM/RDS/3D Hirshfeld Surfaces Combined Study. Molecules, 2023, 28, 3308.	1.7	4
8408	Alkali Tin Halides: Exploring the Local Structure of A₂SnX₆ (A = K, Rb; X = Cl,) Tj ETQq0 0 0 rgBT /Overlock 10 127, 7284-7298.	1.5	1
8409	Four New Sbâ€based Orthophosphates: Cation Regulation to Investigate Diversified Structural Architecture. Chemistry - A European Journal, 0, , .	1.7	1
8410	13C CPMAS NMR as an Alternative Method to Verify the Quality of Dietary Supplements Containing Curcumin. Molecules, 2023, 28, 3442.	1.7	2
8411	Development of a Niâ€“Al reactive force field for Ni-based superalloy: revealing electrostatic effects on mechanical deformation. Journal of Materials Research and Technology, 2023, 24, 4454-4467.	2.6	0
8412	Synthesis of a high-entropy (TiVCrMo)3AlC2 MAX and its tribological properties in a wide temperature range. Journal of the European Ceramic Society, 2023, 43, 4684-4695.	2.8	7
8413	Optimal Design of Mid-Infrared Nonlinear-Optical Crystals: From SrZnSnSe₄ to SrZnSiSe₄. Inorganic Chemistry, 2023, 62, 6549-6553.	1.9	8
8414	Mechanism of AlP modifying the morphology of Si in Al-20Si alloys based on experimental studies and first-principles calculations. International Journal of Cast Metals Research, 2023, 36, 56-64.	0.5	0
8415	Enhancing birefringence of non-Ï€-conjugated sulfate systems through rare-earth metal-centered polyhedra. CrystEngComm, 2023, 25, 2939-2945.	1.3	2
8416	Effect of strontium (Sr) doping on the structural, electronic and optical properties of ZnO, by first-principles calculations. Physica B: Condensed Matter, 2023, 660, 414903.	1.3	4
8417	Unraveling Bonding Mechanisms and Electronic Structure of Pyridine Oximes on Fe(110) Surface: Deeper Insights from DFT, Molecular Dynamics and SCC-DFT Tight Binding Simulations. Molecules, 2023, 28, 3545.	1.7	1

#	Article	IF	Citations
8418	Highly Boosting Circularly Polarized Luminescence of Chiral Metalâ€“Imidazolate Frameworks. Advanced Science, 2023, 10, .	5.6	7
8419	AgIn₅Se₈: a defect diamond-like non-linear optical selenide. Inorganic Chemistry Frontiers, 2023, 10, 3248-3254.	3.0	4
8420	Reasonably optimized structure of iron-doped cobalt hydroxylfluoride for high-performance supercapacitors. Journal of Colloid and Interface Science, 2023, 644, 64-72.	5.0	4
8421	Beyond single tetrahedron physics of the breathing pyrochlore compound <mml:math xmlns:mml="http://www.w3.org/1998/Math/MathML"><mml:msub><mml:mi>Ba</mml:mi><mml:mn>3</mml:mn></mml:msub><mml:mathvariant="normal">O</mml:mi></mml:mrow><mml:mn>11</mml:mn></mml:msub></mml:math>. Physical Review B, 2023, 107, .	1.1	2
8422	DFT based comparative analysis of the physical properties of some binary transition metal carbides XC (X = Nb, Ta, Ti). Journal of Materials Research and Technology, 2023, 24, 4808-4832.	2.6	8
8423	Selective and Sensitive Detection of Formaldehyde at Room Temperature by Tin Oxide Nanoparticles/Reduced Graphene Oxide Composite. ACS Applied Nano Materials, 2023, 6, 7948-7959.	2.4	6
8424	Synthesis and Characterization of Xylazine Hydrochloride Polymorphs, Hydrates, and Cocrystals: A ³⁵Cl Solid-State NMR and DFT Study. Crystal Growth and Design, 2023, 23, 3412-3426.	1.4	3
8425	Unveiling the Transporting Mechanism of (Ti0.2Zr0.2Nb0.2Hf0.2Ta0.2)C at Room Temperature. Crystals, 2023, 13, 708.	1.0	0
8426	Investigating the function and design of molecular materials through terahertz vibrational spectroscopy. Nature Reviews Chemistry, 2023, 7, 480-495.	13.8	10
8427	Insight into physical properties of carbon-doped BeSiP2 and BeGeP2 chalcopyrite: An ab initio study. Journal of Solid State Chemistry, 2023, 323, 124054.	1.4	1
8428	Ab initio predictions of the structural, electronic, optical, elastic, and thermoelectric properties of quasi-two-dimensional BaFZnP. Computational Condensed Matter, 2023, 35, e00809.	0.9	7
8429	Reactive nanostructured membrane with high permeate flux under an ultralow pressure for excellent removal of refractory organic matter in actual water. Applied Catalysis B: Environmental, 2023, 334, 122794.	10.8	8
8430	Selective synthesis of two-dimensional semiconductive coordination polymers with silverâ€“sulfur network. CrystEngComm, 2023, 25, 2990-2994.	1.3	0
8451	Effect of Nitrogen Doping on Optoelectronic Properties of TiO2 Anatase Model for Solar Hydrogen Production: A DFTâ€‰+â€‰U Approach. Springer Proceedings in Energy, 2023, , 61-72.	0.2	0
8475	DFT and MC investigation of EDOT on honeycomb borophene as potential energy storage material. AIP Conference Proceedings, 2023, , .	0.3	1
8477	Pico technology â€“ An advancement in dye degradation. AIP Conference Proceedings, 2023, , .	0.3	0
8507	Tools and software for computer-aided drug design and discovery. , 2023, , 637-661.		1
8551	Hirshfeld atom refinement of metalâ€“organic frameworks for accurate positioning of hydrogen atoms and disorder analysis. Chemical Communications, 2023, 59, 8799-8802.	2.2	0

#	Article	IF	Citations
8597	New perspectives on the multianion approach to adapt electrode materials for lithium and post-lithium batteries. Physical Chemistry Chemical Physics, 2023, 25, 15600-15623.	1.3	2
8606	Engineered Graphene Grain Boundaries as Molecular Sieves for Water Desalination. , 2022, , .		1
8634	Spinâ€“phonon coupling and magnetic relaxation in single-molecule magnets. Chemical Society Reviews, 2023, 52, 4567-4585.	18.7	16
8636	Application of Molecular Simulation Methods in Treating Intrinsic Structures of Energetic Materials. , 2023, , 41-113.		1
8697	Adsorption Study of Carbon Monoxide on Modified Metal and Non-metallic Surface Using Density Functional Theory: A Short Review Towards Functional Materials. , 2023, , 442-458.		0
8809	Computational Insights of Dimensional Organic Materials. , 2023, , 382-473.		2
8811	Two-in-one tecton strategy to construct single crystalline hydrogen-bonded organic framework with high proton conductivity above 100 Â°C. Science China Chemistry, 2023, 66, 2563-2568.	4.2	0
8823	DFT predictions of the electronic, phonon, optical, and thermoelectric characteristics of CaCu2S2. MRS Communications, 0, , .	0.8	0
8849	Simulating excited states in metal organic frameworks: from light-absorption to photochemical CO₂ reduction. Materials Advances, 0, , .	2.6	0
8864	Elucidating mechanochemical reactivity of a ternary halogen-bonded cocrystal system by computational and calorimetric studies. Physical Chemistry Chemical Physics, 2023, 25, 28576-28580.	1.3	1
8945	The Use of DFT-Based ab-initio Technique to Determine the Stability Difference in B2 Ti-PGM Compounds. , 0, , .		0
9084	The design and optimization of heterogeneous catalysts using computational methods. Catalysis Science and Technology, 2024, 14, 515-532.	2.1	0
9208	A UV non-hydrogen pure selenite nonlinear optical material for achieving balanced properties through framework-optimized structural transformation. Materials Horizons, 2024, 11, 1704-1709.	6.4	4
9248	Lifshitz transition and superconducting critical temperature in Fe-based compounds. AIP Conference Proceedings, 2024, , .	0.3	0
9398	Electronic and Electrochemical Properties of Novel Cathode Material NaFeSO4OH by First-Principle Calculations. Lecture Notes in Mechanical Engineering, 2024, , 285-298.	0.3	0